Methods in Molecular Biology 1416

Springer Protocols

Massimiliano Gnecchi *Editor*

Mesenchymal Stem Cells

Methods and Protocols

Second Edition

Humana Press

METHODS IN MOLECULAR BIOLOGY

Series Editor
John M. Walker
School of Life and Medical Sciences
University of Hertfordshire
Hatfield, Hertfordshire, AL10 9AB, UK

For further volumes:
http://www.springer.com/series/7651

Mesenchymal Stem Cells

Methods and Protocols

Second Edition

Edited by

Massimiliano Gnecchi

Department of Molecular Medicine, Unit of Cardiology, University of Pavia, Pavia, Italy
Department of Cardiothoracic and Vascular Sciences – Coronary Care Unit and Laboratory of Clinical and Experimental Cardiology, Fondazione IRCCS Policlinico San Matteo, Pavia, Italy
Laboratory of Experimental Cardiology for Cell and Molecular Therapy, Fondazione IRCCS Policlinico San Matteo, Pavia, Italy
Department of Medicine, University of Cape Town, Cape Town, South Africa

Humana Press

Editor
Massimiliano Gnecchi
Department of Molecular Medicine
Unit of Cardiology
University of Pavia
Pavia, Italy

Department of Cardiothoracic and Vascular
Sciences – Coronary Care Unit and Laboratory
of Clinical and Experimental Cardiology
Fondazione IRCCS Policlinico San Matteo
Pavia, Italy

Laboratory of Experimental Cardiology
for Cell and Molecular Therapy
Fondazione IRCCS Policlinico San Matteo
Pavia, Italy

Department of Medicine
University of Cape Town
Cape Town, South Africa

ISSN 1064-3745 ISSN 1940-6029 (electronic)
Methods in Molecular Biology
ISBN 978-1-4939-3582-6 ISBN 978-1-4939-3584-0 (eBook)
DOI 10.1007/978-1-4939-3584-0

Library of Congress Control Number: 2016936658

Printed on acid-free paper

This Humana Press imprint is published by Springer Nature
The registered company is Springer Science+Business Media LLC New York

Preface

Mesenchymal stem cells (MSC) are adult cells with the capacity for self-renewal and multilineage differentiation. Initially described in the bone marrow, MSC are also present in other organs and tissues. From a therapeutic perspective, because of their straightforward preparation and hypothetical immunologic privilege, MSC emerged as an extremely promising therapeutic agent for tissue regeneration and repair. Currently, there are a significant number of clinical trials underway exploring the use of MSC for the treatment of various diseases including bone defects, graft-versus-host disease, myocardial infarction and heart failure, stroke, Crohn's disease, and wound repair. At the same time, there are still unresolved issues associated with MSC related to their isolation, culture and expansion, phenotypic definition, multipotential differentiation, and mechanisms of action. While researchers should ideally share and use proven methods and protocols to ultimately enable the comparison of results obtained by independent investigators, current MSC research is often considered nonhomogeneous, with different labs using different protocols and definitions.

The present volume aims to outline the current status of the field and to emphasize the need for clearly established and reproducible protocols to better define the identity, function, and use of MSC in cell therapy. In particular, in the first part of the book, a series of state-of-the-art reviews gives the reader a summary on the use of MSC for the treatment of various diseases. Then, in the following three parts, numerous chapters illustrate methods on isolation and characterization of MSC, expansion of MSC for clinical use, and production and definition of the MSC secretome. These protocols include practical advice from researchers who have personalized their methodologies. These insightful tips should dramatically reduce the time and costs involved in setting up MSC protocols in individual labs.

The volume mainly addresses PhD students and postdocs since they are the investigators actively operating in the field of cell and molecular biology, proteomics, and transcriptomics or in the development of clinically compliant manufacturing of therapeutic MSC or their derivatives. However, the state-of-the-art review chapters would be of extreme interest also for more senior investigators.

Pavia, Italy *Massimiliano Gnecchi*

Acknowledgments

I would like to personally thank all of the authors who contributed to this volume for sharing their invaluable knowledge and expertise in this dynamic field of Mesenchymal Stem Cell Applications.

Most of all, I extend a heartfelt thanks to Laurene Kelly, M.Sc., for managing all the correspondence with the authors. Ms. Kelly directly interfaced with each author for approval of her editorial improvements producing a uniform and *user friendly* volume.

Massimiliano Gnecchi

Contents

Contributors

Giulio Alessandri • *Department of Cerebrovascular Diseases, Fondazione IRCCS Neurological Institute Carlo Besta, Milan, Italy*

Gabriella Andriolo • *Lugano Cell Factory, Cardiocentro Ticino - Swiss Institute of Regenerative Medicine (SIRM), Lugano, Switzerland*

Sandra I. Anjo • *CNC – Center for Neuroscience and Cell Biology, University of Coimbra, Coimbra, Portugal; Faculty of Sciences and Technology, University of Coimbra, Coimbra, Portugal*

Stefano Baila • *TerumoBCT, Zaventem, Belgium*

Luigi Balducci • *Medestea Research and Production Laboratories, Consorzio CARSO, Bari, Italy*

Wayne Balkan • *Interdisciplinary Stem Cell Institute, University of Miami Miller School of Medicine, Miami, FL, USA*

Andrea Barbero • *Department of Biomedicine, University Hospital Basel, University of Basel, Basel, Switzerland*

Christina Barckhausen • *Department of Hematology, Oncology and Immunology, University Hospital Giessen and Marburg, Philipps-University Marburg, Marburg, Germany*

Maria Ester Bernardo • *Dipartimento di Emato-Oncologia e Medicina Trasfusionale, IRCCS Ospedale Pediatrico Bambino Gesù, Rome, Italy*

Jonathan Bernhard • *Department of Biomedical Engineering, Columbia University, New York, NY, USA*

Pierre-Olivier Bessette • *Faculté de Médecine, Université de Montréal, Montréal, Canada*

Karen Bieback • *Medical Faculty Mannheim, Institute of Transfusion Medicine and Immunology, Heidelberg University, Heidelberg, Germany; German Red Cross Blood Service Baden-Württemberg – Hessen, Mannheim, Germany*

Francisco J. Blanco • *Rheumatology Division, ProteoRed-PRB2/ISCIII Proteomics Group, INIBIC – Hospital Universitario de A Coruña, A Coruña, Spain; RIER-RED de Inflamación y Enfermedades Reumáticas, INIBIC-CHUAC, A Coruña, Spain; Servicio de Reumatología, Unidad de Investigación, INIBIC-CHU A Coruña, A Coruña, Spain*

Sara Bolis • *Lugano Cell Factory, Cardiocentro Ticino - Swiss Institute of Regenerative Medicine (SIRM), Lugano, Switzerland*

Siddaraju V. Boregowda • *Department of Molecular Therapeutics, The Scripps Research Institute, Jupiter, FL, USA*

Melanie Borie • *Centre de Recherche du Centre Hospitalier de l'Université de Montréal (CRCHUM), Montreal, QC, Canada*

Joaquim M.S. Cabral • *Department of Bioengineering and iBB - Institute for Bioengineering and Biosciences, Instituto Superior Técnico, Universidade de Lisboa, Lisboa, Portugal*

Valentina Calamia • *Rheumatology Division, ProteoRed-PRB2/ISCIII Proteomics Group, INIBIC – Hospital Universitario de A Coruña, A Coruña, Spain*

Arnold I. Caplan • *Skeletal Research Center, Case Western Reserve University, Cleveland, OH, USA*

Joana G. Carmelo • *Department of Bioengineering and iBB - Institute for Bioengineering and Biosciences, Instituto Superior Técnico, Universidade de Lisboa, Lisboa, Portugal*

Matteo Centola • *Department of Biomedicine, University Hospital Basel, University of Basel, Basel, Switzerland*

Steven A.J. Chamuleau • *Division Heart and Lungs, Department of Cardiology, University Medical Center Utrecht, Utrecht, The Netherlands*

Jerry K.Y. Chan • *Experimental Fetal Medicine Group, Department of Obstetrics and Gynaecology, Yong Loo Lin School of Medicine, National University of Singapore, Singapore, Singapore; Department of Reproductive Medicine, KK Women's and Children's Hospital, Singapore, Singapore; Cancer and Stem Cell Biology Program, Duke-NUS Graduate Medical School, Singapore, Singapore*

Andre Choo • *Agency for Science Technology and Research, Bioprocessing Technology Institute, Singapore, Singapore; Division of Bioengineering, Faculty of Engineering, National University of Singapore, Singapore, Singapore*

Maria Chiara Ciuffreda • *Department of Molecular Medicine, Unit of Cardiology, University of Pavia, Pavia, Italy; Department of Cardiothoracic and Vascular Sciences – Coronary Care Unit and Laboratory of Clinical and Experimental Cardiology, Fondazione IRCCS Policlinico San Matteo, Pavia, Italy; Laboratory of Experimental Cardiology for Cell and Molecular Therapy, Fondazione IRCCS Policlinico San Matteo, Pavia, Italy*

Dimas Tadeu Covas • *Hemocentro de Ribeirão Preto, Centro de Terapia Celular, Faculadade de Medicina de Ribeirão Preto, Universidade de São Paulo, Ribeirão Preto, SP, Brazil*

Patrizia Danieli • *Department of Molecular Medicine, Unit of Cardiology, University of Pavia, Pavia, Italy; Department of Cardiothoracic and Vascular Sciences – Coronary Care Unit and Laboratory of Clinical and Experimental Cardiology, Fondazione IRCCS Policlinico San Matteo, Pavia, Italy; Laboratory of Experimental Cardiology for Cell and Molecular Therapy, Fondazione IRCCS Policlinico San Matteo, Pavia, Italy*

Cláudia Lobato da Silva • *Department of Bioengineering and iBB - Institute for Bioengineering and Biosciences, Instituto Superior Técnico, Universidade de Lisboa, Lisboa, Portugal*

Dominique P.V. de Kleijn • *Department of Surgery, Yong Loo Lin School of Medicine, National University of Singapore, Singapore, Singapore; Cardiovascular Research Institute, National University Health System, Singapore, Singapore; Experimental Cardiology, University Medical Center, Utrecht, The Netherlands; Interuniversity Cardiology Institute of the Netherlands, Utrecht, The Netherlands*

Shant Der Sarkissian • *Centre de Recherche du Centre Hospitalier de l'Université de Montréal (CRCHUM) Montreal, QC, Canada; Faculté de Médecine, Université de Montréal, Montreal, QC, Canada*

Pieter A. Doevendans • *Division Heart and Lungs, Department of Cardiology, University Medical Center Utrecht, Utrecht, The Netherlands; Interuniversity Cardiology Institute of the Netherlands (ICIN), Utrecht, The Netherlands*

Annette Ekblond • *Cardiology Stem Cell Centre, The Heart Centre, Rigshospitalet Copenhagen University Hospital, Copenhagen, Denmark*

Vitor Marcel Faça • *Departamento de Bioquímica e Imunologia, Faculdade de Medicina de Ribeirão Preto, Universidade de São Paulo, Ribeirão Preto, SP, Brazil; Hemocentro de Ribeirão Preto, Centro de Terapia Celular, Faculadade de Medicina de Ribeirão Preto, Universidade de São Paulo, Ribeirão Preto, SP, Brazil*

Ana Fernandes-Platzgummer • *Department of Bioengineering and iBB - Institute for Bioengineering and Biosciences, Instituto Superior Técnico, Universidade de Lisboa, Lisboa, Portugal*

Dries A.M. Feyen • *Division Heart and Lungs, Department of Cardiology, University Medical Center Utrecht, Utrecht, The Netherlands*

Fei Gao • *Department of Ophthalmology, Li Ka Shing Faculty of Medicine, University of Hong Kong, Hong Kong, China*

Paolo Giannoni • *Stem Cell Laboratory, Department of Experimental Medicine, University of Genova, Genoa, Italy*

Massimiliano Gnecchi • *Department of Molecular Medicine, Unit of Cardiology, University of Pavia, Pavia, Italy; Department of Cardiothoracic and Vascular Sciences – Coronary Care Unit and Laboratory of Clinical and Experimental Cardiology, Fondazione IRCCS Policlinico San Matteo, Pavia, Italy; Laboratory of Experimental Cardiology for Cell and Molecular Therapy, Fondazione IRCCS Policlinico San Matteo, Pavia, Italy; Department of Medicine, University of Cape Town, Cape Town, South Africa*

Jose Gomez • *Division of Cardiology, Department of Medicine, Duke University Medical Center & Duke Cardiovascular Research Center, Durham, NC, USA*

Lewis Joel Greene • *Hemocentro de Ribeirão Preto, Centro de Terapia Celular, Faculadade de Medicina de Ribeirão Preto, Universidade de São Paulo, Ribeirão Preto, SP, Brazil*

Mandana Haack-Sørensen • *Cardiology Stem Cell Centre, The Heart Centre, Rigshospitalet Copenhagen University Hospital, Copenhagen, Denmark*

Holger Hackstein • *Institute for Clinical Immunology and Transfusion Medicine, University Hospital Giessen and Marburg, Justus-Liebig-University Giessen, Giessen, Germany*

Patrick J. Hanley • *Program for Cell Enhancement and Technologies for Immunotherapy, Center for Cancer and Immunology Research, Washington, DC, USA; Children's National Health System, Washington, DC, USA; Division of Blood and Marrow Transplantation, Washington, DC, USA; Sheikh Zayed Institute for Pediatric Surgical Innovation, Washington, DC, USA; The George Washington University, Washington, DC, USA*

Joshua M. Hare • *Interdisciplinary Stem Cell Institute, University of Miami Miller School of Medicine, Miami, FL, USA*

Jens Kastrup • *Cardiology Stem Cell Centre, The Heart Centre, Rigshospitalet Copenhagen University Hospital, Copenhagen, Denmark*

Satoru Kidoaki • *Laboratory of Biomedical and Biophysical Chemistry, Institute for Materials Chemistry and Engineering, Kyushu University, Fukuoka, Japan*

Veena Krishnappa • *Department of Molecular Therapeutics, The Scripps Research Institute, Jupiter, FL, USA*

Thasaneeya Kuboki • *Laboratory of Biomedical and Biophysical Chemistry, Institute for Materials Chemistry and Engineering, Kyushu University, Fukuoka, Japan*

Ruenn Chai Lai • *Agency for Science Technology and Research, Institute of Medical Biology, Singapore, Singapore*

Paula Lam • *Cancer and Stem Cell Biology Program, Duke-NUS Graduate Medical School, Singapore, Singapore; Department of Physiology, Yong Loo Lin School of Medicine, National University of Singapore, Singapore, Singapore; Laboratory of Cancer Gene Therapy, Division of Cellular and Molecular Research, National Cancer Centre, Humphrey Oei Institute of Cancer Research, Singapore, Singapore*

Qizhou Lian • *Cardiology Division, Department of Medicine, University of Hong Kong, Hong Kong, China; Research Centre of Heart, Brain, Hormone, and Healthy Aging, Li Ka Shing Faculty of Medicine, University of Hong Kong, Hong Kong, China; Department of Ophthalmology, Li Ka Shing Faculty of Medicine, University of China, Hong Kong, China*

Xiaoting Liang • *Cardiology Division, Department of Medicine, University of Hong Kong, Hong Kong, China*

Sai Kiang Lim • *Agency for Science Technology and Research, Institute of Medical Biology, Singapore, Singapore; Department of Surgery, Yong Loo Lin School of Medicine, National University of Singapore, Singapore, Singapore*

Franco Locatelli • *Dipartimento di Emato-Oncologia e Medicina Trasfusionale, IRCCS Ospedale Pediatrico Bambino Gesù, Roma, Italy; Dipartimento di Scienze Pediatriche, Università degli Studi di Pavia, Pavia, Italy*

Viviana Lo Cicero • *Lugano Cell Factory, Cardiocentro Ticino - Swiss Institute of Regenerative Medicine (SIRM), Lugano, Switzerland*

Ana S. Lourenço • *Faculty of Sciences and Technology, University of Coimbra, Coimbra, Portugal; Biocant - Biotechnology Innovation Center, Cantanhede, Portugal*

Marta Magatti • *Centro di Ricerca E. Menni, Fondazione Poliambulanza-Istituto Ospedaliero, Brescia, Italy*

Giuseppe Malpasso • *Department of Molecular Medicine, Unit of Cardiology, University of Pavia, Pavia, Italy; Department of Cardiothoracic and Vascular Sciences – Coronary Care Unit and Laboratory of Clinical and Experimental Cardiology, Fondazione IRCCS Policlinico San Matteo, Pavia, Italy; Laboratory of Experimental Cardiology for Cell and Molecular Therapy, Fondazione IRCCS Policlinico San Matteo, Pavia, Italy*

Bruno Manadas • *CNC – Center for Neuroscience and Cell Biology, University of Coimbra, Coimbra, Portugal; Biocant - Biotechnology Innovation Center, Cantanhede, Portugal*

Ivan Martin • *Department of Biomedicine, University Hospital Basel, University of Basel, Basel, Switzerland*

Matilde N. Melo • *CNC – Center for Neuroscience and Cell Biology, University of Coimbra, Coimbra, Portugal*

Renuka P. Miller • *Program for Cell Enhancement and Technologies for Immunotherapy, Center for Cancer and Immunology Research, Washington, DC, USA; Children's National Health System, Washington, DC, USA*

Maria Mirotsou • *Division of Cardiology, Department of Medicine, Duke University Medical Center & Duke Cardiovascular Research Center, Durham, NC, USA*

Marina Morigi • *IRCCS – Istituto di Ricerche Farmacologiche Mario Negri, Centro Anna Maria Astori, Bergamo, Italy*

Paola Musarò • *Department of Cardiothoracic and Vascular Sciences – Coronary Care Unit and Laboratory of Clinical and Experimental Cardiology, Fondazione IRCCS Policlinico San Matteo, Pavia, Italy; Laboratory of Experimental Cardiology for Cell and Molecular Therapy, Fondazione IRCCS Policlinico San Matteo, Pavia, Italy*

Philipp Netsch • *Medical Faculty Mannheim, Institute of Transfusion Medicine and Immunology, Heidelberg University, Heidelberg, Germany; German Red Cross Blood Service Baden-Württemberg – Hessen, Mannheim, Germany*

Johnathan Ng • *Department of Biomedical Engineering, Columbia University, New York, NY, USA*

Nicolas Noiseux • *Centre de Recherche du Centre Hospitalier de l'Université de Montréal (CRCHUM) Montreal, QC, Canada; Faculté de Médecine, Université de Montréal, Montreal, QC, Canada; Division of Cardiac Surgery, Centre Hospitalier de l'Université de Montréal (CHUM), Montreal, QC, Canada*

Philipp Nold • *Department of Hematology, Oncology and Immunology, University Hospital Giessen and Marburg, Philipps-University, Marburg, Germany*

Willy Noort • *Division Heart and Lungs, Department of Cardiology, University Medical Center Utrecht, Utrecht, The Netherlands; Department of Cell Biology, University Medical Center Utrecht, Utrecht, The Netherlands*

Maristela Delgado Orellana • *Hemocentro de Ribeirão Preto, Centro de Terapia Celular, Faculadade de Medicina de Ribeirão Preto, Universidade de São Paulo, Ribeirão Preto, SP, Brazil*

Jayanthi Padmanabhan • *Agency for Science Technology and Research, Bioprocessing Technology Institute, Singapore, Singapore*

Adam Papadimitropoulos • *Department of Biomedicine, University Hospital Basel, University of Basel, Basel, Switzerland*

Ornella Parolini • *Centro di Ricerca E. Menni, Fondazione Poliambulanza-Istituto Ospedaliero, Brescia, Italy*

Patrice Penfornis • *Cancer Institute, University of Mississippi Medical Center, Jackson, MS, USA*

Donald G. Phinney • *Department of Molecular Therapeutics, The Scripps Research Institute, Jupiter, FL, USA*

Stefano Pianta • *Centro di Ricerca E. Menni, Fondazione Poliambulanza-Istituto Ospedaliero, Brescia, Italy*

Elia Piccinini • *Department of Biomedicine, University Hospital Basel, University of Basel, Basel, Switzerland*

Radhika Pochampally • *Cancer Institute, University of Mississippi Medical Center, Jackson, MS, USA; Department of Biochemistry, University of Mississippi Medical Center, Jackson, MS, USA*

Rodolfo Quarto • *Stem Cell Laboratory, Department of Experimental Medicine, University of Genova, Genoa, Italy*

Marina Radrizzani • *Lugano Cell Factory, Cardiocentro Ticino - Swiss Institute of Regenerative Medicine (SIRM), Lugano, Switzerland*

Giuseppe Remuzzi • *IRCCS – Istituto di Ricerche Farmacologiche Mario Negri, Centro Anna Maria Astori, Bergamo, Italy; Unit of Nephrology and Dialysis, A.O. Papa Giovanni XXIII, Bergamo, Italy*

Brent Rice • *TerumoBCT, Lakewood, CO, USA*

Camillo Ricordi • *Cell Transplant Program and Diabetes Research Institute, University of Miami, Miami, FL, USA*

Beatriz Rocha • *Rheumatology Division, ProteoRed-PRB2/ISCIII Proteomics Group, INIBIC – Hospital Universitario de A Coruña, A Coruña, Spain*

Markus Thomas Rojewski • *Institut für Klinische Transfusionsmedizin und Immungenetik Ulm, DRK-Blutspendedienst Baden-Württemberg – Hessen, Ulm, Germany; Institut für Transfusionsmedizin, Universitätsklinikum Ulm, Ulm, Germany*
Cinzia Rota • *IRCCS – Istituto di Ricerche Farmacologiche Mario Negri, Centro Anna Maria Astori, Bergamo, Italy*
Cristina Ruiz-Romero • *Rheumatology Division, ProteoRed-PRB2/ISCIII Proteomics Group, INIBIC – Hospital Universitario de A Coruña, A Coruña, Spain; CIBER-BBN, INIBIC-CHUAC, A Coruña, Spain*
A.J. Salgado • *Life and Health Sciences Research Institute (ICVS), School of Health Sciences, University of Minho, Braga, Portugal; ICVS/3B's, PT Government Associate Laboratory, Braga/Guimarães, Portugal*
Cristina Sanina • *Interdisciplinary Stem Cell Institute, University of Miami Miller School of Medicine, Miami, FL, USA*
Cátia Santa • *CNC – Center for Neuroscience and Cell Biology, University of Coimbra, Coimbra, Portugal; Institute for Interdisciplinary Research, University of Coimbra (IIIUC), Coimbra, Portugal*
Jeffrey Schmeckpeper • *Division of Cardiology, Department of Medicine, Duke University Medical Center & Duke Cardiovascular Research Center, Durham, NC, USA*
Hubert Schrezenmeier • *Institut für Klinische Transfusionsmedizin und Immungenetik Ulm, DRK-Blutspendedienst Baden-Württemberg – Hessen, Ulm, Germany; Institut für Transfusionsmedizin, Universitätsklinikum Ulm, Ulm, Germany*
R. Wilder Scott • *Department of Cellular and Physiological Sciences and Biomedical Research Centre, University of British Columbia, Vancouver, BC, Canada*
Celeste Scotti • *Department of Biomedicine, University Hospital Basel, University of Basel, Basel, Switzerland; IRCCS Istituto Ortopedico Galeazzi, Milan, Italy*
Luc Sensebé • *UMR5273-U1031 STROMALab, CNRS, INSERM, Université Paul Sabatier Toulouse, EFS, Toulouse, France*
S.C. Serra • *Life and Health Sciences Research Institute (ICVS), School of Health Sciences, University of Minho, Braga, Portugal; ICVS/3B's, PT Government Associate Laboratory, Braga/Guimarães, Portugal*
Antonietta Silini • *Centro di Ricerca E. Menni, Fondazione Poliambulanza-Istituto Ospedaliero, Brescia, Italy*
Joost P.G. Sluijter • *Division Heart and Lungs, Department of Cardiology, University Medical Center Utrecht, Utrecht, The Netherlands; Interuniversity Cardiology Institute of the Netherlands (ICIN), Utrecht, The Netherlands; Experimental Cardiology Laboratory, Department of Cardiology, University Medical Center Utrecht, Utrecht, CX, The Netherlands*
Sabrina Soncin • *Lugano Cell Factory, Cardiocentro Ticino - Swiss Institute of Regenerative Medicine (SIRM), Lugano, Switzerland*
F.G. Teixeira • *Life and Health Sciences Research Institute (ICVS), School of Health Sciences, University of Minho, Braga, Portugal; ICVS/3B's, PT Government Associate Laboratory, Braga/Guimarães, Portugal*
Atanas Todorov • *Department of Biomedicine, University Hospital Basel, University of Basel, Basel, Switzerland*
Beatrice Tonnarelli • *Department of Biomedicine, University Hospital Basel, University of Basel, Basel, Switzerland*
Carlo Tremolada • *Istituto Image, Milan, Italy*

Hung-Fat Tse • *Cardiology Division, Department of Medicine, University of Hong Kong, Hong Kong, China; Research Centre of Heart, Brain, Hormone, and Healthy Aging, Li Ka Shing Faculty of Medicine, University of Hong Kong, Hong Kong, China*

Lucia Turchetto • *Lugano Cell Factory, Cardiocentro Ticino - Swiss Institute of Regenerative Medicine (SIRM), Lugano, Switzerland*

Valentina Turco • *Department of Cardiothoracic and Vascular Sciences – Coronary Care Unit and Laboratory of Clinical and Experimental Cardiology, Fondazione IRCCS Policlinico San Matteo, Pavia, Italy; Laboratory of Experimental Cardiology for Cell and Molecular Therapy, Fondazione IRCCS Policlinico San Matteo, Pavia, Italy*

T. Michael Underhill • *Department of Cellular and Physiological Sciences and Biomedical Research Centre, University of British Columbia, Vancouver, BC, Canada*

Frederieke van den Akker • *Division Heart and Lungs, Department of Cardiology, University Medical Center Utrecht, Utrecht, The Netherlands*

Carlo Ventura • *SWITH (Stem Wave Institute for Tissue Healing), Gruppo Villa Maria (GVM) and Ettore Sansavini Health Science Foundation – ONLUS, Lugo (Ravenna), Italy; National Institute of Biostructures and Biosystems (NIBB) at the S. Orsola – Malpighi Hospital, Institute of Cardiology, University of Bologna, Bologna, Italy*

Minh Quan Vu • *Centre de Recherche du Centre Hospitalier de l'Université de Montréal (CRCHUM), Montreal, QC, Canada; Faculté de Médecine, Université de Montréal, Montreal, QC, Canada*

Gordana Vunjak-Novakovic • *Department of Biomedical Engineering, Columbia University, New York, NY, USA; Departments of Medicine, Columbia University, New York, NY, USA*

Ian A. White • *Interdisciplinary Stem Cell Institute, University of Miami Miller School of Medicine, Miami, FL, USA*

Ronne Wee Yeh Yeo • *Agency for Science Technology and Research, Institute of Medical Biology, Singapore, Singapore*

Yuelin Zhang • *Cardiology Division, Department of Medicine, University of Hong Kong, Hong Kong, China; Department of Ophthalmology, Li Ka Shing Faculty of Medicine, University of Hong Kong, Hong Kong, China*

Part I

Overview of Mesenchymal Stem Cells For Cell Therapy

Chapter 1

Mesenchymal Stromal Cells in Hematopoietic Stem Cell Transplantation

Maria Ester Bernardo and Franco Locatelli

Abstract

Mesenchymal stromal cells (MSCs) comprise a heterogeneous population of multipotent cells that can be isolated from various human tissues and cultured ex vivo for clinical use. Thanks to their secretion of growth factors, immunomodulatory properties and cell-to-cell interactions, MSCs play a key role in the regulation of hematopoiesis and in the modulation of immune responses against allo- and autoantigens. In light of these properties, MSCs have been employed in clinical trials in the context of hematopoietic stem cell transplantation (HSCT) to prevent/treat graft rejection and to treat steroid-resistant acute graft-versus-host disease (GvHD). The available clinical evidence derived from these studies indicates that MSC administration is safe; moreover, promising preliminary results in terms of efficacy have been reported in some clinical trials. This chapter focuses on recent advances in MSC therapy by reporting on the most important relevant studies in the field of HSCT.

Key words Mesenchymal stromal cells, Hematopoietic stem cell transplantation, Engraftment, Graft-versus-host disease, Immune-regulatory properties, Inflammation

1 Introduction

Mesenchymal stromal cells (MSCs) were first described more than 40 years ago by Friedenstein et al. as a population of adherent cells isolated from the bone marrow (BM), which were non-phagocytic, exhibited a fibroblast-like morphology and could be induced to differentiate in vitro into bone, cartilage, adipose tissue, tendon, and muscle [1]. After transplantation under the kidney capsule, MSCs could generate all of the different connective tissue lineages [2].

After their identification in the BM, human MSCs were isolated from a variety of other human tissues, including periosteum, muscle connective tissue, perichondrium, adipose tissue (AT), umbilical cord blood (UCB), and fetal tissues, such as amniotic fluid and placenta [1, 3–5]. One hallmark characteristic of MSCs is their multipotency, defined as the ability to differentiate

Massimiliano Gnecchi (ed.), *Mesenchymal Stem Cells: Methods and Protocols*, Methods in Molecular Biology, vol. 1416,
DOI 10.1007/978-1-4939-3584-0_1,

into several mesenchymal lineages, including bone, cartilage, and adipose tissue (AT) [6]. MSCs display broad and potent immune-modulatory properties which can influence both adaptive and innate immune responses [7–9]. Indeed, recent findings have demonstrated that MSCs actively interact not only with cells belonging to the adaptive immune system, but also with components of the innate immune response and that, through these latter interactions, they display both anti-inflammatory and pro-inflammatory effects. This ability of MSCs to adopt a different phenotype in response to sensing an inflammatory environment is crucial for understanding their therapeutic potential in immune-mediated disorders [10–12]. The exact mechanisms by which MSCs exert their functions, either through cell-to-cell contact or secretion of soluble factors or both, are still not completely understood. Moreover, data on the mechanisms by which MSCs display their immunosuppressive effect have been mainly obtained in in vitro studies [7–9]; the in vivo biological relevance of the in vitro observations needs to be clarified.

Thanks to their immune-modulatory properties, as well as their ability to home to inflamed sites and repair injured tissues [7, 10, 13], MSCs have been recently employed as a therapeutic tool in the context of hematopoietic stem cell transplantation (HSCT), as well as in approaches of immune-regulatory and regenerative cell therapy. Phase I/II clinical trials [11–13], mainly addressing the issues of feasibility and safety of MSC infusions, have been conducted and to date no adverse effects have been registered after MSC administration. In particular, MSCs have been employed to enhance hematopoietic stem cell (HSC) engraftment after HLA-haploidentical, T cell-depleted allografts [14] and UCB transplantation [15], as well as to treat severe, steroid-refractory, acute *graft*-versus-*host* disease (aGvHD) [16]. MSCs have also been successfully used to repair tissue injury, occurring both after allogeneic HSCT [17] and in refractory Crohn's disease (CD) [18].

2 Mesenchymal Stem Cell Characterization and Immunomodulatory Properties

2.1 Characterization of Ex-Vivo Expanded Mesenchymal Stem Cells

Due to the low frequency of mesenchymal progenitors in human tissues, MSCs are extensively ex vivo expanded for clinical use [14–16]. Standard conditions for ex vivo expansion of MSCs are based on the presence of 10 % fetal calf serum (FCS) [14–16]. However, serum-free additives, devoid of the risks connected with the use of animal products, such as platelet lysate (PL), are also being developed with favorable results [19, 20].

Because MSC numbers are limited in human tissues and since they lack specific markers, it has been troublesome to prospectively isolate the most primitive mesenchymal progenitors and MSCs are

still characterized on the basis of their morphology, ability to adhere to plastic and immunophenotype by a combination of positive (CD105, CD73, CD90, and HLA class I) and negative (CD14, CD31, CD34, and CD45) markers [21]. Recently, specific markers have been utilized, such as stage-specific embryonic antigen-4 (SSEA-4), STRO-1, the low-affinity nerve growth factor receptor (CD271), and MCAM/CD146 (Melanoma Cell Adhesion Molecule), for the identification and prospective isolation of human BM-derived mesenchymal progenitors [22–24]. However, none of these markers has demonstrated to be by itself capable of identifying the true mesenchymal stem cell. Moreover, since both ex vivo expansion on plastic surfaces and culture conditions may induce phenotypic and functional changes, it remains uncertain whether culture-expanded MSCs differ from their progenitors in vivo.

During the last decade, several studies have been performed on the risk of transformation of MSCs during ex vivo expansion and on potential tumor formation in vivo after MSC administration [25–28]. However, the occurrence of malignant transformation under routinely used culture conditions has been demonstrated to be an extremely uncommon event, and, to date, tumor formation has never been demonstrated in over 5000 patients treated with MSCs, these findings indicate a safe MSC profile [29]. In particular, genetic studies performed both by conventional karyotyping and molecular techniques (array-CGH), together with the study of several proteins and genes involved in the regulation of the cell cycle, senescence, and tumorigenesis, have been employed to document the absence of chromosomal abnormalities and transformation in ex vivo expanded MSCs [25]. Moreover, French researchers have demonstrated that the occasional presence of aneuploidy in some MSC preparations may be related to the occurrence of senescence, and not to the development of transformation [26].

2.2 Immunomodulatory Properties of Mesenchymal Stem Cells

MSCs display unique immune-modulatory properties that were first demonstrated in vitro and, subsequently, in vivo both in animal models and in humans [7, 8]. The interactions of MSCs with cells of both the adaptive and innate immune system are schematically summarized in Fig. 1.

MSCs were first demonstrated to suppress in vitro T-lymphocyte proliferation induced by alloantigens [30], mitogens [9], CD3 and CD28 agonist antibodies [9, 31, 32]. MSCs have been reported to inhibit the effects of cytotoxic T cells (CTLs), probably due to suppression of CTL proliferation [33]. Since the separation of MSCs and peripheral blood mononuclear cells (PBMCs) by transwell experiments does not completely abrogate the suppressive effect, it is likely that this effect is partly dependent on cell-to-cell contact mechanisms and partly attributed to the secretion of soluble antiproliferative factors (such as TGF-β, hepatocyte growth factor,

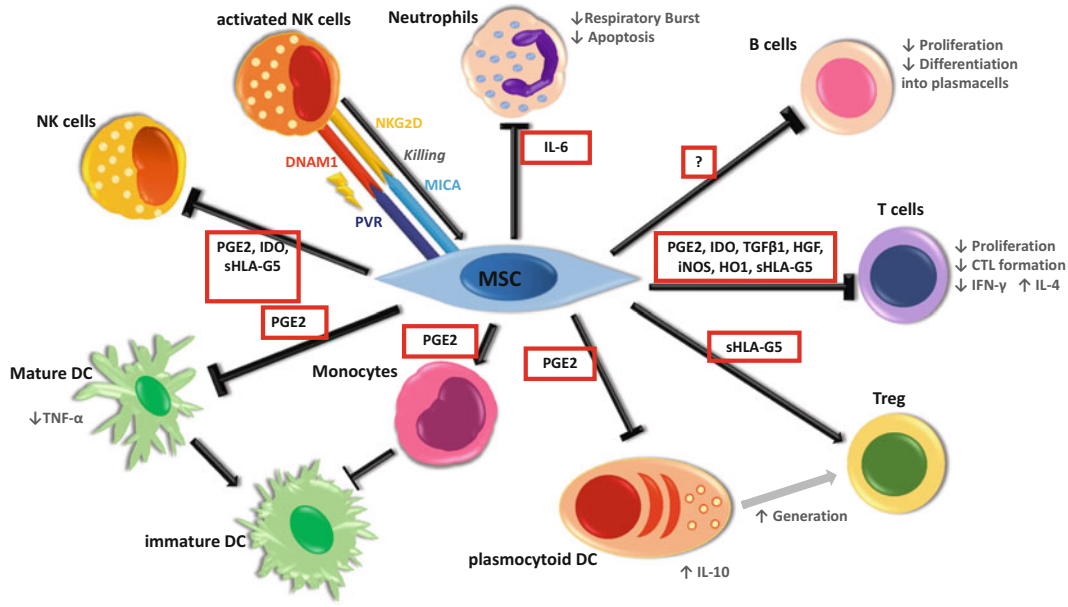

Fig. 1 Schematic representation of MSC interactions with cells of both the adaptive and innate immune system. *NK* natural killer, *DC* dendritic cells, *Treg* regulatory T cells, *PGE2* prostaglandin E2, *IDO* indoleamine 2,3-dioxygenase, *CTL* cytotoxic T lymphocytes

prostaglandin E2 (PGE2), indoleamine 2,3-dioxygenase (IDO), nitric oxide (NO), heme-oxygenase-1 (HO-1)) [34, 35]. Inhibition of lymphocyte proliferation by MSCs has not been associated with the induction of apoptosis, but it is rather interpreted as due to inhibition of cell division, thus preventing T lymphocytes from responding to antigenic triggers, while maintaining these cells in the G0/G1 phase of the cell cycle [30, 31].

Several in vitro and in vivo studies have documented the ability of MSCs to polarize T cells toward a regulatory phenotype [36], which serves as an important mechanism by which MSCs blunt inflammation. In vitro co-incubation of human MSCs with PBMCs induces the differentiation of $CD4^+$ T cells into $CD25^+FoxP3^+$ expressing regulatory T cells (induced Tregs) [37, 38]. The generation of Tregs was reported to be monocyte-dependent and was not observed in co-cultures of MSCs and purified $CD4^+$ T cells or monocyte-depleted PBMCs, but it could be restored by the addition of monocytes [39]. The polarization of T cells toward a Treg phenotype has been also shown in experimental models of autoimmune and inflammatory diseases [40, 41].

A role for monocytes, as an essential intermediary through which (UCB-derived) MSCs mediate their suppressive effects in vitro on T-cell proliferation, has also been reported. Removal of monocytes from human PBMCs was associated with a reduction in the immunosuppressive effects of MSCs on mitogen-induced

T-cell proliferation, and monocytes purified from UCB/MSC co-culture showed significantly reduced accessory cell and allo-stimulatory function when tested in subsequent T-cell proliferation assays [42]. Differentiation of both monocytes and $CD34^+$ progenitors into $CD1a^+$-dendritic cells (DCs) is inhibited in the presence of MSCs, and DCs generated in this latter condition are impaired in their function, in particular in their ability to induce activation of T cells. Moreover, incubation of MSCs with mature DCs has been demonstrated to favor in vitro the induction of regulatory antigen-presenting cells (APCs), through which they could indirectly suppress T-cell proliferation [43, 44].

Conflicting results have been published on the ability of MSCs to interfere in vitro with B-lymphocyte function/proliferation, although the majority of reports suggest that B-cell proliferation, as well as differentiation and expression of cytokines, are inhibited by MSCs [45, 46]. In particular, human MSCs have been demonstrated to suppress in vitro the proliferation of B cells activated with anti-Ig antibodies, soluble CD40 ligand and cytokines, as well as to interfere with differentiation, antibody production and chemotactic behavior of B lymphocytes, through a block of B cells in the G0/G1 phases of the cell cycle [45]. In contrast with these observations, Traggiai et al. have reported that BM-derived MSCs are able to promote proliferation and differentiation into Ig-secreting cells of transitional and *naive* B cells isolated from both healthy donors (highly purified B-cell subsets) and pediatric patients with systemic lupus erythematosus (SLE) [47]. In a recent paper including both healthy subjects and patients with either SLE or experiencing rejection of kidney transplantation, in vitro B-cell proliferation, plasma-cell differentiation, and antibody production were demonstrated to be inhibited by MSCs when peripheral blood lymphocytes were stimulated with CpG, but not when sorted B cells were cultured with MSCs + CpG, thus indicating that the presence of functional T cells is of paramount importance for the MSC-mediated inhibitory effects on B cells [48].

While MSCs are able to suppress natural killer (NK)-cell proliferation and cytotoxicity against K562 targets after stimulation with IL-2 or IL-15, they cannot inhibit the lysis of freshly isolated NK cells in vitro [49, 50]. Due to the expression of ligands that are recognized by activating NK receptors, MSCs are not protected against NK-mediated killing and IL-2-activated both autologous and allogeneic NK cells are therefore capable of effectively lysing MSCs [50]. MSCs can also be lysed by cytotoxic T lymphocytes, when infused into MHC-mismatched mice, resulting in their rejection [51].

Recently, the ability of MSCs to interact with components of the innate immune system and to modify tissue homeostasis and inflammation by adopting a pro- or anti-inflammatory phenotype has been reported both in vitro and in vivo [10, 52]. When exposed

to sufficient levels of Pro-Inflammatory cytokines, MSCs may adopt an immune-suppressive phenotype, promoting both polarization toward anti-inflammatory cells and generation of M2 macrophages in vitro. Co-culture of monocytes with human or mouse BM-MSCs promotes the formation of M2 macrophages [53, 54] and this is dependent on both cellular contact and soluble factors, including PGE2 and kynurenine [53, 55]. Moreover, activation of MSCs with IFN-γ, TNF-α, and lipopolysaccharide (LPS) increases the expression of cyclooxygenase 2 (COX2) and IDO in BM-MSCs, thereby further promoting M2 macrophage polarization [55, 56]. Through the release of chemokine (C-C motif) ligands CCL2, CCL3, and CCL12, human and mouse BM-MSCs can recruit monocytes and macrophages into inflamed tissues and promote wound repair [57]. This polarizing effect of MSCs on M2 macrophages is closely linked with the ability of MSC to favor the emergence of Tregs. M2-polarized macrophages also produce the immune-suppressive cytokine IL-10 and CCL18, which in conjunction with TGF-beta promote the generation of Tregs [58]. Moreover, the production of pro-inflammatory cytokines by M1 macrophages may activate MSCs, and trigger the release of mediators that skew the differentiation of monocytes toward an anti-inflammatory profile and ultimately toward M2 macrophages [10, 54].

Several reports have indicated that MSCs are not constitutively inhibitory, but need to be activated by an inflammatory environment in the host in order to mediate their immune-regulatory effect [12]. Based on this theory, the presence of IFN-γ and/or TNF-α could influence the immune-suppressive effect of MSCs and produce different effects on MSC function [46, 59]. While in the presence of an inflammatory environment MSCs become activated and adopt an immune-suppressive phenotype (MSC2 type) by secreting high levels of soluble factors (IDO, PGE2, NO, TGF-β) that suppress T-cell proliferation, in the absence of an inflammatory environment, MSCs may adopt a pro-inflammatory phenotype (MSC1 type) and enhance T-cell responses by the secretion of chemokines that recruit lymphocytes to sites of inflammation [59–61]. The balance between these two pathways may serve to promote either host defense or tissue repair.

In the majority of studies, the differentiation of MSCs into the resident cell types was not required to obtain a therapeutic effect, which was shown to be associated with their anti-proliferative and anti-inflammatory effect, as well as to the secretion of paracrine mediators (such as HGF, insulin-like growth factor, PGE2, NO, and IDO) produced by the cells and/or by the local microenvironment [10, 11, 34, 35]. Moreover, a sustained engraftment and/or survival of MSCs do not seem to be necessary for their clinical effect [10, 54].

3 Mesenchymal Stem Cell Therapy in Hematopoietic Stem Cell Transplantation

3.1 Mesenchymal Stem Cell Therapy to Promote Hematopoietic Engraftment

Before being employed in the clinical setting, MSCs have been reported, in experimental animal models, to be capable of secreting cytokines that support hematopoiesis and promote engraftment of HSCs [62, 63]. In particular, Almeida-Porada et al. observed that co-transplantation of human MSCs into pre-immune fetal sheep resulted in enhancement of long-term engraftment of human cells in the BM and in higher levels of donor cells in the circulation [62]. Another study performed in NOD/SCID mice demonstrated that co-infusion of fetal lung-derived MSCs and UCB-derived $CD34^+$ cells was associated with enhanced engraftment of human HSCs in the BM of the animals, in particular when relatively low doses of HSCs were infused [63].

In the first clinical trial on the use of MSCs with the scope of accelerating hematological recovery, 28 patients with breast cancer and co-infused with autologous peripheral blood HSCs and MSCs ($1–2 \times 10^6$/kg) were reported; the patients showed a rapid hematopoietic recovery and no toxicity was observed [64]. In a subsequent multicenter, phase I/II trial, 46 patients receiving allogeneic HSCT from an HLA-identical sibling for hematological malignancies were given MSCs. The procedure was not associated with adverse events and hematopoietic recovery was prompt in most patients [65]. In another phase I/II, multicenter clinical study enrolling 14 children given T-cell-depleted HLA-disparate allograft from a relative, infusion of MSCs proved to be safe and all patients showed sustained hematopoietic engraftment, as compared with a 20 % graft failure rate in historical controls [14]. MSCs also promoted a better recovery of NK cells. In a pediatric, phase I–II clinical trial, 8 children, receiving the co-transplantation of unrelated donor UCB cells and ex-vivo expanded MSCs, infusion of MSCs proved to be safe and patients had a neutrophil recovery at a median time of 19 days after the allograft [66]. In another pediatric, phase I/II clinical study, the safety of the co-transplantation of parental MSCs was demonstrated in 13 pediatric patients given UCB-derived HSCs. In contrast with preclinical and clinical results [14, 64], no difference was found in either engraftment rate or speed of hematological recovery between study patients and controls, whereas MSC co-infusion significantly prevented the incidence of life-threatening acute graft-versus-host disease (GvHD) and GvHD-associated transplant-related mortality (TRM) [15]. In the adult setting, the co-infusion of UCB-derived HSCs, third-party donor-mobilized HSCs and MSCs had no effect on the kinetics of UCB cell engraftment, nor on prevention of GvHD [67]. In another study, culture-expanded third-party donor-derived UCB-MSCs were co-transplanted in 21 patients (age 4–31 years) with severe aplastic anemia (SAA) undergoing haplo-HSCT

without T-cell depletion with the double aim of facilitating HSC engraftment and preventing GvHD development. All patients had sustained hematopoietic engraftment without any adverse UCB-MSC infusion-related toxicity; 57 % of patients developed aGvHD (of any grade, 19 % grade III, 5 % grade IV), whereas 10 of 20 (50 %) evaluable patients who survived at least 90 days after transplantation experienced chronic GVHD (which was recorded to be extensive in three patients) [68]. The same Chinese group published results obtained in 50 pediatric and adult patients with refractory/relapsed hematological malignancy undergoing haplo-HSCT with myeloablative conditioning and co-infused with culture-expanded third-party UCB-MSCs. All patients showed sustained hematopoietic engraftment without any adverse infusion-related reaction, the median time to neutrophil and platelet engraftment was 12 and 15 days, respectively. Grade II–IV acute GVHD was observed in 24.0 % of patients, while chronic GVHD was observed in 37.7 % of patients [69].

The data from clinical studies on MSC application to promote engraftment are summarized in Table 1.

Table 1
MSC clinical applications in the promotion of hematopoietic engraftment in phase I/II clinical trials

Clinical context	MSC source	N of pts	Outcome	Reference
Breast cancer; autologous HSCT	BM	28	No tox. Rapid hematopoietic recovery	[64]
Hematological malignancy; allogeneic HSCT	BM	46	No tox. Prompt hematopoietic recovery	[65]
Hematological disorders; haplo-T-cell-depleted HSCT	BM	14 c	No tox. Graft rejection prevention. Accelerated leukocyte recovery	[14]
Hematological disorders; UCBT	BM	8 c	No tox. Prompt hematopoietic recovery	[66]
Hematological disorders; UCBT	BM	13 c	No tox. No effect on engraftment and hematopoietic recovery. GvHD prevention	[67]
Hematological disorders; UCBT+ 3rd-party HSCs	BM	9	No tox. No effect on kinetics of engraftment and GvHD	[15]
SAA, haplo HSCT	UCB	21	No tox. Sustained donor engraftment	[68]
Hematological malignancy; haplo-HSCT	UCB	50 also c	No tox. Sustained donor engraftment	[69]

N of pts number of patients enrolled, *c* children, *HSCT* hematopoietic stem cell transplantation, *BM* bone marrow, *UCB* umbilical cord blood, *tox.* toxicity, *UCBT* umbilical cord blood transplantation, *aGvHD* acute graft-versus-host disease, *SAA* severe aplastic anemia, *HSC* hematopoietic stem cell

In conclusion, published data demonstrate the feasibility and safety of co-transplanting HSCs and MSCs. Moreover, in some contexts (i.e. T-cell-depleted HLA-haploidentical allograft), MSCs may modulate host alloreactivity and/or promote a better engraftment of donor hematopoiesis, reducing the risk of graft failure. The difference between the haploidentical and UCBT settings may be related to the mechanisms underlying graft failure in UCBT, which may be inherent to the low numbers of HSC infused and/or to homing mechanisms; whereas, graft failure in the haploidentical context may be mainly due to immune-mediated mechanisms. MSCs might contribute to the engraftment of donor HSCs not only through immunological mechanisms, but also by contributing to the restoration of the hematopoietic stem cell *niche* and by stimulating the functional recovery of the BM microenvironment through the secretion of paracrine mediators.

MSCs have also been employed to stimulate ex vivo HSC expansion. In particular, culturing UCB-derived HSCs with MSCs was judged successful based on the greater numbers of ex vivo total nucleated cell and hematopoietic progenitor cells expanded, as compared with ex vivo liquid culture of $CD133^+$ cells [70]. The results of a clinical trial in which 31 adult patients with hematological malignancies received transplants with two UCB units, one of which contained cells expanded ex vivo in co-cultures with allogeneic MSCs, have been recently published. The transplantation of UCB cells expanded with MSCs appeared to be safe and effective. Expanded UCB in combination with un-manipulated UCB significantly improved engraftment, as compared with the infusion of un-manipulated cord blood only [71].

3.2 Mesenchymal Stem Cell Therapy to Treat Graft-Versus-Host Disease

MSC therapy in patients with aGvHD occurring after allogeneic HSCT and/or donor lymphocyte infusion has been the most frequent MSC clinical application. Acute GVHD remains a major cause of morbidity and mortality after allogeneic HSCT in both children and adult patients. Although 30–50 % of children respond to corticosteroids as initial therapy, the optimal second-line therapy for steroid-resistant GvHD has not yet been determined. GvHD is caused by engraftment of immunocompetent donor T lymphocytes in an immunologically compromised host which show histocompatibility differences with the donor. These differences between the donor and the host may result in donor T-cell activation against either recipient major histocompatibility complex (MHC) antigens or minor histocompatibility antigens. GVHD is usually subdivided into two forms: acute GVHD, which classically occurs within 100 days after transplantation, and chronic GVHD, which, although related, is a different disease occurring later and displaying some clinical and pathological features which resemble those observed in selected autoimmune disorders (systemic sclerosis, Sjogren syndrome, etc.).

While in the clinical arena MSC treatment has been shown to be effective in preliminary phase I/II studies, the issue of the suppressive effect of MSCs in the context of GvHD prevention/treatment in animal models has produced conflicting results. Indeed, in one study conducted in mice, systemic infusion of AT-derived MSCs early after transplantation of haploidentical HSCs was able to rescue the animals from lethal GvHD [72]. However, a single dose of BM-derived MSCs at the time of allogeneic BM transplantation did not affect the incidence and severity of GvHD in another mouse model [73]. In NOD/SCID mice, UCB-derived MSCs administered at weekly intervals were able to prevent GvHD development after transplantation of allogeneic human PBMCs [74].

In the clinical arena, Le Blanc et al. first reported on a pediatric patient experiencing grade IV refractory acute GvHD of the liver and gut after unrelated donor allogeneic HSCT; the child was rescued by the infusion of BM-derived MSCs isolated from the mother, thus indicating that MSCs act in a non-HLA restricted manner [75]. In a phase II, multicenter clinical trial, 55 adult and pediatric patients with steroid-resistant aGvHD were treated with intravenous infusion/s of third-party MSCs. The median dose of BM-derived MSCs infused was 1.4×10^6 (range $0.4–9 \times 10^6$) cells per kg of patient body weight. Twenty-seven patients received one dose, twenty-two received two doses, and six patients three–five doses of cells obtained from HLA-identical sibling donors ($n = 5$), haploidentical donors ($n = 18$), and third-party HLA-mismatched donors ($n = 69$). Thirty patients had a complete response (CR) and nine showed improvement. No patients had side effects during or immediately after MSC infusions. Patients who achieved CR had a significantly lower transplantation-related mortality 1 year after infusion than patients with partial or no response (37 % versus 72 %, respectively; $p = 0.002$) and better overall survival 2 years after HSCT (53 % versus 16 %, respectively; $p = 0.018$) [16]. In another phase II study, the outcomes of 37 children (some of whom were already reported in the previous study) receiving MSC intravenous infusions for grade III–IV, steroid-refractory, aGVHD have been reported [76]. CR was observed in 59 % of the patients, their transplant-related mortality (TRM) was 14 %; TRM in the remaining children was 60 % ($p = 0.005$). With a median follow-up of 2.3 years, overall survival (OS) was 62 %. Interestingly, children treated after 2009 had received less second-line immune-suppressive treatment and were given MSCs earlier after onset of steroid treatment. This translated into a significantly better OS for children enrolled in the study after 2009 (93 % vs. 65 % for those treated before 2009; $p < 0.05$) [76]. Similar results have been reported in a smaller cohort of pediatric patients (N.11) treated on a compassionate use basis with third-party BM-derived MSCs expanded in the

presence of platelet-lysate (PL) for either acute GVHD or chronic GVHD (cGVHD) [77]. The median MSC dose was 1.2×10^6/kg (range: 0.7–3.7×10^6/kg); no acute or late (up to 18 months) side effects were observed. Overall response was obtained in 71 % of patients, with CR in 24 % of cases. The same 11 children were included in a larger cohort of pediatric and adult patients (total 40, 15 children and 25 adults) experiencing steroid-resistant grade II–IV acute GVHD and treated with third-party BM-derived PL-expanded MSCs. Patients received a median of three MSC infusions after having failed conventional immunosuppressive therapy. A median cell dose of 1.5×10^6/kg per infusion was administered; no acute toxicity was reported. Overall response rate, measured at 28 days after the last MSC injection, was 67.5 %, with 27.5 % CR. Achievement of CR was significantly more frequently recorded in patients experiencing grade II GVHD as compared with those affected by more severe GvHD (61.5 % versus 11.1 %, $p = 0.002$). A trend toward a better response in children as compared with adults was also observed (46.7 versus 16.0 %, $p = 0.065$) [78].

The application of MSCs for acute GvHD has been evaluated in phase II clinical trials, mainly performed by European collaborative groups in the past few years. The only phase III clinical trial (NCT00366145) conducted so far and investigating the use of an industrial MSC product (Prochymal; Osiris Therapeutics, Inc., Columbia, MD, USA) failed to achieve its primary clinical endpoint, i.e. a significant increase of CRs in steroid-resistant GvHD lasting at least 28 days, as compared with placebo. There was a statistical improvement over placebo in patients with gastrointestinal and liver GvHD, but no improvement with Prochymal treatment in patients who develop skin GvHD was observed. These results were reported during an international meeting, however a peer-reviewed publication of the trial has not appeared to date.

The data of the clinical studies on MSC application to treat GvHD are summarized in Table 2.

The first academic, multicenter, phase III study has been recently launched in Europe. Patients with steroid-resistant aGvHD will be randomized to receive a second-line treatment (i.e. mycophenolate mofetil) in combination with either two intravenous infusions of MSCs ($1–2 \times 10^6$/kg 1 week apart) or in combination with two infusions of placebo. This study, which will enroll 150 pediatric and adult patients throughout Europe, will hopefully define the efficacy of MSC treatment in steroid-resistant aGvHD.

Altogether, these clinical data indicate that MSC intravenous infusion is a safe and valuable therapy for patients with severe, refractory aGvHD. Better results may be achieved in children and when MSC treatment is employed early in the disease course. The efficacy of MSC therapy in GvHD management in comparison with other second-line therapies needs to be proven in a prospective randomized trial.

Table 2
MSC clinical applications in the treatment of GvHD

Clinical context	MSC source	N of pts	Outcome	Reference
Grade IV aGvHD after allogeneic HSCT	BM haplo	1 c	Complete resolution of grade IV acute GVHD	[75]
Grade II–IV aGvHD after allogeneic HSCT/DLI	BM 3rd party	55 also c	OR: 69 %; improved OS in responders	[16]
Grade II–IV aGvHD after allogeneic HSCT/DLI	BM 3rd party	37 c	CR 59 %; improved OS, especially if early MSC treatment	[76]
Grade II–IV aGvHD after allogeneic HSCT/DLI	BM 3rd party (PL)	11 c	OR: 71 %; CR: 24 %	[77]
Grade II–IV aGvHD after allogeneic HSCT/DLI	BM 3rd party (PL)	40 also c	OR: 67.5 %; CR: 27.5 %. Better in children and grade II	[78]
Grade II–IV aGvHD after allogeneic HSCT/DLI (phase III)	BM 3rd party	240 also c	No significant increase of CRs as compared with placebo; better if gastrointestinal and liver GvHD	–
Ext. sclerodermatous cGvHD after allogeneic HSCT	BM 3rd party	4	Improvement in signs of cGvHD (intrabone injection)	[80]
Refractory cGvHD after allogeneic HSCT	BM 3rd party	23	OR: 20/23 treated pts. Increase in Bregs	[81]

N of pts number of patients enrolled, *c* children, *HSCT* hematopoietic stem cell transplantation, *DLI* donor leukocyte infusion, *BM* bone marrow, *aGvHD* acute graft-versus-host disease, *cGvHD* chronic graft-versus-host disease, *OR* overall response, *OS* overall survival, *CR* complete response, *PL* platelet lysate expanded MSC, *Ext* extensive

The identification of biomarkers able to predict MSC efficacy is of paramount importance for the development of MSC therapy. Unfortunately, clinical studies on MSC treatment have only rarely been used to identify biomarkers predicting response to MSCs. One approach could be to analyze clinical samples from GvHD patients treated with MSC infusion/s to understand the events underlying patient response in vivo. Dander et al. analyzed plasma levels of two biomarkers associated with acute GvHD development, i.e. interleukin 2 receptor alpha (IL-2Rα) and tumor necrosis factor receptor (TNFR) I, in a group of patients both before and after MSC treatment. While the levels of the two factors were elevated before MSC infusion, they persistently decreased in responder patients, suggesting that these phenomena were related [79]. This observation is in line with several studies indicating that MSCs need to be activated by an inflammatory environment (i.e. such as present during acute GvHD) to deliver their therapeutic effect [12].

The immune-regulatory and anti-inflammatory properties of MSCs make them a potential, interesting candidate also for the treatment of chronic GvHD which is responsible for late morbidity and mortality after allogeneic HSCT. Despite this premise, clinical reports of MSC efficacy in chronic GvHD are scarce. In one report, four patients with sclerodermatous chronic GVHD were treated with intra-BM injection of third-party ex vivo expanded MSCs; the treatment was followed by gradual improvement of the symptoms related to chronic GvHD in all four patients [80]. In a prospective clinical study, 23 patients with chronic GvHD were treated with intravenous infusions (N.3) of third-party BM-derived MSCs at a dose of 1×10^6/kg with a 4-week interval schedule. Twenty of the 23 patients had a CR or partial response in a 12-month follow-up study. The most marked improvements in chronic GVHD symptoms were observed in the skin, oral mucosa, and liver. Clinical improvement was accompanied by a significantly increased number of interleukin-10-producing $CD5^+$ B cells. This study offers a mechanistic explanation for MSC efficacy in chronic GvHD which is based on their ability to promote the survival and proliferation of $CD5^+$ regulatory B cells (Bregs), at least in part through the production of IDO [81].

MSCs have been also employed to treat other complications following allogeneic HSCT and characterized by inflammatory tissue injury. In particular, MSCs have been reported to reverse acute tissue toxicity in selected patients suffering from hemorrhagic cystitis, pneumomediastinum/pneumothorax, and colon perforation [82, 83]. In the first report, a collection of patients with various complications developed after HSCT were treated with MSCs. Twelve patients received intravenous MSC infusions for severe hemorrhagic cystitis after HSCT; in eight of these 12 patients gross hematuria disappeared after a median of 3 (1–14) days. In two

HSCT patients, pneumomediastinum resolved after treatment with MSCs. Colon perforation and peritonitis was reversed in an elderly female with severe gastrointestinal GVHD [82]. Within a phase I trial, two transplanted patients with pneumomediastinum/pneumothorax were treated with intravenous infusions of third-party BM-MSCs at a fixed dose of 2×10^6/kg weekly for three doses and achieved resolution of this complication. Response to MSC infusion was associated with a rapid reduction in inflammatory cytokines [83]. Based on these studies, MSCs might represent a novel treatment to be employed to reverse acute tissue toxicity because of their immune-regulatory and anti-inflammatory effects. These data need to be confirmed in a larger cohort of patients and in randomized trials.

4 Conclusions and Future Directions

In conclusion, MSCs may exert both a direct anti-proliferative effect on T cells, NK cells, and B cells and display indirect modulatory activities by inducing tolerogenic immune responses through the induction of regulatory T cells and tolerogenic DCs. A pro-inflammatory environment may lead to the activation of MSC and may be critical for the induction of suppressive mediators. The central role of the innate immune system in the modulatory effects of MSCs has been recently highlighted; the monocyte/macrophage system deserves particular mention as it has been shown to represent a key player in orchestrating both pro-inflammatory and anti-inflammatory responses by MSCs. The in vivo biological relevance of these findings, mainly collected in in vitro experiments together with MSC mechanisms of action, needs to be further addressed in appropriate animal models and clinical trials.

The role of host factors in activating MSCs to exert their immunomodulatory properties, as well as the functional differences between MSCs derived from different tissue sources and suitable markers for the prospective isolation of MSCs are other issues to be addressed. Identification of such factors may lead to a better understanding of MSC biological and functional properties and, consequently, to the design of novel strategies of MSC therapy in several disorders. Novel molecular tools aimed at defining the MSC secretome, proteome, and transcriptome are being employed to more precisely define the soluble factors that mediate MSC function [84]. These tools include MSC-derived microvesicles or exosomes that can mediate intercellular communication between MSCs and other cells [85].

MSC therapy represents an emerging treatment modality in the modulation of immune responses against alloantigens (and autoantigens); treatment of acute GVHD is already applied in

experienced centers, not only as an experimental treatment but also as a best clinical practice. Prospective randomized studies are needed to translate this concept into a therapeutic reality.

Acknowledgments

This work was partly supported by grants from the Associazione Italiana per la Ricerca sul Cancro (AIRC) IG9062 and the Bando Giovani Ricercatori 2008 to M.E.B.; by the special grant "5 × 1000" from AIRC and a grant from the Regione Lazio (FILAS grant) to F.L.

References

1. Friedenstein AJ, Petrakova KV, Kurolesova AI et al (1968) Heterotopic of bone marrow. Analysis of precursor cells for osteogenic and hematopoietic tissues. Transplantation 6:230–247
2. Friedenstein AJ, Deriglasova UF, Kulagina NN et al (1947) Precursors for fibroblast in different populations of hematopoietic cells as detected by the in vitro colony assay method. Exp Hematol 2:83–92
3. Im GI, Shin YW, Lee KB (2005) Do adipose tissue-derived mesenchymal stem cells have the same osteogenic and chondrogenic potential as bone marrow-derived cells? Osteoarthritis Cartilage 13:845–853
4. Campagnoli C, Roberts IA, Kumar S et al (2001) Identification of mesenchymal stem/progenitor cells in human first-trimester fetal blood, liver, and bone marrow. Blood 98:2396–2402
5. in 't Anker PS, Scherjon SA, Kleijburg-van der Keur C et al (2003) Amniotic fluid as a novel source of mesenchymal stem cells for therapeutic transplantation. Blood 102:1548–1549
6. Pittenger MF, Mackay AM, Beck SC et al (1999) Multilineage potential of adult human mesenchymal stem cells. Science 284:143–147
7. Nauta AJ, Fibbe WE (2007) Immuno modulatory properties of mesenchymal stromal cells. Blood 110:3499–3506
8. Le Blanc K, Ringden O (2007) Immuno modulation by mesenchymal stem cells and clinical experience. J Intern Med 262:509–525
9. Di Nicola M, Carlo-Stella C, Magni M et al (2002) Human bone marrow stromal cells suppress T-lymphocyte proliferation induced by cellular or non specific mitogenic stimuli. Blood 99:3838–3843
10. Le Blanc K, Mougiakakos D (2012) Multipotent mesenchymal stromal cells and the innate immune system. Nat Rev Immunol 12:383–396
11. Prockop DJ, Oh JY (2012) Mesenchymal stem/stromal cells (MSCs): role as guardians of inflammation. Mol Ther 20:14–20
12. Krampera M (2011) Mesenchymal stromal cell 'licensing': a multistep process. Leukemia 25:1408–1414
13. Wang L, Li Y, Chen X et al (2002) MCP-1, MIP-1, IL-8 and ischemic cerebral tissue enhance human bone marrow stromal cell migration in interface culture. Hematology 7:113–117
14. Ball LM, Bernardo ME, Roelofs H et al (2007) Co-transplantation of ex-vivo expanded mesenchymal stem cells accelerates lymphocyte recovery and may reduce the risk of graft failure in haploidentical hematopoietic stem cell transplantation. Blood 110:2764–2767
15. Bernardo ME, Ball LM, Cometa AM et al (2011) Co-infusion of ex vivo expanded, parental mesenchymal stromal cells prevents life-threatening acute GvHD, but does not reduce the risk of graft failure in pediatric patients undergoing allogeneic umbilical cord blood transplantation. Bone Marrow Transplant 46:200–207
16. Le Blanc K, Frassoni F, Ball L et al (2008) Mesenchymal stem cells for treatment of steroid-resistant, severe, acute graft-versus-host disease: a phase II study. Lancet 371:1579–1586
17. Ringden O, Uzunel M, Sundberg B et al (2007) Tissue repair using mesenchymal stem cells for hemorrhagic cystitis, pneumomediastinum and perforated colon. Leukemia 21:2271–2276

18. Ciccocioppo R, Bernardo ME, Sgarella A et al (2011) Autologous bone marrow-derived mesenchymal stromal cells in the treatment of fistulising Crohn's disease. Gut 60:788–798
19. Avanzini MA, Bernardo ME, Cometa AM et al (2009) Generation of mesenchymal stromal cells in the presence of platelet lysate: a phenotypical and functional comparison of umbilical cord blood- and bone marrow-derived progenitors. Haematologica 94:1649–1660
20. Schallmoser K, Bartmann C, Rohde E et al (2007) Human platelet lysate can replace fetal bovine serum for clinical-scale expansion of functional mesenchymal stromal cells. Transfusion 47:1436–1446
21. Dominici M, Le Blanc K, Mueller I et al (2006) Minimal criteria for defining multipotent mesenchymal stromal cells. The International Society for Cellular Therapy position statement. Cytotherapy 8:315–317
22. Gang EJ, Bosnakovski D, Figueiredo CA et al (2007) SSEA-4 identifies mesenchymal stem cells from bone marrow. Blood 109:1743–1751
23. Simmons PJ, Torok-Storb B (1991) Identification of stromal cell precursors in human bone marrow by a novel monoclonal antibody, STRO-1. Blood 78:55–62
24. Battula VL, Treml S, Bareiss PM et al (2009) Isolation of functionally distinct mesenchymal stem cells subsets using antibodies against CD56, CD271, and mesenchymal stem cell antigen-1 (MSCA-1). Haematologica 94:173–184
25. Bernardo ME, Zaffaroni N, Novara F et al (2007) Human bone marrow-derived mesenchymal stem cells do not undergo transformation after long-term *in vitro* culture and do not exhibit telomere maintenance mechanisms. Cancer Res 67:9142–9149
26. Tarte K, Gaillard J, Lataillade J et al (2010) Clinical-grade production of human mesenchymal stromal cells: occurrence of aneuploidy without transformation. Blood 115:1549–1553
27. Vogel G (2010) To scientists' dismay, mixed-up cell lines strike again. Science 329:1004
28. Torsvik A, Røsland GV, Svendsen A et al (2010) Spontaneous malignant transformation of human mesenchymal stem cells reflects cross-contamination: putting the research field on track - letter. Cancer Res 70:6393–6396
29. Barkholt L, Flory E, Jekerle V et al (2013) Risk of tumorigenicity in mesenchymal stromal cell-based therapies—bridging scientific observations and regulatory viewpoints. Cytotherapy 15:753–759
30. Le Blanc K, Tammik L, Sundberg B et al (2003) Mesenchymal stem cells inhibit and stimulate mixed lymphocyte cultures and mitogenic responses independently of the major histocompatibility complex. Scand J Immunol 57:11–20
31. Tse WT, Pendleton JD, Beyer WM et al (2003) Suppression of allogeneic T-cell proliferation by human marrow stromal cells: implications in transplantation. Transplantation 75:389–397
32. Krampera M, Glennie S, Dyson J et al (2003) Bone marrow mesenchymal stem cells inhibit the response of naïve and memory antigen-specific T cells to their cognate peptide. Blood 101:3722–3729
33. Rasmusson I, Ringden O, Sundberg B et al (2003) Mesenchymal stem cells inhibit the formation of cytotoxic T lymphocytes, but not activated cytotoxic T lymphocytes or natural killer cells. Transplantation 76:1208–1213
34. Meisel R, Zibert A, Laryea M et al (2004) Human bone marrow stromal cells inhibit allogeneic T-cell responses by indolamine 2,3-dioxygenase-mediated tryptophan degradation. Blood 103:4619–4621
35. Chabannes D, Hill M, Merieau E et al (2007) A role for heme oxygenase-1 in the immunosuppressive effect of adult rat and human mesenchymal stem cells. Blood 110:3691–3694
36. Burr SP, Dazzi F, Garden OA (2013) Mesenchymal stromal cells and regulatory T cells: the Yin and Yang of peripheral tolerance? Immunol Cell Biol 91:12–18
37. Maccario R, Podestà M, Moretta A et al (2005) Interaction of human mesenchymal stem cells with cells involved in alloantigen-specific immune response favours the differentiation of CD4+ T-cell subsets expressing regulatory/suppressive phenotype. Haematologica 90:516–525
38. English K, Ryan JM, Tobin L et al (2009) Cell contact, prostaglandin E (2) and transforming growth factor beta1 play nonredundant roles in human mesenchymal stem cell induction of CD4 + CD25(High) forkheadbox P3+ regulatory T cells. Clin Exp Immunol 156:149–160
39. Melief SM, Schrama CLM, Brugman MH (2013) Multipotent stromal cells induce human regulatory T cells through a novel pathway involving skewing of monocytes towards anti-inflammatory macrophages. Stem Cells. doi:10.1002/1432
40. Akiyama K, Chen C, Wang D et al (2012) Mesenchymal-stem-cell-induced immunoregulation involves FAS-ligand-/FAS-mediated T cell apoptosis. Cell Stem Cell 10:544–555
41. Duijvestein M, Wildenberg ME, Welling MM et al (2011) Pretreatment with interferon-gamma enhances the therapeutic activity of mesenchymal stromal cells in animal models of colitis. Stem Cells 29:1549–1558

42. Cutler AJ, Limbani V, Girdlestone J et al (2010) Umbilical cord-derived mesenchymal stromal cells modulate monocyte function to suppress T cell proliferation. J Immunol 185:6617–6623
43. Jiang XX, Zhang Y, Liu B et al (2005) Human mesenchymal stem cells inhibit differentiation and function of monocyte-derived dendritic cells. Blood 105:4120–4126
44. Nauta AJ, Kruisselbrink AB, Lurvink E et al (2006) Mesenchymal stem cells inhibit generation and function of both CD34+-derived and monocyte-derived dendritic cells. J Immunol 177:2080–2087
45. Corcione A, Benvenuto F, Ferretti E et al (2006) Human mesenchymal stem cells modulate B cell functions. Blood 107:367–372
46. Krampera M, Cosmi L, Angeli R et al (2006) Role of interferon-gamma in the immunomodulatory activity of human bone marrow mesenchymal stem cells. Stem Cells 24: 386–398
47. Traggiai E, Volpi S, Schena F et al (2008) Bone marrow-derived mesenchymal stem cells induce both polyclonal expansion and differentiation of B cells isolated from healthy donors and systemic lupus erythematosus patients. Stem Cells 26:562–569
48. Rosado MM, Bernardo ME, Scarsella M et al (2015) Inhibition of B-cell proliferation and antibody production by mesenchymal stromal cells is mediated by T cells. Stem Cells Dev 24(1):93–103
49. Sotiropoulou PA, Perez SA, Gritzapis AD et al (2006) Interactions between human mesenchymal stem cells and natural killer cells. Stem Cells 24:74–85
50. Spaggiari GM, Capobianco A, Becchetti S et al (2006) Mesenchymal stem cell-natural killer cell interactions: evidence that activated NK cells are capable of killing MSCs, whereas MSCs can inhibit IL-2-induced NK-cell proliferation. Blood 107:1484–1490
51. Nauta AJ, Westerhuis G, Kruisselbrink AB et al (2006) Donor-derived mesenchymal stem cells are immunogenic in an allogeneic host and stimulate donor graft rejection in a non-myeloablative setting. Blood 108:2114–2120
52. Keating A (2012) Mesenchymal stromal cells: new directions. Cell Stem Cell 10:709–716
53. Eggenhofer E, Hoogduijn MJ (2012) Mesenchymal stem cell-educated macrophages. Transplant Res 1:12
54. Bernardo ME, Fibbe WE (2013) Mesenchymal stromal cells: sensors and switchers of inflammation. Cell Stem Cell 13:392–402
55. Nemeth K, Leelahavanichkul A, Yuen PS et al (2009) Bone marrow stromal cells attenuate sepsis via prostaglandin E 2-dependent reprogramming of host macrophages to increase their interleukin-10 production. Nat Med 15:42–49
56. François M, Romieu-Mourez R, Li M, Galipeau J (2012) Human MSC suppression correlates with cytokine induction of indoleamine 2,3-dioxygenase and bystander M2 macrophage differentiation. Mol Ther 20:187–195
57. Chen L, Tredget EE, Wu PY, Wu Y (2008) Paracrine factors of mesenchymal stem cells recruit macrophages and endothelial lineage cells and enhance wound healing. PLoS One 3, e1886
58. Melief SM, Geutskens SB, Fibbe W et al (2013) Multipotent stromal cells skew monocytes towards an anti-inflammatory IL-10 producing phenotype by production of IL-6. Haematologica 98:888–895
59. Ren G, Zhang L, Zhaon X et al (2008) Mesenchymal stem cell-mediated immunosuppression occurs via concerted action of chemokines and nitric oxide. Cell Stem Cell 2:141–150
60. Li W, Ren G, Huang Y et al (2012) Mesenchymal stem cells: a double-edged sword in regulating immune responses. Cell Death Differ 19:1505–1513
61. Waterman RS, Tomchuck SL, Henkle SL et al (2010) A new mesenchymal stem cell (MSC) paradigm: polarization into a pro-inflammatory MSC1 or an Immunosuppressive MSC2 phenotype. PLoS One 5, e10088
62. Almeida-Porada G, Porada CD, Tran N et al (2000) Co-transplantation of human stromal cell progenitors into pre-immune fetal sheep results in early appearance of human donor cells in circulation and boosts cell levels in bone marrow at later time points after transplantation. Blood 95:3620–3627
63. Noort WA, Kruisselbrink AB, in't Anker PS et al (2002) Mesenchymal stem cells promote engraftment of human umbilical cord blood-derived CD34+ cells in NOD/SCID mice. Exp Hematol 30:870–878
64. Koc ON, Gerson SL, Cooper BW et al (2000) Rapid hematopoietic recovery after co-infusion of autologous-blood stem cells and culture-expanded marrow mesenchymal stem cells in advanced breast cancer patients receiving high-dose chemotherapy. J Clin Oncol 18:307–316
65. Lazarus HM, Koc ON, Devine SM et al (2005) Cotransplantation of HLA-identical sibling culture-expanded mesenchymal stem cells and hematopoietic stem cells in hematologic malignancy patients. Biol Blood Marrow Transplant 11:389–398
66. MacMillan ML, Blazar BR, DeFor TE et al (2008) Transplantation of culture-expanded

haploidentical mesenchymal stem cells to promote engraftment in pediatric recipients of unrelated donor umbilical cord blood: results of a phase I–II clinical trial. Bone Marrow Transplant 43:1–8

67. Gonzalo-Daganzo R, Regidor C, Martìn-Donaire T et al (2009) Results of a pilot study on the use of third-party mesenchymal stromal cells in cord blood transplantation in adults. Cytotherapy 11:278–288
68. Wu Y, Cao Y, Li X et al (2014) Cotransplantation of haploidentical hematopoietic and umbilical cord mesenchymal stem cells for severe aplastic anemia: successful engraftment and mild GVHD. Stem Cell Res 12:132–138
69. Wu Y, Wang Z, Cao Y et al (2013) Cotransplantation of haploidentical hematopoietic and umbilical cord mesenchymal stem cells with a myeloablative regimen for refractory/relapsed hematologic malignancy. Ann Hematol 92:1675–1684
70. Robinson SN, Ng J, Niu T et al (2006) Superior ex vivo cord blood expansion following co-culture with bone marrow-derived mesenchymal stem cells. Bone Marrow Transplant 37:359–366
71. de Lima M, McNiece I, Robinson SN et al (2012) Cord-blood engraftment with ex vivo mesenchymal-cell coculture. N Engl J Med 367:2305–2315
72. Sudres M, Norol F, Trenado A et al (2006) Bone marrow mesenchymal stem cells suppress lymphocyte proliferation in vitro but fail to prevent graft-versus-host-disease in mice. J Immunol 176:7761–7767
73. Tisato V, Naresh K, Girdlestone J et al (2007) Mesenchymal stem cells of cord blood origin are effective at preventing but not treating graft-versus-host disease. Leukemia 21:1992–1999
74. Polchert D, Sobinsky J, Douglas G et al (2008) IFN-gamma activation of mesenchymal stem cells for treatment and prevention of graft versus host disease. Eur J Immunol 38:1745–1755
75. Le Blanc K, Rasmusson I, Sundberg B et al (2004) Treatment of severe graft-versus-host disease with third party haploidentical mesenchymal stem cells. Lancet 363:1439–1441
76. Ball LM, Bernardo ME, Roelofs H et al (2013) Multiple infusions of mesenchymal stromal cells induce sustained remission in children with steroid-refractory, grade III–IV acute graft-versus-host disease. Br J Haematol 163:501–509
77. Lucchini G, Introna M, Dander E et al (2010) Platelet-lysate-expanded mesenchymal stromal cells as a salvage therapy for severe resistant graft-versus-host disease in a pediatric population. Biol Blood Marrow Transplant 16:1293–1301
78. Introna M, Lucchini G, Dander E et al (2014) Treatment of graft versus host disease with mesenchymal stromal cells: a phase I study on 40 adult and pediatric patients. Biol Blood Marrow Transplant 20:375–381
79. Dander E, Lucchini G, Vinci P et al (2012) Mesenchymal stromal cells for the treatment of graft-versus-host disease: understanding the in vivo biological effect through patient immune monitoring. Leukemia 26:1682–1684
80. Zhou H, Guo M, Bian C et al (2010) Efficacy of bone marrow-derived mesenchymal stem cells in the treatment of sclerodermatous chronic graft-versus-host disease: clinical report. Biol Blood Marrow Transplant 16:403–412
81. Peng Y, Chen X, Liu Q et al (2015) Mesenchymal stromal cells infusions improve refractory chronic graft versus host disease through an increase of CD5+ regulatory B cells producing interleukin 10. Leukemia 29(3):636–646
82. Ringden O, Le Blanc K (2011) Mesenchymal stem cells for treatment of acute and chronic graft-versus-host disease, tissue toxicity and hemorrhages. Best Pract Res Clin Haematol 24:65–72
83. Yin F, Battiwalla M, Ito S et al (2014) Bone marrow mesenchymal stromal cells to treat tissue damage in allogeneic stem cell transplant recipients: correlation of biological markers with clinical responses. Stem Cells 32:1278–1288
84. Ranganath SH, Levy O, Inamdar MS et al (2012) Harnessing the mesenchymal stem cell secretome for the treatment of cardiovascular disease. Cell Stem Cell 10:244–258
85. Biancone L, Bruno S, Deregibus MC et al (2012) Therapeutic potential of mesenchymal stem cell-derived microvesicles. Nephrol Dial Transplant 27:3037–3042

Chapter 2

Bone Tissue Engineering: Past–Present–Future

Rodolfo Quarto and Paolo Giannoni

Abstract

Bone is one of the few tissues to display a true potential for regeneration. Fracture healing is an obvious example where regeneration occurs through tightly regulated sequences of molecular and cellular events which recapitulate tissue formation seen during embryogenesis. Still in some instances, bone regeneration does not occur properly (i.e. critical size lesions) and an appropriate therapeutic intervention is necessary. Successful replacement of bone by tissue engineering will likely depend on the recapitulation of this flow of events. In fact, bone regeneration requires cross-talk between microenvironmental factors and cells; for example, resident mesenchymal progenitors are recruited and properly guided by soluble and insoluble signaling molecules. Tissue engineering attempts to reproduce and to mimic this natural milieu by delivering cells capable of differentiating into osteoblasts, inducing growth factors and biomaterials to support cellular attachment, proliferation, migration, and matrix deposition. In the last two decades, a significant effort has been made by the scientific community in the development of methods and protocols to repair and regenerate tissues such as bone, cartilage, tendons, and ligaments. In this same period, great advancements have been achieved in the biology of stem cells and on the mechanisms governing "stemness". Unfortunately, after two decades, effective clinical translation does not exist, besides a few limited examples. Many years have passed since cell-based regenerative therapies were first described as "promising approaches", but this definition still engulfs the present literature. Failure to envisage translational cell therapy applications in routine medical practice evidences the existence of unresolved scientific and technical struggles, some of which still puzzle researchers in the field and are presented in this chapter.

Key words Bone, Mesenchymal stem cells, iPSC, Cell therapy, Biomaterials, Scaffolds

1 Past Cell Therapy

The standard approach proposed in the past implied the delivery of in vitro expanded cells (stem cells, progenitors, etc.) combined with biomaterials of various chemical nature and architecture.

1.1 Cells

Osteoprogenitor cells have been isolated from a variety of tissues, including periostium, bone marrow, spleen, thymus, skeletal muscle, and adipose tissue [1–8]. Osteoprogenitors have also been isolated from other tissues, such as amniotic fluid [9], chorionic villi [10], infrapatellar fat pad [11], synovium [12], and the umbilical cord [13],

Massimiliano Gnecchi (ed.), *Mesenchymal Stem Cells: Methods and Protocols*, Methods in Molecular Biology, vol. 1416,
DOI 10.1007/978-1-4939-3584-0_2,

although their use in tissue engineering is not always straightforward. The most common source of stem cells remains bone marrow. Mesenchymal stem cells (MSC) can be isolated, expanded in culture, and stimulated to differentiate into bone, cartilage, muscle, marrow stroma, tendon, fat, and a variety of other connective tissues [14]. Very large numbers of MSC can be generated in culture from limited marrow samples, making it possible to engineer constructs composed of these cells together with appropriate scaffolds which can be re-introduced into the recipient. In order to obtain large numbers of osteoprogenitors for cell transplantation, culture conditions and the effects of growth factors on proliferation and differentiation of MSC are of great interest and have been investigated by several groups [15–19]. Furthermore, MSC can be transduced with various viral vectors and are, thus, interesting candidates also for somatic gene therapy in local or systemic pathologies [20–22].

One interesting source of osteoprogenitor cells is achievable in large quantities, under local anesthesia, with minimal discomfort [4, 8]. This population can be isolated from human adipose tissue harvested by suction-assisted lipectomy (liposuction) [23]. From this adipocyte-rich fraction, MSC-like cells can be isolated, maintained in vitro for extended periods with low levels of senescence. Immunofluorescence and flow cytometry show that the majority of these cells are of mesodermal or mesenchymal origin with low levels of contaminating pericytes, endothelial cells, and smooth muscle cells. Finally, they can differentiate in vitro into adipogenic, chondrogenic, myogenic, and osteogenic cells in the presence of lineage-specific induction factors [8].

Some, if not all of the problems raised by solid tissue osteoprogenitor cells could be solved by harvesting cells with similar characteristics from peripheral blood. This of course would be the simplest source of cells to harvest and a minimally invasive approach for the donor. Few reports, starting from the historical publication by Luria and coworkers [24], suggest that it is possible to isolate a population of fibroblasts from peripheral blood [25]. These peripheral blood fibrocytes would in principle be the population of cells that reach sites of tissue injury and contribute to connective scar tissue formation. They display a distinct cell surface phenotype (CD34−/CD45−/collagen I+/β1 integrin subunit) and are an abundant source of cytokines and growth factors that function to attract and activate inflammatory and connective tissue cells. However, controversial data are often presented in the literature regarding circulating mesenchymal progenitors; this underlines the lack of incontrovertible proof of this very elusive and limited cell population and the presence of different opinions within the scientific community [26].

1.2 Biomaterials

The right choice of a suitable tridimensional matrix to deliver progenitor cells is of critical importance. Scaffolds are one of the most important elements required to trigger the cascade of events leading to bone repair and to mimic the extracellular matrix in a regenerating bone microenvironment. This concept implies that scaffolds do not simply deliver cells, but that they are somewhat "informative" to the cells and—thus importantly—they should be engineered as such. The primary properties of biomaterials for bone regeneration are osteoconductivity and integration with host bone tissue [27–31]. Their architecture therefore must be permissive for blood vessels to colonize even in larger structures. Finally, they should be biocompatible and resorbable. From this point of view, the new generation of bioceramics are indeed exceptional candidates [32]. Porous bioceramics (hydroxyapatite—HA and tricalcium phosphate—TCP) are osteoconductive, have a favorable bone affinity [33–35], and are free from risks of rejection or infection [31, 33, 36].

An important improvement in this field is represented by synthetic porous scaffolds. In this case in fact, the internal architecture can be intelligently designed and the density, as well as the biomechanical properties of the material, can be predetermined. The result is that the surface available for cell delivery and for consequent tissue regeneration can be maximized and may be rendered extremely wide. As outlined already, bone tissue engineering strategies attempt to provide the injured segment initially with a scaffold of poor mechanical properties, but highly permissive to new bone ingrowth and blood vessel invasion. Scaffolds will have to be eventually resorbed to allow the new bone to gradually remodel, acquiring the required mechanical properties; ideally the scaffold resorption kinetics should correspond to those of new bone deposition. HA-TCP composites have achieved these prerequisites, where HA allows a direct chemical bond with the pre-existing or with the newly deposited bone, and TCP represents the resorbable component. Interestingly, specifically designed studies have shown that neither resorption nor dissolution of TCP or Si-modified TCP would take place in the absence of new bone formation within the defective site. Indeed, orthotopic and ectopic model studies have shown that contemporary phagocytic action by macrophages and osteoclasts and deposition of new osteoid matrix are needed to generate scaffold volumes with varied densities as those seen only in cell-bearing implants. Possibly then, the precursor cells' presence on and within the scaffold, prior to implantation, may influence the ECM proteins' availability on the material surface, thus favoring attachment of the osteoclasts and their resorption activity [37].

1.3 Obstacles

Bone has been one of the most interesting models and target tissues for cell therapy. Many groups around the world have attempted to find the best approach to regenerate it. Theoretical approaches

have been applied with interesting results both in small and large animal models. Even a few clinical studies have been performed with promising results [38]. But still, at present, no routine clinical application exists. What then is the reason for this apparent gap between successful experimental models and their translation to clinical practice? First therapeutic alternatives are available basically in any medium–large sized hospital and usually they represent a consistent approach to solve the problem. However, real life situations are always more complex than any experimental setting. In other words, bone lesions (i.e. in an emergency room setting) are unpredictable in many ways (size, anatomical location, cause of the lesion, health status of the subject, etc.) and of course, they are far from being standard. Moreover, the unavailability of specific off-the-shelf scaffolds contributes to the slow adoption of cell-based tissue regenerative approaches, in spite of the fact that MSC themselves are immune-privileged. These cells, in fact, carry low levels of class 1 and no class 2 Human Leukocyte Antigens [39], properties that prompted their clinical exploitation even in allogeneic hematopoietic stem cell transplantation [40]. MSC are thus particularly advantageous in bone tissue engineering applications, since they neither induce immune nor inflammatory responses in recipient organisms [41], but cells still need time to grow, a requirement that may not match the needs of the patient or the clinical setting. Moreover, a large body of evidence indicates the loss of osteochondrogenic potential of the cells due to several factors, particularly culture conditions, passage number, length of osteogenic induction, age and health conditions of donors, cell loss after implantation and the hostile environment of the injured tissue [42, 43]. Indeed, cell pre-conditioning has been suggested to improve in vivo delivery in many experimental settings [42, 44]. Safety, legal, and ethical issues also play a role, particularly if we consider all the requirements necessary to provide a "certified safe" cell population (in terms of collateral risk-free cell availability, number of cells, and effectiveness of the cells themselves) to any patient in need of treatment [45]. In this respect, several studies are being conducted to provide adequate quantitative parameters that could predict at least the efficacy of cell-based medicinal products, particularly relating to cell viability and osteogenic potency [46]. Still no one can predict the fate of in vitro expanded stem cells a decade after they have been reintroduced in vivo.

2 Present Challenges

2.1 Informative Substrates

An emerging philosophy aims to circumvent the traditional approach of recreating the complexity of living tissues ex vivo. In this context, the most ambitious strategy attempts to develop synthetic materials that establish key interactions with cells in ways that

unlock the body's innate powers of organization and self-repair. The complex cell–biomaterial interaction moves on multiple spatial and temporal scales. Therefore, in order to effectively influence cell behavior, scaffold materials must bear complex information, coded in their *physical* and *chemical* structures. In particular, bio-scaffolds must be properly designed to allow the spatial organization of stem cells and provide the basis for recreating a microenvironment mimicking their physiological *niche*. Stem cell niche is defined as a dynamic microenvironment that balances stem cell ability to maintain tissue homeostasis and repair throughout the lifetime of an organism [47]. In principle, stem cells in their niche make decisions to remain in a quiescent state, undergo self-renewal, or exit the niche upon exposure to local or systemic stimuli. These signals are actively coordinated and presented in a temporally and spatially regulated manner. Proper microenvironmental cues given by the biomaterial may be "informative" for cells, stimulating specific cellular responses.

2.2 Scaffold Physical Properties

Regardless of the chemistry or topography of the scaffolds, and prior to its implantation at the injured site, the primary function that a scaffold provides to the seeded cells is a physical support for adhesion. This implies close contact between cellular (endogenous) or secreted (exogenous) proteins and the scaffold itself. A few macromolecular classes encompass almost all the main extracellular matrix constituents, including collagens, elastin, proteoglycans, hyaluronic acid, and adhesion glycoproteins such as fibrinogen, fibronectin, tenascins, and thrombospondins. Independently of the scaffold, the mechanisms of cell adhesion rely on the deposition of extracellular matrix (ECM) components secreted by the seeded cells [48]. The ECM secretion pattern and the initial sensed resistance of the substrata are coupled to cytoskeletal alterations by a feed-back loop, through the concerted action of selectins, cadherins, and integrins [49, 50]. These mechanosensors and adhesion proteins, in turn, may direct cell differentiation toward a specific lineage. Indeed cells of mesenchymal origin adhere and contract on a variety of different substrates, for example uncoated or collagen-coated acrylamide gels and glass. Such a wide range of recognized surfaces parallels a wide variation in matrix stiffness sensing [51]. The resistance that a cell feels when it deforms the ECM can be measured, and ranges from 0.1 kPa (in soft tissues) to 1.0–20.0 kPa (muscle) to >25.0 kPa for bone. By varying matrix elasticity, Engler and collaborators were able to demonstrate that matrix stiffness can specify the MSC lineage differentiation, regardless of the culturing conditions or nutrients used [52]. Local sensing of force is then actively transduced into biochemical signals that regulate cell shape, growth, differentiation, and even death [53]. Interestingly, nuclear deformations also take place in response to cytoskeletal modifications, cell cycle and division: the nucleus is

quite stiff and resists distortion for brief periods, whereas it undergoes deformation for longer periods, granting the continuous timescale spectrum for varied genome expression kinetics [54] and hence a physiological base for differentiation as a consequence of the adhesion substrate characteristics.

2.3 Topographical Surface Modifications of Scaffolds

Progenitor cell fate is also affected by topographic cues of the scaffolds (i.e. *topological conditioning*). Recently, it has been reported that cells are able to decode the topographic signals of the scaffold and respond to the shape of the microenvironment by priming a specific cell differentiation commitment [55]. Thus, nanostructured biomaterials such as nanoparticles, nanofibers, nanosurfaces, and nanocomposites have gained increasing interest in regenerative medicine, since they offer a temporary ECM for regenerative cells [56–58]. Topography may also be relevant for hydrophilicity and for specific protein adsorption, as shown by the selective take-up of proteins relevant for cell attachment, such as fibronectin and vitronectin, on fibrous meshes with nanoscale fiber diameters [59]. Indeed, the interaction of cells with the surrounding milieu is in the nanometer scale and for prosthetic applications in orthopedics, cell attachment to grooved materials [60] and to nanocrystalline coatings [61] has long been documented. Thus nanoscaled topography of synthetic materials has been tailored to resemble the original surrounding tissue and mammalian cells have demonstrated a response to topographical surface variations [62, 63]. For mesenchymal cells, specific nano-patterning(s) may be compliant with the peculiar distribution(s) of adhesion molecules, mimicking the one that cells would adopt in a specific stiffness/elasticity context of an underlying contact surface. The patterning would "anticipate" the cell response to a specific substratum, thus forcing the consequences of cell adhesion, as in the case of neuronal differentiation of MSC toward neuronal lineages when cultured onto gratings of 350 nm line width [64].

2.4 Micro-environment

The optimization of the interactions between a scaffold matrix and cellular counterparts of the constructs can also be pursued by a contemporary specific biomimetic functionalization and/or nanostructuration of the interface. Clearly, once a cell has somewhat "decoded" its substrate and has ignited a new gene expression program in response to exogenous/endogenous stimuli, the secreted extracellular matrix proteins will modify the microenvironment and further drive the cell along a specific differentiation pathway. Experimental settings, in which passive adsorption of two matrix proteins, vitronectin (VN) and type collagen I (Col I), was tested on polymeric substrates showed that treated substrates mediated MSC adhesion and differently induced activation of mitogen-activated protein kinase (MAPK) and phosphatidylinositol-3-kinase (PI3K) signal transduction pathways [65]. Hence, the de novo synthesis

and deposition of ECM proteins by MSC alters the chemical identity of the polymeric substrate, altering the integrin expression profiles by a feed-back loop mechanism. These changes, in turn, cause modifications in the MAPK and PI3K signaling pathways, ultimately influencing the osteogenic differentiation of the seeded cells. Larger amounts of fibronectin and Col I and lower levels of VN were in fact deposited on poly(lactic) glycolic acid scaffolds over a 28-day period. Accordingly, cells also provided higher levels for α5β1 and α2β1 integrins (receptors for fibronectin and Col 1, respectively), and reduced levels for αVβ3 integrin (VN receptor). Relevant to the osteogenic differentiation of the cells, adhesion to Col I and fibronectin has been shown to induce the MAPK cascade, in particular the activation of the ERK1/2 system, which is critical for the activation of the osteogenic transcriptional factor Runx2 [66, 67]. Specific integrins then seem to be preferred or even required for the osteogenic differentiation of MSC; however a bio-functionalization of a scaffold surface should not focus on the presentation of a uniform coating to engage a single receptor, but rather identify the properties that control the presentation of integrin-specific epitopes within the coatings [68].

Clearly several chemical–physical modifications can be attempted and performed on almost any specific substrata even in a multiple fashion, provided that the proper chemistry is used. Indeed, many different strategies are currently being tested [69], including simple coatings [70], the contemporary use of genetic engineering and structural approaches [71, 72] and combinations of matrix-mimicking ligands and engineered structured nanomatrices [73]. The same natural extracellular matrix is per se able to induce specific cell commitment [74]. It is not surprising then, that the combination of topographical and chemical cues may result in a synergistic effect, in some cases informative enough to directly address adult MSC stem cells to non-canonical differentiation pathways, such as the neuronal one. Interestingly, the effects of a nano-patterned surface were even stronger than single biochemical induction on controls grown on un-patterned surfaces [64]. The cells are, therefore, major players in tissue regeneration approaches and the successful reconstruction of normal tissue depends on the properly simulated activity of the available progenitors.

3 Will Tissue Engineering and Cell Therapy Still Be Valuable?

In a number of studies, autologous marrow samples have been harvested and osteoprogenitors were isolated and expanded in culture [75]. A critical size segmental defect was surgically created in a long bone. The surgical lesion was filled with biomaterials carrying autologous in vitro expanded osteogenic progenitors. Radiographic and histological analysis of the retrieved specimens

revealed excellent integration of the host bone/implants and an amount of neo-formed bone significantly higher in the scaffolds loaded with osteoprogenitors than in acellular control grafts. The results of these studies were in good agreement suggesting an important advantage in bone formation and therefore, in the healing of the segmental defect when marrow-derived osteoprogenitors were delivered together with a proper biomaterial scaffold. It is surprising that, after initial enthusiasm over very encouraging large animal study results, only two pilot clinical studies have been performed [76, 77]. Although material science technology has resulted in clear improvements in the field of regenerative medicine, no ideal bone substitute has been developed yet and hence large bone defects still represent a major challenge for orthopedic and reconstructive surgeons. A number of bone substitute biomaterials are readily available. The intended clinical use defines the desired properties of engineered bone substitutes. Anatomical defects in load bearing long bones, for instance, require devices with high mechanical stability whereas for craniofacial applications, initially injectable or moldable constructs are favorable. Therefore, the most intriguing concept is the priming of the natural processes of bone regeneration driven by cells, through the use of materials able to mimic a specific pre-existing microenvironment.

An intriguing future alternative, given the advancing knowledge on the biology of stem cells, is going to be recruiting and properly addressing resident stem cells toward a regeneration pathway more than toward a reparation process. This in theory should be possible using appropriate soluble signals, able to deviate cells from a path and redirect them in a desired direction. Alternatively, more recent research has prompted the use of inducible pluripotent stem cells (iPSCs) for disease modeling, drug effectiveness evaluation, and therapeutic applications. The enormous potential for the generation of patient-specific stem cells able to differentiate into any lineage has boosted attempts to resolve their limitations in tissue engineering and regenerative medicine applications: random genomic integration of the transgenes, tumorigenic risk associated with the use of *c-myc*, the potential immunogenicity of autologous-derived iPSCs due to insufficient reprogramming and genetic instability. These severe risk factors have sparked a debate on the use of iPSCs for regenerative medicine applications. However, in order to circumvent these aspects, iPSCs could complete an in vitro differentiation into the needed cell type before transplantation, as suggested by the work of Araki et al. [78]. Nonetheless, epigenetic aberration patterns can be generated following directed differentiation. Therefore, in spite of the low immunogenicity of differentiated cells derived from iPSCs of a syngeneic source, immunogenicity must be thoroughly evaluated for each single protocol intended for clinical translation [79]. Screening and reliable protocols to assess the tumorigenic potential of individual iPSC

lines are also needed. Induced mesenchymal stem cells have already been generated and they maintain the potential to differentiate into osteoblasts, chondrocytes, or adipocytes starting from cord blood CD34+ cells [80]. Interestingly iPSC cells transduced according to the traditional Yamanaka protocol [81] were sensitive to nanotopographical patterning of the culture substrate, linking the previously described effects of topographical-induced differentiation pathways to an epigenetic status of the cell [82].

4 Conclusions

As a whole, a scaffold properly designed for tissue engineering applications must bear a structure planned on different spatial scales, in order to mimic the complex MSC niche [83]. Not all aspects of the niche will be needed to enhance stem cell self-renewal, but the simultaneous presence of many of these, such as chemical and multi-scale architectural cues, will be required to prompt specific cell differentiation and tissue ingrowth. Pre-commitment of MSC grown on a specific matrix cannot be overcome by the presence of soluble factors in the growth medium: indeed proper surface sensing has evidenced the existence of new requirements for progenitor cell lineage differentiation. For example, the osteogenic differentiation of MSC seeded onto electrospun poly(ε-caprolactone)/ECM scaffolds is maintained even if the cell culture medium is devoid of dexamethasone, a molecule normally required in standard osteogenic induction of plastic-adherent MSC cultures [84]. This observation as well as the many others in the field are of paramount relevance for MSC tissue engineering applications, particularly for bone reconstruction applications, where several rounds of ex-vivo cell duplications are needed and are normally performed on standard disposable culture plasticware. In this respect, recent lines of research have evidenced that the sensitivity of stem cells to the mechanical microenvironment is indeed a new parameter that must be considered when addressing induction strategies and the physical in vivo and ex vivo microenvironments for tissue engineering applications. All these approaches and specific aspects (scaffold stiffness compliance, surface topography and tri-dimensionality, scaffold chemistry) will have to be integrated into scaffold engineering to properly foster tissue regeneration. Whether this is feasible remains to be seen, given the high level of complexity of the dynamic interactions among the different components. These aspects, however, have become even more relevant, particularly if the same pluripotent progenitor cells are used for multiple tissue repairs within tissue engineered composites, such as in the case of osteochondral defects. Significantly, recent findings have also raised the possibility that an injured microenvironment may lose compliance, due to insufficient sensitivity and remodeling

options of stem cells once in a non-inducing environment, such as a fibrotic scar [85]. Given the influence of the microenvironment on repair outcomes, then, an additional challenge will also need to be addressed: to provide the proper cell "pre-commitment" in vitro to partially overcome an inappropriate pathological microenvironment in vivo, at the lesion site.

References

1. Bosch P, Musgrave DS, Lee JY et al (2000) Osteoprogenitor cells within skeletal muscle. J Orthop Res 18:933–944
2. Doherty MJ, Ashton BA, Walsh S et al (1998) Vascular pericytes express osteogenic potential in vitro and in vivo. J Bone Miner Res 13:828–838
3. Friedenstein AJ, Piatetzky S II, Petrakova KV (1966) Osteogenesis in transplants of bone marrow cells. J Embryol Exp Morphol 16:381–390
4. Huang JI, Beanes SR, Zhu M et al (2002) Rat extramedullary adipose tissue as a source of osteochondrogenic progenitor cells. Plast Reconstr Surg 109:1033–1041, discussion 1042–1043
5. Levy MM, Joyner CJ, Virdi AS et al (2001) Osteoprogenitor cells of mature human skeletal muscle tissue: an in vitro study. Bone 29:317–322
6. Mizuno S, Glowacki J (1996) Three-dimensional composite of demineralized bone powder and collagen for in vitro analysis of chondroinduction of human dermal fibroblasts. Biomaterials 17:1819–1825
7. Schantz JT, Hutmacher DW, Chim H et al (2002) Induction of ectopic bone formation by using human periosteal cells in combination with a novel scaffold technology. Cell Transplant 11:125–138
8. Zuk PA, Zhu M, Mizuno H et al (2001) Multilineage cells from human adipose tissue: implications for cell-based therapies. Tissue Eng 7:211–228
9. Antonucci I, Stuppia L, Kaneko Y et al (2011) Amniotic fluid as a rich source of mesenchymal stromal cells for transplantation therapy. Cell Transplant 20:789–795
10. Poloni A, Maurizi G, Babini L et al (2011) Human mesenchymal stem cells from chorionic villi and amniotic fluid are not susceptible to transformation after extensive in vitro expansion. Cell Transplant 20:643–654
11. Ioan-Facsinay A, Kloppenburg M (2011) An emerging player in knee osteoarthritis: the infrapatellar fat pad. Arthritis Res Ther 15:225
12. Fan J, Varshney RR, Ren L et al (2009) Synovium-derived mesenchymal stem cells: a new cell source for musculoskeletal regeneration. Tissue Eng Part B Rev 15:75–86
13. Corrao S, La Rocca G, Lo Iacono M et al (2013) Umbilical cord revisited: from Wharton's jelly myofibroblasts to mesenchymal stem cells. Histol Histopathol 28:1235–1244
14. Bianco P, Gehron Robey P (2000) Marrow stromal stem cells. J Clin Invest 105:1663–1668
15. Bianco P, Riminucci M, Gronthos S et al (2001) Bone marrow stromal stem cells: nature, biology, and potential applications. Stem Cells 19:180–192
16. Gronthos S, Simmons PJ (1995) The growth factor requirements of STRO-1-positive human bone marrow stromal precursors under serum-deprived conditions in vitro. Blood 85:929–940
17. Lennon DP, Haynesworth SE, Young RG et al (1995) A chemically defined medium supports in vitro proliferation and maintains the osteochondral potential of rat marrow-derived mesenchymal stem cells. Exp Cell Res 219:211–222
18. Locklin RM, Oreffo RO, Triffitt JT (1999) Effects of TGFbeta and bFGF on the differentiation of human bone marrow stromal fibroblasts. Cell Biol Int 23:185–194
19. Quito FL, Beh J, Bashayan O et al (1996) Effects of fibroblast growth factor-4 (k-FGF) on long-term cultures of human bone marrow cells. Blood 87:1282–1291
20. Bartholomew A, Patil S, Mackay A et al (2001) Baboon mesenchymal stem cells can be genetically modified to secrete human erythropoietin in vivo. Hum Gene Ther 12:1527–1541
21. Chuah MK, Van Damme A, Zwinnen H et al (2000) Long-term persistence of human bone marrow stromal cells transduced with factor VIII-retroviral vectors and transient production of therapeutic levels of human factor VIII in nonmyeloablated immunodeficient mice. Hum Gene Ther 11:729–738
22. Daga A, Muraglia A, Quarto R et al (2002) Enhanced engraftment of EPO-transduced

human bone marrow stromal cells transplanted in a 3D matrix in non-conditioned NOD/SCID mice. Gene Ther 9:915–921

23. Mizuno H, Zuk PA, Zhu M et al (2002) Myogenic differentiation by human processed lipoaspirate cells. Plast Reconstr Surg 109: 199–209, discussion 210-211
24. Luria EA, Panasyuk AF, Friedenstein AY (1971) Fibroblast colony formation from monolayer cultures of blood cells. Transfusion 11: 345–349
25. Lange C, Kaltz C, Thalmeier K et al (1999) Hematopoietic reconstitution of syngeneic mice with a peripheral blood-derived, monoclonal CD34-, Sca-1+, Thy-1(low), c-kit+stem cell line. J Hematother Stem Cell Res 8:335–342
26. Hoogduijn MJ, Verstegen MM, Engela AU et al (2014) No evidence for circulating mesenchymal stem cells in patients with organ injury. Stem Cells Dev 23:2328–2335
27. Breton P, Freidel M (1993) Hydroxyapatite in orthognathic surgery. Animal experimentation and clinical applications. Rev Stomatol Chir Maxillofac 94:115–119
28. Chappard D, Zhioua A, Grizon F et al (1993) Biomaterials for bone filling: comparisons between autograft, hydroxyapatite and one highly purified bovine xenograft. Bull Assoc Anat (Nancy) 77:59–65
29. Erickson D (1991) Binding bone. Will new bioceramic coatings improve orthopedic implants? Sci Am 265:101–102
30. Heise U, Osborn JF, Duwe F (1990) Hydroxyapatite ceramic as a bone substitute. Int Orthop 14:329–338
31. Oonishi H (1991) Orthopaedic applications of hydroxyapatite. Biomaterials 12:171–178
32. Langstaff S, Sayer M, Smith TJ et al (1999) Resorbable bioceramics based on stabilized calcium phosphates. Part I: rational design, sample preparation and material characterization. Biomaterials 20:1727–1741
33. Johnson KD, Frierson KE, Keller TS et al (1996) Porous ceramics as bone graft substitutes in long bone defects: a biomechanical, histological, and radiographic analysis. J Orthop Res 14:351–369
34. Kuhne JH, Bartl R, Frisch B et al (1994) Bone formation in coralline hydroxyapatite. Effects of pore size studied in rabbits. Acta Orthop Scand 65:246–252
35. Sartoris DJ, Holmes RE, Resnick D (1992) Coralline hydroxyapatite bone graft substitutes: radiographic evaluation. J Foot Surg 31:301–313
36. Misch CE, Dietsh F (1993) Bone-grafting materials in implant dentistry. Implant Dent 2:158–167
37. Mastrogiacomo M, Papadimitropoulos A, Cedola A et al (2007) Engineering of bone using bone marrow stromal cells and a silicon-stabilized tricalcium phosphate bioceramic: evidence for a coupling between bone formation and scaffold resorption. Biomaterials 28:1376–1384
38. Steinert AF, Rackwitz L, Gilbert F et al (2012) Concise review: the clinical application of mesenchymal stem cells for musculoskeletal regeneration: current status and perspectives. Stem Cells Transl Med 1:237–247
39. Herrmann RP, Sturm MJ (2014) Adult human mesenchymal stromal cells and the treatment of graft versus host disease. Stem Cells Cloning 7:45–52
40. Battiwalla M, Barrett AJ (2014) Bone marrow mesenchymal stromal cells to treat complications following allogeneic stem cell transplantation. Tissue Eng Part B Rev 20:211–217
41. El-Ghannam A (2005) Bone reconstruction: from bioceramics to tissue engineering. Expert Rev Med Devices 2:87–101
42. Giannoni P, Scaglione S, Daga A et al (2010) Short-time survival and engraftment of bone marrow stromal cells in an ectopic model of bone regeneration. Tissue Eng Part A 16: 489–499
43. Martino G, Pluchino S (2006) The therapeutic potential of neural stem cells. Nat Rev Neurosci 7:395–406
44. Sart S, Ma T, Li Y (2014) Preconditioning stem cells for in vivo delivery. Biores Open Access 3:137–149
45. Giannoni P, Cancedda R (2004) Regulatory issues: down to the bare bones. In: Petit H, Quarto R (eds) Engineering bone. Landes Bioscience Publishers, Georgetown, TX, pp 205–219
46. Pietila M, Lehtonen S, Narhi M et al (2010) Mitochondrial function determines the viability and osteogenic potency of human mesenchymal stem cells. Tissue Eng Part C Methods 16:435–445
47. Voog J, Jones DL (2010) Stem cells and the niche: a dynamic duo. Cell Stem Cell 6:103–115
48. Chastain SR, Kundu AK, Dhar S et al (2006) Adhesion of mesenchymal stem cells to polymer scaffolds occurs via distinct ECM ligands and controls their osteogenic differentiation. J Biomed Mater Res A 78:73–85
49. Hamidouche Z, Hay E, Vaudin P et al (2008) FHL2 mediates dexamethasone-induced

mesenchymal cell differentiation into osteoblasts by activating Wnt/beta-catenin signaling-dependent Runx2 expression. FASEB J 22: 3813–3822

50. Lee JW, Juliano R (2004) Mitogenic signal transduction by integrin- and growth factor receptor-mediated pathways. Mol Cells 17: 188–202
51. Discher DE, Janmey P, Wang YL (2005) Tissue cells feel and respond to the stiffness of their substrate. Science 310:1139–1143
52. Engler AJ, Sen S, Sweeney HL et al (2006) Matrix elasticity directs stem cell lineage specification. Cell 126:677–689
53. Vogel V, Sheetz M (2006) Local force and geometry sensing regulate cell functions. Nat Rev Mol Cell Biol 7:265–275
54. Dahl KN, Engler AJ, Pajerowski JD et al (2005) Power-law rheology of isolated nuclei with deformation mapping of nuclear substructures. Biophys J 89:2855–2864
55. Dalby MJ, Gadegaard N, Herzyk P et al (2007) Nanomechanotransduction and interphase nuclear organization influence on genomic control. J Cell Biochem 102:1234–1244
56. Balasundaram G, Sato M, Webster TJ (2006) Using hydroxyapatite nanoparticles and decreased crystallinity to promote osteoblast adhesion similar to functionalizing with RGD. Biomaterials 27:2798–2805
57. Hollister SJ, Maddox RD, Taboas JM (2002) Optimal design and fabrication of scaffolds to mimic tissue properties and satisfy biological constraints. Biomaterials 23:4095–4103
58. Zhang L, Rodriguez J, Raez J et al (2009) Biologically inspired rosette nanotubes and nanocrystalline hydroxyapatite hydrogel nanocomposites as improved bone substitutes. Nanotechnology 20:175101
59. Place ES, Evans ND, Stevens MM (2009) Complexity in biomaterials for tissue engineering. Nat Mater 8:457–470
60. Eisenbarth E, Velten D, Breme J (2007) Biomimetic implant coatings. Biomol Eng 24: 27–32
61. Nicula R, Luthen F, Stir M et al (2007) Spark plasma sintering synthesis of porous nanocrystalline titanium alloys for biomedical applications. Biomol Eng 24:564–567
62. Dalby MJ, McCloy D, Robertson M et al (2006) Osteoprogenitor response to semi-ordered and random nanotopographies. Biomaterials 27:2980–2987
63. Dalby MJ, McCloy D, Robertson M et al (2006) Osteoprogenitor response to defined topographies with nanoscale depths. Biomaterials 27: 1306–1315
64. Yim EK, Pang SW, Leong KW (2007) Synthetic nanostructures inducing differentiation of human mesenchymal stem cells into neuronal lineage. Exp Cell Res 313:1820–1829
65. Kundu AK, Putnam AJ (2006) Vitronectin and collagen I differentially regulate osteogenesis in mesenchymal stem cells. Biochem Biophys Res Commun 347:347–357
66. Franceschi RT, Xiao G (2003) Regulation of the osteoblast-specific transcription factor, Runx2: responsiveness to multiple signal transduction pathways. J Cell Biochem 88:446–454
67. Xiao G, Jiang D, Thomas P et al (2000) MAPK pathways activate and phosphorylate the osteoblast-specific transcription factor, Cbfa1. J Biol Chem 275:4453–4459
68. Keselowsky BG, Collard DM, Garcia AJ (2005) Integrin binding specificity regulates biomaterial surface chemistry effects on cell differentiation. Proc Natl Acad Sci U S A 102:5953–5957
69. Fu RH, Wang YC, Liu SP et al (2011) Differentiation of stem cells: strategies for modifying surface biomaterials. Cell Transplant 20:37–47
70. Uygun BE, Stojsih SE, Matthew HW (2009) Effects of immobilized glycosaminoglycans on the proliferation and differentiation of mesenchymal stem cells. Tissue Eng Part A 15: 3499–3512
71. Benoit DS, Schwartz MP, Durney AR et al (2008) Small functional groups for controlled differentiation of hydrogel-encapsulated human mesenchymal stem cells. Nat Mater 7:816–823
72. Gorsline RT, Tangkawattana P, Lannutti JJ et al (2010) Accelerated chondrogenesis in nanofiber polymeric scaffolds embedded with BMP-2 genetically engineered chondrocytes. J Biomed Sci Eng 3:908–916
73. Anderson JM, Kushwaha M, Tambralli A et al (2009) Osteogenic differentiation of human mesenchymal stem cells directed by extracellular matrix-mimicking ligands in a biomimetic self-assembled peptide amphiphile nanomatrix. Biomacromolecules 10:2935–2944
74. Chen XD, Dusevich V, Feng JQ et al (2007) Extracellular matrix made by bone marrow cells facilitates expansion of marrow-derived mesenchymal progenitor cells and prevents their differentiation into osteoblasts. J Bone Miner Res 22:1943–1956
75. Bianco P, Robey PG (2001) Stem cells in tissue engineering. Nature 414:118–121
76. Quarto R, Mastrogiacomo M, Cancedda R et al (2001) Repair of large bone defects with the use of autologous bone marrow stromal cells. N Engl J Med 344:385–386

77. Vacanti CA, Bonassar LJ, Vacanti MP et al (2001) Replacement of an avulsed phalanx with tissue-engineered bone. N Engl J Med 344:1511–1514
78. Araki R, Uda M, Hoki Y et al (2013) Negligible immunogenicity of terminally differentiated cells derived from induced pluripotent or embryonic stem cells. Nature 494:100–104
79. Nazor KL, Altun G, Lynch C et al (2012) Recurrent variations in DNA methylation in human pluripotent stem cells and their differentiated derivatives. Cell Stem Cell 10: 620–634
80. Meng X, Su RJ, Baylink DJ et al (2013) Rapid and efficient reprogramming of human fetal and adult blood CD34+ cells into mesenchymal stem cells with a single factor. Cell Res 23:658–672
81. Takahashi K, Yamanaka S (2006) Induction of pluripotent stem cells from mouse embryonic and adult fibroblast cultures by defined factors. Cell 126:663–676
82. Downing TL, Soto J, Morez C et al (2013) Biophysical regulation of epigenetic state and cell reprogramming. Nat Mater 12:1154–1162
83. Dellatore SM, Garcia AS, Miller WM (2008) Mimicking stem cell niches to increase stem cell expansion. Curr Opin Biotechnol 19: 534–540
84. Thibault RA, Scott Baggett L, Mikos AG et al (2010) Osteogenic differentiation of mesenchymal stem cells on pregenerated extracellular matrix scaffolds in the absence of osteogenic cell culture supplements. Tissue Eng Part A 16:431–440
85. Berry FB, Mirzayans F, Walter MA (2006) Regulation of FOXC1 stability and transcriptional activity by an epidermal growth factor-activated mitogen-activated protein kinase signaling cascade. J Biol Chem 281:10098–10104

Chapter 3

Mesenchymal Stem Cells for Osteochondral Tissue Engineering

Johnathan Ng, Jonathan Bernhard, and Gordana Vunjak-Novakovic

Abstract

Mesenchymal stem cells (MSC) are of major interest in regenerative medicine, as they are easily harvested from a variety of sources (including bone marrow and fat aspirates) and they are able to form a range of mesenchymal tissues, in vitro and in vivo. We focus here on the use of MSCs for engineering of cartilage, bone, and complex osteochondral tissue constructs, using protocols that replicate some aspects of natural mesodermal development. For engineering of human bone, we discuss some of the current advances, and highlight the use of perfusion bioreactors for supporting anatomically exact human bone grafts. For engineering of human cartilage, we discuss the limitations of current approaches, and highlight engineering of stratified, mechanically functional human cartilage interfaced with bone by mesenchymal condensation of MSCs. Taken together, current advances enable engineering of physiologically relevant bone, cartilage and osteochondral composites, and physiologically relevant studies of osteochondral development and disease.

Key words Cartilage, Bone, Regenerative medicine, Bioreactor, Anatomically shaped grafts

1 Introduction

Bone, cartilage, and their interface are each unique and complex tissues, but together they provide the structure and support systems necessary for load-bearing and movement. Damage to any of these tissues, caused by trauma or diseases such as osteoarthritis, can cause pain, inhibit functionality and restrict mobility of the patient. In the United States alone, there are over 1.7 million osteochondral surgical procedures performed each year [1]. Such invasive surgeries were previously limited to elderly patients suffering from extensive osteoarthritis or brittle bones caused by osteoporosis. However, the last 20 years has seen a substantial increase in the number of corrective procedures performed in younger age groups [2]. Characteristically, this younger age group is more active, and demands higher performance from treatment options [3].

Massimiliano Gnecchi (ed.), *Mesenchymal Stem Cells: Methods and Protocols*, Methods in Molecular Biology, vol. 1416,
DOI 10.1007/978-1-4939-3584-0_3,

Currently, surgical treatments include manufactured, natural, and autologous options. Manufactured options mostly use a combination of metal and plastic. These solutions provide excellent mechanical properties that restore structure and mobility, factors especially important for joint replacements [4]. However, despite extensive research on bio-integration into native tissue, a high percentage of implants still do not fully integrate with the host tissue and eventually experience failure [5]. Currently, the average lifetime of a manufactured implant is 10–15 years [6], meaning younger generations will undergo multiple replacement surgeries during their lifetime. In addition, inert solutions lack the ability to grow and adapt with the native tissue, and in some cases induce negative adaptation, which in turn requires surgical intervention [5].

Natural treatment solutions are based on the use of tissues that are xenogenic (from animals) and allogenic (from other patients). With advancements in removing cellular material, decellularized allografts and xenografts have become a frequent treatment option [7]. Decellularized grafts maintain the original structure, composition, and mechanical properties of the extracellular matrix, while the removal of the cellular components prevents the activation of immune responses and graft rejection [5]. In principle, decellularized tissue grafts provide a natural, non-inflammatory framework for cell infiltration, graft incorporation, and regeneration of the tissue structure. However, in clinical practice these grafts have limited osteogenicity and clinical outcomes are not predictable. Recent research has focused on the use of growth factors doped into these scaffolds to elicit more predictable and robust outcomes [5, 8].

Autologous solutions (tissues harvested from another region in the same patient) are the current gold standard for bone and cartilage repair. Autologous grafts have the advantage of being from the patient's own body, thereby preventing rejection events. In addition, the presence of native cells and vasculature within the tissue should result in predictable regeneration and recovery of the treated tissue [9]. A major disadvantage of the autologous solution is the need to harvest donor tissue, which is always in limited supply [5]. Besides requiring additional time for the patient on the operating table, the harvest site experiences donor-site morbidity [7, 8]. Also, the harvested tissue is not in the correct anatomical shape, so the surgeon must shape the graft.

These limitations in the use of tissue autografts have heightened interest in the fast-developing field of tissue engineering. Tissue engineering proposes to combine the benefits from each of the current solutions to produce an autologous, integrative solution with adequate mechanical properties, thereby providing a customized graft for the osteochondral surgical intervention that does not require tissue harvest. Tissue engineers strive to construct patient-tailored tissue grafts utilizing a combination of three elements: scaffolds, bioreactors, and cells [10]. Scaffolds provide

the main framework of the tissue, and have been created from both synthetic and natural sources [11]. With synthetic scaffolds, engineers are able to control the chemical make-up, degradation rate, isotropy, and mechanical properties of the tissue [11]. Scaffolds derived from natural tissues, such as decellularized allografts, have fantastic biocompatibility and usually contain important factors that aid in the regeneration process [11].

Bioreactors allow engineers to recreate on the benchtop, key aspects of the in vivo environment [10]. Common osteochondral bioreactors include perfusion bioreactors, to replicate vasculature by providing adequate nutrient transport and waste removal, and bioreactors with mechanical stimulation, to replicate the physiological stresses placed on tissues [12–14]. These bioreactors can be used to develop and mature tissue before implantation, and also as highly controllable tools for investigating normal and diseased tissue states [15].

The cells, incorporated in vitro, modify the tissue engineered construct in preparation for implantation, and can have a critical impact on regeneration after placement in vivo. Initially in tissue engineering strategies, primary cells were utilized. These cells had the capacity to create and maintain a desired tissue and have produced exciting results [16–19]. However, sources of these cells can be a problem. Allogeneic sources are readily available and the cells can be easily harvested, but cause tissue rejection when implanted, while autologous cells can only be obtained by sacrificing tissue at another location in the body, similar to tissue harvest for autografts.

In response to problems with the use of primary cells, mesenchymal stem cells (MSC) have been actively explored as a source of cells with a major clinical interest. Residing in the mesoderm that drives the formation of the entire osteochondral tissue, mesenchymal stem cells have been harvested from a variety of tissues (*see* Table 1 for an overview of tissue sources for isolation of MSC),

Table 1
Tissue sources for deriving mesenchymal stem cells for osteochondral tissue engineering

Tissue source	Abbreviation	Citation
Bone marrow	BMSC	Pittenger et al. [20]
Adipose	ASC	Zuk et al. [21]
Dental tissue	DTSC	Seo et al.[22]
Periosteum	PSC	Yoshimura et al. [23]
Amnion	AMSC	Int' Anker et al. [24]
Umbilical cord	UCBSC	Erices et al. [25]

with evidence suggesting that stem cells can be isolated from any vascularized construct [26, 27]. The mesenchymal nature of MSCs provides an ideal solution for engineering osteochondral grafts. These cells enable replication of the natural mesodermal development, leading to the formation of entire osteochondral constructs comprising multiple tissue types from a single batch of easily harvested autologous cells [20, 26, 28].

In this chapter, we focus on the use of MSC for tissue engineering of osteochondral tissues. We also discuss recent developments in engineering of cartilage and bone from human MSCs, and describe potential strategies to unify multiple tissue types into a single, complete osteochondral graft.

2 Mesenchymal Stem Cells for Engineering Bone

Over the last two decades, advancements have been made in determining the appropriate scaffold to influence MSC differentiation. Mechanically stiff substrates [29], the application of mechanical forces [30], and the inclusion of minerals into the scaffold [31] all stimulate osteogenic differentiation and bone formation. A majority of studies have shown satisfactory bone formation in vitro, and many have even shown the ability of engineered bone to regenerate and integrate into the native skeleton [32–35]. The in vivo studies were most commonly performed in the mouse subcutaneous pouch or a rat calvarial defect.

The small size of the animals necessitated the use of similarly small constructs. During cultivation of these small constructs, passive diffusion was sufficient to ensure adequate nutrient delivery and waste removal. However, increasing the complexity and size of the constructs has proven difficult, primarily due to passive diffusion no longer being sufficient for cell cultivation. The lack of nutrition and waste management causes cell death and necrosis in the interior, destroying the scaffold. Current research is focused on resolving this problem, by designing strategies to enhance transport throughout the bone interior, allowing eventually the production of complex, anatomical constructs.

One important strategy enables pre-vascularization of bone grafts facilitating communication with the vasculature of the host. Current research initiatives are pursuing smart scaffold designs, providing structural pathways and growth factors to attract vascular formation [36, 37]. Another research direction utilizes co-culture of MSC/MSC-derived osteoblasts with vascular cells [38–40]. These studies aim to facilitate interactions between the cells and promote the construction of natural vascular pathways. Therefore, upon implantation, the host will integrate with the pre-formed structures, establishing circulation more readily.

In parallel studies, media compositions were developed to differentiate MSC into hypertrophic chondrocytes [41, 42]. Triggering of chondrogenic maturation in vitro resulted, following implantation in vivo, in the formation of bone and bone marrow, replicating the endochondral ossification pathway that is associated with bone development and fracture repair [42, 43]. Hypertrophic chondrocytes are essential for endochondral ossification as they initiate transition from the soft callus to provisional bone by provoking vascular invasion and depositing the bone template [44]. Hypertrophic chondrocytes are an attractive tool for tissue engineering because of their survival in the hypoxic environment of cartilage, thereby withstanding the time delay necessary for vascular development in vivo [42].

A promising route for growing bone grafts in vitro, and maintaining their viability for an extended period of time to allow differentiation and maturation, is with perfusion bioreactors [45–47]. Perfusion bioreactors provide nutrients and—most critically—oxygen to the entire construct, permitting cell growth and maturation regardless of the complexity of the scaffold shape. Perfusion is critically important for engineering bone and other metabolically active, vascularized tissues, as the diffusional depth of oxygen supply is only a fraction of a millimeter.

In the following section, the highlighted paper details the advancement of perfusion bioreactors from those supporting generic, small-size constructs to those designed to engineer anatomically exact human bone grafts. To create these complex grafts, Grayson et al. approached the problem in three separate steps: generation of the anatomically exact scaffold, construction and validation of a unique bioreactor, and integration of the two during cultivation [48].

3 Highlight: "Engineering Anatomically Shaped Human Bone Grafts" Grayson et al. [48]

The exact anatomical dimensions of the mandibular condyle, selected as a model due to its complex shape and need for bone grafting solutions for the temporomandibular joint, were determined by computed tomography scans. Using specialized, commercially available computer software, the 2D slices of the scan were reconstructed into a 3D file that could be imported into computer-aided manufacturing (CAM) software to produce the necessary fabrication steps for the computer-numerical-control (CNC) milling machine. Decellularized trabecular bone was chosen as the scaffold for its structural, biochemical, osteoinductive and mechanical properties, and micromilled to the exact anatomical shape.

Control of perfusion through the bone scaffold was dictated by the design of a specific anatomically shaped perfusion chamber,

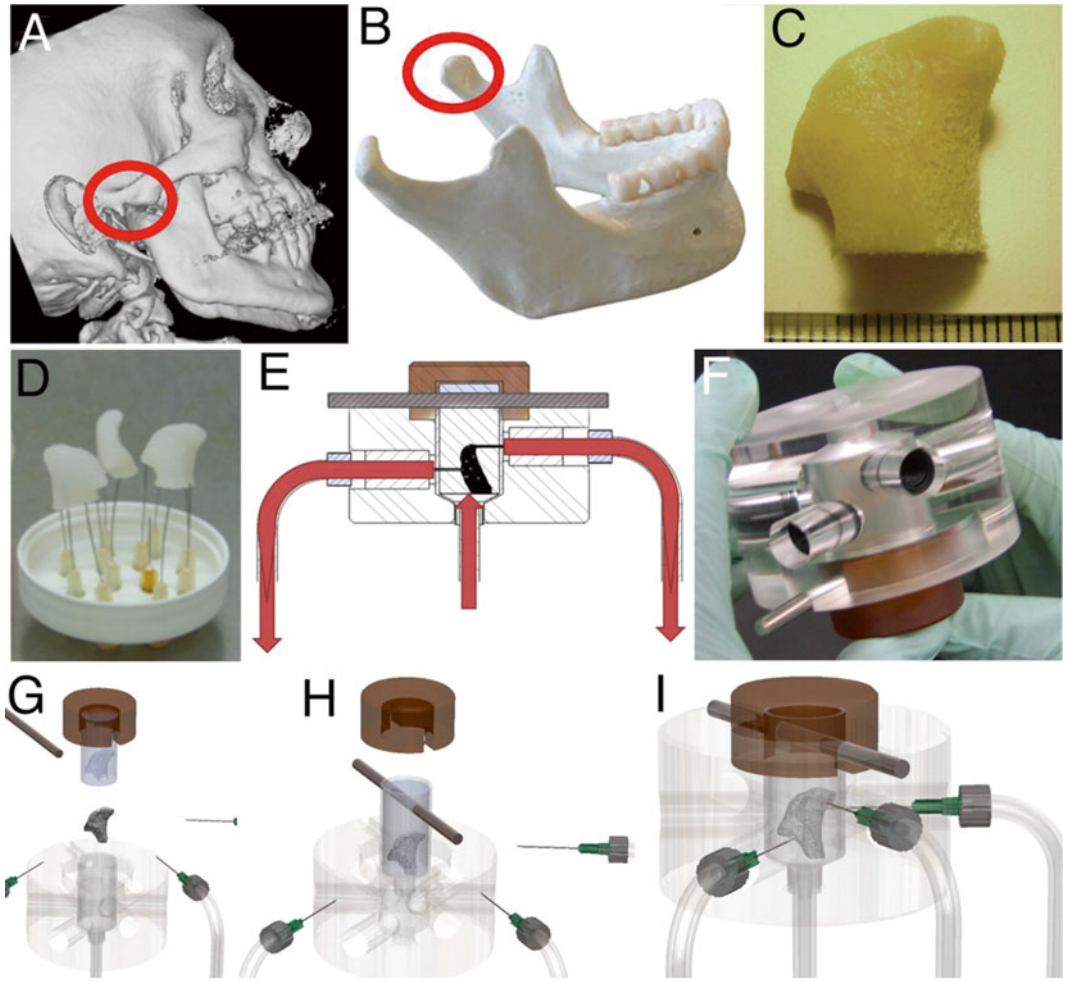

Fig. 1 Tissue engineering of anatomically shaped bone grafts. (**a**–**c**) Scaffold preparation. (**a**, **b**) Clinical CT images were used to obtain high-resolution digital data for the reconstruction of the exact geometry of human temporomandibular joint (TMJ) condyles. (**c**) These data were incorporated into the MasterCAM software to machine TMJ-shaped scaffolds from fully decellularized trabecular bone. (**d**) A photograph illustrating the complex geometry of the final scaffolds that appear markedly different in each projection. (**e**) The scaffolds were seeded in a stirred suspension of hMSC, using three million cells per scaffold (~1 cm^3 volume), pre-cultured for 1 week to allow cell attachment, and cultured with perfusion through the cell-seeded scaffold for an additional 4 weeks. (**f**) A photograph of the perfusion bioreactor used to cultivate anatomically shaped grafts in vitro. (**g**–**i**) Key steps in the bioreactor assembly. Images are reproduced with permission from ref. 48

also created using the converted computed tomography scans. The perfusion chamber—a PDMS negative mold of the scaffold—was compressed by two manifolds to direct the medium flow through the cell-seeded scaffold. Clamps on the flow tubing allowed control of the flow rate. Computational modeling was conducted to verify that the chosen flow rates produced satisfactory perfusion to all areas of the scaffold. The method is shown in Fig. 1.

Human bone marrow stem cells were expanded and seeded into the anatomically shaped scaffolds using the spinner flask method. After loading into the bioreactor, the scaffolds were cultured for 5 weeks in osteogenic medium. After cultivation, constructs under perfusion had a 7.5-fold increase in DNA compared with statically cultured constructs, with histological analysis showing significant cell viability and bone deposition in all parts of the scaffold. In the static controls, the interior of the complex scaffolds was devoid of cells and showed only minimal bone deposition. Temporal evaluation of the constructs using μCT demonstrated a significant increase in bone volume over 5 weeks, and displayed significantly more bone volume than the statically cultivated constructs. Differences in the development and matrix deposition between the two groups are shown in Fig. 2.

In summary, the use of a custom-designed perfusion system allowed successful, development of viable, anatomically shaped engineered tissues, proving their validity and advancing tissue engineered bone grafts toward clinical translation.

4 Engineering Cartilage Using Mesenchymal Stem Cells

Early studies demonstrated the efficacy of synthetic materials, such as polyglycolic acid (PGA) and poly-l-lactic acid (PLLA), as scaffolds for primary chondrocytes both in vitro and in vivo [49, 50]. In addition to the scaffold-based cell carriers, hydrogels such as agarose and alginate, consisting of water-swollen networks, were also widely used as carriers to maintain chondrocyte phenotype and provide local microenvironmental control [51]. While trophic factors such as TGF-β are essential for chondrogenesis, biophysical stimulation such as deformational loading has also been used to modulate cartilage development in vitro [18, 52]. These studies contributed to an overall tissue-engineering paradigm involving three-dimensional environments with tissue-specific biochemical and biophysical stimulation.

Despite their well-established ability to form cartilage in vitro, chondrocytes have limited proliferative ability and are prone to dedifferentiation in vitro. Investigators attempted to extend methods successfully used with chondrocytes to the engineering of cartilage from MSC, but only with limited success. In particular, studies comparing the use of agarose to engineer cartilage from chondrocytes and from MSCs revealed that MSCs formed cartilaginous tissues with subnormal biochemical and mechanical properties [19, 53]. Still, several studies showed that long-term culture with the application of TGF-β, mechanical stimulation, osmotic loading, and enzymatic treatment all improved the properties of cartilage grown from agarose seeded with MSCs [19, 53–55].

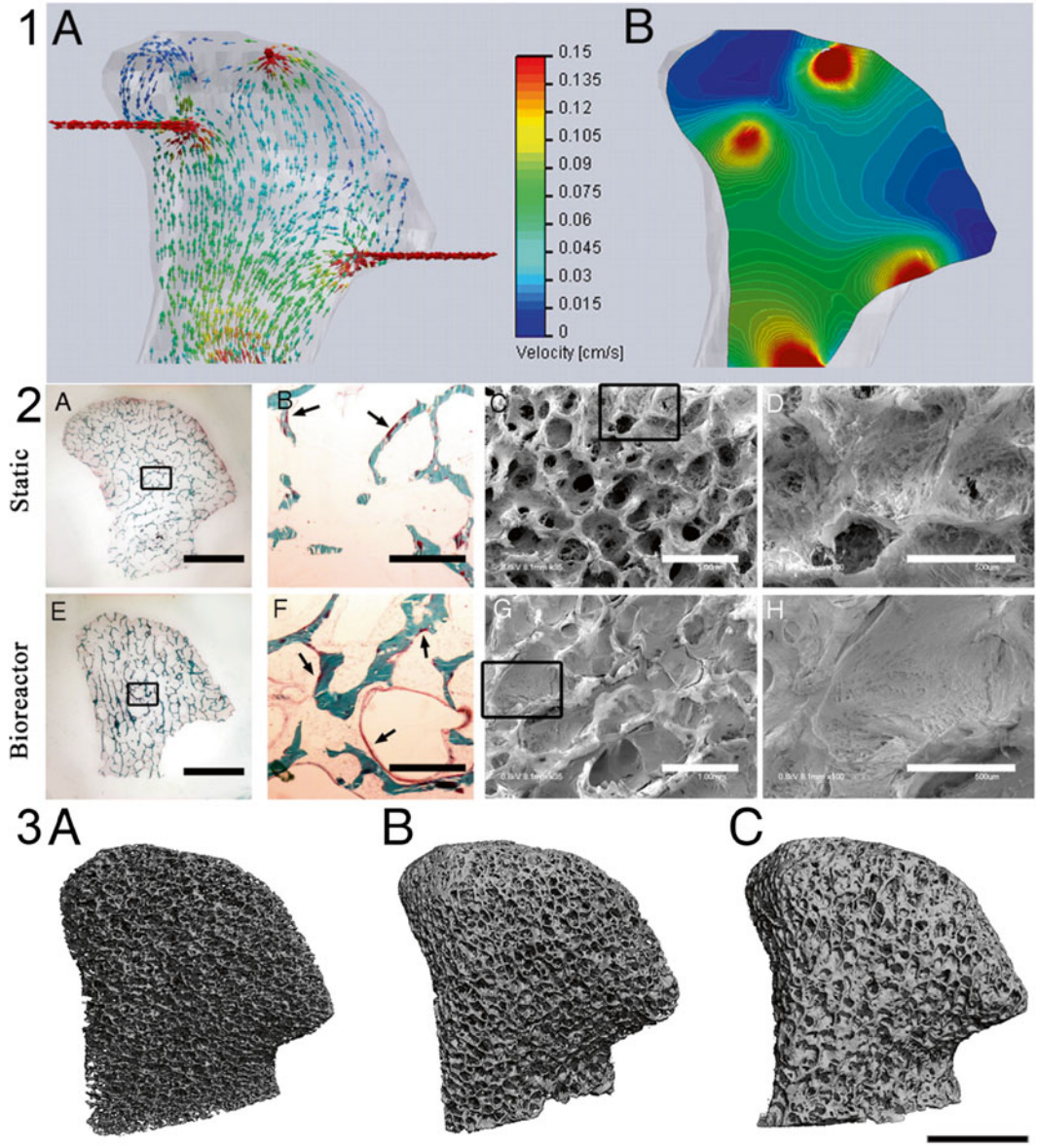

Fig. 2 Effects of perfusion on bone formation in vitro. (**1**) Computational models of medium flow through TMJ constructs during bioreactor cultivation. (**1a**) Color-coded velocity vectors indicate the magnitude and direction of flow through the entire construct based on experimentally measured parameters. (**1b**) Construct is digitally sectioned, and the color-coded contours are used to indicate the magnitude of flow in the inner regions. (**2a**–**h**) Bone formation was markedly enhanced by perfusion, in a manner dependent on the fluid flow pattern. (**2a**–**d**) Constructs cultured under static conditions. (**2e**–**h**) Constructs cultured with medium perfusion. (**2a**, **e**) Trichrome staining of the entire cross-section of scaffolds showing differences in the new matrix distribution (*red*) compared with the original scaffold (*green*) for the static (**2a**) and perfused (**2e**) culture groups. (**2b**, **f**) Major differences in osteoid formation (*arrows*) in the central regions of constructs cultured statically (**2b**) and in perfusion (**2f**). (**2c**, **d**, **g**, **h**) SEM images of the central construct regions. (**2c**, **d**) Statically cultured constructs exhibit empty pore spaces and loosely packed cells. (**2g**, **h**) Constructs cultured in perfusion demonstrate the formation of dense and confluent lamellae of bone tissue that fill entire pore spaces. (Scale bars—**2a**, **e**: 5 mm; **2b**, **c**, **f**, **g**: 1 mm; 2**d**, **h**: 500 μm.) (**3a**–**c**) Architecture of the mineralized bone matrix developed over time and in a manner dependent on culture conditions. The reconstructions of 3D μCT images demonstrate the changes in pore structure (relative to the initial state) that were evident at the end of the fifth week of cultivation. (Scale bar: 5 mm.) Images reproduced with permission from ref. 48

Multiple labs have shown that incorporation of glycosaminoglycans such as hyaluronic acid and chondroitin sulfate by polymerization into hydrogels recreated a biomimetic microenvironment for chondrogenesis [56–58]. Furthermore, scaffold architecture can also be designed to mimic that of native cartilage matrix, as studies showed that interlocking woven polycaprolactone (PCL) supported the formation of cartilaginous tissue [59]. Interestingly, investigators adapted these techniques for making cell-instructive and bioactive scaffolds to further enhance cartilage formation by controlling differentiation of hMSC. For example, Bian et al showed that neo-cartilage formation by hMSC in vivo could be enhanced by incorporating N-cadherin, an intercellular cell binding protein implicated in cell condensation that precedes cartilage formation, into methacrylated HA [60]. Similarly, Brunger et al. showed that a viral vector immobilized on a woven PCL scaffold could mediate transduction of hMSC and drive TGF-β3 expression, thus leading to potent chondrogenic differentiation [61].

5 Highlight: Self-Assembly of Human Mesenchymal Stem Cells into Functional and Stratified Cartilage [62]

While it is evident that biomimetic methods enhance tissue formation by simulating the native microenvironment, the formation of physiological tissue by progenitor cells ultimately required lessons taken from native tissue morphogenesis. Self-assembly has been proposed as an in vitro method for recapitulating mesenchymal condensation that precedes chondrogenesis [63].

Scaffold-free cartilage formation by self-assembly of hMSC was first introduced as the pellet culture, whereby cells centrifuged into high-density aggregates were cultured in chondrogenic medium. This method was shown to recapitulate the progression of chondrogenesis [64, 65]. Still, the proponents of scaffold-based cartilage tissue engineering criticized the use of pellets for their physiologically irrelevant size, geometry, and mechanical properties. Similar to earlier studies with chondrocytes, studies also showed that MSC self-assembled on scaffold formed cartilaginous tissues that resembled hyaline cartilage with dense ECM and zonal organization [66–71].

Our lab recently showed that fusion of condensed mesenchymal bodies (CMBs) on decellularized bone (DCB) can lead to the formation of large, functional, and well organized cartilage grafts [62]. To overcome the limitations in size and geometry of the pellets, numerous CMBs were packed, within a mold, onto the surface of decellularized bone and cultured for up to 5 weeks (Fig. 3). For the first time, centimeter-sized cartilage with physiological stratification, mechanical and tribological properties comparable to native cartilage was successfully grown in vitro from hMSC (Table 2).

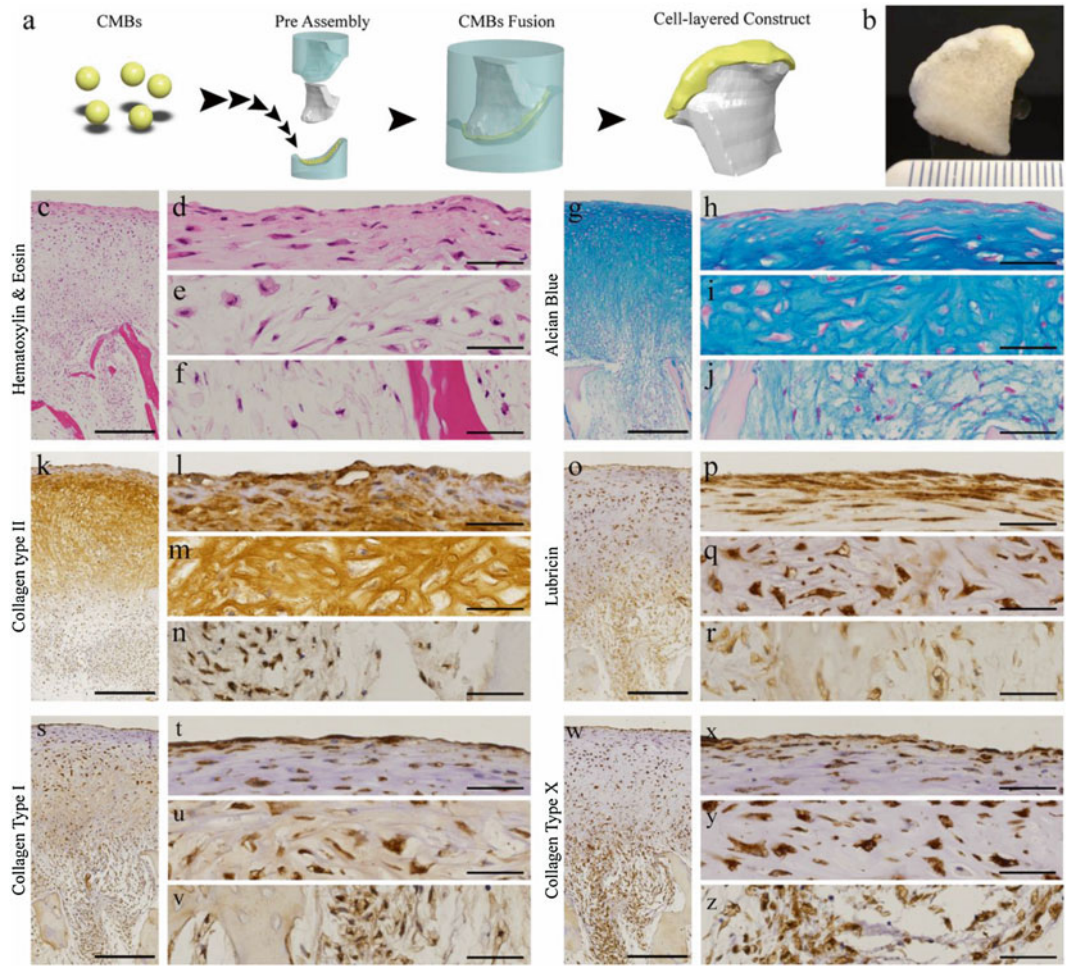

Fig. 3 In vitro formation of physiologically stratified, stiff, and frictionless human cartilage interfaced with a bone substrate. Cartilage was formed from condensed mesenchymal bodies (CMBs) press fit onto a bone substrate, and cultured in vitro, as reported by Bhumiratana et al. [62]. (**a**, **b**) CMBs were press-fitted within molds on a decellularized bone scaffold (DCB), forming cartilage after 5 weeks of chondrogenic induction. Histological and immunohistochemical analysis showing representative stains of (**c**, **f**) H&E, (**g**–**j**) Alcian Blue for GAG, (**k**–**n**) collagen type II, (**o**–**r**) lubricin, (**s**–**v**) collagen type I, and (**w**–**z**) collagen type X. (Scale bar: 500 μm in low-magnification images, 50 μm in high-magnification images)

Table 2
Mechanical properties of human cartilage engineered by CMB fusion

Articular cartilage constructs	Young's modulus, kPa	Minimum friction coefficient, μ_{min}	Equilibrium friction coefficient, μ_{max}
Day 3 CMBs	788 ± 200	0.049 ± 0.008	0.276 ± 0.033
Day 5 CMBs	825 ± 197	0.046 ± 0.010	0.283 ± 0.042
Day 7 CMBs	457 ± 46*	0.064 ± 0.013	0.334 ± 0.053

Interestingly, we also observed that the formation of boundaries around CMBs, indicated by the presence of tenascin-C, limits integration of CMBs that must be fused within 3–5 days following chondrogenic induction to achieve successful integration. The boundaries between CMBs that were fused after 1 week of condensation persisted for a long time in culture, hindered integration, and resulted in formation of cartilage with subnormal mechanical and tribological properties. Other early chondrogenic markers characteristic of mesenchymal condensation were also increasingly expressed during the first week of culture prior to the onset of ECM production. This study showed the feasibility of engineering cartilage by self-assembly of hMSC pellets, using a method that mimics mesenchymal condensation.

6 Engineering Osteochondral Composites Using Mesenchymal Stem Cells

The osteochondral composite consists of a cartilage layer above a bone layer, with a functional interface between the two tissue layers. Engineering such a complex tissue presents significant challenges, as the articular cartilage and the subchondral bone comprise different cell types and different microenvironments. Also, the subchondral bone has a much higher mechanical stiffness than articular cartilage.

The strategies proposed and evaluated for fabrication of osteochondral composites have been summarized in two excellent recent reviews [72, 73]. Broadly, the strategies can be classified according to their selection of the scaffold and cell source for cartilage and bone layers (Fig. 4). Some investigators formed the cartilage layer using chondrocytes, while others chose to form both the cartilage layer and the bone phase using MSCs in order to overcome the limitations of chondrocytes.

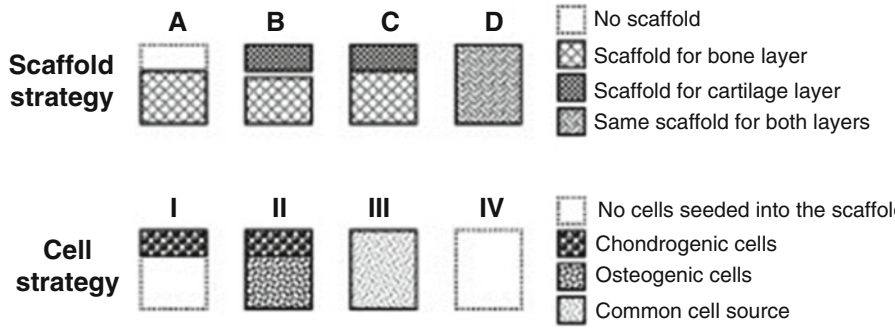

Fig. 4 Approach to assembling osteochondral composites. The schematic shows one of the scaffolds and cell-based strategies for engineering osteochondral composites discussed here, proposed by Martin et al. [72]

Most commonly, investigators used bi-layered scaffolds whereby the cartilage layer comprises a synthetic or natural polymer and the bone layer comprises polymers, ceramics, or metals. The cartilage and bone layers were combined using sutures and adhesives, such as fibrin. Interestingly, several groups used a scaffold-free approach similar to self-assembly methods for culturing cells at high density on top of the bone layer. In these various approaches, desirable outcomes of the in vitro culture and in vivo implantation were generally associated with strong integration between the cartilaginous and bone layer, sometimes with the formation of a calcified transition zone.

In a functional osteochondral unit, the interface needs to recapitulate the transition between bone and cartilage with strong integration between the layers. In the articular cartilage, deep zone collagen fibrils extend into the calcified layer that inter-digitates with the subchondral bone. In addition to integrating the cartilage and bone, the calcified cartilage distributes load across the interface between the biomechanically incompatible non-mineralized cartilage and mineralized subchondral bone.

Depending on the method of seeding and the choice of scaffold for the bone layer, the production of cartilaginous ECM and the transition of this matrix into calcified cartilage at the interface can be enhanced using various methods. For example, Schaefer and colleagues reported that a chondrocyte-seeded PGA mesh sutured with a collagen-hydroxyapatite (Col-HA) sponge had the ability to integrate following long-term implantation [74]. Similarly, Wang and colleagues showed that the scaffold-free, high-density seeding of chondrocytes on top of a porous osteoconductive scaffold resulted in neo-cartilage integration with the collagen-hydroxyapatite (Col-HA) scaffold [75]. Kandel and colleagues showed the formation of mechanically strong cartilage by self-assembly of chondrocytes on calcium polyphosphate (CPP) in a long-term orthotopic sheep model. Finally, Allan and colleagues subsequently showed enhanced cartilage–bone integration with deep zone mineralization of chondrocytes cultured on CPP in the presence of β-glycerophosphate (β-GP) [76, 77]. Thus, it is evident that ECM integration and calcified layer formation are important determinants of the composite outcome.

7 Highlight: Osteochondral Composites and the Calcified Cartilage

Several groups have reported that high-density scaffold-free cultures of chondrocytes on polymer-ceramic bone scaffolds could result in the formation of well-integrated osteochondral composites. Our lab introduced the fusion of scaffold-free mesenchymal bodies with the bone substrate, followed with bioreactor culture of the composite tissue. This new method resulted in the formation of

a physiologically stratified cartilage layer that resembled the stiffness and frictionless properties of native cartilage and was well integrated with the underlying bone matrix [62]. Tuli et al. also showed in an earlier study, the formation of an organized osteochondral composite with distinct cartilage–bone transition by press-coating a PLA scaffold with a chondrogenically induced hMSC pellet [78]. Both investigations reported scaffold-free formation of an organized cartilage layer that was well integrated with the bone substrate. Of note, our use of DCB as the bone layer scaffold is similar to the successful use of Col-HA scaffolds in earlier investigations. Also, we optimized the approach to scaffold-free cartilage formation on an anatomical scale from hMSC by fusion of numerous CMBs (Fig. 5).

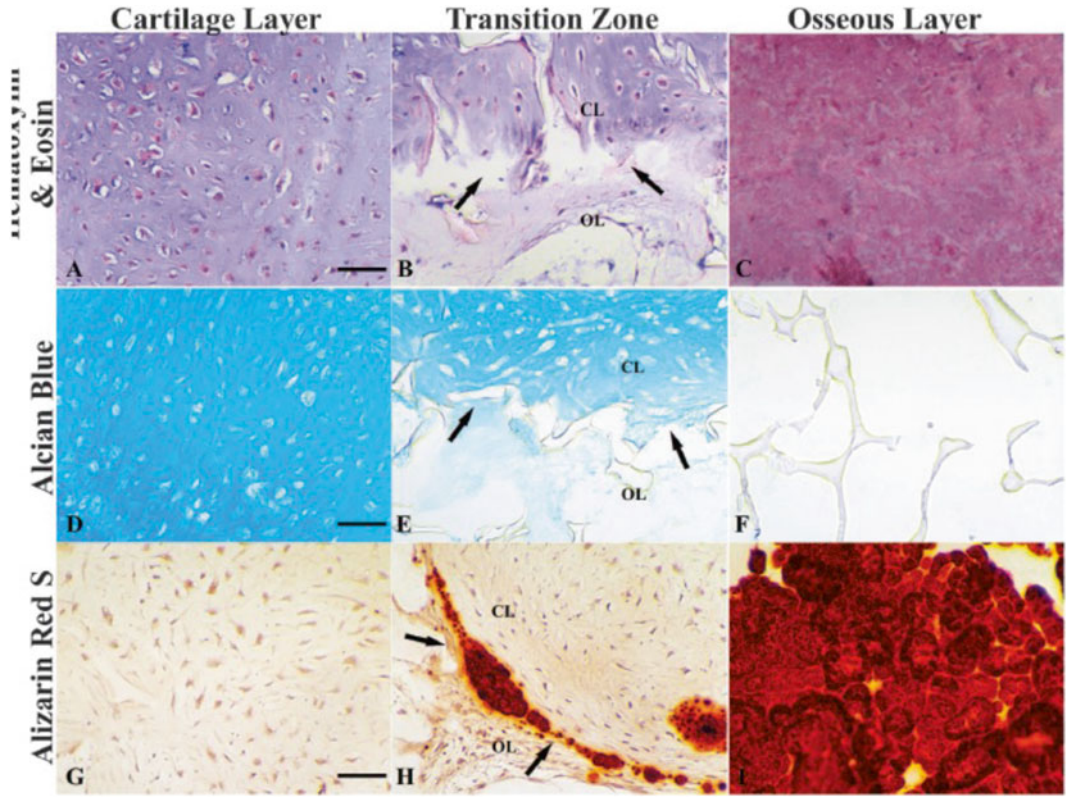

Fig. 5 Osteochondral composites obtained by combining pre-grown cartilage and bone. The panel shows osteochondral constructs cultured for 10 weeks following the assembly of cartilage and bone regions. (**a**–**c**) H&E for the cells and matrix of the cartilage layer (**a**), sharply demarcated transition zone (**b**, *arrows*), and an osseous layer (**c**); (**d**–**f**) Alcian Blue for proteoglycan that is strongly positive in the cartilage layer (**d**), diminishingly positive in the transition zone (**e**, *arrows*), and negative in the osseous layer (**f**); (**g**–**i**) alizarin red staining, for mineralization that was negative in the cartilage layer (**g**), and strongly positive in the transition zone (**h**, *arrows*) and the osseous layer (**i**). *CL* cartilage layer, *OL* osseous layer. Scale bars: 80 μm. Reproduced with permission from Tuli et al. [78]

In our study, we did not observe the formation of calcified cartilage and our bone layer consisted of native bone matrix permeated with cells from the cartilage layer without osteogenic induction. Tuli et al. showed the concomitant formation of a bone layer by separately seeding the bone scaffold with osteogenically induced MSC. Studies by Kandel et al. and Allan et al. observed deep zone hypertrophy and the formation of a calcified layer at the cartilage–bone interface when scaffold-free chondrocytes were cultured on a ceramic scaffold in the presence of a phosphate source (β-GP). Interestingly, Khanarian et al. recently reported enhanced mineralization and matrix deposition by hypertrophic chondrocytes in a hydrogel-ceramic composite containing micro-HA particles that recapitulated the aggregate size and content of the native mineral [79].

Taken together, these studies show that a suitable biomimetic approach to engineering osteochondral composites from hMSC could involve a scaffold-free formation of the cartilage layer by high-density culture of hMSC atop an osteoinductive scaffold seeded with osteogenically induced hMSC. Further, formation of a calcified layer at the interface could be enhanced with a soluble phosphate source and the incorporation of ceramic at the interface as well as in the osteoinductive scaffold.

8 Future Directions

The use of MSC in osteochondral tissue engineering is a highly attractive proposition, as autologous MSCs are easily accessible and readily form bone and cartilage. For the purpose of personalized regenerative medicine, it is evident that cartilage and bone grafts as well as their composites can be entirely derived from MSC taken from each subject, with the application of tissue engineering methods that are inspired by cartilage and bone development. As highlighted above, the pursuit of engineering bone, cartilage, and osteochondral composites from MSC have taken interesting directions, and the progress made is gratifying. Still, there are numerous problems that need to be addressed, as investigators search for biologically inspired regenerative approaches.

For MSC-based bone tissue engineering, concerns remain about the long-term viability of grafts following implantation. It is believed that after implantation, cells in the interior will die before the host vasculature can penetrate the graft, triggering necrosis and graft failure. To address this issue, investigators are using two complementary approaches: promoting pre-vascularization of bioengineered grafts and directing maturation of MSC to recapitulate endochondral ossification. Pre-vascularization of the bone graft is expected to facilitate rapid vascularization following implantation.

Current initiatives are pursuing smart scaffold designs to provide structural pathways and growth factors for connecting the graft to the host vasculature [36, 37], and co-cultures of MSC/MSC-derived osteoblasts with vascular cells [38, 39].

Another fascinating direction emerged from the studies of Mueller et al. and Scotti et al. who developed media for differentiating MSCs toward hypertrophic chondrocytes [42, 80]. Triggering chondrogenic maturation resulted in the formation of bone and bone marrow in vivo, by replicating the endochondral ossification pathway utilized in bone development and long bone fracture repair [42, 43]. Hypertrophic chondrocytes are essential in endochondral ossification as they trigger transition from the soft callus to preliminary bone by provoking vascular invasion and deposition of the initial bone template [44]. Hypertrophic chondrocytes are an attractive tissue engineering tool due to their survival in the hypoxic environment of cartilage, thereby withstanding the time delay necessary for the vascular development they help orchestrate [42]. Tissue-engineered bone grafts are on the verge of clinical translation, and the relentless progression of the field will hopefully produce the most clinically appropriate grafts for treating numerous patients requiring bone grafts. The rapid advancement in bone tissue engineering is likely to convert this exciting bone technology into routine practice.

Similarly, MSC-based cartilage tissue engineering has its unique problems, even though the functional properties of in vitro grown cartilage are increasingly approaching the functional properties of native cartilage. Of note, hMSC-derived cartilage is prone to hypertrophy and mineralization not seen with chondrocyte-based cartilage. Recent investigations have shown that hypertrophy correlates with the tendency to mineralize ectopically in vivo and that cartilage formed by MSC was unstable and could spontaneously mineralize in long-term in vitro cultures [80–83].

Interestingly, the mineralization of cartilage formed by MSC is usually localized, which suggests that MSC could have different chondrogenic fates. Whether the organization and differentiation fate of MSC can be controlled during in vitro cartilage formation is still very much a work in progress. Still, some recent studies have shed light on how we might be able to better control chondrogenic differentiation of hMSC. With the availability of compound libraries and high-throughput screening technology, potent small molecules for chondrogenic differentiation of hMSC are being discovered. Recent studies have shown that these small molecules can enhance the in vitro and in vivo cartilage formation by association with a key transcription factor, RUNX1 [84, 85].

The role of oxygen tension during in vitro chondrogenesis has also been clarified as investigators have shown that sustained hypoxia promoted the formation of cartilage by hMSC with

denser ECM and this construct is less prone to mineralize [86]. Further, the requirements of cartilage homeostasis have also been elucidated as investigators have shown, using in vivo models, that the depletion of either superficial zone progenitors or superficial zone proteins resulted in articular cartilage degradation [87, 88]. These studies have advanced our collective understanding of what drives cartilage formation, maturation, and homeostasis. For tissue engineers, the problem remains to specify cartilage formation effectively and accurately so that cartilage grown in vitro can be used to treat cartilage injuries and diseases as well as restore joint homeostasis.

Osteochondral composites have been proposed as an in vitro model for understanding the pathogenesis of degenerative joint diseases with cartilage and bone etiologies such as osteoarthritis. To recreate osteochondral composites from MSC, accurate spatiotemporal control of trophic factors is essential as the articular cartilage and the subchondral bone consist of different cell types in different microenvironments. We are now moving toward developing bioreactors for optimizing simultaneous chondrogenic and osteogenic differentiation of MSC within a biphasic osteochondral composite. Biophysical cues such as compressive loading and interstitial shear, which have been shown to benefit chondrogenic and osteogenic differentiation, should be made compatible with bioreactor designs [89–92].

Moving forward, the methods for engineering physiologically relevant bone, cartilage, and osteochondral composites from MSC need to be inspired by a keen understanding of the development, maturation, and homeostasis of native cartilage and bone. The interactions between multiple signaling pathways and multiple cell types governing joint morphogenesis and endochondral ossification are just a few aspects of the complexities that are the focus of current undertakings by biologists and clinicians [63, 93–96]. These investigations should provide critical insights into strategies for engineering osteochondral grafts from MSC, and aid development of models for studying osteochondral development and disease.

Acknowledgments

This work was funded by the NIH (grants DE016525, EB002520, and AR061988 to G.V.N.), the A*STAR Graduate Academy in Singapore (graduate fellowship to J.N.), the NSF (graduate fellowship to J.B.), the Whitaker Foundation (fellowship to J.B.), and the Columbia University (Presidential Fellowship to J.B.).

References

1. Inpatient Surgery: National Center for Health Statistics (2013) http://www.cdc.gov/nchs/fastats/inpatient-surgery.htm. Accessed 20 Nov 2014
2. Orthopedic Instrumentation BioMed Trends (2010) http://www.biomedtrends.com/GetDetails.asp?CatName=Orthopedics
3. Minzlaff P, Feucht MJ, Saier T et al (2014) Can young and active patients participate in sports after osteochondral autologous transfer combined with valgus high tibial osteotomy? Knee Surg Sports Traumatol Arthrosc [Epub ahead of print]
4. Hayes JS, Richards RG (2010) The use of titanium and stainless steel in fracture fixation. Expert Rev Med Devices 7:843–853
5. Barone DTJ, Raquez JM, Dubois P (2011) Bone-guided regeneration: from inert biomaterials to bioactive polymer (nano) composites. Polym Adv Technol 22:463–745
6. Hip Fracture: Cleveland Clinic (2014) https://my.clevelandclinic.org/services/orthopaedics-rheumatology/diseases-conditions/hip-fracture. Accessed 20 Nov 2014
7. Giannoudis PV, Dinopoulos H, Tsiridis E (2005) Bone substitutes: an update. Injury 36:20–27
8. Calori GM, Mazza E, Colombo M et al (2011) The use of bone-graft substitutes in large bone defects: any specific needs? Injury 42:S56–S63
9. Salgado AJ, Coutinho OP, Reis RL (2004) Bone tissue engineering: state of the art and future trends. Macromol Biosci 4:743–765
10. Langer R, Vacanti JP (1993) Tissue engineering. Science 260:920–926
11. Hutmacher DW (2000) Scaffolds in tissue engineering bone and cartilage. Biomaterials 21:2529–2543
12. Griffith LG, Naughton G (2002) Tissue engineering – current challenges and expanding opportunities. Science 295:1009–1014
13. Hansmann J, Groeber F, Kahlig A et al (2013) Bioreactors in tissue engineering – principles, applications and commercial constraints. Biotechnol J 8:298–307
14. Martin I, Wendt D, Heberer M (2004) The role of bioreactors in tissue engineering. Trends Biotechnol 22:80–86
15. Vunjak-Novakovic G, Tandon N, Godier A et al (2010) Challenges in cardiac tissue engineering. Tissue Eng Part B Rev 16:169–187
16. Hutmacher DW, Schantz T, Zein I et al (2001) Mechanical properties and cell cultural response of polycaprolactone scaffolds designed and fabricated via fused deposition modeling. J Biomed Mater Res 55:203–216
17. Wang YZ, Blasioli DJ, Kim HJ et al (2006) Cartilage tissue engineering with silk scaffolds and human articular chondrocytes. Biomaterials 27:4434–4442
18. Mauck RL, Nicoll SB, Seyhan SL et al (2003) Synergistic action of growth factors and dynamic loading for articular cartilage tissue engineering. Tissue Eng 9:597–611
19. Mauck RL, Yuan X, Tuan RS (2006) Chondrogenic differentiation and functional maturation of bovine mesenchymal stem cells in long-term agarose culture. Osteoarthritis Cartilage 14:179–189
20. Pittenger MF, Mackay AM, Beck SC et al (1999) Multilineage potential of adult human mesenchymal stem cells. Science 284:143–147
21. Zuk PA, Zhu M, Mizuno H et al (2001) Multilineage cells from human adipose tissue: implications for cell-based therapies. Tissue Eng 7:211–228
22. Seo BM, Miura M, Gronthos S et al (2004) Investigation of multipotent postnatal stem cells from human periodontal ligament. Lancet 364:149–155
23. Yoshimura H, Muneta T, Nimura A et al (2007) Comparison of rat mesenchymal stem cells derived from bone marrow, synovium, periosteum, adipose tissue, and muscle. Cell Tissue Res 327:449–462
24. in't Anker PS, Scherjon SA, Kleijburg-van der Keur C et al (2004) Isolation of mesenchymal stem cells of fetal or maternal origin from human placenta. Stem Cells 22:1338–1445
25. Erices A, Conget P, Minguell JJ (2000) Mesenchymal progenitor cells in human umbilical cord blood. Br J Haematol 109:235–242
26. Caplan AI (1991) Mesenchymal stem-cells. J Orthop Res 9:641–650
27. Crisan M, Yap S, Casteilla L et al (2008) A perivascular origin for mesenchymal stem cells in multiple human organs. Cell Stem Cell 3:301–313
28. Mauney JR, Volloch V, Kaplan DL (2005) Role of adult mesenchymal stem cells in bone tissue-engineering applications: current status and future prospects. Tissue Eng 11:787–802
29. Engler AJ, Sen S, Sweeney HL et al (2006) Matrix elasticity directs stem cell lineage specification. Cell 126:677–689
30. Kreke MR, Huckle WR, Goldstein AS (2005) Fluid flow stimulates expression of osteopontin

and bone sialoprotein by bone marrow stromal cells in a temporally dependent manner. Bone 36:1047–1055

31. Bhumiratana S, Grayson WL, Castaneda A et al (2011) Nucleation and growth of mineralized bone matrix on silk-hydroxyapatite composite scaffolds. Biomaterials 32:2812–2820
32. Cui L, Liu B, Liu G et al (2007) Repair of cranial bone defects with adipose derived stem cells and coral scaffold in a canine model. Biomaterials 28:5477–5486
33. Jukes JM, Both SK, Leusink A et al (2008) Endochondral bone tissue engineering using embryonic stem cells. Proc Natl Acad Sci U S A 105:6840–6845
34. Liu HH, Peng HJ, Wu Y et al (2013) The promotion of bone regeneration by nanofibrous hydroxyapatite/chitosan scaffolds by effects on integrin-BMP/Smad signaling pathway in BMSCs. Biomaterials 34:4404–4417
35. Yuan J, Cui L, Zhang WJ et al (2007) Repair of canine mandibular bone defects with bone marrow stromal cells and porous beta-tricalcium phosphate. Biomaterials 28:1005–1013
36. Kneser U, Polykandriotis E, Ohnolz J et al (2006) Engineering of vascularized transplantable bone tissues: induction of axial vascularization in an osteoconductive matrix using an arteriovenous loop. Tissue Eng 12: 1721–1731
37. Santos MI, Reis RL (2010) Vascularization in bone tissue engineering: physiology, current strategies, major hurdles and future challenges. Macromol Biosci 10:12–27
38. Tsigkou O, Pomerantseva I, Spencer JA et al (2010) Engineered vascularized bone grafts. Proc Natl Acad Sci U S A 107:3311–3316
39. Wang L, Fan HB, Zhang ZY et al (2010) Osteogenesis and angiogenesis of tissue-engineered bone constructed by prevascularized beta-tricalcium phosphate scaffold and mesenchymal stem cells. Biomaterials 31: 9452–9461
40. Correia C, Grayson WL, Park M et al (2011) In vitro model of vascularized bone: synergizing vascular development and osteogenesis. PLoS One 6:9
41. Mueller MB, Tuan RS (2008) Functional characterization of hypertrophy in chondrogenesis of human mesenchymal stem cells. Arthritis Rheum 58:1377–1388
42. Scotti C, Tonnarelli B, Papadimitropoulos A et al (2010) Recapitulation of endochondral bone formation using human adult mesenchymal stem cells as a paradigm for developmental engineering. Proc Natl Acad Sci U S A 107: 7251–7256
43. Scotti C, Piccinini E, Takizawa H et al (2013) Engineering of a functional bone organ through endochondral ossification. Proc Natl Acad Sci U S A 110:3997–4002
44. Olsen BR, Reginato AM, Wang WF (2000) Bone development. Annu Rev Cell Dev Biol 16:191–220
45. Cartmell SH, Porter BD, Garcia AJ et al (2003) Effects of medium perfusion rate on cell-seeded three-dimensional bone constructs in vitro. Tissue Eng 9:1197–1203
46. Grayson WL, Bhumiratana S, Cannizzaro C et al (2008) Effects of initial seeding density and fluid perfusion rate on formation of tissue-engineered bone. Tissue Eng Part A 14: 1809–1820
47. Sikavitsas VI, Bancroft GN, Holtorf HL et al (2003) Mineralized matrix deposition by marrow stromal osteoblasts in 3D perfusion culture increases with increasing fluid shear forces. Proc Natl Acad Sci U S A 100:14683–14688
48. Grayson WL, Frohlich M, Yeager K et al (2010) Engineering anatomically shaped human bone grafts. Proc Natl Acad Sci U S A 107: 3299–3304
49. Freed LE, Marquis JC, Nohria A et al (1993) Neocartilage formation in vitro and in vivo using cells cultured on synthetic biodegradable polymers. J Biomed Mater Res 27:11–23
50. Vunjak-Novakovic G, Martin I, Obradovic B et al (1999) Bioreactor cultivation conditions modulate the composition and mechanical properties of tissue-engineered cartilage. J Orthop Res 17:130–1308
51. Benya PD, Shaffer JD (1982) Dedifferentiated chondrocytes reexpress the differentiated collagen phenotype when cultured in agarose gels. Cell 30:215–224
52. Mauck RL, Soltz MA, Wang CCB et al (2000) Functional tissue engineering of articular cartilage through dynamic loading of chondrocyte-seeded agarose gels. J Biomech Eng 122: 252–260
53. Huang AH, Stein A, Tuan RS et al (2009) Transient exposure to transforming growth factor beta 3 improves the mechanical properties of mesenchymal stem cell-laden cartilage constructs in a density-dependent manner. Tissue Eng Part A 15:3461–3472
54. Sampat SR, Dermksian MV, Oungoulian SR et al (2013) Applied osmotic loading for promoting development of engineered cartilage. J Biomech 46:2674–2681
55. O'Connell GD, Nims RJ, Green J et al (2014) Time and dose-dependent effects of chondroitinase ABC on growth of engineered cartilage. Eur Cell Mater 27:312–320

56. Suh JKF, Matthew HWT (2000) Application of chitosan-based polysaccharide biomaterials in cartilage tissue engineering: a review. Biomaterials 21:2589–2598
57. Varghese S, Hwang NS, Canver AC et al (2008) Chondroitin sulfate based niches for chondrogenic differentiation of mesenchymal stem cells. Matrix Biol 27:12–21
58. Kim IL, Mauck RL, Burdick JA (2011) Hydrogel design for cartilage tissue engineering: a case study with hyaluronic acid. Biomaterials 32:8771–8782
59. Moutos FT, Freed LE, Guilak F (2007) A biomimetic three-dimensional woven composite scaffold for functional tissue engineering of cartilage. Nat Mater 6:162–167
60. Bian L, Guvendiren M, Mauck RL et al (2013) Hydrogels that mimic developmentally relevant matrix and N-cadherin interactions enhance MSC chondrogenesis. Proc Natl Acad Sci U S A 110:10117–10122
61. Brunger JM, Huynh NPT, Guenther CM et al (2014) Scaffold-mediated lentiviral transduction for functional tissue engineering of cartilage. Proc Natl Acad Sci U S A 111: E798–E806
62. Ratana S, Eton RE, Oungoulian SR et al (2014) Large, stratified, and mechanically functional human cartilage grown in vitro by mesenchymal condensation. Proc Natl Acad Sci U S A 111:6940–6945
63. Pacifici M, Koyama E, Shibukawa Y et al (2006) Cellular and molecular mechanisms of synovial joint and articular cartilage formation. In: Zaidi M (ed) Skeletal development and remodeling in health, disease, and aging. Ann N Y Acad Sci 1068:74–86
64. Johnstone B, Hering TM, Caplan AI et al (1998) In vitro chondrogenesis of bone marrow-derived mesenchymal progenitor cells. Exp Cell Res 238:265–272
65. Sekiya I, Vuoristo JT, Larson BL et al (2002) In vitro cartilage formation by human adult stem cells from bone marrow stroma defines the sequence of cellular and molecular events during chondrogenesis. Proc Natl Acad Sci U S A 99:4397–4402
66. Elder SH, Cooley AJ Jr, Borazjani A et al (2009) Production of hyaline-like cartilage by bone marrow mesenchymal stem cells in a self-assembly model. Tissue Eng Part A 15:3025–3036
67. Kandel RA, Boyle J, Gibson G et al (1997) In vitro formation of mineralized cartilagenous tissue by articular chondrocytes. In Vitro Cell Dev Biol Anim 33:174–181
68. Lee WD, Hurtig MB, Kandel RA et al (2011) Membrane culture of bone marrow stromal cells yields better tissue than pellet culture for engineering cartilage-bone substitute biphasic constructs in a two-step process. Tissue Eng Part C Methods 17:939–948
69. Murdoch AD, Grady LM, Ablett MP et al (2007) Chondrogenic differentiation of human bone marrow stem cells in transwell cultures: generation of Scaffold-free cartilage. Stem Cells 25:2786–2796
70. Ofek G, Revell CM, Hu JC et al (2008) Matrix development in self-assembly of articular cartilage. PLoS One 3, e2795
71. Yu HS, Grynpas M, Kandel RA (1997) Composition of cartilagenous tissue with mineralized and non-mineralized zones formed in vitro. Biomaterials 18:1425–1431
72. Martin I, Miot S, Barbero A et al (2007) Osteochondral tissue engineering. J Biomech 40:750–765
73. Nooeaid P, Salih V, Beier JP et al (2012) Osteochondral tissue engineering: scaffolds, stem cells and applications. J Cell Mol Med 16:2247–2270
74. Schaefer D, Martin I, Jundt G et al (2002) Tissue-engineered composites for the repair of large osteochondral defects. Arthritis Rheum 46:2524–2534
75. Wang YZ, Kim UJ, Blasioli DJ et al (2005) In vitro cartilage tissue engineering with 3D porous aqueous-derived silk scaffolds and mesenchymal stem cells. Biomaterials 26:7082–7094
76. Allan KS, Pilliar RM, Wang J et al (2007) Formation of biphasic constructs containing cartilage with a calcified zone interface. Tissue Eng 13:167–177
77. Kandel RA, Grynpas M, Pilliar R et al (2006) Repair of osteochondral defects with biphasic cartilage-calcium polyphosphate constructs in a Sheep model. Biomaterials 27:4120–4131
78. Tuli R, Nandi S, Li WJ et al (2004) Human mesenchymal progenitor cell-based tissue engineering of a single-unit osteochondral construct. Tissue Eng 10:1169–1179
79. Khanarian NT, Haney NM, Burga RA et al (2012) A functional agarose-hydroxyapatite scaffold for osteochondral interface regeneration. Biomaterials 33:5247–5258
80. Mueller MB, Fischer M, Zellner J et al (2010) Hypertrophy in mesenchymal stem cell chondrogenesis: effect of TGF-beta isoforms and chondrogenic conditioning. Cells Tissues Organs 192:158–166
81. Dickhut A, Pelttari K, Janicki P et al (2009) Calcification or dedifferentiation: requirement to lock mesenchymal stem cells in a desired differentiation stage. J Cell Physiol 219:219–226

82. Farrell MJ, Fisher MB, Huang AH et al (2014) Functional properties of bone marrow-derived MSC-based engineered cartilage are unstable with very long-term in vitro culture. J Biomech 47:2173–2182
83. Pelttari K, Winter A, Steck E et al (2006) Premature induction of hypertrophy during in vitro chondrogenesis of human mesenchymal stem cells correlates with calcification and vascular invasion after ectopic transplantation in SCID mice. Arthritis Rheum 54:3254–3266
84. Johnson K, Zhu S, Tremblay MS et al (2012) A stem cell-based approach to cartilage repair. Science 336:717–721
85. Yano F, Hojo H, Ohba S et al (2013) A novel disease-modifying osteoarthritis drug candidate targeting Runx1. Ann Rheum Dis 72:748–753
86. Leijten J, Georgi N, Teixeira LM et al (2014) Metabolic programming of mesenchymal stromal cells by oxygen tension directs chondrogenic cell fate. Proc Natl Acad Sci U S A 111:13954–13959
87. Ruan MZ, Erez A, Guse K et al (2013) Proteoglycan 4 expression protects against the development of osteoarthritis. Sci Transl Med 5:17634
88. Taniguchi N, Carames B, Kawakami Y et al (2009) Chromatin protein HMGB2 regulates articular cartilage surface maintenance via beta-catenin pathway. Proc Natl Acad Sci U S A 106:16817–16822
89. Alexander PG, Gottardi R, Lin H et al (2014) Three-dimensional osteogenic and chondrogenic systems to model osteochondral physiology and degenerative joint diseases. Exp Biol Med 239:1080–1095
90. Grayson WL, Bhumiratana S, Chao PHG et al (2010) Spatial regulation of human mesenchymal stem cell differentiation in engineered osteochondral constructs: effects of pre-differentiation, soluble factors and medium perfusion. Osteoarthritis Cartilage 18:714–723
91. Liu XG, Jiang HK (2013) Preparation of an osteochondral composite with mesenchymal stem cells as the single-cell source in a double-chamber bioreactor. Biotechnol Lett 35:1645–1653
92. Vunjak-Novakovic G, Meinel L, Altman G et al (2005) Bioreactor cultivation of osteochondral grafts. Orthod Craniofac Res 8:209–218
93. Goldring MB, Tsuchimochi K, Ijiri K (2006) The control of chondrogenesis. J Cell Biochem 97:33–44
94. Kusumbe AP, Ramasamy SK, Adams RH (2014) Coupling of angiogenesis and osteogenesis by a specific vessel subtype in bone. Nature 507:323–328
95. Xie H, Cui Z, Wang L et al (2014) PDGF-BB secreted by preosteoclasts induces angiogenesis during coupling with osteogenesis. Nat Med 20:1270–1278
96. Zaidi M (2007) Skeletal remodeling in health and disease. Nat Med 13:791–801

Chapter 4

Mesenchymal Stem Cells in Cardiology

Ian A. White, Cristina Sanina, Wayne Balkan, and Joshua M. Hare

Abstract

Cardiovascular disease (CVD) accounts for more deaths globally than any other single disease. There are on average 1.5 million episodes of myocardial infarction (heart attack) each year in the United States alone with roughly one-third resulting in death. There is therefore a major need for developing new and effective strategies to promote cardiac repair. Intramyocardial transplantation of mesenchymal stem cells (MSCs) has emerged as a leading contender in the pursuit of clinical intervention and therapy. MSCs are potent mediators of cardiac repair and are therefore an attractive tool in the development of preclinical and clinical trials. MSCs are capable of secreting a large array of soluble factors, which have had demonstrated effects on pathogenic cardiac remolding, fibrosis, immune activation, and cardiac stem cell proliferation within the damaged heart. MSCs are also capable of differentiation into cardiomyocytes, endothelial cells, and vascular smooth muscle cells, although the relative contribution of trilineage differentiation and paracrine effectors on cardiac repair remains the subject of active investigation.

Key words Mesenchymal stem cell, Cardiology, Myocardial infarction, Clinical trial, Cardiovascular disease

1 Introduction

While our knowledge of the developmental origin of MSCs is still relatively limited, it is widely believed that MSCs are derived from mesoderm, one of the three germ layers that form at gastrulation during the development of the mammalian embryo [1]. It is from this mesodermal layer that cells destined to form the myocardium of the heart are also derived [2]. During heart tube formation, promyocardial cells migrate from the lateral plate mesoderm to populate the primordium of the left ventricle and sinus venosus. The outflow tract and right ventricle are then simultaneously populated with cells migrating from a second cardiogenic area located posterior to the dorsal wall of the pericardial cavity [3].

Within 3 weeks of gestation the human heart demonstrates the first signs of peristaltic contraction, while mesoderm-derived cells continue to migrate into the heart as it grows. This hyperplastic growth continues until birth at which point the organ has received

Massimiliano Gnecchi (ed.), *Mesenchymal Stem Cells: Methods and Protocols*, Methods in Molecular Biology, vol. 1416,
DOI 10.1007/978-1-4939-3584-0_4,

a full complement of cardiac cells [2, 3]. During the first few days following birth, cardiomyocytes undergo a final round of karyokinesis in the absence of cytokinesis resulting in binucleation and exit from the cell cycle [4, 5]. Postpartum organ growth to adulthood is then primarily the result of cardiomyocyte hypertrophy rather than cellular proliferation. For decades it was believed that this program made the heart a post-mitotic organ, unable to replenish lost cells once depleted [6]. However, during the 1990s several researchers began describing an ability of mature cardiomyocytes to re-enter into the cell cycle in vitro, although this process resulted in rapid apoptosis of the cells [7]. More recently some key studies have expanded on this observation, demonstrating sustained cytokinesis of postpartum mammalian cardiomyocytes in vivo. The first of these studies identified a transient ability of the murine neonatal heart to repair in response to partial resection of the left ventricular apex [8]. Within a finite developmental window, mature cardiomyocytes can undergo sarcomeric disassembly and re-enter mitosis with the resulting progeny contributing directly to recellularization of the injury site. The second study demonstrated an ability of human cardiac tissue to replace between 0.45 and 1 % of cells per year throughout the human lifespan [9], based on abrupt changes in the cellular incorporation of the radioisotope ^{14}C of humans exposed following the Limited Nuclear Test Ban Treaty of 1963. Together these observations have led to a revolution in the perception of cardiovascular disease, dispelling concerns that repair of the mammalian heart was not feasible and giving hope to interventional strategies geared toward promoting endogenous repair mechanisms.

2 Cardiovascular Disease

Cardiovascular disease (CVD) continues to account for more deaths globally than any other single disease. The most recent data show that Americans suffer an average of 1.5 million episodes of acute myocardial infarction (AMI) each year with roughly one-third resulting in death [10]. This rate translates to about one heart attack every 30 seconds and one cardiac-related death every 1.5 minute within the United States alone. Morbidity associated with post-infarction cardiomyopathy is also a significant problem and accounts for approximately 6 million hospital visits per year, thereby contributing significantly to annual healthcare costs.

AMI is the result of blockage to one or more of the main coronary arteries. Upon occlusion, a region of permanent injury containing dead and dying cells, known as an infarct, develops. Blood supply is interrupted within the developing infarct and the area rapidly becomes hypoxic [11]. Cardiomyocytes are comparatively resistant to chronic hypoxia at neutral pH. However, when the

extracellular pH drops below 6.5 cardiomyocytes undergo extensive hypoxia-induced death. Hypoxia in cardiomyocytes causes a switch from oxidative to glycolytic energy generation, resulting in increased glucose consumption, lactic acid production, and lower intracellular pH. Increased plasma lactate levels reflect this metabolic shift and are diagnostic of infarction in ischemic heart disease [12]. Chronic hypoxia in the presence of high glucose leads to progressive acidosis of cardiac myocytes. The resulting hypoxia-acidosis leads to apoptosis of cardiac cells within the infarct zone followed by vascular collapse and extensive tissue necrosis [12, 13]. A typical human infarct can result in the loss of over 1 billion cardiomyocytes [14], the tissue being replaced by the formation of a permanent, avascular collagenous scar, that averts an otherwise inevitable ventricular rupture. This process of cardiac remolding, while rapid in onset, can take several weeks to complete. When completed, these changes lead to significant reduction in cardiac function and ultimately to heart failure and death. While examples exist in nature that demonstrate an innate regenerative ability of cardiovascular tissue following injury [15, 16], this capability has been largely lost in mammalians, possibly as a consequence of increased body mass and greater systemic blood pressure.

Studying large and small animal models of AMI have led to the development of strategies to improve the reparative response of mammalian cardiac tissue. In this regard recent focus has been directed at engaging endogenous repair mechanisms through various interventions including the use of exogenous stem cell transplantation. The rationale for this approach is that the proliferative and multilineage differentiation capacity of stem cells conveys latent potential for organ regeneration through the formation of new tissue and also through the initiation of neovascularization. Pluripotent stem cells, such as embryonic stem cells (ESCs) and induced pluripotent stem cells (iPSCs), were early candidates for regenerative therapy as they retain the most potential for multilineage differentiation and proliferation. However, as a therapeutic cell for cardiac regeneration they are fraught with biological (and in the case of ESCs, ethical) issues, including risk of teratoma formation [17] and have therefore proved to be of little direct use.

The limited differentiation capacity of adult stem cells suggested a more refined approach and in 2003 the first phase I clinical trial using adult skeletal myoblast stem cells was carried out [18]. After initial optimism triggered by cell engraftment and enhancements in left ventricular function, the effects were found not only to be unsustainable, but also to lead to arrhythmias due to a lack of electrical coupling with host cardiomyocytes [19]. However, with the discovery of cardiac stem cells (CSCs) [20] came an exciting opportunity to improve engraftment and enhance functional integration. The recent SCIPIO trial [21] established CSCs as an effective therapeutic cell demonstrating cardiac engraftment,

enhancement of coronary vasculature, and a contemporaneous reduction in scar volume. These initial results are promising, and efforts aimed at increasing cell numbers obtained from tissue biopsies are currently moving forward. In the interim a variety of other adult cell types have been examined in preclinical and clinical trials. Some of the most consistently successful results for the induction of cardiac repair have been seen with the use of MSCs, which have been isolated from bone marrow and adipose tissue, expanded in culture and used successfully in preclinical and clinical trials (*see* Table 1 for list of clinical trials).

3 Mesenchymal Stem Cells

The term "Mesenchymal Stem Cells" (MSCs) was coined by Arnold Caplan in the early 1990s [22, 23], although the cells were first described in the 1970s by Alexander Friedenstein as a population of bone marrow stromal cells capable of mesodermal differentiation and trophic support of hematopoiesis [24, 25]. Since their discovery, there have been over 20,000 publications on the subject of MSC biology and their clinical applications. However, despite this attention a consensus has yet to be reached regarding the exact identity of these cells. In an attempt to standardize the field, the Mesenchymal and Tissue Stem Cell Committee of the International Society for Cellular Therapy (ISCT) set minimal criteria in 2001 for defining MSCs. The primary feature set forth by the committee, as definitively representative of MSCs, is an adherence to plastic substrate together with a capacity for multilineage differentiation toward osteo-, adipo-, and chondrocytic lineages. The committee also recommended that MSCs should express cluster of differentiation (CD) markers: CD90, CD105, CD44, CD106, CD166, CD73, and CD29 while not expressing CD45, CD34, CD14, CD11b, CD19, CD31, and HLA-DR [26]. While broadly accepted, labs have not universally adopted these criteria. Indeed, the designation Mesenchymal Stem Cell and Multipotent Stromal Cell in reference to MSCs is routinely and interchangeably used. This lack of consensus has made navigating the MSC literature and following the development of MSC biology more of a challenge.

MSCs have been isolated from several different species and from nearly every tissue type, suggesting that MSCs likely reside in all postnatal organs [22, 27, 28]. The cells reside within organs in a perivascular distribution where they contribute to niche maintenance and tissue homeostasis [29–31]. MSCs typically do not mobilize to the peripheral blood and constitute only around 1 in 10^8 of the total peripheral mononuclear cell population [32, 33]. Therefore, to obtain sufficient numbers for transplantation it is necessary to isolate MSCs from a tissue or organ and expand them in vitro, using specific protocols [34–39].

Table 1
Clinical trials with mesenchymal stem cells (http://clinicaltrials.gov)

Study	Year/country	Study ID	Phase	Cell type	Delivery method	No. treated	Primary outcome
Prospective randomized study of mesenchymal stem cell therapy in patients undergoing cardiac surgery (PROMETHEUS)	2007–2011/USA	NCT00587990	1–2	Autologous	Intraoperative intramyocardial	45	Safety/efficacy study
Intracoronary autologous mesenchymal stem cells implantation in patients with ischemic dilated cardiomyopathy	2012–Pres./Malaysia	NCT01720888	2	Autologous	Intracoronary	80	Efficacy study
Left ventricular assist device combined with allogeneic mesenchymal stem cells implantation in patients with end-stage heart failure	2012–Pres./Greece	NCT01759212	2–3	Allogeneic	Intraoperative intramyocardial	5	Efficacy study
Allogeneic stem cells implantation combined with coronary bypass grafting in patients with ischemic cardiomyopathy	2012–Pres./Greece	NCT01753440	2–3	Allogeneic	Intraoperative intramyocardial	30	Efficacy study
A phase IIa, single-blind, placebo-controlled, crossover, multicenter, randomized study to assess the safety, tolerability, and preliminary efficacy of a single intravenous dose of ischemia-tolerant allogeneic mesenchymal bone marrow cells to subjects with heart failure of non-ischemic etiology	2012–Pres./USA	NCT02123706	2a	Allogeneic	Intravenous	20	Safety/efficacy study
The percutaneous stem cell injection delivery effects on neomyogenesis pilot study (The POSEIDON-Pilot Study)	2010–2013/USA	NCT01087996	1–2	Allogeneic/ autologous	Transendocardial injection	30	Safety/efficacy study
A phase 1 randomized, double-blind, placebo-controlled, dose escalation, multicenter study to determine the safety of intravenous ex-vivo cultured adult human mesenchymal stem cells (Provacel) following acute myocardial infarction	2005–2009/USA	NCT00114452	1	Allogeneic	Intravenous	53	Safety study

(continued)

Table 1
(continued)

Study	Year/country	Study ID	Phase	Cell type	Delivery method	No. treated	Primary outcome
Randomized clinical trial of intravenous infusion umbilical cord mesenchymal stem cells on cardiopathy (RIMECARD)/dilated cardiomyopathy	2012–Pres./Chile	NCT01739777	1	Allogeneic	Intravenous	30	Safety/efficacy study
Safety and efficacy of intracoronary adult human mesenchymal stem cells after acute myocardial infarction (SEED-MSC)	2007–2010/Korea	NCT01392105	2	Autologous	Intracoronary	80	Safety/efficacy study
"ESTIMATION Study" for endocardial mesenchymal stem cells implantation in patients after acute myocardial infarction	2011–Pres./Russia	NCT01394432	3	Autologous	Transendocardial injection	50	Efficacy study
Umbilical cord-derived mesenchymal stem cells therapy in ischemic cardiomyopathy	2013–2014/China	NCT01946048	1	Allogeneic	Intraoperative intramyocardial	10	Safety/efficacy study
Mesenchymal stem cells and myocardial ischemia (MESAMI)	2010–2014/France	NCT01076920	1, 2	Autologous	Transendocardial injection	10	Safety/efficacy study
Transendocardial autologous cells (hMSC or hBMC) in ischemic heart failure trial (TAC-HFT)	2008–2012/USA	NCT00768066	1, 2	Autologous	Transendocardial injection	67	Safety/efficacy study
TRansendocardial stem cell injection delivery effects on neomyogenesis study (the TRIDENT study)	2013–Pres./USA	NCT02013674	2	Allogeneic	Transendocardial injection	45	Safety/efficacy study
PercutaneOus StEm Cell Injection Delivery Effects On Neomyogenesis in Dilated CardioMyopathy (The POSEIDON-DCM Study)	2011–Pres./USA	NCT01392625	1, 2	Autologous/ allogeneic	Transendocardial injection	36	Safety/efficacy study
Mesenchymal stem cells to treat ischemic cardiomyopathy	2010–2013/Brazil	NCT01913886	1, 2	Autologous	Intracoronary	10	Safety/efficacy study
Combined CABG and stem cell transplantation for heart failure	2006–2010/Finland	NCT00418418	2	Autologous	Intraoperative intramyocardial	60	Efficacy study
A phase II, multicenter, randomized, double-blind, placebo-controlled study to evaluate the safety and efficacy of PROCHYMAL®	2009–2016/USA	NCT00877903	2	Allogeneic	Intravenous	220	Safety/efficacy study

Clinical trial of autologous adipose tissue-derived stromal cell therapy for ischemic heart failure	2012–2014/Japan	NCT01709279	1	Autologous	Intracoronary	6	Safety/efficacy study
Stem cell therapy for vasculogenesis in patients with severe myocardial ischemia	2005–2009/ Denmark	NCT00260338	1, 2	Autologous	Intraoperative intramyocardial	31	Safety/efficacy study
Phase II combination stem cell therapy for the treatment of severe coronary ischemia (CI) MESENDO	2008–2014/USA	NCT00790764	2	Autologous	Intracoronary	60	Safety/efficacy study
Autologous mesenchymal stromal cell therapy in heart failure	2008–2014/ Denmark	NCT00644410	1, 2	Autologous	Transendocardial injection (NOGA)	59	Safety/efficacy study
RELIEF (a randomized, open-labeled, multicenter trial for safety and efficacy of intracoronary adult human mesenchymal stEm Cells Acute Myocardial inFarction)	2013–Pres./ Republic of Korea	NCT01652209	3	Autologous	Intracoronary	135	Safety/efficacy study
Mesenchymal stem cells for idiopathic dilated cardiomyopathy	2013–2016/Spain	NCT01957826	1, 2	Autologous	Transendocardial injection	70	Safety/efficacy study
Stem cell injection to treat heart damage during open heart surgery	2012–2014/USA	NCT01557543	1	Autologous	Intraoperative intramyocardial	24	Safety study
Intracoronary human Wharton's Jelly-derived mesenchymal stem cells (WJ-MSCs) transfer in patients with acute myocardial infarction (AMI)	2011–2012/China	NCT01291329	2	Allogeneic	Intracoronary	160	Safety/efficacy study
Ex vivo cultured bone marrow-derived allogeneic MSCs in AMI	2009–2012/India	NCT00883727		Allogeneic	Intravenous	20	Safety/efficacy study
Intracoronary infusion of autologous bone marrow cells for treatment of idiopathic dilated cardiomyopathy	2008–2010/Spain	NCT00629096	2	Autologous	Intracoronary	27	Efficacy study
A study of allogeneic mesenchymal bone marrow cells in subjects with ST segment elevation myocardial infarction (STEMI)	2013–2017/USA	NCT01770613	2	Allogeneic	Intravenously	50	Safety/efficacy study

(continued)

Table 1
(continued)

Study	Year/country	Study ID	Phase	Cell type	Delivery method	No. treated	Primary outcome
Effect of intramyocardial injection of mesenchymal precursor cells on heart function in people receiving an LVAD	2009–2011/USA	NCT00927784	2	Allogeneic	Intraoperative intramyocardial	10	Safety/efficacy study
The purpose of this study is to evaluate the efficacy and safety of a allogeneic mesenchymal precursor cells (CEP-41750) for the treatment of chronic heart failure	2014–2018/USA	NCT02032004	3	Allogeneic	Transendocardial injection	1730	Safety/efficacy study
Safety study of allogeneic mesenchymal precursor cell infusion in myocardial infarction	2012–2014/New Zealand; Denmark; Belgium; Australia	NCT01781390	2	Allogeneic	Intracoronary	225	Safety/efficacy study

The fact that tissue isolation and culturing techniques appear to contribute to differences in cell characteristics, combined with their apparent ubiquitous distribution, highlights the potential heterogeneity within various MSC isolates. Consequently, several subpopulations of MSCs have been described, some of which are described below:

- Recycling Stem (RS) cells represent the smallest population, and most rapidly dividing in culture. These bone marrow-derived cells are considered the most primitive and exhibit a greater potential to differentiate into osteoblasts, adipocytes, and chondrocytes under standard conditions [40, 41].
- Multipotent Adult Progenitor Cells (MAPCs) are the only MSCs to display immortality in culture, and demonstrate a capacity to differentiate into cells of all three germ layers (endoderm, mesoderm, and ectoderm) [42, 43].
- Human Bone Marrow-derived Multipotent Stem Cells (hBMSCs) [44] also have the capacity to differentiate into cells of all three germ layers.
- Human Marrow-Isolated Adult Multilineage Inducible (MIAMI) cells, which in addition to being multi-potent, express numerous markers found among embryonic stem cells and pancreatic islet cells [45].
- Cardiac Stromal Cells (CStCs) are a novel MSC subpopulation arising from cardiac tissue [46]. Compared to BM-derived MSCs, these cells demonstrate an enhanced ability to express cardiovascular markers and differentiate into cardiomyocytes [46], while exhibiting a reduced ability to differentiate along the osteogenic and adipogenic lineages.
- Subpopulations of c-kit (CD117) positive MSCs. While not a defining characteristic, there is some evidence to suggest that these cells may constitute a more homogeneous group of primitive MSCs exhibiting greater capacity for endodermal differentiation and enhanced multilineage differentiation efficiency [40, 47, 48].

In summary, MSCs comprise a heterogeneous population of multipotent adult mesodermal progenitors. They possess several biological properties, such as a broad differentiation potential, low immunogenicity, an ability to modulate host immune responses, and to produce and secrete an array of factors that promote tissue remodeling. These features make them attractive candidates for cell-based therapies, and will be explored in detail below as they pertain to myocardial infarction as the primary cause of cardiovascular disease in humans.

4 Cardiac Immunobiology

Perhaps one of the most striking features of MSCs is their capacity for immune obscurity [49–51]. This property is (in part) due to the absence of Major Histocompatibility Complex (MHC) class II, CD40 ligand, and CD80/86 (B7 costimulatory molecules) expression [52–54], all of which are involved in allogeneic tissue rejection. MSCs also lack, or express at very low levels, MHC class I, which is typically used by natural killer cells (NK) and cytotoxic T cells (CTLs) to differentiate healthy "self" from unhealthy cells or "non-self." This lack of MHC-I shields MSCs from detection by allogeneic CTLs, but makes them conspicuous to activated NK cells, which exhibit cytolytic activity against both autologous and allogeneic MSCs [55, 56]. Despite the potency of immune modulation exerted by MSCs (or perhaps because of it) a mechanism seems to have evolved that systematically removes autologous MSCs over time whether infection or malignant transformation has occurred or not. Elimination is comparatively enhanced for allogeneic MSCs, the rate of which seems to be dictated by a balance between their relative expression of immunogenic and immunosuppressive factors [57, 58]. While some concerns regarding the relative immunogenicity of allogeneic MSCs might be obviated by using autologous MSCs, there are compelling reasons for developing an "off the shelf" modality for allogeneic MSCs. The low numbers of autologous MSCs that can be isolated from an individual necessitates ex-vivo expansion of cells leading to unavoidable delays between isolation and re-infusion. Moreover, the quantity and quality of MSCs dramatically diminish with age [59], and several genetic diseases preclude the use of autologous MSCs [60]. Furthermore, the effect ex vivo culture has upon the immunogenicity of autologous MSCs has yet to be determined experimentally.

One of the challenges facing the use of MSCs for cell therapies is that their immune evasion is hampered upon differentiation, when the cells upregulate MHC expression, thus compromising their covert status and making them visible to the immune system [61]. Clearly this detectability has implications for their use in the treatment of AMI, where MSC differentiation to cardiomyocytes may play a therapeutic role. In a swine model of chronic ischemic cardiomyopathy, our group and others have reported the capacity of allogeneic MSCs to engraft and undergo multilineage differentiation [62, 63]. However, long-term success of MSC engraftment into post-infarct myocardium has yet to be satisfactorily demonstrated, possibly due to the fact that the cells are being attacked by the immune system upon differentiation. The future success of MSC-based cellular therapies for the treatment of CVD will therefore benefit from studies aimed at exploiting and enhancing the immune evasive properties of MSCs.

The immunomodulatory properties of MSCs have been extensively described throughout the literature and represent arguably one of the principal mechanisms of action against adverse cardiac remodeling following AMI. Immune modulation is not, however, a default function of MSCs and specific activation is required by inflammatory mediators to stimulate the immunomodulatory activity of MSCs [64]. Following AMI, proinflammatory chemokines are rapidly released by tissue-resident macrophages activated by damage-associated molecular patterns (DAMPs) [65]. These chemokines bind to glycosaminoglycans on endothelial cell surfaces and in the extracellular matrix, causing a respiratory burst in neutrophils and their subsequent degranulation [66]. The release of reactive oxygen species, proteases, arachidonic metabolites, and other proinflammatory mediators leads to robust immune activation and severe damage of the vascular endothelium and myocardium [67]. MSCs used in models of lung injury [68], diabetes [69], and sepsis [70] appear to be motivated by this stimulus to adopt a modulatory role, diminishing the apoptosis and degranulation of neutrophils, therefore tempering the magnitude of the innate response.

Once "primed" by pro-immunogenic stimuli, MSCs exhibit modulatory activity on several aspects of the immune system, most notably a major effect on resident macrophages. Macrophages can be broadly separated into two distinct categories. Classically activated (M1) macrophages represent the proinflammatory arm, whereas alternatively activated (M2) macrophages represent an anti-inflammatory, reparative branch [71, 72]. Through the secretion of PGE2, MSCs promote the M2 phonotype even in the presence of heavy proinflammatory stimuli that would normally lead to M1 phenotypes [70, 73, 74]. A shift from an M1 to an M2 phenotype results in decreased production of IFN-γ and TNF-α, potent proinflammatory cytokines, and promotes the production of the anti-inflammatory cytokine IL-10. The effect is a further tempering of neutrophil recruitment and activation. Cardiac fibroblasts, responsible for the production and deposition of collagen leading to the establishment of a permanent scar, respond to an array of proinflammatory cytokines (e.g., tumor necrosis factor-α, interleukin (IL)-1, IL-6, and transforming growth factor-beta (TGF-β) all of which are produced by M1 macrophages in the myocardium post-MI) [73, 75]. The healing process requires a precise balance between removal of debris and regulation of scar formation. Depletion of macrophages in infarcted hearts impairs collagen deposition, however it also inhibits necrotic cell clearance, angiogenesis and predisposes the heart to rupture [76]. The molecular pathways that control the balance between the proinflammatory (M1) and reparative (M2) functions of macrophages therefore represent one potential target for MSC-mediated modulation of pathogenic cardiac remodeling and enhancement of repair [77].

Dendritic cells (DC) are phagocytic antigen-presenting cells, which link the innate immune system to the adaptive immune system. MSCs modulate the function and maturation of DCs in co-culture experiments [78, 79], and hamper migration to lymph nodes in vivo and mitigate their T-cell allostimulatory capacity [80]. Activated MSCs also act directly upon the adaptive immune response by suppressing T-cell proliferation, as demonstrated in mixed lymphocyte reactions, through the release of soluble factors including indoleamine 2,3-dioxygenase (IDO) [81], PGE2 [82], nitric oxide (NO) [83], heme oxygenase-1 (HO-1) [84], hepatocyte growth factor (HGF), and transforming growth factor-β (TGF-β) [54, 85]. In addition to inhibiting T-cell proliferation, MSCs can also influence T-cell lineage commitment. In a rat allograft model, combined intrathymic (i.t.) and intravenous (i.v.) injection of MSCs prolonged survival of the transplanted heart. The allograft survival was associated with a shift in the Th1/Th2 balance, and an upregulation of $CD4^+$, $CD25^+$, and $Foxp3^+$ T regulatory (Treg) cell differentiation. A concordant decrease in the level of proinflammatory cytokines interleukin 2 (IL-2) and interferon-gamma (IFN-γ) and an increase in the levels of anti-inflammatory IL-4 and IL-10 were also reported. The B cell, which produces antibodies, is highly dependent on T cells and MSC inhibition of T-cell activity and proliferation likely contribute a major role in MSC-dependent B-cell modulation [86]. However, human MSCs have been observed to directly inhibit the proliferation, differentiation, and chemotactic behavior of mature B cells when preactivated with exogenous IFN-γ [87]. In an allogeneic co-culture experiment, B cells arrested in the G_0/G_1 phase of the cell cycle, IgM, IgG, and IgA production were significantly impaired and expression of chemotactic receptors CXCR4, CXCR5, and CCR7 was significantly downregulated [88].

Thus, this evidence makes it clear that MSCs have a broad and significant impact on the immune system (Fig. 1). Their capacity for immune modulation and homing to the sites of injury makes them a compelling delivery system for secreted soluble factors that potentially protect the heart from acute injury. However, MSCs are also capable of producing anti-fibrotic factors and matrix metalloproteinases (MMPs) that are able to remodel extracellular matrix. It is thought, therefore, that MSCs have a potential role in chronic cardiac disease through reverse remolding of the scar resulting in sufficient reperfusion and rigidity to promote cardiomyocyte regeneration [89, 90].

5 Cardiomyogenesis and Neoangiogenesis

As previously discussed, MSCs possess several key characteristics that set them apart from other cell types, making them an attractive therapy for cardiomyoplasty. In addition to their immunoregu-

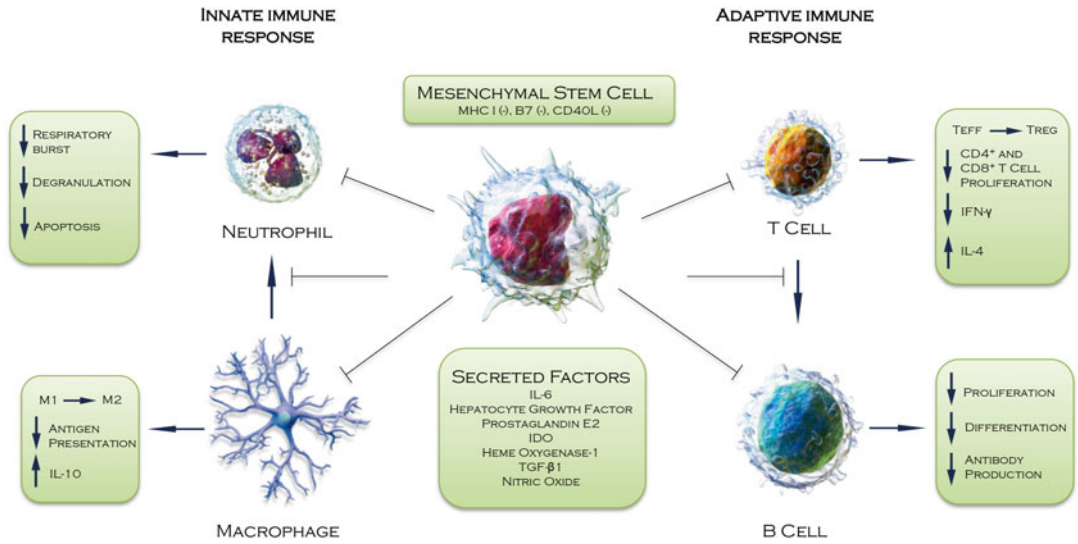

Fig. 1 Paracrine immunomodulation in the infarcted myocardium. MSCs are immune-evasive and modulate the response of both the adaptive and innate immune system during acute inflammation of the ischemic myocardium. Illustration of cells used with permission from Wikimedia commons

latory and homing properties, their genetic stability and ability to be expanded in culture means that vast numbers of cells capable of multilineage differentiation can be generated.

Human MSCs retain sufficient plasticity to adopt cardiac specific characteristics in culture and can be induced to express several cardiomyocyte-specific makers (α-actinin, myosin heavy chain, and troponin-T) and transcription factors (GATA-4 and Nkx2-5) [91–93] when driven by exogenous stimuli. Mechanical strain [94], electrostimulation [95, 96], DNA demethylation using 5-azacytidine [97], culture with pro-cardiogenic factors such as BMP-2 [98], HGF [99], TGF-β [100] and Jagged1 [101], or co-culture with mature xenogeneic cardiomyocytes [92, 102] or cardiomyocyte lysate [103] have each proven efficacious in driving myocyte differentiation in vitro. However, whether the physiological conditions within the heart are sufficient to promote such efficient differentiation of transplanted MSCs toward a myocyte lineage is a topic of discussion. Our group and others have demonstrated cardiac differentiation in vivo, but this has not been observed by others [14, 62, 104–109] possibly due to species differences or distinct handing of the cells, which could affect viability or differentiation frequency toward cardiomyogenesis. Nevertheless, a direct role for transplanted MSCs in neomyogenesis may be of little significant importance from a physiological standpoint. Evidence from our laboratory and others suggests that MSCs may stimulate the proliferation and maturation of resident cardiac stem cells through paracrine signaling, thereby indirectly supporting

innate neomyogenesis [110]. Indeed, such a supporting role would be in concordance with the theory that MSCs, as perivascular cells, function as supportive cells in the maintenance of stem cells within the vascular niche of the organ.

An ideal cell type for use in ischemic AMI would be one that not only promotes cardiomyogenesis, but also supports neoangiogenesis. There appears to be clear evidence that MSCs retain sufficient ability to differentiate into endothelial and vascular smooth muscle cells, both in vitro and in vivo [62, 109, 111–114]. Moreover, MSCs have potent proangiogenic activity, both in vitro and in vivo, through the secretion of VEGF, FGFs, angiopoietins, and extracellular matrix components [89, 115–120]. The significance of the angiogenic action of MSCs in post-ischemic myocardial protection was highlighted specifically by Markel and colleagues using small-interfering RNA (si)RNA directed against VEGF. In these studies knock down of VEGF in transplanted MSCs resulted in a marked negative effect on recovery of myocardial function in a rat model of AMI [121]. This effect was further demonstrated in suicide gene-based studies carried out by Yoon et al. [122]. In this system targeted elimination of cells acquiring a vascular lineage dramatically reduced functional benefits, whereas depletion of cardiomyogenic cells showed no significant effect [122]. Our group recently demonstrated that this effect of VEGF on MSC differentiation toward a vascular phenotype was dependent on the activation of PDGFR via nitric oxide synthase [123]. Thus, accumulating evidence suggests a crucial role for MSCs in neoangiogenesis and vascular homeostasis that might parallel their endogenous role as perivascular cells [124].

While MSCs produce a battery of factors that have a demonstrable biochemical effect on cardiac disease [125], the measurable effects on tissue regeneration have been less than expected. Low engrafting efficiency, low viability, and hostile environmental conditions within the injury site have been implicated as potential explanations [126, 127]. If the medicinal benefit of MSCs is conveyed through recapitulation of their pericytic function, inasmuch as their stimulation of resident cardiac stem cells and induction of angiogenesis, then engraftment of MSCs with host vasculature would be a necessity. However, the ischemic scar tissue is, by its nature, avascular and therefore may not provide the ideal substrate or niche environment for robust engraftment and MSC activation. Recent efforts have therefore been geared toward improving the therapeutic efficiency, engraftment, survival and immune evasion of MSCs, the results of which are several preconditioning approaches and genetic modifications aimed at amplifying existing characteristics and imparting novel capabilities onto the cells.

6 Mesenchymal Stem Cell Modification

In order to utilize MSCs for cardiac repair, it is necessary to expand the cells in vitro and then prepare them as a suspension for injection. However, MSCs are normally grown attached to a substrate, and this adhesion to structural glycoproteins of the extracellular matrix (ECM) is necessary for their survival [128, 129]. Removal of this matrix support, as occurs when the cells are prepared for injection, will therefore lead to increased anoikis, i.e., apoptosis induced by loss of matrix attachments. This lack of matrix, coupled with the fact that infusion of MSCs into the circulation or directly into the infarcted region of the heart exposes them to harsh environmental conditions, means that the number of culture-expanded MSCs engrafting at sites of injury rapidly declines following initial infusion [130]. A number of studies have therefore focused on improving the engraftment efficiency of MSCs following their injection into the damaged heart. As MSCs are capable of long-term transgene expression [131], it has been possible to develop strategies based on genetic engineering to enhance homing efficiency and improve cell survival.

Mangi et al. were the first to demonstrate that genetic modification of MSCs to overexpress the anti-apoptotic transcription factor Akt resulted in a greater resistance to apoptosis both in vitro and in vivo and led to an increase in cardiac function in a rodent model of MI [132, 133]. Transgenic overexpression of another prosurvival gene, Bcl-2 by rat MSCs decreased apoptosis by 32 %, enhanced secretion of VEGF by 60 % under hypoxic conditions and improved capillary density in the infarct border zone [134]. Similarly, transfection of MSCs with basic-fibroblast growth factor (bFGF) enhanced cytoprotection under hypoxic conditions and caused greater neovascularization compared to untransfected MSCs [135]. MSCs overexpressing VEGF demonstrated an improvement in myocardial perfusion and in restoration of heart function compared to control groups [136] and MSCs transduced with hemoxygenase, an enzyme preventing oxidative damage, showed both better engraftment and enhanced cell survival following intra-myocardial delivery relative to non-transduced MSCs [137].

Culture-expanded MSCs demonstrate reduced expression of receptors for chemokines and adhesion molecules such as CXCR4 and CCR1, which significantly compromises homing capacity. Studies in which MSCs were modified to overexpress CXCR4 and CCR1 demonstrated enhanced engraftment and cardiac performance [138, 139]. Overexpression of tissue transglutaminase (tTG), which crosslinks proteins, leads to enhanced adhesion of MSCs and survival of implanted cells via an integrin-dependent mechanism [140]. Indeed, integrin signaling is a critical component

of MSC engraftment and the integrin-linked kinase (ILK) is crucial for hypoxic MSCs to establish cell adhesion with ischemic myocardium [127]. ILK enhances phosphorylation of PKB/Akt, which plays a major role in the regulation of adhesion-mediated cell survival signals. Hypoxic conditions suppress expression of ILK, however forced expression through transfection of the ILK gene results in enhanced MSC survival, decreases in infarct size, and a greater improvement of left ventricular function [127].

Although the engraftment efficiency of MSCs might be enhanced by such genetic modification, these approaches are currently restricted to basic and translational research due to limited clinical experience with gene therapy and genetically modified cell products. However, these ongoing studies will further elucidate the biology of MSCs and will contribute to our understanding of the mechanisms of their reparative action.

7 Mesenchymal Stem Cell Preconditioning

Modifications to MSCs with translational pragmatism include various methods of priming or preconditioning [141]. In this regard, improvements in engraftment of transplanted MSCs have been demonstrated in the absence of direct genetic manipulation, by the use of combinatorial pretreatment with several exogenous growth factors. In a rat model of AMI, pretreatment with insulin-like growth factor-1 (IGF-1), fibroblast growth factor-2 (bFGF) and bone morphogenetic protein-2 (BMP-2) enhanced connexing-43 (Cx43) gap junction formation and imparted cytoprotective effects on cardiomyocytes [98]. Behfar et al. pretreated human MSCs with a recombinant cocktail of transforming growth factor-beta [1], BMP-4, activin-A, retinoic acid, IGF-1, bFGF, alpha-thrombin, and interleukin-6, which directed differentiation of MSCs into cardiopoiesis. These cells were subsequently injected into the myocardium of infarcted murine hearts, which led to functional and structural benefits [142].

Pharmacological pretreatment of MSCs with steroids such as estrogen [143], which influences myocardial remodeling through stimulation of growth hormone production, or statins such as atorvastatin [144, 145], which enhance cell survival and differentiation into cardiomyocytes, have also received attention, as has tadalafil, a phosphodiesterase inhibitor used on adipose-derived MSCs in rat models of cardiomyopathy [146]. Non-biochemical and non-pharmacological treatments such as hypoxic and anoxic preconditioning have also demonstrated significant improvements on MSC survival. Hypoxic preconditioning activates the Akt signaling pathway leading to the expression of several prosurvival and proangiogenic factors such as Bcl-2, Bcl-xL, Hif-1, VEGF, Ang-1, and erythropoietin [147]. Hypoxia preconditioning enhanced

MSCs survival together with improved angiogenesis of the infarct border zone and as a consequence improved cardioprotection following AMI [148]. Similarly anoxic-preconditioned MSCs demonstrated reduced apoptosis, which is thought to be mediated through upregulation of the Bcl-2/Bax ratio and by inhibition of caspase-3 activation in the myocardium [108].

8 Clinical Trials with Mesenchymal Stem Cells for Heart Disease

Thirty-two clinical trials using MSCs to treat different heart conditions including AMI, severe coronary ischemia, ischemic cardiomyopathy, dilated cardiomyopathy, and heart failure are registered on https://clinicaltrials.gov (a web-based service by the US National Institute of Health; *see* Table 1). Most have used or are using adult bone marrow-derived MSCs; while several trials chose cell-based treatment with MSCs derived from adipose tissue or umbilical cord. Many of these studies used allogeneic sources of MSCs from healthy donors, which, as discussed above, is possible due to the immune evasive and immunomodulatory properties exhibited by MSCs. Allogeneic MSCs are an attractive and convenient cell type, the major advantage being their immediate availability. In contrast, autologous cells require expansion for 4–6 weeks prior to treatment, a delay that may reduce the efficacy of stem cell therapy. In addition, their therapeutic ability may be compromised by the health of the donor/patient.

The initial MSC studies for acute and chronic MI in 2004–2008 used intracoronary administration of autologous cells [149, 150]. However, in 2009, the first double-blinded trial on 53 patients with AMI "Osiris"[151] showed that allogeneic intravenous cell infusion was well tolerated and had a significantly greater effect on left ventricular ejection fraction and a lower incidence of arrhythmia and chest pain (Fig. 2). This study began the era of allogeneic MSC use for cardiac pathology, suggesting that allogeneic cell-based therapy is safe and effective. Although autologous MSC treatment was prevalent in ischemic cardiomyopathy (11/15 clinical trials), non-ischemic cardiomyopathy and AMI trials adopted allogeneic MSC treatment early on (Fig. 3). By 2014, an equal number of clinical trials used allogeneic and autologous MSCs (Fig. 4).

Consistent with the registered data from https://clinicaltrials.gov, there are ongoing phase I, II and III clinical trials evaluating MSC safety and efficacy for cardiac regeneration using a variety of delivery systems. The method of stem cell delivery can influence cell-therapy outcome, which is why intracoronary, intravenous, intraoperative/intramyocardial injections, and catheter-based transendocardial injections are currently in use in order to establish the

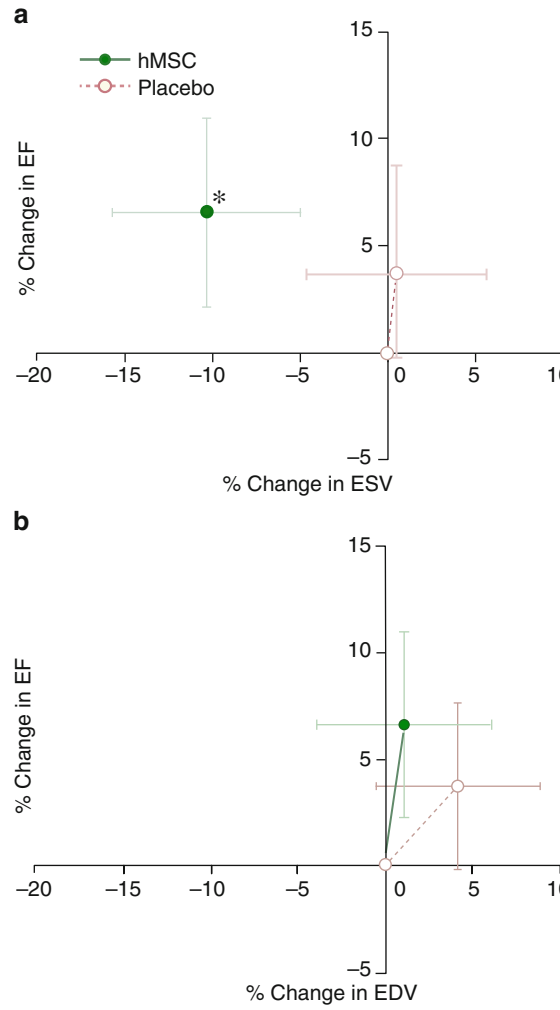

Fig. 2 Impact of hMSC treatment on LV remodeling. Changes in left ventricular (LV) ejection fraction (EF) are plotted against the changes in LV end-systolic volume (ESV) (**a**) and end-diastolic volume (EDV) (**b**) during follow-up. Human mesenchymal stem cell (hMSC) patients ($n=18$ at 12 months) exhibit evidence of reverse remodeling with no increase in LV EDV and a decline in LV ESV, whereas placebo patients ($n=11$ at 12 months) demonstrate evidence of LV chamber enlargement. *$P=0.005$ versus baseline [151]

most efficient stem cell transplantation technique in compliance with heart pathology (Fig. 5).

The first clinical trials for acute and chronic MI [150] used catheter-based intracoronary autologous MSC delivery during percutaneous coronary intervention (PCI). These studies showed no serious adverse events, significantly better regional and global left-ventricular function, up to 10 % increased left ventricular ejection fraction (LVEF), increased exercise capacity, and improvement in

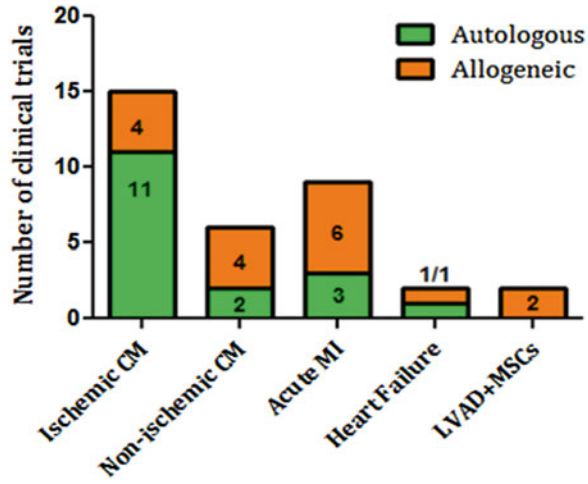

Fig. 3 Autologous and allogeneic mesenchymal stem cell-based treatment according to heart pathology

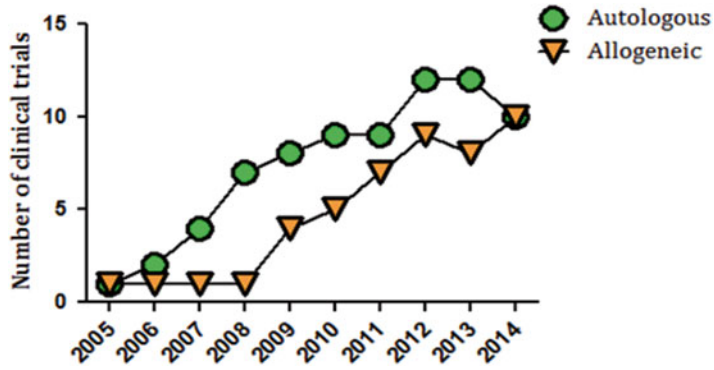

Fig. 4 Progressive growth of allogeneic and autologous mesenchymal stem cell-based clinical trials

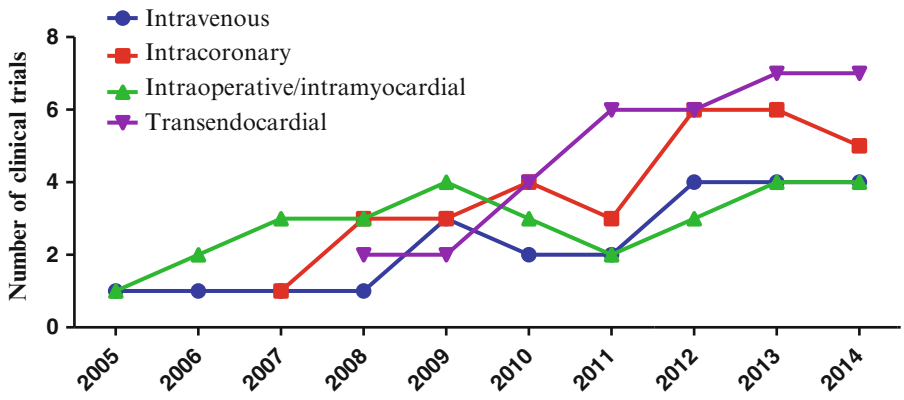

Fig. 5 MSC delivery methods used in clinical trials from 2005 to 2014

New York Heart Association (NYHA) heart failure class. Using the same method of cell delivery, Katritsis et al. [149] combined autologous MSCs with endothelial progenitor cells for AMI treatment and showed better left ventricular function and myocardial perfusion with evidence of regeneration of the previously nonviable infarct scar. A pilot study conducted by Mohyeddin-Bonab et al. in 2007 tested whether intracoronary delivery during PCI or intraoperative/intramyocardial treatment with autologous MSCs is safe and efficient for old myocardial infarction [152]. Their results demonstrated increased LVEF, a change in NYHA class, and significant improvement in viable myocardium in the MSC-treated group. However, there were no data presented (probably because of small sample size) regarding which delivery route was more beneficial. The PROMETHEUS study showed that intraoperative/intramyocardial autologous MSC injections together with Coronary Artery Bypass Grafting (GABG) procedure into akinetic, yet non-revascularized segments, was safe and produced comprehensive regional functional restitution, which in turn drives improvement in global left ventricular function (Fig. 6) [153]. The TAC-HFT trial compared transendocardial injections of autologous MSCs, bone marrow mononuclear cells (BMCs), and placebo in chronic ischemic heart failure [154, 155]. This study again showed safety of the delivery method, and MSCs and BMCs significantly improved regional contractility [156] and increased 6-min walk distance, but only the MSCs reduced scar size (Fig. 7). There were no changes in LVEF or heart chamber volumes [154].

Anastasiadis et al. [157] combined left ventricular mechanical support device (LVAD) implantation with allogeneic MSC injections in a case-report study and showed improved LVEF when the device was turned off. This study from 2012 formed the basis for a recent study with LVAD+ allogeneic MSC treatment for patients with end-stage heart failure. In 2013 our group compared allogeneic vs. autologous bone marrow-derived MSCs delivered by transendocardial injection in patients with ischemic cardiomyopathy: the POSEIDON randomized dose-escalation trial (20, 100, 200 million cells). This study showed that allogeneic and autologous MSCs are safe and reduced mean early enhancement defect (scar size) by 33.21 %. Allogeneic MSCs reduced left ventricular end-diastolic volumes and interestingly, the lowest concentration of MSCs (20 million cells) produced the greatest reductions in left ventricular volume and increased ejection fraction. Notably, allogeneic MSCs did not stimulate significant donor-specific alloimmune reactions [51]. The segmental ejection fraction analysis from the POSEIDON study showed that injected and non-injected segments improved regional contractile performance with the greater scar reduction in injected sites (Fig. 8) [158]. In 2014, Lee et al. [159] published results of a multicenter trial examining the safety and efficacy of intracoronary administration of autologous bone

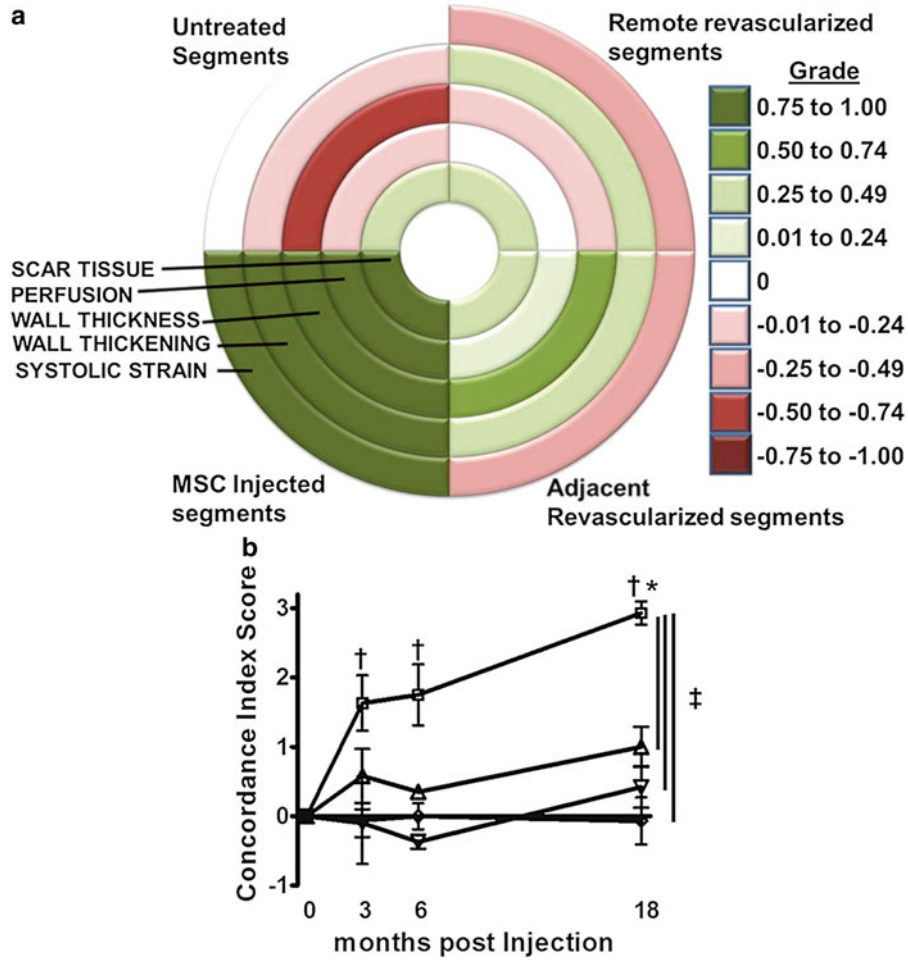

Fig. 6 Concordance index score is an indicator of simultaneous and comprehensive improvement. (PROMETHEUS Trial.) (**a**) Bull's-eye map depicting the concordance of change for each variable used for the concordance index score based on the average grade for each group at 18 months post-treatment. A grade closer to 1 signifies a concordant improvement in the variable and a grade closer to −1 represents deterioration. The concordance index score is then derived by adding the grades for changes in scar tissue size, perfusion, and the average of the grades for changes in wall thickness, wall thickening, and systolic strain. The highest value (3) signifies simultaneous improvement in all five CMR indices and the lowest (−3) a simultaneous deterioration, respectively. (**b**) In the MSCs plus CABG group, the injected non-revascularized segments improved comprehensively and thus had a higher concordance index score compared with all other groups. The effect of the MSCs dissipated by a function of distance from the actual injection site ($P = 0.03$ adjacent vs. remote revascularized and non-treated segments). (*Open square*) MSC injected; (*filled triangle*) adjacent revascularized; (*filled inverted triangle*) remote revascularized; and (*open diamond*) untreated. *$P < 0.05$ 1-way ANOVA repeated measures; †$P < 0.05$ vs. baseline, Bonferroni post-tests; ‡$P < 0.05$ 2-way ANOVA [153]

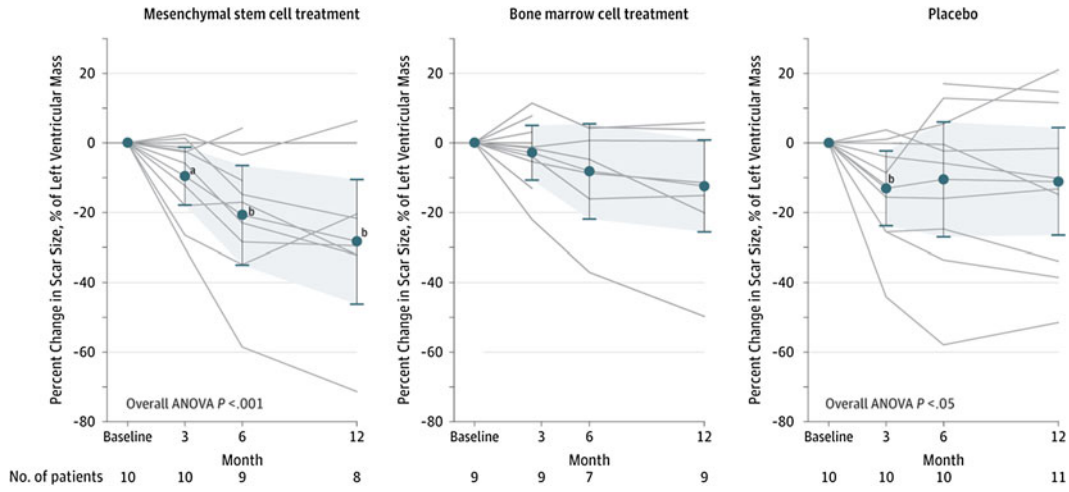

Fig. 7 Impact of transendocardial stem cell injection of mesenchymal stem cells, bone marrow cells, or placebo on the scar size. (TAC-HFT randomized trial.) Significant reduction in scar size as the percentage of left ventricular mass for patients treated with mesenchymal stem cells (MSCs) and those in the placebo group who underwent serial magnetic resonance imaging. Repeated measures of analysis of variance model *P* values: treatment group, $P = 0.99$; time, $P = 0.007$; treatment group × time, $P = 0.22$. Data markers represent means; error bars, 95 % CIs. Analysis of variance (ANOVA) was conducted with repeated measures. [a]Within group, $P < 0.05$ vs. baseline. [b]Within group, $P < 0.01$ vs. baseline [154]

marrow-derived MSCs in patients with AMI and showed improved global LVEF in MSC-treated patients.

Twenty ongoing clinical trials are testing the regenerative potential of MSCs for cardiac disease, in particular ischemic cardiomyopathy and AMI. However, there is still a need for larger clinical trials comparing autologous and allogeneic MSCs in order to answer questions about the most effective dose and frequency for each cardiac pathology, the best cell delivery system, and the use of single vs. multiple cell types.

9 Conclusions

Collectively, the studies using MSCs to treat CVD are numerous and consensus favors MSCs as potent mediators of cardiac repair. MSCs clearly retain significant plasticity and are capable of formidable immunomodulation and neo-angiogenesis. However, a feature common in MSC transplantation is a conspicuous lack of proliferation, differentiation, or engraftment. Several explanations have been presented to explain this and many modifications and pretreatments are being attempted to address it. However, there are other considerations, perhaps more difficult to address and that have not been described as thoroughly. Stem cell division is driven

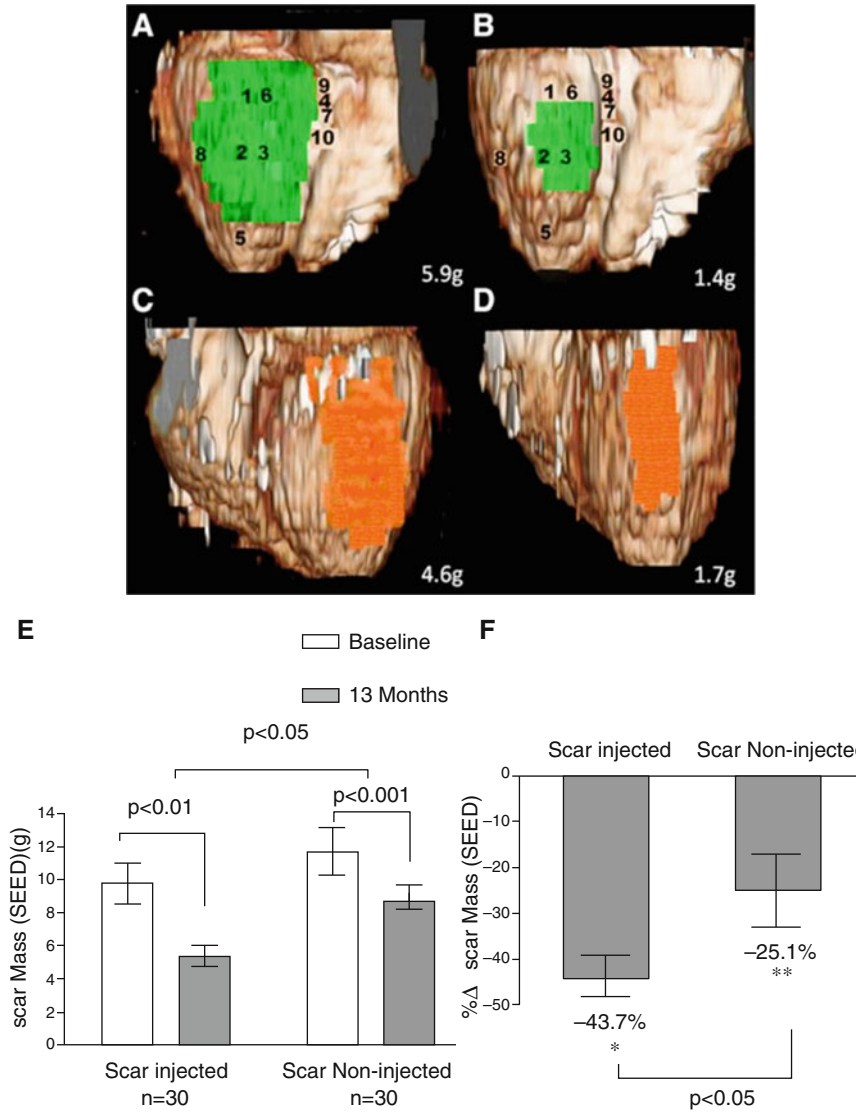

Fig. 8 Volume-rendered three-dimensional (3D) reformats of left ventricle with color encoding of scar tissue. (POSEIDON Trial.) (**a**, **b**) Scar mass (*green*) of inferior segments treated by transendocardial stem cell injection (TESI) at baseline and 13 months after TESI, respectively (numbers represent sites of injection). (**c**, **d**) Scar mass (*orange*) of lateral segments not treated by TESI at baseline and at 13-month follow-up, respectively. Actual scar mass (grams) is depicted in the *lower right corner* of each panel. Three-dimensional reconstructions in this figure correspond to segmental early enhancement defect (SEED) measurements. (**e, f**) Absolute values and percentage changes of scar mass obtained by segmental imaging analysis approach. When considering the autologous and allogeneic groups combined, there is greater scar size reduction in the scar-injected segments (–43.7 ± 4.4 %, from 9.8 ± 1.2 to 5.4 ± 0.7 g; $n = 30$; *$P < 0.01$) when compared with the scar-non-injected segments (–25.1 ± 7.8 %, from 11.7 ± 1.4 to 8.6 ± 1.0 g; $n = 30$; **$P < 0.001$; between-group comparison scar-injected vs. scar-non-injected $P < 0.05$) [158]

by contextual signals from the 3D structure of the niche. MSCs being pericytic or adventitial cells require adhesion to a substrate to maintain viability, which in vivo constitutes perivascular adhesion to sinusoids or large vessels, respectively [29, 160]. In the absence of the niche microenvironment, stem cells can irreversibly lose their inherent stemness [161]. Although they initially survive and retain many stem cell markers, their efficacy can begin to wane very rapidly following transplantation [161]. When MSCs are injected into the myocardium or circulation no such orientation or structure exists and the transplanted cells therefore may not receive the mitogenic signals necessary to initiate cell cycle or drive differentiation. Moreover, a lack of substantive adhesion may cause a loss of cellular identity, anoikis and depletion by NK cells, leading to an irreversible decline in viable cell numbers. It is clear that while we have made significant progress, much work remains as we learn to fully exploit the power of MSCs in cardiac repair.

Moving forward, an exciting prospect aimed at improving stem cell potency, viability, and engraftment involves cell combination therapy. An example includes the use of ex-vivo stromal cell aggregates known as cardiospheres [162]. These floating clusters are comprised of a central core of primitive c-kit$^+$ cardiac stem cells surrounded by layers of early-stage committed differentiating cells, and an outside cell layer of MSCs [163]. Culture of these cells as a 3D structure is thought to potentially recapitulate cardiac niche biology in the in vitro environment [164]. Preclinical models using autologous as well as allogeneic cardiosphere-derived cells (CDCs) have demonstrated a reduction in scar size and improvements in cardiac function after MI, although the mechanism of action is not clear [165–168]. Results from a phase I clinical trial using intracoronary infusion of cardiosphere-derived cells (CADUCEUS) further supports the notion that CDCs are capable of regenerating heart tissue after AMI in humans [169].

Our group recently reported preclinical findings from studies combining MSCs with c-kit$^+$ cardiac stem cells (CSC) [170]. Co-culture with MSCs enhanced CSC proliferation and lineage commitment toward a cardiac phenotype, suggesting that important biological interactions exist between these cells (Fig. 9) [110]. These interactions are dependent on gap junction formation mediated through expression of Cx43 [110, 171]. In a porcine model of AMI, co-injection of human MSCs and human c-kit$^+$ CSCs resulted in a sevenfold greater engraftment of stem cells than with either cell type alone, a significant reduction in scar size and significant restoration of diastolic and systolic function [170]. These observations, together with the success of safety trials of MSCs (POSEIDON) [51] and c-kit$^+$ stem cells (SCIPIO) [21] have created an opportunity for exploring therapeutic enhancement of this combination therapy in humans. As a result, a new

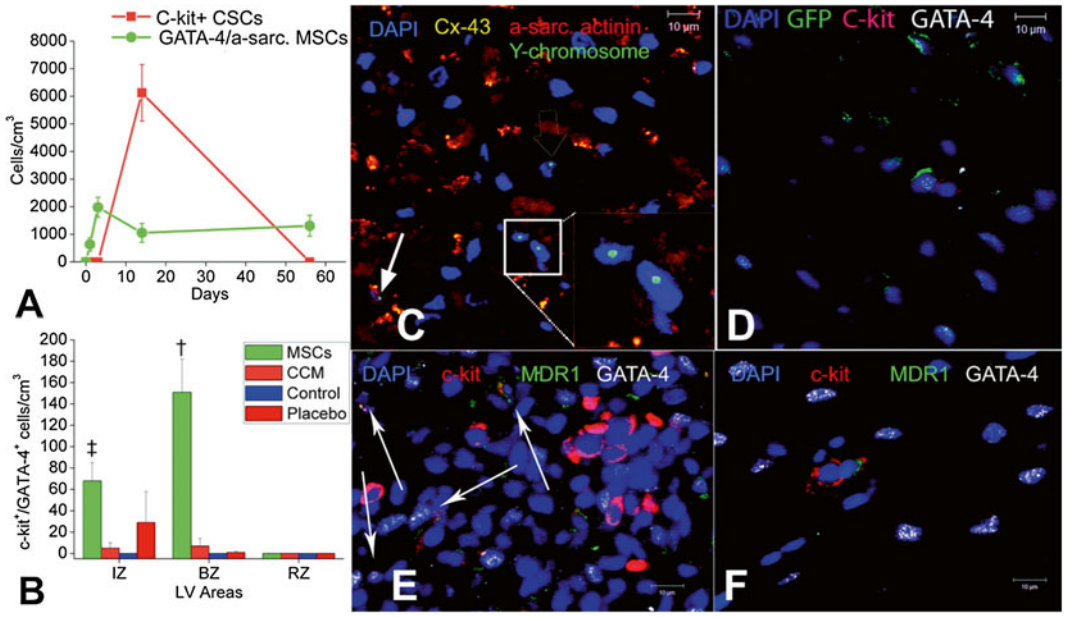

Fig. 9 MSCs stimulate endogenous CSCs. (**a**) The contribution of cardiomyocyte precursors following exogenous administration of MSCs (*green line*) and endogenous CSCs (*orange line*) during cardiac repair after MI. MSC differentiation occurs rapidly after delivery. At 2 weeks, MSCs activate endogenous expansion of c-kit$^+$ CSCs (*orange line*). (**b**) Two weeks following TEI, the number of C-kit$^+$ cells coexpressing GATA-4 is greater in MSCs versus non-MSCs treated hearts. The cardiac precursors are preferentially located in the IZ and BZ of the MI, indicating an active process of endogenous regeneration ($^‡P = 0.019$ and $^†P < 0.0001$). (**c**, **d**) The 2-week-old chimeric myocardium contains mature cardiomyocytes (*open arrow*), immature MSCs (*inset*), and cardiac precursors of MSCs origin (*arrow*), coupled to host myocardium by connexin-43 gap junctions. Interestingly, endogenous c-kit$^+$ CSCs are found in close proximity to MSCs (**d**). (**e**) Cluster of c-kit$^+$ CSCs in an MSC-treated heart; numerous CSCs are committed to cardiac lineage documented by GATA-4 and MDR-1 coexpression (*arrows*). (**f**) Few isolated c-kit$^+$ cells were found in non-MSC-treated animals [110]

phase I clinical trial has recently received regulatory approval from the FDA and is currently in the process of recruiting patients.

The debate enveloping stem cell clinical trials for use against cardiac disease has intensified recently with the publication of two high profile reports [172, 173]. These critical reports clearly have implications for future clinical trials involving bone marrow cells and CSCs and the tide of criticism would seem to also threaten clinical trials utilizing MSCs. However, this criticism will likely not affect MSCs, which stand alone in their unprecedented ability to perform a number of beneficial functions, as discussed above. The data coming from preclinical and clinical trials clearly support a continued effort to exploit the medicinal potential of MSCs. The biochemical activity of MSCs has been demonstrated beyond a doubt with observable results. Our understanding of MSC biology has evolved significantly over the past two decades and significant

advancements have been made, yet much work still remains. Therefore, the focus moving forward will be directed at expanding the current successes through discovery of the critical factors mediating MSC repair and optimization of the system.

References

1. Vodyanik MA, Yu J, Zhang X et al (2010) A mesoderm-derived precursor for mesenchymal stem and endothelial cells. Cell Stem Cell 7:718–729
2. Abu-Issa R, Kirby ML (2007) Heart field: from mesoderm to heart tube. Annu Rev Cell Dev Biol 23:45–68
3. Brand T (2003) Heart development: molecular insights into cardiac specification and early morphogenesis. Dev Biol 258:1–19
4. Montserrat N, Jopling C, Izpisua Belmonte JC (2010) Understanding the molecular basis for cardiomyocyte cell cycle regulation: new insights in cardiac regeneration after injury? Expert Rev Cardiovasc Ther 8:1043–1045
5. Pasumarthi KB, Field LJ (2002) Cardiomyocyte cell cycle regulation. Circ Res 90:1044–1054
6. MacLellan WR, Schneider MD (2000) Genetic dissection of cardiac growth control pathways. Annu Rev Physiol 62:289–319
7. Kang PM, Izumo S (2000) Apoptosis and heart failure: a critical review of the literature. Circ Res 86:1107–1113
8. Porrello ER, Mahmoud AI, Simpson E et al (2011) Transient regenerative potential of the neonatal mouse heart. Science 331:1078–1080
9. Bergmann O, Bhardwaj RD, Bernard S et al (2009) Evidence for cardiomyocyte renewal in humans. Science 324:98–102
10. Go AS, Mozaffarian D, Roger VL et al (2014) Heart disease and stroke statistics—2014 update: a report from the American Heart Association. Circulation 129:e28–e292
11. Jennings RB, Steenbergen C, Reimer KA (1995) Myocardial ischemia and reperfusion. Monogr Pathol 37:47–80
12. Graham RM, Frazier DP, Thompson JW et al (2004) A unique pathway of cardiac myocyte death caused by hypoxia-acidosis. J Exp Biol 207:3189–3200
13. Kubasiak LA, Hernandez OM, Bishopric NH et al (2002) Hypoxia and acidosis activate cardiac myocyte death through the Bcl-2 family protein BNIP3. Proc Natl Acad Sci U S A 99:12825–12830
14. Laflamme MA, Murry CE (2005) Regenerating the heart. Nat Biotechnol 23:845–856
15. Becker RO, Chapin S, Sherry R (1974) Regeneration of the ventricular myocardium in amphibians. Nature 248:145–147
16. Poss KD, Wilson LG, Keating MT (2002) Heart regeneration in zebrafish. Science 298:2188–2190
17. Hatzistergos KE, Blum A, Ince T et al (2011) What is the oncologic risk of stem cell treatment for heart disease? Circ Res 108:1300–1303
18. Menasche P, Hagege AA, Vilquin JT et al (2003) Autologous skeletal myoblast transplantation for severe postinfarction left ventricular dysfunction. J Am Coll Cardiol 41:1078–1083
19. Menasche P (2003) Myoblast-based cell transplantation. Heart Fail Rev 8:221–227
20. Beltrami AP, Barlucchi L, Torella D et al (2003) Adult cardiac stem cells are multipotent and support myocardial regeneration. Cell 114:763–776
21. Bolli R, Chugh AR, D'Amario D et al (2011) Cardiac stem cells in patients with ischaemic cardiomyopathy (SCIPIO):initial results of a randomised phase 1 trial. Lancet 378: 1847–1857
22. Caplan AI (1991) Mesenchymal stem cells. J Orthop Res 9:641–650
23. Caplan AI (1986) Molecular and cellular differentiation of muscle, cartilage, and bone in the developing limb. Prog Clin Biol Res 217B:307–318
24. Friedenstein AJ, Chailakhjan RK, Lalykina KS (1970) The development of fibroblast colonies in monolayer cultures of guinea-pig bone marrow and spleen cells. Cell Tissue Kinet 3:393–403
25. Friedenstein AJ, Chailakhyan RK, Latsinik NV et al (1974) Stromal cells responsible for transferring the microenvironment of the hemopoietic tissues. Cloning in vitro and retransplantation in vivo. Transplantation 17:331–340

26. Dominici M, Le Blanc K, Mueller I et al (2006) Minimal criteria for defining multipotent mesenchymal stromal cells. The International Society for Cellular Therapy position statement. Cytotherapy 8:315–317
27. da Silva Meirelles L, Chagastelles PC, Nardi NB (2006) Mesenchymal stem cells reside in virtually all post-natal organs and tissues. J Cell Sci 119:2204–2213
28. Orbay H, Tobita M, Mizuno H (2012) Mesenchymal stem cells isolated from adipose and other tissues: basic biological properties and clinical applications. Stem Cells Int 2012:461718
29. Crisan M, Yap S, Casteilla L et al (2008) A perivascular origin for mesenchymal stem cells in multiple human organs. Cell Stem Cell 3:301–313
30. Mendez-Ferrer S, Michurina TV, Ferraro F et al (2010) Mesenchymal and haematopoietic stem cells form a unique bone marrow niche. Nature 466:829–834
31. Winkler EA, Bell RD, Zlokovic BV (2011) Central nervous system pericytes in health and disease. Nat Neurosci 14:1398–1405
32. Roufosse CA, Direkze NC, Otto WR et al (2004) Circulating mesenchymal stem cells. Int J Biochem Cell Biol 36:585–597
33. He Q, Wan C, Li G (2007) Concise review: multipotent mesenchymal stromal cells in blood. Stem Cells 25:69–77
34. Caterson EJ, Nesti LJ, Danielson KG et al (2002) Human marrow-derived mesenchymal progenitor cells: isolation, culture expansion, and analysis of differentiation. Mol Biotechnol 20:245–256
35. Chang Y, Hsieh PH, Chao CC (2009) The efficiency of Percoll and Ficoll density gradient media in the isolation of marrow derived human mesenchymal stem cells with osteogenic potential. Chang Gung Med J 32:264–275
36. Harichandan A, Sivasubramaniyan K, Buhring HJ (2013) Prospective isolation and characterization of human bone marrow-derived MSCs. Adv Biochem Eng Biotechnol 129:1–17
37. Lennon DP, Caplan AI (2006) Isolation of human marrow-derived mesenchymal stem cells. Exp Hematol 34:1604–1605
38. Majumdar MK, Banks V, Peluso DP et al (2000) Isolation, characterization, and chondrogenic potential of human bone marrow-derived multipotential stromal cells. J Cell Physiol 185:98–106
39. Wolfe M, Pochampally R, Swaney W et al (2008) Isolation and culture of bone marrow-derived human multipotent stromal cells (hMSCs). Methods Mol Biol 449:3–25
40. Colter DC, Class R, DiGirolamo CM et al (2000) Rapid expansion of recycling stem cells in cultures of plastic-adherent cells from human bone marrow. Proc Natl Acad Sci U S A 97:3213–3218
41. Zhou Z, Jiang EL, Wang M et al (2005) Comparative study on various subpopulations in mesenchymal stem cells of adult bone marrow. Zhongguo Shi Yan Xue Ye Xue Za Zhi 13:54–58
42. Jiang Y, Jahagirdar BN, Reinhardt RL et al (2002) Pluripotency of mesenchymal stem cells derived from adult marrow. Nature 418:41–49
43. Jiang Y, Vaessen B, Lenvik T et al (2002) Multipotent progenitor cells can be isolated from postnatal murine bone marrow, muscle, and brain. Exp Hematol 30:896–904
44. Yoon YS, Wecker A, Heyd L et al (2005) Clonally expanded novel multipotent stem cells from human bone marrow regenerate myocardium after myocardial infarction. J Clin Invest 115:326–338
45. D'Ippolito G, Diabira S, Howard GA et al (2004) Marrow-isolated adult multilineage inducible (MIAMI) cells, a unique population of postnatal young and old human cells with extensive expansion and differentiation potential. J Cell Sci 117:2971–2981
46. Rossini A, Frati C, Lagrasta C et al (2011) Human cardiac and bone marrow stromal cells exhibit distinctive properties related to their origin. Cardiovasc Res 89:650–660
47. Blazquez-Martinez A, Chiesa M, Arnalich F et al (2014) c-Kit identifies a subpopulation of mesenchymal stem cells in adipose tissue with higher telomerase expression and differentiation potential. Differentiation 87(3–4):147–160
48. Varma MJ, Breuls RG, Schouten TE et al (2007) Phenotypical and functional characterization of freshly isolated adipose tissue-derived stem cells. Stem Cells Dev 16: 91–104
49. Abarbanell AM, Coffey AC, Fehrenbacher JW et al (2009) Proinflammatory cytokine effects on mesenchymal stem cell therapy for the ischemic heart. Ann Thorac Surg 88:1036–1043
50. Aggarwal S, Pittenger MF (2005) Human mesenchymal stem cells modulate allogeneic immune cell responses. Blood 105: 1815–1822
51. Hare JM, Fishman JE, Gerstenblith G et al (2012) Comparison of allogeneic vs autologous

bone marrow-derived mesenchymal stem cells delivered by transendocardial injection in patients with ischemic cardiomyopathy: the POSEIDON randomized trial. JAMA 308:2369–2379

52. Le Blanc K, Tammik C, Rosendahl K et al (2003) HLA expression and immunologic properties of differentiated and undifferentiated mesenchymal stem cells. Exp Hematol 31:890–896
53. Majumdar MK, Keane-Moore M, Buyaner D et al (2003) Characterization and functionality of cell surface molecules on human mesenchymal stem cells. J Biomed Sci 10:228–241
54. Tse WT, Pendleton JD, Beyer WM et al (2003) Suppression of allogeneic T-cell proliferation by human marrow stromal cells: implications in transplantation. Transplantation 75:389–397
55. Rasmusson I, Ringden O, Sundberg B et al (2003) Mesenchymal stem cells inhibit the formation of cytotoxic T lymphocytes, but not activated cytotoxic T lymphocytes or natural killer cells. Transplantation 76: 1208–1213
56. Spaggiari GM, Capobianco A, Becchetti S et al (2006) Mesenchymal stem cell-natural killer cell interactions: evidence that activated NK cells are capable of killing MSCs, whereas MSCs can inhibit IL-2-induced NK-cell proliferation. Blood 107:1484–1490
57. Ankrum JA, Ong JF, Karp JM (2014) Mesenchymal stem cells: immune evasive, not immune privileged. Nat Biotechnol 32: 252–260
58. Zangi L, Margalit R, Reich-Zeliger S et al (2009) Direct imaging of immune rejection and memory induction by allogeneic mesenchymal stromal cells. Stem Cells 27: 2865–2874
59. Fan M, Chen W, Liu W et al (2010) The effect of age on the efficacy of human mesenchymal stem cell transplantation after a myocardial infarction. Rejuvenation Res 13:429–438
60. O'Marcaigh AS, Cowan MJ (1997) Bone marrow transplantation for inherited diseases. Curr Opin Oncol 9:126–130
61. Huang XP, Sun Z, Miyagi Y et al (2010) Differentiation of allogeneic mesenchymal stem cells induces immunogenicity and limits their long-term benefits for myocardial repair. Circulation 122:2419–2429
62. Quevedo HC, Hatzistergos KE, Oskouei BN et al (2009) Allogeneic mesenchymal stem cells restore cardiac function in chronic ischemic cardiomyopathy via trilineage differentiating capacity. Proc Natl Acad Sci U S A 106:14022–14027
63. Makkar RR, Price MJ, Lill M et al (2005) Intramyocardial injection of allogenic bone marrow-derived mesenchymal stem cells without immunosuppression preserves cardiac function in a porcine model of myocardial infarction. J Cardiovasc Pharmacol Ther 10:225–233
64. Shi Y, Hu G, Su J et al (2010) Mesenchymal stem cells: a new strategy for immunosuppression and tissue repair. Cell Res 20:510–518
65. Soehnlein O, Lindbom L (2010) Phagocyte partnership during the onset and resolution of inflammation. Nat Rev Immunol 10: 427–439
66. Frangogiannis NG (2012) Regulation of the inflammatory response in cardiac repair. Circ Res 110:159–173
67. Jordan JE, Zhao ZQ, Vinten-Johansen J (1999) The role of neutrophils in myocardial ischemia-reperfusion injury. Cardiovasc Res 43:860–878
68. Ortiz LA, Dutreil M, Fattman C et al (2007) Interleukin 1 receptor antagonist mediates the antiinflammatory and antifibrotic effect of mesenchymal stem cells during lung injury. Proc Natl Acad Sci U S A 104:11002–11007
69. Volarevic V, Al-Qahtani A, Arsenijevic N et al (2010) Interleukin-1 receptor antagonist (IL-1Ra) and IL-1Ra producing mesenchymal stem cells as modulators of diabetogenesis. Autoimmunity 43:255–263
70. Nemeth K, Leelahavanichkul A, Yuen PS et al (2009) Bone marrow stromal cells attenuate sepsis via prostaglandin E(2)-dependent reprogramming of host macrophages to increase their interleukin-10 production. Nat Med 15:42–49
71. Chen L, Tredget EE, Wu PY et al (2008) Paracrine factors of mesenchymal stem cells recruit macrophages and endothelial lineage cells and enhance wound healing. PLoS One 3, e1886
72. Zhang QZ, Su WR, Shi SH et al (2010) Human gingiva-derived mesenchymal stem cells elicit polarization of m2 macrophages and enhance cutaneous wound healing. Stem Cells 28:1856–1868
73. Kim J, Hematti P (2009) Mesenchymal stem cell-educated macrophages: a novel type of alternatively activated macrophages. Exp Hematol 37:1445–1453
74. Gonzalez MA, Gonzalez-Rey E, Rico L et al (2009) Adipose-derived mesenchymal stem cells alleviate experimental colitis by inhibiting

inflammatory and autoimmune responses. Gastroenterology 136:978–989

75. Porter KE, Turner NA (2009) Cardiac fibroblasts: at the heart of myocardial remodeling. Pharmacol Ther 123:255–278
76. van Amerongen MJ, Harmsen MC, van Rooijen N et al (2007) Macrophage depletion impairs wound healing and increases left ventricular remodeling after myocardial injury in mice. Am J Pathol 170:818–829
77. Cho DI, Kim MR, Jeong HY et al (2014) Mesenchymal stem cells reciprocally regulate the M1/M2 balance in mouse bone marrow-derived macrophages. Exp Mol Med 46, e70
78. Jung YJ, Ju SY, Yoo ES et al (2007) MSC-DC interactions: MSC inhibit maturation and migration of BM-derived DC. Cytotherapy 9:451–458
79. Spaggiari GM, Abdelrazik H, Becchetti F et al (2009) MSCs inhibit monocyte-derived DC maturation and function by selectively interfering with the generation of immature DCs: central role of MSC-derived prostaglandin E2. Blood 113:6576–6583
80. Chiesa S, Morbelli S, Morando S et al (2011) Mesenchymal stem cells impair in vivo T-cell priming by dendritic cells. Proc Natl Acad Sci U S A 108:17384–17389
81. DelaRosa O, Lombardo E, Beraza A et al (2009) Requirement of IFN-gamma-mediated indoleamine 2,3-dioxygenase expression in the modulation of lymphocyte proliferation by human adipose-derived stem cells. Tissue Eng Part A 15:2795–2806
82. Najar M, Raicevic G, Boufker HI et al (2010) Mesenchymal stromal cells use PGE2 to modulate activation and proliferation of lymphocyte subsets: combined comparison of adipose tissue, Wharton's Jelly and bone marrow sources. Cell Immunol 264:171–179
83. Ren G, Zhang L, Zhao X et al (2008) Mesenchymal stem cell-mediated immunosuppression occurs via concerted action of chemokines and nitric oxide. Cell Stem Cell 2:141–150
84. Chabannes D, Hill M, Merieau E et al (2007) A role for heme oxygenase-1 in the immunosuppressive effect of adult rat and human mesenchymal stem cells. Blood 110:3691–3694
85. Di Nicola M, Carlo-Stella C, Magni M et al (2002) Human bone marrow stromal cells suppress T-lymphocyte proliferation induced by cellular or nonspecific mitogenic stimuli. Blood 99:3838–3843
86. Uccelli A, Moretta L, Pistoia V (2008) Mesenchymal stem cells in health and disease. Nat Rev Immunol 8:726–736
87. Krampera M, Cosmi L, Angeli R et al (2006) Role for interferon-gamma in the immunomodulatory activity of human bone marrow mesenchymal stem cells. Stem Cells 24: 386–398
88. Corcione A, Benvenuto F, Ferretti E et al (2006) Human mesenchymal stem cells modulate B-cell functions. Blood 107:367–372
89. Merfeld-Clauss S, Gollahalli N, March KL et al (2010) Adipose tissue progenitor cells directly interact with endothelial cells to induce vascular network formation. Tissue Eng Part A 16:2953–2966
90. Traktuev DO, March KL, Tkachuk VA et al (2006) Adipose tissue stromal cells – multipotent cells with therapeutic potential for stimulation of angiogenesis in tissue ischemia. Kardiologiia 46:53–63
91. Makino S, Fukuda K, Miyoshi S et al (1999) Cardiomyocytes can be generated from marrow stromal cells in vitro. J Clin Invest 103:697–705
92. Li X, Yu X, Lin Q et al (2007) Bone marrow mesenchymal stem cells differentiate into functional cardiac phenotypes by cardiac microenvironment. J Mol Cell Cardiol 42:295–303
93. Augello A, De Bari C (2010) The regulation of differentiation in mesenchymal stem cells. Hum Gene Ther 21:1226–1238
94. Pijnappels DA, Schalij MJ, Ramkisoensing AA et al (2008) Forced alignment of mesenchymal stem cells undergoing cardiomyogenic differentiation affects functional integration with cardiomyocyte cultures. Circ Res 103:167–176
95. Genovese JA, Spadaccio C, Chachques E et al (2009) Cardiac pre-differentiation of human mesenchymal stem cells by electrostimulation. Front Biosci (Landmark Ed) 14:2996–3002
96. Wen L, Zhang C, Nong Y et al (2013) Mild electrical pulse current stimulation upregulates S100A4 and promotes cardiogenesis in MSC and cardiac myocytes coculture monolayer. Cell Biochem Biophys 65:43–55
97. Xu W, Zhang X, Qian H et al (2004) Mesenchymal stem cells from adult human bone marrow differentiate into a cardiomyocyte phenotype in vitro. Exp Biol Med (Maywood) 229:623–631
98. Hahn JY, Cho HJ, Kang HJ et al (2008) Pretreatment of mesenchymal stem cells with a combination of growth factors enhances gap junction formation, cytoprotective effect on cardiomyocytes, and therapeutic efficacy for myocardial infarction. J Am Coll Cardiol 51:33–943

99. Forte G, Minieri M, Cossa P et al (2006) Hepatocyte growth factor effects on mesenchymal stem cells: proliferation, migration, and differentiation. Stem Cells 24:23–33
100. Mohanty S, Bose S, Jain KG et al (2013) TGFbeta1 contributes to cardiomyogenic-like differentiation of human bone marrow mesenchymal stem cells. Int J Cardiol 163: 93–99
101. Li H, Yu B, Zhang Y et al (2006) Jagged1 protein enhances the differentiation of mesenchymal stem cells into cardiomyocytes. Biochem Biophys Res Commun 341: 320–325
102. Xu M, Wani M, Dai YS et al (2004) Differentiation of bone marrow stromal cells into the cardiac phenotype requires intercellular communication with myocytes. Circulation 110:2658–2665
103. Xie XJ, Wang JA, Cao J et al (2006) Differentiation of bone marrow mesenchymal stem cells induced by myocardial medium under hypoxic conditions. Acta Pharmacol Sin 27:1153–1158
104. Toma C, Pittenger MF, Cahill KS et al (2002) Human mesenchymal stem cells differentiate to a cardiomyocyte phenotype in the adult murine heart. Circulation 105:93–98
105. Rota M, Kajstura J, Hosoda T et al (2007) Bone marrow cells adopt the cardiomyogenic fate in vivo. Proc Natl Acad Sci U S A 104:17783–17788
106. Wagers AJ, Weissman IL (2004) Plasticity of adult stem cells. Cell 116:639–648
107. Wei F, Wang TZ, Zhang J et al (2012) Mesenchymal stem cells neither fully acquire the electrophysiological properties of mature cardiomyocytes nor promote ventricular arrhythmias in infarcted rats. Basic Res Cardiol 107:274
108. Rose RA, Jiang H, Wang X et al (2008) Bone marrow-derived mesenchymal stromal cells express cardiac-specific markers, retain the stromal phenotype, and do not become functional cardiomyocytes in vitro. Stem Cells 26:2884–2892
109. Silva GV, Litovsky S, Assad JA et al (2005) Mesenchymal stem cells differentiate into an endothelial phenotype, enhance vascular density, and improve heart function in a canine chronic ischemia model. Circulation 111:150–156
110. Hatzistergos KE, Quevedo H, Oskouei BN et al (2010) Bone marrow mesenchymal stem cells stimulate cardiac stem cell proliferation and differentiation. Circ Res 107(7):913–922
111. Wang T, Xu Z, Jiang W et al (2006) Cell-to-cell contact induces mesenchymal stem cell to differentiate into cardiomyocyte and smooth muscle cell. Int J Cardiol 109:74–81
112. Jazayeri M, Allameh A, Soleimani M et al (2008) Molecular and ultrastructural characterization of endothelial cells differentiated from human bone marrow mesenchymal stem cells. Cell Biol Int 32:1183–1192
113. Li Q, Xu X, Wang Z et al (2007) Investigation of canine mesenchymal stem cells differentiation to vascular endothelial cell in vitro. Sheng Wu Yi Xue Gong Cheng Xue Za Zhi 24:1348–1351
114. Oswald J, Boxberger S, Jorgensen B et al (2004) Mesenchymal stem cells can be differentiated into endothelial cells in vitro. Stem Cells 22:377–384
115. Martens TP, See F, Schuster MD et al (2006) Mesenchymal lineage precursor cells induce vascular network formation in ischemic myocardium. Nat Clin Pract Cardiovasc Med 3(Suppl 1):S18–S22
116. Kinnaird T, Stabile E, Burnett MS et al (2004) Local delivery of marrow-derived stromal cells augments collateral perfusion through paracrine mechanisms. Circulation 109: 1543–1549
117. Oskowitz A, McFerrin H, Gutschow M et al (2011) Serum-deprived human multipotent mesenchymal stromal cells (MSCs) are highly angiogenic. Stem Cell Res 6:215–225
118. Tang YL, Zhao Q, Zhang YC et al (2004) Autologous mesenchymal stem cell transplantation induce VEGF and neovascularization in ischemic myocardium. Regul Pept 117: 3–10
119. Rubina K, Kalinina N, Efimenko A et al (2009) Adipose stromal cells stimulate angiogenesis via promoting progenitor cell differentiation, secretion of angiogenic factors, and enhancing vessel maturation. Tissue Eng Part A 15:2039–2050
120. Tang J, Xie Q, Pan G et al (2006) Mesenchymal stem cells participate in angiogenesis and improve heart function in rat model of myocardial ischemia with reperfusion. Eur J Cardiothorac Surg 30:353–361
121. Markel TA, Wang Y, Herrmann JL et al (2008) VEGF is critical for stem cell-mediated cardioprotection and a crucial paracrine factor for defining the age threshold in adult and neonatal stem cell function. Am J Physiol Heart Circ Physiol 295:H2308–H2314
122. Yoon CH, Koyanagi M, Iekushi K et al (2010) Mechanism of improved cardiac function after

bone marrow mononuclear cell therapy: role of cardiovascular lineage commitment. Circulation 121(18):2001–2011

123. Gomes SA, Rangel EB, Premer C et al (2013) S-nitrosoglutathione reductase (GSNOR) enhances vasculogenesis by mesenchymal stem cells. Proc Natl Acad Sci U S A 110:2834–2839
124. Traktuev DO, Merfeld-Clauss S, Li J et al (2008) A population of multipotent CD34-positive adipose stromal cells share pericyte and mesenchymal surface markers, reside in a periendothelial location, and stabilize endothelial networks. Circ Res 102:77–85
125. Ranganath SH, Levy O, Inamdar MS et al (2012) Harnessing the mesenchymal stem cell secretome for the treatment of cardiovascular disease. Cell Stem Cell 10:244–258
126. Strauer BE, Steinhoff G (2011) 10 years of intracoronary and intramyocardial bone marrow stem cell therapy of the heart: from the methodological origin to clinical practice. J Am Coll Cardiol 58:1095–1104
127. Song H, Song BW, Cha MJ et al (2010) Modification of mesenchymal stem cells for cardiac regeneration. Expert Opin Biol Ther 10:309–319
128. Frisch SM, Francis H (1994) Disruption of epithelial cell-matrix interactions induces apoptosis. J Cell Biol 124:619–626
129. Meredith JE, Fazeli B, Schwartz MA (1993) The extracellular matrix as a cell survival factor. Mol Biol Cell 4:953–961
130. Assis AC, Carvalho JL, Jacoby BA et al (2010) Time-dependent migration of systemically delivered bone marrow mesenchymal stem cells to the infarcted heart. Cell Transplant 19:219–230
131. Zhang XY, La Russa VF, Bao L et al (2002) Lentiviral vectors for sustained transgene expression in human bone marrow-derived stromal cells. Mol Ther 5:555–565
132. Gnecchi M, He H, Liang OD et al (2005) Paracrine action accounts for marked protection of ischemic heart by Akt-modified mesenchymal stem cells. Nat Med 11:367–368
133. Mangi AA, Noiseux N, Kong D et al (2003) Mesenchymal stem cells modified with Akt prevent remodeling and restore performance of infarcted hearts. Nat Med 9:1195–1201
134. Li W, Ma N, Ong LL et al (2007) Bcl-2 engineered MSCs inhibited apoptosis and improved heart function. Stem Cells 25:2118–2127
135. Song H, Kwon K, Lim S et al (2005) Transfection of mesenchymal stem cells with the FGF-2 gene improves their survival under hypoxic conditions. Mol Cells 19:402–407
136. Yang J, Zhou W, Zheng W et al (2007) Effects of myocardial transplantation of marrow mesenchymal stem cells transfected with vascular endothelial growth factor for the improvement of heart function and angiogenesis after myocardial infarction. Cardiology 107:17–29
137. Tang YL, Tang Y, Zhang YC et al (2005) Improved graft mesenchymal stem cell survival in ischemic heart with a hypoxia-regulated heme oxygenase-1 vector. J Am Coll Cardiol 46:1339–1350
138. Cheng Z, Ou L, Zhou X et al (2008) Targeted migration of mesenchymal stem cells modified with CXCR4 gene to infarcted myocardium improves cardiac performance. Mol Ther 16:571–579
139. Huang J, Zhang Z, Guo J et al (2010) Genetic modification of mesenchymal stem cells overexpressing CCR1 increases cell viability, migration, engraftment, and capillary density in the injured myocardium. Circ Res 106:1753–1762
140. Song H, Chang W, Lim S et al (2007) Tissue transglutaminase is essential for integrin-mediated survival of bone marrow-derived mesenchymal stem cells. Stem Cells 25:1431–1438
141. Kanashiro-Takeuchi RM, Schulman IH, Hare JM (2011) Pharmacologic and genetic strategies to enhance cell therapy for cardiac regeneration. J Mol Cell Cardiol 51:619–625
142. Behfar A, Yamada S, Crespo-Diaz R et al (2010) Guided cardiopoiesis enhances therapeutic benefit of bone marrow human mesenchymal stem cells in chronic myocardial infarction. J Am Coll Cardiol 56:721–734
143. Ray R, Novotny NM, Crisostomo PR et al (2008) Sex steroids and stem cell function. Mol Med 14:493–501
144. Yang YJ, Qian HY, Huang J et al (2008) Atorvastatin treatment improves survival and effects of implanted mesenchymal stem cells in post-infarct swine hearts. Eur Heart J 29:1578–1590
145. Li N, Zhang Q, Qian H et al (2014) Atorvastatin induces autophagy of mesenchymal stem cells under hypoxia and serum deprivation conditions by activating the mitogen-activated protein kinase/extracellular signal-regulated kinase pathway. Chin Med J (Engl) 127:1046–1051
146. Haider H, Lee YJ, Jiang S et al (2010) Phosphodiesterase inhibition with tadalafil

provides longer and sustained protection of stem cells. Am J Physiol Heart Circ Physiol 299:H1395–H1404

147. Chacko SM, Ahmed S, Selvendiran K et al (2010) Hypoxic preconditioning induces the expression of prosurvival and proangiogenic markers in mesenchymal stem cells. Am J Physiol Cell Physiol 299:C1562–C1570
148. Hu X, Yu SP, Fraser JL et al (2008) Transplantation of hypoxia-preconditioned mesenchymal stem cells improves infarcted heart function via enhanced survival of implanted cells and angiogenesis. J Thorac Cardiovasc Surg 135:799–808
149. Katritsis DG, Sotiropoulou P, Giazitzoglou E et al (2007) Electrophysiological effects of intracoronary transplantation of autologous mesenchymal and endothelial progenitor cells. Europace 9:167–171
150. Chen SL, Fang WW, Ye F et al (2004) Effect on left ventricular function of intracoronary transplantation of autologous bone marrow mesenchymal stem cell in patients with acute myocardial infarction. Am J Cardiol 94:92–95
151. Hare JM, Traverse JH, Henry TD et al (2009) A randomized, double-blind, placebo-controlled, dose-escalation study of intravenous adult human mesenchymal stem cells (prochymal) after acute myocardial infarction. J Am Coll Cardiol 54:2277–2286
152. Mohyeddin-Bonab M, Mohamad-Hassani MR, Alimoghaddam K et al (2007) Autologous in vitro expanded mesenchymal stem cell therapy for human old myocardial infarction. Arch Iran Med 10:467–473
153. Karantalis V, DiFede DL, Gerstenblith G et al (2014) Autologous mesenchymal stem cells produce concordant improvements in regional function, tissue perfusion, and fibrotic burden when administered to patients undergoing coronary artery bypass grafting: The Prospective Randomized Study of Mesenchymal Stem Cell Therapy in Patients Undergoing Cardiac Surgery (PROMETHEUS) trial. Circ Res 114:1302–1310
154. Heldman AW, DiFede DL, Fishman JE et al (2014) Transendocardial mesenchymal stem cells and mononuclear bone marrow cells for ischemic cardiomyopathy: the TAC-HFT randomized trial. JAMA 311:62–73
155. Trachtenberg B, Velazquez DL, Williams AR et al (2011) Rationale and design of the transendocardial injection of autologous human cells (bone marrow or mesenchymal) in chronic ischemic left ventricular dysfunction and heart failure secondary to myocardial infarction (TAC-HFT) trial: a randomized, double-blind, placebo-controlled study of safety and efficacy. Am Heart J 161:487–493
156. Williams AR, Trachtenberg B, Velazquez DL et al (2011) Intramyocardial stem cell injection in patients with ischemic cardiomyopathy: functional recovery and reverse remodeling. Circ Res 108:792–796
157. Anastasiadis K, Antonitsis P, Doumas A et al (2012) Stem cells transplantation combined with long-term mechanical circulatory support enhances myocardial viability in end-stage ischemic cardiomyopathy. Int J Cardiol 155:e51–e53
158. Suncion VY, Ghersin E, Fishman JE et al (2014) Does transendocardial injection of mesenchymal stem cells improve myocardial function locally or globally? An analysis from the percutaneous stem cell injection delivery effects on neomyogenesis (POSEIDON) randomized trial. Circ Res 114:1292–1301
159. Lee JW, Lee SH, Youn YJ et al (2014) A randomized, open-label, multicenter trial for the safety and efficacy of adult mesenchymal stem cells after acute myocardial infarction. J Korean Med Sci 29:23–31
160. Abedin M, Tintut Y, Demer LL (2004) Mesenchymal stem cells and the artery wall. Circ Res 95:671–676
161. Hsu YC, Pasolli HA, Fuchs E (2011) Dynamics between stem cells, niche, and progeny in the hair follicle. Cell 144:92–105
162. Chimenti I, Gaetani R, Barile L et al (2012) Isolation and expansion of adult cardiac stem/progenitor cells in the form of cardiospheres from human cardiac biopsies and murine hearts. Methods Mol Biol 879: 327–338
163. Smith RR, Barile L, Cho HC et al (2007) Regenerative potential of cardiosphere-derived cells expanded from percutaneous endomyocardial biopsy specimens. Circulation 115:896–908
164. Karantalis V, Balkan W, Schulman IH et al (2012) Cell-based therapy for prevention and reversal of myocardial remodeling. Am J Physiol Heart Circ Physiol 303:H256–H270
165. Carr CA, Stuckey DJ, Tan JJ et al (2011) Cardiosphere-derived cells improve function in the infarcted rat heart for at least 16 weeks—an MRI study. PLoS One 6, e25669
166. Lee ST, White AJ, Matsushita S et al (2011) Intramyocardial injection of autologous cardiospheres or cardiosphere-derived cells

preserves function and minimizes adverse ventricular remodeling in pigs with heart failure post-myocardial infarction. J Am Coll Cardiol 57:455–465

167. Li TS, Cheng K, Malliaras K et al (2012) Direct comparison of different stem cell types and subpopulations reveals superior paracrine potency and myocardial repair efficacy with cardiosphere-derived cells. J Am Coll Cardiol 59:942–953
168. Malliaras K, Li TS, Luthringer D et al (2012) Safety and efficacy of allogeneic cell therapy in infarcted rats transplanted with mismatched cardiosphere-derived cells. Circulation 125:100–112
169. Makkar RR, Smith RR, Cheng K et al (2012) Intracoronary cardiosphere-derived cells for heart regeneration after myocardial infarction (CADUCEUS): a prospective, randomised phase 1 trial. Lancet 379:895–904
170. Williams AR, Hatzistergos KE, Addicott B et al (2013) Enhanced effect of combining human cardiac stem cells and bone marrow mesenchymal stem cells to reduce infarct size and to restore cardiac function after myocardial infarction. Circulation 127:213–223
171. Mureli S, Gans CP, Bare DJ et al (2013) Mesenchymal stem cells improve cardiac conduction by upregulation of connexin 43 through paracrine signaling. Am J Physiol Heart Circ Physiol 304:H600–H609
172. Nowbar AN, Mielewczik M, Karavassilis M et al (2014) Discrepancies in autologous bone marrow stem cell trials and enhancement of ejection fraction (DAMASCENE): weighted regression and meta-analysis. BMJ 348:g2688
173. van Berlo JH, Kanisicak O, Maillet M et al (2014) c-kit cells minimally contribute cardiomyocytes to the heart. Nature 509(7500): 337–341

Chapter 5

Mesenchymal Stem Cells in Kidney Repair

Marina Morigi, Cinzia Rota, and Giuseppe Remuzzi

Abstract

Every year 13.3 million people suffer acute kidney injury (AKI), which is associated with a high risk of death or development of long-term chronic kidney disease (CKD) in a substantial percentage of patients besides other organ dysfunctions. To date, the mortality rate per year for AKI exceeds 50 % at least in patients requiring early renal replacement therapy and is higher than the mortality for breast and prostate cancer, heart failure and diabetes combined.

Until now, no effective treatments able to accelerate renal recovery and improve survival post AKI have been developed. In search of innovative and effective strategies to foster the limited regeneration capacity of the kidney, several studies have evaluated the ability of mesenchymal stem cells (MSCs) of different origin as an attractive therapeutic tool. The results obtained in several models of AKI and CKD document that MSCs have therapeutic potential in repair of renal injury, preserving renal function and structure thus prolonging animal survival through differentiation-independent pathways. In this chapter, we have summarized the mechanisms underlying the regenerative processes triggered by MSC treatment, essentially due to their paracrine activity. The capacity of MSC to migrate to the site of injury and to secrete a pool of growth factors and cytokines with anti-inflammatory, mitogenic, and immunomodulatory effects is described. New modalities of cell-to-cell communication via the release of microvesicles and exosomes by MSCs to injured renal cells will also be discussed. The translation of basic experimental data on MSC biology into effective care is still limited to preliminary phase I clinical trials and further studies are needed to definitively assess the efficacy of MSC-based therapy in humans.

Key words MSCs, Tissue regeneration, Kidney, AKI, CKD, Tubules, Glomeruli, Growth factors, Paracrine effect

1 Introduction

The promise of novel stem cell-based therapies for tissue regeneration in intractable diseases and in many other disease conditions has inspired great hope and expectations. In the last years, the unceasing demand of patients and their families has piqued the proliferation of institutions, working often outside the standard clinical trial network, that have performed ineffective and potentially dangerous stem cell treatments without an underlying scientific foundation. The International Society for Stem Cell Research (ISSCR) Task Force on Unproven Stem Cell Treatments

Massimiliano Gnecchi (ed.), *Mesenchymal Stem Cells: Methods and Protocols*, Methods in Molecular Biology, vol. 1416,
DOI 10.1007/978-1-4939-3584-0_5,

was convened in 2010 to delineate the development of web-based resources for patients searching for information on advertised stem cell therapy [1]. The Task Force proposed an inquiry and review process for clinics and suppliers promising therapeutic benefits from the administration of preparations claimed to contain stem cells or derivatives [1]. The pressure to identify new therapeutic indications for the use of stem cells has stimulated numerous clinical trials; however, the lack of clear preclinical results and the absence of systematic approaches have made it difficult to obtain unequivocal proof of clinical benefit. More than 4000 clinical trials employing stem cells of different origin are listed in the website www.clinicaltrials.gov with more than 1750 open studies [2] (Fig. 1). So far, the majority of open trials refers to transplantation of bone marrow (BM)-derived hematopoietic stem cells for the cure of several hematological disorders and hundreds of other trials are testing the safety and effectiveness of BM-mesenchymal stem cells (MSCs) [2], in different diseases such as osteogenesis imperfecta, graft-versus-host disease, Crohn's disease, Hurler syndrome, fracture healing, and bone marrow engraftment. One of the most relevant testing grounds for evaluating the regenerative potential of stem cell therapy rests on studies in acute and chronic cardiovascular diseases [3]. These trials suggested that treatment with stem cells of different origin, including BM cells, were safe but efficacy was very limited [4]. A recent report by Nowbar and colleagues [5] highlights a significant association between the number of discrepancies in 49 randomized controlled trials of autologous BM stem cell therapy in

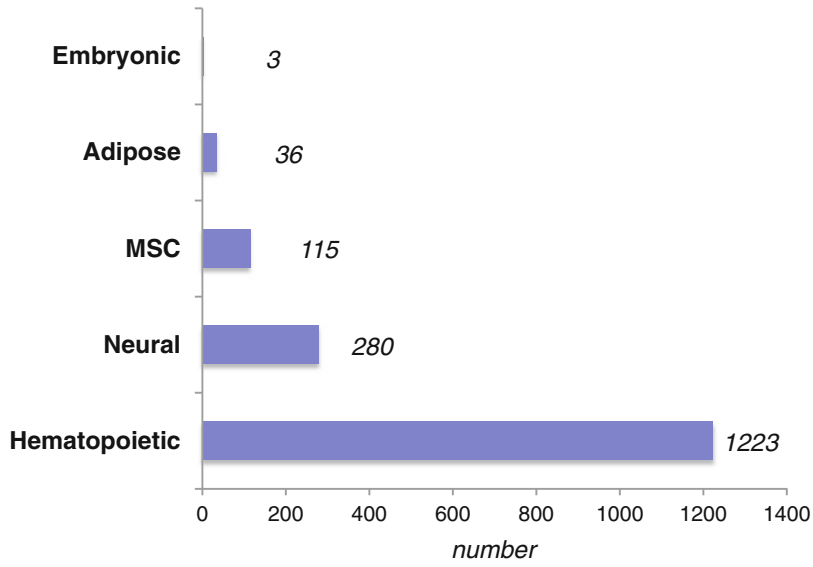

Fig. 1 Stem cell types employed in ongoing clinical trials. Histograms indicating the number of clinical trials testing stem cells of different origin are listed at the website www.clinicaltrials.gov

patients with heart disease and the reported improvement of ejection fraction effect size. Of note, in five trials without errors, the effect of BM cell therapy on ejection fraction was completely absent. In this context, many challenges and technical barriers including cell type, route of administration, timing of intervention, and cell number must be overcome in experimental models before translation of stem cell therapy to the clinic [2, 6].

The use of stem cells as a cure for acute kidney injury (AKI) and chronic kidney diseases (CKD) began in the last decade with pioneering preclinical studies describing the ability of BM-derived cells to regenerate several renal compartments including tubular cells [7], glomerular podocytes, mesangial and endothelial cells [8, 9]. In this chapter, the therapeutic role of MSCs obtained from BM and from other tissues in promoting renal repair and tissue regeneration will be discussed.

2 Mesenchymal Stem Cells

Mesenchymal stem cells (MSCs) were initially identified in the BM by Friedenstein in the 1960s and 1970s; he demonstrated their intrinsic osteogenic potential as documented by heterotopic ossicle generation [10]. The nomenclature for these cells ranges from MSCs which is an alternative to multipotent mesenchymal stromal cells—recommended by the International Society for Cellular Therapy [11]—or, more stringently, to skeletal stem cells [12, 13]. BM-MSCs represent a rare heterogeneous population (0.1–0.001 %) of multipotent cells capable of differentiating into cells of mesodermal lineages such as osteocytes, adipocytes, and chondrocytes [12]. BM-MSCs have been described as spindle-shape, clonogenic cells, able to regulate the self-renewal, maturation, quiescence, and recruitment of hematopoietic stem cells to the vascular compartment through the release of cytokines and growth factors [14]. MSCs were originally isolated from bone marrow; nevertheless, populations of stem cells with a similar phenotype have been identified also in various fetal and adult tissues like placenta, amniotic fluid (AF), umbilical cord blood (CB), Wharton's jelly (WJ), and adipose tissue (AD) [12, 15]. MSCs with similar phenotype have been described to have different gene expression profiles. For example, BM-MSCs and CB-MSCs share a considerable number of transcripts, but CB-MSCs express angiogenic and matrix remodeling genes to a higher extent with respect to BM-MSCs [16]. The finding that MSCs exhibit cell surface markers that are identical to those expressed by pericytes (perivascular cells are present in multiple organs including the kidney) suggest that MSCs are ubiquitous and possibly stabilize the microvascular environment [17, 18].

Even though MSCs are not identified by unique and specific markers, the International Society for Cellular Therapy (ISCT) has proposed a set of standards to define human MSCs including adherence to plastic in culture, fibroblastoid appearance, and multipotency [11]. MSCs are negative for the hematopoietic markers CD45, CD34, and CD14, for the co-stimulatory molecules CD80, CD86, and CD40, and they do not express major histocompatibility complex (MHC) class II. Whereas MSCs are positive for CD105, CD73, CD44, CD90, and CD71 [14]. However, the lack of a marker that unambiguously identifies MSCs in different tissues raises the possibility that the environment in which MSCs reside could influence the cell characteristics [12].

MSC release a broad repertoire of trophic and regulatory proteins including growth factors, proteinases, hormones, cytokines, chemokines referred to as the MSC secretome [3]. It is now generally accepted that MSCs exert their therapeutic effect through the release of these bioactive molecules, which are able to counteract inflammation and to support regeneration of damaged tissue [19]. Moreover, the study of MSC biology has revealed that the release of factors by MSC may be influenced by cytokines produced by resident cells at the site of injury, suggesting that MSCs might be considered as an "intelligent," site-specific multidrug released system [20]. A complete list of MSC-secreted proteins remains to be generated, however several studies using different proteomic techniques have identified the main trophic factors responsible for the MSC therapeutic effect. Extracellular matrix proteins and proteins involved in cell adhesion (Collagen α-1 and α-2 chains, Fibronectin, and Vitronectin), enzymes involved in matrix remodeling such as metalloproteinase (MMP1, MMP2), and metalloproteinase inhibitor (TIMP1, TIMP2) are secreted by MSCs [21] (Fig. 2). Moreover, MSCs are able to produce a large amount of growth factors with anti-apoptotic, pro-survival, and mitogenic effects, for example, fibroblast growth factor (FGF)-II, basic nerve growth factor (bNGF), insulin-like growth factor (IGF)-1, brain-derived neurotrophic factor (BDNF), glial cell line-derived neurotrophic factor (GDNF), platelet-derived growth factor (PDGF)-AB, vascular endothelial growth factor (VEGF), hepatocyte growth factors (HGF), and epidermal growth factor (EGF) [3, 21, 22] (Fig. 2). The MSC secretion profile also includes cytokines and chemokines such as stromal cell-derived factor-1 (SDF-1), interleukin-10 (IL-10), and IL-8 [21]. It has been documented that MSCs secrete high levels of angiogenic factors including angiopoietin-1 (Ang-1), monocyte chemoattractant protein-1 (MCP-1), interleukin-6 (IL-6), and placental growth factor (PLGF) [23] (Fig. 2).

MSCs also exert strong anti-inflammatory and immunomodulatory effects acting on the main immune cell subsets. While MSCs express MHC class I but not MHC class II, the immunosuppressive role of MSCs is independent of the expression of MHC class I

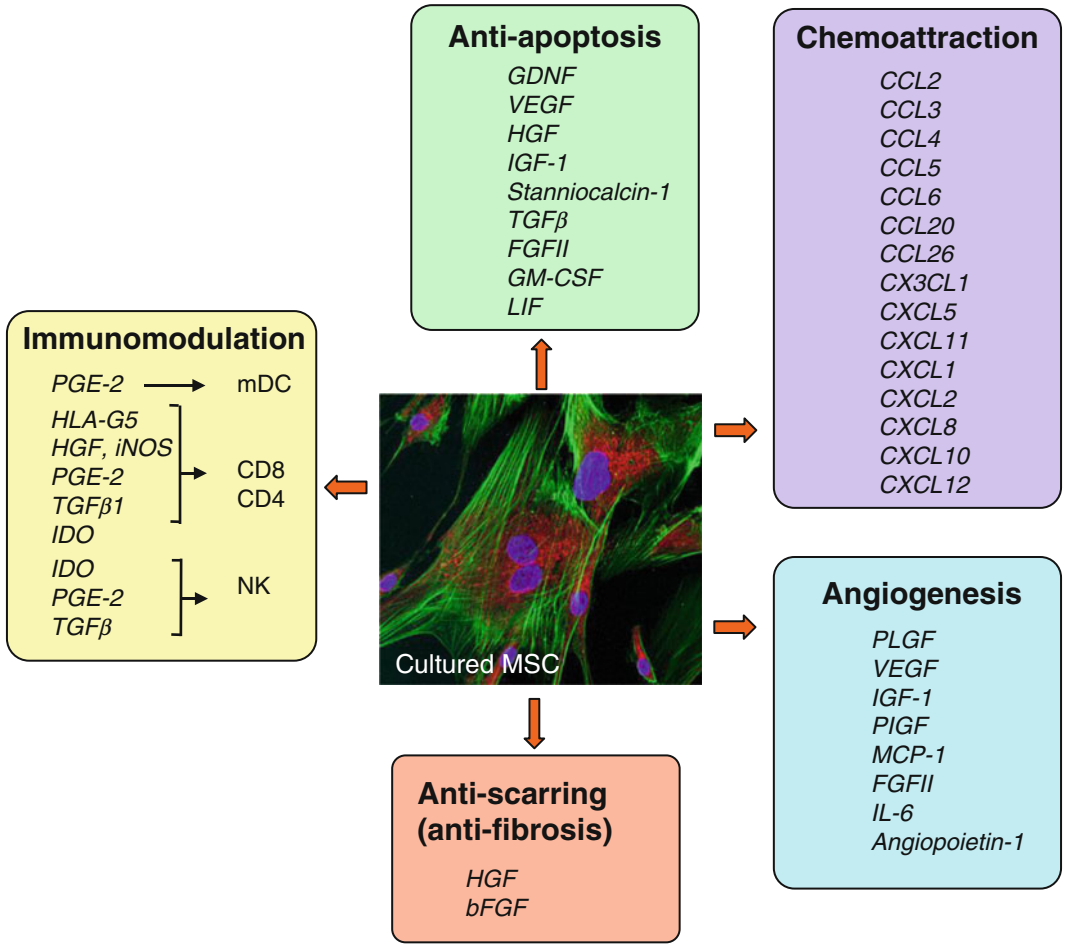

Fig. 2 Proposed MSC mechanism of action. The therapeutic effect of MSCs is credited to a paracrine mechanism based on immunomodulatory, anti-apoptotic, angiogenic, anti-fibrotic, and chemoattractant activity. MSCs release factors such as PGE-2, HLA-G5, HGF, iNOS, IDO, TGF-b, and IL-10 that inhibit the proliferation of CD8+ and CD4+ T lymphocytes, natural killer (NK) cells, and regulatory T cells, and block the maturation of dendritic cells (DCs). Moreover, MSCs exert an anti-apoptotic effect via the production of growth factors such as VEGF, HGF, and IGF-I. In addition, MSCs stimulate local angiogenesis by secreting VEGF, IGF-1, PIGF, MCP-1, bFGF, and IL-6. HGF and bFGF contribute to fibrosis inhibition and several chemokines released by MSCs are responsible for leukocyte migration to the injured area, which is important in normal tissue maintenance

and II molecules [24]. MSCs are also able to alter T-cell effector functions [25] and to suppress T-lymphocyte proliferation and activation in co-culture experiments [26]. Moreover, several in vitro and in vivo studies have documented the ability of MSCs to promote a regulatory phenotype within both adaptive and innate immune cells [27]. This immune regulatory role is due to the capacity of MSCs to release immunosuppressive factors including transforming growth factor beta (TGFβ), prostaglandin E2 (PGE2), nitric oxide (NO), interleukin (IL)-10, indoleamine

2,3-dioxygenase (IDO), and human leukocyte antigen-G5 (HLAG-5) able to induce T-cell suppression and Treg expansion; whereas IL-6, macrophage colony-stimulating factor (M-CSF) in addition to PGE2 and IL-10 are able to suppress antigen-presenting cell (APC) maturation [28] (Fig. 2). Evidence is now emerging that the local microenvironment activates the MSC immunosuppressive effect. Indeed, the above indicated soluble factors are minimally expressed in resting MSCs unless they are activated by several inflammatory cytokines [28].

Although the role of MSCs on T lymphocytes, B lymphocytes, natural killer cells, and dendritic cells has been extensively investigated, very little is known about the MSC–macrophage interaction. Classical proinflammatory M1 macrophages exhibit potent antimicrobial properties and are characterized by the promotion of a Th1 response. In contrast, alternatively activated M2 macrophages secrete less proinflammatory cytokines and are thought to be involved in the resolution of tissue inflammation apart from having immunoregulatory functions [29]. Depending on the microenvironment, macrophages can shift their phenotype to support specific functional activities relevant to different phases of inflammation [29]. Kim and coworkers observed that macrophages (M1) when co-cultured with MSCs exhibit a high level of CD206, a marker of alternatively activated M2 macrophages which express a high level of IL-6 and low level of TNF-α, suggesting that MSCs can shift the macrophage phenotype from an inflammatory to an anti-inflammatory phenotype [29].

Besides their ability to release soluble factors in the microenvironment, MSCs are able to produce more complex structures called microvesicles (MVs) and exosomes (Exo), responsible for the intercellular communication between MSCs and target cells [30, 31]. Exosomes are membrane fragments of 30–90 nm diameter derived from the endosomal membrane compartment after fusion of secretory granules with the plasma membrane [32, 33]. Microvesicles are relatively large vesicles (100 nm to 1 mm diameter) released from the surface membrane of activated cells [32, 33]. MSC-derived MVs and Exo have been identified as a novel mechanism of cell-to-cell communication that allows transfer of membrane receptors, functional proteins, mRNA, microRNA, and organelles (e.g., mitochondria) between cells [32].

3 Mesenchymal Stem Cell-Based Therapy in Acute Kidney Injury

3.1 Acute Kidney Injury

Acute kidney injury (AKI) is a common clinical problem with increasing incidence, serious consequences, unsatisfactory therapeutic options, and an enormous financial burden to society [34]. AKI is a complex disorder that comprises multiple causative factors and occurs with varied clinical manifestations that range from minimal, but sustained elevation in serum creatinine to anuric renal failure.

The incidence of AKI in hospitalized patients has generally been reported to be in the 2–7 % range, with an incidence of 5–10 % in intensive care unit (ICU) patients. Despite advances in preventive strategies and support measures, the incidence of AKI has remained stable, probably due to the therapeutic use of new more aggressive nephrotoxic drugs, more invasive procedures, and increasing age of the patient population. Moreover, AKI has remained associated with high morbidity and mortality, particularly in ICU patients, where mortality rates may exceed 50 %. In addition, patients that survive their acute illness may develop or exacerbate chronic kidney disease [35].

In the last 20 years, there have been extensive advances in the study of AKI pathophysiology, however so far this effort has not translated into an effective pharmacological treatment able to improve survival after an AKI episode. Numerous pharmacological agents have been tested with successful results in preventing or ameliorating experimental AKI [36]. However, treatments with dopamine, furosemide, mannitol, calcium channel blockers, atrial natriuretic peptide, and several other hormonal or pharmacological substances have failed to be successfully translated into clinical practice [37, 38]. AKI is classically characterized by the rapid deterioration of renal function, with at least a 50 % decrease in glomerular filtration rate (GFR) that leads to accumulation of nitrogenous waste such as blood urea nitrogen (BUN) and creatinine [34]. The most common cause of AKI is acute tubular necrosis (ATN) induced by an ischemic or toxic insult. ATN is characterized by a rapid dysfunction and loss of tubular epithelial cell integrity and polarity, with shedding of the proximal tubule brush border, mislocalization of adhesion molecules, and other membrane proteins such as sodium/potassium ATPase [39, 40]. Detachment of injured and necrotic tubular cells from the tubular basement membrane can lead to the obstruction of the tubular lumen, causing an increase in intratubular pressure with a consequent “backleak” of the filtrate [39, 40]. The kidney, in a physiological setting, shows a limited capacity of cell turnover, whereas after injury, tubular cell proliferation can lead to tissue regeneration [41]. In animal models, it has been observed that recovery depends strictly on the replacement of damaged and/or dead epithelium with a new functioning one and on the regenerative potential of surviving tubular cells. One major limitation to restoring structural integrity is the number of surviving cells. Therapeutic strategies to direct the replacement of damaged cells should consider the local supply of new cells.

3.2 Role of Mesenchymal Stem Cells in Acute Kidney Injury

In the attempt to find innovative interventions able to potentiate the regenerative ability of the kidney, MSCs have been studied for their potential to repair acutely damaged tissues in virtue of their trophic, anti-inflammatory, and pro-survival activity [42–48].

In this context our group was the first to demonstrate the renoprotective effect of BM-MSCs. We observed that intravenous injection of murine BM-MSCs protected renal function and structure in mice with AKI induced by the nephrotoxic antitumor drug cisplatin [49]. Murine BM-MSCs limited tubular damage and accelerated proliferation of tubular cells in virtue of their tropism for the damaged kidney [49]. The finding that MSCs can protect renal tubules from acute injury has been supported by data obtained in different models of AKI. Herrera et al. showed, in a glycerol-induced murine rhabdomyolysis model of AKI, that MSCs engrafted in the damaged kidney, promoting morphological and functional recovery [50]. In an experimental model of ischemia/reperfusion injury, Togel and co-workers confirmed the renoprotective capacity of MSCs [51]. The study showed that intracarotid administration of MSCs either immediately or 24 h after renal ischemia resulted in a significant improvement of renal function. However, MSCs were only transiently present in the renal vasculature, and were not detected within the renal parenchyma for up to 3 days after infusion. Examination of gene expression in the kidneys of MSC-treated rats revealed a decrease in proinflammatory cytokines and an increase in several growth factors with mitogenic, pro-survival, and anti-apoptotic effects [51].

Of importance for future treatment prospects, our group has demonstrated the renoprotective effect of human BM-derived MSCs upon infusion in immunodeficient mice with AKI induced by cisplatin [52]. Human BM-MSC injection in cisplatin NOD/SCID mice decreased proximal tubular epithelial cell injury and ameliorated the deficit in renal function, resulting in reduced recipient mortality [52]. Human BM-MSCs were predominantly localized in peritubular areas and acted by reducing renal cell apoptosis and increasing tubular cell proliferation. Moreover, human BM-MSCs reduced leukocyte infiltration preserving microvascular integrity and contributing to improved renal tissue oxygenation [52].

Although bone marrow represents the most common tissue source of MSCs, harvesting BM stem cells is invasive and their number, frequency, differentiation potential, and lifespan decline with the age of the donor. Therefore, the search for new sources of more accessible MSCs, with similar surface expression patterns, is of significant value. For this purpose our group tested the renoprotective effect of human MSCs isolated from adipose tissue (AD), umbilical cord blood (CB), and amniotic fluid (AF) [53, 54]. We studied the effect of human AD-MSCs, isolated from two different donors, in NOD/SCID mice with cisplatin-induced AKI and we observed that human stem cells failed to improve renal function and damage. Conversely, in an experimental model of AKI induced by cisplatin, Kim and coworkers reported that infusion of human AD-MSCs and the corresponding conditioned

medium ameliorated renal function and structure, increasing animal survival. Moreover, human AD-MSCs were able to reduce renal tubular cell apoptosis and inflammation exerting a paracrine-protective effect [55]. Recently, Katsuno et al. demonstrated that human adipose tissue-derived stromal cells (ASCs) cultured in low (2 %) serum (LASCs) secreted high levels of growth factors such as HGF and VEGF with respect to human ASCs cultured in high (20 %) serum [56]. Moreover, when injected in rats with AKI induced by folic acid, human LASCs were able to attenuate renal damage and interstitial fibrosis via a paracrine effect and no evidence of transdifferentiation was observed [56].

Mesenchymal stem cells can be also obtained from umbilical cord. In particular, several studies have indicated that cord blood is an alternative and extremely rich reservoir of MSCs [57–60] and represents a potentially unlimited source of stem cells. Its collection is non-invasive and relatively simple to process and store [61]. Our group has documented that systemic infusion of human CB-MSCs in NOD/SCID mice with cisplatin-induced AKI protected animals from renal function impairment and tubular injury (Fig. 3). Similarly to human BM-MSCs, injected human CB-MSCs reduced tubular cell apoptosis and induced tubular cell proliferation. The renoprotective effect of human CB-MSCs was further confirmed by their ability to inhibit oxidative damage [53]. Of note, human CB-MSCs markedly prolonged animal survival to a more significant extent than other stem cells studied [53]. Recently, other groups have

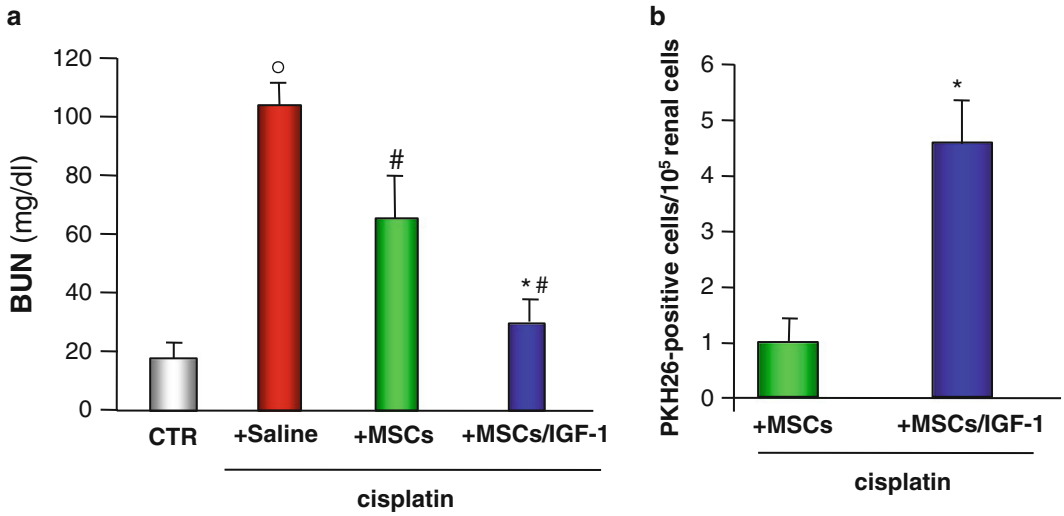

Fig. 3 Preconditioning of BM-MSCs with IGF-1 enhances the therapeutic effect of mouse BM-MSCs and increases their engraftment in mice with cisplatin-induced AKI. (**a**) Renal function evaluated as blood urea nitrogen (BUN) in control (CTR) mice and AKI mice receiving an intravenous injection of saline, unstimulated MSCs or IGF-1-treated MSCs. (**b**) Quantification of engrafted PKH26-positive MSCs in cisplatin-injured renal tissue at 4 days. Data are means ± SEM. *$p < 0.05$ versus MSCs, #$p < 0.05$ versus CTR, #$p < 0.05$ versus saline

investigated the therapeutic effect of MSCs isolated from Wharton's Jelly (WJ-MSCs) in different experimental models of AKI. In an experimental model of ischemia/reperfusion injury, human WJ-MSCs improved renal function, increasing renal tubular cell proliferation and reducing apoptotic events [62]. In parallel, in an experimental model of AKI induced by folic acid, Fang et al. showed that early administration of human WJ-MSCs ameliorated renal function as well as tubular injury of AKI by promoting resident cell proliferation and reducing tubular cell apoptosis [63].

In the last 10 years, amniotic fluid obtained from amniocentesis, has also been extensively studied as a non-controversial source of stem cells with no-tumorigenicity at late passages when injected into immunodeficient mice [64]. In this context, our group has tested the therapeutic effect of human AFS cells, immunoisolated for c-kit, which express intermediate characteristics between embryonic and adult stem cells including MSC markers [54]. Considering the potential plasticity of human AFS cells, we have investigated whether these cells exert their renoprotection through differentiation into resident tubular cells or through local paracrine effects [54]. We observed that human hAFS cells improved renal function and limited tubular damage in NOD/SCID mice with AKI induced by cisplatin. The effect of human AFS cells on animal survival was similar to that observed with human BM-MSCs.

3.3 Mechanism of Action of Mesenchymal Stem Cells

Initially, it was thought that the mechanism by which BM stem cells promoted kidney repair was due to the ability of these stem cells to differentiate and integrate into resident cells, replacing damaged tubular cells [7, 50, 65]. However, subsequent studies by different groups including our own [51, 52, 62, 63, 66] have documented that BM-MSCs were only transiently present in the damaged kidney and they predominantly localized in the peritubular area, suggesting that MSCs protected the kidney via paracrine and/or endocrine activity rather than through direct incorporation into renal tubules. In this context, the finding of Togel and coworkers is considered an important breakthrough [51, 67]. In an ischemia/reperfusion experimental model of AKI, they did not observe differentiation of rat BM-MSCs into a tubular or endothelial cell phenotype. On the contrary, they showed a significant reduction in the expression of proinflammatory cytokines such as IL-1β, TNF-α, IFN-γ, and inducible nitric oxide synthase, in AKI rats receiving rat BM-MSCs. Additionally, the anti-inflammatory cytokines IL-10 and bFGF, TGF-α, and Bcl-2 were highly upregulated in AKI rats given BM-MSC infusion [51]. Moreover, the vasculotropic, paracrine effect of rat BM-MSCs was documented in a study showing that MSC-conditioned medium containing VEGF, HGF, and IGF-1 improved aortic endothelial cell growth and survival [67]. Of note, they observed that MSCs injected in mice with AKI induced by ischemia/reperfusion home to the renal microvascular

circulation decreasing apoptosis of tubular cells [67]. The finding that MSCs exert a renoprotective effect through the release of soluble factors was also demonstrated by in vitro experiments with conditioned media (CM) from cultured bone marrow-derived stromal cells that induced a significant cell death reduction in cisplatin-injured proximal tubule cells [66]. Intraperitoneal injection of CM in mice with AKI limited renal injury and increased proliferation of tubular epithelial cells, thus inducing regeneration of damaged renal tissue [66]. To identify the soluble factors involved in the MSC-mediated renoprotection, we first focused on IGF-1, a growth factor described to have mitogenic effects on tubular cells [68]. Blocking MSC-derived IGF-1 with a specific antibody attenuated the proximal tubular cell proliferation. In agreement with these data, the knocking down of IGF-1 expression in MSCs by small interfering-RNA (siRNA) also resulted in a significant reduction of tubular cell proliferation, while apoptosis was increased when MSCs were co-cultured with proximal tubular cells that had been damaged by cisplatin [69]. Furthermore, in mice with AKI, IGF-1 gene-silenced MSCs failed to exert their protective effect on renal function and tubular structure, thus indicating a key role for IGF-1 produced by MSCs, in promoting regenerative processes in the kidney. Similarly, in an ischemia/reperfusion model of AKI, knocking down of VEGF by siRNA reduced the effect of rat BM-MSCs on renal function recovery and survival. Moreover, AKI rats treated with VEGF knockdown MSCs did not show any increase in renal microvessel density compared with MSC-treated AKI rats [70].

The ability of MSCs to exert a renoprotective effect via the local release of growth and anti-inflammatory factors rather than through differentiation into resident cells has also been described for human CB-MSCs and hAFS cells [53, 54]. Our group has documented that injected human CB-MSCs localized predominantly in peritubular areas of mice with AKI, and were able to create a proregenerative environment through their ability to inhibit oxidative damage and to induce the prosurvival factor Akt in tubular cells [53]. In vitro experiments with human CB-MSCs co-cultured with cisplatin-treated proximal tubular cells in a transwell system documented that stem cells increased the levels of mitogenic and pro-survival factors including FGF, HB-EGF, VEGF, and HGF in the cell supernatant. Moreover, we observed that human CB-MSCs were able to inhibit the release of IL-1β and TNF-α by proximal tubular cells exposed to cisplatin suggesting a regenerative and anti-inflammatory action of stem cell treatment [53].

Similar to human BM-MSCs and CB-MSCs, human AFS cells do not acquire tubular epithelial markers. When injected in AKI mice they exerted a paracrine effect via local release of factors like IL-6, VEGF, and stromal cell-derived factor-1 (SDF-1), which were able to activate Akt, stimulate proliferation and inhibit apoptosis of tubular cells [54].

Based on the data above described, it has become evident that MSCs promote renal regeneration through the local release of mitogenic and vasculotropic factors. Therefore, it is evident that novel strategies to potentiate migration, engraftment, survival, and paracrine effects of administered stem cells by cell preconditioning or genetic modifications may enhance the MSC local effect in damaged tissues [3, 20]. In particular, gene-modified and preconditioned BM-MSCs have shown enhanced therapeutic effects in a preclinical model of AKI. BM-MSCs genetically modified with the serine protease kallikrein by adenovirus transduction were more resistant to oxidative stress-induced apoptosis and secreted high levels of VEGF in culture medium [71]. Injection of kallikrein-modified BM-MSCs in rats with ischemia/reperfusion injury enhanced renal function inhibiting apoptosis and inflammation [71]. Other strategies to improve the ability of stem cells to survive and produce paracrine factors can be achieved by in vitro pre-treatment with melatonin. Mias and coworkers have observed that melatonin is able to increase the resistance of BM-MSCs to hydrogen peroxide-induced apoptosis by promoting overexpression of the antioxidant enzyme catalase and superoxidase dismutase [72]. Moreover, in a rat model of AKI, melatonin preconditioning allowed the long-term survival of BM-MSCs within the damaged kidney improving angiogenesis, proliferation, and recovery of renal function [72]. Our group has shown that pre-incubation of mouse BM-MSCs with TNF-α, IGF-1, and GDNF induced in vitro cytoskeletal rearrangement and increased cell migration [73]. In animals with AKI, infusion of BM-MSCs preconditioned with IGF-1 improved the capacity of MSCs to engraft into the injured kidney and totally restored renal function, suggesting that the preconditioning could be a new strategy to enhance the therapeutic effect of MSCs [73]. In this context, the therapeutic potential of human AFS cells was ameliorated by their pre-exposure with GDNF, which markedly improved renal function and tubular structure by increasing human AFS survival and the expression of the receptors CD44, CXCR4, and SDF-1 involved in cell homing [54].

Recently, the horizontal transfer of mRNAs contained within MSC-derived microvesicles (MVs) and exosomes (Exo) to target cells has been indicated as a new mechanism of cell-to-cell communication by which MSCs protect renal tissue from acute injury [32]. In vitro experiments by Bruno et al. demonstrated that microvesicles derived from human BM-MSCs, when injected in SCID mice with glycerol-induced AKI, restored renal function and structure by inducing proliferation of tubular cells [74]. Microarray analysis and quantitative real-time PCR of MV-derived RNA extracts indicated that MVs activated a proliferative program in tubular cells via the transfer of a specific subset of mRNAs associated with transcription, proliferation, and immunoregulation [74].

Moreover, Collino and coworkers demonstrated that MVs isolated from human BM-MSCs contained ribonucleoproteins involved in the intracellular traffic of mRNAs and a selected pattern of non-coding RNAs, named micro RNAs (miRNAs), that post-transcriptionally modulate the expression of genes involved in the regulation of several cellular processes [75]. In this context, our group has documented that MVs and exosomes (Exo) released from human BM-MSCs are able to induce proliferation of proximal tubular cells damaged by cisplatin, through the transfer of IGF-1R mRNA that was translated into its corresponding protein [31]. The transfer of IGF-1R was peculiar for BM-MSCs, since Exo deriving from normal human dermal fibroblasts did not contain either IGF-1 or its receptor [31]. Moreover, the transport of IGF-1R by the human BM-MSC-derived Exo is a specific process since other receptors, such as the insulin receptor, or the peroxisome proliferator-activated receptor gamma were not detected in the Exo. These findings suggest that horizontal transfer of the mRNA for IGF-1R to tubular cells through Exo potentiates tubular cell sensitivity to locally produced IGF-1, providing a new mechanism underlying the powerful renoprotection of the few BM-MSC observed in vivo [31]. Recently, Lindoso and coworkers observed that extracellular vesicles (EVs), isolated from BM-MSCs were able to transfer and modulate the expression of several miRNAs inside renal proximal tubular epithelial cells (PTECs) in an in vitro model of ischemia–reperfusion injury induced by ATP depletion [76]. They demonstrated that MSC-EV incorporation induced protection from renal tubular cell death. The protective effect was associated with EV-mediated miRNA transfer and with transcriptional modulation of miRNAs expressed by injured PTECs. The MSC-derived MVs shuttle and modulate the expression of several miRNAs in PTECs regulating tissue repair and recovery processes involved in apoptosis, cytoskeleton reorganization, and hypoxia [76].

4 Mesenchymal Stem Cell-Based Therapy in Chronic Kidney Disease

Therapy with MSCs has been shown to improve the outcome of experimental AKI, but whether MSCs can delay renal failure in chronic nephropathies has not been established. Despite technical hurdles such as the difficult choice of optimal treatment timing and the length of therapy [77], treatment with MSCs targeting and stimulating endogenous renal cell populations of the glomerular compartment represents an interesting option. In the CKD model of Alport syndrome, mice deficient for alpha 3-chain type IV collagen developed progressive glomerular damage leading to renal failure. Weekly injections with MSCs limited interstitial fibrosis and loss of peritubular capillaries, but failed to delay the progression of

chronic nephropathy and animal survival [78]. It is intriguing that fetal blood-derived MSCs intrauterinally injected in collagen type 1 alpha 2-deficient fetal mice were able to ameliorate glomerular lesions, thus proving the feasibility of prenatal stem cell treatment for hereditary renal diseases [79]. Infusion of MSCs in 5/6 rats with a nephrectomy partially prevented renal function impairment, attenuated glomerular sclerosis [80, 81] and interstitial fibrosis [82]. Intrarterial infusion of MSCs in rats with anti-Thy1.1 glomerulonephritis accelerated glomerular recovery from mesangiolytic damage [83]. In the same model, the long-term effect of MSC infusion was investigated [84]. Renal function and matrix deposition were markedly reduced on day 60 after MSC infusion; however, 20 % of the glomeruli contained single or clusters of adipocytes at the site of fibrosis, thus pointing to maldifferentiation as a possible side effect of MSC therapy [84]. Interestingly, in systemic lupus erythematosus-like disease in MRL/*Ipr* mice, allogeneic BM-MSC transplantation induced reconstruction of the dysfunctional BM osteoclastic niche and partially reverted multiorgan dysfunction [85].

Our group has studied the effects of repeated injections of rat BM-MSCs in rats with adriamycin (ADR)-induced nephropathy, a model of progressive glomerulosclerosis characterized by early glomerular podocyte damage followed by activation of parietal epithelial cells (PEC), both cells contribute to the formation of synechiae and adhesions of the Bowman's capsule to the glomerular capillary loop [86]. We showed that infusions with BM-MSCs in ADR rats exerted an effective anti-apoptotic effect on podocytes and attenuated podocyte-PEC bridges normalizing the distribution of PEC along the Bowman's capsule, thereby reducing glomerulosclerosis (Fig. 4).

Data that BM-MSCs enhanced glomerular VEGF levels and limited capillary rarefaction (Fig. 4) can explain the pro-survival effects of stem cell therapy. In vitro experiments with MSCs cocultured with adriamycin-damaged podocytes indicated a functional role for stem cell-derived VEGF on the pro-survival pathway [86]. These results indicated that MSC therapy, by reducing podocyte damage, restored PEC regenerative ability, thereby ameliorating glomerular architecture and preventing sclerotic lesions. The fact that MSC therapy failed to reduce proteinuria in ADR rats could be attributed to the limited recovery of the podocyte slit diaphragm proteins that were unable to reestablish normal function of foot processes. Strategies to enhance MSC retention and renoprotection in the damaged kidney by preconditioning or genetic modification could be helpful to increase the MSC local effects thus ameliorating also renal functional parameters.

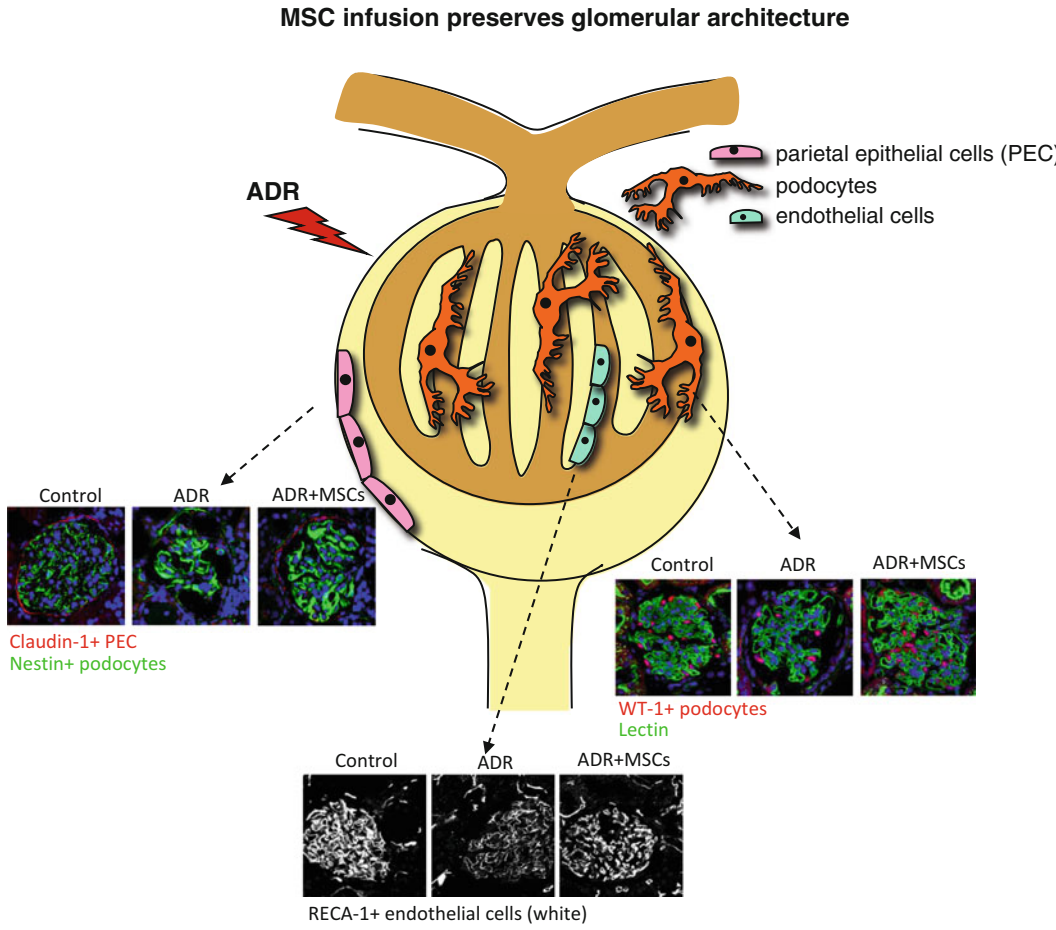

Fig. 4 Repeated infusions of MSCs in ADR-induced nephropathy preserve glomerular architecture. Repeated i.v. injections (at 36 and 60 h and 3, 5, 7, 14, and 21 days) of MSCs in ADR-treated rats limit podocyte loss, attenuate the formation of podocyte-parietal epithelial cell bridges and limit microvascular rarefaction

5 Conclusions

Preclinical studies in AKI have highlighted the potential of MSCs to promote renal regeneration by acting via the local release of cocktails of growth factors, anti-inflammatory and immunomodulatory cytokines. However, the translation of these experimental approaches into effective and safe modalities of care is still limited. In this context, an FDA-approved phase I clinical trial (NCT00733876) is ongoing with the purpose of evaluating the feasibility and safety of allogeneic human BM-MSC administration. Escalating doses of MSCs are given to open-heart surgery patients at high risk of postoperative AKI. Preliminary analysis of the outcomes of these subjects has shown that renal function was

well preserved postoperatively for up to 16 months and none of the patients required hemodialysis. Hospital stays and readmission rates decreased by 40 % whereas 20 % of case controls developed AKI [87, 88]. MSC was safe and no adverse events have been recorded [87, 88]. Our group has designed an explorative study to evaluate the safety of one systemic infusion of ex vivo-expanded BM-MSC to repair the kidney and to ameliorate function in patients with solid organ cancer who develop AKI after treatment with the antitumor drug cisplatin.

Realistically, although preliminary data on the safety of the MSC treatment are encouraging, further studies to test the real efficacy of this novel intervention are needed and we should proceed with prudence and caution.

Acknowledgments

The authors thank Manuela Passera and Antonella Piccinelli for their help in preparing this manuscript.

References

1. Taylor PL, Barker RA, Blume KG et al (2010) Patients beware: commercialized stem cell treatments on the web. Cell Stem Cell 7:43–49
2. Daley GQ (2012) The promise and perils of stem cell therapeutics. Cell Stem Cell 10:740–749
3. Ranganath SH, Levy O, Inamdar MS et al (2012) Harnessing the mesenchymal stem cell secretome for the treatment of cardiovascular disease. Cell Stem Cell 10:244–258
4. Rosenzweig A (2006) Cardiac cell therapy-mixed results from mixed cells. N Engl J Med 355:1274–1277
5. Nowbar AN, Mielewczik M, Karavassilis M et al (2014) Discrepancies in autologous bone marrow stem cell trials and enhancement of ejection fraction (DAMASCENE): weighted regression and meta-analysis. BMJ 348:g2688
6. Weissman I (2012) Stem cell therapies could change medicine… if they get the chance. Cell Stem Cell 10:663–665
7. Poulsom R, Forbes SJ, Hodivala-Dilke K et al (2001) Bone marrow contributes to renal parenchymal turnover and regeneration. J Pathol 195:229–235
8. Ito T, Suzuki A, Imai E et al (2001) Bone marrow is a reservoir of repopulating mesangial cells during glomerular remodeling. J Am Soc Nephrol 12:2625–2635
9. Li B, Morioka T, Uchiyama M et al (2006) Bone marrow cell infusion ameliorates progressive glomerulosclerosis in an experimental rat model. Kidney Int 69:323–330
10. Friedenstein AJ, Chailakhjan RK, Lalykina KS (1970) The development of fibroblast colonies in monolayer cultures of guinea-pig bone marrow and spleen cells. Cell Tissue Kinet 3:393–403
11. Dominici M, Le Blanc K, Mueller I et al (2006) Minimal criteria for defining multipotent mesenchymal stromal cells. The International Society for Cellular Therapy position statement. Cytotherapy 8:315–317
12. Bianco P, Robey PG, Simmons PJ (2008) Mesenchymal stem cells: revisiting history, concepts, and assays. Cell Stem Cell 2:313–319
13. Bianco P, Cao X, Frenette PS et al (2013) The meaning, the sense and the significance: translating the science of mesenchymal stem cells into medicine. Nat Med 19:35–42
14. Uccelli A, Moretta L, Pistoia V (2008) Mesenchymal stem cells in health and disease. Nat Rev Immunol 8:726–736
15. Edwards RG, Hollands P (2007) Will stem cells in cord blood, amniotic fluid, bone marrow and peripheral blood soon be unnecessary in transplantation? Reprod Biomed Online 14:396–401
16. Panepucci RA, Siufi JL, Silva WA Jr et al (2004) Comparison of gene expression of umbilical cord vein and bone marrow-derived mesenchymal stem cells. Stem Cells 22:1263–1278

17. Crisan M, Yap S, Casteilla L et al (2008) A perivascular origin for mesenchymal stem cells in multiple human organs. Cell Stem Cell 3:301–313
18. Caplan AI, Correa D (2011) The MSC: an injury drugstore. Cell Stem Cell 9:11–15
19. Teixeira FG, Carvalho MM, Sousa N et al (2013) Mesenchymal stem cells secretome: a new paradigm for central nervous system regeneration? Cell Mol Life Sci 70:3871–3882
20. Wagner J, Kean T, Young R et al (2009) Optimizing mesenchymal stem cell-based therapeutics. Curr Opin Biotechnol 20:531–536
21. Kupcova Skalnikova H (2013) Proteomic techniques for characterisation of mesenchymal stem cell secretome. Biochimie 95:2196–2211
22. Drago D, Cossetti C, Iraci N et al (2013) The stem cell secretome and its role in brain repair. Biochimie 95:2271–2285
23. Bronckaers A, Hilkens P, Martens W et al (2014) Mesenchymal stem/stromal cells as a pharmacological and therapeutic approach to accelerate angiogenesis. Pharmacol Ther 143:181–196
24. Abumaree M, Al Jumah M, Pace RA et al (2012) Immunosuppressive properties of mesenchymal stem cells. Stem Cell Rev 8:375–392
25. Bartholomew A, Sturgeon C, Siatskas M et al (2002) Mesenchymal stem cells suppress lymphocyte proliferation in vitro and prolong skin graft survival in vivo. Exp Hematol 30:42–48
26. Di Nicola M, Carlo-Stella C, Magni M et al (2002) Human bone marrow stromal cells suppress T-lymphocyte proliferation induced by cellular or nonspecific mitogenic stimuli. Blood 99:3838–3843
27. Casiraghi F, Remuzzi G, Perico N (2014) Mesenchymal stromal cells to promote kidney transplantation tolerance. Curr Opin Organ Transplant 19:47–53
28. English K (2013) Mechanisms of mesenchymal stromal cell immunomodulation. Immunol Cell Biol 91:19–26
29. Kim J, Hematti P (2009) Mesenchymal stem cell-educated macrophages: a novel type of alternatively activated macrophages. Exp Hematol 37:1445–1453
30. Baglio SR, Pegtel DM, Baldini N (2012) Mesenchymal stem cell secreted vesicles provide novel opportunities in (stem) cell-free therapy. Front Physiol 3:359
31. Tomasoni S, Longaretti L, Rota C et al (2013) Transfer of growth factor receptor mRNA via exosomes unravels the regenerative effect of mesenchymal stem cells. Stem Cells Dev 22:772–780
32. Ratajczak J, Wysoczynski M, Hayek F et al (2006) Membrane-derived microvesicles: important and underappreciated mediators of cell-to-cell communication. Leukemia 20:1487–1495
33. Camussi G, Deregibus MC, Bruno S et al (2010) Exosomes/microvesicles as a mechanism of cell-to-cell communication. Kidney Int 78:838–848
34. Devarajan P (2006) Update on mechanisms of ischemic acute kidney injury. J Am Soc Nephrol 17:1503–1520
35. Coca SG, Yusuf B, Shlipak MG et al (2009) Long-term risk of mortality and other adverse outcomes after acute kidney injury: a systematic review and meta-analysis. Am J Kidney Dis 53:961–973
36. Star RA (1998) Treatment of acute renal failure. Kidney Int 54:1817–1831
37. Grino JM (1994) BN 52021: a platelet activating factor antagonist for preventing post- transplant renal failure. A double-blind, randomized study. The BN 52021 Study Group in Renal Transplantation. Ann Intern Med 121:345–347
38. Haug CE, Colvin RB, Delmonico FL et al (1993) A phase I trial of immunosuppression with anti-ICAM-1 (CD54) mAb in renal allograft recipients. Transplantation 55:766–772
39. Bonventre JV (2003) Dedifferentiation and proliferation of surviving epithelial cells in acute renal failure. J Am Soc Nephrol 14(Suppl 1):S55–S61
40. Lameire N, Van Biesen W, Vanholder R (2008) Acute kidney injury. Lancet 372:1863–1865
41. Benigni A, Morigi M, Remuzzi G (2010) Kidney regeneration. Lancet 375:1310–1317
42. Aejaz HM, Aleem AK, Parveen N et al (2007) Stem cell therapy-present status. Transplant Proc 39:694–699
43. Daley GQ, Scadden DT (2008) Prospects for stem cell-based therapy. Cell 132:544–548
44. Lindvall O, Kokaia Z (2006) Stem cells for the treatment of neurological disorders. Nature 441:1094–1096
45. Laflamme MA, Murry CE (2005) Regenerating the heart. Nat Biotechnol 23:845–856
46. Little MH (2006) Regrow or repair: potential regenerative therapies for the kidney. J Am Soc Nephrol 17:2390–2401
47. Cantley LG (2005) Adult stem cells in the repair of the injured renal tubule. Nat Clin Pract Nephrol 1:22–32
48. Morigi M, Benigni A, Remuzzi G et al (2006) The regenerative potential of stem cells in acute renal failure. Cell Transplant 15(Suppl 1):S111–S117
49. Morigi M, Imberti B, Zoja C et al (2004) Mesenchymal stem cells are renotropic, helping to repair the kidney and improve function in acute renal failure. J Am Soc Nephrol 15:1794–1804
50. Herrera MB, Bussolati B, Bruno S et al (2004) Mesenchymal stem cells contribute to the renal repair of acute tubular epithelial injury. Int J Mol Med 14:1035–1041

51. Togel F, Hu Z, Weiss K et al (2005) Administered mesenchymal stem cells protect against ischemic acute renal failure through differentiation-independent mechanisms. Am J Physiol Renal Physiol 289:F31–F42
52. Morigi M, Introna M, Imberti B et al (2008) Human bone marrow mesenchymal stem cells accelerate recovery of acute renal injury and prolong survival in mice. Stem Cells 26:2075–2082
53. Morigi M, Rota C, Montemurro T et al (2010) Life-sparing effect of human cord blood-mesenchymal stem cells in experimental acute kidney injury. Stem Cells 28:513–522
54. Rota C, Imberti B, Pozzobon M et al (2012) Human amniotic fluid stem cell preconditioning improves their regenerative potential. Stem Cells Dev 21:1911–1923
55. Kim JH, Park DJ, Yun JC et al (2012) Human adipose tissue-derived mesenchymal stem cells protect kidneys from cisplatin nephrotoxicity in rats. Am J Physiol Renal Physiol 302:F1141–F1150
56. Katsuno T, Ozaki T, Saka Y et al (2013) Low serum cultured adipose tissue-derived stromal cells ameliorate acute kidney injury in rats. Cell Transplant 22:287–297
57. Flynn A, Barry F, O'Brien T (2007) UC blood-derived mesenchymal stromal cells: an overview. Cytotherapy 9:717–726
58. Sanchez-Ramos J (2006) Stem cells from umbilical cord blood. Semin Reprod Med 24:358–369
59. Erices A, Conget P, Minguell JJ (2000) Mesenchymal progenitor cells in human umbilical cord blood. Br J Haematol 109:235–242
60. Lee OK, Kuo TK, Chen WM et al (2004) Isolation of multipotent mesenchymal stem cells from umbilical cord blood. Blood 103:1669–1675
61. Seres KB, Hollands P (2010) Cord blood: the future of regenerative medicine? Reprod Biomed Online 20:98–102
62. Du T, Cheng J, Zhong L et al (2012) The alleviation of acute and chronic kidney injury by human Wharton's jelly-derived mesenchymal stromal cells triggered by ischemia-reperfusion injury via an endocrine mechanism. Cytotherapy 14:1215–1227
63. Fang TC, Pang CY, Chiu SC et al (2012) Renoprotective effect of human umbilical cord-derived mesenchymal stem cells in immunodeficient mice suffering from acute kidney injury. PLoS One 7, e46504
64. De Coppi P, Bartsch G Jr, Siddiqui MM et al (2007) Isolation of amniotic stem cell lines with potential for therapy. Nat Biotechnol 25:100–106
65. Gupta S, Verfaillie C, Chmielewski D et al (2002) A role for extrarenal cells in the regeneration following acute renal failure. Kidney Int 62:1285–1290
66. Bi B, Schmitt R, Israilova M et al (2007) Stromal cells protect against acute tubular injury via an endocrine effect. J Am Soc Nephrol 18:2486–2496
67. Togel F, Weiss K, Yang Y et al (2007) Vasculotropic, paracrine actions of infused mesenchymal stem cells are important to the recovery from acute kidney injury. Am J Physiol Renal Physiol 292:F1626–F1635
68. Hirschberg R, Ding H (1998) Mechanisms of insulin-like growth factor-I-induced accelerated recovery in experimental ischemic acute renal failure. Miner Electrolyte Metab 24:211–219
69. Imberti B, Morigi M, Tomasoni S et al (2007) Insulin-like growth factor-1 sustains stem cell mediated renal repair. J Am Soc Nephrol 18:2921–2928
70. Togel F, Zhang P, Hu Z et al (2009) VEGF is a mediator of the renoprotective effects of multipotent marrow stromal cells in acute kidney injury. J Cell Mol Med 13:2109–2114
71. Hagiwara M, Shen B, Chao L et al (2008) Kallikrein-modified mesenchymal stem cell implantation provides enhanced protection against acute ischemic kidney injury by inhibiting apoptosis and inflammation. Hum Gene Ther 19:807–819
72. Mias C, Trouche E, Seguelas MH et al (2008) Ex vivo pretreatment with melatonin improves survival, proangiogenic/mitogenic activity, and efficiency of mesenchymal stem cells injected into ischemic kidney. Stem Cells 26:1749–1757
73. Xinaris C, Morigi M, Benedetti V et al (2013) A novel strategy to enhance mesenchymal stem cell migration capacity and promote tissue repair in an injury specific fashion. Cell Transplant 22:423–436
74. Bruno S, Grange C, Deregibus MC et al (2009) Mesenchymal stem cell-derived microvesicles protect against acute tubular injury. J Am Soc Nephrol 20:1053–1067
75. Collino F, Deregibus MC, Bruno S et al (2010) Microvesicles derived from adult human bone marrow and tissue specific mesenchymal stem cells shuttle selected pattern of miRNAs. PLoS One 5, e11803
76. Lindoso RS, Collino F, Bruno S et al (2014) Extracellular vesicles released from mesenchymal stromal cells modulate miRNA in renal tubular cells and inhibit ATP depletion injury. Stem Cells Dev 23(15):1809–1819
77. Kunter U, Rong S, Moeller MJ et al (2011) Mesenchymal stem cells as a therapeutic approach to glomerular diseases: benefits and risks. Kidney Int Suppl 1:68–73

78. Ninichuk V, Gross O, Segerer S et al (2006) Multipotent mesenchymal stem cells reduce interstitial fibrosis but do not delay progression of chronic kidney disease in collagen4A3-deficient mice. Kidney Int 70:121–129
79. Guillot PV, Cook HT, Pusey CD et al (2008) Transplantation of human fetal mesenchymal stem cells improves glomerulopathy in a collagen type I alpha 2-deficient mouse. J Pathol 214:627–636
80. Choi S, Park M, Kim J et al (2009) The role of mesenchymal stem cells in the functional improvement of chronic renal failure. Stem Cells Dev 18:521–529
81. Cavaglieri RC, Martini D, Sogayar MC et al (2009) Mesenchymal stem cells delivered at the subcapsule of the kidney ameliorate renal disease in the rat remnant kidney model. Transplant Proc 41:947–951
82. Semedo P, Correa-Costa M, Antonio Cenedeze M et al (2009) Mesenchymal stem cells attenuate renal fibrosis through immune modulation and remodeling properties in a rat remnant kidney model. Stem Cells 27:3063–3073
83. Kunter U, Rong S, Djuric Z et al (2006) Transplanted mesenchymal stem cells accelerate glomerular healing in experimental glomerulonephritis. J Am Soc Nephrol 17: 2202–2212
84. Kunter U, Rong S, Boor P et al (2007) Mesenchymal stem cells prevent progressive experimental renal failure but maldifferentiate into glomerular adipocytes. J Am Soc Nephrol 18:1754–1764
85. Sun L, Akiyama K, Zhang H et al (2009) Mesenchymal stem cell transplantation reverses multiorgan dysfunction in systemic lupus erythematosus mice and humans. Stem Cells 27:1421–1432
86. Zoja C, Garcia PB, Rota C et al (2012) Mesenchymal stem cell therapy promotes renal repair by limiting glomerular podocyte and progenitor cell dysfunction in adriamycin-induced nephropathy. Am J Physiol Renal Physiol 303:F1370–F1381
87. Gooch A, Doty J, Flores J et al (2008) Initial report on a phase I clinical trial: prevention and treatment of post-operative acute kidney injury with allogeneic mesenchymal stem cell in patients who require on-pump cardiac surgery. Cell Ther Transplant [Online] 1:31–35
88. Togel FE, Westenfelder C (2010) Mesenchymal stem cells: a new therapeutic tool for AKI. Nat Rev Nephrol 6:179–183

Chapter 6

Mesenchymal Stem Cells in Lipogems, a Reverse Story: from Clinical Practice to Basic Science

Carlo Tremolada, Camillo Ricordi, Arnold I. Caplan, and Carlo Ventura

Abstract

The idea that basic science should be the starting point for modern clinical approaches has been consolidated over the years, and emerged as the cornerstone of Molecular Medicine. Nevertheless, there is increasing concern over the low efficiency and inherent costs related to the translation of achievements from the bench to the bedside. These burdens are also perceived with respect to the effectiveness of translating basic discoveries in stem cell biology to the newly developing field of *advanced cell therapy* or Regenerative Medicine. As an alternative paradigm, past and recent history in Medical Science provides remarkable reverse stories in which clinical observations at the patient's bedside have fed major advances in basic research which, in turn, led to consistent progression in clinical practice. Within this context, we discuss our recently developed method and device, which forms the core of a system (Lipogems) for processing of human adipose tissue solely with the aid of mild mechanical forces to yield a microfractured tissue product.

Key words Adipose tissue, Innovative device, Stromal vascular niche, Adipose-derived stem cells, Cryopreservation, Chemical agents, Electromagnetic energy, Lipogems

1 Introduction

Translation of scientific information from the bench to the bedside is a consolidated approach in Science utilized during the last decades, and at the same time it is a concept that has been used so often it risks achieving cliché status. This paradigm has no doubt contributed to the identification of mechanistic bases of a number of diseases, paving the way to modern Molecular Medicine and Therapy. Nevertheless, clinical scientists and public health representatives are increasingly concerned with the low translational efficiency of scientific discoveries of the past generation into tangible clinical improvement. In particular, clinical research is constrained by rising costs, slow results, restrictions in funding, and the need for compliance with cumbersome regulatory issues.

Massimiliano Gnecchi (ed.), *Mesenchymal Stem Cells: Methods and Protocols*, Methods in Molecular Biology, vol. 1416,
DOI 10.1007/978-1-4939-3584-0_6,

The world of stem cells is not immune to these criticisms. So far, human adult stem cells have been isolated from multiple tissues, including bone marrow, dental pulp, placenta, and adipose tissue. Stem cells with attractive features have also been harvested from amniotic fluid and even urinary sediment. A remarkable breakthrough has been seen in our basic knowledge of stem cell biology and the dissection of mechanisms underlying their differentiating potential, paracrine activity, and fate in animal models of disease. Despite this progress, clinical translation of stem cell research to the most challenging diseases currently afflicting society, including heart failure, diabetes, neurodegenerative disorders, stroke, or injuries to the central and peripheral nervous system, is still in its infancy, awaiting affordable strategies and results that may prompt the elevation of cell therapy and regenerative medicine as a consolidated tool to target crucial unmet clinical needs.

Within this context, an urgent question arises: What phenomena do clinicians observe that may attract the attention of basic scientists? Is there any clinical observation from tissue transplantation/cell therapy that is crying for consideration as a novel paradigm in the rescue of damaged tissues, potentially involving laboratory researchers in studies that may lead to further deployment in stem cell biology? Indeed, the relevance of such a reverse, bed-to-bench-side approach, is highlighted by a number of examples, including, just to cite a few: (a) clinical studies showing that cancer-causing retroviruses exert effects similar to AIDS on the human immune system: this helped scientists to identify HIV, a retrovirus in the same family as the cancer-causing retroviruses, as that responsible for the development of AIDS [1]; (b) clinical investigations initially performed on thousands of infants dying annually from a mysterious respiratory ailment: separately, basic studies on surface tension and pulmonary physiology allowed researchers to identify and characterize pulmonary surfactant. As a result, clinical and basic scientists together determined that the deaths were due to a lack of surfactant, which caused the alveoli, or air sacs in the lungs, to collapse [2]. Treatments were then developed in the lab and tested in and applied to patients with great clinical success [3]; (c) clinical research, starting from the anticancer effect of tamoxifen, also demonstrated that the treatment of healthy women can effectively act as a prophylactic strategy to prevent development of breast cancer in high-risk subjects [4]; (d) initial observations linking cardiovascular disease (CVD) to obese patients: over the past several years, these studies fostered an exponential increase in our understanding of adipose biology and its relevance to CVD [5]. Intriguingly, clinical observations in this area still pose remarkable questions for basic scientists: one of the most puzzling is the obesity paradox [5]. How can adipose tissue increase CVD risk factors and yet be protective once CVD develops?

In agreement with these considerations, in the current review we discuss a recently developed method and device, namely Lipogems [6], which yields a microfractured human adipose tissue product that was initially conceived as a device to improve the lipofilling technique for plastic surgery and reconstruction. Since then clinical evidence of unprecedented soft tissue repair after transplantation of the Lipogems product has been observed. Dr. Carlo Tremolada initially invented the method and device to improve our understanding on the inherent features of the tissue product and the putative mechanisms of its rescuing potential through collaboration with basic science research scientists. This reverse story is currently providing novel clues on the mechanisms by which human mesenchymal stem cells (hMSCs)/pericytes residing within the Lipogems product may act to awaken the self-healing patterning by a recipient tissue.

Adhering to the reverse bed-to-bench-side paradigm, the clinical results obtained following the transplantation of the Lipogems product have served as a launching point for subsequent molecular biology studies. Importantly, Lipogems were shown to maintain an intact stromal vascular niche harboring cellular elements with mesenchymal stem cell and pericyte characteristics. Moreover, Lipogems-derived stem cells express transcriptional profiles characterized by self-renewal/stemness patterning, along with a set of genes orchestrating commitment along the neurogenic lineage. Interestingly, the Lipogems product can be reliably cryopreserved, without losing its niche structure and the viability of its embedded stem cells. Further studies have also revealed that the human adipose-derived stem cells (hASCs) residing within the Lipogems product are significantly more responsive to both chemical agents and physical energy than hASCs enzymatically dissociated from the initial lipoaspirate. In particular, exposure to electromagnetic fields induced a significantly higher yield of commitment along the myocardial, endothelial, skeletal muscle, and neural lineages in Lipogems-derived, as compared to enzymatically dissociated hASCs. These findings have helped to unravel several of the mechanistic bases of the healing properties of the Lipogems product and may hopefully serve to further deploy its use in the rescue of damaged tissue.

The fundamental mechanism underlying the clinical efficiency of transplanted freshly obtained Lipogems product (which is basically microfragmeted lipoaspirate thoroughly purified of its oily and hematopoietic components) may involve the secretion of trophic mediators delivering instructive messages that may help create a more compliant “regenerative environment” within the donor tissue. Lipogems may act as a “slow releasing medium” with regenerative factors where they are mostly needed.

2 The Method and the Device

In recent years, surgical techniques including vascular surgery have demonstrated the benefit of transplanted autologous adipose tissue as a filler capable not only of increasing the volume within the tissues receiving vessels compromised by various diseases, but also in restoring the subcutaneous and cutaneous trophisms due to aging or actinic and even radiotherapy damage [7].

A relevant portion of these beneficial effects has been attributed to the rescue-potential of tissue-resident hASCs, sharing consistent phenotypical and transcriptional profiles with hMSCs isolated from different sources, including bone marrow, dental pulp, and term placenta [8, 9]. The use of autologous lipofilling has significantly contributed to the resolution of scarring processes, also favoring engraftment of transplanted skin tissue performed with the aim of optimizing the morphological and functional compliance of the injured soft tissues [8, 9]. In particular, these combined strategies hold promise in promoting the recovery of tissue trophism in a number of challenging conditions, including the diabetic foot, venous leg ulcers, and pressure ulcers.

To date, autologous lipofilling has involved fat harvesting by liposuction usually from the abdomen or inner thigh, followed by centrifugation to partially separate fat from blood, fragments of scarred tissue, and oils released by preadipocytes/adipocytes damaged during the liposuction procedure (Coleman technique) [8]. The processed fat is then placed into syringes with a specially designed blunt cannula for *transplantation*. However, the resulting adipose tissue is a particularly dense product, and it is not suitable for easy passage through narrow needles, which are required to accomplish a delicate subcutaneous graft in extremely fragile or damaged tissues, such as the subcutaneous and cutaneous layers of a diabetic foot or in the delicate and scarred fingers of hands plagued by scleroderma. These clinical presentations require the use of complex and expensive devices (injectors, pumps, specifically designed syringes); nevertheless, they fail to attain a homogenous and finely pliant distribution of transplanted fat tissue [10]. Moreover, results from studies utilizing these current techniques are often variable not only between different patients but even in the same patient and injected area, and rarely is even reabsorption of the injected fat observed (ranging between 20 and 80 %) [10]. This outcome is further worsened by the detrimental effects due to the onset of inflammatory responses triggered by residual oils within the injected fat tissue product.

To overcome these critical problems, Carlo Tremolada and colleagues recently developed and designed a novel method and device (Lipogems™) [6] which: (a) completely resolves the issues associated with the techniques previously utilized for fat

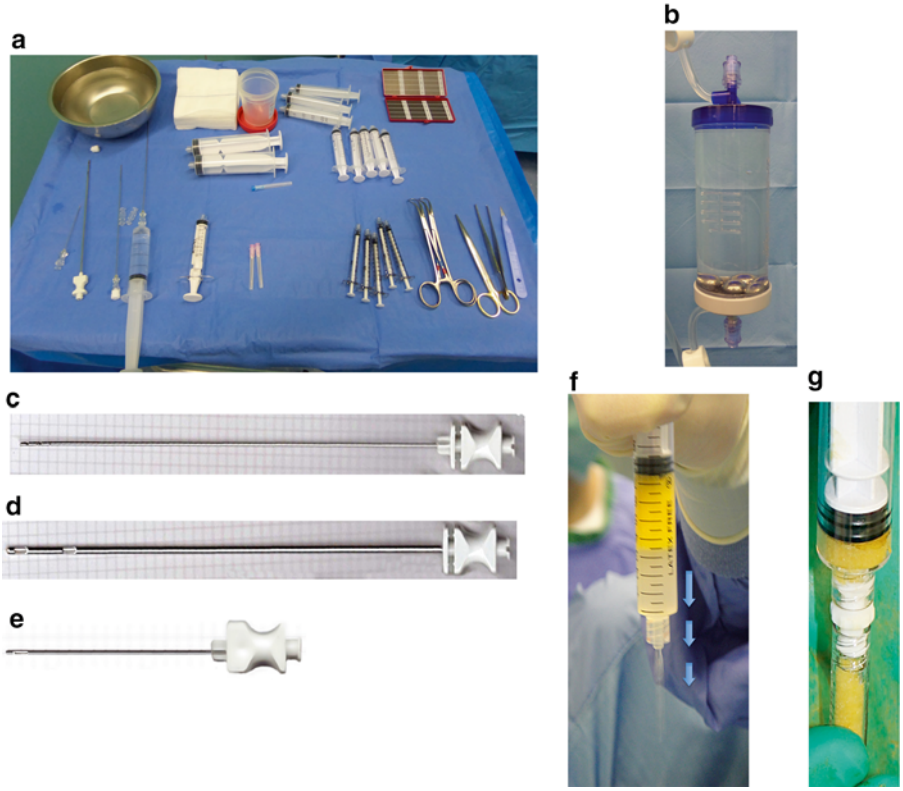

Fig. 1 The Lipogems system. (**a**) Example of the surgical kit provided. (**b**) View of the standard 225-ml device. (**c**) Infiltration cannula (19 G blunt 1 mm multiholes). (**d**) Harvesting cannula (13 G blunt 2 × 3 mm multiholes). (**e**) Injection cannula (19 G blunt 1 × 2 mm hole). (**f**) After collecting lipogems, the syringe is positioned vertically to decant and excess saline is discarded. (**g**) Decanted lipogems tissue is passed from the 10-ml syringe to a 1-ml syringe with a special plastic disposable connector. The 1-ml syringe is ideal for injection into soft tissue

harvesting; (b) facilitates injection through very narrow needles and subsequent homogenous distribution of the fat product (Lipogems product) within the recipient tissue; (c) avoids uneven tissue filling despite a variable rate of volume reabsorption depending on single patients and area of grafting; and (d) avoids post-transplant inflammatory processes.

2.1 The Lipogems Kit

The Lipogems system is a dedicated kit including four sets of instruments that have been optimized to yield the best technical performance and maximize ease of use at each step (Fig. 1a, b).

a. *Anesthesia Kit*: includes a dedicated, disposable blunt 19 G cannula (Fig. 1c) to be attached to any Luer Lock syringe (best 10–60 ml) to infiltrate the adipose tissue before harvesting with saline and diluted epinephrine (1:500,000) with minimal pain and local trauma. This step greatly facilitates subsequent

tissue harvesting through local vasoconstriction and subsequent hemostasis (induced mechanically and by the diluted epinephrine). Local (optional) anesthesia with very diluted lidocaine (0.02 %) may be added to the solution. The harvest area should be infused to obtain a certain degree of tissue firmness (as a general rule, 50 ml per 10×10 cm area of skin), and about 12 min should elapse before collecting the adipose tissue.

b. *Harvesting Kit*: contains a disposable blunt 13 G multi-hole smooth cannula with Luer Lock fitting, specially designed to ensure an optimal compromise between invasiveness and speed of fat tissue harvesting (Fig. 1d). Special autoblocking 10- or 60-ml Luer Lock syringes are provided (optional) to ease the manual harvesting of lipoaspirate which is transferred to larger 60-ml syringes by a special disposable transfer device. The 60-ml syringes are positioned vertically to decant the sample into a tray (a plastic disposable one is also optional) and excess fluid (blood and tumescent solution) is discarded to speed up the next stage.

c. *Processing Kit* (Figs. 2 and 3): this is the true heart of the Lipogems Device and Method. It includes a disposable device with a complete set of fittings and connections for the saline

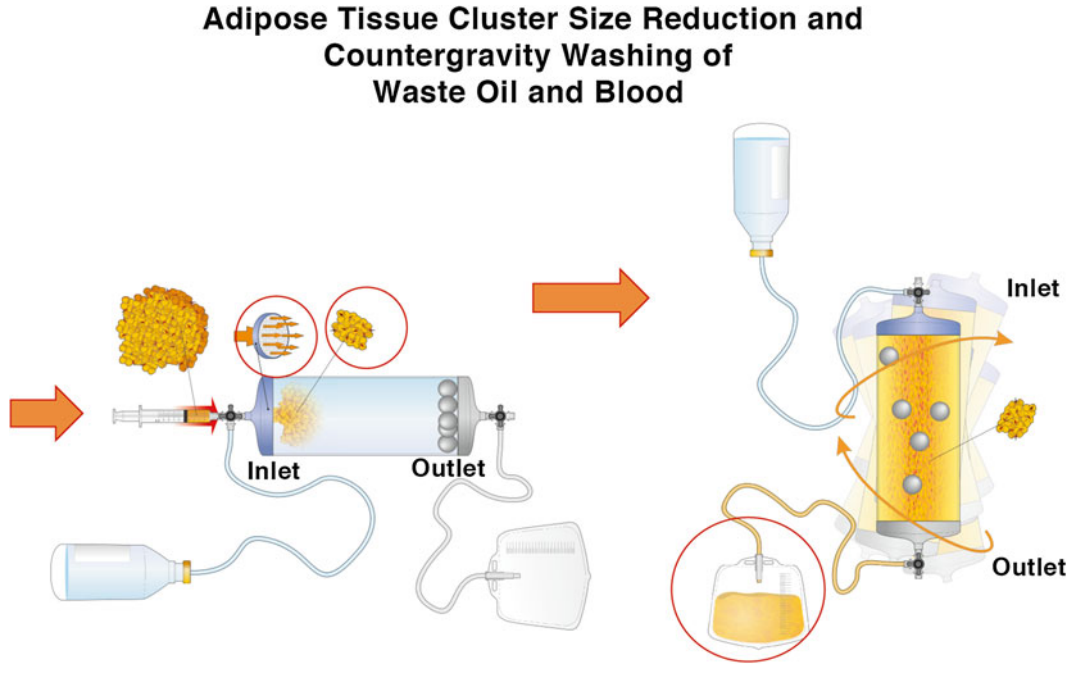

Fig. 2 The Lipogems device: first volumetric cluster reduction and washing of the lipoaspirate. The Lipogems device is powered by gravity and is completely closed and filled with saline. The lipoaspirate is pushed into the inlet (first reduction in volume) and the device is shaked for some minutes to completely wash the Lipogems tissue and remove any waste oil and blood

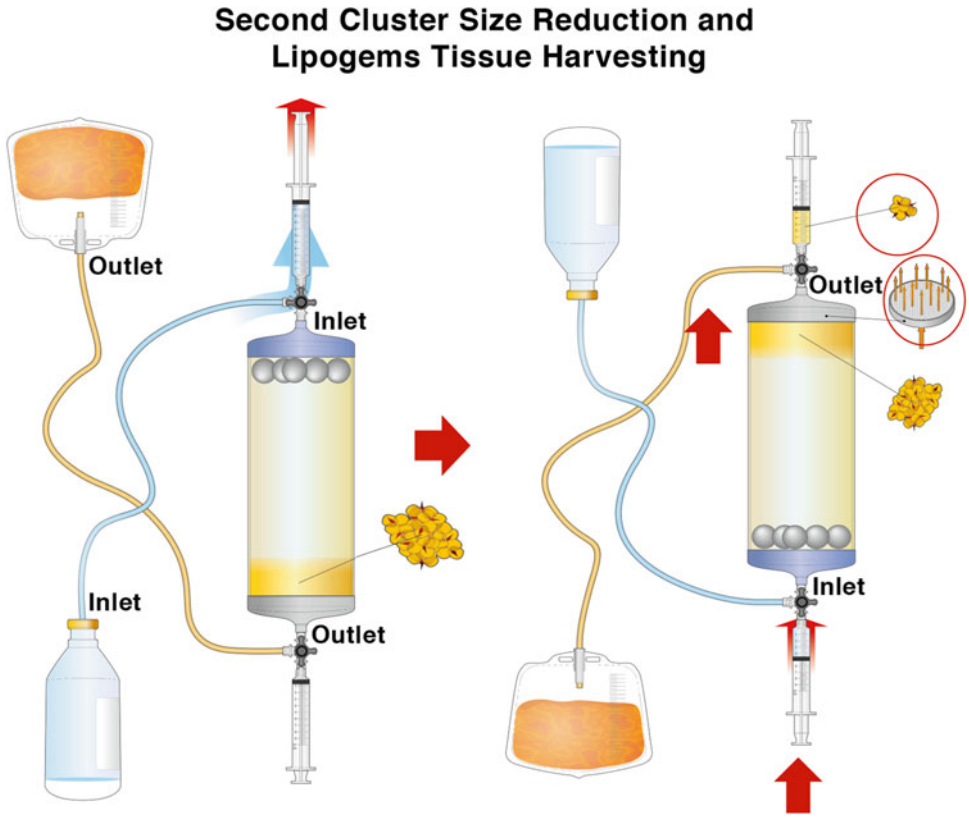

Fig. 3 The Lipogems device: second volumetric reduction of adipose clusters. Once the fat is completely washed and the solution is clear (5–15 min) the device is reversed (*grey cap up*) and a second cluster reduction is performed to obtain the final Lipogems product

bags (1 l saline bags are recommended for the 60-ml device and 3–5 l for the 240-ml device) and a large waste bag. The Lipogems device, aided by the forces of gravity and *minimal tissue manipulation* (as it is defined from a regulatory stand point), allows volumetric reduction (micro-fracturing) of the adipose cluster in the initial lipoaspirate (Figs. 2 and 3).

Between 40 ml and 130 ml of lipoaspirate (ideally 100 ml) are processed during each procedure with the standard 225 ml device (10–25 ml in the 60 ml device). To avoid cell damage, the device is carefully prefilled with saline to avoid the presence of air throughout all the steps, also producing a completely closed system. Tissue processing starts with a first cluster reduction obtained by pushing the aspirated fat from the syringe into the device through a first size reduction filter while allowing a corresponding quantity of saline to exit toward the waste bag (http://youtu.be/wCGM3smxTG8). During a subsequent shaking step, stainless steel marbles inside the device emulsify oil residues which are subsequently removed

together with contaminating blood components and cellular debris by the gravity counter-flow of the saline solution, while the washed reduced fat clusters migrate to the top of the device (http://youtu.be/wCGM3smxTG8). When the solution inside the device appears clear and the lipoaspirate is yellow, the device is turned upside-down by 180°, with the fat tissue product now facing a narrower size reduction filter. The second adipose cluster reduction is obtained by passing the floating adipose clusters through this second-size reduction filter by pushing additional fluid from the lower opening of the device using a 10-ml syringe (http://youtu.be/wCGM3smxTG8). At the end of the procedure, which is performed in a surgical room and only lasts 10–15 min., the device releases a *micro-fractured fluid fat tissue product* (clusters of 300–600 μm in diameter) that can easily flow through a small caliber needle. Lipogems can also easily pass through a standard 25 G sharp needle and homogenously disperse within the recipient tissue after transplantation. The same product can also be subjected to controlled freezing for tissue banking purposes.

The entire procedure is performed manually and sped up by gravity. We are currently developing a fully automated Lipogems device in order to further speed up and simplify the overall process and reduce operator dependent variability.

d. *Infiltration Kit*: If the Lipogems tissue is to be used immediately for clinical purposes, the system includes a specially designed 19 G blunt cannula (Fig. 1e), which permits minimally invasive delivery of the Lipogems product into subcutaneous and cutaneous tissues, as well as intramuscularly, as it has been recently performed at the level of the anal and urethral sphincters, for the correction of fecal incontinency [11]. The cannula is inserted after first puncturing the skin or mucosa with a standard 18 G or larger needle. A 1-ml Luer Lock cannula is recommended for controlling injections especially on the face. Its peculiar small caliber and blunt tip allow the delivery of Lipogems with minimal discomfort. Before infusion, the 10-ml syringe is vertically positioned and excess fluid is discarded (Fig. 1e) and then the Lipogems tissue product is transferred with a 1-ml syringe fitted with a special disposable Luer Lock connector provided in the kit (Fig. 1g).

2.2 Features of the Lipogems Product

Immunohistochemical analysis revealed that the Lipogems product encompasses a remarkably preserved vascular stroma with slit-like capillaries wedged between adipocytes and stromal stalks containing vascular channels with evident lumina. Seventy-two hours following initial fat harvesting, at 4 °C, the Lipogems product still exhibited an intact niche, while unprocessed lipoaspirate from the same donor exhibited an unorganized environment with compressed

and distorted microchannels [6]. The exact mechanism(s) accounting for the niche preservation within the Lipogems product remains to be established. We cannot exclude that maintenance of the adipose stem cell microenvironment is the result of (a) a lipoaspiration performed with an ad-hoc designed cannula more gently impacting with the site of harvest; (b) the mild mechanical forces and low pressure (gravity) applied within the processing device throughout each step; and (c) the prompt removal of oil, cellular debris, and lysates that may chemically act to degrade the niche architecture over time. In fact, comparative immunohistochemistry revealed that at 72 h after harvesting, the expression of CD146 was significantly increased in the Lipogems product, as compared with the unprocessed lipoaspirate; CD34 was similarly expressed in both samples. Since CD34 is a marker of endothelial differentiation and CD146 is co-expressed by endothelial cells and pericytes, these results indicate that pericytes, a mesenchymal cell that is thought to have stem-like properties, explains the significantly increased expression of CD146 found in the Lipogems product. Accordingly, the expression of α-smooth muscle actin (ASMA), a well-established marker of mural cells, was also higher in the Lipogems product than in the unprocessed lipoaspirate [6]. The number of cells expressing S-100 protein, a marker for adipocytes and preadipocytes, was similar in both conditions.

Further phenotypic analyses were performed on freshly harvested Lipogems product, the product previously stored at 4 °C for 24 h, or the product thawed after 7 days of cryopreservation at −180 °C under liquid nitrogen. Following a collagenase digestion to release the stromal vascular fraction (SVF) and to remove adipocytes, cellular viability close to 100 % was observed in all samples, as shown by the trypan blue dye exclusion test, with no differences between groups. Comparative flow cytometry analyses of selected stem cell markers in non-expanded cellular components from the lipoaspirate and the Lipogems product revealed significantly higher expression of the CD146+/90+/34− pattern [6] (identifying cells with pericyte characteristics [12]) in the Lipogems SVF when compared to the original lipoaspirate. The SVF fraction from the Lipogems product also exhibited a significantly higher percentage of CD146+/34+ elements than the unprocessed lipoaspirate. This expression pattern points to a pericyte subset that may be transitional between pericytes and supra-adventitial adipose stromal cells, and/or a set of endothelial (progenitor) cells [13, 14]. The percentage of $CD90^{+}/CD29^{+}/CD34^{-}$ elements, unambiguously identifying the hMSC population, was remarkably higher in the Lipogems product, when compared with the lipoaspirate. In further support of the differences between the two cellular products, the percentage of hematopoietic-like elements positive for CD14, CD34, and CD45 was significantly lower in the Lipogems than in

the unprocessed lipoaspirate [6]. Accordingly, a significantly higher percentage of hMSC-associated expression elements, compared with hematopoietic stem cell-related markers, was recently observed in another independent study on the characterization of the human micro-fragmented fat tissue product obtained with the Lipogems method and device [15].

3 The Expansion of Lipogems-Derived hASCs

We have provided evidence that Lipogems-embedded stem cells can be easily transferred and expanded in culture, without any manipulation. After placing the Lipogems product in regular D-MEM medium, containing 10 % fetal calf serum, hASCs were released from the tissue clusters, attaching to the tissue culture plastic, and reached 70–80 % confluence within 7–12 days [6]. Therefore, even in a GMP setting, the Lipogems product can be immediately transferred to a tissue culture environment for expansion, while in the same setting the conventional enzymatic processing of the lipoaspirate, and related washing of blood and oil contaminants, would require considerably longer periods and additional manipulation (usually 40–50 min per sample), prior to placing the released cells into culture.

Culturing Lipogems-derived hASCs also provided evidence that these cells exhibit the typical developmental potential of hMSCs, including commitment along osteogenic, chondrogenic, and adipogenic lineages [6, 15]. Adipogenic differentiation showed multiple adipocytic multivacuolar cells; the size increased with the time of induction. Osteogenic differentiation was confirmed by morphological changes, as early as the first week of induction and at the end of the induction period, by the formation of mineralized matrix, as demonstrated by Alizarin Red staining. Chondrogenic differentiation was observed after a 3-week induction period, as shown by the appearance of abundant extracellular matrix, and the presence of human type II collagen. The Lipogems tissue itself, not only its derived hMSCs, differentiated toward cartilage in vitro, acting as a natural scaffold and exhibiting interesting mechanical properties [16].

Of particular interest, Lipogems-derived hASCs expanded in culture retained their ability to express a set of genes, including vascular endothelial growth factor (VEGF), KDR, encoding a major VEGF receptor, and hepatocyte growth factor (HGF), involved in the orchestration of vasculogenesis and proper capillary formation [6]. Moreover, Lipogems-derived stem cells were found to express genes that constitute the core circuitry of self-renewal such as Oct4, Sox2, Nanog, and neurogenic lineage genes such as NeuroD1, Pax6, and Sox3 [15].

4 The Lipogems Product Is Efficiently Cryopreserved and Can Be Obtained from Cadaveric Donors

As reported above, the Lipogems product can be cryopreserved even in liquid nitrogen, without altering either the stromal vascular niche structure or the viability of the embedded stem cell elements (hMSCs and pericytes) [6]. Conversely, the release of viable hASCs from cryopreserved lipoaspirates is a rare, low-yield, and non-reproducible phenomenon.

This observation implies that excess Lipogems product resulting after a transplantation procedure, or the product itself, may be subjected to banking for future use, without losing its tissue status.

Intriguingly, a micro-fractured fat tissue product still harboring viable hASCs can also be harvested from cadaveric donors with the Lipogems device [6]. In cadaveric fat tissue (≤30 h post-mortem) there were approximately 75 % fewer total viable cells within the SVF after either enzymatic digestion or Lipogems processing, when compared with adipose tissue harvested from living donors. The yield of cells released from the cell clusters of the Lipogems product following its treatment with collagenase is similar to that observed after a direct enzymatic digestion of the unprocessed lipoaspirate, indicating that Lipogems processing does not affect hASC recovery. Flow cytometry analysis of cultured hASCs derived from cadaveric Lipogems provided evidence that the vast majority (~80 %) of cells expressed characteristic hASC markers, exhibiting phenotypic patterns similar to those detected in hASCs obtained from the Lipogems product of living donors.

Similar to the product derived from living donors, the cadaveric Lipogems product can be cryopreserved; after thawing, viable cells are released and can be grown and expanded in culture.

5 Lipogems-Derived hASCs Vigorously Respond to Both Chemical and Physical Stimuli

An interesting finding in stem cell biology is that stem cell multi-/pluri-potency and fate can be modulated not only by naturally occurring or synthetic chemical agents [17–23], but also by physical energy, as observed following exposure to electromagnetic fields [24–27].

We have previously shown that the expression of vasculogenic genes can be remarkably enhanced following exposure of enzymatically dissociated hASCs to a mixture of natural molecules including hyaluronic, butyric, and retinoic acids [28]. Both Lipogems-derived hASCs and hASCs resulting from enzymatic digestion of lipoaspirates harvested from the same donor were found to spontaneously express VEGF, KDR, and HGF mRNAs

to a similar extent. However, exposure of Lipogems hASCs to the above mixture resulted in significantly higher transcription of these genes, as compared to the effect yielded from enzymatically dissociated stem cells. Studies are currently in progress to assess whether such a greater vasculogenic potential may result in enhanced tissue healing in animal models of vascular disease.

Lipogems-derived hASCs were also highly responsive to the action of electromagnetic fields. In particular, exposure of Lipogems-derived hASCs to a Radio Electric Asymmetric Conveyer (REAC), an innovative device designed to asymmetrically convey radioelectric fields of 2.4 GHz to either the human body [29, 30] or cultured cells [26, 27], remarkably enhanced the transcription program of multilineage, tissue-restricted genes [27], including: (a) cardiogenic genes prodynorphin, GATA-4, and Nkx-2.5; (b) vasculogenic transcripts VEGF, HGF, and von Willebrand factor (vWF); (c) neurogenin-1, and (d) myoD, involved in neurogenic and skeletal myogenic commitment, respectively.

Stem cell exposure to REAC also finely tuned the expression of stemness-related genes, inducing an early increase in Nanog, Sox2, and Oct4 transcription during the first 4–12 h, followed by a significant down-regulation of transcript levels below the control value after 24 h of treatment [27]. It is now evident that the down-regulation of stemness genes after their initial induction is a critical step in cell progression toward a differentiated state [31–35]. Relevant to these observations, comparative transcriptional analyses in REAC-exposed cells revealed that both the early overexpression and the subsequent inhibition of stemness genes were significantly more pronounced in Lipogems-derived hASCs than in the enzymatically dissociated counterpart [27]. This distinctive feature was reflected in the differentiating ability of Lipogems-derived hASCs. In a stem cell population exposed to the electromagnetic field, flow cytometry analysis of β-3-tubulin, myoD, and α-sarcomeric actinin highlighted a neural, skeletal myogenic, and cardiogenic commitment, respectively; and provided evidence that the percentage of each lineage commitment from Lipogems-derived hASCs significantly exceeded the percentage detected from enzymatically dissociated hASCs [27].

On the whole, these data indicate that the Lipogems product may be an ideal source of stem cells capable of optimizing their multipotency expression and differentiation potential in the presence of either chemical or physical stimuli. The mechanisms underlying these results still remain to be elucidated. We are currently investigating the possibility that lipoaspirate processing with the Lipogems device (avoiding the use of collagenase and other enzymes) may have preserved the cell surface environment and glycocalyx composition better than other methods based on enzymatic dissociation. This would account for the enhanced hASC responsiveness to chemical and physical interventions.

6 Future Directions

It is increasingly evident that a multidisciplinary approach to basic and clinical research should accelerate translation to the bedside. While basic research findings drive the development of clinical research studies, and data from these studies improve our understanding of human health and disease; it is also true that data collected in the clinical setting may guide the direction of basic research questions and hypotheses. Ultimately, both would be expected to lead to improvements in medical treatment, diagnostics, and preventive care.

Studies are in progress to verify whether the Lipogems product by itself, or the chemical/physical preconditioning of the product (or its expanded hASCs) prior to transplantation, may result in improved tissue rescue in defined animal models of disease, including heart failure, neurodegenerative diseases, skeletal muscle dystrophy, diabetes, bone, and cartilage defects.

In the affirmative, the Lipogems method and device may become an attractive *system* for multifaceted tissue/cell therapy interventions.

Weblink to Supplemental Animation. Lipoaspirate processing with the Lipogems device. http://youtu.be/wCGM3smxTG8

References

1. Gallo RC, Montagnier L (2003) The discovery of HIV as the cause of AIDS. N Engl J Med 349:2283–2285
2. Clements JA (1997) Lung surfactant: a personal perspective. Annu Rev Physiol 59:1–21
3. Clements JA, Avery ME (1998) Lung surfactant and neonatal respiratory distress syndrome. Am J Respir Crit Care Med 157(4 Pt 2):S59–S66
4. Jensen EV, Jordan VC (2003) The estrogen receptor: a model for molecular medicine. Clin Cancer Res 9:1980–1989
5. Turer AT, Hill JA, Elmquist JK et al (2012) Adipose tissue biology and cardiomyopathy: translational implications. Circ Res 111: 1565–1577
6. Bianchi F, Maioli M, Leonardi E et al (2013) A new nonenzymatic method and device to obtain a fat tissue derivative highly enriched in pericyte-like elements by mild mechanical forces from human lipoaspirates. Cell Transplant 22:2063–2077
7. Rigotti G, Marchi A, Galiè M et al (2007) Clinical treatment of radiotherapy tissue damage by lipoaspirate transplant: a healing process mediated by adipose-derived adult stem cells. Plast Reconstr Surg 119:1409–1422
8. Coleman SR (2006) Structural fat grafting: more than a permanent filler. Plast Reconstr Surg 118(3 Suppl):108S–120S
9. Reckhenrich AK, Kirsch BM, Wahl EA et al (2014) Surgical sutures filled with adipose-derived stem cells promote wound healing. PLoS One 9, e91169
10. Tremolada C, Palmieri G, Ricordi C (2010) Adipocyte transplantation and stem cells: plastic surgery meets regenerative medicine. Cell Transplant 19:1217–1223
11. Giori A, Tremolada C, Vailati R et al (2015) Recovery of Function in Anal Incontinence after Micro-Fragmented Fat Graft (Lipogems®) Injection: Two Years Follow Up of the First 5 Cases. CellR4 3 (2): e1544
12. Olson LE, Soriano P (2011) PDGFRβ signaling regulates mural cell plasticity and inhibits fat development. Dev Cell 20:815–826
13. Yoshimura K, Shigeura T, Matsumoto D et al (2006) Characterization of freshly isolated and cultured cells derived from the fatty and fluid portions of liposuction aspirates. J Cell Physiol 208:64–76
14. Zimmerlin L, Donnenberg VS, Pfeifer ME et al (2010) Stromal vascular progenitors in adult human adipose tissue. Cytometry A 77:22–30

15. Carelli S, Messaggio F, Canazza A et al (2015) Characteristics and properties of mesenchymal stem cells derived from micro-fragmented adipose tissue. Cell Transplant 24(7):1233–1252
16. Bosetti M, Borrone A, Follenzi A et al (2015) Human lipoaspirate as autologous injectable active scaffold for one-step repair of cartilage defects. Cell Transplant, Sep 21. [Epub ahead of print]
17. Ventura C, Maioli M (2000) Opioid peptide gene expression primes cardiogenesis in embryonal pluripotent stem cells. Circ Res 87: 189–194
18. Ventura C, Zinellu E, Maninchedda E, Maioli M (2003) Dynorphin B is an agonist of nuclear opioid receptors coupling nuclear protein kinase C activation to the transcription of cardiogenic genes in GTR1 embryonic stem cells. Circ Res 92:623–629
19. Ventura C, Zinellu E, Maninchedda E et al (2003) Protein kinase C signaling transduces endorphin-primed cardiogenesis in GTR1 embryonic stem cells. Circ Res 92:617–622
20. Ventura C, Maioli M, Asara Y et al (2004) Butyric and retinoic mixed ester of hyaluronan: a novel differentiating glycoconjugate affording a high-throughput of cardiogenesis in embryonic stem cells. J Biol Chem 279: 23574–23579
21. Ventura C, Cantoni S, Bianchi F et al (2007) Hyaluronan mixed esters of butyric and retinoic acid drive cardiac and endothelial fate in term placenta human mesenchymal stem cells and enhance cardiac repair in infarcted rat hearts. J Biol Chem 282:14243–14252
22. Lionetti V, Cantoni S, Cavallini C et al (2010) Hyaluronan mixed esters of butyric and retinoic acid affording myocardial survival and repair without stem cell transplantation. J Biol Chem 285:9949–9961
23. Maioli M, Santaniello S, Montella A et al (2010) Hyaluronan esters drive Smad gene expression and signaling enhancing cardiogenesis in mouse embryonic and human mesenchymal stem cells. PLoS One 5(11), e15151
24. Ventura C, Maioli M, Pintus G (2000) Elf-pulsed magnetic fields modulate opioid peptide gene expression in myocardial cells. Cardiovasc Res 45:1054–1064
25. Ventura C, Maioli M, Asara Y et al (2005) Turning on stem cell cardiogenesis with extremely low frequency magnetic fields. FASEB J 19:155–157
26. Maioli M, Rinaldi S, Santaniello S et al (2012) Radiofrequency energy loop primes cardiac, neuronal, and skeletal muscle differentiation in mouse embryonic stem cells: a new tool for improving tissue regeneration. Cell Transplant 21:1225–1233
27. Maioli M, Rinaldi S, Santaniello S et al (2014) Radio electric asymmetric conveyed fields and human adipose-derived stem cells obtained with a non-enzymatic method and device: a novel approach to multipotency. Cell Transplant 23(12):1489–1500
28. Cavallari G, Olivi E, Bianchi F et al (2012) Mesenchymal stem cells and islet cotransplantation in diabetic rats: improved islet graft revascularization and function by human adipose tissue-derived stem cells preconditioned with natural molecules. Cell Transplant 21: 2771–2781
29. Castagna A, Fontani V, Rinaldi S et al (2011) Radio electric tissue optimization in the treatment of surgical wounds. Clin Cosmet Investig Dermatol 4:133–137
30. Fontani V, Castagna A, Mannu P et al (2011) Radioelectric asymmetric stimulation of tissues as treatment for post-traumatic injury symptoms. Int J Gen Med 4:627–634
31. Yoon DS, Kim YH, Jung HS et al (2011) Importance of Sox2 in maintenance of cell proliferation and multipotency of mesenchymal stem cells in low-density culture. Cell Prolif 44:428–440
32. Baal N, Reisinger K, Jahr H et al (2004) Expression of transcription factor Oct-4 and other embryonic genes in CD133 positive cells from human umbilical cord blood. Thromb Haemost 92:767–775
33. Goodell MA (2003) Stem-cell "plasticity": befuddled by the muddle. Curr Opin Hematol 10:208–213
34. Lang KC, Lin IH, Teng HF et al (2009) Simultaneous overexpression of Oct4 and Nanog abrogates terminal myogenesis. Am J Physiol Cell Physiol 297:C43–C54
35. Park SB, Seo KW, So AY et al (2012) SOX2 has a crucial role in the lineage determination and proliferation of mesenchymal stem cells through Dickkopf-1 and c-MYC. Cell Death Differ 19:534–545

Chapter 7

Paracrine Mechanisms of Mesenchymal Stem Cells in Tissue Repair

Massimiliano Gnecchi, Patrizia Danieli, Giuseppe Malpasso, and Maria Chiara Ciuffreda

Abstract

Tissue regeneration from transplanted mesenchymal stromal cells (MSC) either through transdifferentiation or cell fusion was originally proposed as the principal mechanism underlying their therapeutic action. However, several studies have now shown that both these mechanisms are very inefficient. The low MSC engraftment rate documented in injured areas also refutes the hypothesis that MSC repair tissue damage by replacing cell loss with newly differentiated cells. Indeed, despite evidence of preferential homing of MSC to the site of myocardial ischemia, exogenously administered MSC show poor survival and do not persist in the infarcted area. Therefore, it has been proposed that the functional benefits observed after MSC transplantation in experimental models of tissue injury might be related to the secretion of soluble factors acting in a paracrine fashion. This hypothesis is supported by pre-clinical studies demonstrating equal or even improved organ function upon infusion of MSC-derived conditioned medium (MSC-CM) compared with MSC transplantation. Identifying key MSC-secreted factors and their functional role seems a reasonable approach for a rational design of nextgeneration MSC-based therapeutics. Here, we summarize the major findings regarding both different MSC-mediated paracrine actions and the identification of paracrine mediators.

Key words Mesenchymal stem cells, Soluble factors, Paracrine mechanisms, Tissue repair, Angiogenesis, Cytoprotection, Conditioned medium, Tissue regeneration, Rigenerative medicine, Cell therapy

1 Introduction

Tissue regeneration from transplanted mesenchymal stromal cells (MSC) either through transdifferentiation or cell fusion was originally proposed as the principal mechanism underlying their therapeutic action [1–9]. However, several studies have now shown that both these mechanisms are very inefficient. For instance, in vitro differentiation of MSC into contractile cardiomyocytes (CMC) is very rare unless chemical compounds are used to prime the cells [10, 11]. Recently, we were able to demonstrate that it is possible to differentiate human MSC of fetal origin by overexpressing specific miRNAs

Massimiliano Gnecchi (ed.), *Mesenchymal Stem Cells: Methods and Protocols*, Methods in Molecular Biology, vol. 1416,
DOI 10.1007/978-1-4939-3584-0_7,

[12]. However, even in this case, cell manipulation is required. An alternative is represented by co-culture of MSC with native CMC, but in the case of human cells this method is obviously not applicable on a large scale [13–16]. Cell fusion of bone marrow (BM)-derived donor cells with recipient CMC has been reported [17], but the low frequency of this mechanism rules out its substantial involvement in MSC-mediated cardiac repair [16].

Also transdifferentiation of MSC into renal cells is not considered an attainable goal in cell therapy. For instance, after ischemic injury the intravenous injection of BM-MSC reduced functional renal impairment but without obvious evidence of cell differentiation into tubular cells [18]. The therapeutic action of BM-MSC was evaluated also in a rat model of ischemia/reperfusion-induced acute kidney injury (AKI): iron-labeled BM-MSC were predominantly located in the glomerular capillaries, while kidney tubular cells showed no iron labeling, indicating the absence of transdifferentiation into tubular cells [19]. Togel and coworkers confirmed that there is no evidence of rat BM-MSC differentiation into tubular or endothelial cells (EC) in the same experimental model of AKI [20, 21]. In a brain stroke experimental study, only 3 % of MSC administered intravenously expressed neuronal markers in vivo, further supporting the concept that tissue replacement is not likely to be a functionally relevant mechanism of action for this cell type [22]. Some reports testing a wound repair model suggest that MSC differentiate into epidermal keratinocytes, EC, pericytes, and sebocytes in areas adjacent to the wound [23–25]. These events seem to be due to MSC differentiation rather than MSC fusion with local resident cells [23–25]. However, other investigators reported that there is no evidence that MSC transdifferentiate into phenotypes typical of resident cutaneous cells in the wound healing model [26]. So, also in this setting there is no certainty that regeneration from exogenous cells does occur.

The low MSC engraftment rate documented in injured areas also refutes the hypothesis that MSC repair tissue damage by replacing cell loss with newly differentiated cells. Despite evidence of preferential homing of MSC to the site of myocardial ischemia [27], exogenously administered MSC show poor survival and do not persist in the infarcted area [28, 29], probably because of the harsh ischemic microenvironment, characterized by oxidative stress, inflammation, cytotoxic cytokines and in some instances an absence of extracellular matrix (ECM) for MSC attachment [30, 31]. Other investigators have failed to detect permanent engraftment of transplanted BM-derived MSC (BM-MSC) in infarcted hearts [32]. Human adipose tissue-derived MSC (AD-MSC) can improve blood perfusion in mice with hind limb ischemia, a model of peripheral artery disease (PAD) [33, 34], but the incorporation rate of MSC into the host vascular structures resulted lower than

1 %, indicating that other effects likely account for the observed beneficial effects [34]. The infusion of MSC in AKI animal models has demonstrated that few cells are able to engraft in the damaged renal tissue and that these cells are preferentially localized at the peritubular level and, less frequently, in the tubular epithelium [2, 4]. Imberti and colleagues also confirmed that the engraftment of BM-MSC in damaged kidney was low and the percentage of cells inside the tubular epithelium was negligible (<5–8 % of total engrafted cells) [35]. However, the renal protective effects in terms of functional restoration and animal survival were significant, supporting the notion that MSC act through a transdifferentiation-independent mechanism [5]. Togel and co-workers confirmed the renal protective capacity of MSC in an experimental model of renal ischemia/reperfusion injury, with a significant improvement in renal function [20]. Again, MSC were only transiently present in the renal vasculature and were not detected within the renal parenchyma three days after infusion.

In brain stroke studies, MSC have been found to home preferentially to the ischemic boundary [36, 37]. Nonetheless, it has been shown that few cells survive after 2 weeks and long-term cell engraftment results are negligible. Few cells have been shown to survive in the studies of xenogeneic cell implantation: with no immunosuppression, cell survival at 2 weeks was very poor [38]. Also long-term cell engraftment has not been detected after intravenous administration [22]. In another study, out of 3×10^6 MSC delivered intravenously, only 3 % expressed neuronal markers in vivo, further supporting the concept that tissue replacement is not likely to be a functionally relevant mechanism of action for this cell type [39].

All this evidence questions the plasticity of transplanted MSC. In general, regardless of whether stem cells transdifferentiate via fusion-dependent or fusion-independent mechanisms, it has been shown that in many cases the amount of newly generated tissue is too limited to justify functional improvements. Therefore, it has been proposed that the functional benefits observed after MSC transplantation in experimental models of tissue injury might be related to the secretion of soluble factors acting in a paracrine fashion [4, 5, 7–9, 20, 40–44]. This hypothesis is supported by recent pre-clinical studies demonstrating equal or even improved organ function upon infusion of MSC-derived conditioned medium (MSC-CM) compared with MSC transplantation [7–9, 40, 45–54]. Therefore, identifying key MSC-secreted factors and their functional role seems a reasonable approach for a rational design of next-generation MSC-based therapeutics.

We now summarize the major findings regarding different MSC-mediated paracrine actions.

2 Paracrine Effects

The array of potential therapeutic mechanisms mediated by the MSC secretome spans from cytoprotection and tissue repair (anti-apoptotic and pro-mitotic) to neovascularization, anti-inflammatory, and anti-fibrotic effects. In some instances, restoration of cell metabolism also plays a role.

2.1 Cytoprotective Effect

Extensive data from a wide array of pathological conditions demonstrate that MSC exert powerful cytoprotective and anti-apoptotic actions through the release of soluble active mediators. For instance, our group was the first to demonstrate that medium conditioned by hypoxic MSC can reduce apoptosis and necrosis of isolated rat CMC exposed to low oxygen tension [40]. The cytoprotective effect was greatly enhanced in MSC overexpressing the gene Akt-1 (Akt-MSC). More importantly, the paracrine-protective properties of the Akt-MSC were validated in vivo by injecting CM obtained from Akt-MSC in a rat experimental model of permanent coronary occlusion. The infarct size and the CMC apoptotic index were significantly lower in animals treated with concentrated Akt-MSC-CM compared with controls. In a follow-up study, we were able to document that infarct size reduction was matched by the preservation of cardiac function [41]. The data obtained with CM injection essentially replicated the results observed with MSC transplantation both in terms of infarct size and cardiac function, confirming that cytoprotection was the main mechanism of stem cell action in this experimental model. These findings were also successfully replicated in pigs [55]. Other groups have confirmed the paracrine cytoprotective effects exerted by BM-derived stem cells on ischemic CMC [56–58]. Our group has recently demonstrated that also MSC of human origin derived from the amniotic membrane of the placenta (hAMC) mediate powerful cardioprotective effects following MI. Indeed, the injection of CM from hAMC (hAMC-CM) into infarcted rat hearts limited infarct size, reduced CMC apoptosis and ventricular remodeling and resulted in improved cardiac function compared with controls [59].

It has also been shown that human BM-MSC mediate renal protection. The infusion of BM-MSC in immune-deficient NOD/SCID mice with AKI induced by cisplatin decreased proximal tubular epithelial cell injury and reduced renal function impairment, increasing the survival of the recipient [4]. In an experimental model of renal ischemia/reperfusion injury, the intracarotid administration of MSC resulted in a significant improvement of renal function, although MSC were only transiently present in the renal vasculature, confirming the renoprotective action of MSC [20]. Interestingly, the kidneys of MSC-treated rats revealed a decrease in gene expression of pro-inflammatory cytokines and an increase in several growth factors

with mitogenic, pro-survival, and anti-apoptotic effects [20]. The same authors also demonstrated that in mice with AKI induced by ischemia/reperfusion, MSC home to the renal microvascular circulation preventing tubular cell apoptosis [21]. Another study showed that intraperitoneal injection of BM-MSC-CM in a mouse model of tubular injury resulted in a significant decrease of tubular cell apoptosis, increased survival, and renal function improvement [44]. Finally, CM produced by MSC genetically modified to overexpress Lnc2 prevented apoptosis and increased the expression of growth factors when administered to cisplatin-treated HEK 293 kidney cells [60].

The beneficial effects of MSC therapy documented in brain injury models are also mediated by paracrine mechanisms [61]. For instance, the administration of male MSC in female rats who experienced stroke resulted in a decrease in the number of apoptotic neurons, with a limited number of transplanted cells differentiating into neural cells [62]. This evidence of brain protection was accompanied by a rise in beta fibroblast growth factor (bFGF) levels. The anti-apoptotic effect was further demonstrated using human MSC, which induce functional amelioration, reduce infarct volume, and promote neuroprotection in rodents with experimental stroke [7]. Increased levels of insulin-like growth factor (IGF-1) as well as vascular endothelial growth factor (VEGF), epidermal growth factor (EGF), and bFGF were observed in the brain of treated rats, as compared with controls. In particular, the IGF-1 levels were upregulated exclusively in vivo, suggesting a very specific and regulated mechanism [7]. The use of MSC seems then to lead to improvement of function and to enhance plasticity of the remaining tissue, particularly tissue in the boundary zone of the ischemic lesion. Thus, when injected intravenously, MSC enter and engraft in the brain and evoke the expression of growth and trophic factors from endogenous cells, primarily astrocytes and endothelial cells.

Also the intracerebroventricular administration of CM from MSC resulted in reduced infarct volume in mice with ischemia/reperfusion brain injury, by a mechanism of neuroprotection that was dependent on secreted tissue inhibitor of metalloproteinase-1 (TIMP-1) and progranulin [63]. The direct intravenous infusion of CM from MSC derived from adipose tissue induced behavioral and learning recovery in rats with experimental hypoxia ischemia brain injury, while markedly reducing long-term functional cognitive and motor skill impairment by a mechanism regulated by secreted IGF-1 and brain-derived neurotrophic factor (BDNF) [64].

2.2 Provasculogenic Effects

Post-natal neovascularization is another important biological process positively influenced by MSC in a paracrine fashion. Despite evidence that BM-MSC incorporate into vascular structures, only

a small number of vessels have been shown to contain donor cells. However, several studies demonstrated that MSC represent a source of paracrine proangiogenic and proarteriogenic factors [41, 65, 66]. Kinnaird et al. were the first to demonstrate that MSC-CM can stimulate EC proliferation and migration in vitro and that the injection of MSC-CM into mice that had undergone hindlimb ischemia was sufficient to mediate restoration of blood flow in the injured limb [9]. Gene expression profiling of MSC grown under normal conditions or under hypoxia stimulation revealed that these cells express a wide range of arteriogenic cytokines at baseline and that several of these cytokines are upregulated by hypoxia [65]. Other studies testing MSC transplantation in experimental MI models reported an increase in capillary density in treated animals compared with controls, despite the presence of few EC of donor origin [67–69]. In all these cases, even though not directly proven, a proangiogenic paracrine mechanism seems the most reasonable explanation for the effects observed. On the contrary, a recent study by our group has convincingly demonstrated that the injection of hAMC-CM resulted in a significant increase of vascular density after cardiac ischemia/reperfusion injury [59].

When infused in immunodeficient NOD/SCID mice with AKI, human BM-MSC preserved microvascular integrity contributing to improved renal tissue oxygenation [4]. Togel and coworkers further documented the vasculotropic, paracrine effect of rat BM-MSC with MSC-CM containing VEGF, hepatocyte growth factor (HGF), and IGF-1 [21]. And as evidenced by Rehman et al. the transplantation of human AD-MSC can enhance angiogenic and neurogenic processes through secretion of VEGF, HGF, and transforming growth factor β (TGF-β) [33].

It has also been shown that during the wound healing process, MSC increase angiogenesis through paracrine mechanisms [23–26, 70, 71]. In particular, MSC-CM acts in vivo as a chemoattractant recruiting macrophages and EC to the wound [72] and even in a liver fibrosis model, improved microcirculation after MSC injection has been reported [73].

2.3 Anti-inflammatory Effect

The anti-inflammatory effect of MSC has also been noted in many studies and documented to be mediated through paracrine mechanisms [74, 75]. MSC, when used in models of lung, renal, cardiac or hepatic injury as well as in models of burn injury of different organs have repeatedly shown beneficial effects [76–79]. All of these conditions are typically accompanied by a strong inflammatory response; this observation was an incentive to study the effect of MSC on inflammation. We now know that MSC mediate anti-inflammatory effects; however, the main mechanism behind this beneficial effect remains unclear. One of the main pro-inflammatory cytokines is tumor necrosis factor-alpha (TNF-α). It has been

demonstrated that administration of MSC reduces the level of TNF-α in vitro. In the model of cisplatin-induced acute renal injury, levels of pro-inflammatory cytokines such as TNF-α, interleukin (IL)-1β, IL-6, and others were significantly increased [80–82]. When MSC were co-cultured with the proximal tubular cell line (human kidney-2) and pre-treated with cisplatin, significant reductions in TNF-α and IL-1β were also detected [83]. In an in vivo model of lung injury, a decline in the levels of TNF, IL-6, and interferon-gamma (IFN-γ) in the serum was also detected in the group pre-treated with MSC compared with controls [84]. The anti-inflammatory properties of MSC have also been suggested by their capacity to inhibit T- and B-cell proliferation [85, 86] and H_2O_2 production from neutrophils [87], as well as by their ability to suppress T and NK cytotoxicity [88].

Inflammatory bowel disease (IBD) in humans refers to a family of disorders characterized by destructive inflammation of the colon or small intestine. Damage caused by chronic inflammation leads to debilitating gastrointestinal manifestations such as severe cramps and abdominal pain, diarrhea, and weight loss. While the causes of IBD are not well understood, $CD4^+$ T cells are thought to play a key role in pathogenesis of the disease [89]. Therapies using MSC have been largely successful in treating IBD in animal models. MSC appear to suppress the disease through multiple mechanisms. Several studies have reported that MSC infusion increases the frequency of regulatory T cells accompanied by a reduction in T cells secreting inflammatory cytokines [90, 91]. In a model of colitis, MSC from mice deficient in Fas ligand (FasL) were unable to suppress the disease [92, 93]. FasL and its receptor Fas are both essential molecules for maintaining T-cell homeostasis, and signaling downstream of Fas leads to the rapid induction of apoptosis in susceptible cells, including activated effector T cells.

Anti-inflammatory action is also exerted by MSC in experimental models of acute myocarditis [94, 95]. Ohnishi et al. demonstrated that MSC transplantation attenuated the increase in $CD68^+$ inflammatory cells and monocyte chemoattractant protein (MCP)-1 expression in the myocardium and improved cardiac function in mice with myocarditis. Adult rat ventricular cardiomyocytes cultured under standard conditions were injured by MCP-1, which may play an important role in myocarditis [96]. In contrast, in the presence of MSC-CM, MCP-1-induced injury was significantly attenuated.

Anti-inflammatory effects play an important role in brain disease. For instance, in a murine model mimicking Krabbe's disease (KD), the intra-cerebral-ventricular administration of either BM- or AD-MSC was shown to ameliorate motor function impairment and limit overall deterioration by reducing cerebral inflammation, including a significant decrease in the numbers of central nervous system-infiltrating macrophages, and activated microglial cells

implicated in KD progression [97]. Other studies have also confirmed the immune modulatory properties of MSC after systemic cell injection in rodents affected by experimental autoimmune encephalomyelitis, as a model of multiple sclerosis. The systemic injection of both BM-MSC and AD-MSC led to inhibition of autoreactive T-cell responses via immune regulatory and neurotrophic mechanisms [98, 99]. Additionally, it has been shown that intrastriatal transplanted AD-MSC limit the progression of Parkinson's disease in mice [100]. Histological, electrophysiological, neurochemical, and gene expression studies suggested that the likely mechanisms by which AD-MSC grafts rescued the nigrostriatal function involved little direct differentiation of the stem cell into functional dopaminergic neurons, rather the improvement was the result of indirect modulation of the oxidative stress-induced neuroinflammatory environment via the secretion of BDNF, glial cell line-derived neurotrophic factor (GDNF), and nerve growth factor (NGF) at the level of the lesioned substantia nigra [100].

MSC exert immunomodulatory effects also by inducing neighboring cells to secrete anti-inflammatory cytokines [101–103], which may be useful in inhibiting excessive inflammation. For instance, a significant reduction in the expression of pro-inflammatory cytokines such as IL-1β, TNF-α, IFN-γ, inducible nitric oxide synthase, and a concomitant remarkable upregulation of anti-inflammatory cytokines (IL-10 and bFGF, TGF-α, Bcl-2) were observed in AKI rats receiving BM-MSC infusion [20].

2.4 Effects on Endogenous Regeneration

One of the most intriguing hypotheses regarding the therapeutic effects mediated by MSC is that factors produced and released by these cells may induce endogenous regeneration by stimulating resident progenitor cells. In the case of the heart, there is evidence suggesting that MSC transplantation may activate resident cardiac progenitor cells (CPC) and/or stimulate CMC replication via paracrine action, thus improving endogenous cardiac regeneration [15, 104]. The demonstration that rat BM-MSC secrete trophic factors able to induce activation and proliferation of CPC in vitro supports this hypothesis [105]. It has also been shown that intramyocardial administration of HGF and IGF-1 at the infarct border zone can induce CPC migration, proliferation, and differentiation [106]. Since MSC release both HGF and IGF-1, particularly under hypoxic stimulation [41], it is reasonable to hypothesize that MSC injected into ischemic hearts may attract and activate resident CPC through the release of these molecules. MSC injected into infarcted pig hearts resulted in newly formed CMC, some of which stained positive for c-kit and others for Ki67 [107]. More direct evidence that BM-MSC trigger proliferation and differentiation of endogenous CPC has been produced [15]. Transendocardial injection of GFP-MSC was performed in a pig model of ischemia–reperfusion injury and a detailed tissue analysis showed that MSC stimulate

endogenous CMC regeneration by stimulating endogenous c-kit$^+$ CPC and by enhancing native CMC cell cycling.

In mice with AKI induced by cisplatin, BM-MSC homed to the damaged kidney and boosted proliferation of tubular cells [2]. Similar results were replicated in immunodeficient NOD/SCID mice with AKI, where human BM-MSC acted mainly by diminishing renal cell apoptosis and by increasing tubular cell proliferation [4].

BM-MSC-secreted factors present in the CM promoted proliferation and increased the expression of glial fibrillary acidic protein (GFAP) of neural stem/precursor cells (NPC) in vitro suggesting an effect toward their differentiation into astrocytes [108]. It has also been suggested that MSC-secreted factors may induce oligodendroglial differentiation/maturation of adult NPC, as shown by treatment of NPC with rat MSC-CM [109]. In rodents affected by experimental autoimmune encephalomyelitis, a model of multiple sclerosis, the systemic injection of BM-MSC led to inhibition of the autoreactive T-cell response as well as the stimulation of endogenous oligodendrogenesis via immune regulatory and neurotrophic mechanisms [98, 99, 110–112]. Key factors responsible for the observed therapeutic effects have been identified, these include: HGF [113, 114], bFGF, BDNF, and platelet derived-growth factor (PDGF) [110].

In a wound healing setting, several studies have indicated that MSC accelerate epithelialization and increase granulation tissue formation [23–26, 70, 71]. Also MSC-CM, similar to MSC, accelerated epithelialization in wound repair [72, 115, 116]. MSC secrete pro-mitotic factors that stimulate proliferation of keratinocytes, dermal fibroblasts, and EC in vitro [26, 115–117]. Further investigation has shown that dermal fibroblasts secrete increased amounts of collagen type I [115] and alter gene expression in response to either MSC or MSC-CM [117]. Overall, these data suggest that MSC therapeutically applied to the wound stimulate proliferation and migration of the predominant cell types in skin healing.

2.5 Antifibrotic Effect

It has been demonstrated that MSC transplantation decreases fibrosis in the heart [118] and other organs such as the liver [119], kidney [120], and lung [121]. In the heart, factors released by MSC alter the extracellular matrix and inhibit fibrosis through paracrine actions, resulting in a more favorable post-infarction healing process and strengthening of the infarct scar [122]. Direct injection of human MSC into ischemic rat hearts limited fibrosis and left ventricular dilatation, without evidence of myocardial regeneration [123]. Consistently, it has been shown that MSC express a number of molecules involved in the biogenesis of ECM such as collagens, metalloproteinases (MMP), serine proteases, and serine protease inhibitors [66]. For example, Xu et al. showed

that transplantation of MSC into infarcted rat hearts significantly attenuated the cardiac expression of collagen types I and III, tissue inhibitor of metalloproteinase (TIMP)-1, and TGF-β compared with infarcted control hearts [124]. Other researchers found that MSC-CM significantly attenuated cardiac fibroblast proliferation and inhibited type I and type III collagen expression in cardiac fibroblasts [125]. Nagaya and colleagues injected BM-MSC into the myocardium of rats in which dilated cardiomyopathy was produced by inducing experimental myocarditis [118]. MSC administration significantly decreased the collagen deposition in the myocardium, resulting in decreased LV end-diastolic pressure and increased LV maximum dP/dt. Of note, relative quantification of cardiac proteins showed that MMP-2 and MMP-9 significantly increased in control hearts, whereas after MSC treatment MMP levels were comparable to sham.

Several in vivo studies have been performed to evaluate the therapeutic potential of MSC in the context of liver disease [8, 73, 126–132]. A decrease in liver fibrosis with improved hepatic function was reported. Following liver injury, hepatic stellate cells (HSC) were activated into proliferative, α-SMA-positive, myofibroblast-like, and ECM-producing cells [133]. Several in vitro studies have demonstrated the ability of MSC to indirectly modulate HSC activation via paracrine mechanisms. Using indirect coculture systems, Parekkadan et al. showed that human BM-MSC could inhibit collagen synthesis in activated rat HSC [134]. Moreover, MSC inhibited HSC proliferation, even if HSC did not revert to a quiescent state. The underlying mechanisms in the modulation of HSC activity were attributed to IL-10, TNF-α, and HGF secretion by MSC.

Historically, idiopathic pulmonary fibrosis (IPD) has been viewed as the result of ongoing inflammation with subsequent activation and proliferation of resident mesenchymal elements in the lung. Since effective therapies are not available, the anti-fibrotic properties of MSC have been tested in this setting [135]. Initial reports indicated that BM-MSC could ameliorate experimental bleomycin-induced lung fibrosis by improving survival and lung inflammation. These beneficial effects were not accounted by lung regeneration, but rather through a paracrine mechanism [121, 136]. In a follow-up study, Ortiz et al. [137] found that a subpopulation of mouse MSC produced IL-1 receptor antagonist, an anti-inflammatory soluble factor that was capable of attenuating the severity of bleomycin-induced lung injury and capable of reducing fibrosis. The combination of cell and gene therapy also attenuated histological damage and reduced the collagen content of the lung [138]. Despite this evidence, the role of MSC in lung fibrosis is still debated since there is the possibility that circulating fibrocytes can contribute to the pathophysiology of fibrotic lung diseases [139–141].

2.6 Effects on Metabolism

Relevant changes in cardiac metabolism occur in the acute and subacute phase after myocardial infarction. These changes greatly influence infarct size and ventricular structural remodeling. Feygin and co-workers showed that the border zone of infarcted pig hearts is affected by significant bioenergetic abnormalities and that MSC administration can partially attenuate this metabolic remodeling [142]. Since the authors observed low rates in cell engraftment, they hypothesized that MSC did not provide a structural contribution to the damaged heart, but that the beneficial effects were likely the result of paracrine mechanisms. This observation was further extended by the demonstration that Akt-MSC significantly prevent metabolic remodeling in infarcted rat hearts [143]. In particular, treatment with Akt-MSC spared phosphocreatine stores and limited the increase in 2-DG uptake in the residual intact myocardium compared with saline. Furthermore, Akt-MSC-treated hearts had a normal pH, whereas low pH was measured in control groups.

3 Characterization of the Stem Cell Secretome

The new emerging view, which is to foster the repair of damaged tissue by harnessing paracrine factors instead of using whole cells, introduces a different dimension to therapeutic application of MSC in regenerative medicine. This has directed the scientific community to the challenging investigation of the molecules that make up the stem cell secretome. Irregardless of whether these molecules are soluble or delivered by extracellular vesicles, they may be responsible for some of the beneficial effects observed after stem cell transplantation.

The first and most intuitive approach used was to measure the concentration of those proteins known to play a role in tissue repair. For instance, it has been shown that concentrations of proteins such as VEGF, bFGF, HGF, IGF-1, BDNF, MMP-2 and MMP-9, just to name a few, are significantly increased in injured tissues receiving MSC treatment [100, 118, 122, 144]. However, this simplistic approach is too limited and does not allow full elucidation of the MSC secretome nature. Indeed, besides already recognized proteins and cytokines involved in tissue protection, angiogenesis and repair mechanisms, other known or unknown factors might be responsible for all or at least some of the multiple aspects influenced by MSC in a paracrine fashion. The tools available for studying secretome expression in vitro more in depth include both transcriptomic and proteomic analysis techniques. Genome wide arrays have been utilized to better characterize the identity of putative paracrine factors. Even though this approach can only be performed on cells and not the secretome itself, it adds useful information on the nature of putative reparative factors since

it explores a larger number of candidates and, importantly, may reveal a particular gene whose product's action is still totally or partially unknown. For instance, by comparing Akt-MSC and control MSC it has been shown that the secreted frizzled related protein 2 (Sfrp2) was most significantly upregulated in Akt-MSC. Most importantly, Sfrp2 was shown to exert cytoprotection on ischemic CMC and the pro-survival effect of Akt-MSC was markedly attenuated upon knockdown of Sfrp2 with siRNA [145]. The cardioprotective and additional beneficial properties of Sfrp2 have subsequently been confirmed [71]. Transcriptomics was also used to identify the factors responsible for tissue repair observed after intravenous injection of human MSC in a mouse model of acute MI [146]; this procedure resulted in a large number of cells trapped predominantly in the lung. Gene expression analysis of lung tissue indicated that 451 human transcripts of human MSC origin were upregulated. Among them, TNFAIP6 (TSG-6), known for its powerful anti-inflammatory effects, emerged as one of the most solid candidates, with a 47-fold increase. Knock-down experiments showed that the intravenous injection of human MSC, but not human MSC transduced with TSG-6 siRNA, limited the inflammatory response and infarct size [146]. Moreover, the intravenous administration of recombinant TSG-6 also reduced the inflammatory response and infarct size, confirming the importance of this soluble factor in tissue repair. More recently, a comparative gene array analysis of fetal human AMC and human fibroblasts led to the identification of 32 genes encoding for secreted factors overexpressed by human AMC. Among these, Midkine and Secreted Protein Acidic and Rich in Cysteine (SPARC) were upregulated, also at the protein level [59].

The proteomic tools available for studying secretome expression include multiplex antibody-based techniques, such as antibody arrays. These assays offer high sensitivity (typically 1–10 pg/ml) as well as high specificity, reproducibility across a broad range of concentrations, and the potential for high-throughput analysis. This multiplex methodology can be used on a planar microspot array (e.g. RayBio cytokine arrays) or bead-based assays (e.g. Luminex. xMAP technology). There is however a limitation in the targeted antibody-based methods, which lies in the preselection of the analytes included in the assay and the exclusion of those molecules for which specific antibodies are not commercially available. Using this technique, at least 40 proteins with high expression levels varying from 10 to 110 % spot intensity relative to the negative control and normalized to a positive control were identified as putative paracrine mediators able to increase the survival of mice with fulminant hepatic failure [147]. Antibody arrays have also been employed to assess the identity of MSC-derived factors contributing to cardiac improvement in a swine MI model; angiogenic (VEGF, endothelin, and epiregulin), anti-apoptotic (Galectin-3,

Smad-5, sRFP-1, and sRFP-4) and anti-remodeling factors were identified [148]. The impact of human MSC tissue origin on secretome characteristics (bone marrow versus umbilical cord) has also been examined using antibody arrays [149]. IL-6, IL-8, TIMP-2, MCP-1, VEGF, and OPG were found to be common to BM-MSC of three different donors, and also similar but not identical to that of umbilical cord blood-derived MSC, suggesting that the trophic nature of MSC might depend on the cell origin.

Other commonly used proteomic approaches for identifying secreted proteins include gel-based (2-D or 2-D Fluorescence Difference Gel Electrophoresis) or gel-independent (1-D or 2-D LC-MS/MS) techniques [150]. However, the highly bioactive molecules secreted in the stem cell secretomes (SCS) are often difficult to identify using conventional gel-based techniques. LC-MS/MS is the current preferred approach, and is often used in conjunction with isobaric quantification with stable isotope labeling with amino acids in cell culture (SILAC), isobaric tag for relative and absolute quantitation (iTRAQ) or isotope-coded affinity tag (ICAT) labeling [151]. The SCS of mouse and human MSC were recently characterized mostly using LC-MS/MS [152–158]. Using this technique, it was possible to identify 258 proteins specifically expressed by murine MSC, 54 of which were classified as secreted proteins [153]. Sarojini et al. applied the LC-MS/MS approach to MSC-CM and identified 19 secreted proteins including extracellular matrix structural proteins, collagen processing enzymes, pigment epithelium-derived factor (PEDF), and cystatin C (Cys C). MSC SCS has been shown to induce the chemotactic response in human fibroblasts, with PEDF being the most abundant protein in the SCS and the predominant fibroblast chemoattractant in the CM evaluated by immunodepletion and reconstitution experiments [157]. In another study, using LC-MS/MS the authors successfully demonstrated that preconditioning of human AD-MSC with TNF-α leads to increased expression of cytokines and chemokines such as IL-6, IL-8, MCP-1, MMPs, PTX3, and Cathepsin L [159]. However, many cytokines and growth factors that were present in low concentrations were not detectable by LC-MS/MS. Another more systematic integrated approach to human MSC secretome analysis was utilized by Sze et al.; they included LC-MS/MS detection, antibody arrays, microarrays, and bioinformatics through which 201 unique proteins were identified (132 using LC-MS/MS and 72 using antibody arrays) [160]. Importantly, computational analysis predicted that these factors are involved with three major groups of biological processes: metabolism, defense response, and tissue differentiation; and the latter included vascularization, hematopoiesis, and skeletal development. The spectrum of the identified proteins was consistent with the reported paracrine effects of whole (parental) MSC on different cellular systems and diseases, strengthening the molecular basis for the use of MSC-CM in modulating repair after injury.

A definitive list of constitutively expressed BM-MSC secretome factors has yet to be generated, even though with current proteomic techniques it is possible to detect the majority of factors that are expressed when present at high levels [149]. Various deficiencies in current techniques are responsible for this lag in advancement in the characterization of the MSC secretome. These technical weaknesses include limited sensitivity for gel-based and LC-MS/MS assays when searching for molecules at low concentrations (10–20 fmol), and the limited availability of antibodies to detect secreted proteins for ELISA and microarray analyses. Therefore, the current general consensus is that an integrated approach is necessary. In one study, this issue was partially overcome by using antibody arrays together with LC-MS/MS increasing the reproducibility of the results [156]. The resulting proteomic profiling of the MSC-SCS included almost all the cytokines and chemokines that were previously reported to be secreted by MSC, such as epithelial-derived neutrophil-activating peptide 78 (ENA78), growth factors (VEGF, HGF), growth factor-binding proteins such as insulin-like growth factor binding protein 2 (IGFBP2), cytokines (IL-1 β, IL-6, IL-8, TGF-β), and TIMP 1 and 2. From a total of 201 unique proteins (132 using LC-MS/MS and 72 using antibody array) identified in the cultured medium, more than 85 % were validated at the mRNA level by cDNA microarrays or quantitative RT-PCR. In addition, computational analyses were used to predict the role of the identified protein in metabolism, angiogenesis, immune response or differentiation [156].

As a last note, new approaches are necessary to directly quantify the dynamic expression profile of MSC-secreted factors both locally and systemically. Particularly in light of the fact that the secretome is known to depend on spatial/temporal factors; for example, some proteins are expressed only during the cell death phase. And certainly, the greatest challenge will be to accurately profile the secretome in vivo distinguishing between host and transplanted MSC-secreted proteins [150].

4 Exosomes

Recently, it has been proposed that the beneficial paracrine effects observed after MSC therapy might be mediated, at least in part, by exosomes [161]. Exosomes are membrane bound vesicles (~30–100 nm) originally deriving from endosomes as intraluminal vesicles, which contain various molecular constituents including proteins and RNAs from maternal cells. Among these constituents, there are microRNAs (miRNAs), small non-coding RNA molecules which have a prominent role in gene regulation and biological function. Both the release and the content of the MSC-derived exosomes are modified by environmental conditions. The

hypothesis proposed is that via exosomes, MSC transfer their content to recipient cells, alter local gene expression and thereby promote therapeutic responses. Recently, MSC-derived exosomes have been found to be efficacious in an increasing number of animal models for the treatment of diseases such as liver fibrosis [162], liver injury [163], hypoxic pulmonary hypertension [164], acute lung injury [165, 166], acute kidney injury [167–169], and cardiovascular diseases [170].

For example, it has been shown that the beneficial paracrine effects observed after MSC therapy in acute MI might be mediated by exosomes [170]. Through size fractionation studies, it was proposed that the active component in CM was a large complex, 50–200 nm in size. Exosomes obtained from CM of MSC derived from human embryonic stem cells (hESC) by size exclusion using high-performance liquid chromatography reduced infarct size in a murine model, while the CM deprived of exosomes did not. The secretion of cardioprotective exosomes is not unique to hESC-MSC and was also found in MSC derived from different sources. Besides cytoprotection, it has also been suggested that exosomes act directly through the ligand/receptor interaction or indirectly on angiogenesis by modulating soluble factor production involved in endothelial and progenitor cell differentiation, proliferation, migration, and adhesion [171]. For instance, exosomes generated from platelets play an interesting beneficial proangiogenic role in a model of myocardial ischemia by delivering a cocktail of proangiogenic proteins, such as VEGF, bFGF, and PDGF [172]. Microvesicles released by BM-MSC can also restore renal function after glycerol-induced injury by activating the proliferation of tubular epithelial cells [173]. This regenerative activity was attributed to: specific mRNAs encoding for proteins responsible for the control of cell proliferation, transcription, and immune response [174]; ribonucleoproteins involved in the intracellular traffic of mRNA; and a selected pattern of microRNA modulating the expression of genes involved in the regulation of several cellular processes [175]. Intravenous infusion of microvesicles in rats immediately after renal ischemia/reperfusion injury reduced apoptosis and increased the cellular proliferation of tubular cells. Inactivation of microvesicle cargos with RNAase blunted the protective effects [167]. Tomasoni and coworkers documented that microvesicles and exosomes released by human BM-MSC induce proliferation of proximal tubular cells damaged by cisplatin, through the transfer of IGF-1R mRNA that was translated into its corresponding protein [169]. Administration of exosomes generated from BM-MSC promoted functional recovery and neurovascular remodeling in rats after traumatic brain injury (TBI) [176]. Compared with the saline-treated group, exosome-treated rats with TBI showed significant improvement in spatial learning and sensorimotor functional recovery. Exosome treatment significantly

increased the number of newly generated endothelial cells in the lesion boundary zone and dentate gyrus and significantly increased the number of newly formed immature and mature neurons in the dentate gyrus as well as reducing neuroinflammation. It has also been shown that MSC-derived exosomes can elicit hepato-protective effects against toxicant-induced injury, mainly through the activation of proliferative and regenerative responses [163].

Even though MSC-derived exosomes are clearly on the forefront of becoming one of the most sought after pharmaceutical delivery agents, thorough clinical investigation is lacking. For requisite pharmaceutical characterization and before they can be safely translated to clinical application, we will need to develop assays to evaluate the complex structure of naturally derived exosomes. Technical issues such as purification and mass exosome production and isolation need to be first addressed and then animal models set up to evaluate their potential off-target effects and possible toxicities. In the end as with the decision to use whole MSC cell preparations or defined MSC-secreted proteins, here too it is quite possible that not all components of exosomes are required for their proper function, and an alternative strategy would be to develop exosome mimetics and load them with synthetic effector molecules [177, 178].

5 Protein and Molecular Therapies

The demonstration that stem cells secrete therapeutic factors provides a potential breakthrough in that, rather than administering whole cell preparations, specific proteins could be administered for therapeutic purposes. However, transplantation of stem cells for their paracrine effects still represents a reasonable strategy since their beneficial factors remain partly unidentified and because multiple factors might function synergistically. However, if specific paracrine cell-derived factors are identified, then protein-based therapy might be more easily translated into clinical benefits. The most obvious limitation of protein therapy is the necessity to maintain therapeutic concentrations to induce the desired effect for the necessary length of time. Establishing the threshold concentration and the necessary time remains to be determined and represents a difficult task. Protein stability and pharmacokinetics may be problematic. To overcome these hurdles, a variety of strategies have emerged for manipulating protein properties: stability, specificity, immunogenicity, and pharmacokinetics [179]. Mechanisms for altering these properties include manipulation of the primary structure, incorporation of chemical and post-translation modifications, and utilization of fusion partners. Protein and peptide therapeutics have already achieved the status of an important class of drugs through advancements in molecular biology and recombinant technology.

Another major consideration is that most therapeutic proteins are administered by the parenteral route, which has many drawbacks. Various delivery strategies have evolved over the past few years to improve delivery of proteins and peptides, including the use of biopolymers and nanomaterials for controlled release of proteins [180, 181], as well as delivery via non-invasive routes such as subcutaneous injection or dermal patches. Development of an oral preparation still represents the most desirable delivery form for protein therapeutics, but involves greater challenges. Even though the road to reach optimal protein therapy is full of hurdles, we anticipate that the persistent development and application of rational protein design technology will enable significant improvements in the efficacy and safety of existing protein therapeutics, as well as allow the generation of entirely novel classes of proteins with diverse modes of action.

Acknowledgments

We acknowledge Laurene Kelly for expert editorial support. This work was supported by the Ministero Italiano della Sanità [Grant number GR-2008-1142781 and GR-2010-2320533], the Fondazione Cariplo [Grant number 2007-5984], and the Ministero Italiano degli Affari Esteri [Grant number ZA11GR2].

References

1. Tomita S, Li RK, Weisel RD et al (1999) Autologous transplantation of bone marrow cells improves damaged heart function. Circulation 100:II247–II256
2. Morigi M, Imberti B, Zoja C et al (2004) Mesenchymal stem cells are renotropic, helping to repair the kidney and improve function in acute renal failure. J Am Soc Nephrol 15:1794–1804
3. Pittenger MF, Martin BJ (2004) Mesenchymal stem cells and their potential as cardiac therapeutics. Circ Res 95:9–20
4. Morigi M, Introna M, Imberti B et al (2008) Human bone marrow mesenchymal stem cells accelerate recovery of acute renal injury and prolong survival in mice. Stem Cells 26:2075–2082
5. Morigi M, De Coppi P (2014) Cell therapy for kidney injury: different options and mechanisms—mesenchymal and amniotic fluid stem cells. Nephron Exp Nephrol 126:59
6. Uccelli A, Moretta L, Pistoia V (2008) Mesenchymal stem cells in health and disease. Nat Rev Immunol 8:726–736
7. Wakabayashi K, Nagai A, Sheikh AM et al (2010) Transplantation of human mesenchymal stem cells promotes functional improvement and increased expression of neurotrophic factors in a rat focal cerebral ischemia model. J Neurosci Res 88:1017–1025
8. Jung KH, Shin HP, Lee S et al (2009) Effect of human umbilical cord blood-derived mesenchymal stem cells in a cirrhotic rat model. Liver Int 29:898–909
9. Kinnaird T, Stabile E, Burnett MS et al (2004) Local delivery of marrow-derived stromal cells augments collateral perfusion through paracrine mechanisms. Circulation 109:1543–1549
10. Makino S, Fukuda K, Miyoshi S et al (1999) Cardiomyocytes can be generated from marrow stromal cells in vitro. J Clin Invest 103:697–705
11. Martin-Rendon E, Sweeney D, Lu F et al (2008) 5-Azacytidine-treated human mesenchymal stem/progenitor cells derived from umbilical cord, cord blood and bone marrow do not generate cardiomyocytes in vitro at high frequencies. Vox Sang 95:137–148
12. Pisano F, Altomare C, Cervio E et al (2015) Combination of miRNA499 and miRNA133

exerts a synergic effect on cardiac differentiation. Stem Cells 33:1187–1199
13. Rangappa S, Entwistle JW, Wechsler AS et al (2003) Cardiomyocyte-mediated contact programs human mesenchymal stem cells to express cardiogenic phenotype. J Thorac Cardiovasc Surg 126:124–132
14. Xu M, Wani M, Dai YS et al (2004) Differentiation of bone marrow stromal cells into the cardiac phenotype requires intercellular communication with myocytes. Circulation 110:2658–2665
15. Hatzistergos KE, Quevedo H, Oskouei BN et al (2010) Bone marrow mesenchymal stem cells stimulate cardiac stem cell proliferation and differentiation. Circ Res 107:913–922
16. Loffredo FS, Steinhauser ML, Gannon J et al (2011) Bone marrow-derived cell therapy stimulates endogenous cardiomyocyte progenitors and promotes cardiac repair. Cell Stem Cell 8:389–398
17. Noiseux N, Gnecchi M, Lopez-Ilasaca M et al (2006) Mesenchymal stem cells overexpressing Akt dramatically repair infarcted myocardium and improve cardiac function despite infrequent cellular fusion or differentiation. Mol Ther 14:840–850
18. Duffield JS, Park KM, Hsiao LL et al (2005) Restoration of tubular epithelial cells during repair of the postischemic kidney occurs independently of bone marrow-derived stem cells. J Clin Invest 115:1743–1755
19. Lange C, Togel F, Ittrich H et al (2005) Administered mesenchymal stem cells enhance recovery from ischemia/reperfusion-induced acute renal failure in rats. Kidney Int 68:1613–1617
20. Togel F, Hu Z, Weiss K et al (2005) Administered mesenchymal stem cells protect against ischemic acute renal failure through differentiation-independent mechanisms. Am J Physiol Renal Physiol 289:F31–F42
21. Togel F, Weiss K, Yang Y et al (2007) Vasculotropic, paracrine actions of infused mesenchymal stem cells are important to the recovery from acute kidney injury. Am J Physiol Renal Physiol 292:F1626–F1635
22. Chen J, Li Y, Wang L et al (2001) Therapeutic benefit of intravenous administration of bone marrow stromal cells after cerebral ischemia in rats. Stroke 32:1005–1011
23. Wu Y, Chen L, Scott PG et al (2007) Mesenchymal stem cells enhance wound healing through differentiation and angiogenesis. Stem Cells 25:2648–2659
24. Sasaki M, Abe R, Fujita Y et al (2008) Mesenchymal stem cells are recruited into wounded skin and contribute to wound repair by transdifferentiation into multiple skin cell type. J Immunol 180:2581–2587
25. Li H, Fu X, Ouyang Y et al (2006) Adult bone-marrow-derived mesenchymal stem cells contribute to wound healing of skin appendages. Cell Tissue Res 326:725–736
26. Javazon EH, Keswani SG, Badillo AT et al (2007) Enhanced epithelial gap closure and increased angiogenesis in wounds of diabetic mice treated with adult murine bone marrow stromal progenitor cells. Wound Repair Regen 15:350–359
27. Williams AR, Hare JM (2011) Mesenchymal stem cells: biology, pathophysiology, translational findings, and therapeutic implications for cardiac disease. Circ Res 109:923–940
28. Iso Y, Spees JL, Serrano C et al (2007) Multipotent human stromal cells improve cardiac function after myocardial infarction in mice without long-term engraftment. Biochem Biophys Res Commun 354: 700–706
29. Terrovitis JV, Smith RR, Marban E (2010) Assessment and optimization of cell engraftment after transplantation into the heart. Circ Res 106:479–494
30. Rodrigues M, Griffith LG, Wells A (2010) Growth factor regulation of proliferation and survival of multipotential stromal cells. Stem Cell Res Ther 1:32
31. Song H, Cha MJ, Song BW et al (2010) Reactive oxygen species inhibit adhesion of mesenchymal stem cells implanted into ischemic myocardium via interference of focal adhesion complex. Stem Cells 28:555–563
32. Muller-Ehmsen J, Krausgrill B, Burst V et al (2006) Effective engraftment but poor mid-term persistence of mononuclear and mesenchymal bone marrow cells in acute and chronic rat myocardial infarction. J Mol Cell Cardiol 41:876–884
33. Rehman J, Traktuev D, Li J et al (2004) Secretion of angiogenic and antiapoptotic factors by human adipose stromal cells. Circulation 109:1292–1298
34. Moon MH, Kim SY, Kim YJ et al (2006) Human adipose tissue-derived mesenchymal stem cells improve postnatal neovascularization in a mouse model of hindlimb ischemia. Cell Physiol Biochem 17:279–290
35. Imberti B, Morigi M, Tomasoni S et al (2007) Insulin-like growth factor-1 sustains stem cell mediated renal repair. J Am Soc Nephrol 18:2921–2928
36. Horita Y, Honmou O, Harada K et al (2006) Intravenous administration of glial cell line-derived neurotrophic factor gene-modified human mesenchymal stem cells protects against injury in a cerebral ischemia model in the adult rat. J Neurosci Res 84:1495–1504
37. Kang SK, Lee DH, Bae YC et al (2003) Improvement of neurological deficits by

intracerebral transplantation of human adipose tissue-derived stromal cells after cerebral ischemia in rats. Exp Neurol 183:355–366
38. Mora-Lee S, Sirerol-Piquer MS, Gutierrez-Perez M et al (2012) Therapeutic effects of hMAPC and hMSC transplantation after stroke in mice. PLoS One 7, e43683
39. Chopp M, Li Y (2002) Treatment of neural injury with marrow stromal cells. Lancet Neurol 1:92–100
40. Gnecchi M, He H, Liang OD et al (2005) Paracrine action accounts for marked protection of ischemic heart by Akt-modified mesenchymal stem cells. Nat Med 11: 367–368
41. Gnecchi M, He H, Noiseux N et al (2006) Evidence supporting paracrine hypothesis for Akt-modified mesenchymal stem cell-mediated cardiac protection and functional improvement. FASEB J 20:661–669
42. Du T, Cheng J, Zhong L et al (2012) The alleviation of acute and chronic kidney injury by human Wharton's jelly-derived mesenchymal stromal cells triggered by ischemia-reperfusion injury via an endocrine mechanism. Cytotherapy 14:1215–1227
43. Fang TC, Pang CY, Chiu SC et al (2012) Renoprotective effect of human umbilical cord-derived mesenchymal stem cells in immunodeficient mice suffering from acute kidney injury. PLoS One 7, e46504
44. Bi B, Schmitt R, Israilova M et al (2007) Stromal cells protect against acute tubular injury via an endocrine effect. J Am Soc Nephrol 18:2486–2496
45. Kanki S, Segers VF, Wu W et al (2011) Stromal cell-derived factor-1 retention and cardioprotection for ischemic myocardium. Circ Heart Fail 4:509–518
46. Timmers L, Lim SK, Hoefer IE et al (2011) Human mesenchymal stem cell-conditioned medium improves cardiac function following myocardial infarction. Stem Cell Res 6:206–214
47. Beohar N, Rapp J, Pandya S et al (2010) Rebuilding the damaged heart: the potential of cytokines and growth factors in the treatment of ischemic heart disease. J Am Coll Cardiol 56:1287–1297
48. Aejaz HM, Aleem AK, Parveen N et al (2007) Stem cell therapy-present status. Transplant Proc 39:694–699
49. Daley GQ, Scadden DT (2008) Prospects for stem cell-based therapy. Cell 132:544–548
50. Lindvall O, Kokaia Z (2006) Stem cells for the treatment of neurological disorders. Nature 441:1094–1096
51. Laflamme MA, Murry CE (2005) Regenerating the heart. Nat Biotechnol 23: 845–856
52. Little MH (2006) Regrow or repair: potential regenerative therapies for the kidney. J Am Soc Nephrol 17:2390–2401
53. Cantley LG (2005) Adult stem cells in the repair of the injured renal tubule. Nat Clin Pract Nephrol 1:22–32
54. Morigi M, Benigni A, Remuzzi G et al (2006) The regenerative potential of stem cells in acute renal failure. Cell Transplant 15(Suppl 1):S111–S117
55. Lim BK, Choi JH, Nam JH et al (2006) Virus receptor trap neutralizes coxsackievirus in experimental murine viral myocarditis. Cardiovasc Res 71:517–526
56. Takahashi M, Li TS, Suzuki R et al (2006) Cytokines produced by bone marrow cells can contribute to functional improvement of the infarcted heart by protecting cardiomyocytes from ischemic injury. Am J Physiol Heart Circ Physiol 291:H886–H893
57. Uemura R, Xu M, Ahmad N et al (2006) Bone marrow stem cells prevent left ventricular remodeling of ischemic heart through paracrine signaling. Circ Res 98:1414–1421
58. Xu M, Uemura R, Dai Y et al (2007) In vitro and in vivo effects of bone marrow stem cells on cardiac structure and function. J Mol Cell Cardiol 42:441–448
59. Danieli P, Malpasso G, Ciuffreda MC et al (2015) Conditioned medium from human amniotic mesenchymal stromal cells limits infarct size and enhances angiogenesis. Stem Cells Transl Med 4:448–458
60. Halabian R, Roudkenar MH, Jahanian-Najafabadi A et al (2015) Co-culture of bone marrow-derived mesenchymal stem cells overexpressing lipocalin 2 with HK-2 and HEK293 cells protects the kidney cells against cisplatin-induced injury. Cell Biol Int 39:152–163
61. Drago D, Cossetti C, Iraci N et al (2013) The stem cell secretome and its role in brain repair. Biochimie 95:2271–2285
62. Chen J, Li Y, Katakowski M et al (2003) Intravenous bone marrow stromal cell therapy reduces apoptosis and promotes endogenous cell proliferation after stroke in female rat. J Neurosci Res 73:778–786
63. Egashira Y, Sugitani S, Suzuki Y et al (2012) The conditioned medium of murine and human adipose-derived stem cells exerts neuroprotective effects against experimental stroke model. Brain Res 1461:87–95
64. Wei X, Du Z, Zhao L et al (2009) IFATS collection: the conditioned media of adipose stromal cells protect against hypoxia-ischemia-induced brain damage in neonatal rats. Stem Cells 27:478–488
65. Kinnaird T, Stabile E, Burnett MS et al (2004) Marrow-derived stromal cells express

genes encoding a broad spectrum of arteriogenic cytokines and promote in vitro and in vivo arteriogenesis through paracrine mechanisms. Circ Res 94:678–685
66. Ohnishi S, Yasuda T, Kitamura S et al (2007) Effect of hypoxia on gene expression of bone marrow-derived mesenchymal stem cells and mononuclear cells. Stem Cells 25: 1166–1177
67. Jiang S, Haider HK, Idris NM et al (2006) Supportive interaction between cell survival signaling and angiocompetent factors enhances donor cell survival and promotes angiomyogenesis for cardiac repair. Circ Res 99:776–784
68. Nagaya N, Fujii T, Iwase T et al (2004) Intravenous administration of mesenchymal stem cells improves cardiac function in rats with acute myocardial infarction through angiogenesis and myogenesis. Am J Physiol Heart Circ Physiol 287:H2670–H2676
69. Tomita S, Mickle DA, Weisel RD et al (2002) Improved heart function with myogenesis and angiogenesis after autologous porcine bone marrow stromal cell transplantation. J Thorac Cardiovasc Surg 123:1132–1140
70. McFarlin K, Gao X, Liu YB et al (2006) Bone marrow-derived mesenchymal stromal cells accelerate wound healing in the rat. Wound Repair Regen 14:471–478
71. Alfaro MP, Pagni M, Vincent A et al (2008) The Wnt modulator sFRP2 enhances mesenchymal stem cell engraftment, granulation tissue formation and myocardial repair. Proc Natl Acad Sci U S A 105:18366–18371
72. Chen L, Tredget EE, Wu PY et al (2008) Paracrine factors of mesenchymal stem cells recruit macrophages and endothelial lineage cells and enhance wound healing. PLoS One 3, e1886
73. Wang Y, Lian F, Li J et al (2012) Adipose derived mesenchymal stem cells transplantation via portal vein improves microcirculation and ameliorates liver fibrosis induced by CCl4 in rats. J Transl Med 10:133
74. English K (2013) Mechanisms of mesenchymal stromal cell immunomodulation. Immunol Cell Biol 91:19–26
75. Klinker MW, Wei CH (2015) Mesenchymal stem cells in the treatment of inflammatory and autoimmune diseases in experimental animal models. World J Stem Cells 7:556–567
76. Iyer SS, Rojas M (2008) Anti-inflammatory effects of mesenchymal stem cells: novel concept for future therapies. Expert Opin Biol Ther 8:569–581
77. Zhu XY, Lerman A, Lerman LO (2013) Concise review: mesenchymal stem cell treatment for ischemic kidney disease. Stem Cells 31:1731–1736
78. Gnecchi M, Danieli P, Cervio E (2012) Mesenchymal stem cell therapy for heart disease. Vascul Pharmacol 57:48–55
79. Puglisi MA, Tesori V, Lattanzi W et al (2011) Therapeutic implications of mesenchymal stem cells in liver injury. J Biomed Biotechnol 2011:860578
80. Eliopoulos N, Zhao J, Bouchentouf M et al (2010) Human marrow-derived mesenchymal stromal cells decrease cisplatin renotoxicity in vitro and in vivo and enhance survival of mice post-intraperitoneal injection. Am J Physiol Renal Physiol 299:F1288–F1298
81. Ramesh G, Reeves WB (2002) TNF-alpha mediates chemokine and cytokine expression and renal injury in cisplatin nephrotoxicity. J Clin Invest 110:835–842
82. Zhang B, Ramesh G, Norbury CC et al (2007) Cisplatin-induced nephrotoxicity is mediated by tumor necrosis factor-alpha produced by renal parenchymal cells. Kidney Int 72:37–44
83. Morigi M, Rota C, Montemurro T et al (2010) Life-sparing effect of human cord blood-mesenchymal stem cells in experimental acute kidney injury. Stem Cells 28:513–522
84. Yagi H, Soto-Gutierrez A, Navarro-Alvarez N et al (2010) Reactive bone marrow stromal cells attenuate systemic inflammation via sTNFR1. Mol Ther 18:1857–1864
85. Duffy MM, Ritter T, Ceredig R et al (2011) Mesenchymal stem cell effects on T-cell effector pathways. Stem Cell Res Ther 2:34
86. Franquesa M, Hoogduijn MJ, Bestard O et al (2012) Immunomodulatory effect of mesenchymal stem cells on B cells. Front Immunol 3:212
87. Raffaghello L, Bianchi G, Bertolotto M et al (2008) Human mesenchymal stem cells inhibit neutrophil apoptosis: a model for neutrophil preservation in the bone marrow niche. Stem Cells 26:151–162
88. Spaggiari GM, Capobianco A, Abdelrazik H et al (2008) Mesenchymal stem cells inhibit natural killer-cell proliferation, cytotoxicity, and cytokine production: role of indoleamine 2,3-dioxygenase and prostaglandin E2. Blood 111:1327–1333
89. Corridoni D, Arseneau KO, Cominelli F (2014) Inflammatory bowel disease. Immunol Lett 161:231–235
90. Gonzalez MA, Gonzalez-Rey E, Rico L et al (2009) Adipose-derived mesenchymal stem cells alleviate experimental colitis by inhibiting inflammatory and autoimmune responses. Gastroenterology 136:978–989
91. Zhang Q, Shi S, Liu Y et al (2009) Mesenchymal stem cells derived from human gingiva are capable of immunomodulatory functions and ameliorate inflammation-

related tissue destruction in experimental colitis. J Immunol 183:7787–7798
92. Zhao Y, Wang L, Jin Y et al (2012) Fas ligand regulates the immunomodulatory properties of dental pulp stem cells. J Dent Res 91:948–954
93. Akiyama K, Chen C, Wang D et al (2012) Mesenchymal-stem-cell-induced immunoregulation involves FAS-ligand-/FAS-mediated T cell apoptosis. Cell Stem Cell 10:544–555
94. Ohnishi S, Yanagawa B, Tanaka K et al (2007) Transplantation of mesenchymal stem cells attenuates myocardial injury and dysfunction in a rat model of acute myocarditis. J Mol Cell Cardiol 42:88–97
95. Van Linthout S, Savvatis K, Miteva K et al (2011) Mesenchymal stem cells improve murine acute coxsackievirus B3-induced myocarditis. Eur Heart J 32:2168–2178
96. Fuse K, Kodama M, Hanawa H et al (2001) Enhanced expression and production of monocyte chemoattractant protein-1 in myocarditis. Clin Exp Immunol 124:346–352
97. Yang CC, Shih YH, Ko MH et al (2008) Transplantation of human umbilical mesenchymal stem cells from Wharton's jelly after complete transection of the rat spinal cord. PLoS One 3, e3336
98. Gerdoni E, Gallo B, Casazza S et al (2007) Mesenchymal stem cells effectively modulate pathogenic immune response in experimental autoimmune encephalomyelitis. Ann Neurol 61:219–227
99. Zappia E, Casazza S, Pedemonte E et al (2005) Mesenchymal stem cells ameliorate experimental autoimmune encephalomyelitis inducing T-cell anergy. Blood 106:1755–1761
100. McCoy MK, Martinez TN, Ruhn KA et al (2008) Autologous transplants of adipose-derived adult stromal (ADAS) cells afford dopaminergic neuroprotection in a model of Parkinson's disease. Exp Neurol 210:14–29
101. Aggarwal S, Pittenger MF (2005) Human mesenchymal stem cells modulate allogeneic immune cell responses. Blood 105:1815–1822
102. Francois M, Romieu-Mourez R, Li M et al (2012) Human MSC suppression correlates with cytokine induction of indoleamine 2,3-dioxygenase and bystander M2 macrophage differentiation. Mol Ther 20:187–195
103. Prockop DJ, Oh JY (2012) Mesenchymal stem/stromal cells (MSCs): role as guardians of inflammation. Mol Ther 20:14–20
104. Karantalis V, Hare JM (2015) Use of mesenchymal stem cells for therapy of cardiac disease. Circ Res 116:1413–1430
105. Nakanishi C, Yamagishi M, Yamahara K et al (2008) Activation of cardiac progenitor cells through paracrine effects of mesenchymal stem cells. Biochem Biophys Res Commun 374:11–16
106. Linke A, Muller P, Nurzynska D et al (2005) Stem cells in the dog heart are self-renewing, clonogenic, and multipotent and regenerate infarcted myocardium, improving cardiac function. Proc Natl Acad Sci U S A 102:8966–8971
107. Amado LC, Saliaris AP, Schuleri KH et al (2005) Cardiac repair with intramyocardial injection of allogeneic mesenchymal stem cells after myocardial infarction. Proc Natl Acad Sci U S A 102:11474–11479
108. Galindo LT, Filippo TR, Semedo P et al (2011) Mesenchymal stem cell therapy modulates the inflammatory response in experimental traumatic brain injury. Neurol Res Int 2011:564089
109. Rivera FJ, Kandasamy M, Couillard-Despres S et al (2008) Oligodendrogenesis of adult neural progenitors: differential effects of ciliary neurotrophic factor and mesenchymal stem cell derived factors. J Neurochem 107:832–843
110. Constantin G, Marconi S, Rossi B et al (2009) Adipose-derived mesenchymal stem cells ameliorate chronic experimental autoimmune encephalomyelitis. Stem Cells 27:2624–2635
111. Zhang J, Li Y, Chen J et al (2005) Human bone marrow stromal cell treatment improves neurological functional recovery in EAE mice. Exp Neurol 195:16–26
112. Zhang J, Li Y, Lu M et al (2006) Bone marrow stromal cells reduce axonal loss in experimental autoimmune encephalomyelitis mice. J Neurosci Res 84:587–595
113. Bai L, Lennon DP, Caplan AI et al (2012) Hepatocyte growth factor mediates mesenchymal stem cell-induced recovery in multiple sclerosis models. Nat Neurosci 15:862–870
114. Voulgari-Kokota A, Fairless R, Karamita M et al (2012) Mesenchymal stem cells protect CNS neurons against glutamate excitotoxicity by inhibiting glutamate receptor expression and function. Exp Neurol 236:161–170
115. Kim WS, Park BS, Sung JH et al (2007) Wound healing effect of adipose-derived stem cells: a critical role of secretory factors on human dermal fibroblasts. J Dermatol Sci 48:15–24
116. Lee EY, Xia Y, Kim WS et al (2009) Hypoxia-enhanced wound-healing function of adipose-derived stem cells: increase in stem cell proliferation and up-regulation of VEGF and bFGF. Wound Repair Regen 17:540–547
117. Smith AN, Willis E, Chan VT et al (2010) Mesenchymal stem cells induce dermal fibroblast responses to injury. Exp Cell Res 316:48–54

118. Nagaya N, Kangawa K, Itoh T et al (2005) Transplantation of mesenchymal stem cells improves cardiac function in a rat model of dilated cardiomyopathy. Circulation 112: 1128–1135
119. Oyagi S, Hirose M, Kojima M et al (2006) Therapeutic effect of transplanting HGF-treated bone marrow mesenchymal cells into CCl4-injured rats. J Hepatol 44:742–748
120. Ninichuk V, Gross O, Segerer S et al (2006) Multipotent mesenchymal stem cells reduce interstitial fibrosis but do not delay progression of chronic kidney disease in collagen4A3-deficient mice. Kidney Int 70:121–129
121. Ortiz LA, Gambelli F, McBride C et al (2003) Mesenchymal stem cell engraftment in lung is enhanced in response to bleomycin exposure and ameliorates its fibrotic effects. Proc Natl Acad Sci U S A 100:8407–8411
122. Gnecchi M, Zhang Z, Ni A et al (2008) Paracrine mechanisms in adult stem cell signaling and therapy. Circ Res 103:1204–1219
123. Berry MF, Engler AJ, Woo YJ et al (2006) Mesenchymal stem cell injection after myocardial infarction improves myocardial compliance. Am J Physiol Heart Circ Physiol 290:H2196–H2203
124. Xu X, Xu Z, Xu Y et al (2005) Effects of mesenchymal stem cell transplantation on extracellular matrix after myocardial infarction in rats. Coron Artery Dis 16:245–255
125. Ohnishi S, Sumiyoshi H, Kitamura S et al (2007) Mesenchymal stem cells attenuate cardiac fibroblast proliferation and collagen synthesis through paracrine actions. FEBS Lett 581:3961–3966
126. Nasir GA, Mohsin S, Khan M et al (2013) Mesenchymal stem cells and Interleukin-6 attenuate liver fibrosis in mice. J Transl Med 11:78,5876–11-78
127. Li Q, Zhou X, Shi Y et al (2013) In vivo tracking and comparison of the therapeutic effects of MSCs and HSCs for liver injury. PLoS One 8, e62363
128. Chang YJ, Liu JW, Lin PC et al (2009) Mesenchymal stem cells facilitate recovery from chemically induced liver damage and decrease liver fibrosis. Life Sci 85:517–725
129. Rabani V, Shahsavani M, Gharavi M et al (2010) Mesenchymal stem cell infusion therapy in a carbon tetrachloride-induced liver fibrosis model affects matrix metalloproteinase expression. Cell Biol Int 34:601–605
130. Zhao DC, Lei JX, Chen R et al (2005) Bone marrow-derived mesenchymal stem cells protect against experimental liver fibrosis in rats. World J Gastroenterol 11:3431–3440
131. Abdel Aziz MT, Atta HM, Mahfouz S et al (2007) Therapeutic potential of bone marrow-derived mesenchymal stem cells on experimental liver fibrosis. Clin Biochem 40:893–899
132. Tanimoto H, Terai S, Taro T et al (2013) Improvement of liver fibrosis by infusion of cultured cells derived from human bone marrow. Cell Tissue Res 354:717–728
133. Friedman SL (2008) Hepatic stellate cells: protean, multifunctional, and enigmatic cells of the liver. Physiol Rev 88:125–172
134. Parekkadan B, van Poll D, Megeed Z et al (2007) Immunomodulation of activated hepatic stellate cells by mesenchymal stem cells. Biochem Biophys Res Commun 363: 247–252
135. Toonkel RL, Hare JM, Matthay MA et al (2013) Mesenchymal stem cells and idiopathic pulmonary fibrosis. Potential for clinical testing. Am J Respir Crit Care Med 188:133–140
136. Rojas M, Xu J, Woods CR et al (2005) Bone marrow-derived mesenchymal stem cells in repair of the injured lung. Am J Respir Cell Mol Biol 33:145–152
137. Ortiz LA, Dutreil M, Fattman C et al (2007) Interleukin 1 receptor antagonist mediates the antiinflammatory and antifibrotic effect of mesenchymal stem cells during lung injury. Proc Natl Acad Sci U S A 104:11002–11007
138. Aguilar S, Scotton CJ, McNulty K et al (2009) Bone marrow stem cells expressing keratinocyte growth factor via an inducible lentivirus protects against bleomycin-induced pulmonary fibrosis. PLoS One 4, e8013
139. Epperly MW, Guo H, Gretton JE et al (2003) Bone marrow origin of myofibroblasts in irradiation pulmonary fibrosis. Am J Respir Cell Mol Biol 29:213–224
140. Hashimoto N, Jin H, Liu T et al (2004) Bone marrow-derived progenitor cells in pulmonary fibrosis. J Clin Invest 113:243–252
141. Phillips RJ, Burdick MD, Hong K et al (2004) Circulating fibrocytes traffic to the lungs in response to CXCL12 and mediate fibrosis. J Clin Invest 114:438–446
142. Feygin J, Mansoor A, Eckman P et al (2007) Functional and bioenergetic modulations in the infarct border zone following autologous mesenchymal stem cell transplantation. Am J Physiol Heart Circ Physiol 293: H1772–H1780
143. Gnecchi M, He H, Melo LG et al (2009) Early beneficial effects of bone marrow-derived mesenchymal stem cells overexpressing Akt on cardiac metabolism after myocardial infarction. Stem Cells 27: 971–979
144. Yoon YS, Wecker A, Heyd L et al (2005) Clonally expanded novel multipotent stem

cells from human bone marrow regenerate myocardium after myocardial infarction. J Clin Invest 115:326–338
145. Mirotsou M, Zhang Z, Deb A et al (2007) Secreted frizzled related protein 2 (Sfrp2) is the key Akt-mesenchymal stem cell-released paracrine factor mediating myocardial survival and repair. Proc Natl Acad Sci U S A 104:1643–1648
146. Lee RH, Pulin AA, Seo MJ et al (2009) Intravenous hMSCs improve myocardial infarction in mice because cells embolized in lung are activated to secrete the anti-inflammatory protein TSG-6. Cell Stem Cell 5:54–63
147. Parekkadan B, van Poll D, Suganuma K et al (2007) Mesenchymal stem cell-derived molecules reverse fulminant hepatic failure. PLoS One 2, e941
148. Nguyen BK, Maltais S, Perrault LP et al (2010) Improved function and myocardial repair of infarcted heart by intracoronary injection of mesenchymal stem cell-derived growth factors. J Cardiovasc Transl Res 3:547–558
149. Park CW, Kim KS, Bae S et al (2009) Cytokine secretion profiling of human mesenchymal stem cells by antibody array. Int J Stem Cells 2:59–68
150. Skalnikova H, Motlik J, Gadher SJ et al (2011) Mapping of the secretome of primary isolates of mammalian cells, stem cells and derived cell lines. Proteomics 11:691–708
151. Ranganath SH, Levy O, Inamdar MS et al (2012) Harnessing the mesenchymal stem cell secretome for the treatment of cardiovascular disease. Cell Stem Cell 10:244–258
152. Choi YA, Lim J, Kim KM et al (2010) Secretome analysis of human BMSCs and identification of SMOC1 as an important ECM protein in osteoblast differentiation. J Proteome Res 9:2946–2956
153. Estrada R, Li N, Sarojini H et al (2009) Secretome from mesenchymal stem cells induces angiogenesis via Cyr61. J Cell Physiol 219:563–571
154. Kim JM, Kim J, Kim YH et al (2013) Comparative secretome analysis of human bone marrow-derived mesenchymal stem cells during osteogenesis. J Cell Physiol 228:216–224
155. Li N, Sarojini H, An J et al (2010) Prosaposin in the secretome of marrow stroma-derived neural progenitor cells protects neural cells from apoptotic death. J Neurochem 112:1527–1538
156. Liu CH, Hwang SM (2005) Cytokine interactions in mesenchymal stem cells from cord blood. Cytokine 32:270–279
157. Sarojini H, Estrada R, Lu H et al (2008) PEDF from mouse mesenchymal stem cell secretome attracts fibroblasts. J Cell Biochem 104:1793–1802
158. Tasso R, Gaetani M, Molino E et al (2012) The role of bFGF on the ability of MSC to activate endogenous regenerative mechanisms in an ectopic bone formation model. Biomaterials 33:2086–2096
159. Lee MJ, Kim J, Kim MY et al (2010) Proteomic analysis of tumor necrosis factor-alpha-induced secretome of human adipose tissue-derived mesenchymal stem cells. J Proteome Res 9:1754–1762
160. Sze SK, de Kleijn DP, Lai RC et al (2007) Elucidating the secretion proteome of human embryonic stem cell-derived mesenchymal stem cells. Mol Cell Proteomics 6: 1680–1689
161. Cervio E, Barile L, Moccetti T et al (2015) Exosomes for intramyocardial intercellular communication. Stem Cells Int 2015:482171
162. Li T, Yan Y, Wang B et al (2013) Exosomes derived from human umbilical cord mesenchymal stem cells alleviate liver fibrosis. Stem Cells Dev 22:845–854
163. Tan CY, Lai RC, Wong W et al (2014) Mesenchymal stem cell-derived exosomes promote hepatic regeneration in drug-induced liver injury models. Stem Cell Res Ther 5:76
164. Lee C, Mitsialis SA, Aslam M et al (2012) Exosomes mediate the cytoprotective action of mesenchymal stromal cells on hypoxia-induced pulmonary hypertension. Circulation 126:2601–2611
165. Sdrimas K, Kourembanas S (2014) MSC microvesicles for the treatment of lung disease: a new paradigm for cell-free therapy. Antioxid Redox Signal 21:1905–1915
166. Zhu YG, Feng XM, Abbott J et al (2014) Human mesenchymal stem cell microvesicles for treatment of Escherichia coli endotoxin-induced acute lung injury in mice. Stem Cells 32:116–125
167. Gatti S, Bruno S, Deregibus MC et al (2011) Microvesicles derived from human adult mesenchymal stem cells protect against ischaemia-reperfusion-induced acute and chronic kidney injury. Nephrol Dial Transplant 26: 1474–1483
168. Reis LA, Borges FT, Simoes MJ et al (2012) Bone marrow-derived mesenchymal stem cells repaired but did not prevent gentamicin-induced acute kidney injury through paracrine effects in rats. PLoS One 7, e44092
169. Tomasoni S, Longaretti L, Rota C et al (2013) Transfer of growth factor receptor mRNA via exosomes unravels the regenerative

effect of mesenchymal stem cells. Stem Cells Dev 22:772–780
170. Lai RC, Arslan F, Lee MM et al (2010) Exosome secreted by MSC reduces myocardial ischemia/reperfusion injury. Stem Cell Res 4:214–222
171. Martinez MC, Andriantsitohaina R (2011) Microparticles in angiogenesis: therapeutic potential. Circ Res 109:110–119
172. Janowska-Wieczorek A, Wysoczynski M, Kijowski J et al (2005) Microvesicles derived from activated platelets induce metastasis and angiogenesis in lung cancer. Int J Cancer 113:752–760
173. Ratajczak J, Wysoczynski M, Hayek F et al (2006) Membrane-derived microvesicles: important and underappreciated mediators of cell-to-cell communication. Leukemia 20: 1487–1495
174. Bruno S, Grange C, Deregibus MC et al (2009) Mesenchymal stem cell-derived microvesicles protect against acute tubular injury. J Am Soc Nephrol 20:1053–1067
175. Collino F, Deregibus MC, Bruno S et al (2010) Microvesicles derived from adult human bone marrow and tissue specific mesenchymal stem cells shuttle selected pattern of miRNAs. PLoS One 5, e11803
176. Zhang Y, Chopp M, Meng Y et al (2015) Effect of exosomes derived from multipluripotent mesenchymal stromal cells on functional recovery and neurovascular plasticity in rats after traumatic brain injury. J Neurosurg 122:856–867
177. EL Andaloussi S, Mager I, Breakefield XO et al (2013) Extracellular vesicles: biology and emerging therapeutic opportunities. Nat Rev Drug Discov 12:347–357
178. Lai RC, Yeo RW, Tan KH et al (2013) Exosomes for drug delivery – a novel application for the mesenchymal stem cell. Biotechnol Adv 31:543–551
179. Malik DK, Baboota S, Ahuja A et al (2007) Recent advances in protein and peptide drug delivery systems. Curr Drug Deliv 4:141–151
180. Zhang G, Nakamura Y, Wang X et al (2007) Controlled release of stromal cell-derived factor-1 alpha in situ increases c-kit + cell homing to the infarcted heart. Tissue Eng 13: 2063–2071
181. Segers VF, Tokunou T, Higgins LJ et al (2007) Local delivery of protease-resistant stromal cell derived factor-1 for stem cell recruitment after myocardial infarction. Circulation 116:1683–1692

Part II

Isolation and Characterization of Mesenchymal Stem Cells

Chapter 8

Protocols for *in vitro* Differentiation of Human Mesenchymal Stem Cells into Osteogenic, Chondrogenic and Adipogenic Lineages

Maria Chiara Ciuffreda*, Giuseppe Malpasso*, Paola Musarò, Valentina Turco, and Massimiliano Gnecchi

Abstract

Mesenchymal stem cells (MSC) possess high plasticity and the potential to differentiate into several different cell types; this characteristic has implications for cell therapy and reparative biotechnologies. MSC have been originally isolated from the bone marrow (BM-MSC), but they have been found also in other tissues such as adipose tissue, cord blood, synovium, skeletal muscle, and lung. MSC are able to differentiate in vitro and in vivo into several cell types such as bone, osteocytes, chondrocytes, adipocytes, and skeletal myocytes, just to name a few.

During the last two decades, an increasing number of studies have proven the therapeutic potential of MSC for the treatment of neurodegenerative diseases, spinal cord and brain injuries, cardiovascular diseases, diabetes mellitus, and diseases of the skeleton. Their immuno-privileged profile allows both autologous and allogeneic use. For all these reasons, the scientific appeal of MSC is constantly on the rise.

The identity of MSC is currently based on three main criteria: plastic-adherence capacity, defined epitope profile, and capacity to differentiate in vitro into osteocytes, chondrocytes, and adipocytes. Here, we describe standard protocols for the differentiation of BM-MSC into the osteogenic, chondrogenic, and adipogenic lineages.

Key words Mesenchymal stem cells, Bone marrow, Adipocytes, Chondrocytes, Osteocytes

1 Introduction

The first evidence of the presence of non-hematopoietic stem cells in bone marrow was reported by Cohnheim in 1867 [1]. In the late 1960s, Friedenstein and coworkers were the first to isolate and culture this cell type from the bone marrow [2]. These cells were able to form colonies deriving from single cells that after few days exhibited a heterogeneous appearance. Thereafter, they began to proliferate and differentiate into mature cells of mesenchymal

*Maria Chiara Ciuffreda and Giuseppe Malpasso have equally contributed.

Massimiliano Gnecchi (ed.), *Mesenchymal Stem Cells: Methods and Protocols*, Methods in Molecular Biology, vol. 1416,
DOI 10.1007/978-1-4939-3584-0_8,

lineages such as osteoblasts [3]. The initial clones of adherent cells expanded into round-shaped colonies composed of fibroblastoid cells, thus the term "Colony Forming Unit-fibroblasts" was coined [2, 4]. Subsequent experiments revealed the multi-potentiality of marrow cells and how their fate was determined by environmental cues [5]. For instance, culturing marrow stromal cells in the presence of osteogenic stimuli such as ascorbic acid, inorganic phosphate, and dexamethasone promotes their differentiation into osteoblasts [6]; in contrast, the addition of transforming growth factor-beta (TGF-β) induces differentiation into chondrocytes [7]. Furthermore, it has been shown that these cells can differentiate into adipocytes, tendons, and muscle [8, 9]. Since stromal cells were shown to possess self-renewal and differentiation capacity, characteristics typically associated with stem cells, many investigators started to refer to cultured stromal cells isolated from the bone marrow as mesenchymal stem cells (BM-MSC).

Successively, MSC were found in different adult tissues [5, 10–12]. For instance, several groups have isolated a population of cells with biological characteristics similar to BM-MSC from the adipose tissue [13, 14]. Moreover, it has been demonstrated that it is possible to isolate MSC also from cord blood, placenta, skeletal muscle, and other tissues [15]. The MSC population is heterogeneous and comprises a varying amount of committed cells; therefore, to address the inconsistencies between the nomenclature and the biological properties of this heterogeneous cell population, the International Society for Cellular Therapy has defined specific requirements that a cell population must have in order to be defined as MSC [16, 17].

In particular, the cells must:

1. Maintain plastic-adherence when cultured under standard conditions.
2. Exhibit the capacity for osteogenic, adipogenic, and chondrogenic differentiation.
3. Express CD73, CD90, and CD105 surface markers and lack the expression of CD14, CD11b, CD34, CD45, CD19, CD79, and HLAII.

The discovery of a specific marker exclusively expressed by MSC would obviously reduce the problems related with the isolation and identification of these cells. However, all of the markers described to date are expressed also by other cell populations within the human body. More details on the MSC surface marker profile can be found elsewhere in this book. Here, we describe comprehensive protocols for osteo-chondro-adipogenic differentiation of human BM-MSC. Furthermore, we provide protocols to confirm MSC differentiation at RNA level.

In particular, MSC induced toward osteogenic differentiation begin to express genes and proteins associated with the osteoblastic

phenotype (i.e. osteopontin, cathepsin K, and bone sialoprotein) and acquire a morphology similar to osteoblasts. Afterward, they begin to deposit extracellular matrix enriched with deposits of hydroxy-1-epatite, which is characteristic of bone tissue. Osteogenic differentiation can be evaluated using Von Kossa, which stains the calcium deposits present in the extracellular matrix or by evaluating the alkaline phosphatase activity [5, 6].

When MSC differentiate into adipocytes they start to express genes such as peroxisome proliferator-activated receptor γ, glucose transporter type 4, adipose differentiation-related protein, and glycerol-3-phosphate dehydrogenase, and lipid vacuoles start to accumulate in the cytoplasm [5].

Finally, when MSC are appropriately stimulated to differentiate into chondrocytes, they produce an extracellular matrix primarily composed of collagen II, X, and proteoglycan aggrecan. The assay usually utilized to assess chondrocyte differentiation is Alcian blue staining. Osteogenic, adipogenic, and chondrogenic differentiation can be also confirmed by gene expression, targeting genes specifically expressed by osteocytes, adipocytes, and chondrocytes, respectively.

2 Materials

2.1 Equipment

1. Safety hood and CO_2 incubator.
2. Hemocytometer or electric field multichannel cell counting system.
3. Cell culture dishes or flasks.
4. 6-well plates.
5. Polypropylene 96-well plates.
6. 15 and 50 ml centrifuge tubes.
7. Motorized and manual pipetting systems.
8. Pipettes and tips.
9. 1.5 ml microcentrifuge tubes.
10. Vortex.
11. –20 °C freezer.
12. Inverted light microscope equipped with phase contrast filter.
13. Refrigerated centrifuge.
14. PCR thermocycler.
15. Electrophoresis equipment.
16. Agarose.
17. UV transilluminator.

2.2 Cell Culture of MSC

1. Sterile-filtered, heat-inactivated Fetal Bovine Serum (FBS).
2. 100 U/ml Penicillin and 100 μg/ml Streptomycin (P/S).
3. 10× trypsin-EthyleneDiaminetetraAcetic acid (EDTA).
4. Dulbecco's Modified Eagle Medium (DMEM) High Glucose.
5. Complete growth medium: DMEM High Glucose supplemented with 10 % FBS and 1 % P/S.
6. Dulbecco's Phosphate-Buffered Saline (PBS) 1× sterile, without calcium and magnesium.
7. Trypan blue.

2.3 Osteogenic Differentiation

The medium consists of DMEM High Glucose supplemented with:

2.3.1 Osteogenic Medium (See **Note 1**)

1. 10 % FBS.
2. 1 % P/S.
3. 100 nM dexamethasone (*see* **Note 2**).
4. 10 mM sodium β-glycero phosphate (*see* **Note 3**).
5. 0.05 mM ascorbic acid (*see* **Note 4**).

2.3.2 Alkaline Phosphate Staining (Early Differentiation)

1. Fast Blue RR capsules containing 12 mg of diazonium salt.
2. Naphthol AS-MX phosphate alkaline solution.
3. Mayer's hematoxylin solution.

Preparation of alkaline dye solution: dissolve contents of one Fast Blue RR capsule in 48 ml distilled water (a magnetic stirrer may be helpful) and add 2 ml of naphthol AS-MX phosphate alkaline.

2.3.3 Von Kossa Staining (Late Differentiation) (See **Note 5**)

1. 10 % formaldehyde.
2. 5 % silver nitrate.

2.4 Chondrogenic Differentiation

The chondrogenic medium consists of DMEM high glucose supplemented with

2.4.1 Chondrogenic Medium

1. 1 % P/S.
2. 100 nM dexamethasone (*see* **Note 6**).
3. 10 % insulin-transferrin-selenium (ITS-Premix).
4. 1 μg/ml ascorbic acid (*see* **Note 7**).
5. 1 % sodium pyruvate.
6. 10 ng/ml Human Transforming Growth Factor β1 (*see* **Note 8**).

2.4.2 Alcian Blue Staining

1. 10 % formalin.
2. Acetic acid.
3. Absolute ethanol.

4. Alcian blue 8GX.
5. Filter paper.
   Preparation of Alcian blue solution: dissolve 10 g of Alcian blue 8GX in a mixture of 60 ml absolute ethanol and 40 ml of acetic acid. Solution is stable for 1 year.
   Preparation of de-staining solution: mix 120 ml of absolute ethanol with 80 ml acetic acid.

2.5 Adipogenic Differentiation

2.5.1 Adipogenic Medium (See **Note 9**)

The medium consists of DMEM High Glucose supplemented with:

1. 10 % FBS.
2. 1 % P/S.
3. Dimethyl sulfoxide (DMSO).
4. 1 mM dexamethasone (*see* **Note 10**).
5. 0.5 mM isobutylmethylxanthine (IBMX) (*see* **Note 11**).
6. 50 μM indomethacin (*see* **Note 12**).

2.5.2 Oil Red O Staining

1. 4 % paraformaldehyde.
2. Oil Red O.
3. Filter paper.
   Preparation of oil Red solution: dissolve 0.05 g of Oil Red O in 10 ml isopropyl alcohol and filter with filter paper. Prepare fresh before use.

2.6 RNA Isolation and Gene Expression Analysis

1. Agarose.
2. TRIzol reagent.
3. 70 % Ethanol.
4. Isopropanol.
5. Chloroform.
6. Nuclease-free water.
7. Upstream and downstream specific primer for:
   (a) osteocyte genes (i.e. osteopontin, cathepsin K, and bone sialoprotein).
   (b) chondrocyte genes (i.e. collagen I, III, X, and aggrecan).
   (c) adipocyte genes (i.e. peroxisome proliferation-activated receptor γ and adipose differentiation-related protein).

3 Methods

3.1 Osteogenic Differentiation Protocol

1. Detach 80 % confluent MSC with 1× trypsin-EDTA.
2. Collect the trypsinized cells by centrifugation (5 min at 300 × *g* at room temperature (RT)) and resuspend in fresh complete growth medium. This will remove the trypsin from the culture.

3. Combine 10 μl of the cell suspension with 10 μl trypan blue in a 1.5 ml microcentrifuge tube to determine the cell number and viability (count unstained cells).
4. Re-plate the cells in complete growth medium at a seeding density of 5×10^3 cells/cm^2 in 6-well culture plates.
5. When the cells are 60 % confluent, start the osteogenic differentiation protocol by replacing the complete growth medium with the osteogenic medium. In parallel, grow the control undifferentiated MSC in standard complete medium.
6. Cultivate the cells for 3–5 weeks (early and late differentiation time points, respectively) at 37 °C in a humidified 5 % CO_2 atmosphere.
7. Change the osteogenic medium twice a week.

3.1.1 Alkaline Phosphatase Staining (Early Differentiation)

1. After 3 weeks, remove osteogenic medium and wash the cells three times with 1× PBS.
2. Add the alkaline dye solution to cells and incubate at RT for 30 min. As a result of phosphatase activity, naphthol AS-MX is liberated and immediately coupled with a diazonium salt, forming an insoluble, brown pigment at sites of phosphatase activity. Protect from direct light.
3. Discard alkaline dye solution and rinse in distilled water for 2 min. Do not allow 6-well plates to dry.
4. Add Mayer's hematoxylin solution for 10 min at RT.
5. Rinse counterstained 6-well plates for 3 min in distilled water. This will result in red violet nuclear staining.
6. Observe the alkaline phosphate activity using a bright field light microscope.

3.1.2 Von Kossa Staining (Late Differentiation)

1. After 5 weeks of culture, rinse the cells three times with 1× PBS.
2. Fix the cells with 10 % formaldehyde at RT for 30 min.
3. Rinse the fixed cells three times with distilled water.
4. Add 5 % silver nitrate solution and subsequently expose to UV light for 30 min (*see* **Note 13**).
5. Rinse the cells three times with distilled water.
6. The presence of mineralized calcium deposits is confirmed with black color staining, which is readily observable under bright field light microscope.

3.2 Chondrogenic Differentiation Protocol

1. Repeat **steps 1–3** reported in Subheading 3.1.
2. Centrifuge cell suspension at 300 × *g* for 5 min at RT.
3. Resuspend cells in chondrogenic medium at 1.25×10^6 cells/ml. In parallel grow control BM-MSC in the presence of complete growth medium.

4. Dispense 0.2 ml aliquots of the cell suspension (corresponding to 2.5×10^5 cells) for each well of a polypropylene 96-well plate.
5. Spin plates at $500 \times g$ for 5 min.
6. Place the multi-well plate in the incubator at 37 °C in a humidified 5 % CO_2 atm for at least 3 weeks (*see* **Note 14**).
7. Change the chondrogenic medium daily. Be careful to not aspirate the aggregates.

3.2.1 Alcian Blue Staining

1. Remove the polypropylene 96-well plate from the incubator and carefully aspirate the medium. Be careful to not aspirate the aggregates.
2. Carefully wash the cell aggregates twice with PBS, add 10 % of formalin and incubate 1 h at RT.
3. Remove the formalin and wash twice with distilled water. Be careful and do not aspirate aggregates.
4. Add enough Alcian blue solution to cover the cell aggregates and incubate overnight at RT in the dark.
5. Aspirate Alcian blue solution and wash twice with de-staining solution for 20 min each time.
6. Carefully aspirate the de-staining solution and add $1 \times$PBS.
7. Cartilage aggregates will stain in dark-blue.

3.3 Adipogenic Differentiation Protocol

1. Repeat **steps 1–3** reported in Subheading 3.1.
2. Seed cells at the density of 2×10^4 cells/cm^2 in 6-well culture plates.
3. When the cells are 80 % confluent, carefully remove the medium from the wells and add the adipogenic medium.
4. Replace the medium every 3–4 days for 3 weeks.

3.3.1 Oil Red O Staining

1. After 3 weeks, remove the adipogenic medium and wash the cells three times with 1× PBS.
2. Fix the cells with 10 % formaldehyde at RT for 15 min (*see* **Note 15**).
3. Rinse the cells once with distilled water.
4. Cover the monolayer with Oil Red O solution and incubate for 5 min at RT.
5. Remove Oil Red O solution and wash the cells three times with distilled water.
6. Red lipid vacuoles will be observable using an inverted microscope.

3.4 Expression Analysis of Osteo-Chondro-Adipo Specific Genes

3.4.1 RNA Isolation

1. Repeat **steps 1–3** reported in Subheading 3.1.
2. Re-plate the cells at an appropriate seeding (*see* Subheading 3.1, 3.2 and 3.3).
3. Start the differentiation protocol (*see* Subheadings 3.1, 3.2 and 3.3).
4. At the end of the differentiation treatment, rinse the cells three times with 1× PBS.
5. Add 1 ml/well of TRIzol reagent directly to the cells in the 6-well plates (*see* **Note 16**).
6. Shake gently for 5 min at RT.
7. Lyse the cells directly inside the 6-well plate by pipetting the cells up and down several times, then transfer the cell lysate into a 1.5 ml microcentrifuge tube.
8. Add 0.2 ml of chloroform for each ml of TRIzol.
9. Vortex the tubes for 15 s and incubate for 10 min at RT.
10. Centrifuge the sample at 12,000 × *g* for 15 min at 4 °C (*see* **Note 17**).
11. Aspirate the aqueous phase and transfer it to a clean tube.
12. Add 0.5 ml of isopropanol for each ml of TRIzol.
13. Mix well and incubate at RT for 10 min.
14. Freeze at −20 °C (at least overnight, can keep longer).
15. Centrifuge at 12,000 × *g* for 10 min at 4 °C.
16. Carefully discard supernatant and wash the RNA pellet by adding 1 ml of 70 % ethanol for each ml of TRIzol.
17. Shake the tubes gently and then centrifuge at 7500 × *g* for 5 min at 4 °C.
18. Discard the ethanol and air-dry the pellet.
19. Resuspend the RNA pellet in nuclease-free water.

3.4.2 RT-PCR Analysis

1. Perform RT-PCR with SuperScript II Reverse Transcriptase enzyme following the manufacturer's instructions.
2. Perform PCR amplification using the obtained cDNA and appropriate specific primers (*see* Subheading 2.4).
3. Analyze the PCR product by electrophoresis system (agarose gel).
4. Check the agarose gel under an UV transilluminator and acquire a picture for analysis.

4 Notes

1. Some investigators add 1,25-dihydroxy vitamin D_3 to the osteogenic medium [18, 19].
2. Prepare 1 mM stock solution in absolute ethanol. Aliquot and store at −20 °C.
3. Prepare a 100× stock solution dissolving 2.16 g in 10 ml DMEM without FBS.
4. Prepare a 1000× solution dissolving 50 mg in 10 ml of DMEM/10 mM HEPES without FBS. Store at 4 °C.
5. For the analysis of osteogenic differentiation, Alizarin Red S solution can be used. This stain is used to evaluate calcium deposit formation.
6. Prepare 1 mM stock solution in absolute ethanol. Aliquot and store at −20 °C.
7. Prepare a 5000× solution dissolving 50 mg in 10 ml of DMEM/10 mM HEPES without FBS. Store at 4 °C.
8. Prepare 1 μg/ml stock solution (100×) in 4 mM hydrochloric acid and 1 % FBS.
9. In some differentiation protocols, the adipogenic medium also contains insulin at different concentrations [18, 19].
10. Prepare 1 mM stock solution in absolute ethanol. Aliquot and store at −20 °C.
11. IBMX 0.05 M stock solution is prepared in DMSO. Aliquoted and stored at −20 °C.
12. Prepare concentrated stock solution in DMSO.
13. Care must be taken with the reaction times, as the color may become intense and turn the dish very black, making it difficult to read. After 15 min of incubation, we suggest to check the reaction every 5 min.
14. Twenty-four hours after the beginning of differentiation protocol cell aggregates should start floating inside the wells. The formation of these cell aggregates is necessary for the differentiation of BM-MSC into chondrocytes.
15. After formaldehyde fixation, plates can be immediately assessed or stored in 1× PBS at 4 °C overnight or longer.
16. For the chondrogenic differentiation protocol, pool the cell aggregates and transfer them into a 1.5 ml microcentrifuge tube. Add 1.5 ml/tube TRIzol and homogenize the pooled aggregates to dissolve them (**step 7** can be skipped in this case).
17. The mixture separates into a lower red phenol-chloroform phase, an interphase, and a colorless upper aqueous phase. Only the aqueous phase contains RNA.

References

1. Cohnheim JF (1867) Über Entzündung und Eiturung. Path Anat Physiol Klin Med 40:1–79
2. Friedenstein AJ, Piatetzky-Shapiro II, Petrakova KV (1966) Osteogenesis in transplants of bone marrow cells. J Embryol Exp Morphol 16:381–390
3. Friedenstein AJ, Chailakhjan RK, Lalykina KS (1970) The development of fibroblast colonies in monolayer cultures of guinea-pig bone marrow and spleen cells. Cell Tissue Kinet 3:393–403
4. Friedenstein AJ, Deriglasova UF, Kulagina NN et al (1974) Precursors for fibroblasts in different populations of hematopoietic cells as detected by the in vitro colony assay method. Exp Hematol 2:83–92
5. Pittenger MF, Mackay AM, Beck SC et al (1999) Multilineage potential of adult human mesenchymal stem cells. Science 284:143–147
6. Jaiswal N, Haynesworth SE, Caplan AI et al (1997) Osteogenic differentiation of purified, culture-expanded human mesenchymal stem cells in vitro. J Cell Biochem 64:295–312
7. Johnstone B, Hering TM, Caplan AI et al (1998) In vitro chondrogenesis of bone marrow-derived mesenchymal progenitor cells. Exp Cell Res 238:265–272
8. Wakitani S, Saito T, Caplan AI (1995) Myogenic cells derived from rat bone marrow mesenchymal stem cells exposed to 5-azacytidine. Muscle Nerve 18:1417–1426
9. Digirolamo CM, Stokes D, Colter D et al (1999) Propagation and senescence of human marrow stromal cells in culture: a simple colony-forming assay identifies samples with the greatest potential to propagate and differentiate. Br J Haematol 107:275–281
10. De Bari C, Dell'Accio F, Tylzanowski P et al (2001) Multipotent mesenchymal stem cells from adult human synovial membrane. Arthritis Rheum 44:1928–1942
11. Sabatini F, Petecchia L, Tavian M et al (2005) Human bronchial fibroblasts exhibit a mesenchymal stem cell phenotype and multilineage differentiating potentialities. Lab Invest 85:962–971
12. Zvaifler NJ, Marinova-Mutafchieva L, Adams G et al (2000) Mesenchymal precursor cells in the blood of normal individuals. Arthritis Res 2:477–488
13. Baer PC, Geiger H (2012) Adipose-derived mesenchymal stromal/stem cells: tissue localization, characterization, and heterogeneity. Stem Cells Int 2012:812693
14. Gimble JM, Katz AJ, Bunnell BA (2007) Adipose-derived stem cells for regenerative medicine. Circ Res 100:1249–1260
15. Gnecchi M, Danieli P, Cervio E (2012) Mesenchymal stem cell therapy for heart disease. Vascul Pharmacol 57:48–55
16. Horwitz EM, Le Blanc K, Dominici M et al (2005) Clarification of the nomenclature for MSC: the international society for cellular therapy position statement. Cytotherapy 7: 393–395
17. Dominici M, Le Blanc K, Mueller I et al (2006) Minimal criteria for defining multipotent mesenchymal stromal cells. The international society for cellular therapy position statement. Cytotherapy 8:315–317
18. Baksh D, Yao R, Tuan RS (2007) Comparison of proliferative and multilineage differentiation potential of human mesenchymal stem cells derived from umbilical cord and bone marrow. Stem Cells 25:1384–1392
19. Bosnakovski D, Mizuno M, Kim G et al (2005) Isolation and multilineage differentiation of bovine bone marrow mesenchymal stem cells. Cell Tissue Res 319:243–253

Chapter 9

Colony Forming Unit Assays

Patrice Penfornis and Radhika Pochampally

Abstract

Mesenchymal stem/stromal cells (MSCs) have been extensively investigated for their potential to regenerate tissue, to modulate the immune system, and their wound healing properties in over 350 clinical trials worldwide. MSCs from various tissues such as adipose, bone, and others are currently being studied in clinical trials in indications for ischemic, inflammatory, autoimmune, and degenerative disorders. As a result, numerous isolation protocols have been published. This chapter provides a simple protocol whereby a total of 80–100 million human MSCs, with an average viability greater than 90 %, can be produced from a relatively small (1–3 mL) bone marrow aspirate in 14–20 days using double stack culture chambers. MSCs were originally referred to as fibroblastoid colony forming cells because one of their characteristic features is adherence to tissue culture plastic and generation of colonies when plated at low densities. The efficiency with which they form colonies still remains an important assay for the quality of cell preparations. To assess the quality of cell preparations, two different colony forming unit (CFU) assays are also provided.

Key words MSCs, Isolation, Expansion, Culture, Colony forming unit assay

1 Introduction

The recent explosion of interest in developing cell and gene therapies using adult stem/progenitor cells from human bone marrow can be partly attributed to the ease of isolation and expansion of cells from this source in vitro. In addition, the possibility of generating genetically manipulated bone marrow-derived stem cells to introduce specific genes of interest makes them attractive vehicles for gene therapy [1–6].

hMSCs are the most attractive and most viable source of cells for cell therapeutic applications. The intrinsic properties of these cells make them attractive for clinical applications; for example, they can be safely expanded in vitro and are not susceptible to malignant transformation, thus rendering them suitable for cell therapy approaches [7–9]. Since tissue matching between MSC donor and recipient does not appear to be required, MSC may be the first cell type which could be used as an "off-the-shelf"

Massimiliano Gnecchi (ed.), *Mesenchymal Stem Cells: Methods and Protocols*, Methods in Molecular Biology, vol. 1416,
DOI 10.1007/978-1-4939-3584-0_9,

therapeutic product [10, 11]. Moreover, the possibility of storing these cells without compromising their phenotype enhances their practicality in therapeutic use [12, 13].

Despite the attractive aspects of MSCs, the field is restricted by unresolved issues such as inherent inter- and intra-laboratory heterogeneity in preparations [14, 15]. This heterogeneity stems from various factors such as donor variability, the biopsy from right or left side, isolation conditions at initial harvest, and culture conditions. Human MSCs are highly sensitive to plating density and early progenitors are rapidly lost if cultures are grown to confluence [16, 17]. Although the most recent definition of MSCs includes the expression of CD105, CD90, and CD73 surface antigens as potential biomarkers for MSCs, they alone are not sufficient to isolate cells directly from human bone marrow [18]. Therefore, it is important to devise standardized assays for isolating and characterizing MSCs.

For the primary isolation of bone marrow-derived MSCs, critical steps include the isolation of mononucleated cells from a marrow aspirate by centrifugation on a density gradient followed by recovery and expansion of cells that adhere to tissue culture plastic in standard serum-containing medium (passage zero cells). Passage zero cells are subsequently expanded by plating at a low density, which enhances the percentage of rapidly proliferating spindle-shaped cells. These cells would be replaced by large, flat and thereby more mature hMSCs if the passage zero cells were plated at higher density or continually passaged for more than four to six times (Fig. 1). Mature hMSCs will expand more slowly and have less multi-lineage differentiation potential, but still retain the ability

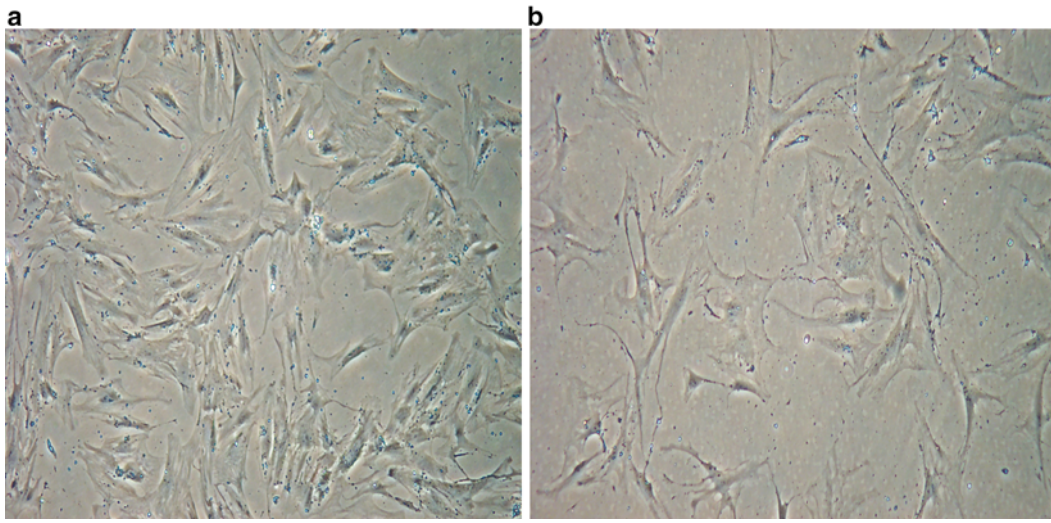

Fig. 1 Representative phase contrast microscopic images of cultures with (**a**) rapidly proliferating early passage MSCs and (**b**) slowly proliferating late passage MSCs

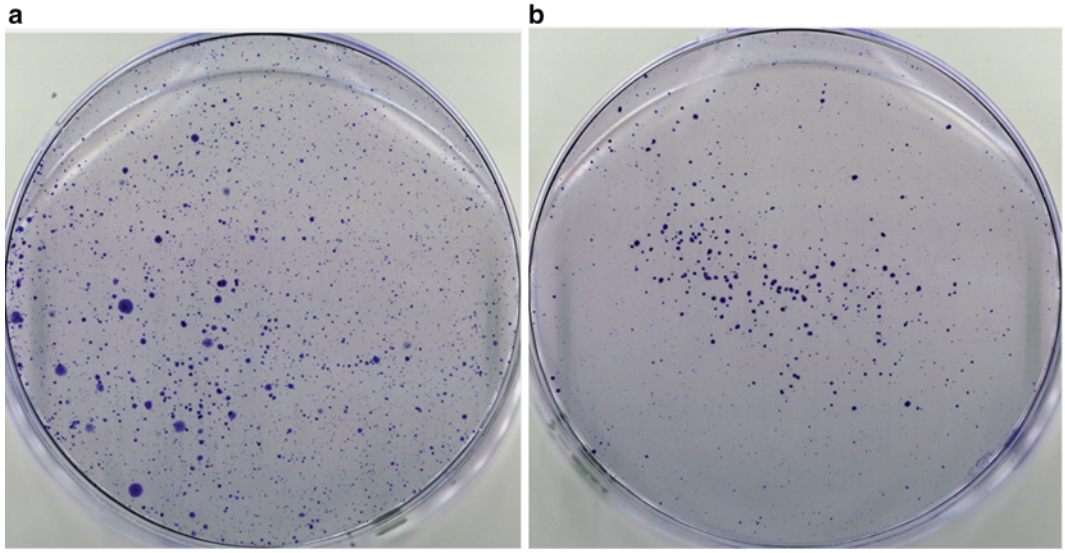

Fig. 2 Crystal violet stained plates of CFU-F assays performed on (**a**) rapidly proliferating early passage MSCs and (**b**) slowly proliferating late passage MSCs

to differentiate into mineralizing osteoblasts and secrete factors that enhance the growth of hematopoietic stem cells and perhaps other cells [19].

The efficiency with which hMSCs form colonies still remains an important assay for the quality of cell preparations. This chapter also describes two methods used to assay the colony forming ability of MSCs: (a) a traditional assay for colony forming units (CFU-F, Fig. 2) and (b) single-cell colony forming unit assay (sc-CFU, Fig. 3). In the traditional CFU assay, cells are plated at low density in large plates and discrete colonies are counted after 2–3 weeks. While with human MSCs, a single cell generates each colony, notably with rat or mouse MSCs, single cells can generate more than one colony because the cells can detach as they expand and re-seed the plate [20, 21]. In this chapter, we also describe a refined assay in which single MSCs are plated using a fluorescent flow cytometer with an automated cell sorter (FACSVantage SE with Clonesort accessory; Becton-Dickinson) to plate single cells into individual wells of a 96-well microtiter plate as described in Smith et al. [22]. The cells are incubated in complete medium for 10–14 days and visible colonies are assayed by staining the plates with Crystal Violet. With the sc-CFU assay, it is possible to distinguish the colony forming potential of two distinct kinds of MSCs present in early passage cultures: (1) spindle-shaped cells that are rapidly self-replicating that are predominant in the first few days after plating the cells at low density, and (2) broader, slowly replicating cells that predominate as colonies or cultures become confluent. The proliferative spindle-shaped cells can be distinguished from larger,

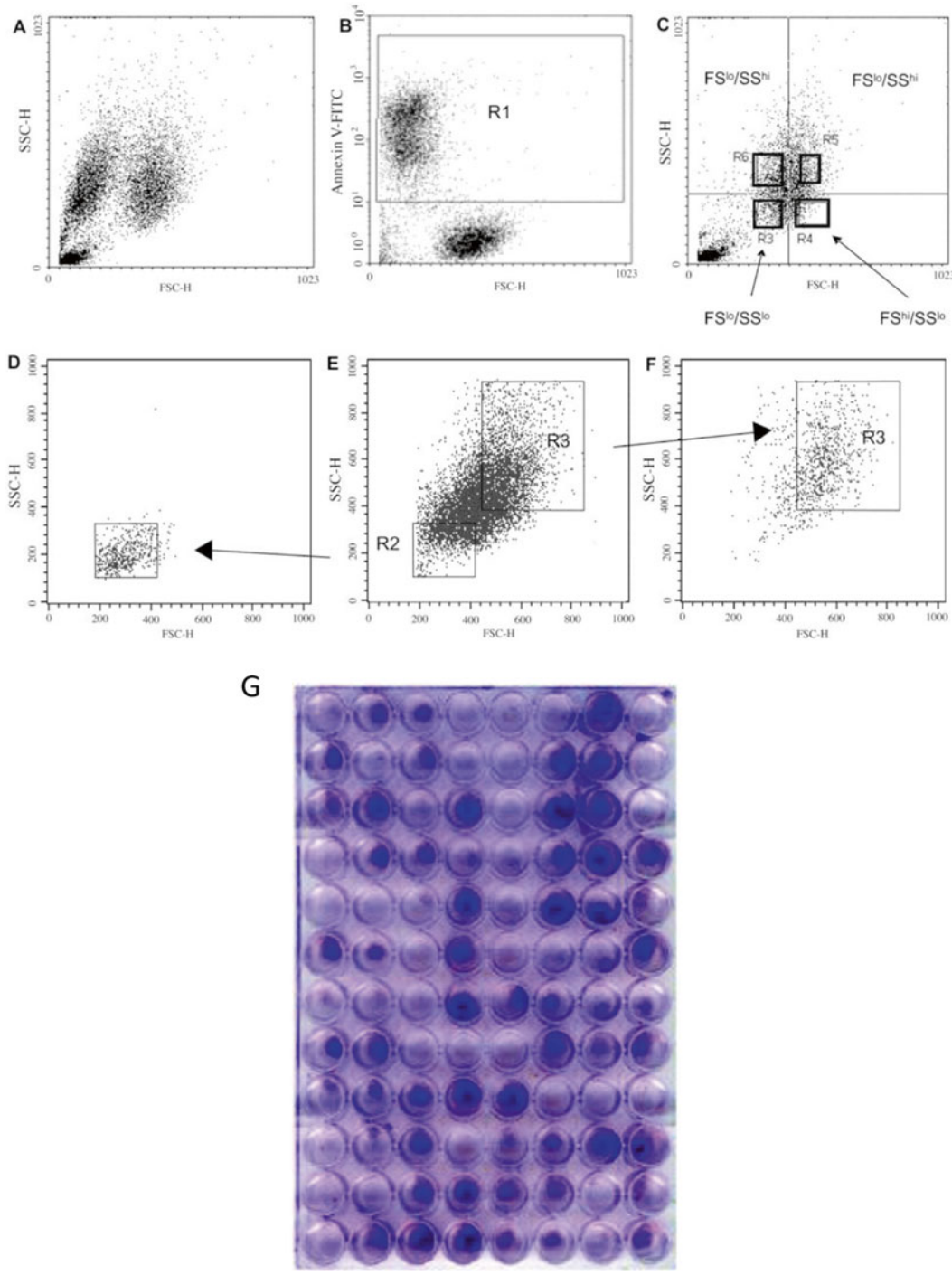

Fig. 3 Representative assay of FS/SS of passage 2 hMSCs initially plated at 500 cells per cm^2 and incubated for 6 days to obtain high-density P3 cells. The cells were detached with trypsin/EDTA and assayed on the open stream flow cytometer. (**a**) Uncorrected plot of FS/SS. (**b**) Same sample stained with Annexin V-FITC (R1). (**c**) Same sample after gating out Annexin V^+ events. A small fraction of very low FS/SS events was Annexin V^- debris. (**e**) Cell sorting based on FS/SS results in fractions (**d**, **f**) that differ at a subsequent analysis for FS/SS with the same instrument settings. *FITC* fluorescein isothiocyanate, *FS* forward scatter, *SS* side scatter. (**g**) Representative single cell assay in a 96-well plate (reproduced with permission from Stem Cells Journal)

slower proliferating cells by their lower forward scatter (FS^{lo}) and lower side light scatter (SS^{lo}). As the delineation of subpopulations based upon FS/SS is somewhat difficult to standardize (Fig. 2), the sc-CFU assay is more useful in estimating the proportion of early progenitors in different preparations of MSCs.

2 Materials

2.1 Isolation and Culture of Human Bone Marrow-Derived MSCs

1. Complete Culture Medium (CCM): α-MEM containing 16.5 % (v/v) Fetal Bovine Serum (FBS) and 1 % (v/v) Penicillin (10,000 units/mL)-Streptomycin (10,000 μg/mL).
2. Hank's Balanced Salt Solution (HBSS) without Ca^{2+} and Mg^{2+}.
3. Ficoll-Paque.
4. Phosphate Buffered Saline (PBS), pH 7.4.
5. Trypsin-EDTA in Hank's Balanced Salt Solution.
6. Trypan blue, 0.4 %.
7. Phosphate Buffered Saline (PBS), pH 7.4.
8. Cryopreservation Medium: α-MEM containing 30 % FBS and 5 % (v/v) DMSO.
9. Bleach.
10. 175 cm^2 flasks or 150-mm tissue culture dishes.
11. Cryo 1 °C Freezing Container.
12. Biological Safety cabinet Class II equipped with a vacuum system.
13. Water bath set at 37 °C.
14. Water-jacketed CO_2 incubator with HEPA filter system in humidified atmosphere and set at 37 °C, 5 % CO_2.
15. Bench centrifuge with swinging bucket rotor and brake ON/OFF option.
16. Inverted phase microscope.
17. Hemocytometer.
18. Sterile cell culture plastic pipets individually wrapped (2, 5, 10, and 25 mL).
19. Pipet-Aid.
20. Sterile conical centrifuge tubes (15 and 50 mL).
21. Pipetman 200–1000 μL and sterile filter tips.
22. CellSTACK (2-stack) culture chambers—1272 cm^2 cell growth area.

2.2 Colony Forming Unit Assay

1. Crystal Violet (3 %) in methanol. Filter through 25 μm filter paper and store at room temperature. Before use, dilute to 0.5 % in PBS.

2. Annexin V-FITC apoptosis detection kit.
3. Flow Cytometry Microbead Standards.
4. 96-well tissue culture plate.
5. EPICS FC500 flow cytometer running with CXP software.
6. FACSvantage SE with FACSDiva Option.

3 Methods

3.1 Isolation and Culture of Human Bone Marrow-Derived MSCs

1. Source bone marrow aspirates from the iliac crest and place in 10 mL heparinized tubes pre-filled with 3 mL of α-MEM. It is recommended to process samples as soon as possible, meanwhile samples can be kept at +4 °C with gentle agitation (e.g. tube rotator).
2. Transfer each aspirate into a 50 mL conical tube and dilute to 15 mL with Hank's Balanced Salt Solution (HBSS).
3. Rinse aspirate twice with 5 mL of HBSS and combine with the diluted aspirate (25 mL total volume).
4. For each aspirate, place 10 mL of pre-warmed (37 °C) Ficoll-Paque into a separate 50 mL conical tube.
5. Gently overlay each aspirate onto the Ficoll. Take care to angle the tube containing Ficoll at ≈170° and very slowly pipet onto the diluted aspirate over the border of the Ficoll meniscus. Once done, gently return the tube to a vertical position (*see* **Note 1**).
6. Centrifuge tubes at 1800 × *g* for 30 min at room temperature in a swinging bucket rotor with the brake turned OFF (*see* **Note 2**).
7. After centrifugation, carefully collect the buffy coat, located at the Ficoll–HBSS interface, and transfer cells into a clean 50 mL conical tube.
8. Dilute each sample to 25 mL with HBSS and invert the tube 3–5 times to mix (*see* **Note 3**).
9. Centrifuge tubes at 1000 × *g* for 10 min in a swinging bucket rotor with the brake turned ON.
10. Remove the supernatant by vacuum aspiration and resuspend the cells with 30 mL of pre-warmed Complete Culture Medium (CCM).
11. Count viable cells with a hemocytometer using Trypan blue and plate at a cell density of 50–100 cells/cm^2 in 175 cm^2 flasks or 150 mm dishes.
12. Incubate the cells at 37 °C in a humidified 5 % CO_2 atmosphere for 24 h to allow adherent cells to attach.

13. After 24 h, remove the media and non-adherent cells (*see* **Note 4**).
14. Add 10 mL of pre-warmed PBS to the culture, rock gently to cover the entire surface area and aspirate. Repeat the wash two additional times (*see* **Note 5**).
15. Add 30 mL of fresh CCM to the flask and return flasks to the incubator.
16. Examine cultures daily by phase microscopy.
17. Every 3 days, remove the medium and rinse the flask with 10 mL of pre-warmed PBS. Aspirate the wash and feed cultures with 30 mL of fresh CCM. Continue until the cells reach 70–80 % confluence (*see* **Note 6**).
18. To harvest cultures, remove the media and rinse the flask with 30 mL PBS and aspirate.
19. Add 10 mL of pre-warmed trypsin-EDTA solution to the flask. Distribute the trypsin across the surface area of the flask. Incubate the flask for 2–5 min at 37 °C. Examine the cells by phase microscopy.
20. After 80–90 % of the cells have rounded up or become detached, gently tap the sides of the flask to dislodge any remaining attached cells.
21. Add 10 mL of CCM to the flask. Rock the flask back and forth to swirl the media around the flask and transfer the entire cell suspension into a clean 50 mL conical tube.
22. Rinse the flask with 30 mL of PBS and combine with the cell suspension.
23. Centrifuge at $1000 \times g$ for 10 min in a swinging bucket rotor with the brake ON.
24. Remove the supernatant and resuspend the cells in 1–2 mL of pre-warmed PBS.
25. Count the cells with a hemocytometer and Trypan Blue or preferred method (*see* **Note 7**).
26. Re-seed harvested cells at a density of 50–100 viable cells/cm^2 in an appropriate culture vessel. The resultant hMSC cultures can usually be successfully expanded through passage 3 or 4 without significant loss of the stem cell phenotype.

The remainder of this procedure will describe the expansion of hMSCs in a Corning CellSTACK (2-stack) culture chamber (total surface = 1272 cm^2).

27. In order to obtain between 0.8 and 1×10^8 cells, we recommend using five 2-stack culture chambers. Add 300 mL of CCM per double stack culture chamber and place each chamber in the incubator for at least 2 h before seeding (*see* **Note 8**).

28. Plate 6×10^4 cells per stack and carefully distribute cells evenly by gentle agitation using solid caps.
29. Grow cells for 2–3 weeks with complete medium changes every 3–4 days. To remove medium, use a vacuum aspirator and a Pasteur pipet. Gently angle the culture chambers to avoid bubbling. The bottom stack can be monitored by using a regular inverted microscope.
30. To harvest cells, wash stacks with 100 mL PBS per stack and aspirate. Add 15 mL Trypsin-EDTA per stack and incubate for 5 min. Follow cell detachment with the microscope, stop trypsinization when almost all cells are detached, re-incubate an additional minute if needed, but no more than 7 min.
31. Use the harvested cells for experimental purposes or re-seed additional flasks or stacks at a density of 50–100 cells/cm^2. It is recommended to determine expanded MSC quality by using the colony forming unit (CFU) assays (*see* Subheadings 3.1 and 3.2).
32. Cryopreserve unused expanded hMSCs in Cryopreservation Medium (*see* Subheading 2.1) at 10^6 cells/ml (*see* **Note 9**).

3.2 Colony Forming Unit Assays

The efficiency with which MSCs form colonies still remains an important assay for the quality control of MSC preparations. This section describes two methods to assay the colony forming ability of MSCs including (1) a traditional assay for colony forming units—fibroblast assay (CFU-F) and (2) a single-cell colony forming unit assay (sc-CFU).

3.2.1 Colony Forming Unit: Fibroblast Assay (CFU-F)

1. Expand hMSC cultures to 70–80 % confluence and harvest with trypsin-EDTA (*see* Subheading 3.1).
2. To ensure cell separation, a glass Pasteur pipet can be flamed to create a narrow tip. Draw cells through the narrowed pipet several times (s*ee* **Note 10**).
3. Count the number of cells using a hemocytometer.
4. Dilute cells in CCM and plate at 100 cells per 100-mm tissue culture dish or ten cells per well in a 6-well plate.
5. Incubate for 10–14 days at 37 °C in a humidified 5 % CO_2 incubator.
6. Wash plates with PBS and stain with 0.5 % (v/v) Crystal Violet solution for 5–10 min at room temperature.
7. Wash thoroughly with water and count visible colonies with a diameter greater than 1 mm (Fig. 1).

3.2.2 Colony Forming Unit: Single Cell Assay (sc-CFU)

Rapidly self-renewing MSCs are characterized by low forward scatter (FS^{lo}) and low side scatter (SS^{lo}) light. The following protocol describes the isolation of FS^{lo}/SS^{lo} MSCs that are rapidly self-renewing.

It is also a rapid, standardized assay for FS/SS, a useful protocol to identify preparations of MSCs enriched for proliferative cells that will expand rapidly during subsequent passage in culture. The use of the assay should help to resolve discrepancies in data obtained by different laboratories with presumably similar preparations of hMSCs.

1. Standardize the closed stream flow cytometer (EPICS FC500 running CXP software) using microbeads with known uniform diameters (i.e. 6, 10, 15, and 20 μm).
2. Adjust the gains and voltages on the photomultiplier tubes so that the mean value of the FS peak for the 20 mm bead is about 650 and the peak of the SS for the 6 μM bead is about 450. With these settings, the standard deviation for FS of the largest bead should be less than ±0.4 % ($n = 3$) of the mean and the slope of FS on a linear scale of 0 to 1023 of at least 41 (*see* **Note 11**).
3. For the assay, detach cells expanded as described in Subheading 3.1 with trypsin/EDTA and centrifuge in CCM at $450 \times g$ for 10 min (*see* **Note 12**).
4. Count cells on a hemocytometer and resuspend in cold PBS (4 °C) at a concentration of about 5×10^5 cells/mL. The assay should be run shortly thereafter.
5. Stain cells with the Annexin V-FITC (using the manufacturer's recommended protocol) and maintain at 4 °C to prevent aggregation due to the presence of calcium and reagent-induced toxicity. Staining with Annexin V-FITC identifies events in the upper left of the plot as cell debris and dead cells (R1 in Fig. 2b). To obtain sub-fractions of cells, the Annexin V^+ events are gated out and four subpopulations are defined on the basis of FS and SS (Fig. 3c).
6. Analyze cells using the above method and sort single FS^{lo}/SS^{lo} cells per well of a 96-well plate using the FACSVantage instrument. Isolate distinct fractions on the basis of FS and SS (Fig. 3) and divide the Annexin V^- events into four quadrants on the basis of FS and SS. Offset the sort gates from the boundaries (*see* **Note 13**).
7. Incubate the microtiter plates with one hMSC per well in 0.15 mL CCM at 37 °C and 5 % CO_2.
8. Every 4–5 days, aspirate CCM from each well and replace with 0.15 mL of fresh medium.
9. After 2 weeks in culture, remove the medium and wash the wells with PBS. Incubate samples with 0.5 % Crystal Violet solution for 5–10 min, wash with water and count colonies with diameters greater than 1 mm using an inverted phase contrast microscope with a 4× objective.

4 Notes

1. If the Ficoll and HBSS cell suspension layers are mixed, the mononuclear cells will not completely and efficiently separate during centrifugation.
2. The brake is left off to allow a slow deceleration that helps to avoid disturbance of the Ficoll–HBSS cell suspension interface.
3. It is recommended to dilute the collected buffy coat with HBSS at a 3:1 volume ratio.
4. If the non-adherent cells are not removed, hematopoietic cells may become attached and contaminate the hMSC culture.
5. There may not be many adherent cells seen at this point.
6. To preserve progenitor cell phenotype, do not allow the cells to become confluent. Because hMSCs are not evenly distributed in the marrow, some aspirates do not have enough hMSCs to obtain large cultures. If a sample does not grow well or does not have good morphology by the eighth day, discard it.
7. A typical yield from a 175 cm^2 primary culture flask is between 1×10^6 and 3×10^6 total cells, with an average viability usually greater than 90 %.
8. It is important to allow the chambers containing CCM to equilibrate to 37 °C and 5 % CO_2 before use.
9. Freeze at a rate of minus 1 °C per minute using a Nalgene Cryo 1 °C freezing container placed at −80 °C. After 24 h, transfer vials to liquid nitrogen for long-term storage.
10. It is critical that the cells are well dissociated.
11. The variation in values for log (%G/%T) should be established against samples containing 0.5 or 1 million MSCs per mL when the following parameters are varied: (a) the flow rate was 250, 500, or 900 cells per second; (b) the FS was assayed with 67 or 122 volts and a gain of 2 or with 353 volts and a gain of 1; and (c) the peak for FS of the 20 μm bead was set at 550, 650, or 750; and (d) the peak for SS for the 7 μm bead was set at 350, 450, or 550.
12. Cell culture confluence is important and cells should be harvested when they are less than 80 % confluent.
13. The accuracy of sorting single cells into each well of a microtiter plate should be verified routinely by sorting fluorescent beads (i.e. Flowchek; Beckman-Coulter) into a test plate and examining the wells with an epifluorescence microscope.

References

1. Tanavde V, Vemuri MC, Pochampally R (2014) Mesenchymal stromal cells: novel methods for characterization, understanding differentiation, and function. Stem Cells Int 2014:630936
2. Liechty KW, MacKenzie TC, Shaaban AF et al (2000) Human mesenchymal stem cells engraft and demonstrate site-specific differentiation after in utero transplantation in sheep. Nat Med 6:1282–1286
3. Kopen GC, Prockop DJ, Phinney DG (1999) Marrow stromal cells migrate throughout forebrain and cerebellum, and they differentiate into astrocytes after injection into neonatal mouse brains. Proc Natl Acad Sci U S A 96: 10711–10716
4. Azizi SA, Stokes D, Augelli BJ et al (1998) Engraftment and migration of human bone marrow stromal cells implanted in the brains of albino rats—similarities to astrocyte grafts. Proc Natl Acad Sci U S A 95:3908–3913
5. Pereira RF, Halford KW, O'Hara MD et al (1995) Cultured adherent cells from marrow can serve as long-lasting precursor cells for bone, cartilage, and lung in irradiated mice. Proc Natl Acad Sci U S A 92:4857–4861
6. Hansen F, Gjermo P, Eriksen HM (1975) The effect of a chlorhexidine-containing gel on oral cleanliness and gingival health in young adults. J Clin Periodontol 2:153–159
7. Penfornis P, Pochampally R (2011) Isolation and expansion of mesenchymal stem cells/multipotential stromal cells from human bone marrow. Methods Mol Biol 698:11–21
8. Tarte K, Gaillard J, Lataillade JJ et al (2010) Clinical-grade production of human mesenchymal stromal cells: occurrence of aneuploidy without transformation. Blood 115: 1549–1553
9. Bernardo ME, Zaffaroni N, Novara F et al (2007) Human bone marrow derived mesenchymal stem cells do not undergo transformation after long-term in vitro culture and do not exhibit telomere maintenance mechanisms. Cancer Res 67:9142–9149
10. Schallmoser K et al (2008) Rapid large-scale expansion of functional mesenchymal stem cells from unmanipulated bone marrow without animal serum. Tissue Eng Part C Methods 14:185–196
11. Brooke G, Cook M, Blair C et al (2007) Therapeutic applications of mesenchymal stromal cells. Semin Cell Dev Biol 18:846–858
12. Badowski M, Muise A, Harris DT (2014) Mixed effects of long-term frozen storage on cord tissue stem cells. Cytotherapy 16: 1313–1321
13. Chatzistamatiou TK, Papassavas AC, Michalopoulos E et al (2014) Optimizing isolation culture and freezing methods to preserve Wharton's jelly's mesenchymal stem cell (MSC) properties: an MSC banking protocol validation for the Hellenic Cord Blood Bank. Transfusion. doi:10.1111/trf.12743
14. Sivasubramaniyan K, Lehnen D, Ghazanfari R et al (2012) Phenotypic and functional heterogeneity of human bone marrow- and amnion-derived MSC subsets. Ann N Y Acad Sci 1266:94–106
15. Vogel W, Grünebach F, Messam CA et al (2003) Heterogeneity among human bone marrow-derived mesenchymal stem cells and neural progenitor cells. Haematologica 88:126–133
16. Sekiya I, Larson BL, Smith JR et al (2002) Expansion of human adult stem cells from bone marrow stroma: conditions that maximize the yields of early progenitors and evaluate their quality. Stem Cells 20:530–541
17. Colter DC, Class R, DiGirolamo CM et al (2000) Rapid expansion of recycling stem cells in cultures of plastic-adherent cells from human bone marrow. Proc Natl Acad Sci U S A 97:3213–3218
18. Dominici M, Le Blanc K, Mueller I et al (2006) Minimal criteria for defining multipotent mesenchymal stromal cells. International society for cellular therapy position statement. Cytotherapy 8:315–317
19. Prockop DJ (1997) Marrow stromal cells as stem cells for nonhematopoietic tissues. Science 276:71–74
20. Peister A, Zeitouni S, Pfankuch T et al (2006) Novel object recognition in Apoe(−/−) mice improved by neonatal implantation of wild-type multipotential stromal cells. Exp Neurol 201:266–269
21. Javazon EH, Colter DC, Schwarz EJ et al (2001) Rat marrow stromal cells are more sensitive to plating density and expand more rapidly from single-cell-derived colonies than human marrow stromal cells. Stem Cells 19: 219–225
22. Smith JR, Pochampally R, Perry A et al (2004) Isolation of a highly clonogenic and multipotential subfraction of adult stem cells from bone marrow stroma. Stem Cells 22:823–831

Chapter 10

Methods and Strategies for Lineage Tracing of Mesenchymal Progenitor Cells

R. Wilder Scott and T. Michael Underhill

Abstract

Mesenchymal progenitors (MP) are found to varying extents in most tissues and organs. Their relationship to bone marrow-derived mesenchymal stem cells (MSCs) remains unclear, however, both populations appear to share a number of properties as defined by functional assays, clonogenic activity, and genetic and cell surface markers. MSCs were originally defined by their in vitro colony forming unit-fibroblast (CFU-F) activity and their ability to contribute to various mesenchymal lineages (i.e. cartilage, bone, and fat). MSCs also appear to exhibit some unique properties, in that expanded clones in the absence of bone-inducing factors generate bone spicules/organs in vivo. Subsequent analysis of these elements has demonstrated that the transplanted cells directly contribute to multiple mesenchymal lineages. Our ability to study MP and/or MSC behavior and lineage potential in vivo has been hampered by a lack of suitable Cre lines in which to effectively genetically mark and follow the fate and activity of these cells in development, growth, homeostasis and following injury or in disease. The emergence of several new genetic lines is enabling us to now address critical questions regarding MP/MSC location, behavior, function, and fate. The use of these lines and others in conjunction with suitable reporter lines will be described for MP/MSC cell fate analysis.

Key words Cre lines, Tissue processing, Reporter genes, Immunofluorescence

1 Introduction

Over 40 years ago, Friedenstein and colleagues described the isolation and characterization of a population of bone marrow (BM)-derived cells with colony forming activity [1–3]. The colonies derived from these cells appeared fibroblastic in nature, and hence they were termed colony forming unit-fibroblast (CFU-F). Subsequent studies demonstrated that cells from a single CFU-F could variably contribute to various mesenchymal lineages, including but not limited to white adipocytes, chondrocytes, and osteoblasts. Based on these properties and others, bone marrow CFU-Fs were later proposed to derive from mesenchymal stem cells (MSCs) [4, 5]. The first MSC isolation from human bone marrow was described in the late 1990s by Pittenger et al., and these cells were

Massimiliano Gnecchi (ed.), *Mesenchymal Stem Cells: Methods and Protocols*, Methods in Molecular Biology, vol. 1416,
DOI 10.1007/978-1-4939-3584-0_10,

found to have similar properties to that of previously described non-human MSCs [6]. As these cells were thought to represent endogenous stem cells with the ability to contribute to multiple lineages (even across germ layers), it was thought that they would represent an excellent source of stem cells to affect tissue regeneration. As a result, methods for their collection and expansion were quickly developed, and initial preclinical and clinical applications rationally targeted regeneration of skeletal tissues. MSC-based treatments have subsequently been expanded and they are now being "tested" in a myriad of conditions involving diverse tissues and organs. For the most part, MSC-based strategies have not delivered on the promise, and it is anticipated that a better understanding of MSC biology will enable development of more efficacious MSC therapeutics [7]. In this regard, the MSC moniker has now been used to suggest that MSCs represent medicinal signaling cells, which can deliver a variety of factors and molecules to coordinate multiple facets of tissue regeneration, including immunomodulation, stem/progenitor cell function and activity, mechanical stabilization, innervation, and revascularization [8].

1.1 Are Mesenchymal Stem Cells Real Stem Cells?

The stem cell connotation brings with it a number of critical and well-defined criteria, which minimally include demonstration of extensive self-renewal activity and uni- or multi-lineage contribution. Until recently, these criteria, especially rigorous demonstration of self-renewal, were not satisfied for tissue-resident MSCs. Evidence for self-renewal of BM-MSCs comes from studies showing that in vitro clonally expanded MSCs when transplanted into a recipient were sufficient to recapitulate many aspects of bone, including osteoblasts, chondrocytes, marrow stromal cells, and marrow adipocytes [9, 10]. In this regard, these MSC-derived bone spicules or organs were generated through endochondral ossification from donor MSCs and produced a bone marrow microenvironment sufficient to support hematopoiesis of recipient hematopoietic stem cells (HSCs). To more properly reflect the location, function, and activity of these cells, some groups have proposed that at least a subset of bone marrow-derived "MSCs" be termed skeletal stem cells (SSCs), as this more accurately reflects their self-renewal and lineage potentials [11].

MSC-like cells, in terms of clonogenecity and in vitro multipotency, have been found in other tissues and organs; however, their relationship to BM-MSCs and SSCs has remained unclear [12]. Furthermore, the self-renewal potential of these extra-medullary MSC-like cells has not been determined. Thus, pending consensus on the nature and relationship of these various mesenchymal cells, and consistent with their well-defined in vitro properties (CFU-F activity and mesenchymal lineage potential), these cells will be referred herein to as mesenchymal progenitors (MPs). This population shares many properties, markers, and activities

with other described tissue-resident MPs that have been termed mesenchymal stromal cells, mesenchymal progenitor cells (MPCs), or fibro-adipo progenitors (FAPs) [13, 14]. However, these various descriptions of MP-like cell types indicate that they do in fact share a constellation of surface markers including Sca1 and Cd140a (platelet-derived growth factor receptor α, Pdgfra), and are negative for blood (Ter119 and CD45) and endothelial (CD31) lineage markers (Lin^-). Within the BM, SSCs are located in the perivascular space in close association with sinusoids or arterioles [7]. Similarly, extramedullary MPs are also located in the perivascular space [15]. To complicate matters further, within various adipose depots, vessel-associated adipogenic progenitors also express several MP-associated markers (CD140a and Sca1) and exhibit overlapping lineage potential [16]. The extent of overlap between, and heterogeneity within these various mesenchymal populations remains to be determined.

1.2 Mesenchymal Stem Cells and Stem Cell Niches

Over the past few years, a number of groups have established that BM-resident MPs play a vital role in maintenance and regulation of hematopoiesis as an integral part of the HSC niche (reviewed in refs. 17, 18). In this context, MPs provide trophic factor support that involves expression of SCF, CXCL12 and other cytokines, molecules and factors. Conditional deletion of *Cxcl12* within various proposed niche-associated cell types, demonstrated that perivascular $Lepr^+$ MPs are essential for maintenance of HSC quiescence and re-populating activity [19]. More recent studies have shown that HSCs are found in close association with quiescent nestinGFP^{hi} MPs [20]. In contrast, Greenbaum et al. showed that nestin –ve MPs within the bone marrow were important for HSC maintenance [21]. These seemingly contradictory results may in part reflect our evolving understanding of the complexities of the HSC niche and/or the limitations of the various genetic tools used to define these entities. Nonetheless, these studies have provided unparalleled insights into the composition of the HSC niche and the contribution of MPs. The role of MPs in other stem/progenitor niches is beginning to emerge, and these studies will benefit greatly from the paradigms developed to interrogate MP function in the HSC niche.

1.3 Mesenchymal Progenitors and Mesenchymal Stem Cells in Tissue Regeneration

MSCs have been studied for the longest time in the context of bone. Transplant studies have provided an important framework for defining the nature and potential of these populations, and genetic lineage tracing methodology has now enabled us to identify, track, and study MPs in situ with minimal experimental intervention. Under steady state conditions these cell populations exist in a quiescent state and following exposure to the appropriate stimuli they take on an activated phenotype. In this regard, both BM-MSCs and SSCs expand following injury and their progeny directly contribute to the regenerated bone [22, 23]. Ablation of

BM-MSC or SSCs severely compromises bone regeneration, however, it is assumed that this is a consequence of both direct (i.e. direct contribution to the skeleton) and indirect activities including potentially more generic regenerative functions [22–24]. In many respects, extramedullary MPs exhibit similar activities and responses to injury. In skeletal muscle, a number of groups have shown that MPs participate in muscle regeneration by providing trophic factor support for other muscle stem cells, such as satellite stem cells, and that their partial ablation impacts the timing of satellite cell differentiation and consequently myofiber regeneration [13, 14, 25]. Similarly in the mammalian heart and kidney (labeled with other markers), a tissue-resident MP population is quickly activated following injury [26, 27]. Regeneration is incomplete in these models, the progeny of these cells become myofibroblasts that in part underlie the excess connective tissue deposition associated with tissue repair and fibrosis. Interestingly, MP-like cells within the liver, hepatic stellate cells (HSCs), also exhibit similar functional properties following injury and can also contribute to tissue fibrosis in this organ [28]. In all of these situations, a quiescent MP-like cell is activated in response to injury and participates directly in the regenerative and/or reparative process. Furthermore, BM-MSC/SSC and MPs share the expression of many markers and exhibit overlapping enforced lineage potentials at least in vitro [7, 29, 30]. Not surprisingly, however, BM-MSC/SSCs in comparison to MPs have unique properties, most notably the ability to generate an entire bone organ from clonally expanded transplanted cells [7]. In this regard, BM-MSC/SSC appear to exhibit "higher" intrinsic bone organ-forming activity, and this may in part reflect their biological function. Under pathological conditions such as in *fibrodysplasia ossificans progressiva* (FOP), MPs in other sites can also contribute to endochondral bone formation [31], but this may partly reflect enforced differentiation that is accompanied by expression of activated ALK2 receptor [11]. Heterotopic bone formation is also observed in various diseases and following injury, and presumably tissue-resident MPs participate in this process, but this requires further study. In short, there are numerous functional parallels between BM-MSC/SSCs and extramedullary MPs, but also distinct differences and it is expected that strategies involving new and existing genetic tools will be crucial to furthering our understanding of these important stem/progenitor populations.

The aforementioned studies have relied greatly on genetic methods for the in situ labeling of MPs, coupled with the ability to track their progeny. Minimally, this involves the use of a Cre (or other recombinase such a FRT) to induce the stable expression of a unique reporter gene [32, 33]. In this case, expression of the reporter is absolutely dependent on Cre and following Cre-mediated genome modification the reporter is expressed and continues to be expressed irrespective of the cellular context (i.e. stem,

progenitor, differentiated cell, etc.). Typically, the promoter driving the reporter is widely expressed in most, if not all, cell types. For these purposes, the Rosa26 promoter or the CAG promoter have proven popular and reasonably effective. A number of the more common reporter lines are highlighted in Table 1. The latter combines a CMV-derived enhancer with the chicken beta actin promoter, and provides high-level expression in a wide variety of cell types. In the absence of Cre, the reporter of interest is not transcribed and following Cre-mediated deletion of an upstream cassette or inversion of the region, reporter expression ensues. Importantly, the Cre-modified locus is inherited in all progeny, thereby enabling individual cells to be labeled and their progeny followed over time. The promoter driving the Cre determines which cell type(s) the Cre is expressed in. A large number of Cre lines have been generated, which can be used to label various MPs in various tissue compartments (see below). The addition of a modified estrogen ligand-binding domain (ER or ERT2) to the Cre has provided temporal control of nuclear Cre activity [32]. In this manner, tamoxifen (TAM) treatment drives the translocation of the CreER/ERT2 from the cytoplasm into the nucleus thereby initiating the desired genome modification, in this case reporter gene expression. For lineage tracing there are advantages and disadvantages to constitutive and inducible Cres, however, the ability to temporally control Cre activity provides a major benefit in being able to carry out pulse-chase experiments at any age, where animals are briefly exposed to TAM and the fate of labeled cells can be assessed after days, months, or even years.

A wide variety of Cre lines have been generated, some of which have been successfully applied to the study of MPs and BM-MSC/SSC/MPs. Many of these were used to study BM-MSC/SSCs, but may also have utility in investigating extramedullary MPs. At present, Cre lines that universally and specifically label MPs in all tissues and organs have not been identified. This may reflect the possibility that such markers do not exist or we have yet to identify them.

1.4 Nestin and BM-MSCs

Until recently, our understanding of MP, BM-MSC and SSC biology relied extensively on their isolation, culture, and transplantation [29, 42]. In the past few years, several new genetic strategies have been used to identify these cell types in situ. Analysis of nestin-GFP transgenic mice identified a rare population of GFP+ cells within the bone marrow [10, 20]. Further analysis of this population showed that they had appreciable CFU-F activity and in vitro contributed to several mesenchymal lineages. More significantly, this population was found to reside in close proximity to blood vessels and HSCs, forming an important component of the HSC niche. Subsequent studies have demonstrated that the GFP+ cells could be separated into GFP^{hi} and GFP^{lo} with the former repre-

Table 1
Summary of recombinase-dependent reporter lines useful for lineage tracing studies

Reporter line	5′ Component	3′ Component	Promoter	Insertion locus	Advantages	Disadvantages	Availability[a]	References
Confetti	Multiple FPs	Multiple FPs	CAG	Rosa26	– Multicolor, stochastic deletion to aid clonal analysis – Homozygous reporter mice can be used to create additional colors – Can be used for re-tracing of clones – Membrane-localized FP enables visualization of cell morphology	– Requires strong Cre activity for good recombination – Some of the FPs are weaker and more difficult to detect – Requires cryosectioning to maintain FP activity – Requires moderate Cre activity for efficient recombination	Jax strain 017492	[34]
mTomato/mEGFP	mTomato	mEGFP	CAG	Rosa26	– Good for FCM and FACS, as "cleaner" populations can be identified – Useful for clonal analysis with low-dose TAM – FP expression appears to be well tolerated – Under certain conditions, membrane-bound FP may contribute to the ECM	– High levels of FP may be toxic in some cell types	Jax strain 007676	[35]
nTomato/nEGFP	nTomato	nEGFP	CAG	Rosa26	– Nuclear localized FP – Good for FCM and FACS, as "cleaner" populations can be identified – Useful for clonal analysis with low-dose TAM	– Typically requires moderate Cre activity for efficient recombination – High levels of FP may be toxic in some cell types	Jax strain 023035	[36]

Reporter line	5′ Component	3′ Component	Promoter	Insertion locus	Advantages	Disadvantages	Availability[a]	References
LSL-tdTomato	stop cassette	dTomato	CAG	Rosa26	– Strong FP expression – Very efficient deletion with even weak Cre activity	– High levels of FP may be toxic in some cell types – Potential for greater leakiness due to efficient Cre-mediated recombination	Jax strain 007914	[37]
LSL-LacZ	stop cassette	LacZ	Rosa26	Rosa26	– No autofluorescence issues – Stable signal post-processing, that is suitable for paraffin-embedding	– Endogenous beta-galactosidase activity can be an issue – Detection in adult tissues with antibodies can be difficult – Requires specialized processing of tissue to maintain LacZ activity – Detection can be challenging depending on the tissue – Typically requires a decent Cre driver for good deletion	Jax strain 003474	[38]
LSL-EYFP	stop cassette	EYFP	CAG	Rosa26	– Efficient Cre-mediated recombination and reporter expression	– Weaker FP, fluorescence overlaps with autofluorescence	Jax strain 012567	[39]

(continued)

Table 1
(continued)

Reporter line	5′ Component	3′ Component	Promoter	Insertion locus	Advantages	Disadvantages	Availability[a]	References
LSL-ZsGreen1	stop cassette	ZsGreen1	CAG	Rosa26	– Strong green FP, efficient Cre deletion with lower Cre expression	– Potential for greater leakiness due to efficient Cre-mediated recombination	Jax strain 007906	[40]
FSF-LSLtdTomato	2 stop cassettes	tdTomato	CAG	Rosa26	– Reporter gene expression requires both Cre and Flp recombinase—allows labeling of cells based on two markers	– Requires mice lines that express both recombinases	Jax strain 021875	[38]
LSL-GFP-NLSLacZ	stop cassette	GFP-NLS-LacZ	Rosa26	Rosa26	– Dual reporter with GFP and LacZ	– Endogenous Rosa26 promoter used resulting in lower reporter expression	Jax strain 008606	[41]

[a]Availability of mice is shown for the C57BL/6 background and is subject to change

senting quiescent BM-MSCs within the HSC niche [20]. The nestin GFP transgenic lines have been useful for identifying BM-MSCs [18], but nestin itself as a marker has proven unreliable. Furthermore, lineage tracing with a Nestin^{CreER} line has proven uninformative as it labels multiple populations within the bone marrow including CD31^{+} endothelial cells [22, 23, 43].

1.5 LepR and BM-MPs

The leptin receptor (LepR) has been recently identified as a useful marker for identifying MP cells in BM [19, 23]. LepR-expressing cells within the bone marrow were originally shown to overlap significantly with a group of BM cells defined by high levels of the cytokine CXCL12, these were termed CXCL12-abundant reticular cells or CARs [19]. Deletion of CXCL12 in LepR-expressing cells using a LepR^{Cre} line demonstrated that CARs provided an essential source of several HSC maintenance factors including in addition to CXCL12, also scatter cell factor (SCF or Kit ligand). The LepR^{Cre} has recently been used to systematically study the nature of LepR+ cells within the bone marrow, and these analyses demonstrated that this population overlaps extensively with what previously would be considered a BM-MSC [23]. Consistent with previous reports, isolated LepR^{Cre}-marked cells are positive for a number of MP/MSC-associated markers including Cd140a, Cd140b (Pdgfrβ), CD105, CD51, but are low for Nes^{GFP}. Interestingly, LepR^{+} cells exhibit limited contribution to pre-natal skeletal cells and post-natal skeletal growth, but afterward contribute substantially to newly forming osteoblasts during skeletal turnover [23]. Furthermore, with aging, a large proportion of the adipocytes derive from a LepR^{+} cell. Following skeletal injury, the LepR^{+} cells contribute to both chondrocytic and osteogenic cells in the fracture callus. In vitro analyses demonstrated that LepR^{+}-derived cells represented the bulk of CFU-F activity within the BM and tested clones exhibited variable mesenchymal lineage potential. Analysis of the LepR^{Cre} line has provided a valuable new marker for studying MP/MSC biology, however, the non-inducible nature of the Cre has precluded more sophisticated lineage tracing approaches involving pulse-chase labeling and analysis. LepR was originally identified from the choroid plexus, which is rich in MP-like cells [44] and was found to be subsequently expressed in the hypothalamus and other brain regions, with limited expression in other tissues. However, it remains unclear if LepR represents a more generic marker of tissue-resident MP/MSCs. Furthermore, it remains to be determined if LepR expression in bone marrow stromal cells defines the entire, or a subset, of the BM MP population and/or is associated with a specific BM MP function. These comments notwithstanding, analysis of the LepR^{Cre} mouse has provided important insights into the nature of BM MPs, their contribution to bone renewal and regeneration, and their in vivo lineage potential.

1.6 Pdgfra and Sca1: MP and "MSC" Lineage Markers

The stem cell antigen-1 (Sca1) surface marker has been identified on a number of stem and progenitor cells. Mice deficient for Sca1 display an osteopenic phenotype consistent with disruption of the MP/MSC compartment in bone [45]. The utility of Sca1 as an MP/MSC marker is problematic due to its widespread expression in other cell types including $CD31^+$ endothelial cells. In recent studies, prospective isolation of mouse MP/MSCs has been achieved using Sca1 in combination with Pdgfra co-staining [46, 47]. Pdgfra is expressed in mesenchymal cells [48]. The Pdgfra-Sca1 doubly positive population (PαS) exhibited much higher CFU-F forming activity than either singly-positive population [47]. The PαS fraction also exhibited many of the standard properties associated with BM-MSCs, such as extensive in vitro expansion, multi-lineage potential, and localization to the perivascular space in vivo. *Pdgfra* expression has also been used to identify MPs in several other tissues, including in skeletal muscle, lung, heart, and fat depots [14, 26, 49, 50]. In the brain, *Pdgfra* is also expressed in oligodendrocyte progenitors as well as in other sites both in the brain and body [48, 51]. Several groups have demonstrated that *Pdgfra* is a useful marker for identifying both white and brown adipogenic progenitor cells (APCs) [49, 52]. Studies carried out with $Pdgfra^{Cre}$ and $Pdgfra^{CreERT2}$ have demonstrated that the majority of white adipocytes in both subcutaneous and epididymal fat can be labeled. The relationship of pre-adipocytes to MPs is still being resolved, however, it is likely that APCs at least are a component of the adipose vascular stromal fraction, which has been shown to contain MPs with multi-potent lineage activity. The expression in these other cell populations limits the usefulness of *Pdgfra* as a pan-MP/MSC marker, however, the degree of expression in some tissue compartments may be negligible thereby making the $Pdgfra^{Cre}$-based genetic tools useful for studying MPs with the noted caveats.

1.7 Gremlin 1 and BM-MSC/ SSCs

A promising marker that has recently emerged for possibly identifying BM-MSC/SSCs is Gremlin1 (Grem1) [22, 53]. Gremlin1 (Grem1) acts as an extracellular bone morphogenetic protein (BMP) binding antagonist, with increased preference for BMP2 and BMP4 [54]. Genetic deletion of *Bmp2* has limited impact on skeletal development, however, these mice exhibit increased fracture rates and a greatly reduced ability to initiate fracture repair [55]. In earlier studies, *Grem1* expression was associated with BM-MSCs [53] and to further examine the utility of this marker for identifying BM-MSCs, a mouse line harboring a $Grem1^{CreERT}$ transgenic BAC was generated [22]. Consistent with other studies, these cells exhibited variable expression of a number of MP/MSC markers including CD105 (endoglin) [22]. In contrast to findings with $LepR^{Cre}$ mice, $Grem1^{CreERT}$ mice enabled labeling of a pre-natal population with high skeletogenic potential.

Similarly to *LepR*^{Cre} mice, both lines identified a population that contributed substantially to the fracture callus following bone injury and normal bone turnover. Interestingly, unlike labeling with the *LepR*^{Cre} mice, lineage tracing with the *Grem1CreERT* line yielded very few label$^+$ BM adipocytes [22]. Moreover, this line was also used to identify rare MP-like intestinal reticular cells associated with the vascular plexus within villi and also contributing to the periepithelial mesenchymal sheath. The relationship between the Grem1$^+$ and LepR$^+$ BM populations needs additional study. The in vitro properties of both populations overlap greatly; however, lineage tracing studies have demonstrated several unique features not evident in the in vitro studies. Together, analyses with the various Cre lines further support the idea of a heterogeneous BM mesenchymal stem/progenitor cell population that participates in overlapping but not completely redundant BM functions. In this regard, the BM-MP/MSC/SSC compartment can be minimally fractionated into at least two complementary populations Grem1$^+$ and LepR$^+$. The former population is associated with bone development, growth, renewal, and regeneration (SSC) [56], while the later has a potentially more prominent role in the HSC niche, but also participates in post-natal bone regeneration and renewal. At this time, it remains unclear if the LepR$^+$ cells represent a heterogeneous population, some of which inhabit the HSC niche.

1.8 Gli1 and Tissue-Resident MPs

The hedgehog (HH) pathway plays an important role in multiple facets of stem/progenitor cell biology [57]. Gli1, a constituent of the HH signaling pathway, has recently been identified as a useful marker for identifying perivascular MPs [58]. *Gli1*^{CreERT2} mice were used to effectively label MPs in multiple tissues including kidney, liver, lung, heart, muscle, and BM [58]. Across these various tissues labeled cells were found to co-express CD29, Sca1, CD44, and CD105, with variable expression of Pdgfrb, and were negative for CD45 and CD31. In the bone marrow, as in other tissues, the Gli1$^+$ cells were found in the perivascular space. In liver, lung, and heart damage models, Gli1-labeled cells acquired an activated phenotype following injury. In some of these models, Gli1 progeny gave rise to a large number of aSMA$^+$ myofibroblasts that provided a substantial contribution to tissue fibrosis. Numerous studies have shown an important role for transforming growth factor β (TGFβ) in driving the emergence of aSMA+ myofibroblasts in fibrosis [59]. Consistent with these observations, Gli1$^+$ MPs isolated from various tissues efficiently formed myofibroblasts following exposure to TGFβ1 [58]. Together, these findings and others indicate that MPs play an important role in tissue repair and fibrosis following injury and presumably in chronic disease. Similar to other MP markers, Gli1 is also expressed in other cell types especially within the brain [60, 61], and this needs to be considered when using this line for lineage analysis of MPs.

1.9 Mesenchymal Lineage Markers

MPs contribute to a number of mesenchymal lineages that are characterized by the expression of lineage-associated (but not always defining) transcription factors such as RUNX2, SOX9, SP7 (Osterix), peroxisome proliferation-activated receptor γ (PPARG), and Scleraxis (SCX). *Runx2* and *Sp7* are expressed within the osteogenic lineage in addition to hypertrophic chondrocytes, whereas *Pparg* and *Scx* are more restricted to the adipogenic and tendogenic lineages, respectively. *Sox9* is critically important in chondrogenesis, but also appears in a number of disparate cell types across other germ layers [62]. Lineage tracking with *Osx* has been useful for identifying MP/MSC/SSCs with osteogenic potential within the BM, and in turn these studies have yielded important insights into MP behavior and contribution within bone [43, 63]. The utility of these various markers for studying MP activity outside the BM remains to be defined. *Prrx1* is a pan-MP marker, and transgenic Cre lines harboring a portion of the *Prrx1* promoter have been used extensively for studying MPs in limb skeletal development [64]. *Prrx1* is expressed in adult MPs and thus provides a potentially useful tool for studying post-natal MP biology [65–67]. Interestingly, *Prrx1*-labeled MPs contribute to subcutaneous fat, but provide a limited contribution to visceral white or brown fat [68, 69]. Thus, *Prrx1* may be useful for identifying and studying MPs within specific anatomical compartments.

Summary—Lineage analysis has provided numerous important insights into MP biology in health and disease. As highlighted above, the different CREs exhibit advantages and disadvantages for the effective and specific labeling of MPs within various tissues and organs. The methodology described below pertains to lineage tracking analyses both within and outside the MP compartment, and is designed around the detection of native fluorescent protein (FP) or LacZ reporter activity.

2 Materials

2.1 Tamoxifen Preparation and Administration

1. TAM preparation—Prepare a 25 mg/ml solution of TAM in sunflower oil (optional—can be pre-warmed to 37 °C to expedite dissolution) in a sterile 15 ml conical centrifuge tube. If the crystals are large, crush before addition. The sunflower oil should be sterile and added to the pre-weighed TAM in a biological safety cabinet (BSC). Vortex well and place in a rotating incubator at 37 °C overnight or until no trace of crystals are visible (can be as little as 4 h). Aliquot into daily administration amounts maintaining sterility and store away from light at 4 °C for up to 2 weeks (*see* **Note 1**).
2. 4-OH TAM preparation—warm 100 % ethanol and sunflower oil to 37 °C. Add desired amount of 4-OH TAM powder to

the appropriate volume of 100 % ethanol. At least 30 μl of ethanol is required for the effective dissolution of each mg of 4-OH TAM. Vortex well and allow to dissolve at 37 °C, vortexing frequently. Once the 4-OH TAM is dissolved and the ethanol is fully cleared, add the ethanol solution to pre-warmed sunflower oil in a ratio of 4-OH TAM/ethanol:sunflower oil of 1:5 for pups or 1:9 for adults, and vortex well. Solution will initially appear cloudy, but should clear with mixing. If not, return to 37 °C incubation to fully dissolve with periodic vortexing. It is necessary to prepare fresh all components before each use (*see* **Note 2**).

3. TAM chow—for continuous or longer-term reporter induction, animals can be fed chow-containing tamoxifen (i.e. Harlan Laboratories). However, there may be some aversion to the food leading to decreased food consumption. Following introduction of the new chow, food intake should be monitored to ensure adequate consumption.
4. 1 ml syringes, 25 G 5/8 needles, and gavage needles.

2.2 Tissue Fixation, Collection, Processing, and Cryosectioning

1. Dissection tools, including tweezers and large forceps.
2. Microtome blades.
3. Phosphate-buffered saline (PBS).
4. Paraformaldehyde (PFA)—4 % PFA (EM grade), dissolved in PBS on a hot plate at ~60 °C until the powder is clearly dissolved. Following dissolution, allow to cool and aliquots can be stored at −20 °C. To prepare a 2 % working solution mix with an equal amount of PBS. *As PFA is an irritant and suspected carcinogen, experiments involving PFA should be carried out in a fume hood.*
5. 60 ml syringes (2), two-way valve with tubing for perfusion.
6. 25 G 5/8 needles.
7. Agarose embedding, prepare a 5 % low-melting point agarose solution in PBS by melting in a microwave. Once melted, transfer to a 37 °C water bath to cool solution before use.
8. Tissue-tek optimum cutting temperature (OCT) compound.
9. Embedding molds.
10. Stainless steel 200 ml beaker, 2-methylbutane (isopentane), and liquid N_2.
11. Cryostat.

2.3 Detection of Native FP and Immunofluorescence

1. Terminal anesthetic stock solution is generated by making a 1.6 mg/ml solution of 2,2,2,tribromoethanol in tert amyl alcohol (formerly known as Avertin). This is done by adding 25 g of 2,2,2,tribromoethanol into 15.5 ml of tert amyl alcohol or the desired amount following the same formulation. Dissolve overnight in the dark with vigorous stirring in a fume

hood. Before proceeding, ensure that all powder is dissolved. This stock can be stored for up to a year in the dark at RT. Make up a working solution of 25 mg/ml in PBS by stirring overnight at 37 °C in the dark then filter sterilize. This solution can be stored at 4 °C for up to a month.

2. Microcentrifuge tubes (1.5 ml) and/or 5 ml polypropylene tubes.
3. Humidified chamber box (i.e. paper towels soaked in water in an opaque 100 slide box or equivalent).
4. Numerous factors contribute to higher background and/or artifacts in IF and even histological staining. Most importantly, all solutions should be free of particulate matter and care should be taken not to introduce foreign matter (i.e. debris contaminants, hair, fibers, antibody aggregates, etc.), as this can potentially compromise both imaging quality and subsequent interpretation. In this regard, pre-cleaned glass slides should be used and solutions filtered and mixed well before use, or for small volumes filtered or centrifuged.
5. Sodium borohydride—Immediately before use, make up a 10 mg/ml solution of sodium borohydride in PBS by dissolving an appropriate amount of sodium borohydride in 1× PBS. Properly prepared and fresh sodium borohydride should produce a bubbling reaction following PBS addition. If no bubbling is observed or the stock crystals have aggregated (sodium borohydride is highly hygroscopic), a fresh stock of material should be obtained.
6. Immunofluorescence (IF) block solution is prepared by adding BSA to 2.5 % in PBS. Dissolve slowly to prevent excess foaming. Once dissolved, serum from the secondary antibody species is added to 2.5 %. Store at 4 °C up to 1 month.
7. Anti-CD31 (PECAM1), Clone MEC 13.3 or similar, for detection of endothelial cells.
8. Anti-Laminin, for detection of laminin in basement membranes, which is generally useful for defining tissue architecture as well as the perivascular space.
9. Secondary goat anti-rabbit IgG Alexa 488.
10. Secondary goat anti-rat IgG Alexa 647.
11. A DAPI solution is made-up in ddH_2O at a concentration of 300 μM and aliquots are frozen at −20 °C. Once thawed, store at 4 °C for up to several months—if staining intensity decreases make fresh. Always protect from light. A 300–600 nM working solution is made fresh before each use by diluting stock 1:500–1:1000 in PBS.
12. Aqua polymount mounting media.
13. Coverslips and nail polish.

2.4 In Situ and Whole-Mount LacZ Staining

1. LacZ fixative solution—100 mM $MgCl_2$, 0.2 % glutaraldehyde, and 5 mM ethylene glycol tetraacetic acid (EGTA, from stock 0.5–1.0 M) in 1× PBS. Add all components to a predetermined amount of water (desired amount) and add sufficient volume of 10× PBS to produce a 1× solution and pH to ~7.3. For short-term fixation (<90 min), 4 % PFA can be substituted for LacZ fixative solution.
2. LacZ stock solutions—10× $MgCl_2$ 20 mM (store at rt); 10× detergent solution, sodium deoxycholate 0.1 %, NP-40 0.2 % (store at rt); 20× (100 mM) potassium ferricyanide (store at 4 °C); 20× (100 mM) potassium ferrocyanide (store at 4 °C). All the above solutions are made-up in ddH_2O. Forty times (40 mg/ml) 5-bromo-4-chloro-3-indolyl-β-D-galatopyranoside (X-gal) solution is prepared in dimethylformamide and aliquoted in appropriate "experiment-size" aliquots and stored at −20 °C.
3. LacZ washing and permeabilization solution—To prepare the LacZ washing/permeabilizing solution from LacZ stock solutions, first warm Ferri and Ferro solutions in a 37 °C water bath. Add 10× $MgCl_2$ and detergent solution to 1× in PBS. Appropriate amounts of pre-warmed Ferri and Ferro solutions should be mixed together prior to addition to the $MgCl_2$/detergent solution. Mix solution gently to prevent bubbles, giving final concentrations of 2 mM $MgCl_2$, 0.01 % Deoxycholate, 0.02 % NP40, 5 mM potassium ferricyanide, and 5 mM potassium ferrocyanide. Pre-warming of solutions reduces subsequent crystal formation.
4. LacZ Staining solution—LacZ Staining solution is prepared by adding X-gal (or other LacZ substrates, Bluo-Gal, Salmon-gal, Red-gal, etc.) stock solution to fresh LacZ washing and permeablization solution to a final concentration of 1 mg/ml. Use immediately and minimize exposure to light.
5. Nuclear Fast Red counterstain solution or other counterstains.
6. Ethanol, xylene, and Cytoseal 60 or similar.

3 Methods

3.1 Reporter Gene Induction with Tamoxifen

1. Appropriate mouse lines are interbred to generate progeny containing one copy of Cre along with a single copy of the Cre-dependent reporter gene. A number of the more commonly used Cre-dependent reporters are outlined in Table 1. In some instances, it may be beneficial to use reporter and/or Cre homozygous animals. For effective induction of recombination and Cre-dependent reporter gene expression, consideration should be given to which tissues will be labeled. For instance, both gavage and intraperitoneal (IP) injection of

TAM should be evaluated for induction of "desired" reporter gene activity. IP injection is useful for inducing Cre translocation in most tissues and organs, but can also be effective for reporter gene induction in embryos [70]. Local TAM injection can also be used for regional activation of reporter gene expression, with the caveat that reporter expression may be induced at other sites (*see* **Notes 3** and **4**).

2. Inject mice with ~100 μl TAM IP (~2.5 mg/25 g mouse; the volume can be adjusted up for larger mice and the dose can also be adjusted up or down depending on desired outcome, *see* **Note 5**), with a BD 1 ml syringe and BD 25 G 5/8 needle at approximately the same time every day for:
   (a) 1 day, low recombination for clonal studies or efficient CREs.
   (b) Up to 5 days for induction of maximal recombination.
3. It is important to provide a washout period of at least 1 week after the final TAM administration, but ideally >2 weeks to ensure that minimal residual TAM remains within mouse tissues. The length of this washout period is often a compromise and dictated by the nature of the experiment (i.e. are the population of interest relatively stable over this washout period).
4. For embryonic recombination, pregnant dams are carefully (avoid uterus) injected IP with one dose of 100–250 μl TAM at various times (reporter and Cre dependent) during gestation. Injection timing should be based on reporter used, considering that it typically takes at least 6 h-post TAM injection to visualize reporter activity (*see* **Note 6**).
5. For induction in pups (P1–P7), ~50–60 μl of 4OH TAM preparation can be carefully injected into the peritoneal cavity or directly into the stomach using the milk band as a reference (*see* **Note 7**).
6. As mentioned in Subheading 3.1, **step 1**, for some experiments oral gavage delivery is preferred. TAM is prepared the same as in Subheading 2.1, **item 1**. However, it may be useful to work with higher concentrations. Up to 10 mg TAM in 100–300 μL doses can be administered successfully via gavage as single or multiple 10 mg doses over a serious of days. This delivery technique requires some training and practice, as it can be ineffective and/or harmful to the animals if performed incorrectly.
7. TAM dosing is usually adjusted to maximize CRE-mediated labeling of the population of interest (*see* **Note 8**).
8. For many lineage-tracking experiments, we typically use a pulse-chase strategy. A typical experimental paradigm is shown in Fig. 1. This involves analysis of labeled cells shortly after the last TAM injection (1–3 days post-TAM) and comparing the

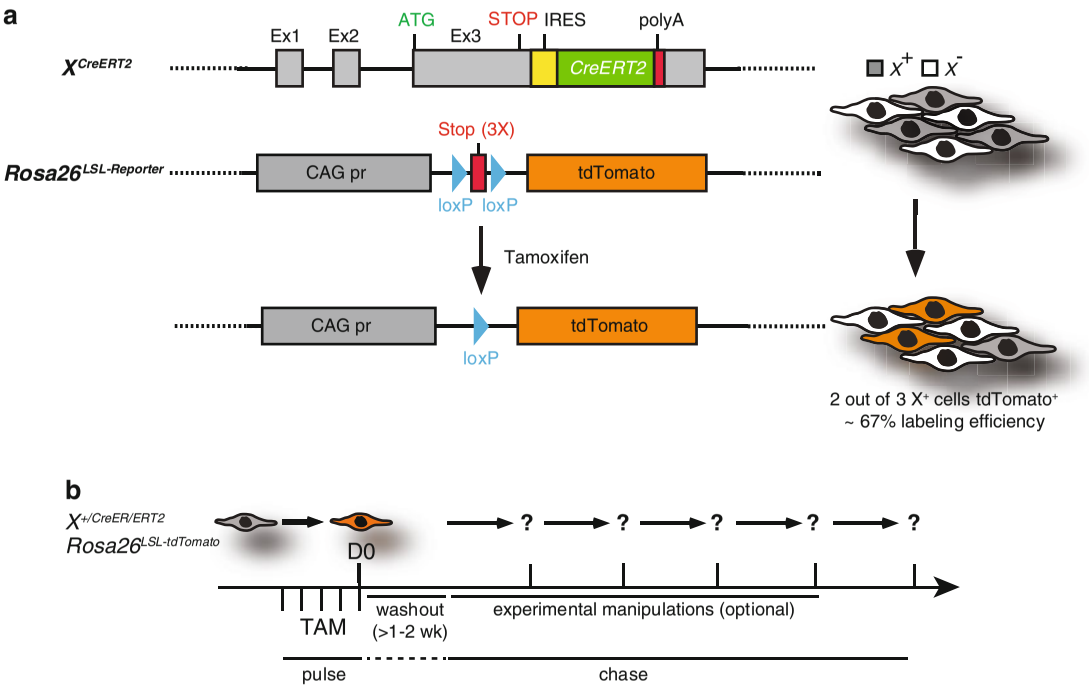

Fig. 1 Overview of a generic lineage tracing strategy. (**a**) A mouse line harboring a knock-in allele of a TAM-inducible Cre into *Gene X* ($X^{CreERT2}$) is interbred with a reporter line (*Rosa26LSL-Reporter*) to generate $X^{CreERT2}$; $Rosa26^{LSL\text{-}Reporter}$ mice. In this case, the CreERT2 cassette contains an internal ribosome entry (IRES) site to enable its translation, and this entire cassette is knocked-in to the 3′ un-translated region of *Gene X*. In the absence of TAM, the cells expressing *Gene X* are reporter negative. If the CreERT2 is leaky (activity in the absence of TAM), reporter$^+$ cells will be observed without TAM treatment. Following TAM administration, the CreERT2 shuttles into the nucleus where it induces recombination at the LoxP sites, thereby deleting the LoxP-Stop-LoxP (LSL) cassette, resulting in reporter expression (tdTomato) in the recombined cells. In this example, not all of the *Gene X*-expressing cells undergo recombination (2 out 3), which yields a labeling efficiency of ~67 %. Labeling efficiency can be typically increased or decreased by modifying the dose of TAM. (**b**) A typical pulse-chase experiment is shown in which TAM is used to induce reporter expression in the cells of interest (*Gene X*-expressing) within embryos or post-natal animals. Day 0 can be defined as the first or last day of TAM treatment, and tissues can be collected at various points (indicated by *?* in the figure) after TAM treatment to determine the fate of reporter-expressing cells. In this manner, the pulse period includes the TAM treatment period, and then tissues are collected at various times after the TAM treatment (chase period) and analyzed. Experimental manipulation (i.e. injury) can sometimes result in additional recombination within the cells of interest as well as in other populations that now express *Gene X* (even in low TAM). Thus, it is always advised to provide a washout period such that residual TAM does not lead to unanticipated cell labeling

frequency, distribution, and fate of labeled cells at various times thereafter (up to a couple of years). Furthermore, various experimental manipulations (injury, etc.) can be performed after the washout period to study the consequences on MP biology and fate. *An important control for fate-mapping studies involves the inclusion of an oil (oil/ethanol) alone control, as this allows assessment of the degree of leaky CreER activity in the absence of TAM.*

3.2 Tissue Processing for Detection of Native FP Fluorescence

1. The methodology described focuses on the detection of native FP fluorescence and does not require the use of anti-FP antibodies (*see* **Note 9**).
2. Tissue processing for retention of native FP fluorescence begins with the collection of tissues at the desired time-post TAM or oil injection. End-point anesthesia is accomplished by IP injection of Terminal anesthetic stock solution (avertin) (300–500 mg/kg; usually this equates to 400–500 μl of 25 mg/ml solution for a 25 g mouse) and surgical plane anesthesia is verified by pedal reflex test before proceeding. If surgical plane is not evident after 5 min, additional avertin (0.25–0.5 dose) can be injected. As avertin is fat soluble, avoid injecting avertin into fat depots and fatter mice may require an increased dose.
3. Transcardial perfusion is performed using a valved syringe apparatus to circulate >10–15 ml PBS with 10 mM EDTA followed immediately by >10–15 ml 2–4 % PFA. Complete systemic circulation is verified when tail spasms are observed.
4. The tissues of interest should be rapidly collected into ice-cold PBS.
5. Slice tissue into pieces of ~4 mm^3 using microtomy blade. For some tissues (i.e. brain, skeletal muscle), it may be necessary to encase the tissue in agarose to aid cutting. For this purpose, submerge the tissue in 5 % low melt agarose in PBS and transfer to −20 °C freezer on a level surface to expedite solidification, but do not allow to freeze. Once solid, place in ice-cold PBS and slice into appropriately sized pieces as described above.
6. To ensure maximal retention of endogenous FP activity, unless otherwise noted, perform all subsequent incubations in the dark.
7. Immerse tissues in ~ 20X tissue volume of 2–4 % PFA for 24–48 h at 4 °C in a 15 or 50 ml conical centrifuge tube or smaller. Depending on the application, different tissues can be either separated or processed together. To minimize adherence to other tissues and the plastic vessel, during this period the tissues should be gently agitated in a roller bottle format or similar.

8. After fixation, carry out 3 × 30 min washes of the tissues in cold PBS at 4 °C.
9. The tissues are incubated in a series of increasing concentrations of sucrose starting at 10 % at 4 °C. Once the tissue no longer floats (1 h to overnight), it can be transferred to a 20 % sucrose solution, followed by 30 %. For optimal preservation of tissue architecture these steps should not be rushed, and incubations involving higher concentrations of sucrose take longer. As noted above, for heart and muscle, higher concentrations (up to 50 %) of sucrose minimize tissue-freezing artifacts (i.e. swiss cheese).
10. Label tissue molds in advance, as it is much more difficult to label them after freezing.
11. Prepare an isopentane slurry by submerging a stainless steel beaker containing several inches of isopentane in approximately the same depth of liquid N_2 in an ice bucket (i.e. styrofoam box).
12. Remove tissue from sucrose solution, blot dry with KimWipe or equivalent being careful not to distort the structure of the tissue as it can stick to the KimWipe if mishandled.
13. Submerge the tissue in OCT compound and allow the OCT to completely cover the tissue surface. If necessary, use tweezers to move the tissue around to ensure complete coverage. This can be done in tissue-culture plates, petri dishes or their lids, tube lids, etc.
14. Once all surfaces of the tissue are thoroughly coated with OCT transfer to a pre-filled cryomold. The cryomold should contain sufficient OCT to ensure that the tissue is completed submerged. Using tweezers, position tissue as desired, and then use large forceps to dip the cryomold into the isopentane slurry such that the OCT surface is level with the isopentane crust.
15. Blocks are submerged and allowed to solidify until a 0.5 cm^2 area on top remains liquid and subsequently, transferred to –20 °C freezer for short-term storage (for up to month). For longer-term storage, blocks should be stored at –80 °C. Once the blocks have been cut, recover open surface with OCT to increase the useful lifespan of stored blocks.
16. For best results, cryosections should be prepared within a reasonable time-frame (weeks–months) after freezing.
17. For cryosectioning, equilibrate the block to chamber temperature by placing it in the chamber for at least 30 min if from –80 °C or 5 min if samples were stored at –20 °C. Place desired number of specimen holders in the chamber to cool at this time.
18. To remove the block from the mold, press the button on the bottom of the mold then squeeze the angled edges together to release the cryo block.

19. Add a generous drop of OCT to the grooved surface of a pre-cooled block holder and place the frozen block on the spreading drop. If possible, align and level the block within the cryostat chamber. If this proves insufficient, the block can be quickly adjusted by removing it from the chamber and rotating it at eye level to ensure that the cutting surface is reasonably parallel to the holder surface. This should be done before the OCT freezes, and once adjusted return the sample-holder to the cryostat chamber.
20. Allow sufficient time for the OCT to solidify and to be sufficiently bonded to the specimen holder. The OCT should appear white and homogeneous similar to that of the block and be immobilized relative to the specimen holder before proceeding.
21. Due care and attention needs to be exercised when preparing and cutting sections on a cryostat as the blade is incredibly sharp. Please refer to the owner's manual for safety information and proper use of the cryostat.
22. Carefully load a blade into the blade holder in the cryostat, align the block face to the knife and begin sectioning (*see* **Note 10**).
23. Cryoblocks are typically sectioned at between −16 and −20 °C and 5–10 μm sections are generated for regular microscopy and 20–100 μm thick sections are typically used for confocal microscopy. To transfer the newly generated section to a slide, gently touch a slide kept at room temperature (RT) to the freshly cut section on the cold stage, and allow the section to adhere outside the chamber at RT for ~30 s. Once complete, store the slides at < −20 °C. Under these conditions, FP activity is retained for months and possibly years. These slides can be used for subsequent IF staining (go to Subheading 3.3) or processed and visualized.
24. For immediate visualization without IF, thaw and dry the slides at up to 30 min at RT (or longer and/or on <37 °C slide warmer if tissue adherence is a concern). To ensure maximal retention of endogenous FP activity, this should be done in the dark.
25. Wash the slides 3 × 10 min in excess PBS to remove OCT compound and then the slides can be immediately counterstained with an appropriate dye, cover-slipped and visualized (*see* Subheading 3.3, **steps 13–18**).

3.3 Combined FP Reporter Visualization with Immunofluorescence

1. Remove slides from freezer and allow to dry for 30–60 min at RT or on a 37 °C slide warmer in the dark. Wash 3 × 10 min with excess PBS in the dark to remove OCT compound.
2. For subsequent **steps 4–15** place slides into a slide box containing wet (water) paper towels or similar. All incubations should be carried out in the dark in an opaque slide box (*see* **Note 11**).

3. Aldehyde-based fixatives (glutaraldehyde > paraformaldehyde) will contribute to tissue autofluorescence (AF). One method that works well to reduce AF is to treat the slides with a solution of sodium borohydride (*see* **Note 12**).
4. Add sufficient borohydride solution to the tissue samples to adequately bathe the sections. Recommended incubations are typically up to 10 min, however, we typically incubate up to an hour with no adverse effect on FP activity, and find this leads to an appreciable decrease in AF (*see* **Note 12**).
5. After 1 h remove sodium borohydride solution, and wash two or more times in PBS until no fizzing is observed.
6. Remove PBS and replace with IF blocking solution. Allow to incubate for 60–90 min at RT or overnight at 4 °C. Do not wash after blocking step.
7. During the last few minutes of the blocking step, prepare the primary antibody solution(s) or cocktail(s). This protocol includes a description of immunodetection of laminin and CD31, however, it is also applicable with minor modifications to the detection of other proteins (*see* **Note 13**). Dilute the primary antibodies to the predetermined working concentration in IF blocking solution, Ab:Block Solution—1:50 and 1:100 for anti-CD31 and anti-Laminin, respectively. Anticipate that a single slide is going to require ~500 μl for reasonable coverage, however, as antibodies are costly, it is best to minimize the antibody solution or cocktail. Thicker sections (>10 μm) may benefit from additional volume of antibody solution or cocktail and increased incubation time (*see* **Note 14**).
8. Remove blocking solution and replace with primary antibody cocktail and incubate for 60–180 min at RT or 4 °C overnight (*see* **Note 15**).
9. Following incubation, carry out three washes >5 min in PBS. Usually a gentle rinse is performed prior to the wash steps. A rinse consists of removing most of the solution, adding PBS as surface tension will allow and removing it. The next addition of PBS begins the first wash.
10. During the third wash, prepare the secondary antibody cocktail. In this case, the primary antibodies were generated in rat and rabbit for CD31 and Laminin, respectively. As they are from different species, it is possible to dilute the two secondary antibodies together in IF blocking solution (*see* **Note 16**).
11. Remove the third PBS wash, and replace with a sufficient amount of secondary antibody cocktail to cover the appropriate section(s) and incubate for 45–60 min at RT.
12. Repeat the washes as described in **step 9**.

13. During the third wash prepare the DAPI counterstain solution for staining of nuclei. Other nuclear dyes can be substituted for DAPI, such as Hoechst dyes, TOTO3, cell cycle dyes, etc.
14. Remove the third PBS wash and replace with DAPI working solution ensuring even coverage of tissue sections and incubate for 5 min at RT.
15. Carry out 2 × 2 min washes in PBS at RT.
16. Dry glass as much as possible without drying tissue sections, and this can be done by gently blotting the excess solution away with a KimWipe or similar.
17. Apply a small drop of Aquapolymount or equivalent to each tissue section and slowly tilt the coverslip onto the slide allowing gravity to work any air out before finally setting it in place. Allow several hours to overnight RT for mounting media to solidify before imaging and to preserve fluorescence (days to a few weeks), slides should be subsequently stored at 4 °C in the dark (*see* **Note 17**).
18. Once coverslipped, slides should be stored in the dark at 4 °C to maximize signal retention. For hardset mounting media (i.e. Aquapolymount) slides should be allowed to dry overnight at RT in the dark and then stored at 4 °C. For mounting media (non-hardset), seal the edges (longer-term storage) or tack the corners (shorter-term storage) with nail polish.
19. Slides can be visualized and/or imaged using a variety of microscopes (i.e. epi-fluorescent, confocal, etc.) equipped for visualization of fluorescence (*see* **Note 18**).

3.4 Whole-Mount LacZ Reporter Staining

1. For some purposes, it may be beneficial to use a LacZ-based reporter, as with due attention, LacZ expression can be effectively analyzed in whole-mount and in sections (*see* **Note 19**).
2. Anesthetize animal as described in Subheading 3.2 (**step 1**) and set up components for perfusion fixation (Subheading 3.2, **step 2**).
3. Transcardial perfusion is performed using a 3-way or T-valved syringe apparatus to circulate >10–15 ml PBS with 10 mM EDTA followed by >10–15 ml LacZ fixative (as above, this should be performed in a fume hood to minimize exposure to aldehydes).
4. Dissect tissue(s) of interest into ice-cold PBS.
5. Slice tissue(s) into ~4 mm^3 pieces using a microtomy blade. As described in Subheading 3.2, **step 5**, tissues can be embedded in agarose to facilitate more precise cubing.
6. Fix tissue in LacZ fixative for 30–120 min at 4 °C in a roller bottle or similar.

7. To ensure maximal retention of β-galactosidase activity and preservation of histological architecture, perform all incubations at 4 °C unless otherwise indicated.
8. Wash tissues 3 × 30 min with PBS.
9. Incubate in LacZ washing/permeabilization solution overnight in a roller bottle or similar (*see* **Note 20**).
10. Replace LacZ wash/permeabilization solution with fresh LacZ staining solution and incubate for 2–24 h in the dark until "reasonable" staining can be observed (*see* **Note 21**).
11. Once desired staining intensity is achieved, remove the staining solution, wash once briefly with PBS, followed by 3 × 30 min washes in PBS (*see* **Note 22**).
12. Post-fix tissues in 4 % PFA at 4 °C for 24–48 h.
13. Remove fix, wash briefly with PBS, followed by 3 × 30 min washes in PBS.
14. For visualization, transfer to 70 % ethanol, this helps intensify the stain and aids crystal dissolution if present. If crystals persist, change solution. With whole-mount staining tissues are typically visualized with a dissection microscope coupled with a digital camera for image collection. Samples can be stored at 4 °C almost indefinitely in 70 % ethanol in a properly sealed container.
15. For additional analyses, the tissues can be paraffin-embedded, sectioned, and processed for immunodetection using standard methodology.

3.5 LacZ In Situ Reporter Staining

1. Process and harvest tissues as described above in Subheading 3.4, **steps 1–4**.
2. Incubate tissue pieces in LacZ fixative for 30–120 min at 4 °C with gentle agitation in a roller bottle or similar.
3. To ensure maximal retention of transgenic β-galactosidase activity, the following incubations, unless otherwise noted, should be performed at 4 °C.
4. Wash tissues 3 × 30 min in PBS.
5. The tissues are incubated in a series of increasing concentrations of sucrose starting at 10 %. Once the tissue no longer floats (1 h to overnight), it can be transferred to a 20 % sucrose solution, followed by 30 %. For optimal preservation of tissue architecture these steps should not be rushed. As noted above, for heart and muscle, higher concentrations (up to 50 %) of sucrose minimize tissue-sectioning artifacts (i.e. swiss cheese).
6. The next few steps are identical to that described for the preparation of cryosections (Subheading 3.2, **steps 21–23**). Section as soon as possible after processing to maximize retention of LacZ activity.

7. Prepare sections on a cryostat (−16 to −20 °C) as described in Subheading 3.2 (**step 23**) and transfer to a fisher Superfrost slide (or similar). Once melted, refreeze immediately typically by placing in the cryostat chamber and then store at −20 °C.
8. For staining, thaw and allow the slides to dry at RT for 30–60 min.
9. Wash the slides 3 × 10 min in PBS to remove OCT compound. During the third wash, prepare the LacZ staining solution.
10. While ensuring the tissue does not dry out, dry all other surfaces of the slide as much as possible by blotting with a KimWipe.
11. Place slides in a darkened humidified chamber. A 100-slide box nicely holds 12 slides and wet paper towels are used to coat the bottom surface.
12. Carefully cover the tissue sections with LacZ staining solution. However, as the staining solution contains detergent and has reduced surface tension, too much solution will drain/wick from the slide (especially if the edges of the slides are in contact with the slide box) leading to dry areas on the sections.
13. Incubate in a dark humidified 37 °C incubator (place an open vessel of H_2O in the incubator) for >4 h until appreciable staining becomes apparent (*see* **Note 21**).
14. Upon completion, pour excess solution into an appropriate cyanide waste, place slides into a slide rack and wash by dipping into a 200 ml beaker of ddH_2O. Replace ddH_2O until clear, then change to PBS if proceeding to IF staining or proceed directly to the next step for histological staining.
15. For counterstaining of LacZ stained cells, we often use nuclear fast red. For this purpose, stain slides in a staining tray for 5 min with nuclear fast red solution and then wash under tap water until the water is clear. This staining solution can be reused, replace when the staining intensity begins to fade.
16. Coverslip as described above in Subheading 3.3, **step 17**. For long-term storage and retention of chromogenic staining, dehydrate with an ethanol dehydration series to 100 % ethanol, xylene, mount with Cytoseal 60 and coverslip.

3.6 Combination IF and LacZ In Situ Staining

1. Chromogenic LacZ product can be visualized alongside IF staining (Fig. 2). In this case, a shortened LacZ incubation and/or a treatment to reduce AF allows for the detection of both signals and subsequent composite image creation (*see* **Note 23**).
2. Slides from Subheading 3.5, **step 14**, are subsequently processed for detection of various antigens using IF.

3. After LacZ incubation, wash slides 3 × 30 min with PBS.
4. For this protocol we routinely treat with sodium borohydride as described above (Subheading 3.3, **steps 3–5**), as glutaraldehdye fixation typically generates increased AF.
5. Once completed the slides can be processed as described above for IF staining at Subheading 3.3, **steps 6–19**. Widefield bright (LacZ staining) and epi-fluorescence images should be collected for all the channels. These can be collected in monochrome or color, with color images being subsequently converted to monochrome to enable merging of images. In order to merge the various images, all images need to be acquired with identical image dimensions. For this purpose, it is easiest if both widefield bright and fluorescence images are collected with the same camera.
6. Save each layer/color as a tagged image format (TIFF). Multiple software platforms are capable of performing the following operations using a similar approach to the one described below for Image J.
7. Open Image J 64 and drag and drop individual image layer tif files onto the Image J 64 header or alternatively each image can be opened separately. The dropped or opened files will open in separate windows. Open the *Merge Channels* window from the *Image* J menu, *Color* submenu and assign each TIF file to the desired color. The gray channel is used for LacZ. Ensure *create composite image* box is checked and select *OK*. The composite will appear as a new file, however, this will require further processing. The gray LacZ channel will require the LUT to be inverted in order for the LacZ signal to appear as white on a black background. To invert the LUT, first select the gray channel while *color* is selected on the *channels tool* window menu. Next, select the *more* icon in the *channels tool* window to reveal the menu. Select *Edit LUT* to open the *LUT editor* window and select the invert icon. The final step is simply aesthetic adjustment of each channel of the composite image. Open the *Channels Tool* window in the *Image* menu, *Color* submenu and select *color* from the dropdown menu to adjust each channel LUT separately. Open the Brightness/Contrast window from the *Image* menu, *Adjust* submenu to adjust LUT for selected channel. Change the selection in the *channels tool* window back to *composite* to view in the context of all colors. Repeat until satisfied with the appearance of the composite image. Adjust LUTs for the other channels. Save composite document as TIFF or select *Copy to System* from the *Edit* menu and paste into desired software. Each separate layer can be adjusted and saved using the same approach.

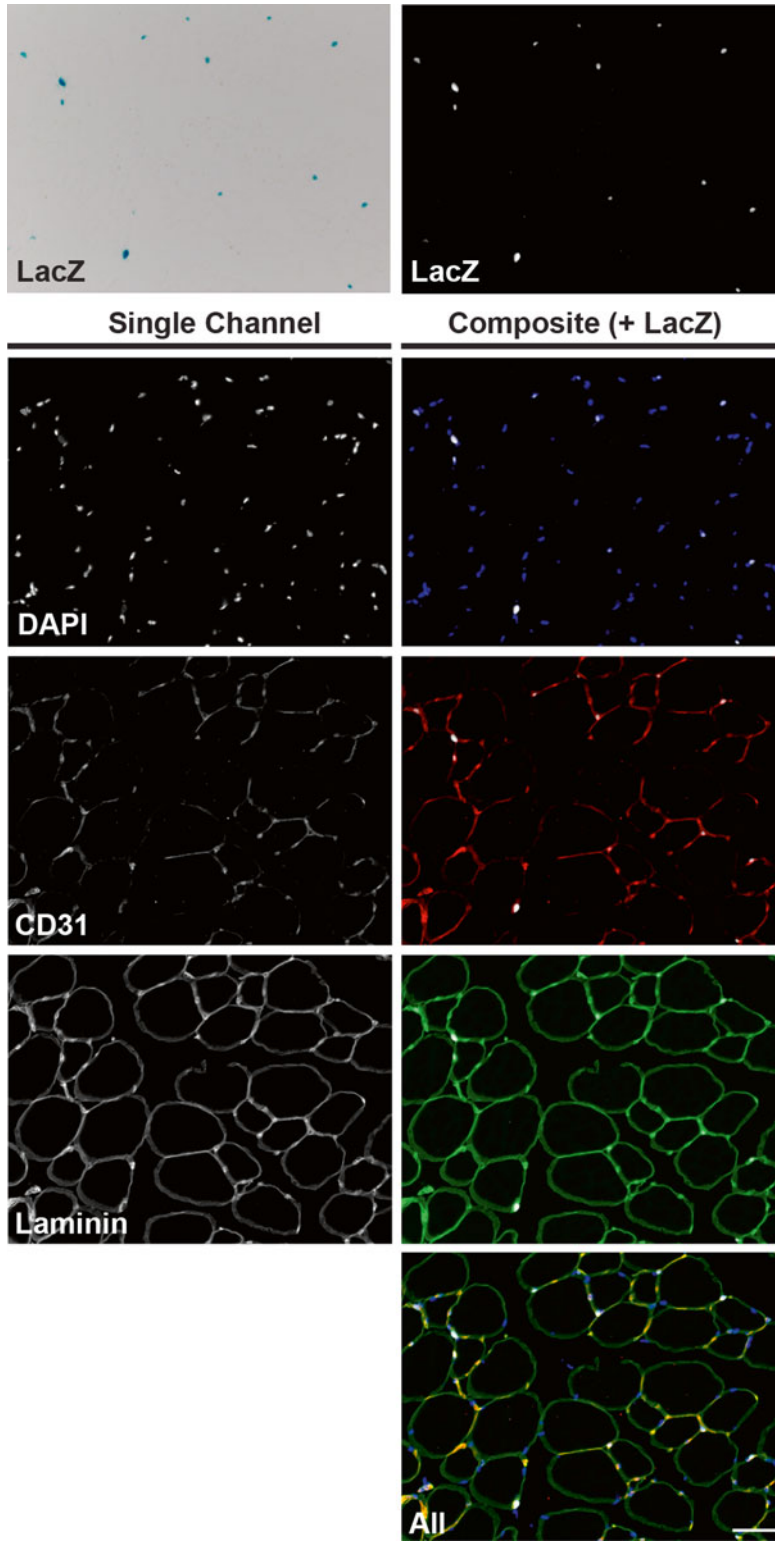

Fig. 2 An example of LacZ in situ stained slide combined with immunodetection of CD31 and Laminin. In this case, MPs are labeled with nuclear LacZ. Tissues were collected from *tibialis anterior* muscle, processed, cryosectioned and reacted with X-gal solution. Subsequently, IF was carried out on this slide with antibodies

4 Notes

1. If precipitate forms during storage, warm suspension to 37 °C before administration. If warming does not re-dissolve crystals, discard and make a fresh lot.
2. TAM versus 4-OH TAM. For activation of the CreER/ERT2, TAM needs to be metabolized to its active form 4-OH TAM. To induce more robust and faster CreER/ERT2 translocation in applications where limited doses are desired (pregnant dams or pups) or potentially greater CreER/ERT2 activity is required, 4-OH TAM is often preferred [70]. As TAM is considerably cheaper than 4-OH TAM and is adequate under most circumstances, TAM is typically the tamoxifen of choice. The newer versions of CreER such as CreERT2 require less TAM to drive recombination.
3. For determining the short- or long-term fate of reporter labeled cells, it may be useful to incorporate other non-Cre-dependent reporters in the breeding program. For instance, for following the ability of reporter-labeled cells to become osteoblasts, many groups use a GFP-based reporter based on a 2.3 kb fragment of the type I collagen promoter (Col2.3-GFP) [71]. Other reporter lines are available to monitor the contribution of labeled cells to other mesenchymal lineages.
4. In some instances, where robust short-term reporter gene expression is desired, two copies of the reporter gene can be used. This is particularly useful for carrying out short-term labeling studies in the embryo or adult. However, as increased reporter gene expression can sometimes contribute to cytotoxicity, care should be taken when more than a single reporter is used. In addition, where possible, homozygous Cre mice can also be used to increase labeling efficiency. For instance, efficient labeling with confetti mice typically requires higher Cre activity, so where possible mice harboring two copies of the Cre increase labeling efficiency.
5. The suggested dose of tamoxifen provides a good starting point. However, to decrease or increase labeling efficiency the dose should be adjusted lower or higher, respectively. Please note, higher doses may be associated with increased side-effects and morbidity, and longer washout periods may also be required.

Fig. 2 (continued) to Laminin and CD31, and finally stained with DAPI. To combine the images, the LacZ image was converted to monochrome and the LUT was inverted (LacZ nuclei now appear white). These images were combined with various single channels to generate composites, and the *bottom image* shows the complete composite image. Note the nuclei of the labeled MPs can be found in close proximity to $CD31^+$ blood vessels. The X-gal product will also lead to some fluorescence quenching, so the resulting fluorescence intensity of X-gal stained structures is typically attenuated. Magnification bar, 40 μm

6. Injection into pregnant dams is associated with a number of complications including dystocia, increased levels of resorption, and late-term abortions. For these purposes, high concentrations and multiple doses should be avoided [70]. Furthermore, it may be beneficial to deliver pups by cesarean section and place with a foster mother (CD1/ICR mice are good foster mothers). In some instances, co-administration with progesterone has reduced late fetal abortion [72].
7. Injection into pups (especially IP) is normally associated with a high level of neo-natal mortality. Under these conditions, larger numbers of pups need to be injected. When done properly there is lower mortality associated with injection into the milk band.
8. Labeling efficiency is typically determined by examining the overlap of CRE-induced reporter expression with that of an endogenous marker reflective of the labeled population. For these purposes, immunodetection of the protein associated with the Cre allele or a suitable definitive marker of the labeled population is suitable. In this manner, the number of marker and FP doubly positive cells versus marker alone can be enumerated. Under these circumstances the number of FP alone cells should be very low, whereas efficient labeling will generate numerous (>80 %) marker and FP doubly-positive cells.
9. Numerous antibodies have been optimized for detection of epitopes following paraffin-processing. However, as FP activity does not survive paraffin-embedding, under these situations, it would be necessary to detect FPs with an appropriate anti-FP antibody. This methodology also provides the opportunity to carry out immunohistochemistry instead of IF.
10. Preparing good cryosections is a bit of an art and requires extensive practice. Furthermore, the nature of the tissue (fat, brain versus muscle) will impact the methods used to generate acceptable sections. Describing these methods is beyond the scope of this protocol, however, there are numerous on-line resources that provide insights into generating high-quality cryosections. For instance, cryosectioning and subsequent staining of adipose tissue is typically challenging, and I would refer the reader to an excellent recent review on this topic [73].
11. Solutions are typically transferred with a P1000 pipette or P200 for more delicate or less adherent specimens. If tissue adherence is not at risk a vacuum can be used for removing waste solutions, however, in both cases subsequent turbulence should be minimized. The pipettors or other tools should never touch the tissue itself, nor should the tissue be left to dry at any time during solution transfers. Also ensure all of the tissue is evenly covered in solution during each incubation. This

can require from 200 μL to over 1 ml/slide. For these purposes, antibody solutions (due to cost and availability) are conserved while wash solutions are used in excess. It is advantageous to limit the amount of liquid on the slide to an area surrounding the tissue including a buffer zone of 2–3 mm outside the tissue to minimize drying and to enhance even staining. As detergent and protein containing solutions have lower surface tension, they may spread more and be more difficult to properly remove.

12. Many tissues such as bone marrow, heart, and lung have significant endogenous AF that can confound analysis. Several methods exist to reduce AF. Radicals in particular, from certain cell types, connective tissues, and fixation methods can cause AF in biological specimens. Glycine and sodium borohydride in solution can be used to attempt to quench these species. Here, a sodium borohydride solution is applied to slides for 1 h to reduce endogenous fluorescence without compromising the intensity of FP fluorescence activity. However, this treatment can be rather aggressive on certain tissues and compromise histology. Thus, it is necessary to test on a small expendable sample before use and/or titrate the concentration and/or exposure/incubation time.
13. As noted above, detection of cell fate can be performed by detection of the expression of other introduced reporters (i.e. Col2.3-GFP). However, in many situations, it is more desirable or efficient to follow cell fate using immunodetection with select antibodies (i.e. aSMA, perilipin, SOX9, etc.). In addition to the described immunodetection of PECAM1 and Laminin, we have used the protocol to detect a number of other proteins. For each new antibody, the conditions for achieving *bona fide* signal over background need to be optimized.
14. The working dilutions of primary antibodies needs to be optimized to maximize signal:noise ratio. This is typically determined empirically using as a guide either published and/or manufacturer's recommendations. This needs to be done for every primary antibody and combinations thereof.
15. Detection of low abundance proteins sometimes benefits from longer primary antibody incubation time (i.e. overnight). In addition, some antibodies for various reasons also perform better with longer incubation times. However, the length of the incubation time has to be balanced with the chance for increased non-specific binding and higher background.
16. In some cases, co-staining with combined secondaries can cause higher background. To minimize this, the dilutions of both secondaries should be determined empirically. In addition, the concentration of the secondary should be optimized

to maximize the signal–noise ratio. For this we typically start with the manufacturer's suggested dilutions or those reported in publications, and bracket this dilution with lower and higher secondary antibody concentrations. There are numerous excellent on-line resources to guide in optimization of primary and secondary antibody dilutions and corresponding incubation buffers. In most instances, 1:500 is sufficient for Alexa-conjugated goat anti-rat/rabbit IgG to generate a robust signal. Under some conditions, these dilutions may need to be optimized. The Alexa 488, 594, and 647 antibody-conjugated fluorophores are used in combination with endogenous FP detection. DAPI is often used for nuclear identification however pacific blue-conjugated secondary antibodies can be used to identify other proteins of interest. Furthermore, if mouse primary antibodies are being used, then additional steps need to be considered to block secondary binding to endogenous mouse antibodies (i.e. Vector Labs, Mouse on Mouse or M.O.M.).

17. Several factors contribute to the deterioration of the fluorescence signal, so for best results the mounted samples should be visualized and imaged as soon as possible. The use of specialized mounting media that can enhance and extend the activity of FPs and other fluorophores is recommended (i.e. Vectashield ProLong Gold antifade, etc.).
18. There are a number of excellent resources that discuss methods for fluorescence detection and imaging, and strategies for maximizing signal-of-interest intensity while minimizing photobleaching [74].
19. While FP reporters are commonly used for lineage tracing studies, there are instances where a LacZ-based reporter can provide an advantage (i.e. tissues with high AF, whole-mount analyses, stable chromogenic read-out, etc.). Some tissues show very limited or no endogenous β-galactosidase activity, however, other tissues such as some glands, bone, and bone marrow have higher intrinsic β-galactosidase activity. Furthermore, senescent cells exhibit higher levels of endogenous β-galactosidase activity. Thus, for all experiments it is important to include a non-LacZ expressing control for comparative purposes.
20. Effective and complete whole-mount LacZ staining of adult tissues or embryos >12 d.p.c. is challenging as there is limited and variable penetration of the reagents into the tissue. Incubation with LacZ permeabilization and staining solution increases tissue staining, but in some instances this is not sufficient. In all cases, we would recommend validating whole-mount staining with section in situ staining to ensure that the

whole-mount staining is adequately identifying all $LacZ^+$ cells. The in situ LacZ staining protocol also typically provides much greater sensitivity than the whole-mount protocol.

21. For monitoring the extent of LacZ staining, we will remove the staining samples from the incubator and carefully check their progress by careful examination under a dissection microscope. This is done under low light illumination. For longer staining, it is sometimes useful to replace the staining solution after 24 h. Try to minimize exposure of the staining solutions to light as this leads to higher background.
22. With whole-mount LacZ staining we typically allow the tissues to stain as long as reasonably possible (compare to non-LacZ containing tissue to ensure increased staining time does not lead to appreciable background). While the staining will appear dark in whole-mount, prepared tissue sections often exhibit relatively weak and difficult to visualize chromogenic material.
23. Combination LacZ and IF provides better results if more intensely stained nuclear and/or cytoplasmic X-gal reacted sections are used.

References

1. Friedenstein AJ, Chailakhjan RK, Lalykina KS (1970) The development of fibroblast colonies in monolayer cultures of guinea-pig bone marrow and spleen cells. Cell Tissue Kinet 3:393–403
2. Friedenstein A, Kuralesova AI (1971) Osteogenic precursor cells of bone marrow in radiation chimeras. Transplantation 12:99–108
3. Friedenstein AJ, Deriglasova UF, Kulagina NN et al (1974) Precursors for fibroblasts in different populations of hematopoietic cells as detected by the in vitro colony assay method. Exp Hematol 2:83–92
4. Caplan AI (1991) Mesenchymal stem cells. J Orthop Res 9:641–650
5. Caplan AI (1994) The mesengenic process. Clin Plast Surg 21:429–435
6. Pittenger MF, Mackay AM, Beck SC et al (1999) Multilineage potential of adult human mesenchymal stem cells. Science 284:143–147
7. Bianco P, Cao X, Frenette PS et al (2013) The meaning, the sense and the significance: translating the science of mesenchymal stem cells into medicine. Nat Med 19:35–42
8. Caplan AI, Correa D (2011) The MSC: an injury drugstore. Cell Stem Cell 9:11–15
9. Sacchetti B, Funari A, Michienzi S et al (2007) Self-renewing osteoprogenitors in bone marrow sinusoids can organize a hematopoietic microenvironment. Cell 131:324–336
10. Mendez-Ferrer S, Michurina TV, Ferraro F et al (2010) Mesenchymal and haematopoietic stem cells form a unique bone marrow niche. Nature 466:829–834
11. Bianco P, Robey PG (2015) Skeletal stem cells. Development 142:1023–1027
12. Caplan AI (2008) All MSCs are pericytes? Cell Stem Cell 3:229–230
13. Joe AW, Yi L, Natarajan A et al (2010) Muscle injury activates resident fibro/adipogenic progenitors that facilitate myogenesis. Nat Cell Biol 12:153–163
14. Uezumi A, Fukada S, Yamamoto N et al (2010) Mesenchymal progenitors distinct from satellite cells contribute to ectopic fat cell formation in skeletal muscle. Nat Cell Biol 12:143–152
15. Crisan M, Yap S, Casteilla L et al (2008) A perivascular origin for mesenchymal stem cells in multiple human organs. Cell Stem Cell 3:301–313
16. Berry R, Jeffery E, Rodeheffer MS (2014) Weighing in on adipocyte precursors. Cell Metab 19:8–20
17. Kfoury Y, Scadden DT (2015) Mesenchymal cell contributions to the stem cell niche. Cell Stem Cell 16:239–253

18. Mendez-Ferrer S, Scadden DT, Sanchez-Aguilera A (2015) Bone marrow stem cells: current and emerging concepts. Ann N Y Acad Sci 1335:32–44
19. Ding L, Saunders TL, Enikolopov G et al (2012) Endothelial and perivascular cells maintain haematopoietic stem cells. Nature 481:457–462
20. Kunisaki Y, Bruns I, Scheiermann C et al (2013) Arteriolar niches maintain haematopoietic stem cell quiescence. Nature 502: 637–643
21. Greenbaum A, Hsu YM, Day RB et al (2013) CXCL12 in early mesenchymal progenitors is required for haematopoietic stem-cell maintenance. Nature 495:227–230
22. Worthley DL, Churchill M, Compton JT et al (2015) Gremlin 1 identifies a skeletal stem cell with bone, cartilage, and reticular stromal potential. Cell 160:269–284
23. Zhou BO, Yue R, Murphy MM et al (2014) Leptin-receptor-expressing mesenchymal stromal cells represent the main source of bone formed by adult bone marrow. Cell Stem Cell 15:154–168
24. Park D, Spencer JA, Koh BI et al (2012) Endogenous bone marrow MSCs are dynamic, fate-restricted participants in bone maintenance and regeneration. Cell Stem Cell 10:259–272
25. Mathew SJ, Hansen JM, Merrell AJ et al (2011) Connective tissue fibroblasts and Tcf4 regulate myogenesis. Development 138:371–384
26. Chong JJ, Chandrakanthan V, Xaymardan M et al (2011) Adult cardiac-resident MSC-like stem cells with a proepicardial origin. Cell Stem Cell 9:527–540
27. Humphreys BD, Lin SL, Kobayashi A et al (2010) Fate tracing reveals the pericyte and not epithelial origin of myofibroblasts in kidney fibrosis. Am J Pathol 176:85–97
28. Mederacke I, Hsu CC, Troeger JS et al (2013) Fate tracing reveals hepatic stellate cells as dominant contributors to liver fibrosis independent of its aetiology. Nat Commun 4:2823
29. Bianco P, Robey PG, Simmons PJ (2008) Mesenchymal stem cells: revisiting history, concepts, and assays. Cell Stem Cell 2:313–319
30. Bianco P (2014) "Mesenchymal" stem cells. Annu Rev Cell Dev Biol 30:677–704
31. Wosczyna MN, Biswas AA, Cogswell CA et al (2012) Multipotent progenitors resident in the skeletal muscle interstitium exhibit robust BMP-dependent osteogenic activity and mediate heterotopic ossification. J Bone Miner Res 27:1004–1017
32. Kretzschmar K, Watt FM (2012) Lineage tracing. Cell 148:33–45
33. Blanpain C, Simons BD (2013) Unravelling stem cell dynamics by lineage tracing. Nat Rev Mol Cell Biol 14:489–502
34. Snippert HJ, van der Flier LG, Sato T et al (2010) Intestinal crypt homeostasis results from neutral competition between symmetrically dividing Lgr5 stem cells. Cell 143:134–144
35. Muzumdar MD, Tasic B, Miyamichi K et al (2007) A global double-fluorescent Cre reporter mouse. Genesis 45:593–605
36. Rinkevich Y, Walmsley GG, Hu MS et al (2015) Skin fibrosis identification and isolation of a dermal lineage with intrinsic fibrogenic potential. Science 348:2151
37. Prigge JR, Wiley JA, Talago EA et al (2013) Nuclear double-fluorescent reporter for in vivo and ex vivo analyses of biological transitions in mouse nuclei. Mamm Genome 2:24022199
38. Madisen L, Zwingman TA, Sunkin SM et al (2010) A robust and high-throughput Cre reporting and characterization system for the whole mouse brain. Nat Neurosci 13:133–140
39. Soriano P (1999) Generalized lacZ expression with the ROSA26 Cre reporter strain. Nat Genet 21:70–71
40. Madisen L, Mao T, Koch H et al (2012) A toolbox of Cre-dependent optogenetic transgenic mice for light-induced activation and silencing. Nat Neurosci 15:793–802
41. Stoller JZ, Degenhardt KR, Huang L et al (2008) Cre reporter mouse expressing a nuclear localized fusion of GFP and beta-galactosidase reveals new derivatives of Pax3-expressing precursors. Genesis 46:200–204
42. Bianco P (2015) Stem cells and bone: a historical perspective. Bone 70:2–9
43. Ono N, Ono W, Mizoguchi T et al (2014) Vasculature-associated cells expressing nestin in developing bones encompass early cells in the osteoblast and endothelial lineage. Dev Cell 29:330–339
44. Tartaglia LA, Dembski M, Weng X et al (1995) Identification and expression cloning of a leptin receptor, OB-R. Cell 83:1263–1271
45. Bonyadi M, Waldman SD, Liu D et al (2003) Mesenchymal progenitor self-renewal deficiency leads to age-dependent osteoporosis in Sca-1/Ly-6A null mice. Proc Natl Acad Sci U S A 100:5840–5845
46. Houlihan DD, Mabuchi Y, Morikawa S et al (2012) Isolation of mouse mesenchymal stem cells on the basis of expression of Sca-1 and PDGFR-alpha. Nat Protoc 7:2103–2111
47. Morikawa S, Mabuchi Y, Kubota Y et al (2009) Prospective identification, isolation, and systemic transplantation of multipotent mesenchymal stem cells in murine bone marrow. J Exp Med 206:2483–2496

48. Hoch RV, Soriano P (2003) Roles of PDGF in animal development. Development 130: 4769–4784
49. Berry R, Rodeheffer MS (2013) Characterization of the adipocyte cellular lineage in vivo. Nat Cell Biol 15:302–308
50. Rock JR, Barkauskas CE, Cronce MJ et al (2011) Multiple stromal populations contribute to pulmonary fibrosis without evidence for epithelial to mesenchymal transition. Proc Natl Acad Sci U S A 108:E1475–E1483
51. Rivers LE, Young KM, Rizzi M et al (2008) PDGFRA/NG2 glia generate myelinating oligodendrocytes and piriform projection neurons in adult mice. Nat Neurosci 11: 1392–1401
52. Lee YH, Petkova AP, Konkar AA et al (2015) Cellular origins of cold-induced brown adipocytes in adult mice. FASEB J 29:286–299
53. Quante M, Tu SP, Tomita H et al (2011) Bone marrow-derived myofibroblasts contribute to the mesenchymal stem cell niche and promote tumor growth. Cancer Cell 19:257–272
54. Church RH, Krishnakumar A, Urbanek A et al (2015) Gremlin1 preferentially binds to bone morphogenetic protein-2 (BMP-2) and BMP-4 over BMP-7. Biochem J 466:55–68
55. Tsuji K, Bandyopadhyay A, Harfe BD et al (2006) BMP2 activity, although dispensable for bone formation, is required for the initiation of fracture healing. Nat Genet 38:1424–1429
56. Kassem M, Bianco P (2015) Skeletal stem cells in space and time. Cell 160:17–19
57. Petrova R, Joyner AL (2014) Roles for Hedgehog signaling in adult organ homeostasis and repair. Development 141:3445–3457
58. Kramann R, Schneider RK, DiRocco DP et al (2015) Perivascular Gli1+ progenitors are key contributors to injury-induced organ fibrosis. Cell Stem Cell 16:51–66
59. Nakagawa N, Duffield JS (2013) Myofibroblasts in fibrotic kidneys. Curr Pathobiol Rep 1:PMC3810972
60. Brownell I, Guevara E, Bai CB et al (2011) Nerve-derived sonic hedgehog defines a niche for hair follicle stem cells capable of becoming epidermal stem cells. Cell Stem Cell 8:552–565
61. Carney RS, Mangin JM, Hayes L et al (2010) Sonic hedgehog expressing and responding cells generate neuronal diversity in the medial amygdala. Neural Dev 5:14
62. Akiyama H, Kim JE, Nakashima K et al (2005) Osteo-chondroprogenitor cells are derived from Sox9 expressing precursors. Proc Natl Acad Sci U S A 102:14665–14670
63. Mizoguchi T, Pinho S, Ahmed J et al (2014) Osterix marks distinct waves of primitive and definitive stromal progenitors during bone marrow development. Dev Cell 29:340–349
64. Logan M, Martin JF, Nagy A et al (2002) Expression of Cre recombinase in the developing mouse limb bud driven by a Prxl enhancer. Genesis 33:77–80
65. Kawanami A, Matsushita T, Chan YY et al (2009) Mice expressing GFP and CreER in osteochondro progenitor cells in the periosteum. Biochem Biophys Res Commun 386:477–482
66. Murao H, Yamamoto K, Matsuda S et al (2013) Periosteal cells are a major source of soft callus in bone fracture. J Bone Miner Metab 31:390–398
67. Ouyang Z, Chen Z, Ishikawa M et al (2013) Prx1 and 3.2kb Col1a1 promoters target distinct bone cell populations in transgenic mice. Bone 58:138–145
68. Krueger KC, Costa MJ, Du H et al (2014) Characterization of Cre recombinase activity for in vivo targeting of adipocyte precursor cells. Stem Cell Rep 3:1147–1158
69. Sanchez-Gurmaches J, Hsiao WY, Guertin DA (2015) Highly selective in vivo labeling of subcutaneous white adipocyte precursors with Prx1-Cre. Stem Cell Rep 4(4):541–550
70. Hayashi S, McMahon AP (2002) Efficient recombination in diverse tissues by a tamoxifen-inducible form of Cre: a tool for temporally regulated gene activation/inactivation in the mouse. Dev Biol 244:305–318
71. Kalajzic Z, Liu P, Kalajzic I et al (2002) Directing the expression of a green fluorescent protein transgene in differentiated osteoblasts: comparison between rat type I collagen and rat osteocalcin promoters. Bone 31:654–660
72. Nakamura E, Nguyen MT, Mackem S (2006) Kinetics of tamoxifen-regulated Cre activity in mice using a cartilage-specific CreER(T) to assay temporal activity windows along the proximodistal limb skeleton. Dev Dyn 235:2603–2612
73. Berry R, Church CD, Gericke MT et al (2014) Imaging of adipose tissue. Methods Enzymol 537:47–73
74. Brown CM (2007) Fluorescence microscopy—avoiding the pitfalls. J Cell Sci 120:1703–1705

Chapter 11

Isolation of Mouse Bone Marrow Mesenchymal Stem Cells

Siddaraju V. Boregowda, Veena Krishnappa, and Donald G. Phinney

Abstract

Mesenchymal stem cells (MSCs) were initially characterized as connective tissue progenitors resident in bone marrow, but have now been isolated from a variety of tissues and organs and shown to also exhibit potent tissue regenerative properties mediated largely via paracrine actions. These findings have spurred the development of MSC-based therapies for treating a diverse array of nonskeletal diseases. Although genetic and experimental rodent models of disease represent important tools for developing efficacious MSC-based therapies, development of reliable methods to isolate MSCs from mouse bone marrow has been hampered by the unique biological properties of these cells. Indeed, few isolation schemes afford high yields and purity while maintaining the genomic integrity of cells. We recently demonstrated that mouse MSCs are highly sensitive to oxidative stress, and long-term expansion of these cells in atmospheric oxygen selects for immortalized clones that lack a functional p53 protein. Herein, we describe a protocol for the isolation of primary MSCs from mouse bone marrow that couples immunodepletion with culture in a low-oxygen environment and affords high purity and yield while preserving p53 function.

Key words Mesenchymal stem cells, Marrow stromal cells, Immunodepletion, Low oxygen, Oxidative stress, p53

1 Introduction

Mesenchymal stem cells (MSCs) were first isolated from bone marrow by Friedenstein and coworkers [1] and characterized based on their ability to differentiate into connective tissue cell lineages [2]. More recently, MSCs have been shown to function as supportive cells within the hematopoietic stem cell niche [3] and secrete paracrine-acting factors that affect angiogenesis, cell survival, inflammation, and immune cell function [4–6]. Increased awareness of the complex biological functions of MSCs has spurred the rapid development of MSC-based therapies for treating various nonskeletal disorders. Despite these advances, most laboratories still enrich MSCs from bone marrow by exploiting their plastic-adherent properties. This approach relies on the fact that contaminating hematopoietic and endothelial cell lineages in bone marrow fail to

Massimiliano Gnecchi (ed.), *Mesenchymal Stem Cells: Methods and Protocols*, Methods in Molecular Biology, vol. 1416,
DOI 10.1007/978-1-4939-3584-0_11,

thrive under conditions that support large-scale MSC expansion [7–9]. However, this approach has proved problematic for isolating MSCs from mouse bone marrow for several reasons. First, studies investigating the hematopoiesis-supporting activity of MSCs demonstrated that hematopoietic progenitors from mouse bone marrow readily adhere to tissue culture plastic, MSCs, or the matrix molecules they secrete [10–12]. Second, plastic-adherent mouse bone marrow cultures support granulopoiesis and B-cell lymphopoiesis in vitro in the absence of added growth factors and cytokines [13, 14], and these adherent cells are as effective as whole bone marrow in reconstituting the hematopoietic system of lethally irradiated mice [15]. Early studies also indicated that the growth and colony-forming unit-fibroblast (CFU-F) activity of mouse MSCs are impaired by atmospheric oxygen [16, 17]. However, due to the need for specialized equipment, cell culture in low oxygen has not been routinely adopted by the larger scientific community. Therefore, selecting for plastic-adherent cells under standard culture conditions is not an effective means to fractionate hematopoietic lineages and MSCs from the bone marrow of mice irrespective of strain.

These limitations have impacted the field of MSC research in several important ways. First, numerous studies have employed cell lines derived from embryonic mesoderm (NIH 3T3, C3H-10T1/2), newborn mouse calvaria (MC3T3), or muscle (C2C12) tissue as a surrogate for marrow-derived MSCs despite obvious differences in the ontogeny and biology of these populations. Second, many laboratories enrich MSCs from marrow by culturing plastic-adherent populations long term over many passages to dilute away contaminating cell lineages. This approach often yields rapidly dividing subpopulations that survive in culture for over 50 passages without evidence of cellular senescence [18–23] and therefore exhibit properties of immortalized cell lines. This outcome is anticipated based on the fact that rodent cells exhibit a high frequency of immortalization as compared to human cells due to differences in checkpoint control mechanisms [24]. Indeed, mouse MSCs have been reported to display high chromosomal instability even following short-term culture [25] and exhibit tumorigenic potential in vivo [26–28]. Therefore, even laboratories that procure their own marrow-derived MSCs may in actuality generate cell lines that are genetically unstable and exhibit different properties than primary cells.

Previously, we developed a protocol based on immunodepletion to fractionate MSCs from mouse bone marrow [29–31]. Recently, we showed that the poor growth of immunodepleted MSCs is due to intracellular oxidative stress induced by exposure to atmospheric oxygen and that oxygen-induced growth inhibition in these cells is p53 dependent [32]. Owing to the fact that the tumor suppressor p53 is mutated in most immortalized rodent cell

lines [33], these results provide a direct link between oxidative stress and cell immortalization. This conclusion is consistent with studies demonstrating that $p53^{-/-}$ MSCs divide incrementally faster than populations isolated by long-term (~80 days) expansion in atmospheric oxygen [34] and that late passage mouse MSCs express high levels of mutant p53 protein [35].

Herein we describe a detailed method to isolate primary MSCs from bone marrow that employs immunodepletion coupled with low-oxygen culture. The approach provides high yields of cells from the bone marrow of only a few mice. The resulting cell populations are devoid of contaminating hematopoietic and endothelial cell lineages, exhibit tri-lineage differentiation potential, and also retain a functional p53 protein. The latter is demonstrated by the fact that cells undergo p53-mediated growth arrest in response to radiation exposure.

2 Materials

2.1 Isolation and Culture of Murine Bone Marrow

1. 10 cc syringes with 22-gauge needles, a 30 cc syringe with an 18-gauge needle, surgical forceps (straight and curved), surgical scissors.
2. Dulbecco's minimum essential medium, alpha modification (α-MEM) with l-glutamine and without ribonucleosides, and ribonucleotides (*see* **Note 1**).
3. Fetal bovine serum (FBS) (*see* **Note 2**).
4. Harvest buffer: Hanks' balanced salt solution (HBSS), 100 U/ml penicillin, 100 μg/ml streptomycin.
5. Cell strainers (70 μm).
6. Tissue culture dishes (100 mm).
7. Complete culture medium: α-MEM, 10 % FBS, 100 U/ml penicillin, 100 μg/ml streptomycin.
8. Modular airtight chamber connected to ProOx model 360 oxygen controller (BioSpherix Ltd., Lacona, NY).
9. Forma Series II Water Jacketed Incubator—Model 3130.

2.2 Harvesting Plastic-Adherent Marrow Cells

1. 0.25 % trypsin-EDTA.
2. Teflon cell scrapers.
3. Serum-free medium: α-MEM, 100 U/ml penicillin, 100 μg/ml streptomycin.
4. Complete culture medium: α-MEM, 10 % FBS, 100 U/ml penicillin, 100 μg/ml streptomycin.
5. Rotator at 4 °C.

2.3 Preparation of Antibody-Conjugated Dynabeads®

1. Dynabeads® M-280 Streptavidin or CELLection™ Biotin Binder Kit (Dynal Biotech).
2. Dynal MPC®-S magnetic particle concentrator (Dynal Biotech).
3. Biotinylated rat anti-mouse antibodies.
   (a) Biotinylated rat anti-mouse CD11b.
   (b) Biotinylated rat anti-mouse CD34.
   (c) Biotinylated rat anti-mouse CD45 antibodies.
4. Antibody diluent: α-MEM, 0.1 % BSA.
5. Complete culture medium: α-MEM, 10 % FBS, 100 U/ml penicillin, 100 μg/ml streptomycin.

2.4 Immuno-depletion

1. Dynal MPC®-S magnetic particle concentrator.
2. Conjugated Dynabeads®.
   (a) Anti-CD11b.
   (b) Anti-CD34.
   (c) Anti-CD45.
3. α-MEM.
4. 0.25 % solution trypan blue.
5. T-75 culture flasks.

2.5 Phenotypic Characterization of Immunodepleted Murine MSCs (IDmMSCs)

1. Wash buffer: HBSS, 1 % BSA, 0.025 % sodium azide.
2. 0.25 % solution trypsin-EDTA.
3. 2 % paraformaldehyde.
4. Methanol (ice-cold).
5. Mouse Fc Block™, anti-mouse CD16/CD32 monoclonal antibody.
6. Fluorescent-conjugated primary and/or secondary antibodies of interest.

2.6 Differentiation

2.6.1 Adipogenic Differentiation

1. Six-well plates or 35 mm tissue culture dishes.
2. Working solution of AdipoRed™ Assay Reagent (Lonza, Walkersville, MD) (*see* **Note 3**).
3. DAPI BioChemica (PanReac AppliChem)—1:500 dilution in PBS.
4. Methanol (ice-cold).
5. Adipogenic induction medium: α-MEM, 10^{-8} M dexamethasone, 20 μM ETYA (5,8,11,14-Eicosatetraynoic acid), 25 μg/ml insulin, 10 % rabbit serum.

2.6.2 Chondrogenic Differentiation

1. ITS-plus premix: 6.25 μg/ml bovine insulin, 6.25 μg/ml transferrin, 6.25 μg/ml selenous acid, 5.33 μg/ml linoleic acid, and 1.25 mg/ml bovine serum albumin.
2. Chondrogenic induction medium: high-glucose DMEM, 10 ng/ml TGF-β3, 100 nM dexamethasone, 50 μg/ml ascorbic acid-2-phosphate, 100 nM sodium pyruvate, 40 μg/ml proline, ITS-plus premix.
3. Hypertrophic medium: high-glucose DMEM, 1 nM dexamethasone, 50 μg/ml ascorbic acid-2-phosphate, 100 nM sodium pyruvate, 40 μg/ml proline, 20 nM β-glycerol phosphate, 50 ng/ml thyroxine, ITS-plus premix.
4. Fixative solution: 20 % formaldehyde, 1× PBS.
5. 1 % toluidine blue solution.
6. 1 % sodium borate solution.
7. 1 % acetic acid solution.
8. 1 % light green solution.
9. 0.1 % Safranin O solution.

2.6.3 Osteogenic Differentiation

1. 2 % solution of Alizarin Red S (*see* **Note 4**).
2. Osteo-inductive medium: high-glucose DMEM, 10 % FBS, 10 mM β-glycerol phosphate, 50 μg/ml ascorbic acid, 10^{-8} M dexamethasone.

2.6.4 Radiation-Induced Growth Arrest

1. Gammacell 40 exactor (Best Theratronics).

3 Methods

3.1 Isolation and Culture of Murine Bone Marrow

1. Typically, bone marrow is harvested from the long bones of 4–6 male mice at 4–6 weeks of age. At this age the long bones are less likely to splinter, and total cellularity is greater as compared to older mice, thereby producing higher cell yields.
2. Mice are euthanized by exposure to carbon dioxide gas. The carcass is then rinsed liberally with 70 % ethanol, an incision is made around the perimeter of the hind limbs where they attach to the trunk, and the skin is removed by pulling toward the foot, which is cut at the ankle bone. This eliminates further contact of the hind limb with the animal's fur, which is a source of contaminating bacteria. The hind limbs are then dissected from the body trunk by cutting along the spinal cord using care not to damage the femur. Limbs are stored on ice in HBSS supplemented with 1× penicillin/streptomycin while awaiting further dissection.
3. Dissection of the hind limbs is done in a sterile cabinet. Each hind limb is bisected by cutting through the knee joint, and

the connective tissue is removed from both the tibia/fibula and the femur. We find it easiest to pull muscle and connective tissue attached at the ankle toward the growth plate, which can then be easily removed by gently prying. Removing muscle and connective tissue from the femur is more tedious, but scraping the diaphysis of the bone clean then pulling the tissue toward each end is effective. Detachment of the growth plate and the ball joint at each end of the bone facilitates this process. After cleaning, the bones are stored in harvest buffer on ice in a 50 ml conical tube (*see* **Note 5**).

4. Extrusion of the bone marrow is performed in a standard biosafety cabinet (BL-2) using proper sterile technique. The ends of the tibia and femur are cut just below the end of the marrow cavity, which is evident by the transition from a red to white coloration in the bone using a pair of sharp scissors. Be careful not to splinter the bones during the cutting process. A 22-gauge needle attached to a 10 cc syringe containing complete medium is then inserted into the spongy bone exposed by removal of the growth plate. The marrow plug is then flushed from the bone with 0.5 ml of complete medium and collected in a 50 ml conical tube on ice (*see* **Note 6**). Marrow plugs are dissociated into a single cell suspension by repeated passage (3×) through an 18-gauge needle attached to a 30 ml syringe. The cell suspension is then filtered through a 70 μm strainer to remove any bone spicules. Cell yield and viability are determined by trypan blue exclusion and counting on a hemocytometer. Typically, we obtain ~5×10^8 bone marrow cells from 4 to 6 mice.
5. Bone marrow cells are diluted in complete medium to a density of 5×10^6 cells/ml, and aliquots (8 ml) are distributed into 100 mm culture dishes at a plating density of 1.45×10^6 cell/cm^2. The plates are cultured undisturbed at 37 °C with 5 % CO_2 and 5 % O_2 in a humidified chamber. After 72 h, the non-adherent cells that accumulate on the surface of the dish are re-suspended by gentle swirling, aspirated, and replaced with 8 ml of complete medium (*see* **Note 7**). All cell manipulations are done using an airtight, oxygen-controlled chamber in 5 % oxygen.
6. After an additional 4 days of culture, the plates are washed with serum-free medium and fed with 8 ml of complete medium. At this stage the cultures typically exhibit one of two characteristics. First, plates may contain distinct colonies of fibroblastic cells that vary in size and composition with small numbers of hematopoietic cells interspersed between the colonies. Cultures with these characteristics typically produce good yields of MSCs (>15 %). Alternatively, plates may contain small colonies of fibroblastic cells that are intermixed within dense patches of cells that take on a "cobblestone" appearance. Cultures with these characteristics typically produce poor yields of MSCs (<5 %).

7. Plates are cultured a total of 8–10 days prior to immunodepletion. Typically, cultures are harvested when distinct fibroblastic colonies greater than 5 mm in diameter are evident on the plates. Plates containing predominantly small colonies or loose aggregates of fibroblastoid cells can be cultured for several additional days to increase yields (*see* **Note 8**).

3.2 Harvesting Plastic-Adherent Marrow Cells

1. Plates are washed with 10 ml of serum-free medium and incubated for approximately 5 min at 37 °C with 4 ml of 0.25 % trypsin/EDTA. Trypsinization is a critical step that determines the yield and overall quality of MSCs after immunodepletion. Rapid but thorough trypsinization is necessary to obtain a single cell suspension after harvest and eliminate the formation of cell aggregates, which dramatically reduces cell yield and viability. Therefore, the use of a freshly thawed trypsin solution is highly recommended. A small amount of FBS (0.5 ml) is then added to inactivate the trypsin. Cells are collected by gentle scraping using a cell scraper (*see* **Note 9**). After scraping, each plate is rinsed once with a small amount of complete medium to remove residual cells. Cells are pooled and stored on ice in a 50 ml conical tube.
2. Cells are collected by centrifugation at $500\times g$ for 15 min at 4 °C and the cell pellet is suspended in 20 ml of α-MEM. It is important to suspend the cell pellet by flicking the bottom of the tube repeatedly using moderate force before adding medium. The pellet contains a large amount of extracellular matrix that will cause the cells to clump together into an insoluble aggregate if medium is directly added to it.
3. Cells are washed 2× as described above, suspended in 20 ml of α-MEM, and then counted on a hemocytometer. Collect the cells a final time by centrifugation.
4. Each depletion reaction can accommodate up to 40×10^6 cells and is performed in a final volume of 1 ml. Therefore, suspend up to 40×10^6 cells in 1 ml of α-MEM. If the yield is greater than 40×10^6 cells, divide the sample into two or more equal aliquots, each suspended in 1 ml of α-MEM. Transfer each aliquot to a 1.5 ml Eppendorf tube and incubate on a rotator for approximately 45 min at 4 °C.
5. Depending upon the number of plates to scrape, harvesting of MSCs can take up to 2 h.

3.3 Preparation of Antibody-Conjugated Dynabeads®

1. We currently use Dynabeads® M-280 Streptavidin superparamagnetic polystyrene beads to perform the immunodepletion (*see* **Note 10**). These are supplied as a suspension containing 6.7×10^8 Dynabeads® per ml (10 mg/ml). One mg of Dynabeads® is saturated by incubating with 5–10 μg of biotinylated antibody assuming 100 % of the antibody is biotinylated. We use five beads

per cell for each immunodepletion and perform three successive rounds using antibodies against CD11b, CD34, and CD45 (*see* **Note 11**).

2. Aliquot the appropriate amount of streptavidin-conjugated Dynabeads® into three separate 1.5 ml Eppendorf tubes labeled CD11b, CD34, and CD45. Place the tubes on the magnetic particle concentrator (MPC) for approximately 1 min. Slowly remove the liquid using a P-200 pipette. Be careful not to aspirate the beads, which may roll down the sides of the tube during removal of the liquid.

Sample Calculation

40×10^6 cells $\times$ 5 Dynabeads®/cell = 200×10^6 Dynabeads®

200×10^6 Dynabeads® $\times$ 1 ml/6.7×10^8 Dynabeads® = 298.5 µl Dynabeads®

3. Wash the Dynabeads® 3× by removing the tubes from the MPC, suspending the beads in 500 µl of PBS, returning the tubes to the MPC, and slowly aspirating the liquid.
4. Dilute each biotinylated antibody (5–10 µg/mg Dynabeads®) to the appropriate concentration in a total volume of 100 µl of antibody diluent. Suspend the Dynabeads® (calculated from above) in the respective antibody solution (calculated from below) and incubate for 30 min at 4 °C with gentle agitation every 5 min.

Sample Calculation

298.5 µl Dynabeads® $\times$ 10 mg/ml = 2.985 mg Dynabeads®

2.985 mg Dynabeads® $\times$ 10 µg antibody/mg = 29.85 µg antibody

29.85 µg antibody $\div$ 0.5 mg/ml = 59.7 µl antibody

5. Place the Eppendorf tubes on the MPC and remove the antibody solution. Wash the beads 7× as described above with 500 µl of antibody diluent. Store the antibody-conjugated Dynabeads® in 500 µl of antibody diluent at 4 °C until ready for use (*see* **Note 12**).
6. Preparation of antibody-conjugated Dynabeads® requires approximately 45 min.

3.4 Immunodepletion

1. Place the Eppendorf tube containing the anti-CD11b-conjugated Dynabeads® on the MPC, remove the buffer by aspiration, and remove the tube from the MPC. Retrieve the suspension of marrow cells from the rotator and then add to the Eppendorf tube containing the anti-CD11b-conjugated Dynabeads®. Thoroughly mix the cells and anti-CD11b-conjugated Dynabeads® using a pipette (P-1000). Incubate the suspension at 4 °C on the rotator for approximately 45 min.
2. Repeat the procedure using the anti-CD34 and then the anti-CD45-conjugated Dynabeads® as follows. Retrieve the

Eppendorf tube containing the anti-CD11b Dynabeads® suspension from the rotator and place in the MPC. Retrieve the anti-CD34-conjugated Dynabeads® from the refrigerator, place on the MPC, and remove the buffer by aspiration. Transfer the cell suspension from the Eppendorf tube containing the anti-CD11b-conjugated Dynabeads® to the Eppendorf tube containing the pellet of anti-CD34-conjugated Dynabeads®. Mix the latter thoroughly and incubate at 4 °C on a rotator for 45 min. Repeat the procedure using the anti-CD45-conjugated Dynabeads®.

3. Transfer the cell suspension to a 50 ml conical tube and dilute to a final volume of 20 ml with α-MEM. Remove an aliquot of cells (10 μl), mix with 15 μl of α-MEM and 25 μl of 0.25 % trypan blue, and count the number of viable cells on a hemocytometer.
4. Collect the remaining cells by centrifugation, suspend in complete medium (remember to disperse the pellet by agitation prior to adding the buffer), and plate 1×10^6 IDmMSCs per T-75 flasks. Culture the cells at 37 °C with 5 % CO_2 and 5 % O_2 in a humidified chamber with medium changes 2–3× weekly (*see* **Note 13**).
5. A typical yield of IDmMSCs from FVB/n mice is typically 15–20 % of the total number of plastic-adherent cells harvested (*see* **Note 14**). Cell viability is always greater than 90 %. Note that yields of plastic-adherent cells, $CD44^+/CD45^-$ cells, and IDmMSCs are significantly greater from populations procured and expanded in 5 % vs. 21 % oxygen (Fig. 1).

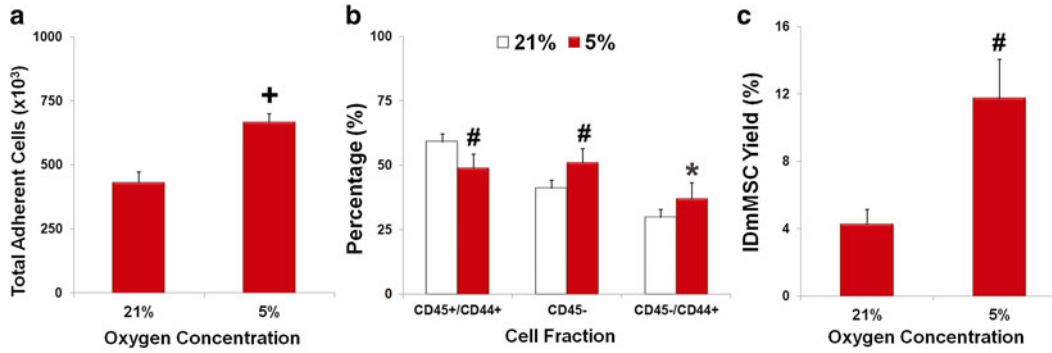

Fig. 1 Expansion of mouse bone marrow in low oxygen enhances yield of IDmMSCs. (**a**) The total yield of plastic-adherent cells from bone marrow cultures expanded in 21 % vs. 5 % oxygen for 7 days was determined by counting. (**b**) Flow cytometric analysis of $CD45^{+ve}/CD44^{+ve}$, $CD45^{-ve}$, and $CD45^{-ve}/CD44^{+ve}$ percentage in bone marrow cultures propagated in 21 % vs. 5 % oxygen. Note that most $CD45^{+ve}$ cells are also $CD44^{+ve}$. (**c**) Total yield of MSCs obtained by immunodepletion from plastic-adherent cultures expanded for 8 days in 21 % vs. 5 % oxygen. Plotted data (mean ± SD) represent results from at least five marrow preparations from each experimental condition. Note that procurement and culture expansion of IDmMSCs in 5 % vs. 21 % resulted in a ~2300-fold increase in cumulative cell yield by the 4th passage. $^*P < 0.05$, $^{\#}P < 0.005$, $^{+}P < 0.001$. Reprinted with modifications from [32]

3.5 Phenotypic Characterization of IDmMSCs

1. The expression profile of surface antigens on IDmMSCs can be evaluated by flow cytometry. Typically, IDmMSCs are cultured for approximately 5 days prior to analysis to ensure good cell viability during the sorting procedure (*see* **Note 15**).
2. IDmMSCs are harvested by incubation in trypsin-EDTA (0.25 %) (*see* **Note 16**). Cells recovered by centrifugation are suspended in wash buffer and counted on a hemocytometer. Cell density is adjusted to 5×10^5 cells/ml, and aliquots (0.5 ml) are transferred to 1.5 ml Eppendorf tubes and incubated for 30 min on a rotator at 4 °C.
3. IDmMSCs are collected by centrifugation at $500 \times g$ for 10 min at 4 °C, and the wash buffer is removed using a pipette (P-1000). The pellet is suspended in 50 μl of wash buffer containing 0.25 μg per 1×10^6 cells of Mouse Fc Block™ (add 0.0625 μg to 50 μl of wash buffer for 2.5×10^5 cells) and incubated on ice for 5 min (*see* **Note 17**).
4. Cells are then incubated with the appropriate dilution of primary antibody prepared in 50 μl of wash buffer, which is added directly to the cell suspension. Removal of the Fc-block is not necessary. Also, multiple antibodies can be added to the cells simultaneously provided that their detection systems are compatible. The cell suspension is incubated for 30 min at 4 °C in the dark with gentle agitation every 10 min.
5. Cells are collected by centrifugation and washed 2× with 500 μl of wash buffer (or 3× if a biotin-conjugated primary antibody is used). After each wash, agitate the cell pellet prior to addition of fresh buffer or antibody solution.
6. If using a fluorescent-conjugated secondary antibody, dilute it in wash buffer (100 μl), add it to the cell pellet, and incubate for 20 min at 4 °C in the dark.
7. Cells are collected by centrifugation and washed 2× as described above. After the final wash, suspend the cell pellet in 0.5–1.0 ml of wash buffer for analysis.
8. If data cannot be acquired immediately after staining, suspend the cell pellet in 250 μl of wash buffer, mix, and then add an equal volume of 2 % paraformaldehyde. Store tubes wrapped in foil at 4 °C overnight and analyze within several days. Remember to use the appropriate isotype controls for each fluorescent-conjugated antibody evaluated.
9. To detect expression of intracellular antigens, cells must be fixed and then permeabilized prior to staining. We typically fix cells in paraformaldehyde (2 %) and permeabilize them by incubation in ice-cold methanol for 15 min. Cells are then washed several times and incubated with Fc-block followed by the appropriate primary and/or secondary antibodies.

10. IDmMSCs lack expression of CD11b, CD31, CD34, CD45, CD90, and CD117, uniformly express CD9, CD29, and CD81, and are also positive for expression of CD44, CD106, and Sca1.

3.6 Differentiation of IDmMSCs into Connective Tissue Lineages In Vitro

1. IDmMSCs are typically cultured for 5–7 days prior to exposure to medium formulations that induce differentiation toward connective tissue cell lineages (*see* **Note 15**). Cells maintained in 5 % vs. 21 % oxygen during the expansion and differentiation phases exhibit more robust adipogenic, osteogenic, and chondrogenic differentiation (Fig. 2).

3.6.1 Adipogenic Differentiation of IDmMSCs

1. IDmMSCs are plated in the appropriate tissue culture vessel (we typically use 6-well plates or 35 mm dishes) at a density that achieves 90 % confluence and cultured in complete culture medium.
2. The following day the medium is replaced with adipogenic induction medium, and the cells are cultured continuously for several weeks with medium changes 2–3× weekly. Accumulation of fat droplets becomes apparent after 4–7 days (*see* **Note 18**).
3. To visualize adipocytes, cultures are washed with PBS, fixed in ice-cold methanol for 2 min and then stained with a working solution of AdipoRed and analyzed within 30 min. Cultures are then rinsed with tap water and counterstained with DAPI (1:500).

3.6.2 Chondrogenic Differentiation of IDmMSCs

1. IDmMSCs are induced to differentiate into chondrocytes by exposing the cells to TGF-β3 in a three-dimensional culture system (micromass) using procedures initially described by Johnstone et al. [36] and MacKay et al. [37].

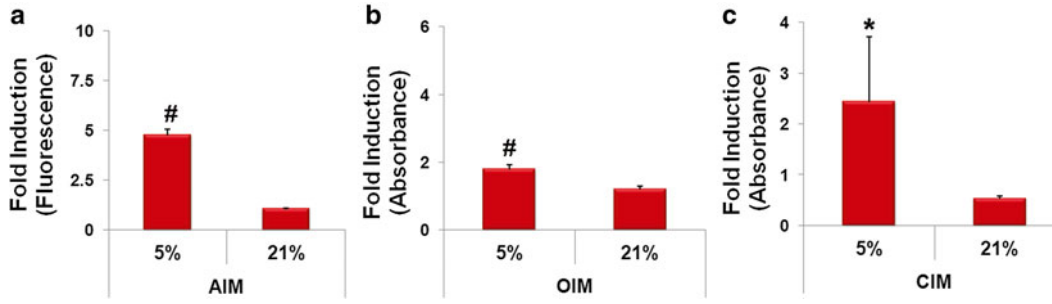

Fig. 2 Effects of oxygen on tri-lineage differentiation of IDmMSCs. (**a**–**c**) IDmMSCs were expanded in 5 % or 21 % oxygen for 5 days and then cultured for an additional 14–21 days in complete culture medium or the appropriate induction medium, and the extent of adipogenic (**a**), osteogenic (**b**), and chondrogenic (**c**) differentiation was quantified as described in the experimental methods. Differentiation data (mean ± SD) were calculated from experiments performed in triplicate. Plotted values represent fold increase of induced vs. control cultures. $^{*}P < 0.05$, $^{\#}P < 0.005$

2. IDmMSCs (500,000 cells/ml) are suspended in an appropriate volume of chondrogenic induction medium, and aliquots (5 ml, 2.5×10^5 cells) are transferred to 15 ml Falcon tubes. The tubes are centrifuged at $500 \times g$ for 10 min at 4 °C to pellet the cells (*see* **Note 19**).
3. The Falcon tubes containing the cell pellets are removed from the centrifuge, wiped thoroughly with 70 % ethanol, placed in a rack in a tissue culture incubator, and incubated at 37 °C in a humidified chamber with 5 % CO_2 for 4 weeks. Be careful to loosely attach the lids to the tubes so that gas exchange can occur. Medium is changed 2–3× weekly. Use every precaution so that the cell pellets are not disturbed during medium changes.
4. After 4 weeks of continuous culture, a significant increase in the size of the micromass pellet should be notable by visual inspection (*see* **Note 20**). Pellets can be harvested for histological analysis at this stage if desired.
5. To induce hypertrophy of the chondrocytes, remove the medium, replace with hypertrophic medium, and culture the pellets for an additional 3–4 weeks.
6. At the end of the culture period, carefully collect the pellets, incubate in fixative solution overnight, and then process in paraffin or glycol methacrylate (GMA) using standard protocols.
7. Histological sections (3–4 μm) are deparaffinized, hydrated, and then stained with 1 % toluidine blue (with or without 1 % sodium borate) for 5 min. Sections are then dehydrated, treated with a hydrophobic clearing agent, and a cover slip is applied. Toluidine blue stains proteoglycans a metachromatic red-purple color and nuclei blue. Inclusion of sodium borate intensifies the blue color.
8. Alternatively, deparaffinized sections can be stained with hematoxylin for 7 min, washed in running tap water for 10 min, stained with 1 % light green for 4–5 min, slowly dipped in 1 % acetic acid four times, and stained with 0.1 % Safranin O for 8 min. Sections are then dehydrated and treated with a hydrophobic clearing agent and a cover slip is applied. Safranin O stains proteoglycans a yellow-red color and nuclei red (*see* **Note 21**).
9. Microscopic evaluation of the pellets should reveal oat-shaped chondrocytes within lacunae interspersed by a significant amount of extracellular matrix. Pellets can also be stained with an antibody specific for type II collagen, which is expressed exclusively in cartilage.

3.6.3 Osteogenic Differentiation of IDmMSCs

1. IDmMSCs are plated in the appropriate tissue culture vessel (we typically use 6-well plates or 60 mm dishes) at a density that achieves approximately 60 % confluence and cultured in complete culture medium.

2. In the following day, complete culture medium is replaced with osteo-inductive medium, and the cells are cultured continuously for up to 3 weeks with medium changes 2–3× weekly (*see* **Note 22**).
3. To evaluate the extent of mineralization, cell monolayers are washed with PBS, fixed for 10 min in 10 % formaldehyde at room temperature, and washed with distilled water. The cell monolayer is then stained 5 min with a 2 % solution of Alizarin Red S and washed with water.
4. The extent of osteogenic differentiation can be determined by quantifying the amount of Alizarin Red S dye [38] or the amount of calcium [29] bound to the extracellular matrix as previously described.

3.7 Radiation-Induced Growth Arrest Assay

1. IDmMSCs obtained from congenic and p53 null C57BL/6 mice are plated in T-25 flasks at a density of 2000 cells/cm^2 and cultured in 5 % or 21 % oxygen for 3 days.
2. To induce p53, flasks are irradiated at the dose of 4Gy using a Gammacell 40 exactor.
3. Cells are fed with fresh medium and cultured an additional 4 days.
4. Cell monolayers are photographed, and then the viability, growth kinetics, and cell cycle status of cells are evaluated as described previously [32].
5. Irradiation impairs the growth and survival of congenic IDmMSCs cultured in hypoxia but not p53 null MSCs (Fig. 3).

4 Notes

1. α-MEM medium containing ribonucleosides and ribonucleotides is toxic to IDmMSCs although the reason for this remains unclear. We once mistakenly used this medium formulation, and after approximately 1 week in culture, essentially all IDmMSCs were no longer viable.
2. FBS is lot selected to optimize cell growth and limit the extent of cellular differentiation. MSCs are cultured for 2 weeks in medium supplemented with 10 % FBS from sample lots obtained from the appropriate vendor. The extent of cell proliferation is measured every few days to generate a growth curve. Levels of alkaline phosphatase (ALP), a marker of osteoblast differentiation, are also measured using a commercial kit. Lots that stimulate strong cell growth but fail to induce significant ALP activity are selected for further use.

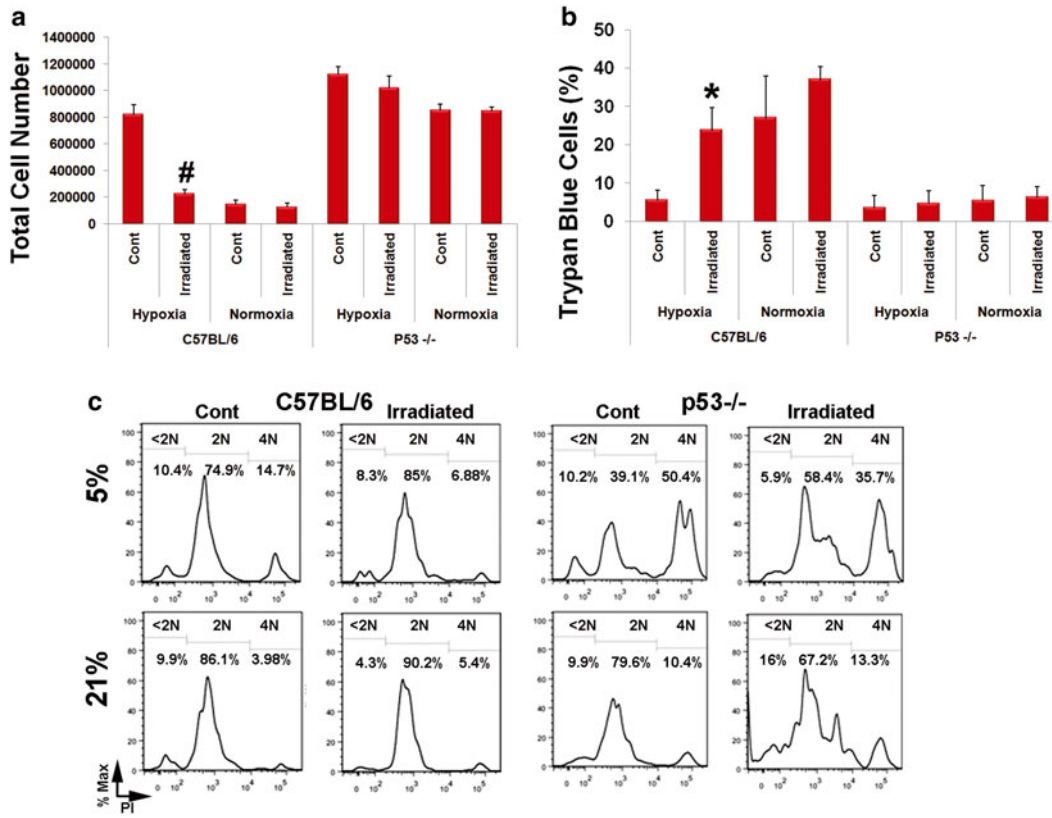

Fig. 3 Radiation-induced growth arrest of wild-type and p53$^{-/-}$ IDmMSCs. (**a, b**) Equal numbers of IDmMSCs (P1) procured from C57BL/6 and B6.129S2-Trp53<tm1Tyj mice and expanded initially in 5 % oxygen were plated at 2000 cells/cm^2, incubated in 5 % or 21 % oxygen for 3 additional days, and then briefly irradiated (4Gy). Cells were cultured expanded for an additional 4 days post-irradiation during which time cell growth (**a**) and viability (**b**) were determined by counting and trypan blue exclusion, respectively. (**c**) Irradiated IDmMSCs were stained with PI and their DNA content was determined by flow cytometric analysis. *$P < 0.05$, #$P < 0.005$. Reprinted with modifications from [32]

3. A working solution of AdipoRed is prepared by dissolving 280 μl of dye in 10 ml of PBS. The solution is used immediately.
4. A working solution (2 %) of Alizarin Red S is prepared by dissolving the dye in distilled water and adjusting the pH to 4.1 with ammonium hydroxide. The solution is then passed through a 0.22 μm filter to remove particulates.
5. Surgical instruments used to dissect the hind limbs are typically replaced with clean, sterile instruments after every 5–10 mice. We generally use a dry bead sterilizer to sterilize instruments between animals.
6. A method was published that employs high-speed centrifugation to harvest marrow from the long bones of mice [39]. We do not recommend this procedure because it strips off the

periosteal layer of the bone, thereby contaminating the cultures with periosteal cells, which due to their rapid growth and reduced oxygen sensitivity, outgrow the IDmMSCs.

7. Do not vigorously wash the culture plates at this time. Removal of the majority of hematopoietic cells at this stage will severely curtail the growth of the fibroblastoid cells thereby dramatically reducing the overall yield of IDmMSCs.
8. It is important to familiarize oneself with the morphology of the plastic-adherent cultures at different stages of expansion. For example, initially after plating, the vast majority of cells in the culture are non-adherent, and only a small number of stellate-shaped cells are seen attached to the culture dish. After the first medium change, many more adherent cells are visible. These cells adopt a spindle-shaped morphology and begin to migrate together to form clusters. After 5–6 days, cells within clusters begin to proliferate rapidly forming large fibroblastoid colonies. Some colonies are comprised of a morphologically homogeneous population of fibroblastoid cells, whereas others appear heterogeneous and may contain a large number of hematopoietic cell types. Finally, the total culture time of the plastic-adherent populations is limited because fibroblastoid cells within the interior of expanding colonies begin to differentiate along the osteoblastic lineage.
9. Based on our experience, one of the most challenging aspects of this procedure for the novice is harvesting adherent cells from dishes prior to immunodepletion. Unfortunately, exposure of cells to trypsin alone is not sufficient to detach the cells from the dishes (we have explored many chemical/biological alternatives without success). Therefore, a physical method such as scraping must also be employed. Unfortunately, the binding avidity and flattened morphology of the cells make them susceptible to physical injury and death if too much force is applied during the scraping procedure. Consequently, most procedural failures can be traced back to low cell yields during this harvest step. Typically, cells are lost due to physical destruction via overaggressive scraping. The use of a freshly thawed bottle of trypsin can circumvent this problem. We do not recommend trypsin stored in the refrigerator or trypsin that was frozen and thawed earlier. Alternatively, ineffective scraping may leave the majority of cells attached to the plates, which are then discarded. Therefore, it is essential to monitor the harvest procedure closely by visual inspection of the plates. Finally, the scraping procedure can be quite time consuming. Therefore, it is also imperative to ensure that the pH of the culture medium does not become excessively alkaline during this process, which may reduce cell viability. Consequently, only a few plates should be harvested at one time until some level of proficiency is

obtained. We recommend that harvesting of cells should be performed in a closed chamber in low oxygen (2–5 %).

10. Alternatively, if one desires to recover the immunodepleted cell populations for further analysis, the immunodepletion can be performed using the CELLection™ Biotin Binder Kit (Dynal Biotech). With this kit, biotinylated antibodies are attached to CELLection™ Dynabeads® via a DNA linker, which provides a cleavable site to remove the beads from the cells.
11. Often people inquire whether we have used automated systems to purify MSCs directly from bone marrow, e.g., MACS (Miltenyi Biotec). We feel this method is ineffective for the following reason: according to the literature, the frequency of MSCs in bone marrow ranges from 1 cell in 10^5 to 10^6 marrow cells. Since we typically obtain approximately 5×10^8 marrow cells from 4 to 6 donor animals, separation at this stage would yield 10^3–10^4 MSCs. This anticipated low yield is the main reason why plastic-adherent populations are expanded ex vivo as a first step toward enrichment of MSCs.
12. Antibody-conjugated Dynabeads® can be prepared 1 day prior to use and stored overnight at 4 °C.
13. A distinguishing characteristic of IDmMSCs is their slow growth in atmospheric oxygen. Populations undergo only one or two population doublings following the first week of culture after immunodepletion. Culture expansion and immunodepletion in 5 % oxygen increase growth and survival [32, 40].
14. The yield of IDmMSCs varies significantly between different inbred strains of mice [41]. These differences, in part, parallel differences in bone mineral density between strains. We prefer to use the FVB/n as marrow donors due to their high yield of IDmMSCs.
15. Based on our experience, freshly isolated IDmMSCs exhibit poor viability when subjected to sheer forces during analysis by flow cytometry or fluorescent-activated cell sorting (FACS). Consequently, we typically culture IDmMSCs for 4–5 days post immunodepletion prior to analyzing their cell surface phenotype by flow cytometry. Reduced viability is likely due to the repeated and prolonged manipulation of cells during the immunodepletion process. Similarly, we typically culture IDmMSCs for 3–5 days in complete culture medium prior to analysis of their differentiation potential, even though their differentiation capacity is not significantly altered by the immunodepletion process.
16. IDmMSCs are harvested by washing the cell monolayer with serum-free α-MEM, incubating with trypsin-EDTA (0.25 %) for 3–5 min at room temperature, and collecting the cells by washing repeatedly with medium. Physical scraping is not required to harvest IDmMSCs.

17. When staining IDmMSCs (or any mouse cells) with antibodies generated in mice, it is essential to block low-affinity Fc-mediated binding of antibodies to the mouse Fc receptor. This is done by incubating cells for several minutes with the Mouse Fc Block™ (anti-mouse CD16/CD32 monoclonal antibody). This assures that any observed staining is due to the interaction of the antigen-binding portion of the antibody with an antigen on the cell surface.
18. Another distinguishing feature of IDmMSCs culture expanded in atmospheric oxygen is their limited capacity for adipogenic differentiation. Therefore, although adipocytes become visible after 4–7 days post-induction, only a small fraction of the total cell population (<20 %) will differentiate into adipocytes using the methods we describe. This contrasts with IDmMSCs cultured in 5 % oxygen, which typically show enhanced adipogenic differentiation (Fig. 2).
19. Suspending IDmMSCs in chondrogenic induction medium prior to centrifugation eliminates the need to change the medium immediately after formation of the micromass pellet. After several days in culture, the pellets are less fragile, thereby facilitating subsequent medium changes.
20. The micromass pellet increases in size due to the secretion by chondrocytes of a large amount of proteoglycans into the extracellular space. Furthermore, these proteoglycans are hydrophilic and therefore have a high water content (recall that cartilage is mostly water, which enhances its shock absorbing capacity). Lack of detectable changes in pellet size may indicate a failure of cells to differentiate.
21. Safranin O is typically preferred over toluidine blue for staining cartilage due to its linear saturation response with increasing proteoglycan content. Accordingly, it provides a more accurate measure of the extent of chondrocyte differentiation.
22. The optimal plating density of IDmMSCs for osteogenic differentiation should be determined empirically. Plating density must be high enough to promote osteogenic commitment but also allow for expansion of the osteoprogenitor cells during the differentiation time course. If cells are plated at too high a density, the cell monolayer may become so dense that it detaches from the culture dish and rolls up into an insoluble aggregate.

Acknowledgments

The authors would like to thank previous members of the Phinney lab for assistance with development of this protocol including

Dr. Gene C. Kopen, Maria Dutreil, and Melody Baddoo. This work is supported by a grant to DGP (1 R24-OD018254-01) from the Director's Office at NIH, which provides funds to distribute IDmMSCs prepared from strains of interest to researchers worldwide. Contact dphinney@scripps.edu for more information.

References

1. Friedenstein AJ, Petrakova KV, Kurolesova AI et al (1968) Heterotopic of bone marrow. Analysis of precursor cells for osteogenic and hematopoietic tissues. Transplantation 6:230–247
2. Prockop DJ (1997) Marrow stromal cells as stem cells for nonhematopoietic tissues. Science 276:71–74
3. Mendez-Ferrer S, Michurina TV, Ferraro F et al (2010) Mesenchymal and haematopoietic stem cells form a unique bone marrow niche. Nature 466:829–834
4. Phinney DG (2007) Biochemical heterogeneity of mesenchymal stem cell populations: clues to their therapeutic efficacy. Cell Cycle 6:2884–2889
5. Caplan AI, Correa D (2011) The MSC: an injury drugstore. Cell Stem Cell 9:11–15
6. Boregowda SV, Phinney DG (2013) MSCs: Paracrine Effects. In: Keating A, Hematti P (eds) Mesenchymal stromal cells: biology and clinical applications. Humana Press, Totowa, NJ, pp 145–168
7. Sotiropoulou PA, Perez SA, Salagianni M et al (2006) Characterization of the optimal culture conditions for clinical scale production of human mesenchymal stem cells. Stem Cells 24:462–471
8. Digirolamo CM, Stokes D, Colter D et al (1999) Propagation and senescence of human marrow stromal cells in culture: a simple colony-forming assay identifies samples with the greatest potential to propagate and differentiate. Br J Haematol 107:275–281
9. Thirumala S, Goebel WS, Woods EJ (2013) Manufacturing and banking of mesenchymal stem cells. Expert Opin Biol Ther 13:673–691
10. Bearpark AD, Gordon MY (1989) Adhesive properties distinguish sub-populations of haemopoietic stem cells with different spleen colony-forming and marrow repopulating capacities. Bone Marrow Transplant 4:625–628
11. Kerk DK, Henry EA, Eaves AC et al (1985) Two classes of primitive pluripotent hemopoietic progenitor cells: separation by adherence. J Cell Physiol 125:127–134
12. Simmons PJ, Zannettino A, Gronthos S et al (1994) Potential adhesion mechanisms for localisation of haemopoietic progenitors to bone marrow stroma. Leuk Lymphoma 12:353–363
13. Witte PL, Robinson M, Henley A et al (1987) Relationships between B-lineage lymphocytes and stromal cells in long-term bone marrow cultures. Eur J Immunol 17:1473–1484
14. Deryugina EI, Muller-Sieburg CE (1993) Stromal cells in long-term cultures: keys to the elucidation of hematopoietic development? Crit Rev Immunol 13:115–150
15. Gordon MY, Bearpark AD, Clarke D et al (1990) Haemopoietic stem cell subpopulations in mouse and man: discrimination by differential adherence and marrow repopulating ability. Bone Marrow Transplant 5(Suppl 1):6–8
16. Gupta V, Rajaraman S, Costanzi JJ (1987) Effect of oxygen on the clonal growth of adherent cells (CFU-F) from different compartments of mouse bone marrow. Exp Hematol 15:1153–1157
17. Ren H, Cao Y, Zhao Q et al (2006) Proliferation and differentiation of bone marrow stromal cells under hypoxic conditions. Biochem Biophys Res Commun 347:12–21
18. Sun S, Guo Z, Xiao X et al (2003) Isolation of mouse marrow mesenchymal progenitors by a novel and reliable method. Stem Cells 21:527–535
19. Meirelles Lda S, Nardi NB (2003) Murine marrow-derived mesenchymal stem cell: isolation, in vitro expansion, and characterization. Br J Haematol 123:702–711
20. Peister A, Mellad JA, Larson BL et al (2004) Adult stem cells from bone marrow (MSCs) isolated from different strains of inbred mice vary in surface epitopes, rates of proliferation, and differentiation potential. Blood 103:1662–1668
21. Tropel P, Noel D, Platet N et al (2004) Isolation and characterisation of mesenchymal stem cells from adult mouse bone marrow. Exp Cell Res 295:395–406
22. Li Y, Zhang C, Xiong F et al (2008) Comparative study of mesenchymal stem cells

from C57BL/10 and mdx mice. BMC Cell Biol 9:24

23. Wu X, Chen S, Orlando SA et al (2011) p85alpha regulates osteoblast differentiation by cross-talking with the MAPK pathway. J Biol Chem 286:13512–13521
24. Prowse KR, Greider CW (1995) Developmental and tissue-specific regulation of mouse telomerase and telomere length. Proc Natl Acad Sci U S A 92:4818–4822
25. Josse C, Schoemans R, Niessen NA et al (2010) Systematic chromosomal aberrations found in murine bone marrow-derived mesenchymal stem cells. Stem Cells Dev 19:1167–1173
26. Tolar J, Nauta AJ, Osborn MJ et al (2007) Sarcoma derived from cultured mesenchymal stem cells. Stem Cells 25:371–379
27. Jeong JO, Han JW, Kim JM et al (2011) Malignant tumor formation after transplantation of short-term cultured bone marrow mesenchymal stem cells in experimental myocardial infarction and diabetic neuropathy. Circ Res 108:1340–1347
28. Miura M, Miura Y, Padilla-Nash HM et al (2006) Accumulated chromosomal instability in murine bone marrow mesenchymal stem cells leads to malignant transformation. Stem Cells 24:1095–1103
29. Baddoo M, Hill K, Wilkinson R et al (2003) Characterization of mesenchymal stem cells isolated from murine bone marrow by negative selection. J Cell Biochem 89:1235–1249
30. Kopen GC, Prockop DJ, Phinney DG (1999) Marrow stromal cells migrate throughout forebrain and cerebellum, and they differentiate into astrocytes after injection into neonatal mouse brains. Proc Natl Acad Sci U S A 96:10711–10716
31. Phinney DG (2008) Isolation of mesenchymal stem cells from murine bone marrow by immunodepletion. Methods Mol Biol 449:171–186
32. Boregowda SV, Krishnappa V, Chambers JW et al (2012) Atmospheric oxygen inhibits growth and differentiation of marrow-derived mouse mesenchymal stem cells via a p53-dependent mechanism: implications for long-term culture expansion. Stem Cells 30:975–987
33. Harvey DM, Levine AJ (1991) p53 alteration is a common event in the spontaneous immortalization of primary BALB/c murine embryo fibroblasts. Genes Dev 5:2375–2385
34. Armesilla-Diaz A, Elvira G, Silva A (2009) p53 regulates the proliferation, differentiation and spontaneous transformation of mesenchymal stem cells. Exp Cell Res 315:3598–3610
35. Li H, Fan X, Kovi RC et al (2007) Spontaneous expression of embryonic factors and p53 point mutations in aged mesenchymal stem cells: a model of age-related tumorigenesis in mice. Cancer Res 67:10889–10898
36. Johnstone B, Hering TM, Caplan AI et al (1998) In vitro chondrogenesis of bone marrow-derived mesenchymal progenitor cells. Exp Cell Res 238:265–272
37. Mackay AM, Beck SC, Murphy JM et al (1998) Chondrogenic differentiation of cultured human mesenchymal stem cells from marrow. Tissue Eng 4:415–428
38. Gregory CA, Gunn WG, Peister A et al (2004) An Alizarin red-based assay of mineralization by adherent cells in culture: comparison with cetylpyridinium chloride extraction. Anal Biochem 329:77–84
39. Dobson KR, Reading L, Haberey M et al (1999) Centrifugal isolation of bone marrow from bone: an improved method for the recovery and quantitation of bone marrow osteoprogenitor cells from rat tibiae and femurae. Calcif Tissue Int 65:411–413
40. Krishnappa V, Boregowda SV, Phinney DG (2013) The peculiar biology of mouse mesenchymal stromal cells – oxygen is the key. Cytotherapy 15:536–541
41. Phinney DG, Kopen G, Isaacson RL et al (1999) Plastic adherent stromal cells from the bone marrow of commonly used strains of inbred mice: variations in yield, growth, and differentiation. J Cell Biochem 72:570–585

Chapter 12

Isolation of Pig Bone Marrow-Derived Mesenchymal Stem Cells

Dries A.M. Feyen, Frederieke van den Akker, Willy Noort, Steven A.J. Chamuleau, Pieter A. Doevendans, and Joost P.G. Sluijter

Abstract

Large animal models are an important preclinical tool for the evaluation of new interventions and their translation into clinical practice. The pig is a widely used animal model in multiple clinical fields, such as cardiology and orthopedics, and has been at the forefront of testing new therapeutics, including cell-based therapies. In the clinic, mesenchymal stem cells (MSCs) are used autologously, therefore isolated, and administrated into the same patient. For successful clinical translation of autologous approaches, the porcine model needs to test MSC in a similar manner. Since a limited number of MSCs can be isolated directly from the bone marrow, culturing techniques are needed to expand the population in vitro prior to therapeutic application. Here, we describe a protocol specifically tailored for the isolation and propagation of porcine-derived bone marrow MSCs.

Key words MSC, Bone marrow, Porcine, Isolation, Expansion, Cell culture

1 Introduction

Mesenchymal stem cells (MSCs) are one of the most attractive translational stem cell types, because of their ease of collection and expansion from individual patients. They are defined by their plastic adherent properties and expression of specific cell surface makers, such as CD105, CD90, and CD73. Furthermore, they exhibit multipotency by differentiating into osteoblasts, adipocytes, and chondrocytes [1]. An additional feature of these cells includes a robust paracrine profile that can promote cell growth and survival [2, 3] and immunomodulatory properties by which they can influence the activation and proliferation of a variety of immune cells [4].

MSC has garnered much attention as candidates to repair and regenerate damaged tissue. In the heart, cell-based therapies have utilized MSCs to promote cardiomyocyte protection, increase angiogenesis, and reduce fibrosis after myocardial infarction

Massimiliano Gnecchi (ed.), *Mesenchymal Stem Cells: Methods and Protocols*, Methods in Molecular Biology, vol. 1416,
DOI 10.1007/978-1-4939-3584-0_12,

leading to better functional recovery after injury [1, 5]. Delivery of MSC with scaffolds has improved cartilage [6] and bone repair [7] strategies, most likely through the combined paracrine activity and differentiation ability of the cells. Furthermore, MSC have also been extensively studied for their ability to prevent and treat graft-versus-host disease [8] and reduce the risk of graft rejection [9] through their immunosuppressive capabilities.

Although very promising results have been achieved with MSC in rodent preclinical models, the therapeutic benefits of stem cell-based therapy must be carefully investigated in a clinically relevant large animal model, such as the pig. For example, the porcine heart shares similarities with the human heart in terms of size, structure, and function [10]. Therefore, pigs are great models for studying cardiac injury and testing new interventions to treat the damaged heart, such as MSC-based therapies [11, 12]. Furthermore, the resemblance of the porcine coronary system to that of humans [13] makes this animal model ideal for testing novel cell delivery catheters and imaging modalities necessary for the implementation of cell-based therapies in the clinic. In addition, the articular cartilage in pigs is similar in thickness to its human counterpart [14] and is therefore preferred in the evaluation of novel MSC-engineered cartilage in orthopedic research. Since in clinical practice, MSC will be derived from an autologous source, for successful translation, a similar approach needs to be undertaken in preclinical porcine models.

This chapter describes the isolation of MSC from pig bone marrow, for which we have set up a simple and robust protocol. Although the major steps in the procedure are similar to that of human MSC isolation, we have adapted and refined it to ensure the derivation of porcine MSCs with similar in vitro and in vivo functions compared to human counterpart MSC [15].

2 Materials

2.1 List of Reagents and Materials

- Ficoll-Paque Plus.
- Plastic blood collection tubes with lithium heparin.
- Phosphate-buffered saline (PBS), pH 7.4.
- MEM alpha cell culture media, fetal bovine serum (FBS), penicillin-streptomycin, and 0.25 % trypsin/EDTA.
- Gelatin A from porcine skin.
- Ascorbic acid (vitamin C).
- Basic fibroblast growth factor (bFGF).
- DMSO.
- 50 ml sterile conical centrifuge tubes.

- Six-well tissue culture dishes and T75 tissue flasks.
- Sterile cell culture plastic pipettes of 2, 5, 10, and 25 ml and pipette aid.
- Controlled rate cell-freezing container.
- Bench top centrifuge with brake ON/OFF option.
- Inverted phase microscope.
- Automated cell counter.

2.2 Preparation of Materials

1. Gelatin coating: for 1 % gelatin stock, dissolve 5 g of gelatin in 500 ml of Milli-Q and autoclave to sterilize. Add 55 ml of the 1 % sterilized gelatin stock to 500 ml DPBS to make 0.1 % gelatin coating.
2. MSC basic medium: 500 ml MEM alpha, 55 ml FBS (10 %), 5.5 ml p/s (1 %).
3. MSC culture medium: 500 ml MEM alpha, 55 ml FBS (10 %), 5.5 ml p/s (1 %), bFGF (1 ng/ml) vitamin C (0.2 ng/ml) (*see* **Note 1**).
4. bFGF stock (25 μg/ml): dissolve bFGF powder in 1 ml of MSC basic medium and make aliquots. Keep stock at −80 °C. Do not refreeze, but store at 4 °C after thawing.
5. Vitamin C stock (5 mg/ml): dissolve 0.1 g vitamin C in 20 ml Milli-Q. Sterilize by filtering with 0.2 μm filter. Keep stock at −20 °C. Vitamin C will breakdown under the influence of light.
6. Freezing medium: MSC basic medium + 20 % DMSO.

3 Methods

3.1 Bone Marrow Collection

1. The bone marrow can be collected from the iliac crest or sternum of the pig.
2. Using a sharp, strong needle and a 50 cc syringe, aspirate 10–25 ml of bone marrow (BM) (*see* **Notes 2** and **3**).
3. BM needs to be collected in tubes containing an anticoagulant, such as lithium heparin (*see* **Notes 4** and **5**).

3.2 Isolation of Porcine Mononuclear Cells (pMNCs)

1. Gently resuspend obtained BM.
2. Perform a cell count on the whole BM by transferring 50–100 μl into an Eppendorf tube, and count cells using an automated cell counter, preferably one that can differentiate between nucleated and nonnucleated cell types (*see* **Note 6**).
3. Divide whole BM into 50 ml tubes, preferably 10 ml in each tube (*see* **Note 7**).
4. Dilute the 10 ml whole BM with PBS to 30 ml and mix well making sure no cells stick to the tube (*see* **Note 8**).

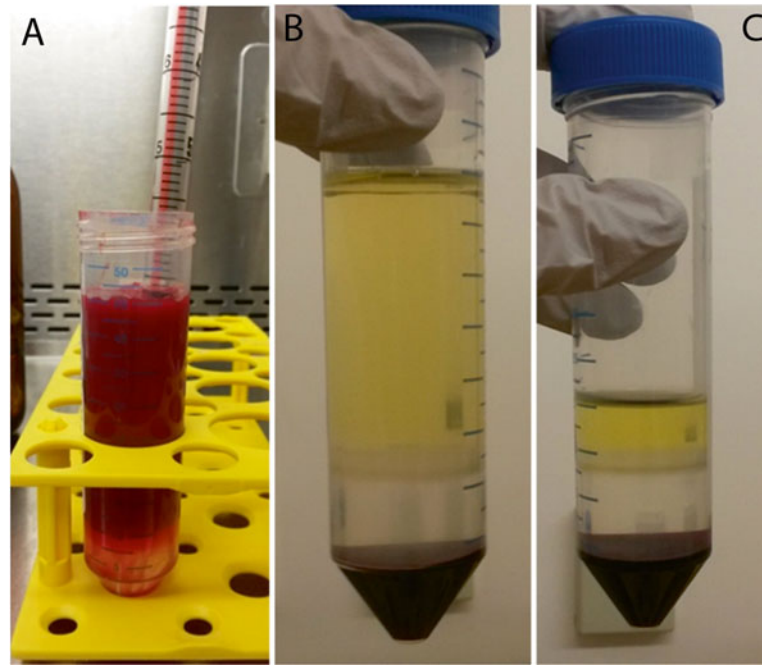

Fig. 1 Ficoll separation of aspirated bone marrow. Two separate layers are visible (**a**); a clear Ficoll layer at the bottom and red fluid at the top. After centrifugation, three distinct layers are formed (**b**) with the white ring containing the MSCs. Before collecting the mononuclear fraction, remove most of the plasma layer (**c**)

5. Add 10 ml Ficoll-Paque Plus slowly to the bottom of the 50 ml tube (*see* **Note 9** and Fig. 1a).
6. Centrifuge the tubes at 20 °C for 30 min at 400 × *g* with slow acceleration (one third of full speed) and no brake. Three distinct layers are formed (*see* Fig. 1b). The MSCs are located in the floating white ring.
7. Remove the upper layer (plasma) as far as possible, until ~1 cm above the white ring (Fig. 1c).
8. Using a 5 ml pipette, collect the majority of the MNC fraction from the middle layer. Do this slowly, and move your pipette horizontally through the ring to improve your yield. Try not to aspirate too much Ficoll as this will harm the cells (*see* **Note 10**).
9. Using a 1 ml pipette, collect the last traces of the white ring.
10. Transfer the MNC fraction from the 50 ml tube into a new 50 ml tube containing 25 ml PBS, mix gently but well.
11. Centrifuge at RT, 7 min at 350 × *g* and remove the supernatant.
12. Resuspend the cell pellets and pool together in 1 ml of PBS if multiple tubes are used.
13. Perform cell count as before (*see* **Note 11**).

3.3 Seeding and Culturing Porcine Mesenchymal Stem Cells (pMSCs)

1. Coat 6-well plates with 0.1 % gelatin and leave in the incubator (37 °C) for 10–15 min before use.
2. Before use, remove the gelatin.
3. Seed 5×10^6 cells per well in 2 ml of MSC basic medium and place in the incubator (37 °C).
4. Refresh the medium once every 3 days. Use MSC growth medium after day three for the remainder of the cell culture to expand the cell population (*see* **Note 12**).
5. After 7–10 days, colonies of MSCs will be visible (Fig. 2a) (*see* **Note 13**).
6. After the cells reach a 50–60 % confluence, collect cells from 2 wells and replate them into a T75 flask.
7. To do so, wash the cells with PBS and add 160 μl of trypsin per well. Leave in the incubator for several minutes (*see* **Note 14**).
8. Once cells have detached, neutralize with 840 μl of ML growth medium.
9. Collect cell suspensions into a 50 ml tube by using a 1 ml pipette.
10. Add 7 ml ML complete medium and replate into a 0.1 % gelatin coated T75 flask.
11. Place in the incubator; these cells are referred to as passage 1.
12. Continue culturing by splitting cells (usually these cells prefer a 1:3 surface ratio). For a T75 flask, use 1 ml of trypsin and neutralize with 7 ml of ML complete medium (*see* **Note 15** and Fig. 2b).
13. Apart from culturing, freeze cells from earlier passages to create a stock of cells.

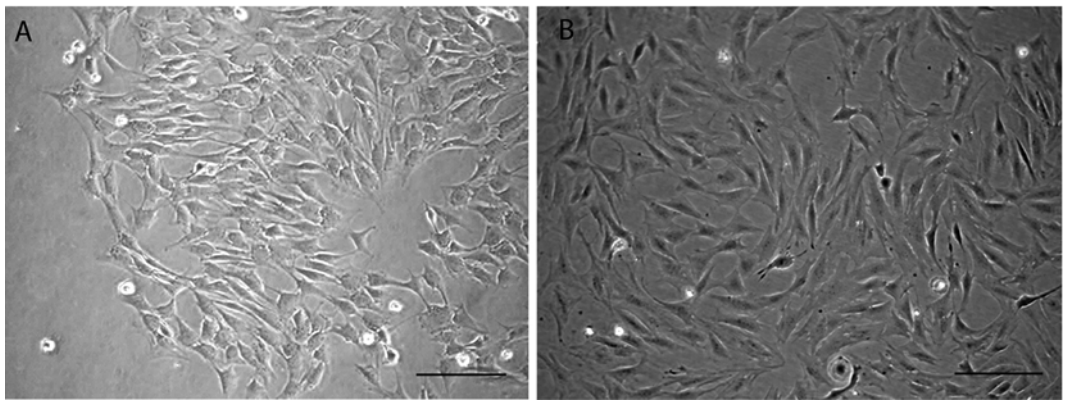

Fig. 2 Representative microscopic images of porcine MSC. MSC colony formation (a) as observed 7 days after isolation and plating. At later passages, such as passage 5 (b), porcine MSCs tend to be less elongated and spindled shape than human MSCs. At this confluence (b) MSCs are ready to be passaged. Scale bar, 50 μm

14. Since this MSC isolation protocol can yield heterogeneous cell populations, characterize the isolated cells at this stage for:
    (a) Cell surface markers.
    (b) Clonogenicity, via colony-forming unit (CFU) assay.
    (c) Differentiation potential into the adipogenic, chondrogenic, and osteogenic lineages.

3.4 Freezing/ Storing Mesenchymal Stem Cells

1. Resuspend trypsinized MSC pellet in 0.5 ml of ML basic medium at the desired concentration (*see* **Note 16**).
2. Put cells on ice during the following freezing steps.
3. Pipette dropwise 0.5 ml of freezing medium (4 °C) onto the cells.
4. Put the vials in a freezing container and place in a −80 °C freezer (*see* **Note 17**).
5. The next day, transfer cells from the −80 °C to liquid nitrogen for long-term storage.

4 Notes

1. Always add fresh bFGF and vitamin C to the MSC culture medium before use, since the growth factor and vitamin C (light sensitive) are unstable in the medium. Furthermore, do not refreeze bFGF and vitamin C after thawing from stock. Instead store at 4 °C.
2. By creating a vacuum using the plunger, the tube will slowly fill with bone marrow.
3. 10–15 million mononuclear cells can be extracted from 10 ml of bone marrow. After plating and culturing, this amount yields approximately two to four million passage 1 MSCs.
4. Alternatively to using specific anticoagulant blood collection tubes, it is possible to use 50 ml tubes with heparin.
5. Keep the collected BM at room temperature, and do not cool on ice or in the fridge.
6. Nonnucleated cells include red blood cells and platelets, while nucleated cells are in the white blood cell fraction containing the MSCs.
7. Do not store less than 7 ml whole BM since the white blood cell ring might be too thin to recognize later in the isolation.
8. Do not use filter tubes (Leucosep), since the white mononuclear cell ring from pig BM has a tendency to precipitate partly on the filter.
9. Addition of Ficoll to BM:

(a) Pipette 13 ml of Ficoll-Paque Plus into a pipette, and insert the pipette into the 50 ml tube containing the diluted bone marrow, with the tip at the bottom of the tube.

(b) Remove the pipette from the pipetting aid. This will cause the Ficoll to be slowly released at the bottom of the tube.

(c) When the fluid level in the pipette and the tube have leveled, lift the pipette slightly and close the tip with your finger when there is only 3 ml left in the pipette. Remove the pipette slowly, keeping your finger firmly in place.

(d) Two separate layers are visible: a clear Ficoll layer at the bottom and the red fluid above that.

10. If you remove a lot of Ficoll when collecting your white ring, you can add 10 % FBS to the tube. This improves the viability of the collected cells.
11. Yield should be ~25–30 %, compared with the initial whole BM measurement.
12. The reason for not adding bFGF and vitamin C during the first 3 days is to further prevent attachment of fibroblasts and other unwanted cell types, which is already diminished by using MEM alpha instead of DMEM medium.
13. Check colony formation daily from day 7 onwards, as this differs between donors.
14. These newly isolated MSC are rather well attached. While 2 min is usually sufficient to detach them, increase trypsin exposure time up to 5 min, but check every 2 min. If still attached, use an additional 75 μl fresh trypsin.
15. To preserve the functionality of the cells, do not allow the MSC to become too confluent. Try to harvest the cells when they reach 80 % confluency.
16. Freeze MSCs in the same manner as when passaging them. Therefore, if the MSCs are cultured in a T75, freeze 1/3 of the flask in each vial, which is around 0.75 million cells per 0.5 ml. For thawing, simply use one vial for one T75. The flask will be full and MSCs ready to use in several days.
17. These containers control the freezing rate at −1 °C per min for optimal preservation of MSCs.

Acknowledgments

This work is part of the Project P1.04 SMARTCARE of the BioMedical Materials institute, co-funded by the Dutch Ministry of Economic Affairs, Agriculture and Innovation. The financial contribution of the Dutch Heart Foundation is gratefully

acknowledged. This work was further supported by a grant from the Alexandre Suerman program for MD/PhD students of the University Medical Center Utrecht, the Netherlands, the ZonMw-TAS program (#116002016) and the Netherlands CardioVascular Research Initiative (CVON): the Dutch Heart Foundation, Dutch Federation of University Medical Centers, the Netherlands Organization for Health Research and Development, and the Royal Netherlands Academy of Sciences.

References

1. Pittenger MF, Martin BJ (2004) Mesenchymal stem cells and their potential as cardiac therapeutics. Circ Res 95:9–20
2. Gnecchi M, He H, Noiseux N et al (2006) Evidence supporting paracrine hypothesis for Akt-modified mesenchymal stem cell-mediated cardiac protection and functional improvement. FASEB J 20:661–669
3. Gnecchi M, Zhang Z, Ni A et al (2008) Paracrine mechanisms in adult stem cell signaling and therapy. Circ Res 103:1204–1219
4. van den Akker F, de Jager SC, Sluijter JP (2013) Mesenchymal stem cell therapy for cardiac inflammation: immunomodulatory properties and the influence of toll-like receptors. Mediators Inflamm 2013:181020
5. Noort WA, Feye D, Van Den Akker F et al (2010) Mesenchymal stromal cells to treat cardiovascular disease: strategies to improve survival and therapeutic results. Panminerva Med 52:27–40
6. Magne D, Vinatier C, Julien M et al (2005) Mesenchymal stem cell therapy to rebuild cartilage. Trends Mol Med 11:519–526
7. Knight MN, Hankenson KD (2013) Mesenchymal stem cells in bone regeneration. Adv Wound Care (New Rochelle) 2:306–316
8. Le Blanc K, Frassoni F, Ball L et al (2008) Mesenchymal stem cells for treatment of steroid-resistant, severe, acute graft-versus-host disease: a phase II study. Lancet 371:1579–1586
9. Ball LM, Bernardo ME, Roelofs H et al (2007) Cotransplantation of ex vivo expanded mesenchymal stem cells accelerates lymphocyte recovery and may reduce the risk of graft failure in haploidentical hematopoietic stem-cell transplantation. Blood 110:2764–2767
10. Dixon JA, Spinale FG (2009) Large animal models of heart failure: a critical link in the translation of basic science to clinical practice. Circ Heart Fail 2:262–271
11. van der Spoel TI, Jansen of Lorkeers SJ, Agostoni P et al (2011) Human relevance of pre-clinical studies in stem cell therapy: systematic review and meta-analysis of large animal models of ischaemic heart disease. Cardiovasc Res 91:649–658
12. van der Spoel TI, Vrijsen KR, Koudstaal S et al (2012) Transendocardial cell injection is not superior to intracoronary infusion in a porcine model of ischaemic cardiomyopathy: a study on delivery efficiency. J Cell Mol Med 16:2768–2776
13. Sahni D, Kaur GD, Jit H et al (2008) Anatomy & distribution of coronary arteries in pig in comparison with man. Indian J Med Res 127:564–570
14. Li WJ, Chiang H, Kuo TF et al (2009) Evaluation of articular cartilage repair using biodegradable nanofibrous scaffolds in a swine model: a pilot study. J Tissue Eng Regen Med 3:1–10
15. Noort WA, Oerlemans MI, Rozemuller H et al (2012) Human versus porcine mesenchymal stromal cells: phenotype, differentiation potential, immunomodulation and cardiac improvement after transplantation. J Cell Mol Med 16:1827–1839

Chapter 13

Isolation, Culture, and Phenotypic Characterization of Mesenchymal Stromal Cells from the Amniotic Membrane of the Human Term Placenta

Marta Magatti, Stefano Pianta, Antonietta Silini, and Ornella Parolini

Abstract

During the past several years, the human placenta and in particular the amniotic fetal membrane have attracted much attention as a possible source of cells to be used in cell therapy approaches due to its putative stem cell potential associated with its early embryonic origin and its immunomodulatory potential associated with its role in fetomaternal tolerance.

Within the human amniotic membrane, it is possible to isolate two main cell populations: amniotic epithelial cells (from the epithelial layer of the amniotic membrane) and amniotic mesenchymal cells (from the mesenchymal layer of the amniotic membrane). In this chapter, we will describe a method for the isolation of mesenchymal stromal cells (hAMSCs). We will also describe their optimal culture conditions and the phenotypic characterization of cells after passaging.

Key words Mesenchymal stromal cells, Human term placenta, Amniotic membrane, Cell isolation, Phenotype, Chang Medium® C

1 Introduction

The human term placenta is a fetomaternal organ comprised of a fetal component which includes the chorion frondosum, chorion laeve, amniotic membrane, and Wharton's jelly of the cord string and a maternal component referred to as the decidua, which is derived from the endometrium [1].

The amnion forms a fluid-filled, membranous sac that surrounds the fetus, comprised of a thin, avascular membrane composed of an epithelial monolayer, a thick basement membrane, and an avascular stroma [2–4].

The amniotic epithelium (AE) is a continuous, single layer of flat, cuboidal, and columnar epithelial cells in contact with the amniotic fluid. A narrow basement membrane is located directly underneath the epithelial cells, and this is composed of collagen, fibronectin, and laminin (Fig. 1). An underlying, thick, acellular

Massimiliano Gnecchi (ed.), *Mesenchymal Stem Cells: Methods and Protocols*, Methods in Molecular Biology, vol. 1416,
DOI 10.1007/978-1-4939-3584-0_13,

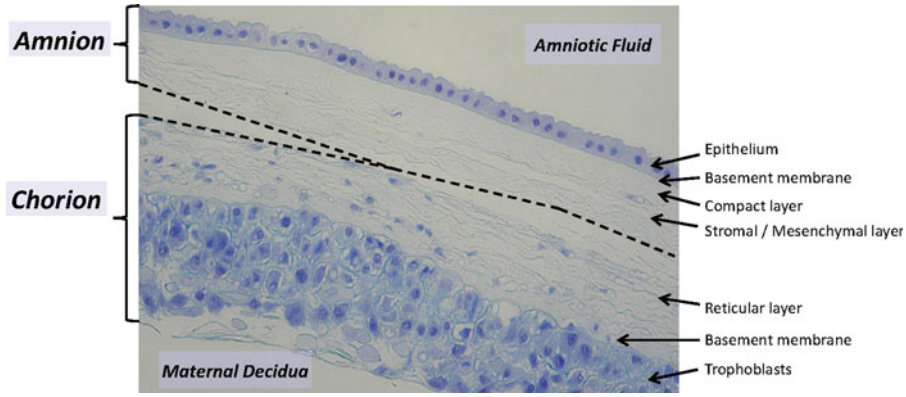

Fig. 1 Histological cross section showing the structure of the amnion and chorion

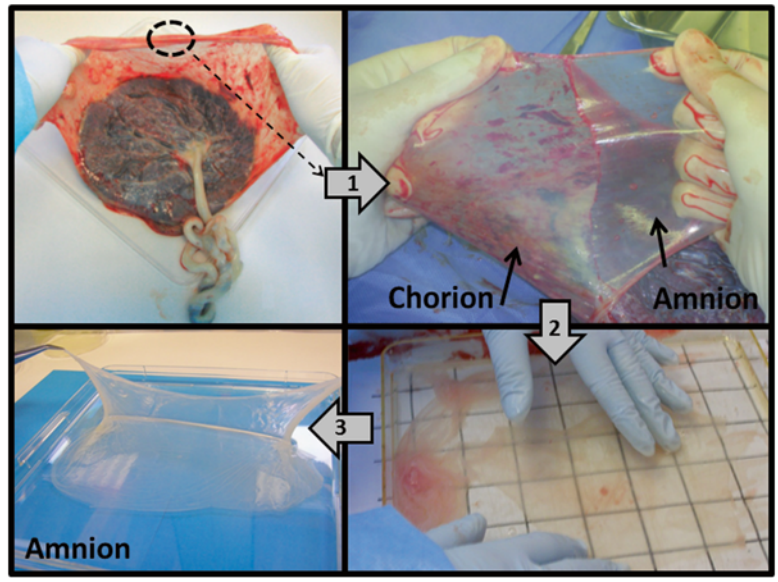

Fig. 2 Flow diagram showing the preparation of the amniotic membrane for cell isolation from the human placenta

compact layer, composed of collagen and fibronectin, is distinguishable underneath the basement membrane [3]. Deeper in the amniotic membrane, a network of dispersed fibroblast-like mesenchymal cells and rare macrophages is observed. A spongy layer of loosely arranged collagen fibers separates the amnion from the chorionic membrane [2].

This chapter will focus on mesenchymal cells from the stromal layer of the amniotic membrane (hAMSC). The amniotic membrane is obtained by gently peeling it off from the underlying chorion (Fig. 2), followed by washing, sterilization, and a series of enzymatic digestions. Isolation protocols and characterization of

AEC are not the purpose of this chapter and have been described elsewhere [5–7].

hAMSC shares many characteristics that are typical of mesenchymal stromal (stem) cells obtained from other sources such as the bone marrow and umbilical cord. The consensus from the *First International Workshop on Placenta-Derived Stem Cells* established that hAMSC should be of fetal origin, adheres to plastic, form fibroblast-like colony-forming units and possesses differentiation potential toward one or more lineages, including osteogenic, adipogenic, or chondrogenic lineages [8]. Furthermore, the consensus identified specific cell surface antigen expression from passages 2 to 4, namely, the positive (≥95 %) expression of CD90, CD73, and CD105 and the lack of (≤2 %) CD45, CD34, CD14, and HLA-DR [8]. After cell isolation (P0), there may be a percentage of cells (ranging from 5 to 15 %) expressing CD45, CD14, and HLA-DR. Considering that mesenchymal stromal cells should be negative for these markers, cells at P0 have been referred to as human amniotic mesenchymal tissue cells (hAMTCs) [9]. After cell culture, the percentage of cells expressing CD45, CD14, and HLA-DR are greatly reduced (<2 %), and the phenotype meets the established consensus criteria for nomenclature; thus, they are referred to as human amniotic mesenchymal stromal cells (hAMSCs). For the sake of simplicity, throughout the text, we will refer to cells isolated from the human amniotic membrane stromal layer as hAMSC.

Herein, we will describe a protocol for the isolation, cryopreservation, and culture of hAMSC. Moreover, we will also describe the phenotypic characterization of hAMSC at different passages.

2 Materials

2.1 Isolation of Mesenchymal Stromal Cells

1. Appropriate surgical and cell culture facilities.
2. Sterilized materials: scalpel blades, forceps, and sterile gloves.
3. Tissue culture supplies and sterile disposable supplies including a plastic sterile dish (245x245mm), motorized pipettor, micropipettes, micropipette tips (1mL, 200μL, 20μL), graduate pipettes (5, 10, 25mL), centrifuge tubes (30, 50mL), and 100mL beaker.
4. Cell counting materials such as Bürker chamber and Trypan blue.
5. Phosphate-buffered saline (PBS), 1× without calcium chloride and magnesium chloride.
6. Physiological salt solution, 0.9 % w/v NaCl.
7. RPMI 1640 without L-glutamine.

8. Hanks' balanced salt solution (HBSS).
9. Heat-inactivated fetal bovine serum (FBS).
10. L-glutamine 200 mM.
11. Penicillin-streptomycin (P/S): 10,000 U penicillin and 10 mg streptomycin per mL in 0.9 % NaCl.
12. Betadine® 10 % povidone-iodine.
13. Cefamezin: cefazolin 100 mg/mL.
14. Amphotericin B (Amph B) 250 μg/mL.
15. Collagenase A.
16. Dispase.
17. DNase.
18. Physiological salt solution + P/S + Amph B: physiological salt solution 0.9 % NaCl addition of P/S [penicillin (final concentration 100 U/mL) and streptomycin (final concentration 100 μg/mL)] and Amph B (final concentration 2.5 μg/mL).
19. PBS + P/S + Amph B + Cefamezin: PBS + P/S [penicillin (final concentration 500 U/mL) and streptomycin (final concentration 500 μg/mL)], Amph B (final concentration 12.5 μg/mL) and Cefamezin (final concentration 1.87 mg/mL).
20. Enzyme solution 1: HBSS + dispase (final concentration 2.5 U/mL).
21. Complete RPMI 1640: RPMI 1640 supplemented with 10 % FCS + P/S [penicillin (final concentration 500 U/mL) and streptomycin (final concentration 500 μg/mL)] + L-glutamine (final concentration 1 mM).
22. Collagenase A solution: prepare a 7.5 mg/mL stock solution in PBS and filter.
23. Enzyme solution 2: complete RPMI 1640 supplemented with collagenase A solution (final concentration 0.9 mg/mL) + DNase (final concentration 0.01 mg/mL).

2.2 Cell Expansion

1. Standard culture supplies and sterile disposable supplies including a motorized pipettor, micropipettes, micropipette tips (1mL, 200μL, 20μL), graduate pipettes (5, 10, 25mL), centrifuge tubes (30, 50mL), and flasks (25, 75, 150 cm^2).
2. Cell counting materials such as Bürker chamber and Trypan blue.
3. PBS 1× without calcium chloride and magnesium chloride.
4. Chang Medium® C.
5. L-glutamine 200 mM.
6. P/S with 10,000 U penicillin and 10 mg streptomycin per mL in 0.9 % NaCl.

7. 0.25 % trypsin EDTA solution: 2.5 g porcine trypsin and 0.2 g EDTA.
8. PBS + P/S: PBS supplemented with 1 % P/S [penicillin (final concentration 100 U/mL) and streptomycin (final concentration 100 μg/mL)].
9. Complete Chang Medium® C: prepare as described by the manufacturer, and supplement with 2 mM L-glutamine and 1 % P/S.

2.3 Characterization: Immuno-phenotyping

1. Standard culture supplies and disposable supplies including a motorized pipettor, micropipettes, micropipette tips (1mL, 200μL, 20μL), graduate pipettes (5, 10, 25mL), and centrifuge tubes (30, 50mL).
2. Micronic tubes (1.4 mL round-bottom polypropylene tubes).
3. Flow cytometer and analysis software.
4. Antihuman, fluorochrome-conjugated antibodies suitable for use in flow cytometry:
   (a) CD13-PE (clone L138).
   (b) CD44-FITC (clone L178).
   (c) CD73-PE (clone AD2).
   (d) CD90-FITC (clone 5E10).
   (e) CD105-FITC (clone SN6).
   (f) CD117-PE (clone 104D2).
   (g) CD326-APC (clone EBA-1).
   (h) Stage-specific embryonic antigen-4 (SSEA-4)-PE (clone MC813-70).
   (i) CD49a-Alexa 488 (clone TS2/7).
   (j) CD49b-FITC (clone AK-7).
   (k) CD49c-PE (clone C3 II.1).
   (l) CD49d-PE (clone 9F10).
   (m) CD45-APC (clone 2D1).
   (n) HLA-ABC-FITC (clone G46-2.6).
   (o) HLA-DR-PE (clone TU36).
   (p) CD34-PE (clone 581).
5. Isotype control antibodies:
   (a) Mouse IgG1,k-PE isotype control (clone X40).
   (b) Mouse IgG1,k-FITC isotype control (clone X40).
   (c) Mouse IgG1,k-APC Isotype Control (clone X40).
   (d) Mouse IgG3,k-PE isotype control (clone A112-3).
   (e) Mouse IgG1-Alexa 488 Isotype control.
   (f) Mouse IgG2b,k-PE (clone 27–35) isotype control.

6. PBS 1× without calcium chloride and magnesium chloride.
7. 10 % bovine serum albumin (BSA).
8. 20 % sodium azide.
9. Polyglobin.
10. Propidium iodide (PI) 1 μg/mL.
11. Staining buffer: PBS with 0.02 % sodium azide and 0.1 % BSA.
12. Polyglobin solution: 20 mg/mL polyglobin in PBS with 1 % BSA.

3 Methods

3.1 Isolation of Amniotic Mesenchymal Stromal Cells

Steps 1–3 are intended to macroscopically evaluate the placental tissues in order to verify their suitability for subsequent tissue processing. The procedures described in this section should be performed at room temperature and under sterile conditions. The total time from stripping of the tissue to the final cell pellet is approximately 5 h (*see* **Note 1**).

Macroscopic evaluation:

1. In order to minimize contamination of the work area and facilitate cleaning at the end of the procedure, we suggest preparing the laminar flow hood by spreading absorbent paper on the work area. Wear sterile gloves and sleeves when handling the placenta.
2. Gently pull the placenta from the container in which it is transported and place it on the tray.
3. Proceed with the macroscopic evaluation of the placenta initially assessing the degradation state of the membranes. Use forceps and a scalpel to handle the placenta. Make sure that the amniotic membrane and chorion are attached. Discard the pieces of amnion that have already separated from the chorion.
4. Detach the amnion from the chorion by simple, mechanical traction (Fig. 2). The amnion is the innermost membrane of the placenta starting from the fetal side.
5. Wash the amnion with 1 % P/S + 1 % Amph B in physiological saline solution.
6. Manually remove blood clots and highly gelatinous areas.
7. Using a sterile scalpel, cut the amniotic membrane into 3 × 3 cm pieces, and place the pieces in a sterile container containing 50 mL of 1 % P/S+ 1 % Amph B in physiological saline solution for 5 min.

Sterilization phase:

8. Sterilize the membranes by placing them in a sterile beaker containing the physiological saline solution+0.25 % povidone-iodine for 1–2 s. Then, immediately remove and incubate for 3 min in a beaker containing PBS + P/S + Amph B + Cefamezin.
9. Using sterile tweezers, transfer the pieces into a beaker containing sterile PBS+P/S.

Enzymatic digestion:

10. Transfer the membrane pieces into a sterile beaker containing the enzyme solution 1. We suggest keeping a ratio of 0.4 mL enzyme solution 1/piece.
11. Incubate for 9 min at 37 °C in a water bath with agitation.
12. Transfer the partially digested fragments to sterile beakers with 40 mL of complete RPMI 1640 for 3 min at room temperature.
13. Transfer the membranes to one or more sterile beakers containing the enzyme solution 2. We suggest 32 mL of enzyme solution 2 for a maximum of 25–30 pieces.
14. Incubate for 2.5–3 h at 37 °C in a water bath with agitation (*see* **Note 2**).
15. Transfer the digested membranes in the enzyme solution 2–50 mL sterile tubes, and mix the membranes by inverting the tubes five times.
16. Centrifuge at 150 × *g* for 3 min at room temperature.
17. Pour the supernatant through a sterile metal strainer (100 μm) (*see* **Note 3**).
18. Collect the cell pellets into one tube and bring to volume with PBS+P/S.
19. Centrifuge 150 × *g* for 3 min at room temperature.
20. Pour the supernatant through a sterile metal strainer (100 μm). Discard the cell pellet (*see* **Note 4**).
21. Dilute the filtered cells 1:2 with PBS+P/S and distribute the supernatant obtained into different 50 mL tubes.
22. Centrifuge the tubes at 300 × *g* for 10 min at room temperature.
23. Aspirate the supernatants.
24. Resuspend the cell pellets by gently tapping the bottom of the tube.
25. Collect the cell pellets into one tube, filter the cells through a sterile strainer (70 μm) and bring to volume to 50 mL with complete RPMI 1640.
26. Centrifuge the cells at 300 × *g* for 10 min at room temperature.
27. Aspirate the supernatants.

28. Add complete RPMI 1640 (we suggest a maximum of 5 mL per tube) and count the cells. We suggest counting with a Bürker chamber using Trypan blue stain to discriminate between dead and live cells (*see* **Note 5**).
29. The hAMSC can be frozen (*see* **Note 6**), plated for cell expansion (*see* Subheading 3.2), or characterized by immunophenotypic analysis (*see* Subheading 3.3).

3.2 Cell Expansion

All procedures described in Subheading 3.2 should be performed under sterile conditions.

1. Plate hAMSC after isolation (designated as P0 cells) at a density of $10 \times 10^3/cm^2$ in complete Chang Medium® C (*see* **Note 7**).
2. Check the cells daily and change the medium every 3 days. Remove half of the volume and replace it with fresh medium. The cells can be split when they reach 80–90 % confluency (*see* **Note 8**).
3. Aspirate the culture medium (*see* **Note 9**) and wash the cell monolayer twice with PBS+P/S.
4. Aspirate all the PBS+P/S and add prewarmed trypsin (*see* **Note 10**).
5. Place the flask in the 37 °C incubator for 2 min (*see* **Note 11**).
6. Add complete Chang Medium® C to deactivate the trypsin. We suggest adding at least five times the volume of trypsin.
7. Collect the cells in a tube and centrifuge at $300 \times g$ for 10 min at +20 °C.
8. Aspirate the supernatant and resuspend the pellet in complete Chang Medium® C.
9. Count the cells with a Bürker chamber, and use Trypan blue stain to discriminate between dead and live cells. These are passage one (P1) cells (*see* **Note 12**).
10. Plate P1 hAMSC at a density of $10 \times 10^3/cm^2$.
11. Check the cells daily and split them when they reach 80–90 % confluency (*see* **Note 13**).

3.3 Characterization: Immuno-phenotyping

Cells can be analyzed by immunophenotyping immediately after isolation (P0), after two passages (P2), or after having been thawed. To ensure that the different cell preparations are comparable with each other in terms of their immunophenotype, we recommend cryopreserving batches of each cell preparation after isolation (P0) and after passaging (P2) and then thawing and analyzing both P0 and P2 by flow cytometry:

1. Harvest hAMSC single-cell suspensions and count cells with a Bürker chamber using Trypan blue stain to discriminate between dead and live cells.

2. Wash cells with staining buffer.
3. Aliquot 2.5×10^5 cells/50 μL into Micronic tubes (*see* **Note 14**).
4. Add 40 μL/sample of polyglobin solution to block nonspecific binding.
5. Add conjugated antibody or isotype control and vortex (*see* **Note 15**).
6. Incubate cells for 20 min at 4 °C protected from light (*see* **Note 16**).
7. Wash the cells twice with 0.5 mL of staining buffer to remove any unbound antibody. Centrifuge cells at $300 \times g$ for 5 min. Carefully aspirate supernatants.
8. Resuspend the cells in 0.2 mL of staining buffer.
9. Add 30 μL/sample of propidium iodide (1 μg/mL) to discriminate dead cells during analysis.
10. Acquire and analyze cells with flow cytometer (*see* **Note 17**).
11. hAMSC cells are characterized by the expression of markers reported in Fig. 3.

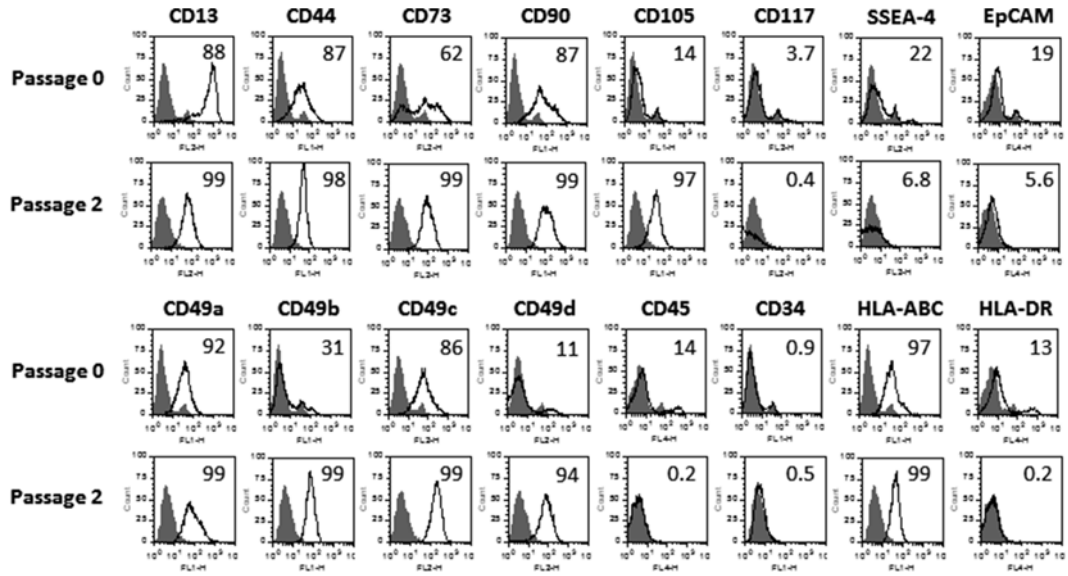

Fig. 3 Immunophenotype of hAMSC at different culture passages. *Markers at P0:* Cells are positive for CD13, CD44, CD73, CD90, CD49a, CD49b, CD49c, and HLA-ABC. Cells are negative for CD117 and CD34. There is a small percentage of cells expressing CD105, EpCAM, SSEA-4, CD45, and HLA-DR. *Markers at P2*: Cells remain positive for markers observed at P0 and also for CD105. Among these markers, the expression of CD73, CD90, CD105, CD49b, CD49c, and CD49d increases significantly compared to P0. Cells remain negative for CD117 and CD34, while the expression of EpCAM, SSEA-4, CD45, and HLA-DR significantly decreases compared to P0. The percentage of positive cells is indicated in each plot. Samples were acquired and analyzed with FACSCalibur and CellQuest Software (BD Biosciences)

4 Notes

1. This protocol can be used for isolating hAMSC from term placentas obtained from cesarean section procedures or from spontaneous deliveries. The time between the delivery of the placenta and the cell isolation procedure is critical for optimal cell preparation/recovery. The tissue should be kept at 4 °C during transportation and up until the start of the isolation protocol. We suggest performing cell isolation within 12 h from delivery.
2. Check the membrane digestion and slightly mix the suspension. We suggest not exceeding 3 h of digestion.
3. After digestion with enzyme solution 2, the amniotic membrane pieces release a lot of collagen, thus making the suspension very viscous.
4. The cell pellet is enriched with epithelial cells from the amniotic membrane (hAEC).
5. The yield of hAMSC from the one term placenta is usually in the range of $10–30 \times 10^6$ cells. The viability of freshly isolated hAMSC should be over 80 %.
6. The cells should be frozen using standard cryogenic techniques (FBS+10 % DMSO, rate of temperature decrease equal to −1 °C/min). If the cells are prepared and then frozen for future use, we suggest freezing $3–5 \times 10^6$ cells/vial, which should be sufficient for subsequent quality testing.
7. We suggest using complete Chang Medium® C for cell growth, as previously reported for the expansion of MSC from chorionic villi [10]. Following indications given in this protocol, cells can be cultured up to passage 6 without reaching senescence. Cells show a duplication time (DT), calculated as $t^*\log 2/\log n$ (t = time between two consecutive passages; n = cell number of detached cells divided by the initial number of seeded cells) of 3.24 ± 1.07 at P1 at 1.44 ± 0.39 at P2 which is maintained without significant variations until passage 5 (DT at passage 5 of 1.61 ± 0.48 days). The cumulative population doublings (PD, calculated as $\log n/\log 2$; n = cell number of detached cells divided by the initial number of seeded cells) at passage 1 are 2.49 ± 0.41; at passage 3, PD are 8.04 ± 1.60 and at passage 5, 13.03 ± 2.65. For expansion protocols using other culture media, refer to [11].
8. After isolation, cells usually require 6–8 days to reach 80–90 % confluency.
9. Be gentle when adding the wash solutions and avoid touching the cell monolayer with the pipette. Rotate the dish orbitally to assure thorough washing.

10. 10. Prewarm trypsin to 37 °C. We recommend using 1, 2.5, and 4 mL of trypsin for T25, T75, and T150 flasks, respectively.
11. Check the cells under the microscope to assure detachment. Cells become round once detached. Usually, 2 min will suffice, but you can tap the flask gently on the benchtop to dislodge the cells, or put the flask in the incubator once again for a few more minutes.
12. At P1 we usually obtain a fivefold average increase in the number of P0 cells plated in complete Chang Medium® C.
13. Cells usually require 3–4 days to reach 80–90 % confluency. At P2, we usually obtain an eightfold average increase in P1 cells plated in complete Chang Medium® C.
14. We suggest a minimum of 5×10^4 and a maximum of 2.5×10^5 cells in 50 μL of staining buffer for each sample.
15. We recommend using 2 μL antibody/2.5×10^5 cells. We suggest performing an antibody titration to identify the optimal amount. Start with the suggested concentration given in the product datasheet, and dilute the antibody in staining buffer.
16. Fluorochromes bound to antibodies are photosensitive, so they must be protected from light.
17. We recommend a minimum of 5×10^4 cells per antibody or isotype control. For the negative control, a separate aliquot of cells should be stained with the appropriate isotype control antibody. First, run cells with isotype control and use isotype controls to adjust the photomultiplier tube (PMT) voltages. Second, use a second aliquot of cells with only one antigen to perform compensation in multiparameter staining. Use forward scatter and side scatter analyses to exclude debris and add propidium iodide to exclude dead cells from the analysis. We recommend a minimum of 10,000 events in the live-cell gate (exclusion of debris and propidium iodide-negative cells) for characterization.

Acknowledgments

The authors would like to thank all the CREM personnel who contributed to the optimization of these protocols.

References

1. Moore KL, Persaud TVN, Torchia MG (2013) The developing human: clinically oriented embryology, 9th edn. Elsevier Saunders, Philadelphia, PA
2. Benirschke K, Kaufmann P (2000) Pathology of the human placenta. Springer, New York
3. Niknejad H, Peirovi H, Jorjani M et al (2008) Properties of the amniotic membrane for potential use in tissue engineering. Eur Cell Mater 29:88–99
4. Mamede AC, Carvalho MJ, Abrantes AM et al (2012) Amniotic membrane: from structure

and functions to clinical applications. Cell Tissue Res 349:447–458

5. Miki T, Marongiu F, Ellis E et al (2007) Isolation of amniotic epithelial stem cells. Curr Protoc Stem Cell Biol. Chapter 1: Unit 1E.3. Wiley
6. Miki T, Marongiu F, Dorko K et al (2010) Isolation of amniotic epithelial stem cells. Curr Protoc Stem Cell Biol. Chapter 1: Unit 1E.3. Wiley
7. Barbati A, Grazia Mameli M, Sidoni A et al (2012) Amniotic membrane: separation of amniotic mesoderm from amniotic epithelium and isolation of their respective mesenchymal stromal and epithelial cells. Curr Protoc Stem Cell Biol 20:1E.8.1–1E.8.15
8. Parolini O, Alviano F, Bagnara GP et al (2008) Concise review: isolation and characterization of cells from human term placenta: outcome of the first international workshop on placenta derived stem cells. Stem Cells 26:300–311
9. Magatti M, De Munari S, Vertua E et al (2012) Amniotic membrane-derived cells inhibit proliferation of cancer cell lines by inducing cell cycle arrest. J Cell Mol Med 16:2208–2218
10. Roselli EA, Lazzati S, Iseppon F et al (2013) Fetal mesenchymal stromal cells from cryopreserved human chorionic villi: cytogenetic and molecular analysis of genome stability in long-term cultures. Cytotherapy 15:1340–1351
11. Lindenmair A, Hatlapatka T, Kollwig G et al (2012) Mesenchymal stem or stromal cells from amnion and umbilical cord tissue and their potential for clinical applications. Cells 12:1061–1088

Chapter 14

Isolation, Culture, and Characterization of Human Umbilical Cord Blood-Derived Mesenchymal Stromal Cells

Karen Bieback and Philipp Netsch

Abstract

Umbilical cord blood (CB) is considered one of the youngest available sources of adult stem cells. Besides hematopoietic stem cells, CB has been shown to contain endothelial progenitor cells as well as mesenchymal stromal/stem cells (MSC). To isolate MSC from cord blood, CB is collected into a sterile bag containing the anticoagulant citrate-phosphate-dextrose (CPD). The CB is then processed by density-gradient centrifugation to obtain mononuclear cells (MNC). These are cultured until the outgrowth of fibroblastoid cell colonies appears. After reaching a subconfluent stage, cells are harvested, expanded, and characterized as cord blood mesenchymal stromal cells (CB-MSC) according to standard criteria: plastic adherence, fibroblast morphology, CFU-f assay, proliferation potential, immune phenotype, and differentiation potential.

Apparently, the frequency of MSC in CB is extremely low. Thus, not every CB unit will provide adequate MSC isolation yields. Different strategies have been proposed aiming to optimize the isolation success by selecting CB units of optimal quality. It is commonly agreed on that a high CB volume, a high cellular content, and a short time frame between birth and MSC isolation are criteria that will enhance the MSC isolation success.

The procedures in this chapter are standardized protocols that were established and optimized in the authors' research laboratory; however, various modifications of the protocols are possible.

Key words Mesenchymal stromal cells, Mesenchymal stem cells, Cord blood, Umbilical cord blood, Isolation, Culture, Characterization, Differentiation, Immune phenotype

1 Introduction

Mesenchymal stromal/stem cells (MSC) are cell culture-expanded, adherent, fibroblastoid, multipotent stemlike cells [1–4]. They are capable of extensive proliferation in ex vivo culture and differentiation into various tissues—probably even beyond the mesodermal germ layer [1, 5, 6]. Taking advantage of their relative ease of isolation, the therapeutic capacities of MSC have been intensely investigated for a variety of human diseases [2, 5].

Although initially isolated from bone marrow (BM), a large variety of different tissue sources have been identified that allow for the isolation of MSC with varying frequencies [7, 8]. Their broad

Massimiliano Gnecchi (ed.), *Mesenchymal Stem Cells: Methods and Protocols*, Methods in Molecular Biology, vol. 1416,
DOI 10.1007/978-1-4939-3584-0_14,

tissue occurrence may relate to the recently revealed in vivo origin of MSC: similar to pericytes, MSC reside in close proximity to blood vessels [9]. This localization may explain why MSC cannot be isolated from the peripheral blood or only from patients where MSC have been mobilized to circulate [10].

In contrast, CB has been identified as a source of MSC, albeit with an extremely low frequency (0–2.3 colony-forming cells per 1×10^8 MNC) and a markedly reduced isolation success between 20 and 30 % for full-term CB units [7, 8, 11, 12]. MSC may circulate especially in early developmental phases such as first and mid-trimester fetal blood; preterm CB as well contain higher numbers of MSC than full-term blood [11, 13–16]. Thus, most likely, MSC circulate at early gestational phases, but where they home to at the end of gestation remains unclear.

Nevertheless, CB (as well as other perinatal tissues, such as umbilical cord) appears as an attractive MSC source as it can be harvested without any harm to the donor and it contains young/highly immature cells that are less susceptible to viral infections [12].

To improve the isolation success, we defined the following critical parameters that have allowed us to increase the isolation success rate of full-term CB units from approximately 30 % to over 60 % [11]:

- The time from collection to isolation of less than 15 h
- A net blood volume greater than 33 ml
- An MNC count greater than 1×10^8 MNC

Confirming our data, the isolation success rate has been further increased to 90 % by processing only CB units that have a net volume ≥90 ml and a storage time between birth and isolation procedure ≤2 h [17]. Success rates of 100 %, which are commonly reported for other tissue sources like bone marrow and adipose tissue, however have never been achieved with CB [7].

Considering their low frequency and limited isolation success, the clinical suitability of CB-MSC, at least for autologous use, has been questioned. MSC appear to be immunoprivileged and immunomodulatory [18]; accordingly, allogeneic MSC have been suggested for the clinical setting due to their immediate availability, better standardization, and lower costs. In fact, administration of allogeneic MSC to human subjects has been achieved without severe immunological complications within clinical trials [19]. Yet, whether the use of allogeneic MSC, with MSC from perinatal tissues being the youngest available, is really advantageous in the clinical setting needs to be thoroughly investigated [18, 20].

In early studies, researchers were mainly interested in utilizing the stromal capacity of MSC to support hematopoiesis. Later, the multi-lineage, mesodermal differentiation potential attracted MSC researchers to grow/regenerate bone, cartilage, and adipose tissue.

Because clinical success was much lower than expected based on in vitro data, and because transplanted MSC were rarely detectable in patients, it was suggested that therapeutic success was mainly related to the immune suppressive and trophic activities of MSC [1, 3, 4]. Usually MSC expanded from different tissue sources share these capacities. MSC derived from fetal/perinatal tissues, however, appear to differ significantly from MSC derived from adult tissues. The most striking difference is the lack/largely reduced adipogenic differentiation potential of CB-MSC [7, 11, 21–23] (*see* also **Note 6** and Fig. 2).

A number of projects have compared CB-MSC with MSC from other tissue sources. Some indicated that CB-MSC rival other MSC in some clinically important features. For example, some authors claim that immune suppression or the bone-forming capacity of CB-MSC exceeds that of other MSC sources. However, other authors claim the exact opposite [7, 21, 24–34]. These discrepancies suggest that not only the culture conditions but also the experimental setup of assays significantly influence the characteristics of expanded cells and indicate that further comparative analyses are needed.

Surface proteins have been used to characterize MSC [32]. Initial minimal criteria included the expression of CD105, CD73, and CD90 and the lack of expression of CD45, CD34, CD14 or CD11b, CD79alpha or CD19, and HLA-DR [33]. Of note, it is now widely accepted that even expanded MSC comprise a heterogeneous cell population. Comparing expanded CB-MSC to MSC from bone marrow and adipose tissue, we detected little variance in the expression pattern of these markers. The mean fluorescence expression intensity of CD105 (endoglin), however, was lower in CB-MSC compared to the two other MSC types. Similar findings were obtained when trying to quantify MSC in fresh CB or BM using a seven-color, single-tube flow cytometric assay [35]. MSC here were identified by the phenotype CD71+CD105+CD184+CD34-CD133-CD45-CD44+NGFR+. Interestingly, using these markers a comparably high frequency of MSC was detected in both cell suspensions with 13.2 ± 5.8 MSC/1×10^6 BM-MNC and 8.8 ± 4.3 MSC/ 1×10^6 CB-MNC.

MSC have potent anti-inflammatory and immunomodulatory properties, while they evoke only minimal immune responses. As this is an invaluable therapeutic characteristic, a number of studies have compared the immunomodulatory capacities of MSC from different tissue sources. Nonstimulated and stimulated MSC from bone marrow, adipose tissue, Wharton's jelly, and CB appear to express similar types and levels of cytokines [36]. In this study, MSC from the different tissues did not exert significant differences in the suppression of mitogen-stimulated T-cell proliferation. Comparable immune suppressive activities of CB- and BM-MSC were also observed in

another study, where interestingly placenta-derived MSC stood out for their reduced immune suppressive activity [25].

It is beyond the scope of this chapter to cover all the publications investigating the preclinical and clinical potential of CB-MSC. However, there are some highly promising data that have led to the exploration of CB-MSC clinical potential in clinical trials, mainly phase I and phase II trials.

The following studies are listed at www.clinicaltrials.gov (search date 26.06.14):

- Safety and efficacy study of CB-MSC to promote engraftment of unrelated hematopoietic stem cell transplantation (study completed)
- CB-MSC for the treatment of steroid-refractory acute or chronic graft-versus-host disease (status unknown)
- Safety and efficacy evaluation of Pneumostem® treatment in premature infants with bronchopulmonary dysplasia (first study completed, follow-up studies recruiting and planned)
- Study to compare the efficacy and safety of Cartistem® and microfracture in patients with knee articular cartilage injury or defect (first study completed, follow-up studies recruiting and planned)
- The safety and the efficacy evaluation of Neurostem®-AD in patients with Alzheimer's disease (first study completed, follow-up studies recruiting and planned)

2 Materials

2.1 Isolation

1. CB units in a multiple bag system containing citrate-phosphate-dextrose (CPD) (collected from the placenta in utero, written informed consent must be obtained before procurement) (*see* **Note 1**).
2. 15- and 50-ml polypropylene tubes.
3. Pasteur pipettes.
4. Ficoll-Paque Plus (1.078 g/ml).
5. Phosphate-buffered saline (PBS).
6. PBS-EDTA: PBS, 2 mM EDTA.

2.2 Culture

1. Six-well standard tissue culture plates.
2. T25, T75, or T175 cm^2 standard tissue culture flasks.
3. 15- and 50-ml polypropylene tubes.
4. Fetal bovine serum (FBS) (*see* **Note 2**).

5. Mesenchymal stem cell growth medium BulletKit (MSCGM™, commercially available MSC growth medium from Lonza) (*see* **Note 3**).
6. Trypsin/EDTA (0.04 %/0.03 %).

2.3 Cryopreservation of Expanded CB-MSC

1. Freezing medium: FBS/10 % DMSO (*see* **Note 4**).
2. 15- and 50-ml polypropylene tubes.
3. 2 ml cryotubes.
4. Freezing container with a freeze rate of −1 °C/min.

2.4 Characterization

2.4.1 CFU-f

1. Methanol.
2. Giemsa's azur eosin methylene blue solution.
3. Deionized water.

2.4.2 Flow Cytometry

1. Antibodies for flow cytometry (panel suggested to check for MSC markers and markers of contaminating cells (hematopoietic, endothelial)): Lineage (CD3, CD14, CD19, CD45, CD235a), CD29, CD31, CD73, CD90, CD105, CD106, HLA-ABC, HLA-DR (*see* **Note 5**).
2. 15- and 50-ml polypropylene tubes.
3. FACS tubes.
4. FcR blocking reagent.
5. 7-Aminoactin(7AAD).

2.4.3 Differentiation

1. Eight-chamber slides.
2. 15- and 50-ml polypropylene tubes.

   The following are commercially available Media (*see* **Notes 3** and **6**).
3. Osteogenic Induction Medium (hMSC Osteogenic BulletKit): Basal medium supplemented with SingleQuots of dexamethasone, l-glutamine, ascorbate, penicillin/streptomycin, MCGS, b-glycerophosphate in hMSC differentiation basal medium—osteogenic.
4. Adipogenic Induction Medium (hMSC Adipogenic Induction Medium): Basal medium supplemented with SingleQuots of h-insulin (recombinant), l-glutamine, MCGS, dexamethasone, indomethacin, IBMX (3-isobuty-l-methyl-xanthine), GA-1000.
5. Adipogenic Maintenance Medium (hMSC Adipogenic Maintenance): Basal medium supplemented with SingleQuots of h-insulin (recombinant), l-glutamine, MCGS, GA-1000.
6. Chondrogenic Induction Medium (hMSC Chondrogenic Induction): Basal medium supplemented with SingleQuots of dexamethasone, ascorbate, ITS + supplement, GA-1000, sodium pyruvate, proline, l-glutamine, freshly add TGF-b3 at a final concentration of 10 ng/ml.

7. 10 % formalin.
8. 5 % silver nitrate.
9. 1 % pyrogallol.
10. 5 % sodium thiosulfate.
11. Oil Red O Stock solution: 0.3 % Oil Red O in isopropanol, working solution: 0.18 % in distilled water; use within 30 min.
12. Mayer's hematoxylin.
13. Acetone.
14. 0.1 % aqueous Safranin O.
15. Weigert's iron hematoxylin.

3 Methods

3.1 Isolation

1. Decontaminate the external surfaces of the CB blood bag with 70 % ethanol.
2. Transfer 25 ml of CB from the collection bag to a 50-ml polypropylene tube.
3. Add 25 ml of PBS/EDTA. When appropriate, remove a small aliquot for cell counting and for sterility testing.
4. Add 10 ml of Ficoll-Paque Plus to a 50-ml polypropylene tube and carefully layer 25 ml of 1:1 diluted UCB on top.
5. Centrifuge 30 min at 430 × *g*, low acceleration and no brake.
6. Remove the plasma phase.
7. Using a sterile Pasteur pipette, carefully transfer the buffy coat interface into a new 50-ml polypropylene tube, and fill the tube with PBS/EDTA (*see* **Note 7**).
8. Centrifuge 10 min at 430 × *g*.
9. Wash with PBS/EDTA two to three times until the supernatant is clear (*see* **Note 8**).
10. Suspend the pellet in 10 ml complete medium and remove a small aliquot for counting mononuclear cells (MNC).
11. Seed the MNC at a density of 1×10^6 cells/cm^2 plastic surface into FBS-precoated 6-well plates.
12. Discard the non-adherent cells after 1–3 days of incubation and add fresh MSCGM™ every 3–4 days.
13. Monitor the culture for the presence of individual adherent fibroblastoid cells by phase-contrast microscopy for 14–30 days (*see* Fig. 1). Passage cells when they have reached 70 % confluency in primary culture.
14. If no colonies of fibroblastoid cells appear within 4–6 weeks, discard the culture.

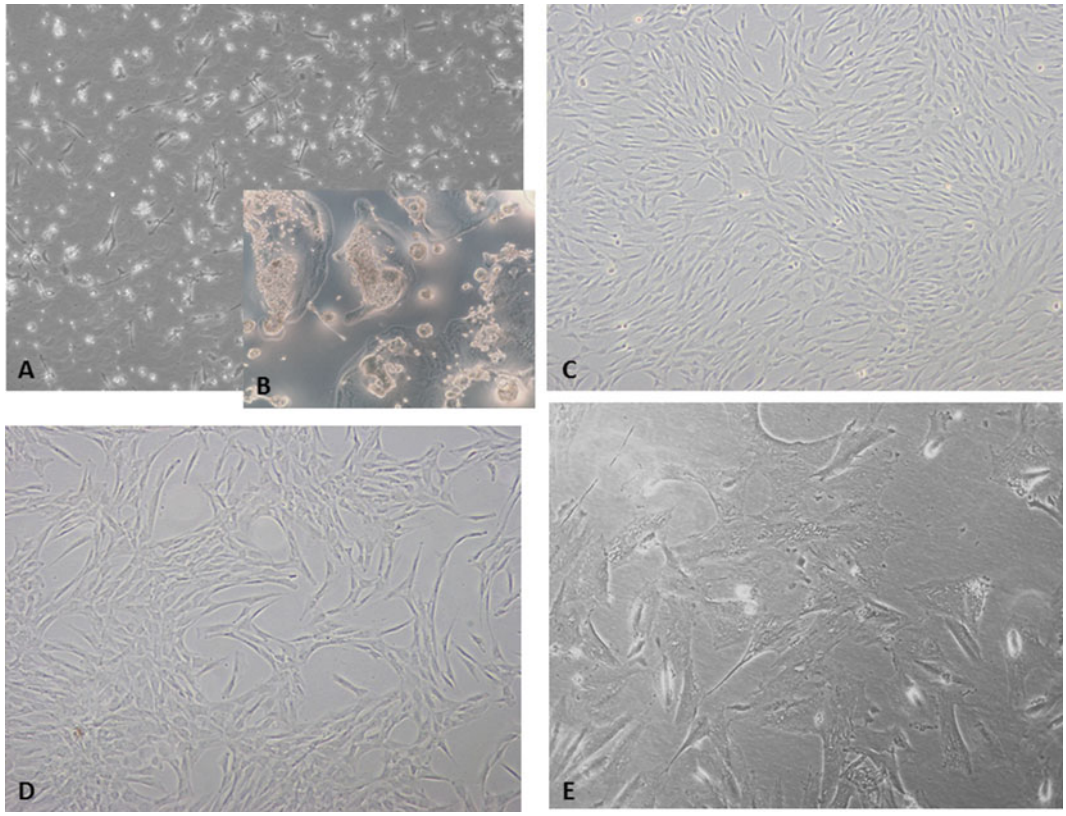

Fig. 1 Morphology of CB-MSC. (**a**) Micrograph of a CB-MNC culture approximately 7 days post-seeding—without FBS precoating. A variety of small, very slim cells have attached. These are mostly cells of the hematopoietic/myeloid lineages, which fuse to form (**b**) the osteoclast-like cells. Precoating with FBS can alter the adherence kinetics of these cells and enables the removal of a majority of contaminating cells. (**c**) Phenotype 1 of CB-MSC: typical MSC-like morphology. (**d**) Phenotype 2 of CB-MSC: more cuboidal shape, cells typically grow more mesh-like. (**e**) Senescent phenotype of CB-MSC indicated by larger cell size, abundance of stress fibers, reduced proliferation rates after approximately 40 cumulative population doublings

3.2 Culture

1. When cells reach approximately 70–80 % confluency, cells should be passaged (*see* **Note 9**).
2. Discard the used culture medium.
3. Rinse the cell layer once with pre-warmed PBS.
4. Add trypsin/EDTA to completely wet the monolayer and incubate at 37 °C for 5–10 min.
5. Add complete medium to neutralize the trypsin, and remove a small aliquot of the cell suspension for cell counting.
6. Replate cells at all subsequent passages with 700–1000 cells/cm^2 in MSCGM™ (*see* **Note 10**).

3.3 Cryopreservation (*See* **Note 4**)

1. When cells reach a subconfluent stage, detach cells using trypsin/EDTA (see above).
2. Count the cells.
3. Mix cells (1×10^6 CB-MSC) with 1-ml cold freezing medium.
4. Equilibrate cells for a few minutes.
5. Transfer cells into a freezing container that allows for a 1 °C/min cooling rate, and place in a −80 °C freezer for max. 24 h.
6. For long-term storage, transfer cells to liquid nitrogen containers, and store in the vapor phase of liquid nitrogen (−180 °C).

3.4 Characterization

3.4.1 Morphology and Phenotype (*See* **Note 2**)

1. Cultures should be continuously monitored to check phenotypic alterations or contaminants. MSC appear as spindle-shaped fibroblastoid cells.
2. As MSC reach a senescent stage, their shape becomes flatter, with the appearance of stress fibers (*see* Fig. 1e).

3.4.2 Expansion Potential

1. Perform cell counting and viability testing at each subculture.
2. To calculate fold expansion of cells, the total number of cells at different time points is divided by the number of cells used to initiate each culture.
3. To calculate cumulative population doublings, the population doubling rate is determined at each passage by using the following formula:

$$X = \left[\log 10(\mathrm{NH}) - \log 10(\mathrm{N1})\right] / \log 10(2)$$

where N1 is the plated cell number and NH is the cell number at harvest.

3.4.3 CFU-F Assay

1. The CFU-F assay can be performed with MSC at passage 1 or later to assess the precursor frequency. Plate serial dilutions (cell concentrations need to be optimized according to the individual conditions) into 6-well plates or T25 tissue culture-treated flasks in complete medium and incubate for 14 days.
2. Stain by removing medium, fixing the monolayer with methanol (5 min at room temperature), and then adding Giemsa solution.
3. Enumerate CFU-F colonies containing 40 or more cells microscopically.

3.4.4 Flow Cytometry (*See* **Note 5**)

1. At subculture, about 10^5 MSC per FACS tube are stained with the appropriate antibodies to detect the MSC phenotype as well as possible contamination with hematopoietic or endothelial cells.
2. Preincubate cells with FcR blocking reagent.

3. Stain with pre-titrated antibodies for 15–30 min at 4 °C.
4. Wash two times with PBS or FACS buffer.
5. Add titrated concentration of 7AAD; incubate for 10 min.
6. Measure the cells using a flow cytometer.

3.4.5 Differentiation Assays (Osteogenic, Adipogenic, Chondrogenic) (See **Note 6***)*

1. Evaluation of the differentiation potential of each culture at early and later time points is recommended.
2. For osteogenic and adipogenic induction, seed the appropriate number of MSC into well plates or chamber slides in complete medium: $3.1 \times 10^3/\text{cm}^2$ cells (osteogenesis) or $2.1 \times 10^4/\text{cm}^2$ (adipogenesis) MSC on to eight-chamber slides.
3. Upon reaching a subconfluent (osteogenesis) or postconfluent (adipogenesis) stage, half of the cultures are subjected to the inducing conditions. The other half of the cultures is maintained in MSCGM™ to serve as a negative control.
4. For osteogenesis, after 3 weeks with biweekly change of medium, fix the cells with 10 % formalin for 15 min at room temperature, and stain for 10–15 min with 5 % silver nitrate. Develop the stain in 1 % pyrogallol and then fix with 5 % sodium thiosulfate for 5 min.
5. For adipogenesis, perform three cycles of induction/maintenance. For each cycle, feed the MSC with adipogenic induction medium and culture for 3–4 days, and then switch to adipogenic maintenance medium for 3–4 days. Adipogenic differentiation is indicated by the formation of neutral lipid-vacuoles stainable with Oil Red O. For the Oil Red O stain, fix the cells with 10 % formalin, wash, and stain with a working solution of 0.18 % Oil Red O for 5 min. Remove staining solution with tap water. Counterstain the nuclei with Mayer's hematoxylin solution.
6. For chondrogenic differentiation, cells are cultured in a micromass culture. Therefore, 2.5×10^5 cells are centrifuged in a 15-ml polypropylene tube at $150 \times g$ to form a free-floating pellet. Culture the micromass without disturbing the pellet for 4 weeks in 0.5 ml of complete chondrogenic differentiation medium including 10 ng/ml TGFb-3. Feed the cells twice a week. After the culture period, make cryosections and stain with Safranin O. For the staining, fix the sections with ice-cold acetone and stain with 0.1 % aqueous Safranin O for 5 min. Counterstain the nuclei with Weigert's iron hematoxylin.

Further assays can be performed to quality control CB-MSC. In-process, sterility controls are recommended, including mycoplasma testing. It has recently become routine to perform karyotype analyses to check for chromosomal abnormalities. Depending on the final goal, some groups assess the immunomodulatory capacities or test differentiation into other lineages.

4 Notes

1. CB-MSC isolation is hampered by low recovery frequency. As already indicated in the introduction, we suggest using CB units as fresh as possible and as large and cell rich as possible. Select units of good quality without thrombi and signs of hemolysis [11]. A 90 % isolation success has been achieved by selecting cord blood units larger than 90 ml and stored less than 2 h after birth [17].
2. CB-MSC isolation is hampered by the adherence of myeloid cells forming osteoclast-like cells (Fig. 1a, b). We validated that FBS precoating improves the MSC isolation efficiency by altering the adherence kinetics of myeloid cells [11]. For the plastic precoating, add a sufficient volume of FBS to wet the entire bottom of the culture plate or flask. Incubate the plate/flask for 30 min at room temperature. Then remove all FBS, use the plate directly, or store it for max of 1 week at 4 °C.

   An alternative method is to deplete contaminating cells by, e.g., immunomagnetic strategies. Methods include the depletion of CD34+, or lineage marker-positive cells by RosetteSep™ (CD3, CD14, CD19, CD38, CD66b, and glycophorin A; StemCell Technologies), which in fact reduce the number of osteoclast-like cells. Other strategies focus on enriching putative precursors, e.g., CD271+ cells. Both methods, however, fail to significantly modify the isolation success of CB-MSC [17, 37, 38].

   CB-MSC can grow in two slightly differing morphologies and densities. One is the typical fibroblastoid morphology. These cells in general grow to form a confluent monolayer. The other type is a more cuboidal shape, and most often these cells grow in a more mesh-like pattern and do not form confluent layers (Fig. 1c, d). Compared to MSC from other tissue sources, CB-MSC are smaller (diameter is approx. 18–19 μm compared to 20–21 μm for BM-MSC, Fig. 2a, b).
3. A variety of different commercial MSC media kits are on the market, both for expansion and differentiation. We initially tested a few and achieved better success rates with the MSCGM™ medium. Detailed protocols for using the respective media can be found at the manufacturer's homepages.

   To avoid the use of fetal bovine serum, it is also possible to isolate CB-MSC in cell culture medium (DMEM or alpha-MEM) supplemented with pooled human platelet lysate [39]. Fully GMP-compliant processing procedures have been developed [40, 41].
4. It is recommended to bank early passages of MSC by cryopreservation. A cell density of 1×10^6 CB-MSC in 1 ml of freezing medium works well in our hands. Densities, however,

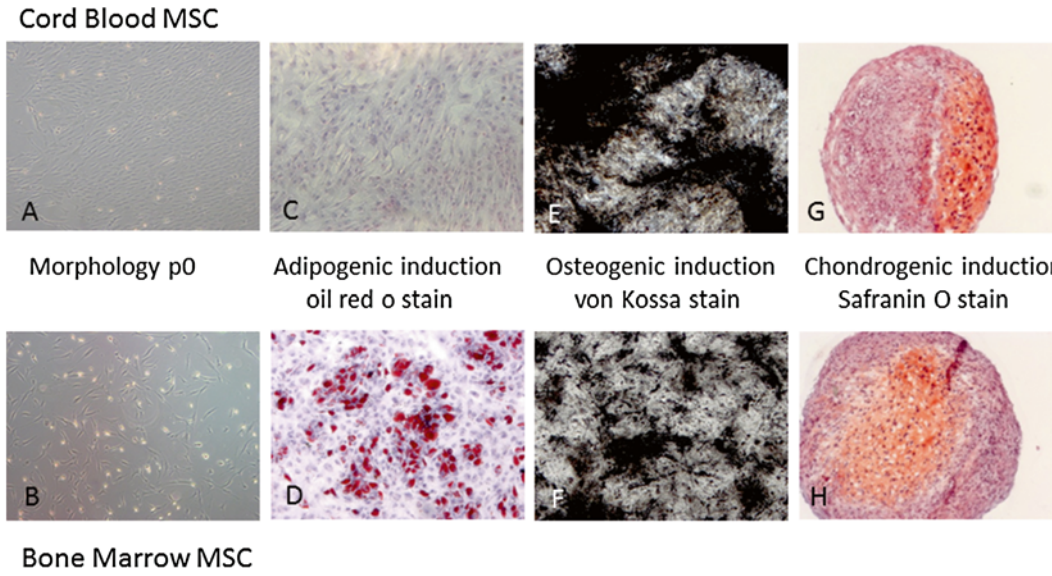

Fig. 2 Adipogenic and osteogenic differentiation. Top row **a**, **c**, **e**, **g**: CB-MSC. Bottom row **b**, **d**, **f**, **h**: BM-MSC. (**a**, **b**) CB-MSC are smaller than BM-MSC. This figure also illustrates the higher proliferation of MSC at very subconfluent stages comparing **b** to **a**: small, round cells and slightly detached cells prepare to undergo mitosis. (**c**, **d**) Oil Red O stain of cells after 3 weeks of adipogenic induction: no occurrence of lipid-filled vacuoles in CB-MSC. Of note, even in BM-MSC, only a fraction of the cells responds to adipogenic stimuli with the production of lipid-filled vacuoles. (**e**, **f**) von Kossa staining of calcium deposits after osteogenic induction. (**g**, **h**) Safranin O binds to glycosaminoglycans after chondrogenic induction showing an *orange-red* color. Please note that not all areas in the micromass pellet have generated glycosaminoglycans

should be optimized according to your needs. The same holds true for the freezing medium. We use 10 % DMSO in FBS, but 10 % DMSO in MSCGM™ medium works as well.

Some publications indicate that it is even possible to isolate MSC from cryopreserved CB units [42].

5. Surface proteins are used to characterize MSC and to check for the presence of contaminating cells such as endothelial or hematopoietic cells [43]. Initial minimal criteria included the expression of CD105, CD73, and CD90 and the lack of expression of CD45, CD34, CD14 or CD11b, CD79alpha or CD19, and HLA-DR [44]. We have added more markers in order to identify possible similarities and differences between cord blood, adipose tissue, and bone marrow-derived MSC.
6. As mentioned in **Note 3**, a number of different commercial suppliers offer medium solutions for MSC characterization. These also include MSC differentiation media. Detailed protocols for the use of the media as well as staining protocols are available online as well.

   In contrast with MSC from other tissue sources, CB-MSC fail to differentiate into the adipogenic lineage, or, if at all, very

rarely and with only a few cells [7, 11, 12, 21]. *See* Fig. 2c, d for adipogenic induction and e, f for osteogenic induction.

7. Careful harvest of the buffy coat interface significantly improves the isolation efficacy of CB-MSC. Take care to collect as little as possible of the plasma and the Ficoll fluid phase.
8. If there is a high contamination with erythrocytes, one can add ammonium chloride lysis buffer (10×: 1.55 M NH_4Cl; 0.1 M NH_4HCO_3; 1 mM EDTA in 1 l distilled water). Fill the tube with fresh cold lysis buffer, invert for ~10 min at room temperature until the liquid phase is clear red, and centrifuge at 4 °C for 10 min at 430 × *g*.
9. The MSC are contact inhibited and thus should be subcultured before entering a confluent stage. We recommend that the monolayer reaches 70–80 % confluency when cells are passaged.
10. Seeding the MSC at low cell densities better maintains the multipotent mesenchymal progenitor cells and enables high proliferation rates within one cell passage [45]. We thus recommend seeding CB-MSC at a density of 700–1000 cells/cm^2. Depending on your conditions, seeding densities should be optimized.

Acknowledgment

This work was supported by the German Jose-Carreras Leukemia-Foundation e.V., DJCLS-R03/18, the German Ministry of Education and Research (BMBF) 01GN0531 and 01GN0939, and by the European Community, LSHB-CT-2005-018999.
We greatly acknowledge the work of Susanne Pilopp née Kern, Andrea Hecker, Cora Ecker, Susanne Elvers-Hornung, and Stephanie Uhlig. P.N. was supported by the "Stiftung Transfusionsmedizin und Immunhämatologie."

References

1. Bieback K, Wuchter P, Besser D et al (2012) Mesenchymal stromal cells (MSCs): science and F(R)Iction. J Mol Med (Berl) 90: 773–782
2. Keating A (2012) Mesenchymal stromal cells: new directions. Cell Stem Cell 10:709–716
3. Prockop DJ, Oh JY (2012) Medical therapies with adult stem/progenitor cells (MSCs): a backward journey from dramatic results in vivo to the cellular and molecular explanations. J Cell Biochem 113:1460–1469
4. Phinney DG, Sensebe L (2013) Mesenchymal stromal cells: misconceptions and evolving concepts. Cytotherapy 15:140–145
5. Sherman LS, Munoz J, Patel SA et al (2011) Moving from the laboratory bench to patients' bedside: considerations for effective therapy with stem cells. Clin Transl Sci 4:380–386
6. Lee OK, Kuo TK, Chen WM et al (2004) Isolation of multipotent mesenchymal stem cells from umbilical cord blood. Blood 103:1669–1675

7. Kern S, Eichler H, Stoeve J et al (2006) Comparative analysis of mesenchymal stem cells from bone marrow, umbilical cord blood, or adipose tissue. Stem Cells 24:1294–1301
8. Bieback K, Brinkmann I (2010) Mesenchymal stromal cells from human perinatal tissues: from biology to cell therapy. World J Stem Cells 2:81–92
9. Crisan M, Yap S, Casteilla L et al (2008) A perivascular origin for mesenchymal stem cells in multiple human organs. Cell Stem Cell 3:301–313
10. Roufosse CA, Direkze NC, Otto WR et al (2004) Circulating mesenchymal stem cells. Int J Biochem Cell Biol 36:585–597
11. Bieback K, Kern S, Klueter H et al (2004) Critical parameters for the isolation of mesenchymal stem cells from umbilical cord blood. Stem Cells 22:625–634
12. Bieback K, Klueter H (2007) Mesenchymal stromal cells from umbilical cord blood. Curr Stem Cell Res Ther 2:310–323
13. Wexler SA, Donaldson C, Denning-Kendall P et al (2003) Adult bone marrow is a rich source of human mesenchymal "stem" cells but umbilical cord and mobilized adult blood are not. Br J Haematol 121:368–374
14. Romanov YA, Svintsitskaya VA, Smirnov VN (2003) Searching for alternative sources of postnatal human mesenchymal stem cells: candidate MSC-like cells from umbilical cord. Stem Cells 21:105–110
15. Javed MJ, Mead LE, Prater D et al (2008) Endothelial colony forming cells and mesenchymal stem cells are enriched at different gestational ages in human umbilical cord blood. Pediatr Res 64:68–73
16. Perdikogianni C, Dimitriou H, Stiakaki E et al (2008) Could cord blood be a source of mesenchymal stromal cells for clinical use? Cytotherapy 10:452–459
17. Zhang X, Hirai M, Cantero S et al (2011) Isolation and characterization of mesenchymal stem cells from human umbilical cord blood: reevaluation of critical factors for successful isolation and high ability to proliferate and differentiate to chondrocytes as compared to mesenchymal stem cells from bone marrow and adipose tissue. J Cell Biochem 112: 1206–1218
18. Lee M, Jeong SY, Ha J et al (2014) Low immunogenicity of allogeneic human umbilical cord blood-derived mesenchymal stem cells in vitro and in vivo. Biochem Biophys Res Commun 446:983–989
19. Hare JM, Fishman JE, Gerstenblith G et al (2012) Comparison of allogeneic vs autologous bone marrow-derived mesenchymal stem cells delivered by transendocardial injection in patients with ischemic cardiomyopathy: the Poseidon randomized trial. JAMA 308:2369–2379
20. Alagesan S, Griffin MD (2014) Autologous and allogeneic mesenchymal stem cells in organ transplantation: what do we know about their safety and efficacy? Curr Opin Organ Transplant 19:65–72
21. Karagianni M, Brinkmann I, Kinzebach S et al (2013) A comparative analysis of the adipogenic potential in human mesenchymal stromal cells from cord blood and other sources. Cytotherapy 15:76–88
22. Ragni E, Vigano M, Parazzi V et al (2013) Adipogenic potential in human mesenchymal stem cells strictly depends on adult or foetal tissue harvest. Int J Biochem Cell Biol 45:2456–2466
23. Kluth SM, Buchheiser A, Houben AP et al (2010) Dlk-1 as a marker to distinguish unrestricted somatic stem cells and mesenchymal stromal cells in cord blood. Stem Cells Dev 19:1471–1483
24. Kim J, Shin JM, Jeon YJ et al (2012) Proteomic validation of multifunctional molecules in mesenchymal stem cells derived from human bone marrow, umbilical cord blood and peripheral blood. PLoS One 7:e32350
25. Castro-Manrreza ME, Mayani H, Monroy-Garcia A et al (2014) Human mesenchymal stromal cells from adult and neonatal sources: a comparative in vitro analysis of their immunosuppressive properties against T cells. Stem Cells Dev 23:1217–1232
26. Pievani A, Scagliotti V, Russo FM et al (2014) Comparative analysis of multilineage properties of mesenchymal stromal cells derived from fetal sources shows an advantage of mesenchymal stromal cells isolated from cord blood in chondrogenic differentiation potential. Cytotherapy 16:893–905
27. Stubbendorff M, Deuse T, Hua X et al (2013) Immunological properties of extraembryonic human mesenchymal stromal cells derived from gestational tissue. Stem Cells Dev 22:2619–2629
28. Ragni E, Montemurro T, Montelatici E et al (2013) Differential microrna signature of human mesenchymal stem cells from different sources reveals an "environmental-niche memory" for bone marrow stem cells. Exp Cell Res 319:1562–1574
29. Lv F, Lu M, Cheung KM et al (2012) Intrinsic properties of mesenchymal stem cells from human bone marrow, umbilical cord and umbilical cord blood comparing the different sources of Msc. Curr Stem Cell Res Ther 7:389–399
30. Kang BJ, Ryu HH, Park SS et al (2012) Comparing the osteogenic potential of canine mesenchymal stem cells derived from adipose tissues, bone marrow, umbilical cord blood, and Wharton's Jelly for treating bone defects. J Vet Sci 13:299

31. Jin HJ, Bae YK, Kim M et al (2013) Comparative analysis of human mesenchymal stem cells from bone marrow, adipose tissue, and umbilical cord blood as sources of cell therapy. Int J Mol Sci 14:17986–18001
32. Bosch J, Houben AP, Hennicke T et al (2013) Comparing the gene expression profile of stromal cells from human cord blood and bone marrow: lack of the typical "bone" signature in cord blood cells. Stem Cells Int 2013:631984
33. Akimoto K, Kimura K, Nagano M et al (2013) Umbilical cord blood-derived mesenchymal stem cells inhibit, but adipose tissue-derived mesenchymal stem cells promote, glioblastoma multiforme proliferation. Stem Cells Dev 22:1370–1386
34. Secunda R, Vennila R, Mohanashankar AM et al (2014) Isolation, expansion and characterisation of mesenchymal stem cells from human bone marrow, adipose tissue, umbilical cord blood and matrix: a comparative study. Cytotechnology 2014 May 6. [Epub ahead of print]
35. Martins AA, Paiva A, Morgado JM et al (2009) Quantification and immunophenotypic characterization of bone marrow and umbilical cord blood mesenchymal stem cells by multicolor flow cytometry. Transplant Proc 41:943–946
36. Yoo KH, Jang IK, Lee MW et al (2009) Comparison of immunomodulatory properties of mesenchymal stem cells derived from adult human tissues. Cell Immunol 259:150–156
37. Hutson EL, Boyer S, Genever PG (2005) Rapid isolation, expansion, and differentiation of osteoprogenitors from full-term umbilical cord blood. Tissue Eng 11:1407–1420
38. Attar A, Ghalyanchi Langeroudi A, Vassaghi A et al (2013) Role of Cd271 enrichment in the isolation of mesenchymal stromal cells from umbilical cord blood. Cell Biol Int 37:1010–1015
39. Reinisch A, Bartmann C, Rohde E et al (2007) Humanized system to propagate cord blood-derived multipotent mesenchymal stromal cells for clinical application. Regen Med 2:371–382
40. Aktas M, Buchheiser A, Houben A et al (2010) Good manufacturing practice-grade production of unrestricted somatic stem cell from fresh cord blood. Cytotherapy 12:338–348
41. Pham PV, Vu NB, Pham VM et al (2014) Good manufacturing practice-compliant isolation and culture of human umbilical cord blood-derived mesenchymal stem cells. J Transl Med 12:56
42. Lee MW, Choi J, Yang MS et al (2004) Mesenchymal stem cells from cryopreserved human umbilical cord blood. Biochem Biophys Res Commun 320:273–278
43. Rojewski MT, Weber BM, Schrezenmeier H (2008) Phenotypic characterization of mesenchymal stem cells from various tissues. Transfus Med Hemother 35:168–184
44. Dominici M, Le Blanc K, Mueller I et al (2006) Minimal criteria for defining multipotent mesenchymal stromal cells. The International Society for Cellular Therapy position statement. Cytotherapy 8:315–317
45. Sekiya I, Larson BL, Smith JR et al (2002) Expansion of human adult stem cells from bone marrow stroma: conditions that maximize the yields of early progenitors and evaluate their quality. Stem Cells 20:530–541

Chapter 15

Isolation, Expansion, and Immortalization of Human Adipose-Derived Mesenchymal Stromal Cells from Biopsies and Liposuction Specimens

Luigi Balducci and Giulio Alessandri

Abstract

Human adipose tissue has proven to be an abundant, accessible, and rich source of adult mesenchymal stromal cells, suitable for tissue engineering and regenerative medicine. However, a major complication in fully investigating these cells may derive from their limited life span.

Although methods to isolate, expand, and immortalize these cells have been widely reported in the literature, exhaustive explanations on the problems that can be encountered during these processes and how these can be solved have never been described. It is of fundamental importance to follow a common protocol to achieve reliable and reproducible results. Here, we describe a protocol to isolate and expand human adipose stromal cells from specimens obtained from tissue biopsies and liposuction surgical interventions. Finally, we broadly describe the cell immortalization technique, and particular attention is paid to some of the apparently "secondary" aspects.

Key words Human adipose tissue, Fat biopsy, Liposuction, Enzymatic digestion, Isolation, Stromal vascular fraction, Adipose-derived stromal cells, Expansion, Immortalization

1 Introduction

Human adipose tissue represents an abundant and accessible source of mesenchymal stromal cells (MSCs) [1]. The advantages of isolating and expanding human adipose-derived stromal cells (hASCs) is linked to the possibility of obtaining large amounts of fat biopsies with minimally invasive procedures and greater stem cell yields compared to other tissue sources such as the bone marrow [2], skeletal muscle [3], skin [4], and periodontal ligaments [5]. Moreover, the adipose tissue obtained from liposuction interventions that are routinely discarded represents another source of fat specimens [6].

Massimiliano Gnecchi (ed.), *Mesenchymal Stem Cells: Methods and Protocols*, Methods in Molecular Biology, vol. 1416,
DOI 10.1007/978-1-4939-3584-0_15,

Many efforts have been made and still continue to be made to further characterize hASCs and to ascertain their potential applications in regenerative medicine [7, 8].

hASCs can be easily isolated and expanded by using a general protocol in three main steps: a digestion process, a neutralization procedure, and a centrifugation phase. After sample mincing, the fragments are digested with collagenase I at 37 °C for at least 30 min. The digestion time is affected by several factors (tissue weight or volume, tissue composition, fragment size, etc.). Following the neutralization of the enzyme, a stromal vascular fraction (SVF) is obtained. The SVF consists of a heterogeneous mesenchymal cell population comprising not only hASCs but also endothelial cells, erythrocytes, fibroblasts, lymphocytes, macrophages, and pericytes [9, 10]. A double wash and centrifugation partially eliminates erythrocytes, lymphocytes, and macrophages from the digested material. Finally, the SVF is then seeded into culture resulting in the adhesion of a subset of elongated cells which can be further purified over time to obtain hASCs. This cell population includes multipotent cells with the ability to differentiate into osteoblasts, adipocytes, and chondroblasts [9, 11, 12].

Although the isolation and expansion of hASCs seem quite simple, their limited life span hampers not only their investigation in preclinical studies but also the exhaustive evaluation of their therapeutic potential. Indeed, like all adult cell types, these cells significantly decrease cell growth after a limited number of in vitro cell passages due to a cellular process termed replicative senescence [13, 14]. Thus, immortalization represents an interesting methodology to overcome this problem. As a consequence, it is possible to obtain cells with a prolonged life span with similar phenotypic and functional characteristics of primary hASCs [15, 16]. Therefore, immortalized hASCs may be very useful to expand preclinical findings and to further understand their therapeutic efficacy.

In this chapter, we will describe the isolation and expansion procedures in detail, step by step from either biopsies or liposuction samples. Moreover, we will report two possible methodologies to immortalize hASCs. Although both approaches are based on a lentiviral cotransduction system, some differences between the two are evidenced.

Finally, we list several notes that come from our own experience and other literature data for successful hASC isolation, expansion, and immortalization.

2 Materials

1. PBS 1×: phosphate-buffered saline, without Ca and Mg, pH 7.4. Sterile filtered for cell culture.

2. PBS+P/S: PBS containing 5 % penicillin/streptomycin (v/v). Add 25 ml of penicillin (10,000 U/ml) and streptomycin (10 mg/ml) solution to 475 ml of sterile PBS 1×.
3. Surgical scissors and tongs: sterilize by autoclaving. Alternatively, wrap the surgical devices with aluminum foil and heat at 200 °C for 2 h in a laboratory oven.
4. Collagenase I digestion solution 0.25 % (w/v): dissolve the lyophilized enzyme in PBS 1× to obtain a 0.25 % solution (i.e., 0.25 g in 100 ml PBS 1×). Add 0.25 g of bovine serum albumin (BSA) to further stabilize the enzyme after reconstitution. Sterilize the solution under a flow laminar cabinet by filtering through a 0.22 μm filter membrane. Aliquot and store at −20 °C. Avoid repeated freezing and thawing since enzyme activity decreases after reconstitution. By adding an equal volume of collagenase I digestion solution 0.25 % to the sample, a 0.13 % (w/v) working solution is obtained.
5. DNase I solution: prepare a DNase I stock solution (2344 U/ml) by dissolving the lyophilized enzyme in DMEM medium. Prepare a working solution by diluting the stock solution 1:100. Aliquot and store at −20 °C. Avoid repeated freezing and thawing. Add 0.2 ml of working solution to the sample.
6. Orbital shaker or rotator: pre-warm an orbital shaker at 37 °C to perform the digestion. A rotation of 250 rpm should be applied to ensure thorough mixing. Alternatively, use a rotator in a 37 °C incubator.
7. Cell strainer: sterile 70 μm pore size strainer for use with falcon 50 ml conical tubes.
8. Culture medium: DMEM/F-12 supplemented with 10 % FBS, 100 U/ml penicillin, 0.1 mg/ml streptomycin, 2 mM l-glutamine, and 2 ng/ml of b-FGF.
9. Trypsin/EDTA solution 0.25 mg/ml.
10. Freezing medium (FM): 90 % FBS and 10 % dimethyl sulfoxide (DMSO). For a total volume of 10 ml FM, add 1 ml DMSO to 9 ml FBS. Store at −20 °C until use. Thaw immediately before use.
11. Lentiviral vectors: pLenti-hTERT (human telomerase reverse transcriptase gene), pLenti-SV40 (simian virus 40 gene), and pLenti-HPV-16 E6/E7 (human papillomavirus-16 E6/E7 genes).
12. Hexadimethrine bromide (polybrene): prepare a stock solution by dissolving the powder into PBS 1× to obtain a 8 mg/ml final concentration. Sterilize the solution by filtering with a 0.22 μm filter. Store at +4 °C until use.

3 Methods

It is mandatory to preserve sterility throughout the entire process. Thus, the use of sterile tools and reagents, as well as antibiotics, is strongly recommended. Whenever possible, sterile single-use devices (falcon tubes, Petri dishes, pipettes, etc.) should be employed.

3.1 Informed Consent

Before human specimen sampling, it is necessary to obtain informed written consent from patients.

In addition, the privacy of human donors undergoing surgical procedures must be maintained (*see* **Note 1**).

3.2 Sample Delivery and Storage

Place the human adipose tissue biopsy into a falcon tube containing about 20 ml DMEM/F-12 supplemented with antibiotics (*see* **Note 2**). Screw the cap and put the tube into a refrigerated container.

Lipoaspirates deriving from tumescent liposuction (*see* **Note 3**) are collected in single-use sterile bags by using a sterile cannula. Put the bag into a refrigerated container.

In general, keep the human sample refrigerated during delivery (*see* **Note 4**).

If not immediately processed, both the biopsies and the lipoaspirates can be stored at 2–8 °C but for no longer than 24 h before use.

3.3 Nomenclature and Processing

Before processing, assign an acronym to the sample for unambiguous identification.

For lipoaspirate:

1. Record its volume (*see* **Note 5**).
2. Dilute the lipoaspirate sample with an equal volume of PBS+P/S and aliquot the suspension into falcon tubes.
3. Centrifuge at 700 × *g* for 5 min (*see* **Note 6**).
4. Recover the lipid phase from the top and dilute with an equal volume of PBS+P/S.
5. Centrifuge at 700 × *g* for 5 min.
6. Collect the lipid phase and perform the enzymatic digestion (see below).

For tissue biopsy:

1. Weigh the sample under sterile conditions and record its weight.
2. Place the sample in a Petri dish with 10 ml of PBS+P/S.
3. By using sterile tongs and scissors or single-use scalpels, remove the connective tissue.

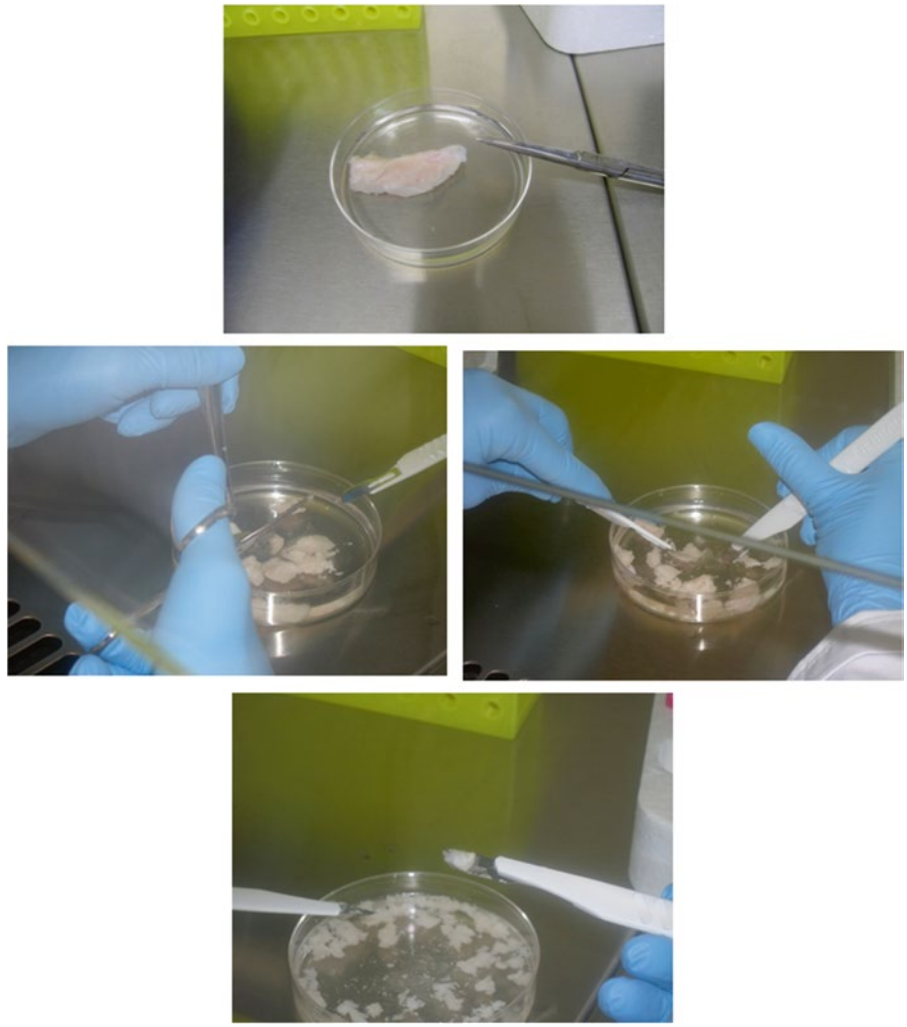

Fig. 1 Adipose tissue processing. After connective tissue removal, the sample is minced using sterile tongs, scissors, and scalpels to obtain small fragments

4. Wash with PBS+P/S three times to remove red blood cells.
5. Add 10 ml PBS+P/S.
6. Mince the sample to obtain small tissue fragments (Fig. 1).
7. Pipette the sample up and down with a 25 ml pipette several times to further homogenize.
8. Centrifuge at 700 × *g* for 5 min.
9. After centrifugation, three phases will be distinguishable: an upper yellow phase (fat), a middle red phase, and a lower pellet (Fig. 2a). Discard the middle red phase with a 10 ml pipette (Fig. 2b).
10. Measure the resting volume and perform the enzymatic digestion (see below).

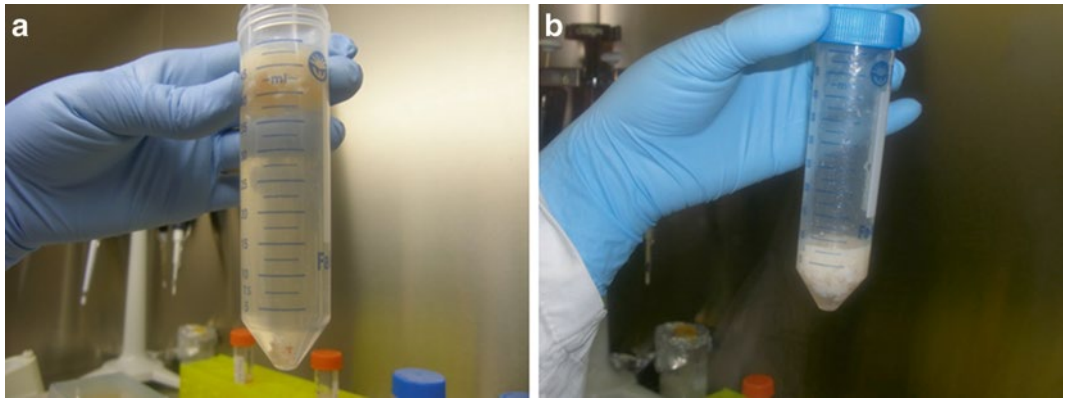

Fig. 2 Adipose tissue after centrifugation. (**a**) *Upper yellow*, middle, and lower pellet distinguishable phases. (**b**) Discard remaining material after middle phase

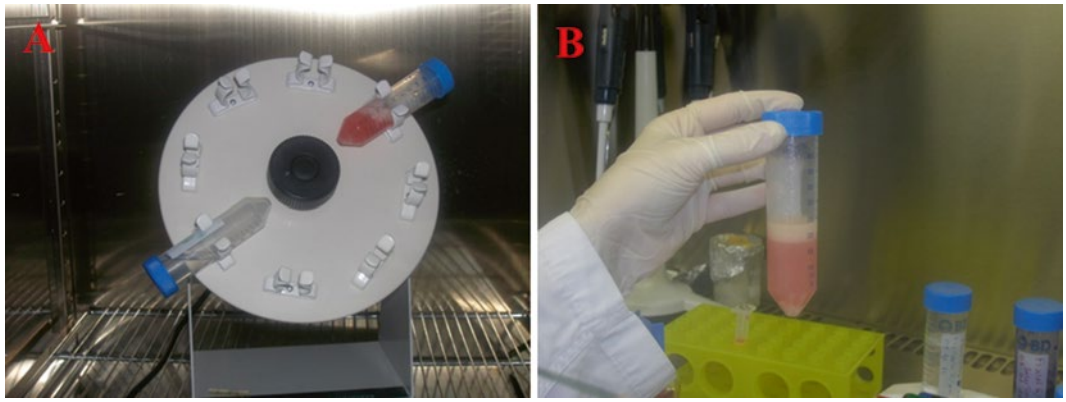

Fig. 3 Enzymatic digestion. (**a**) The mixture supplemented with collagenase I is put on an orbital shaker to ensure thorough mixing and incubated at 37 °C for 1 h. (**b**) Digested material after 1 h is incubated at 37 °C

3.4 Enzymatic Digestion

1. After the lipid fraction volume (either lipoaspirate or tissue sample) has been measured, add an equal amount of collagenase I digestion solution 0.25 % (w/v) (*see* **Note 7**).
2. Add 0.2 ml DNase I working solution (*see* **Note 8**).
3. Incubate the mixture at 37 °C for 1 h (*see* **Note 9**). Put the mixture on an orbital shaker or a rotator to ensure through mixing (Fig. 3).

3.5 Neutralization

1. After incubation, add an equal volume of DMEM/F-12 supplemented with 20 % FBS to neutralize the collagenase I activity.
2. Filter the cell suspension by using a 70 μm cell strainer to eliminate the undigested fragments (Fig. 4).

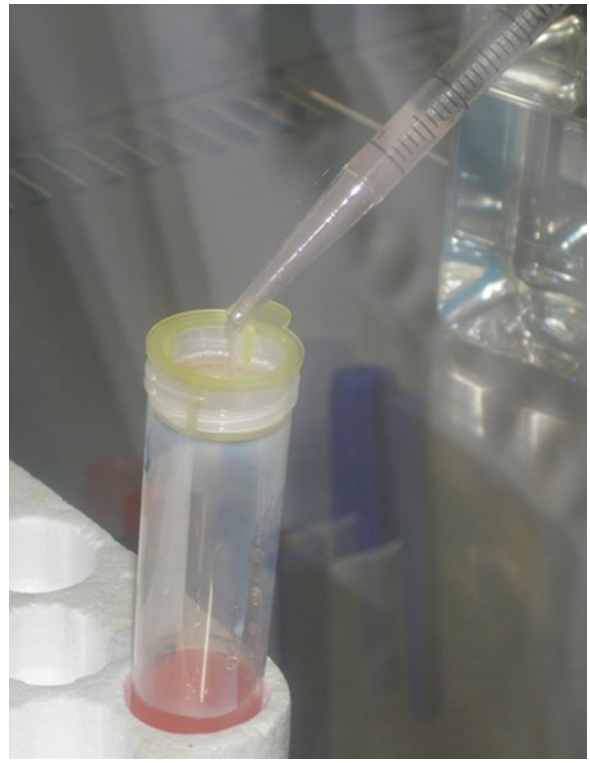

Fig. 4 Filtering. After enzymatic digestion and neutralization, the cell suspension is filtered through a 70 μm cell strainer to eliminate the undigested fragments

3.6 Centrifugation and Resuspension

1. Centrifuge at 700 × *g* for 5 min.
2. Aspirate and discard the supernatant.
3. Resuspend the pellet in 10 ml of culture medium.
4. Centrifuge at 700 × *g* for 5 min.
5. Aspirate and discard the supernatant.
6. Depending by the size of the pellet, resuspend it in an adequate volume of culture medium (5–10 ml) (Fig. 5).
7. Take an aliquot of cell suspension (0.02 ml) to observe under an inverted microscope (*see* **Note 10**).

3.7 Plating

Depending on the cell number, plate the cell suspension as follows:

1. 2 ml/well of cell suspension in a 12 well plate (*see* **Note 11**).
2. Alternatively, 5 ml/T25 flask of cell suspension.
3. Incubate at 37 °C, 5 % CO_2.

3.8 Culture and Expansion

1. After 72 h, gently aspirate the medium and add fresh medium.
2. Observe the cells under an inverted microscope.

Fig. 5 Residual material after centrifugation. After two washes, the remaining pellet is resuspended in an adequate volume of culture medium

3. Incubate at 37 °C, 5 % CO_2 and allow the cells to reach ~80 % confluence.
4. At confluence, aspirate the medium and gently wash cells once with pre-warmed 1× PBS.
5. Add trypsin/EDTA solution 0.25 mg/ml (1 ml/well or 3 ml/T25 flask).
6. Incubate for 2 min at 37 °C, 5 % CO_2 to detach cells (*see* **Note 12**).
7. Add an equal volume of FBS 20 % (v/v).
8. Transfer the cell suspension to a falcon tube.
9. Centrifuge at 700 × *g* for 5 min.
10. Aspirate and discard the supernatant.
11. Resuspend the pellet in 10 ml of culture medium (*see* **Note 13**).
12. Take an aliquot of cell suspension (0.02 ml) and count cells by staining with trypan blue and using a hemocytometer.
13. Seed at a cell density of 16,000 cells/cm^2.
14. Incubate at 37 °C, 5 % CO_2.
15. Change the medium every 48 h (Fig. 6).

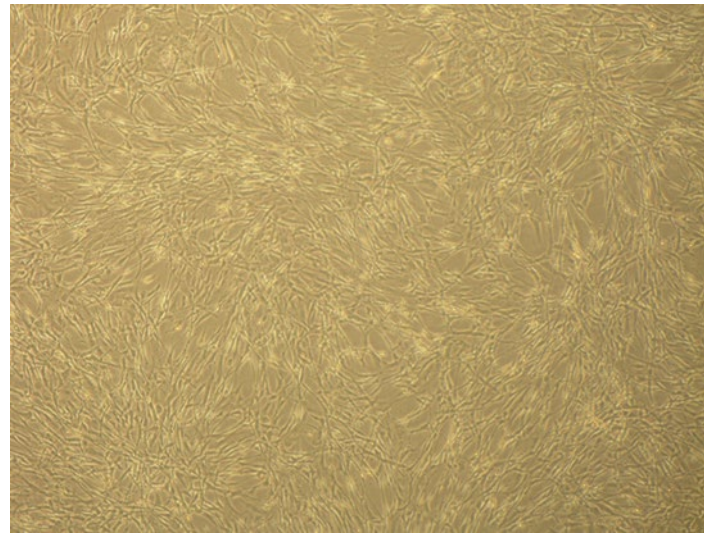

Fig. 6 hASCs in culture. Representative image of cells after 5 weeks of culture. Magnification 4×

3.9 Freezing and Thawing

hASCs should be harvested at 80 % confluence for freezing.

1. Remove the culture medium.
2. Wash twice with pre-warmed 1× PBS.
3. Add trypsin/EDTA solution 0.25 mg/ml (3 ml/T25 flask, 4 ml/T75 flask).
4. Incubate for 2 min at 37 °C, 5 % CO_2 to detach cells.
5. Add an equal volume of FBS 20 % (v/v).
6. Transfer the cell suspension to a falcon tube.
7. Centrifuge at 700 × *g* for 5 min.
8. Aspirate and discard the supernatant.
9. Resuspend the pellet in 10 ml of culture medium.
10. Count cells as described above.
11. Centrifuge at 700 × *g* for 5 min.
12. Discard the medium and gently shake the pellet.
13. Resuspend the pellet to obtain 1.7–2.0 × 10^6 cells/ml FM.
14. Aliquot cell suspension at 1 ml/vial.
15. Freeze at –20 °C for 2 h (*see* **Note 14**).
16. Freeze at –80 °C for 4 h (*see* **Note 15**).
17. Store the vials in liquid nitrogen.
18. Before starting the thawing procedure, prepare a 37 °C pre-warmed bath.

19. Depending on the number of cells to be thawed, prepare one or more T75 flasks.
20. Add 10 ml/T75 culture medium.
21. Incubate the flask(s) at 37 °C, 5 % CO_2 for at least 10 min.
22. Rapidly extract the cryovial(s) from liquid nitrogen.
23. Put the cryovial(s) in the 37 °C pre-warmed bath (*see* **Note 16**).
24. Aspirate with a 2 ml pipette the cell suspension and put in T75 flask.
25. Observe the cell suspension under an inverted microscope.
26. Incubate the flask(s) at 37 °C, 5 % CO_2.
27. After 3–4 h, observe cells under an inverted microscope.
28. Change the medium after 24 h (*see* **Note 17**).

3.10 Cell Transduction and Immortalization

1. Prepare a cell suspension as follows: 0.3×10^6 cells in 12 ml culture medium.
2. Seed 2 ml/well of cell suspension, in each well of a six-well tissue culture plate to obtain a 5.0×10^3 cells/cm^2 cell density (~ 50.0×10^3 cells/well).
3. Incubate at 37 °C, 5 % CO_2 until they reach 70–80 % confluence, and then perform viral transduction as reported below (*see* **Note 18**).
4. Immediately prior to transduction procedure, thaw the lentiviral supernatant in a 37 °C water bath (*see* **Note 19**).
5. Prepare 12 ml pLenti-hTERT transduction mix by resuspending the viral supernatant in pre-warmed fresh culture medium to obtain a 20 MOI (multiplicity of infection) final value (*see* **Note 20**).
6. Add 8 μg/ml polybrene (*see* **Note 21**).
7. Replenish the cell culture medium with 2 ml/well transduction mix.
8. Incubate for 24 h at 37 °C, 5 % CO_2 (*see* **Note 22**).
9. The next day, remove the transduction mix and add 2 ml/well fresh pre-warmed medium.
10. Incubate transduced cells at 37 °C, 5 % CO_2 for 3 days.
11. After this incubation, remove the culture medium.
12. Wash twice with pre-warmed 1× PBS and detach cells with 1 ml/well trypsin/EDTA.
13. As previously reported, neutralize trypsin with 20 % FBS, centrifuge, and resuspend cells in fresh medium.
14. Count the cells.

15. Take 0.6×10^6 hTERT-transduced cells and resuspend in a final volume of 24 ml culture medium (*see* **Note 23**).
16. Seed 2 ml/well cell suspension, in each well of two six-well tissue culture plates. Incubate at 37 °C, 5 % CO_2 until they reach 65–70 % confluence.
17. Immediately prior to the transduction procedure, thaw the pLenti-SV40 and pLenti-HPV-16 E6/E7 viral supernatants in a 37 °C water bath.
18. Prepare 12 ml pLenti-SV40 transduction mix and 12 ml pLenti-HPV-16 E6/E7 transduction mix (20 MOI for each mix).
19. Add 8 μg/ml polybrene.
20. Take one six-well tissue culture plate containing hTERT-transduced cells.
21. Replenish the cell culture medium with 2 ml/well pLenti-SV40 transduction mix. Incubate for 24 h at 37 °C, 5 % CO_2.
22. Take the second six-well tissue culture plate containing hTERT-transduced cells.
23. Replenish the cell culture medium with 2 ml/well pLenti-HPV-16 E6/E7 transduction mix. Incubate for 24 h at 37 °C, 5 % CO_2.
24. The next day, remove the transduction mix from both plates and add 2 ml/well fresh pre-warmed medium.
25. Incubate cotransduced cells at 37 °C, 5 % CO_2 for 3 days.
26. After this incubation, remove the culture medium.
27. Culture and expand cotransduced cells as reported in Subheading 3.8.
28. Calculate the PDL (population doubling level) values at each passage (*see* **Note 24**).

4 Notes

1. An informed consent signed by the patient is mandatory before obtaining human specimens. This document should be approved by an ethical committee and should describe in depth the purpose of the procedure. Moreover, it should clarify that there are no risks for the donors.

   To assure donor privacy, a document reporting the sample code and the medical record number, but not the donor name and surname, should be used. In addition, this document should report donor age and gender, negativity for potential infectious hazardous agents (i.e., viruses), and the signature of the surgeon performing the surgical intervention.

2. It is particularly important to supplement the medium with antibiotics whenever the sampling site is affected by an inflammatory process. It is possible to add 10 % antibiotics (v/v) to secure the sample.
3. Ultrasound-assisted liposuction partially damages the adipose tissue, thus yielding a lower frequency of proliferating hASCs compared to tissue resection and tumescent liposuction [17].
4. Low temperature (+4 °C) will delay damaging processes and better preserves the sample integrity. Do not use dry ice to deliver the sample, since this will freeze the specimen!
5. The volume or weight recording allows an estimation of the final yield, and this parameter can be applied to other procedures. However, it should be kept in mind that other parameters (i.e., donor age and gender) other than volume or weight can affect the final yield.
6. According to some investigators, using a centrifugation speed of $1200 \times g$ allows optimal cell recovery [18]. Based on our own experience, a lower centrifugation speed ($700 \times g$) is sufficient to separate the three phases.
7. It is possible to double the amount of collagenase I, thus reaching a working concentration of ~0.17 % (w/v). This increase does not affect tissue digestion and may be useful when the sample contains a lot of fibrotic tissue.
8. DNase I hydrolyzes DNA deriving from broken nuclei. This DNA could cause cell clustering and, at least in part, hamper the subsequent filtration.
9. The incubation time at 37 °C to perform the enzymatic digestion can range from 0.5 to 2 h. Indeed, it is mainly related to the quantity of tissue that must be digested and the relatively high presence of fibrotic tissue. Control the digestion process at regular intervals. Do not exceed 2 h.
10. The presence of contaminating elements (i.e., undigested fibers, other cell types, etc.) might hamper microscope observation. However, it may provide a partial estimate of the cell number, thus avoiding too low of a cell density during the plating phase.
11. When a multiwell plate is used to seed the cell suspension, fill the untapped wells with 1× PBS. This will counteract growth medium evaporation and potential contamination at the same time.
12. Be careful when incubating the cells with trypsin. Indeed, too long of an incubation can damage the cells.
13. The FBS contained in the growth medium can be increased to 25 %; however, this may promote premature adipogenesis [19]. Moreover, in the presence of high FBS percentages, cells

may retain some FBS protein in their cytoplasm; and this may elicit an immunologic response in vivo [20]. Based on our own experience, using a 10 % final concentration of FBS is an optimal cell culture condition.

14. Pay extreme attention to not exceed two hours at –20 °C. In fact, this may irreversibly damage the cells and, anyhow, strongly reduce cell viability. To avoid this, freezing boxes are commercially available.
15. Contrary to the above reported note, the incubation time at –80 °C is not critical and can be prolonged. However, storing the cell suspension in liquid nitrogen will assure cell viability for long periods and avoid problems due to electricity blackouts.
16. Be extremely careful during this operation since the cryovial might explode! The thawing time must not exceed 3 min. Do not entirely thaw the cell suspension, and leave a small amount frozen.
17. DMSO is potentially toxic to cells and may alter their metabolism. Alternatively, cells can be diluted in culture medium, centrifuged at 700 × *g* for 5 min, and resuspended in fresh medium prior to plating.
18. Do not exceed confluence percentage, as too high of values could negatively affect transduction efficiency.
19. Remove the lentiviral supernatant from the bath immediately when thawed. Indeed, prolonged heating may damage lentiviral particles and decrease transduction efficiency. In addition, very concentrated lentiviral supernatants (small volumes and high titers) are also commercially available. If using such viral suspensions, they can be rapidly thawed at room temperature and immediately used to prepare the transduction mix.
20. Although lentiviruses are safer than retroviruses, using a biosafety level 2 (BL2) facility is strongly recommended.

    The MOI represents the ratio of viral particles infecting a single cell. Obviously, this value only defines a statistical distribution, since some cells may receive more lentiviral particles than others and vice versa. According to our own experience with hASC transduction, an MOI of 20 represents a good compromise between effective transduction and cell viability. Indeed, too high of an MOI may be toxic for the cells.
21. Polybrene is a small, positively charged molecule that binds to cell surfaces and neutralizes surface charge and greatly enhances transduction by lentiviruses. However, it can be toxic for cells. Avoid high polybrene concentrations and prolonged exposure times.

22. During the incubation, remove the plate from the incubator every hour and gently rock the plate by hand for approximately 15–20 s, taking care not to spill the transduction mix. This procedure allows a higher transduction efficiency.
23. Several findings could explain why a cotransduction procedure is mandatory to obtain immortalized hASCs. First, we previously reported that our attempt to use hTERT alone to immortalize hASCs failed [15]. Additional bibliographic evidence has well established that ectopic expression of viral oncogenes such as SV-40 allows primary cells to overcome replicative senescence only for a limited time before entering into a second non-replicative phase called "crisis" [21]. This limitation in the immortalization process of human cells can be circumvented by the reconstitution of the telomerase activity. Indeed, it has been shown that overexpression of hTERT allows SV40 T-Ag-transformed cells, derived from different tissues, to bypass the crisis step and to promote an indefinite life span [22]. Similarly, the E7 oncoprotein from the human papillomavirus type 16 (HPV E7) has also been reported as a factor promoting human cell immortalization [23], but immortalization by HPV-E7 is a rare event. In contrast, co-expression of HPV E7 and hTERT was shown to increase the frequency of immortalization of human keratinocytes [24].

    Finally, at least in part, our suggested order of cotransducing the cells (with hTERT first and then SV-40 or E6/E7) is

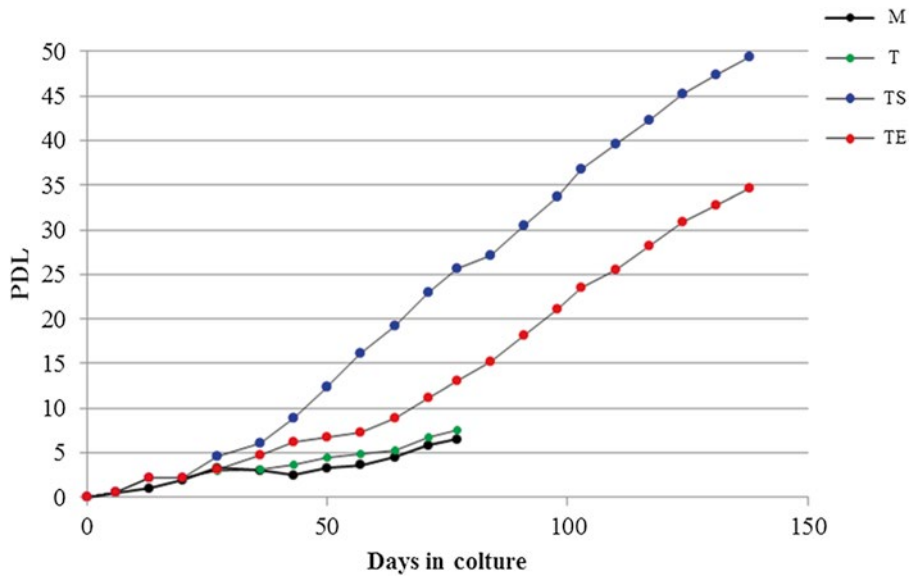

Fig. 7 PDL performance over time. Schematic diagram obtained calculating the PDL of not transduced (M), hTERT-transduced (T), hTERT/SV40-cotransduced (TS), and hTERT/E6-E7-cotransduced cells. Note that TS and TE cells increase their PDL value over time, while M and T cells do not

based on previous studies showing that the order and timing of gene transduction influences genomic stability [25].

24. The PDL calculation is fundamental to verify that cell immortalization has been successfully performed (Fig. 7). Indeed, passage number (n) refers only to cell transfer from one culture vessel to another but not necessarily to cell proliferation. Instead, a constant increase in PDL values confirms that cells have a prolonged life span and do not senesce.

    Calculate the PDL with the following formula:

$$\mathrm{PDL} = \sum \mathrm{PD}$$

$$\mathrm{PD}_{\left[N/(N-1)\right]} = \left[\log\left(Nn / Nn - 1\right)\right] / \log 2$$

where PD = population doubling gained at each passage, n = cell passage, $n-1$ = previous cell passage, Nn = cell number at passage n, and $Nn-1$ = number of cells plated at passage $n-1$.

References

1. Zuk PA, Zhu M, Ashjian P et al (2002) Human adipose tissue is a source of multipotent stem cells. Mol Biol Cell 13:4279–4295
2. Friedenstein AJ, Petrakova KV, Kurolesova AI et al (1968) Heterotopic of bone marrow. Analysis of precursor cells for osteogenic and hematopoietic tissue. Transplantation 6:230–247
3. Alessandri G, Pagano S, Bez A et al (2004) Isolation and culture of human muscle-derived stem cells able to differentiate into myogenic and neurogenic cell lineages. Lancet 364: 1872–1883
4. Toma JG, McKenzie IA, Bagli D et al (2005) Isolation and characterization of multipotent skin-derived precursors from human skin. Stem Cells 23:727–737
5. Seo BM, Miura M, Gronthos S et al (2004) Investigation of multipotent postnatal stem cells from human periodontal ligament. Lancet 364:149–155
6. Gimble J, Guilak F (2003) Adipose-derived adult stem cells: isolation, characterization, and differentiation potential. Cytotherapy 5:362–369
7. Bourin P, Bunnell BA, Casteilla L et al (2013) Stromal cells from the adipose tissue-derived stromal vascular fraction and culture expanded adipose tissue-derived stromal/stem cells: a joint statement of the International Federation for Adipose Therapeutics and Science (IFATS) and the International Society for Cellular Therapy. Cytotherapy 15:641–648
8. Mizuno H, Tobita M, Uysal AC (2012) Concise review: adipose-derived stem cells as a novel tool for future regenerative medicine. Stem Cells 30:804–810
9. Zuk PA, Zhu M, Muzuno H et al (2001) Multilineage cells from human adipose tissue: implications for cell-based therapies. Tissue Eng 7:211–228
10. Astori G, Vignati F, Bardelli S et al (2007) "In vitro" and multicolor phenotypic characterization of cell subpopulations identified in fresh human adipose tissue stromal vascular fraction and in the derived mesenchymal stem cells. J Transl Med 5:55
11. Li H, Zimmerlin L, Marra KG et al (2011) Adipogenic potential of adipose stem cell subpopulations. Plastic Recon Surg 128:663–672
12. Erickson GR, Gimble JM, Franklin DM et al (2002) Chondrogenic potential of adipose tissue-derived stromal cells in vitro and in vivo. Biochem Biophys Res Commun 290:763–769
13. Serrano M, Blasco MA (2001) Putting the stress on senescence. Curr Opin Cell Biol 13:748–753
14. Campisi J (2001) Cellular senescence as a tumor-suppressor mechanism. Trends Cell Biol 11:S27–S31
15. Balducci L, Blasi A, Saldarelli M et al (2014) Immortalization of human adipose-derived

stromal cells: production of cell lines with high growth rate, mesenchymal marker expression and capability to secrete high levels of angiogenic factors. Stem Cell Res Ther 5:63

16. Clynes M (2014) Cell culture models for study of differentiated adipose cells. Commentary Stem Cell Res Ther 5:137
17. Oedayrajsingh-Varma MJ, van Ham SM, Knippenberg M et al (2006) Adipose tissue-derived mesenchymal stem cell yield and growth characteristics are affected by the tissue-harvesting procedure. Cytotherapy 8:166–177
18. Yoshimura K, Shigeura T, Matsumoto D et al (2006) Characterization of freshly isolated and cultured cells derived from the fatty and fluid portions of liposuction aspirates. J Cell Physiol 208:64–76
19. Bunnell BA, Flaat M, Gagliardi C et al (2008) Adipose-derived stem cells: isolation, expansion and differentiation. Methods 45:115–120
20. Spees JL, Gregory CA, Singh H et al (2004) Internalized antigens must be removed to prepare hypoimmunogenic mesenchymal stem cells for cell and gene therapy. Mol Ther 9:747–756
21. Shay JW, Wright WE, Werbin H (1991) Defining the molecular mechanisms of human cell immortalization. Biochim Biophys Acta 1072:1–7
22. Halvorsen TL, Leibowitz G, Levine F (1999) Telomerase activity is sufficient to allow transformed cells to escape from crisis. Mol Cell Biol 19:1864–1870
23. Zwerschke W, Jansen-Durr P (2000) Cell transformation by the E7 oncoprotein of human papillomavirus type 16: interactions with nuclear and cytoplasmic target proteins. Adv Cancer Res 78:1–29
24. Kiyono T, Foster SA, Koop JI et al (1998) Both Rb/p16INK4a inactivation and telomerase activity are required to immortalize human epithelial cells. Nature 396:84–88
25. O'Hare MJ, Bond J, Clarke C et al (2001) Conditional immortalization of freshly isolated human mammary fibroblasts and endothelial cells. Proc Natl Acad Sci U S A 98:646–651

Chapter 16

Optimization of Mesenchymal Stem Cells to Increase Their Therapeutic Potential

Minh Quan Vu, Shant Der Sarkissian, Melanie Borie, Pierre-Olivier Bessette, and Nicolas Noiseux

Abstract

The heart which has limited renewal and regenerative capacity is a prime target for cellular therapy. Stem cell transplantation has emerged as a promising therapeutic strategy to improve healing of the ischemic heart, repopulate the injured myocardium, and restore cardiac function. However, clinical usefulness is impacted by the quality and quantity of delivered cells, the suboptimal manipulations prior to transplantation, and the general poor viability of the cells transferred particularly to an ischemic microenvironment. Focus is now on developing new ways to enhance stem cell renewal and survival capacity before transplant. This can be done by physical, chemical, pharmacological, or genetic manipulation of cells followed by accurate evaluation of conditioning methods by validated tests.

This chapter covers the proper handling of mesenchymal stem cells (human and rat lines) and methodologies to evaluate efficacy and the translational potential of conditioning methods. Specifically, we will cover stem cell culture methods, preconditioning protocols, viability assessment in hypoxic and oxidative challenges as encountered in an ischemic microenvironment, and the proliferative capacity of cells.

Key words Preconditioning, Mesenchymal stem cells, Regenerative medicine, Viability, Proliferation, Myocardial infarct, Cardiovascular disease

1 Introduction

Despite medical advances and improvements in drug therapy, cardiac surgery and cardiology, cardiac injury is usually irreversible. As a therapeutic option, transplantation of stem cells can repair the infarcted heart and improve cardiac function as shown in animal and human studies. Many mechanisms have been proposed to explain improvements in cardiac function including paracrine factors [1–5], which are found in the stem cell culture medium (CM) [6, 7] and are responsible for activating important cellular pathways promoting angiogenesis [8], reducing apoptosis, and improving survival of resident cells in a stressed environment and promoting repair of the infarcted heart.

Massimiliano Gnecchi (ed.), *Mesenchymal Stem Cells: Methods and Protocols*, Methods in Molecular Biology, vol. 1416,
DOI 10.1007/978-1-4939-3584-0_16,

1.1 Limitation of Cell Therapy

A major limitation of stem cell therapy is the poor survival of cells once transplanted. Studies show that less than 1% of transplanted cells survive within a week after injection [9–11], and this may be due to the hostile ischemic microenvironment characterized by active inflammation, protein denaturation and proteases, massive necrosis, and lack of oxygen and nutrients [9–11].

A prime objective is to develop methods to optimize cell survival for transplantation thus improving their therapeutic effect. These methods include genetic manipulation [12, 13], physical or chemical means, or treatment with various medications. Pharmacological treatment includes exposing stem cells to compounds that activate mechanisms that can enhance their survival in stressful environments and/or increase their proliferative capacity for scalability purposes. This process, known as preconditioning, attempts to maximize the biological and functional properties of transplanted stem cells. Many molecules have been proposed as useful preconditioning agents such as oxytocin [14–21] or celastrol [22–24].

This chapter summarizes protocols that we have developed on handling mesenchymal stem cells and evaluating conditioning compounds for clinical translation. We cover methods for isolating and culturing stem cells, testing the efficacy of conditioning molecules in enhancing stem cell viability after oxidative and hypoxic challenges, evaluating the proliferative capacity of stem cells treated with conditioning molecules, and assessing the safety of conditioning compounds by evaluating maintenance of stem cell differentiation potential and cell surface markers.

Our objective with this chapter is to guide future research in stem cell therapy optimization and enable testing and discovery of novel conditioning compounds and methods.

1.2 Mesenchymal Stem Cells

In areas of cardiovascular regeneration, mesenchymal stem cells (MSCs) are widely used, and many advantages support their use. These include:

- MSCs show low immunogenicity [25], allowing autologous and allogeneic transplantation.
- The most common source for isolating MSCs is the bone marrow (BM) [26], but they may also be isolated from other sources such as skeletal muscle biopsies or fetal cardiomyocytes [27]. BM-MSCs are present at a ratio of 1:10,000 bone marrow mononuclear cells [28].
- MSCs are easily expandable ex vivo, providing almost unlimited pools of transplanted cells and can be genetically engineered.
- MSCs are multipotent and able to differentiate into multiple mesodermal lineages depending on the environment

(adipocytes, osteocytes, and chondrocytes [29]). This translineage transformation property is called *plasticity*. Evidence suggests that they may transdifferentiate into cardiomyocytes and vascular cells [30].

- To date, MSCs have been used safely [31] without any report of malignant transformation.
- MSCs secrete a variety of biological factors that promote angiogenesis and establish a favorable regenerative environment at the site of tissue injury/damage. Paracrine signaling is a proposed mechanism of these therapeutic effects [1, 3]. Growth factors and cytokines released in the MSC culture medium (MSC-CM) can also be concentrated and used therapeutically.

MSC characteristics:

- Negative for hematopoietic surface markers (CD34, CD45, CD14, CD19, CD133, CD31, CD79a, HLA-DR [31, 32]).
- Positive for CD63, CD166, CD54, CD55, CD13, and CD44, with high levels (>95 %) of CD105, CD73, and CD90 [28].
- MSCs attach to plastic surfaces and proliferate under standard culture conditions.
- MSCs grow more rapidly when passaged at low densities.
- MSCs differentiate in vitro to osteocytes, adipocytes, or chondrocytes under specific well-defined differentiation conditions.

2 Materials

2.1 MSCs Isolated from

1. Sprague-Dawley male rats from *Charles-Rivers Laboratories*.
2. Isolated from human donor marrow or purchased from *Lonza*.

2.2 Media

1. Culture medium: Minimum Essential Medium alpha (αMEM) or Dulbecco's Modified Eagle Medium (DMEM) supplemented with 10 % fetal bovine serum (FBS) and 1 % penicillin-streptomycin (P-S). For cell conditioning, use αMEM supplemented with 0.2 % serum (αMEM 1×, 0.2 % FBS, 1 % P-S). For the oxidative challenge, use αMEM supplemented with 1 % serum (αMEM 1×, 1 % FBS, 1 % P-S).
2. Human mesenchymal stem cell basal medium (MSCBM): commercially available and used for human MSC maintenance and expansion.
3. Adipogenic induction medium: DMEM high glucose, 10 % FBS, L-glutamine, P-S, 10 μg/mL of Humulin R 100 U/mL, 1 μM of dexamethasone, 0.5 μM IBMX (3-isobutyl-1-methylxanthine), and 60 μM indomethacin.

4. Adipogenic maintenance medium: DMEM high glucose, 10 % FBS, L-glutamine, P-S, 10 μg/mL Humulin R 100 U/mL.
5. Osteogenic induction medium: DMEM high glucose, 10 % FBS, L-glutamine, P-S, 0.1 μM dexamethasone, 10 mM β-glycerophosphate, and 50 μM ascorbic acid:

2.3 Other Materials

1. Dimethylsulfoxide (DMSO).
2. Phosphate-buffered saline, pH 7.4 (PBS).
3. Ficoll-Paque.
4. Trypsin (TrypLE express).
5. Plastic culture plates/dishes: 10 cm petri dishes, 24-, 48-, and 96-well plates.
6. P20-1000 pipettes and multichannel pipettes.
7. Water-jacketed incubator kept at 37 °C and 21 % O_2, 5 % CO_2.
8. Airtight hypoxia chamber.
9. LIVE/DEAD® Viability/Cytotoxicity Assay Kit.
10. PrestoBlue® Cell Viability Reagent.
11. CyQUANT® Cell Proliferation Assay Kit.
12. Hoechst 33342 dye.
13. Trypan blue.
14. Fluorescence-activated cell sorting (FACS) reagents:
    - PBS Buffer, pH 7.4, 0.1 % sodium azide, and 0.02 % BSA.
    - Human FcR blocking reagent.
    - Polystyrene tube (sterilized) 12 × 75 mm.
    - Antibodies (antihuman): CD31, CD34, CD45, CD133/1, CD133/2, CD144
15. Differentiation kits (chondrogenic, adipogenic, and osteogenic).
16. Conditioning molecules (synthetic, natural).

3 Methods

3.1 Isolation and Culture of Rat MSCs (Same Principle for Mice)

1. MSCs are isolated from adult Sprague-Dawley male rat hindlimb bone marrow. Aspirate bone marrow using 18G needles and transfer aspirate to a 50 mL tube containing 10 mL of αMEM medium supplemented with 10 % FBS.
2. Bone marrow mononuclear cells (BMNCs) are isolated by Ficoll-Paque gradient centrifugation:
    - Filter medium containing bone marrow cells with 100 μm filter.
    - Complete with 35 mL sterile PBS.

- Add 14 mL of Ficoll-Paque, and centrifuge for 30 min at 400 × *g*.
- Collect the interphase (approximately 15 mL), and add PBS to interphase to bring volume to 50 mL.
- Centrifuge for 10 min at 100–200 × *g*.
- Discard supernatant and wash the pellet with PBS; centrifuge at 100–200 × *g* for 5 min.
- Repeat wash centrifugation step.
- Resuspend the pellet in 10 mL of αMEM containing 10 % FBS and transfer to 10 mm culture dish (*see* **Note 1**).
- After 48 h, the medium is aspirated and non-adherent cells are discarded.

3. Subculturing: Stem cells are expanded in αMEM containing 10 % FBS.
   - Aspirate the medium, wash once with warm PBS, add 3 mL pre-warmed TrypLE express trypsin (into 10 centimeters petri dishes), and return to the incubator for 5 min. Added trypsin has to fully cover the platted cell surface.
   - Gently tap the culture dish to dislodge cells and visualize detachment under a microscope.
   - When >90 % of cells are detached, add 7 mL of pre-warmed αMEM containing 10 % FBS to the trypsinated cell suspension and transfer the medium to a 15 mL tube:
     - Centrifuge 200 × *g* for 10 min.
     - Resuspend the pellet in 1 mL of pre-warmed αMEM containing 10 % FBS.
   - At this point, determine the total number of cells and percent viability using a hemocytometer, cell counter, and trypan blue exclusion.
   - Cell culture can now be expanded and seeded at a density of 5000/cm^2 in 10 cm petri dishes in 10 mL αMEM containing 10 % FBS . Cells are passaged every 2–3 days (*see* **Note 2**) or frozen for future use.
4. Freezing cells: Following trypsinization and counting steps as described above, aliquot cells at the desired density, add DMSO (dilute 1:10) to the cellular concentrate and transfer to labeled cryovials. Place cryovials in freezing container and transfer to −80 °C overnight and later transfer to −150 °C (*see* **Note 3**).
5. Thawing cells: Rewarm frozen cells briefly (*see* **Note 4**). Gently pour pre-warmed culture medium on top of the frozen aliquot. Centrifuge 200 × *g* for 3 min, aspirate the supernatant, and resuspend cells in pre-warmed αMEM containing 10 % FBS.

3.2 Isolation and Culture of Human MSCs

1. Bone marrow-derived cells can be harvested after obtaining written consent from the donor according to protocols approved by the ethics review board.
2. Bone marrow aspirates are taken from the patient's iliac crest under local anesthesia, collected into heparinized normal saline solution, and processed the same day.
3. Isolation is performed by Ficoll-Paque gradient centrifugation in the same manner as for murine bone marrow-derived stem cells (steps described in Subheading 1.2) (*see* **Note 5**).
4. Subculturing, freezing, and thawing steps are identical to those described above for murine cells except that cells are maintained in human mesenchymal stem cell basal medium (MSCBM).
5. Bone-marrow-derived human MSCs can also be commercially purchased, subcultured, frozen, and thawed according to the steps described above using human mesenchymal stem cell basal medium (MSCBM).

3.3 Conditioning

1. MSC maintained in αMEM containing 10 % FBS is trypsinated, plated using a multichannel pipette into 96-well plates at a density of 4000 cells per well, and incubated at 37 °C (*see* **Note 6**).
2. The next day, the medium is gently aspirated and replaced with low-serum αMEM (0.2 % FBS, 1 % P-S) for synchronization (*see* **Note 7**).
3. Conditioning agent is added to the culture medium (1×10^{-10} M to 1×10^{-6} M). Because serum may affect cellular responses and mask effects specific from the conditioning, molecules are diluted in low or no serum medium.
4. Different exposure times are evaluated to search for the optimal response (*see* **Note 8**).
5. Each experimental and control condition is assayed in triplicate at least.

3.4 Testing the Efficacy of the Conditioning Agents

In order to test the efficacy of the conditioning molecules, following the conditioning step, MSCs are oxygen and serum deprived (<1 % O_2 and 0–0.2 % FBS) or incubated in medium containing H_2O_2 in order to reproduce the hypoxic and oxidative ischemic myocardium environment.

3.4.1 Oxidative Challenge (H_2O_2)

Following the conditioning step, wells are gently washed three times with pre-warmed αMEM containing 1 % FBS.

- Cells are allowed to recuperate for 30 min in αMEM containing 1 % FBS.
- Cells are then challenged by incubation with αMEM supplemented with 1 % FBS and containing 0 mM to 4 mM H_2O_2 for 60 min.

- Cells are then gently washed twice with warm αMEM containing 1 % FBS and allowed to recuperate for 30 min before the viability assay.

3.4.2 Hypoxic Challenge

Following the conditioning step, wells are gently washed three times with pre-warmed αMEM containing 1 % FBS. Control and treated cells are incubated under normoxic or hypoxic conditions in αMEM containing 0–0.2 % FBS (*see* **Note 9**).

- Hypoxia (<1 % oxygen) is achieved by placing culture plates in an airtight hypoxia chamber and flushed twice for 10 minutes with an hour interval in between at a flow rate of 10–15 L per minute with a gas mixture of 5 % CO_2 balanced with 95 % N_2 [33].
- After 24, 48, and 72 h of incubation, plates are assayed for viability.

3.5 Viability Assay

The LIVE/DEAD Viability/Cytotoxicity Assay Kit offers visual results and allows quantification of viability as well as mortality. Many alternatives exist such as the trypan blue exclusion protocol or PrestoBlue cell viability reagent, and these may be used following the manufacturer's protocol.

LIVE/DEAD kit

This assay is applicable to most eukaryotic cell types; calcein AM (*see* **Note 10**) recognizes intracellular esterase activity in living cells, and the ethidium homodimer (*see* **Note 11**) assesses plasma membrane integrity by entering damaged membranes and binding to nucleic acids:

1. Cell preparation and staining:
   - Adherent cells are cultured as described previously.
   - Test for the optimal concentration of LIVE\DEAD reagent. We found that the concentrations of 2 μM calcein AM and 4 μM EthD-1 solution for MSC prepared in αMEM containing 1 % FBS are optimal.
2. Perform the viability assay:
   - After challenge with stressors (as described above), replace medium with 100 μL of the prepared LIVE/DEAD assay solution in each well using a multichannel pipette (*see* **Note 12**).
   - Incubate cells for 60 min at 37 °C (*see* **Note 13**).
3. View using a fluorescence microscope:
   - Optimal filters used: Calcein is compatible using fluorescein optical filter 530 ± 12.5 nm, and EthD-1 is compatible with 645 ± 20 nm.

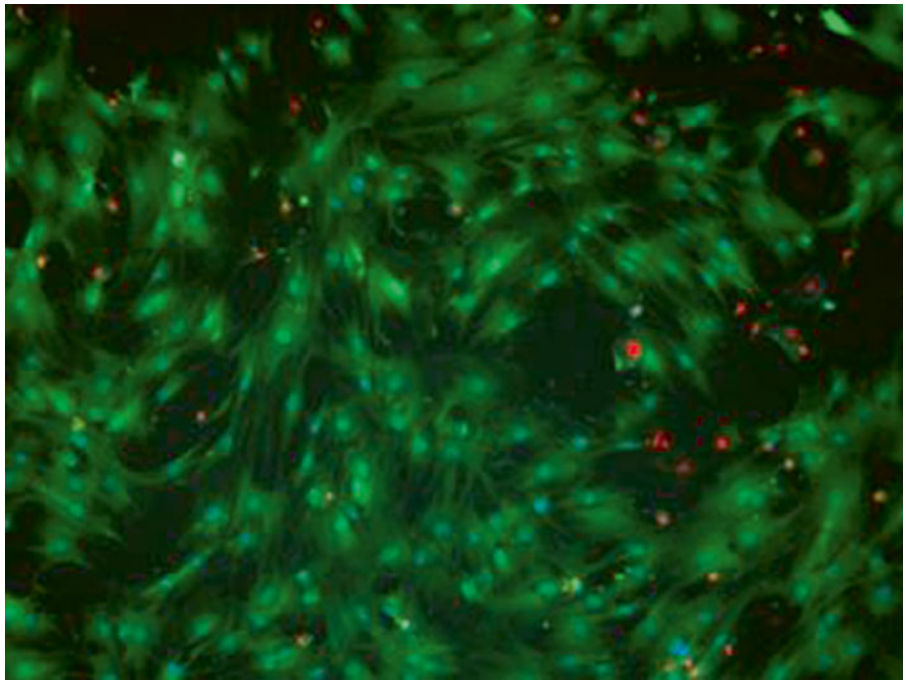

Fig. 1 Representative fluorescent images of LIVE/DEAD viability assay in MSC incubated under hypoxic conditions for 48 h. Living cells are *green* and dead cells are *red*

4. Pictures of living cells (green) and dead cells (red) are taken using a camera mounted on a fluorescence microscope (*see* Fig. 1).
5. Results are quantified using *Image J* software (http://rsbweb.nih.gov/ij/).
6. Cell count (green for living cells and red for dead cells) is done by *Image J*.
7. The relative measure of viability/mortality is calculated according to the total number of cells visualized by Hoechst staining (*see* **Note 14**).
8. Tests are conducted at least three times and values averaged: PrestoBlue.
9. After challenge with stressors (as described above), add 10 μL of PrestoBlue Cell Viability Reagent (*see* **Note 15**) to 90 μL of αMEM containing 1 % FBS.
10. After 60 min of incubation, viability is quantified by fluorescence acquisition using a plate reader equipped with appropriate excitation and emission filters.

3.6 Proliferation Assay

As viability is important to assess the response of stem cells to stress, it is also important to quantify their proliferative capacity as stem cells.

Hoechst nuclei count:

Blue fluorescent Hoechst dyes (*see* **Note 16**) are nucleic acid stains. Their applications include DNA detection, cell number determination, and chromosome sorting:

1. Solid dyes are dissolved with water, DMSO, or dimethylformamide (DMF) to obtain concentrated solutions of 10 mg/mL.
2. Add Hoechst stains to normal culture medium:
   - Live animal cells: 0.2–5 μg/mL and incubate for 20–30 min.
3. Fluorescence emission is in the 510–540 nm range.

CyQUANT® Cell Proliferation Assay Kit:

This kit uses a green fluorescent dye that binds to cellular nucleic acids and is used for determining the density of cells in culture. The protocol can be followed as per the manufacturer's instructions.

Trypan Blue exclusion test:

Population doubling is evaluated at each passage using the following equation:

$$[\log(\text{harvested cells})/\log(\text{seeded cells})]/\log 2$$

Cumulative population doubling is the sum of the population doubling values for all passages.

3.7 Characterization

The safety of the conditioning method is as important as treatment efficacy. It is crucial to verify whether cells maintain their characteristic features following the conditioning steps. In the case of mesenchymal stem cells, it is important that cells maintain their phenotype and plasticity (differentiation capacity). Hence, we proceed with analysis of cell surface markers by FACS and evaluation of the maintenance of the differentiation potential by testing commitment to adipocyte, osteocyte, or chondrocyte lineages.

3.7.1 Differentiation Protocol

hMSC multilineage differentiation is confirmed by in vitro assays for tri-potentiality with adipogenic, osteogenic, and chondrogenic differentiation kits. Here, we provide protocols for adipogenic and osteogenic differentiation.

Adipocyte Differentiation

1. Plate 2.1×10^4 hMSC/cm^2 of culture surface area in 10 cm culture plates. Make sure cells reach 100 % confluence.
2. Add 10 mL of adipogenic induction medium to plates and incubate undisturbed at 37 °C for 3 days.
3. Maintenance—replace induction medium with adipogenic maintenance medium and incubate undisturbed at 37 °C for 3 days.
4. Repeat induction and maintenance cycle three times.

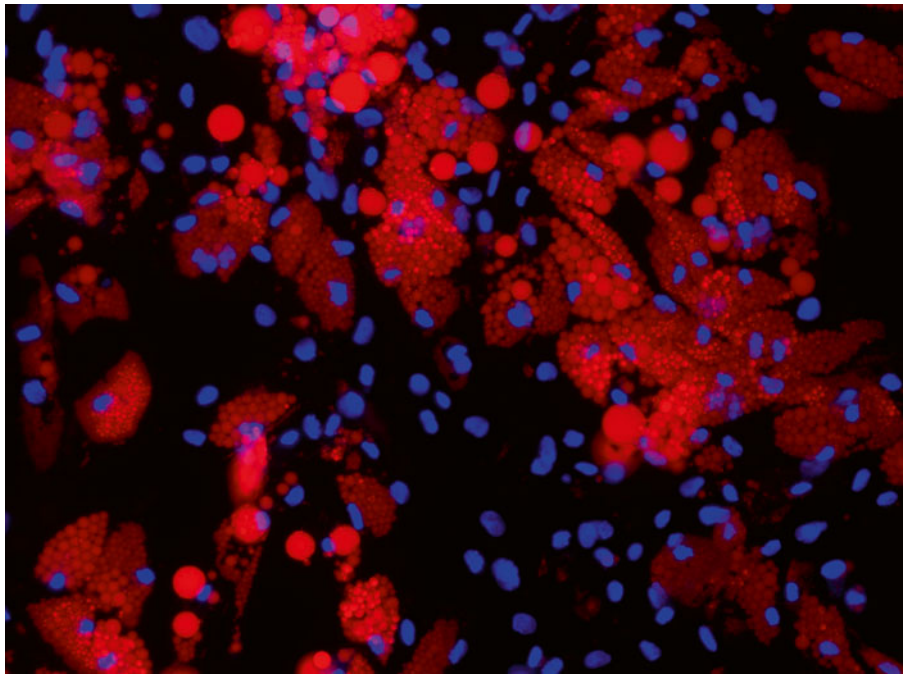

Fig. 2 Adipogenic differentiation of hMSC: vacuoles are stained by Oil Red and *blue* nuclei stained by Hoechst 33342

5. After completion of the cycles, culture for an additional 7 days with maintenance medium, replacing medium every 2–3 days.
6. Color adipocytes with Oil Red staining according to the manufacturer's protocol (*see* Fig. 2).

Osteogenic Differentiation

1. Plate 3.1×10^3 hMSCs/cm^2 in MSCGM at 37 °C, 5 % CO_2 and allow them to adhere to the plastic culture surface.
2. Induce osteogenesis by replacing the culture medium with osteogenic induction medium.
3. Replace with fresh osteogenic induction medium every 3–4 days for 2–3 weeks (*see* **Note 17**).
4. Staining is done according to the *Von Kossa*'s staining protocol with Alizarin Red S (*see* Fig. 3).

3.7.2 FACS

Following the conditioning of MSCs

1. Count the cells (*see* **Note 18**).
2. Centrifuge the cells and suspend the pellet in PBS at a concentration of $0.1–1 \times 10^6$ cells/90 µL.
3. Add 10 µL of FcR blocking reagent, mix, and incubate for 20 min at 4 °C.

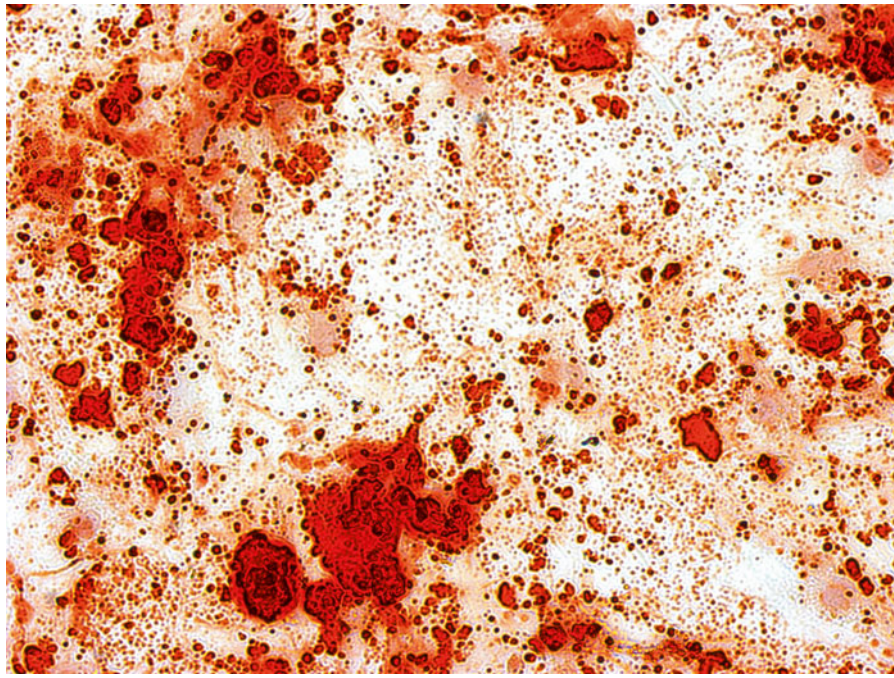

Fig. 3 Osteogenic differentiation of hMSC: free calcium deposits are stained by Alizarin Red

4. Add the antibody to the tubes, mix, and incubate 20 min at room temperature (in the dark).
5. Wash twice with 3–4 mL of FACS buffer followed by centrifugation for 5 min at 350 × *g* and resuspend the pellet in 0.3 mL of FACS buffer solution.
6. Keep cells on ice and in the dark.
7. Analysis should be done by FACS within the hour.

3.8 In Vivo Tests and Future Perspectives

The aim of identifying and developing priming molecules for stem cells is to enhance their survival and functional capacity once transplanted in vivo, thus improving their clinical efficacy [34, 35]. Once molecules have been identified, optimal concentration and timing of conditioning has been established, and safety has been tested; the ideal conditions are applied to MSCs and tested in animal models. Functional assessments and histologic studies are conducted to evaluate their efficacy in in vivo models. Another important issue is proper cell tracking to assess the fate of implanted cells. The latter is beyond the scope of this chapter, although this constitutes the next step in evaluating the efficacy of priming molecules.

4 Notes

1. One rat should yield enough cells to seed a 10 mm petri dish.
2. For in vitro experiments, MSC can be used between passages four and ten.
3. After adding DMSO solution, place the cryopreservation tubes in a Nalgene freezing container and quickly place at –80°C as keeping longer at room temperature is cytotoxic. After 24 hours, transfer cells to –150°C for extended storage.
4. Rewarm just until the solution starts to liquefy; cells will die if left in warmed DMSO for an extended period.
5. Human MSCs can be cultured in human plasma-based serum.
6. Plating reproducibility and cell confluence are crucial to the experiment since variability in cell density will affect assay results. Make sure to thoroughly mix cell suspensions between each plating step, since cells rapidly sediment in solution. Always plate cells in a systematic manner such as by alternating between control and experimental wells until both plates are finished simultaneously. This will ensure plating homogeneity.
7. This step can be omitted for viability studies.
8. Conditioning agents can be used in short burst stimulation protocols (typically 1 h of treatment) or may require several hours or continuous treatment for optimal conditioning. For each conditioning agent, optimal exposure time and dose responses should be determined.
9. The percentage of serum should be validated in preliminary studies.
10. Calcein AM solutions are used within 1 day of preparation because it is susceptible to hydrolysis when exposed to moisture.
11. EthD-1 is stable and not sensitive to moisture; therefore, prepared solutions can be kept frozen for 1 year.
12. Alternatively, prepare 2× concentrate of LIVE/DEAD reagent and add 100 μL of this solution to the 100 μL of culture medium. This will prevent removal of dead/dying cells by aspiration and allow for a more precise quantification of viability.
13. A shorter incubation time is possible with a higher dye concentration or increased incubation temperature.
14. LIVE/DEAD has the advantage of allowing the calculation of a ratio of living cells or dead cells with respect to the total cellular count and thus, objectively comparing the experiments.
15. The PrestoBlue method uses the reducing power of living cells to modify the resazurin-based solution into a highly fluorescent form.

16. Hoechst stains are mutagens and should be handled carefully.
17. Osteogenic-induced cells will change from a spindle shape to cuboid shape as they mineralise. As they start to differentiate, they will begin to delaminate, and it is possible at this time to proceed immediately with differentiation analysis.
18. For FACS analysis, counting more cells yields more accurate results. Use more than one million cells if possible.

References

1. Gnecchi M, He H, Liang OD et al (2005) Paracrine action accounts for marked protection of ischemic heart by Akt-modified mesenchymal stem cells. Nat Med 11:367–368
2. Gnecchi M, He H, Noiseux N et al (2006) Evidence supporting paracrine hypothesis for Akt-modified mesenchymal stem cell-mediated cardiac protection and functional improvement. FASEB J 20:661–669
3. Gnecchi M, Zhang Z, Ni A et al (2008) Paracrine mechanisms in adult stem cell signaling and therapy. Circ Res 103:1204–1219
4. Mansour S, Roy DC, Bouchard V et al (2010) COMPARE-AMI trial: comparison of intracoronary injection of CD133+ bone marrow stem cells to placebo in patients after acute myocardial infarction and left ventricular dysfunction: study rationale and design. J Cardiovasc Transl Res 3:153–159
5. Burdon TJ, Paul A, Noiseux N et al (2011) Bone marrow stem cell derived paracrine factors for regenerative medicine: current perspectives and therapeutic potential. Bone Marrow Res 2011:207326
6. Angoulvant D, Ivanes F, Ferrera R et al (2011) Mesenchymal stem cell conditioned media attenuates in vitro and ex vivo myocardial reperfusion injury. J Heart Lung Transplant 30:95–102
7. Li H, Zuo S, He Z et al (2010) Paracrine factors released by GATA-4 overexpressed mesenchymal stem cells increase angiogenesis and cell survival. Am J Physiol Heart Circ Physiol 299:H1772–H1781
8. Gnecchi M, He H, Melo LG et al (2009) Early beneficial effects of bone marrow-derived mesenchymal stem cells overexpressing Akt on cardiac metabolism after myocardial infarction. Stem Cells 27:971–979
9. Pagani FD, DerSimonian H, Zawadzka A et al (2003) Autologous skeletal myoblasts transplanted to ischemia-damaged myocardium in humans. Histological analysis of cell survival and differentiation. J Am Coll Cardiol 41:879–888
10. Song H, Song BW, Cha MJ et al (2010) Modification of mesenchymal stem cells for cardiac regeneration. Expert Opin Biol Ther 10:309–319
11. Toma C, Pittenger MF, Cahill KS et al (2002) Human mesenchymal stem cells differentiate to a cardiomyocyte phenotype in the adult murine heart. Circulation 105:93–98
12. Dzau VJ, Gnecchi M, Pachori AS (2005) Enhancing stem cell therapy through genetic modification. J Am Coll Cardiol 46:1351–1353
13. Melo LG, Pachori AS, Gnecchi M et al (2005) Genetic therapies for cardiovascular diseases. Trends Mol Med 11:240–250
14. Noiseux N, Borie M, Desnoyers A et al (2012) Preconditioning of stem cells by oxytocin to improve their therapeutic potential. Endocrinology 153:5361–5372
15. Danalache BA, Gutkowska J, Slusarz MJ et al (2010) Oxytocin-Gly-Lys-Arg: a novel cardiomyogenic peptide. PLoS One 5:e13643
16. Gutkowska J, Jankowski M (2012) Oxytocin revisited: its role in cardiovascular regulation. J Neuroendocrinol 24:599–608
17. Gutkowska J, Jankowski M, Antunes-Rodrigues J (2014) The role of oxytocin in cardiovascular regulation. Braz J Med Biol Res 47:206–214
18. Jankowski M, Bissonauth V, Gao L et al (2010) Anti-inflammatory effect of oxytocin in rat myocardial infarction. Basic Res Cardiol 105:205–218
19. Jankowski M, Gonzalez-Reyes A, Noiseux N et al (2012) Oxytocin in the heart regeneration. Recent Pat Cardiovasc Drug Discov 7:81–87
20. Gassanov N, Devost D, Danalache B et al (2008) Functional activity of the carboxyl-terminally extended oxytocin precursor peptide during cardiac differentiation of embryonic stem cells. Stem Cells 26:45–54
21. Kim YS, Ahn Y, Kwon JS et al (2012) Priming of mesenchymal stem cells with oxytocin enhances the cardiac repair in ischemia/reperfusion injury. Cells Tissues Organs 195:428–442

22. Der Sarkissian S, Le Huu A, Borie M et al (2012) Priming of stem cells with celastrol to enhance survival for cell therapy. Can J Cardiol 28:S297
23. Der Sarkissian S, Borie M, Hamet P et al (2011) Pre-conditioning of stem cell with celastrol to enhance their therapeutical potential. Circulation 124:A14198
24. Der Sarkissian S, Cailhier JF, Borie M et al (2014) Celastrol protects ischemic myocardium through heat shock response with upregulation of heme oxygenase-1. Br J Pharmacol 171(23):5265–5279
25. Aggarwal S, Pittenger MF (2005) Human mesenchymal stem cells modulate allogeneic immune cell responses. Blood 105: 1815–1822
26. Le Blanc K, Pittenger M (2005) Mesenchymal stem cells: progress toward promise. Cytotherapy 7:36–45
27. Melo LG, Pachori AS, Kong D et al (2004) Molecular and cell-based therapies for protection, rescue, and repair of ischemic myocardium: reasons for cautious optimism. Circulation 109:2386–2393
28. Jones EA, Kinsey SE, English A et al (2002) Isolation and characterization of bone marrow multipotential mesenchymal progenitor cells. Arthritis Rheum 46:3349–3360
29. Mackay AM, Beck SC, Murphy JM et al (1998) Chondrogenic differentiation of cultured human mesenchymal stem cells from marrow. Tissue Eng 4:415–428
30. Orlic D, Hill JM, Arai AE (2002) Stem cells for myocardial regeneration. Circ Res 91: 1092–1102
31. Gruenloh W, Kambal A, Sondergaard C et al (2011) Characterization and in vivo testing of mesenchymal stem cells derived from human embryonic stem cells. Tissue Eng Part A 17:1517–1525
32. Chamberlain G, Fox J, Ashton B et al (2007) Concise review: mesenchymal stem cells: their phenotype, differentiation capacity, immunological features, and potential for homing. Stem Cells 25:2739–2749
33. Noiseux N, Gnecchi M, Lopez-Ilasaca M et al (2006) Mesenchymal stem cells overexpressing Akt dramatically repair infarcted myocardium and improve cardiac function despite infrequent cellular fusion or differentiation. Mol Ther 14:840–850
34. Forcillo J, Stevens LM, Mansour S et al (2011) IMPACT-CABG trial: implantation of CD133(+) stem cells in patients undergoing coronary bypass surgery-presentation of the first treated patient. Case Rep Transplant 2011:685394
35. Forcillo J, Stevens LM, Mansour S et al (2013) Implantation of CD133+ stem cells in patients undergoing coronary bypass surgery: IMPACT-CABG pilot trial. Can J Cardiol 29:441–447

Chapter 17

Directed Differentiation of Human-Induced Pluripotent Stem Cells to Mesenchymal Stem Cells

Qizhou Lian, Yuelin Zhang, Xiaoting Liang, Fei Gao, and Hung-Fat Tse

Abstract

Multipotent stromal cells, also known as mesenchymal stem cells (MSCs), possess great potential to generate a wide range of cell types including endothelial cells, smooth muscle cells, bone, cartilage, and lipid cells. This protocol describes in detail how to perform highly efficient, lineage-specific differentiation of human-induced pluripotent stem cells (iPSCs) with an MSCs fate. The approach uses a clinically compliant protocol with chemically defined media, feeder-free conditions, and a CD105 positive and CD24 negative selection to achieve a single cell-based MSCs derivation from differentiating human pluripotent cells in approximately 20 days. Cells generated with this protocol express typical MSCs surface markers and undergo adipogenesis, osteogenesis, and chondrogenesis similar to adult bone marrow-derived MSCs (BM-MSCs). Nonetheless, compared with adult BM-MSCs, iPSC-MSCs display a higher proliferative capacity, up to 120 passages, without obvious loss of self-renewal potential and constitutively express MSCs surface antigens. MSCs generated with this protocol have numerous applications, including expansion to large scale cell numbers for tissue engineering and the development of cellular therapeutics. This approach has been used to rescue limb ischemia, allergic disorders, and cigarette smoke-induced lung damage and to model mesenchymal and vascular disorders of Hutchinson-Gilford progeria syndrome (HGPS).

Key words Mesenchymal stem cells, Induced pluripotent stem cells, Differentiation

1 Introduction

Over the past decade, accumulating evidence has demonstrated that mesenchymal stem cells (MSCs) are a promising tool for tissue repair and treatment of many disorders owing to some of their unique properties, such as ease in isolation and expansion, immune privilege, and rare formation of teratoma [1–4]. Despite the availability of many sources of MSCs, bone marrow (BM) and adipose tissue represent the major sources. Nonetheless, these types of MSCs are inherently limited by invasive techniques required for their isolation, a limited capacity for proliferation and impaired differentiation capacity with culture passages [5–7]. Their function also declines with age; thus, the therapeutic efficacy

Massimiliano Gnecchi (ed.), *Mesenchymal Stem Cells: Methods and Protocols*, Methods in Molecular Biology, vol. 1416,
DOI 10.1007/978-1-4939-3584-0_17,

of these types of MSCs is limited [8, 9]. These major issues prompted us to explore new alternative sources of MSCs.

Generation of induced pluripotent stem cells (iPSCs) from somatic cells represents a milestone in stem cell research [10, 11]. Similar to embryonic stem cells (ESCs), iPSCs can grow infinitely and give rise to any human cell type. In addition, iPSCs that are derived autologously overcome some of the disadvantages of ESCs, including ethical issues and immune rejection. Thus, iPSCs are a potentially invaluable source of consistent MSCs. We have successfully derived MSCs from iPSCs [12] and ESCs [13] and also shown that the characteristics of iPSC-MSCs are similar to those of BM-MSCs. Moreover, compared with BM-MSCs, iPSC-MSCs can be expanded for more than 120 passages without obvious senescence or loss of differentiation capacity [12]. Our previous studies demonstrated that iPSC-MSCs are superior to BM-MSCs in attenuation of hind limb ischemia [12], cigarette smoke-induced lung damage [14], and prevention of airway inflammation [15].

In this study, we optimized our previously established protocol [12] to achieve more efficient MSCs generation with a three-stage approach. Briefly, at the first stage, we remove the Geltrex-coated condition from iPSC culture on a gelatin-coated plate to induce spontaneous differentiation in 5–7 days. Next, we trypsinize the differentiating hESC/iPSCs into a single cell and culture with the following supplements: 10 % knockout serum replacement medium, 10 ng/mL basic fibroblast growth factor (bFGF), 10 ng/mL platelet-derived growth factor AB (PDGFAB), and 10 ng/mL epidermal growth factor (EGF) for enrichment of MSCs outgrowth in 10–20 days. In the third stage, the highly enriched MSC-like cells are purified by CD24-/CD105+ sorting and cultured in a single cell-based 96-well culture plate. The single cell-based MSC-like colonies are identified and expanded for the establishment of MSC lines in 15–20 days.

In this chapter, we describe a method for deriving MSCs from iPSCs and characterize the resulting iPSC-MSCs.

2 Materials

2.1 Reagents

All solutions and reagents were prepared at room temperature (unless indicated otherwise).

1. Dulbecco's modified eagle medium: Nutrient Mixture F-12 (DMEM-F12) medium.
2. Knockout serum replacement (KSR).
3. l-glutamine.
4. Nonessential amino acids (NEAA).
5. Human basic fibroblast growth factor (bFGF).

6. Human epidermal growth factor (EGF).
7. Platelet-derived growth factor AB (PDGFAB).
8. Phosphate-buffered saline (PBS).
9. 100× penicillin-streptomycin stock solution (10,000 U/mL; 10,000 μg/mL streptomycin).
10. 2-mercaptoethanol.
11. 0.1 % Gelatin.
12. DMEM/High Glucose.
13. Essential 8™ Medium.
14. 0.05 % Trypsin.
15. Oil red O.
16. Alizarin red S.
17. Alcian blue 8GX.18. Y27632

2.2 Equipment and Supplies

1. 37 °C, 5 % CO_2 incubator.
2. Hood equipped with stereomicroscope.
3. Light microscope.
4. Centrifuge.
5. Biosafety cabinet.
6. Flow cytometer.
7. Centrifuge tubes, pipettes, and sterile cell culture plasticware.

2.3 Media

All media are filter sterilized and stored at 4 °C for no more than 2 weeks.

The media used in this study are as follows:

1. iPSC growth medium: DMEM/F12, 2 % Essential 8™ Medium.
2. iPSC-MSCs medium: DMEM/High Glucose, 10 % FBS, 100 μM NEAA, 5 ng/mL bFGF, 5 ng/mL EGF, 55 μM 2-mercaptoethanol, 100 IU/mL penicillin, 100 μg/mL streptomycin.
3. MSCs differentiation medium: Knockout DMEM, 10 % Knockout serum replacement, 10ng/mL bFGF, 10 ng/mL PDGFAB, 10 ng/mL EGF.
4. Adipogenic differentiation medium: DMEM/High Glucose, 10 % FBS, 100 IU/mL penicillin, 100 μg/mL streptomycin, 1 μM dexamethasone, 10 μg/mL Insulin, 100 μM Indomethacin, 0.5 mM Isobutylmethylxanthine, 2.0 mM l-glutamine.
5. Osteogenic differentiation medium: DMEM/High Glucose, 10 % FBS, 100 IU/mL penicillin, 100 μg/mL streptomycin, 100 nM dexamethasone, 50 μM ascorbic acid, 10 mM β-glycerophosphate, 2.0 mM l-glutamine.

6. Chondrogenic differentiation medium: DMEM/High Glucose, 100 IU/mL penicillin, 100 μg/mL streptomycin, ITS+ (0.01 mg/mL insulin, 0.0055 mg/mL transferrin, 0.005 μg/mL sodium selenite), 100 nM dexamethasone, 50 μM ascorbic acid, 1 mM sodium pyruvate, 10 ng/mL TGF-β3, 2.0 mM l-glutamine.

2.4 Staining Solutions

All staining solutions are filter sterilized and stored at room temperature.

1. Alizarin red s staining solution: Dissolve 1 g alizarin red s in 50 mL deionized H_2O and filter. Adjust pH to 4.1–4.3 with 1 N ammonium hydroxide.
2. Oil red O stock solution: Dissolve 150 mg oil red O in 50 mL isopropanol and store in the dark.
3. Oil red O stock staining solution: Mix three parts of the oil red O stock solution with two parts distilled water and filter the mixture using a syringe filter.
4. Alcian blue staining solution: Dissolve 0.5 g Alcian blue 8GX in 50 mL deionized H_2O and filter.

3 Methods

3.1 Feeder-Free Maintenance and Expansion of Human iPSC Lines

1. Prepare Geltrex-coated plates. Thaw one vial of human ESC-qualified Geltrex on ice and add 1.5 mL per well to a 6-well plate. Swirl the plate to ensure the solution is evenly spread. Keep everything on ice and ensure that all plates are pre-cooled.
2. Maintain the coated plate in an incubator at 37 °C for 1 h and then at room temperature for 1 h prior to use (*see* **Note 1**).
3. Warm the iPSC growth medium before use (*see* **Note 2**).
4. Gently remove the Geltrex solution by aspiration.
5. Immediately add 1 mL iPSC medium with 10μM Y27632/well to a 6-well plate prior to iPSC seeding.
6. Remove a vial of iPSC from liquid nitrogen and thaw quickly in a 37 °C water bath.
7. Transfer the cells to a 15 mL conical tube containing 10 mL iPSC growth medium and centrifuge at 300 × *g* for 5 min at room temperature.
8. After centrifugation, discard the supernatant and resuspend the cells with 1 mL iPSC growth medium with 10μM Y27632. Plate the cells on the coated 6-well plate (*see* **Note 3**).
9. Twenty-four hours later, change the medium and continue culturing until the cells reach 80 % confluence (*see* **Note 4**).

10. When the cells reach 80 % confluence, identify the iPSC clones under the microscope and mark the clones with a lens marker on the bottom of the 6-well plate.
11. Remove medium from the iPSC culture and wash with 2 mL PBS.
12. Add 2 mL/well iPSC growth medium and gently scrape off colonies using a pipette tip (*see* **Note 5**).
13. Harvest the detached cell aggregates and transfer into a 15 mL conical tube and centrifuge at 300 × *g* for 5 min.
14. Discard the supernatant and resuspend the cells with 1 mL iPSC growth medium with 10μM Y27632. Plate the cells on the coated 6-well plate (*see* **Note 6**). Label the new 6-well plate with the cell line name, new passage number, date, split ratio, and your name (*see* **Note 7**).
15. Place the plate in the 37 °C incubator (*see* **Note 8**).

3.2 Derivation of Single Cell-Derived MSC Culture from Human iPSCs

The schematic protocol for differentiating iPSCs into MSCs is shown in Fig. 1.

1. Prepare a confluent 6-well plate of iPSCs without feeders as described above (*see* **Note 9**).

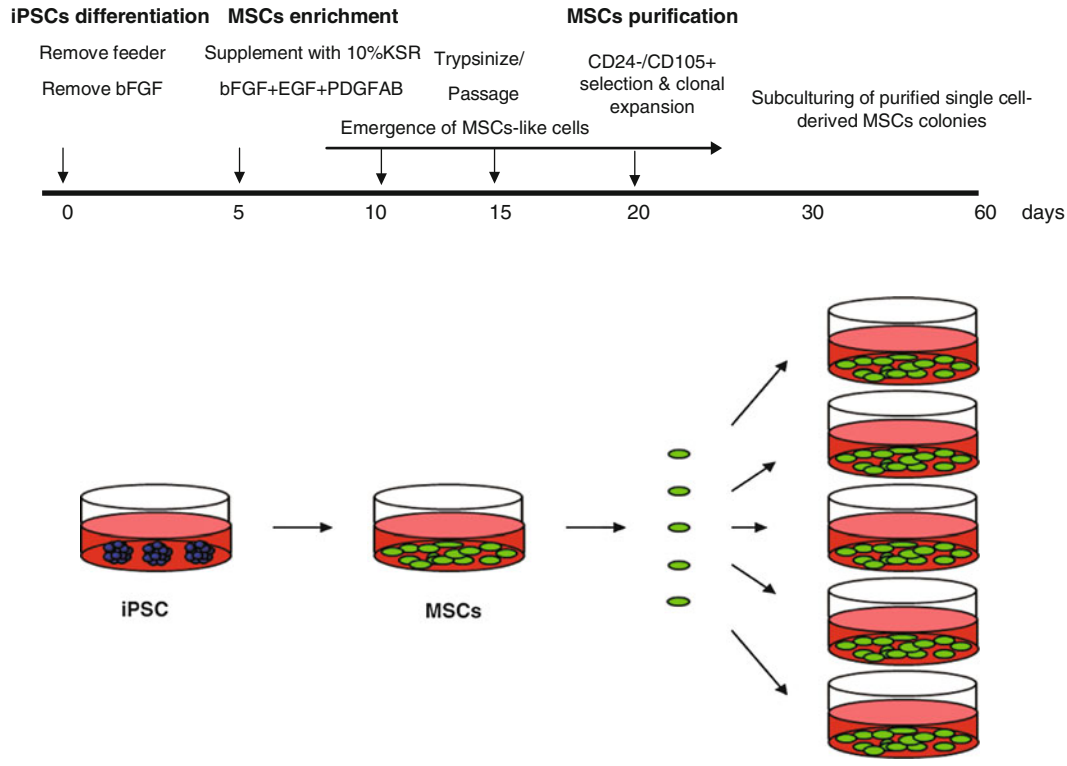

Fig. 1 Schematic protocol for differentiating iPSCs into MSCs

2. Add 10 mL 0.1 % Gelatin to a 10 cm dish, swirl the plate to ensure even spread of the solution and incubate at 37 °C for 1 h before use.
3. Trypsinize a confluent 6-well plate of iPSCs and plate the cells on a 0.1 % Gelatin-coated 10 cm dish containing MSCs differentiation medium.
4. Two week later, harvest the differentiating iPSCs and incubate with CD24-PE and CD105-FITC for 1 h at room temperature.
5. Wash the cells twice with DPBS to remove excess antibodies. Sort $CD24^{-}CD105^{+}$ iPSC-MSCs using a fluorescence-activated cell sorting (FACS) system.
6. Harvest $CD24^{-}CD105^{+}$ cells and seed in a 6-well plate. Add 2 mL DMEM plus 10 % FBS, bFGF (5 ng/mL), PDGFAB (10 ng/mL), and EGF (10 ng/mL) (*see* **Note 10**).
7. When $CD24^{-}CD105^{+}$ cells reach confluence, select wells containing a single cell visualized under light microscopy.
8. Reseed the cells from each well into 1 well of a 6-well plate and then reseed in 25-, 75-, and 175-cm^2 tissue culture flasks.
9. Freeze some cells as stocks when the cells reach 75 % confluence in 175 cm^2 tissue culture flasks (*see* **Note 11**).
10. Achieve eight clone lines in this manner.

MSCs differentiation from iPSCs in three stages: iPSC differentiation, MSCs enrichment, and MSCs purification are shown in Fig. 2.

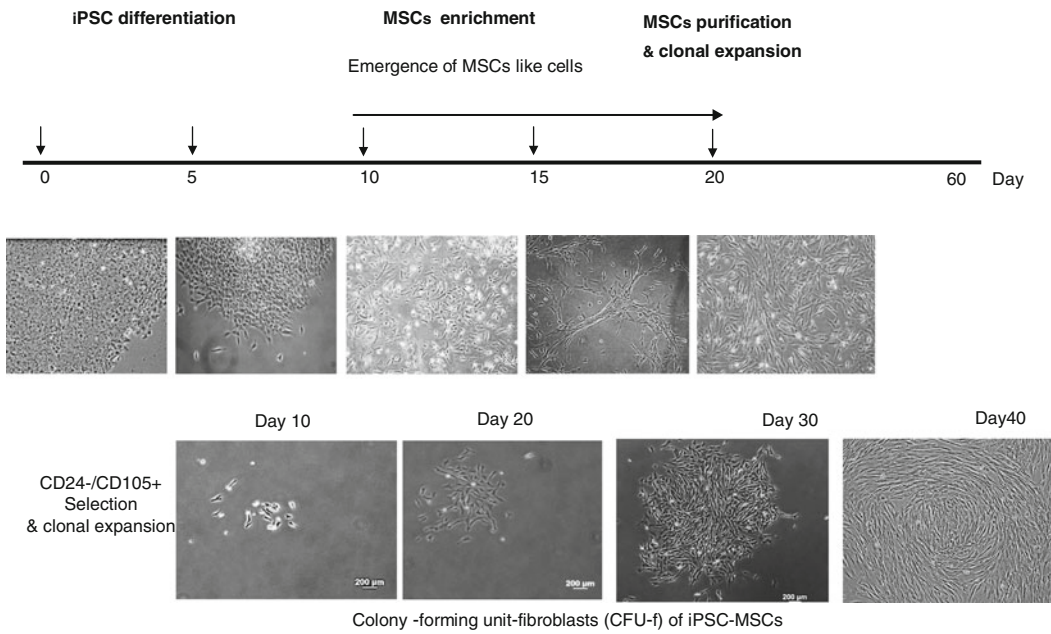

Fig. 2 Microphotographs showing MSCs differentiation from iPSCs at three stages: iPSC differentiation, MSCs enrichment, MSCs purification

3.3 Surface Antigen Analysis of iPSC-MSCs

1. Culture iPSC-MSCs with iPSC-MSCs medium in 75 cm^2 tissue culture flasks.
2. Trypsinize, centrifuge, and resuspend cells in PBS.
3. Incubate 1.5×10^5 cells with each of the following conjugated monoclonal antibodies: TRA-1-80-PE, CD29-PE, CD34-PE, CD44-FITC, CD45-PE, CD49a-PE, CD105-FITC, and CD166-PE at room temperature in the dark for 30 min.
4. Wash cells twice with PBS to remove excess antibodies.
5. Data are analyzed on a BD FACSAria using FlowJo 8.8.4 software (Fig. 3a).

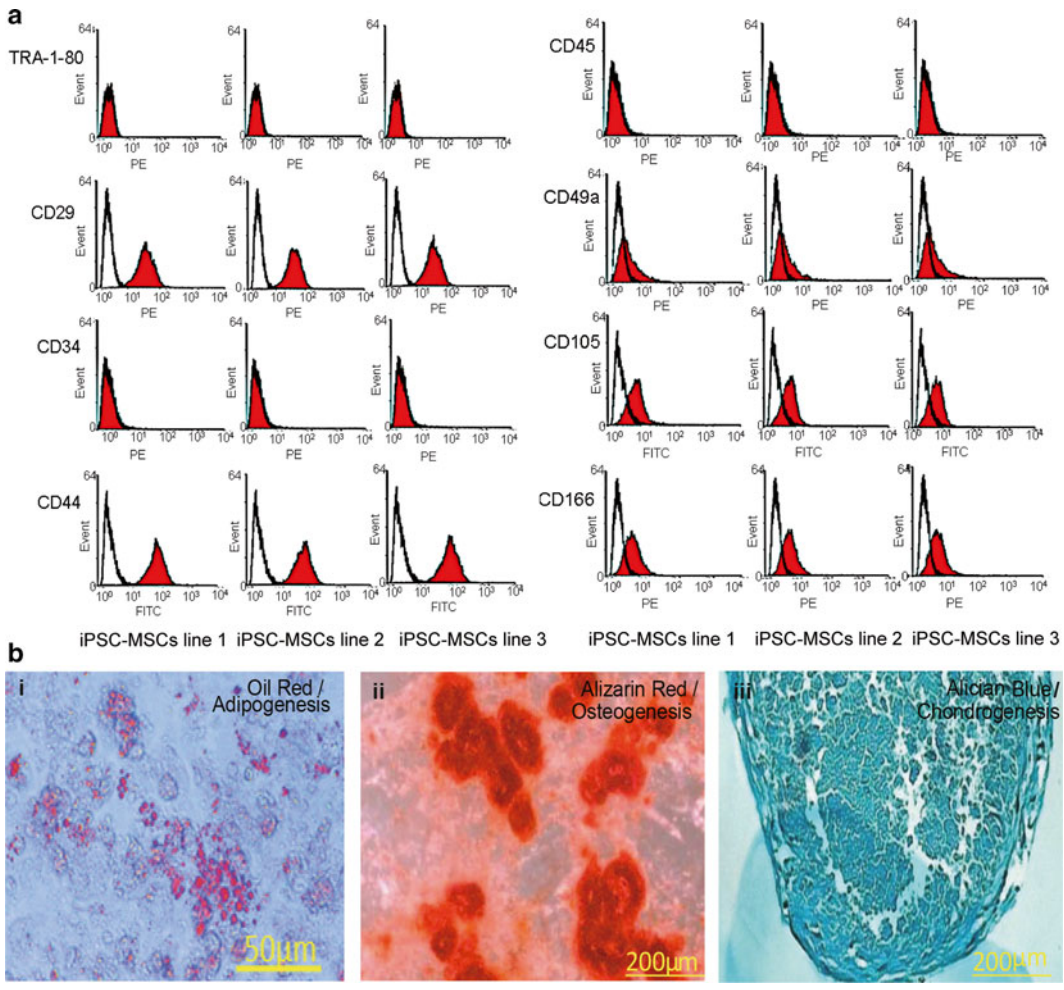

Fig. 3 Functional characterization of MSCs generated from hiPSCs. (**a**) Surface antigen profiling by FACS in 3 lines of iPSC-MSCs cultures for CD29, CD34, CD44, CD45, CD49a, CD105, CD166, and TRA-1-80. (**b**) Differentiation capacity of iPSC-MSCs. Oil red O staining for adipogenesis (i); Alizarin red staining for osteogenesis (ii); Alcian blue staining for chondrogenesis (iii)

3.4 Differentiation of Human iPSC-MSCs: Adipogenesis, Osteogenesis, and Chondrogenesis

3.4.1 Adipogenesis

1. Culture iPSC-MSCs with iPSC-MSCs medium in a 6-well plate.
2. Ensure cells reach 100 % confluence before changing the medium to adipogenic differentiation medium.
3. Culture cells for 2–3 weeks and refresh medium every 3–4 days (*see* **Note 12**).
4. After PBS washing, fix cells with 4 % paraformaldehyde solution for half an hour.
5. Aspirate the fixation buffer and wash cells with distilled water. Carefully aspirate the water and add enough 60 % isopropanol to cover the cell monolayer. Incubate for 5 min at room temperature.
6. Aspirate the 60 % isopropanol and add enough oil red O staining solution to cover the cell monolayer. Incubate at room temperature for 15 min. Intracellular lipid vesicles in mature adipocytes stain bright red (Fig. 3b-i).

3.4.2 Osteogenesis

1. Culture iPSC-MSCs with iPSC-MSCs medium in a 6-well plate.
2. Ensure cells reach 100 % confluence before changing the medium to osteogenesis differentiation medium.
3. Change medium every 3–4 days and culture cells for 2–3 weeks.
4. Fix cells with 4 % paraformaldehyde solution for half an hour and then repeat washing with deionized H_2O. Be gentle, as cell monolayers and calcium deposits are easily dislodged.
5. Remove water and stain cells with 2 % alizarin red staining solution for 3 min at room temperature. Repeat washing with water to remove excess stain. Calcium deposits appear as irregular red-orange crystals (Fig. 3b-ii).

3.4.3 Chondrogenesis

1. Expand iPSC-MSCs in a T-25 or T-75 flask with iPSC-MSCs medium.
2. Determine the total number and suspend the cells in chondrogenic induction medium at a concentration of 8×10^6 cells per mL (*see* **Note 13**).
3. Add 2–3 × 10 μL droplets (8×10^4 cells per droplet) to the center of a 24-well plate.
4. Carefully transfer the plates to an incubator. Allow cells to remain still for 2–4 h (*see* **Note 14**).
5. Carefully flood cells with chondrogenic induction medium (suggested volume for a 24-well plate is 1 mL per well).
6. Change medium every 3 days and culture cells for 2 weeks. Do not disturb the micromasses.

7. Chondrogenic pellets may be formalin fixed and paraffin embedded for Alcian blue staining.
8. Deparaffinize slides and hydrate with distilled water. Stain in 1 % Alcian blue solution for 30 min (*see* **Note 15**). Destain with 0.1 N HCl with repeated washes until excess stain is removed. Visualize under light microscope. Blue staining indicates synthesis of proteoglycans by chondrocytes (Fig. 3b-iii).

4 Notes

1. Do not let the Geltrex solution evaporate, and use the coated plate immediately. If not used immediately, the coated plate must be sealed to prevent evaporation of the Geltrex solution, and it can be stored at 4 °C for up to 7 days after coating.
2. Warm medium to insure the highest viability of iPSCs.
3. The cells must be placed slowly and drop by drop, to ensure even distribution on the plate. The final volume in each well should be 2 mL.
4. The iPSC growth medium must be changed daily.
5. Pipette gently to minimize bubbles.
6. The iPSC can be passaged at 1:6 to 1:10 splits every 5–7 days when the clones reach an optimal density.
7. To maintain pluripotency of human iPSCs, do not keep in culture without passaging for long periods.
8. Move the plate in a forward to back and quick side to side motion to ensure even distribution of iPSC clumps in the wells.
9. The size of iPSC colonies affects the differentiation process such as efficiency and variability during differentiation. Use homogeneously sized iPSC colonies for MSCs differentiation.
10. Basic-FGF, EGF, and PDGFAB are required for enrichment of MSC outgrowth.
11. Set the cells as passage 1 at this stage.
12. Do not disturb the cell monolayer. Intracellular lipid vesicles should be observed after 7 days.
13. TGF-β3 should be added fresh to the medium before each medium change.
14. Do not allow droplets to dry out. Add some sterile water to other unused wells of the 24-well plate to maintain a humid environment.
15. If there is a large proportion of cartilage, overnight staining may be required.

Acknowledgment

This work was supported by HKU Small Project Funding (201409126251 to Dr Lian Q); National Natural Science Foudation of China (No 31270967, 31571407 to Q Lian); Shenzhen Technology project (No JCYJ20140828163633995 to Q Lian); Science and Technology Foundation of Guangdong of China (No 2015B020225001 to Q Lian); Hong Kong Research Grant Council General Research Fund (HKU772510M to Dr Lian Q) and Innovation and Technology Support Programme (ITS/150/12 to Dr Lian Q).

References

1. Zhang Y, Liao S, Yang M et al (2012) Improved cell survival and paracrine capacity of human embryonic stem cell-derived mesenchymal stem cells promote therapeutic potential for pulmonary arterial hypertension. Cell Transplant 21:2225–2239
2. Zhu XY, Urbieta-Caceres V, Krier JD et al (2013) Mesenchymal stem cells and endothelial progenitor cells decrease renal injury in experimental swine renal artery stenosis through different mechanisms. Stem Cells 31:117–125
3. Williams AR, Hare JM (2011) Mesenchymal stem cells: biology, pathophysiology, translational findings, and therapeutic implications for cardiac disease. Circ Res 109:923–940
4. Foronjy RF, Majka SM (2012) The potential for resident lung mesenchymal stem cells to promote functional tissue regeneration: understanding microenvironmental cues. Cells 1:874
5. Zhang Y, Liang X, Lian Q et al (2013) Perspective and challenges of mesenchymal stem cells for cardiovascular regeneration. Expert Rev Cardiovasc Ther 11:505–517
6. Li O, Tormin A, Sundberg B et al (2013) Human embryonic stem cell-derived mesenchymal stroma cells (hES-MSCs) engraft in vivo and support hematopoiesis without suppressing immune function: implications for off-the shelf ES-MSC therapies. PLoS One 8:e55319
7. Uccelli A, Moretta L, Pistoia V (2008) Mesenchymal stem cells in health and disease. Nat Rev Immunol 8:726–736
8. Madonna R, Taylor DA, Geng YJ et al (2013) Transplantation of mesenchymal cells rejuvenated by the overexpression of telomerase and myocardin promotes revascularization and tissue repair in a murine model of hind limb ischemia. Circ Res 113:902–914
9. Gharibi B, Farzadi S, Ghuman M et al (2014) Inhibition of Akt/mTOR attenuates age-related changes in mesenchymal stem cells. Stem Cells 32(8):2256–2266
10. Takahashi K, Yamanaka S (2006) Induction of pluripotent stem cells from mouse embryonic and adult fibroblast cultures by defined factors. Cell 126:663–676
11. Yu J, Vodyanik MA, Smuga-Otto K et al (2007) Induced pluripotent stem cell lines derived from human somatic cells. Science 318:1917–1920
12. Lian Q, Zhang Y, Zhang J et al (2010) Functional mesenchymal stem cells derived from human induced pluripotent stem cells attenuate limb ischemia in mice. Circulation 121:1113–1123
13. Lian Q, Lye E, Suan Yeo K et al (2007) Derivation of clinically compliant MSCs from CD105+, CD24- differentiated human ESCs. Stem Cells 25:425–436
14. Li X, Zhang Y, Yeung SC et al (2014) Mitochondrial transfer of induced pluripotent stem cells-derived MSCs to airway epithelial cells attenuates cigarette smoke-induced damage. Am J Respir Cell Mol Biol 51(3):455–465
15. Sun YQ, Deng MX, He J et al (2012) Human pluripotent stem cell-derived mesenchymal stem cells prevent allergic airway inflammation in mice. Stem Cells 30:2692–2699

Part III

Mesenchymal Stem Cells for Clinical Use

Chapter 18

Isolation and Manufacture of Clinical-Grade Bone Marrow-Derived Human Mesenchymal Stromal Cells

Renuka P. Miller and Patrick J. Hanley

Abstract

Mesenchymal stromal cells (MSCs) are multipotent cells with both regenerative and immunomodulatory capacities. These unique properties make them appealing as a biologic, with multiple phase 1–3 clinical trials currently testing their safety and efficacy. Although expanding MSCs does not require extensive manipulation, expanding MSCs for use in clinical trials does require the knowledge and safety that are delineated in current good manufacturing practices (GMPs). Here we briefly detail the characteristics of MSCs and considerations for expanding them for clinical use. We then include a step-by-step protocol for expanding MSCs for early phase clinical trials, with important notes to consider during the expansion of these MSCs.

Key words Mesenchymal stromal cells, Clinical grade, Good manufacturing practices, Cell therapy

1 Introduction

Originally isolated from the bone marrow (BM), mesenchymal stromal cells (MSCs) are spindle-shaped, non-hematopoietic, progenitor cells that possess multipotent differentiation capacity. Generally, MSCs in BM remain in the resting phase, but in the appropriate in vivo environment or given the proper stimuli, these cells have the ability to differentiate into cells of mesodermal origin such as adipocytes, chondrocytes, and osteoblasts [1]. In BM, MSCs are a rare population comprising only 0.01–0.001 % of BM cells [2]. While BM-derived MSCs are the most well-characterized source of MSCs, similar populations have also been isolated from other sources such as adipose tissue, where they comprise of a greater percentage of cells [3].

In the last decade, MSC clinical applications have expanded rapidly with multiple clinical trials investigating these cells therapeutically. Due to many inherent properties such as hypo-immunogenicity, immunomodulation, and the ability to differentiate into various cell types, MSCs have great potential for cell-based therapies.

Massimiliano Gnecchi (ed.), *Mesenchymal Stem Cells: Methods and Protocols*, Methods in Molecular Biology, vol. 1416,
DOI 10.1007/978-1-4939-3584-0_18,

Although there is conflicting evidence surrounding the immunogenicity of MSCs, most studies agree that these cells are hypoimmunogenic and overall lack stable expression of MHC class II molecules [4]. Furthermore, these cells do not appear to express the co-stimulatory molecules necessary for effector T-cell induction [5, 6]; the absence of MHC class II and co-stimulatory molecules allows MSCs to escape early recognition by multiple facets of the immune response in vivo, making them an ideal candidate for use as an off-the-shelf therapy. MSCs have the potential to inhibit the differentiation of monocytes into dendritic cells and the maturation of immature dendritic cells into mature dendritic cells [7]. MSCs also inhibit T cells directly by releasing soluble factors like indoleamine 2,3-dioxygenase (IDO), which depletes available tryptophan needed by T cells and also transforming growth factor β (TGF-β) and prostaglandin E2 (PGE-2) [8]. In the therapeutic setting, the immunosuppressive effects of MSCs have been shown to be beneficial in the treatment of graft-versus-host disease (GvHD). MSCs have been given to patients after allogeneic hematopoietic stem cell transplantation in an attempt to inhibit the reaction of donor T lymphocytes to recipient antigens, leading to improved resolution of steroid-resistant GvHD [9, 10]. In addition to reducing GVHD, several early phase trials have suggested that MSCs enhance engraftment after stem cell transplant [11]. Furthermore, MSCs have shown promise in inflammatory bowel disease [12] among other inflammatory or autoimmune diseases. Beyond immune modulation, MSCs have been used to restore healing of long bone fractures, to effectively treat children with osteogenesis imperfecta, and they have been used clinically to accelerate wound healing [13, 14].

The interest in MSCs for these and other applications—both autologous and allogeneic—coupled with their more-than-minimal manipulation has created demand for manufacturing of MSCs in accordance with current good manufacturing practices (GMPs). GMP manufacturing of cellular therapy products focuses on core components such as safety, purity and identity, and quality, in addition to good tissue practice (GTP) regulations aimed at preventing the introduction, transmission, or spread of communicable diseases. For this reason, it is imperative that standards are set for core GMP and GTP components, including donor selection, source of starting material, and culture processes.

With regard to choosing donors, the process of screening, testing, and determination of eligibility is similar among product manufacturing for all cell therapies. However, when developing large MSC banks for allogeneic use, finding donors suitable for a variety of recipients may prove challenging. In particular, the age of the donor is an important consideration for determining suitability. Slower growth rates and fewer population doublings have been seen in MSCs derived from older donors when compared with younger donors [15]. In addition, increased age has been shown

to be directly related to decreased proliferation and multipotency [16]. The donor source is also worth considering; here we describe the use of MSCs derived from bone marrow, but some studies suggest that adipose-derived MSCs may have unique characteristics worth investigating [17].

In addition to setting standards for donor eligibility and suitability and deciding the source of MSCs, choosing the optimal expansion paradigm is important [18]. Traditional MSCs rely on adherence to plastic for expansion (although it should be noted that 3D expansion methods have been reported). In order to expand a large number of cells, sufficient surface area is required. Using classic cell culture flasks is an effective method for cell expansion, but one must consider the requirements for space, personnel, and technician times. Some companies such as Corning and Nunc offer multilayered flask systems, which increase the amount of surface area in a compact design. These systems may alleviate the need for additional space, but the amount of labor necessary and technician times are still factors that should be considered. Another option for culturing MSCs is the use of bioreactors. Bioreactors such as the Quantum Cell Expansion System from Terumo BCT [19], the Wave by GE [20], and the Xpansion system by ATMI provide large surface areas over a small footprint and offer varying degrees of automation. Additionally, these systems, along with the multilayered flasks mentioned above, can be functionally closed, meaning that the risk of disease transmission is lower because the cells are not exposed to the environment during their expansion. Nevertheless, here we present a method of manufacturing MSCs that is quickly translatable to early phase clinical trials and is feasible using routine laboratory equipment (Fig. 1).

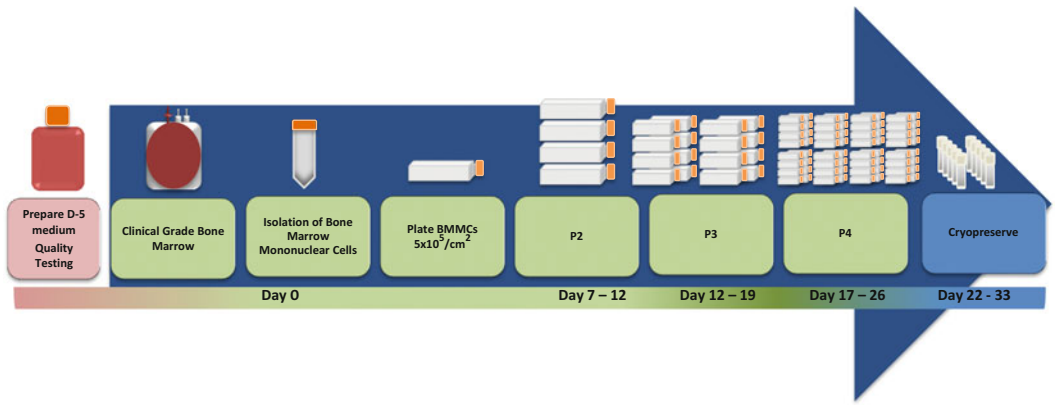

Fig. 1 Expansion of human MSCs in flasks. D5 medium is prepared prior to initiation. Bone marrow mononuclear cells are isolated from bone marrow of an eligible donor and plated in T-175 flasks. After 10–15 days (or when 80–90 % confluent), adherent cells are dislodged, harvested, and split from one flask into four flasks and returned to the incubator for 5–7 days (or when 80–90 % confluent). Again, dislodge cells, harvest, and split them from one flask into four flasks. Repeat until enough cells are expanded to reach desired dosing. At this point cells can be cryopreserved and, upon release, given clinically

When manufacturing cells for clinical trials, it is important to establish specific standards (typically with the Food and Drug Administration (FDA) or a comparable regulatory agency) that must be met before the product is released by a responsible person for therapeutic use (Table 1). These release criteria are important for monitoring safety and efficiency of cell therapy products.

Table 1
Quality testing performed on the MSCs

Stage of manufacture	Test	Performed by	Specification
Bone marrow	Sterility (fungal, bacterial)	CETI/CNMC Microbiology Laboratory	Negative at 4 days
Bone marrow	Cell count	CETI	Total nucleated cells
Bone marrow	Phenotype	CETI	CD73, CD90, CD105
BMMC fraction	Sterility	CETI	Negative at 4 days
BMMC fraction	CFU-F	CETI	Number of CFU
Passage 1	Sterility	CETI	Negative at 4 days
Passage 1	Phenotype	CETI	CD73, CD90, CD105
Passage 1	Viability	CETI	>70 % viable by trypan blue or 7AAD
Passage 2	Sterility	CETI	Negative at 4 days
Passage 2	Phenotype	CETI	CD73, CD90, CD105
Passage 2	Viability	CETI	>70 % viable by trypan blue or 7AAD
Passage 3	Sterility	CETI	Negative at 4 days
Passage 3	Phenotype	CETI	CD73, CD90, CD105
Passage 3	Viability	CETI	>70 % viable by trypan blue or 7AAD
Final product	Sterility	CETI	Negative at 4 days Negative at 21 days
Final product	Phenotype	CETI	>95 % CD73+, CD90+, CD105+; <2 % CD45+, CD34+, CD14+, CD19+; <5 % HLA-DR+
Final product	Viability	CETI	>70 % viable by trypan blue or 7AAD
Final product	Tri-lineage potential	CETI	Adipogenic, chondrogenic, and osteogenic differentiation
Final product	Endotoxin	CETI	<0.05 EU/mL
Final product	Mycoplasma	CETI	Negative
Final product	CFU-F	CETI	# of CFU

Phenotyping, sterility tests, and functional analyses are examples of release criteria testing that are important to consider for MSCs (Table 1). The International Society for Cellular Therapy (ISCT) has proposed minimal criteria to define MSCs that include adherence; the ability to differentiate into osteoblasts, chondroblasts, and adipocytes; and the expression of CD105, CD73, and CD90. Furthermore, MSCs should lack expression of CD45, CD34, CD14 or CD11b, and CD79α or CD19 [21]. Phenotyping not only confirms the identity of the cells as MSCs; it is also an indicator of the purity of the culture.

2 Materials

2.1 D5 Medium

1. D5 Medium: Dulbecco's Modified Eagle's Medium, high glucose without L-glutamine, 2 U/mL heparin, 5 % platelet lysate, 2 mM GlutaMAX, and 10 mM *N*-acetylcysteine.
2. VacuCap filters.
3. Filter Storage Receiver Bottle.
4. Human bone marrow from an eligible donor.
5. Human platelet lysate.
6. 60 mL syringe.
7. 1 or 2 L bottle.

2.2 Isolation of Bone Marrow Mononuclear Cells

1. 1 mL syringe.
2. 5 mL syringe.
3. 16G needle.
4. 30 and 60 mL syringe.
5. Sterile transfer pipette.
6. Sterile centrifuge tubes.
7. Sterile serological pipettes.
8. Sterile cell transfer bag.
9. Trypan blue.
10. Lymphoprep.
11. Aspirating pipette.
12. BacT/Alert anaerobic culture bottle.
13. BacT/Alert aerobic culture bottle.
14. Isolator tube (fungal culture).
15. TrypLE Select.
16. Phosphate-buffered saline (without Mg, Ca).
17. Sterile transfer pipette.

2.3 Plating of Bone Marrow Mononuclear Cells, Mesenchymal Stem Cell Culture, and Cryopreservation

1. Sterile tissue culture-treated T-175 flasks with vented cap.
2. Sterile conical tubes.
3. Plasmalyte A.
4. 25 % flexbumin.
5. Cryovials.
6. Dimethyl sulfoxide.
7. Freezing medium: 20 % DMSO 5 % HSA and 75 % plasmalyte (final concentration of 10 % DMSO).

2.4 Release Testing

1. CD73.
2. CD90.
3. CD105.
4. CD45, CD34, CD14 or CD11b, CD79α or CD19, HLA-DR.
5. EndoSafe.
6. MycoAlert.

3 Methods

3.1 Preparing Expired Platelet Lysate

1. Obtain expired human platelets (often available from a hospital blood bank). Ensure that platelet donors have undergone infectious disease testing and risk assessment (*see* **Notes 1–3**).
2. Using a 60 mL syringe, remove the platelets from the platelet bag and place in a large, sterile 1–2 L bottle.
3. Aliquot 35–40 mL in 50 mL centrifuge tubes. Ensure that the tubes are labeled appropriately and donor information can be tracked if needed. If testing of platelet lysate is not complete, place a biohazard label on the tubes.
4. Transfer platelets to an −80 °C freezer.
5. The next day, or once the platelets are completely frozen, remove them from the freezer and place in a 37 °C water bath to thaw.
6. Once completely thawed, dry the outside of the tubes and centrifuge the platelets at 900×*g* for 10 min at ambient temperature.
7. Collect the supernatant—this is the lysate—into 50 mL tubes labeled "platelet lysate." Include the manufacturing information (from the pooled units) including the date, expiration date, blood type, and lot number. Approximately 25–30 mL of lysate will be required for each 500 mL of D5 Medium.

3.2 Release Testing of Platelet Lysate

1. This is performed on the aliquot of platelets from which the lysate has been obtained above.
2. Using a 37 °C water bath, thaw one vial of frozen MSCs that has been designated by quality control for testing of platelet lysate.

3. Seed the cells at 5000 cells/cm^2 in six well plates in medium prepared (see below) using the test lysate. When possible, a previously qualified lot of lysate-containing medium should be used in parallel.
4. Observe the cultures from day 3 through day 5. Harvest, count, and measure the viability of the cells when 85–95 % confluent or at day 5, whichever comes first.
5. To meet the release testing criteria, the cells grown using the test lysate must show all the following characteristics; lysate that does not meet the criteria must be discarded:
   (a) 85 % confluence must be reached by day 5 of culture.
   (b) The cell density must reach 15,000 cells/cm^2 by day 5 of culture.
   (c) The viability of the cells must be 70 % at the time of harvest.

3.3 Preparation of D5 Medium

DMEM, 2 U/mL heparin, 5 % platelet lysate, 2 mM GlutaMAX, 10 mM *N*-acetylcysteine (*see* **Note 4**):

1. Allow the DMEM to come to room temperature.
2. Mix the components using a sterile bottle. The heparin *must* be added before the platelet lysate to avoid clumping.
3. Filter the mixture through a 0.2 μm filter. Multiple filters may be required.
4. To the filtered medium, add 1 % volume/volume GlutaMAX and 10 mM *N*-acetylcysteine.
5. Generate a batch record to register details of the lot of medium created, including reagents and supplies used, their manufacturer, lot number, and expiration date.
6. Store at 2–8 °C.

3.4 Isolating Bone Marrow Mononuclear Cells from Whole Bone Marrow

1. Obtain 25–50 mL of bone marrow from an eligible donor according to 21CFR part 1271, subpart C. Ensure that all donor eligibility paperwork and other institutional-specific documentation have been completed by requisite physicians, laboratory directors, and quality assurance (*see* **Note 5**).
2. If BM is provided in a cell transfer bag with ports, proceed to **step 3**. If BM is provided in tubes, connect a sterile aspirating pipette to a 30 mL syringe, and draw up the BM into the syringe one tube at a time, adding the BM to a cell culture bag after drawing up BM from each tube.
3. Once BM is pooled in a cell transfer bag, mix the bag well.
4. Prepare anaerobic, aerobic, and fungal sterility bottles (e.g., BacT/Alert) by removing caps and wiping with ethanol. Ensure that bottles are labeled with appropriate product information.

5. Using three 1 mL syringes and a 5 mL syringe, move 0.5 mL from the bag into each 1 mL syringe and move 3–5 mL of BM into the 5 mL syringe.
6. Carefully place a needle on the tip of the 1 mL syringe and dispense BM into the fungal bottle. Repeat using the 1 mL syringes for anaerobic and aerobic sterility bottles.
7. From the 5 mL syringe, submit 1–2 mL of BM for phenotypic analysis and cell counting (*see* **Note 6**). Aliquot the remainder in 2–3 cryovials for archiving, colony-forming unit assays, and karyotyping, if desired.

3.5 Plating Bone Marrow Mononuclear Cells

1. Using a 25 mL sterile serological pipette, aliquot 10 mL of Lymphoprep into the number of required 50 mL centrifuge tubes. One tube (10–15 mL) of Lymphoprep is required for every 10 mL of bone marrow (*see* **Note 7**).
2. For every 10 mL of bone marrow, dilute the bone marrow by adding 10 mL of PBS or RPMI 1640.
3. Slowly layer 20–30 mL of diluted bone marrow for every 10–15 mL of Lymphoprep.
4. Centrifuge the cells at $800 \times g$ for 20 min at ambient temperature with minimal acceleration and brake (*see* **Note 8**).
5. After centrifugation, use a sterile transfer pipette or a sterile serological pipette to harvest the interface containing the bone marrow mononuclear cells (BMMCs). Place the BMMC in a new 50 mL centrifuge tube.
6. Dilute the BMMC 2:1 in PBS or RPMI 1640.
7. Centrifuge the cells at $450 \times g$ for 10 min at ambient temperature.
8. Aspirate the supernatant. Resuspend cells in RPMI or PBS at an estimated concentration of 1×10^6 cells/mL. Remove a sample (<1 mL) for counting.
9. Centrifuge cells at $400 \times g$ for 5 min at ambient temperature.
10. During centrifugation, count the cells using trypan blue. Dilute the cells if necessary.
11. Aspirate the supernatant and resuspend the cells at 1×10^7 cells/mL in D5 medium. Calculate the number of flasks needed. For approximately every ten million cells, one T-175 cm^2 flask is required.
12. Add ~29 mL of D5 medium to each flask.
13. Plate cells in T-175 cm^2 flasks at 5×10^5 cells/cm^2. For a T-175 cm^2 flask, add ~8.75×10^7 cells or ~1 mL to the 30 mL of D5 medium already in the flask. Gently mix and place flask in 37 °C incubator with 5 % CO_2 air.

14. After 4–7 days, remove the nonadherent cells by using an aspirating pipette or a serological pipette to remove the medium. Replace with 30 mL of fresh D5 medium. Harvested cells can be placed in a T-175 cm^2 flask as a control.

3.6 Passaging Mesenchymal Stem Cells

1. After 10–15 days from initiation (very donor dependent), the MSCs should be split upon reaching 80–90 % confluence (*see* **Notes 9–13**).
2. Using an aspirating pipette, aspirate the medium in each flask.
3. Rinse flask with 5–10 mL of sterile PBS.
4. Aspirate the PBS from each flask.
5. Add 3–5 mL of TrypLE Select to each flask. Rotate flask to cover entire surface.
6. Incubate cells for 5–10 min at 37 °C in the incubator.
7. Check flasks under microscope to ensure that the cell monolayer is no longer adherent. Gently tap flasks if still adherent.
8. Once cells are non-adherent, add 5–10 mL of D5 medium to each flask and harvest the cells into a sterile bottle or conical tube.
9. Remove a small aliquot of cells for counting, for sterility testing, and for phenotyping.
10. Count cells as in "Plating BMMC" above.
11. Submit phenotyping and sterility samples as in "isolating BMMC from whole BM."
12. Centrifuge cells at 800 × *g* for 15 min in conical tubes.
13. Transfer 25 mL of fresh D5 medium to each new flask.
14. Aspirate supernatant from centrifuged cells and resuspend in 5 mL of D5 medium for each flask into which they will be transferred. (For example, if there were four flasks that were harvested, there will be 16 flasks that the cells are passaged into, so the centrifuged cells will be resuspended in 80 mL of D5 medium).
15. Add 5 mL of cells to each new flask. Gently rotate each flask to mix cells and return to incubator.
16. Repeat **steps 2–15** every 5–7 days or when cells reach 75–85 % confluence.
17. Save at least 20 million cells for release testing on the final product.

3.7 Cryopreservation

1. Once cells are harvested, centrifuge at 800 × *g* for 15 min at room temperature. The supernatant should be saved for sterility, mycoplasma, and endotoxin testing (*see* **Notes 14–15**).

2. Resuspend cells in a wash medium containing plasmalyte and 5 % human serum albumin.
3. Centrifuge the cells again at $800 \times g$ for 15 min at room temperature.
4. Resuspend the cells in wash medium at ½ the freezing concentration (e.g., if freezing at 1×10^7/mL in 1 mL, add 0.5 mL of wash medium per 1×10^7 cells).
5. Place the cells on ice for 10 min.
6. Add 2× freeze medium.
7. Aliquot cells into cryovials or freezing bags at a concentration of $1–2.5 \times 10^7$ cells/mL.
8. Freeze using a controlled-rate freezer with a program intended for cryopreservation of BM products.
9. Transfer frozen product to liquid nitrogen dewar for long-term storage.

4 Notes

1. All release testing and manufacturing processes reported here are the opinions of the authors and the Program for Cell Enhancement and Technologies for Immunotherapy—they *do not* supersede federal regulations; all products undergoing more-than-minimal manipulation and that are intended for human use should be approved by proper regulatory and institutional bodies.
2. All products intended for therapeutic use should be manufactured under good manufacturing practices (GMPs)/good tissue practices (GTPs).
3. Lots of platelets should be pooled to prevent variability between lots of medium.
4. Alternative media can be used, including substituting human platelet lysate for FBS; however, in our experience, D5 medium is associated with the best expansion.
5. Donor variability is considerable when expanding MSCs. If possible, obtain bone marrow aspirates from multiple donors and grow for one or two passages to determine the best donor for MSCs.
6. An automated cell counter can be used to establish a more accurate total nucleated cell (TNC) count.
7. Although it is recommended that products intended for clinical use are manufactured in a controlled environment in a clean room, we still recommend using closed systems whenever possible. One alternative to manual BMMC isolation is to use the Sepax device by Biosafe.

8. Allow the centrifuge to accelerate/decelerate slowly during BMMC isolation to avoid disrupting the gradient.
9. To limit the number of flasks and to considerably close the system, investigators should consider the use of cell factories or bioreactors such as the WAVE by GE, the Quantum by Terumo, and the Xpansion by ATMI.
10. When dealing with large numbers of flasks, passages and the harvest can be split into batches to prevent cells from being exposed to disassociation reagents and suboptimal conditions for extended periods of time.
11. Typical yield from a T-175 flask is $2–3 \times 10^6$ MSCs meaning that to obtain yields for large clinical trials, multiple incubators will be required.
12. MSCs should not be allowed to reach confluence—they should be split or harvested and cryopreserved before full confluence.
13. MSCs can be cryopreserved at any passage without significantly affecting their viability or subsequent expansion.
14. Cells at the final cryopreservation will require release testing such as mycoplasma, endotoxin, phenotyping, tri-lineage potential, T-cell suppression, sterility, and identity testing. These tests should be performed by certified laboratories using validated and approved assays (Table 1).
15. We recommend the phenotypic markers outlined by the position paper of the international society of cell therapy (ISCT), but other markers associated with distinct lineages can also be used.

Acknowledgments

The authors would like to thank our collaborators at the Baylor College of Medicine, namely, Dr. Adrian Gee, Dr. Zhuyong Mei, and Dr. Helen Heslop. We would also like to thank the Program for Cell Enhancement and Technologies for Immunotherapy (CETI) director, Dr. Catherine Bollard, for her support and guidance.

References

1. Friedenstein AJ, Deriglasova UF, Kulagina NN et al (1974) Precursors for fibroblasts in different populations of hematopoietic cells as detected by the in vitro colony assay method. Exp Hematol 2:83–92
2. Hanley PJ, Mei Z, da Graca Cabreira-Hansen M et al (2013) Manufacturing mesenchymal stromal cells for phase I clinical trials. Cytotherapy 15:416–422
3. Zuk PA, Zhu M, Ashjian P et al (2002) Human adipose tissue is a source of multipotent stem cells. Mol Biol Cell 13: 4279–4295
4. Ryan JM, Barry FP, Murphy JM et al (2005) Mesenchymal stem cells avoid allogeneic rejection. J Inflamm (Lond) 2:8
5. Majumdar M, Keane-Moore M, Buyaner D et al (2003) Characterization and functionality

of cell surface molecules on human mesenchymal stem cells. J Biomed Sci 10:228–241

6. Tse WT, Pendleton JD, Beyer WM et al (2003) Suppression of allogeneic T-cell proliferation by human marrow stromal cells: implications in transplantation. Transplantation 75:389–397
7. Li YP, Paczesny S, Lauret E et al (2008) Human mesenchymal stem cells license adult CD34+ hemopoietic progenitor cells to differentiate into regulatory dendritic cells through activation of the Notch pathway. J Immunol 180:1598–1608
8. Abumaree M, Al Jumah M, Pace RA et al (2012) Immunosuppressive properties of mesenchymal stem cells. Stem Cell Rev 8:375–392
9. Le Blanc K, Rasmusson I, Sundberg B et al (2004) Treatment of severe acute graft-versus-host disease with third party haploidentical mesenchymal stem cells. Lancet 363: 1439–1441
10. Yin F, Battiwalla M, Ito S et al (2014) Bone marrow mesenchymal stromal cells to treat tissue damage in allogeneic stem cell transplant recipients: correlation of biological markers with clinical responses. Stem Cells 32:1278–1288
11. Lazarus HM, Koc ON, Devine SM et al (2005) Cotransplantation of HLA-identical sibling culture-expanded mesenchymal stem cells and hematopoietic stem cells in hematologic malignancy patients. Biol Blood Marrow Transplant 11:389–398
12. Forbes GM, Sturm MJ, Leong RW et al (2014) A phase 2 study of allogeneic mesenchymal stromal cells for luminal Crohn's disease refractory to biologic therapy. Clin Gastroenterol Hepatol 12:64–71
13. Horwitz EM, Gordon PL, Koo WK et al (2002) Isolated allogeneic bone marrow-derived mesenchymal cells engraft and stimulate growth in children with osteogenesis imperfecta: Implications for cell therapy of bone. Proc Natl Acad Sci 99:8932–8937
14. Wu Y, Chen L, Scott PG et al (2007) Mesenchymal stem cells enhance wound healing through differentiation and angiogenesis. Stem Cells 25:2648–2659
15. Baxter MA, Wynn RF, Jowitt SN et al (2004) Study of telomere length reveals rapid aging of human marrow stromal cells following in vitro expansion. Stem Cells 22:675–682
16. Stolzing A, Jones E, McGonagle D et al (2008) Age-related changes in human bone marrow-derived mesenchymal stem cells: consequences for cell therapies. Mech Ageing Dev 129: 163–173
17. Kern S, Eichler H, Stoeve J et al (2006) Comparative analysis of mesenchymal stem cells from bone marrow, umbilical cord blood, or adipose tissue. Stem Cells 24:1294–1301
18. Hanley PJ (2014) Finessing the manufacture of mesenchymal stromal cells. Cytotherapy 16: 711–712
19. Hanley PJ, Mei Z, Durett AG et al (2014) Efficient manufacturing of therapeutic mesenchymal stromal cells with the use of the Quantum Cell Expansion System. Cytotherapy 16:1048–1058
20. Timmins NE, Kiel M, Günther M et al (2012) Closed system isolation and scalable expansion of human placental mesenchymal stem cells. Biotechnol Bioeng 109:1817–1826
21. Dominici M, Le Blanc K, Mueller I et al (2006) Minimal criteria for defining multipotent mesenchymal stromal cells. The International Society for Cellular Therapy position statement. Cytotherapy 8:315–317

Chapter 19

Quality Control Assays for Clinical-Grade Human Mesenchymal Stromal Cells: Methods for ATMP Release

Marina Radrizzani, Sabrina Soncin, Viviana Lo Cicero, Gabriella Andriolo, Sara Bolis, and Lucia Turchetto

Abstract

Mesenchymal stromal/stem cells (MSC) are promising candidates for the development of cell-based therapies for various diseases and are currently being evaluated in a number of clinical trials (Sharma et al., Transfusion 54:1418–1437, 2014; Ikebe and Suzuki, Biomed Res Int 2014:951512, 2014). MSC for therapeutic applications are classified as advanced therapy medicinal products (ATMP) (Regulation (EC) No 1394/2007 of the European Parliament and of the Council of 13 November 2007 on advanced therapy medicinal products and amending Directive 2001/83/EC and Regulation (EC) No 726/2004) and must be prepared according to good manufacturing practices (http://ec.europa.eu/health/documents/eudralex/vol-4). They may be derived from different starting materials (mainly bone marrow (BM), adipose tissue, or cord blood) and applied as fresh or cryopreserved products, in the autologous as well as an allogeneic context (Sharma et al., Transfusion 54:1418–1437, 2014; Ikebe and Suzuki, Biomed Res Int 2014:951512, 2014; Sensebé and Bourin, Transplantation 87(9 Suppl):S49–S53, 2009). In any case, they require an approved and well-defined panel of assays in order to be released for clinical use.

This chapter describes analytical methods implemented and performed in our cell factory as part of the release strategy for an ATMP consisting of frozen autologous BM-derived MSC. Such methods are designed to assess the safety (sterility, endotoxin, and mycoplasma assays) and identity/potency (cell count and viability, immunophenotype and clonogenic assay) of the final product. Some assays are also applied to the biological starting material (sterility) or carried out as in-process controls (sterility, cell count and viability, immunophenotype, clonogenic assay).

The validation strategy for each analytical method is described in the accompanying Chapter 20.

Key words Mesenchymal stromal/stem cell, Advanced therapy medicinal product, Good manufacturing practices, Analytical methods, Cell-based medicinal product

1 Introduction

Mesenchymal stromal/stem cells (MSC) are promising candidates for the development of cell-based therapies and are currently being evaluated in a number of clinical studies addressing various diseases [1–3]. MSC for therapeutic applications are classified as advanced

Massimiliano Gnecchi (ed.), *Mesenchymal Stem Cells: Methods and Protocols*, Methods in Molecular Biology, vol. 1416,
DOI 10.1007/978-1-4939-3584-0_19,

therapy medicinal products (ATMP) [4] and must be prepared according to good manufacturing practice (GMP) standards [5].

In this context, the development and validation of properly designed cell manufacturing and testing methods [6, 7] are of paramount importance for successful translational research.

The manufacturing process has to be carefully defined and validated to ensure product consistency [6]. In addition, to ensure product sterility, the production has to be performed in classified areas [8]. In particular, critical cell manipulation steps are conducted under laminar flow hoods (class A areas), located in class B rooms; and a system for particle and microbiological monitoring should be in place. MSC can be prepared from different starting materials such as bone marrow (BM), adipose tissue, cord blood or amniotic fluid; they can be applied as fresh or cryopreserved products, in autologous as well as allogeneic settings [1–3]. Detailed protocols for MSC production have been published elsewhere [9–11]; Fig. 1 summarizes our method for the manufacturing of autologous frozen BM-derived MSC.

A suitable quality control (QC) strategy has to be designed for each specific ATMP, with the aim of evaluating its safety, identity, purity, and potency [6, 7, 12]. Safety testing should encompass sterility, lack of endotoxin, and, at least for cultured cells, the absence of mycoplasma. The identity test panel includes cell morphology and immunophenotype. These tests also provide information on ATMP purity, as they may detect undesirable impurities such as contaminating cell types. Potency is defined as a measure of biological activity. A potency assay should be based on a defined biological effect closely related to the mechanism(s) responsible for the functional benefits [6]. Cell viability is an important component of the potency of cell-based ATMP, but additional parameters of biological activity should also be tested [12]. In particular, specific potency assays should be developed for any given product and its clinical indication.

Release specifications (i.e., acceptance criteria required for the ATMP before administration to the patient) need to be defined for safety parameters, generally evaluated by assays described in the European Pharmacopoeia (EP) (compendial assays) and for other crucial parameters such as cell viability.

For other important parameters (e.g., specific potency assays based on clonogenic potential or gene expression), mostly evaluated by non-compendial assays developed on a product-specific basis, data may be collected during the initial phases of clinical development as additional product information: in these cases, defined release specifications are not needed.

To complete the release panel, several other tests should also be performed at least during process validation [6], in order to prove genetic stability/absence of tumorigenicity (e.g., karyotype, telomerase activity, soft agar test), evaluate cellular senescence

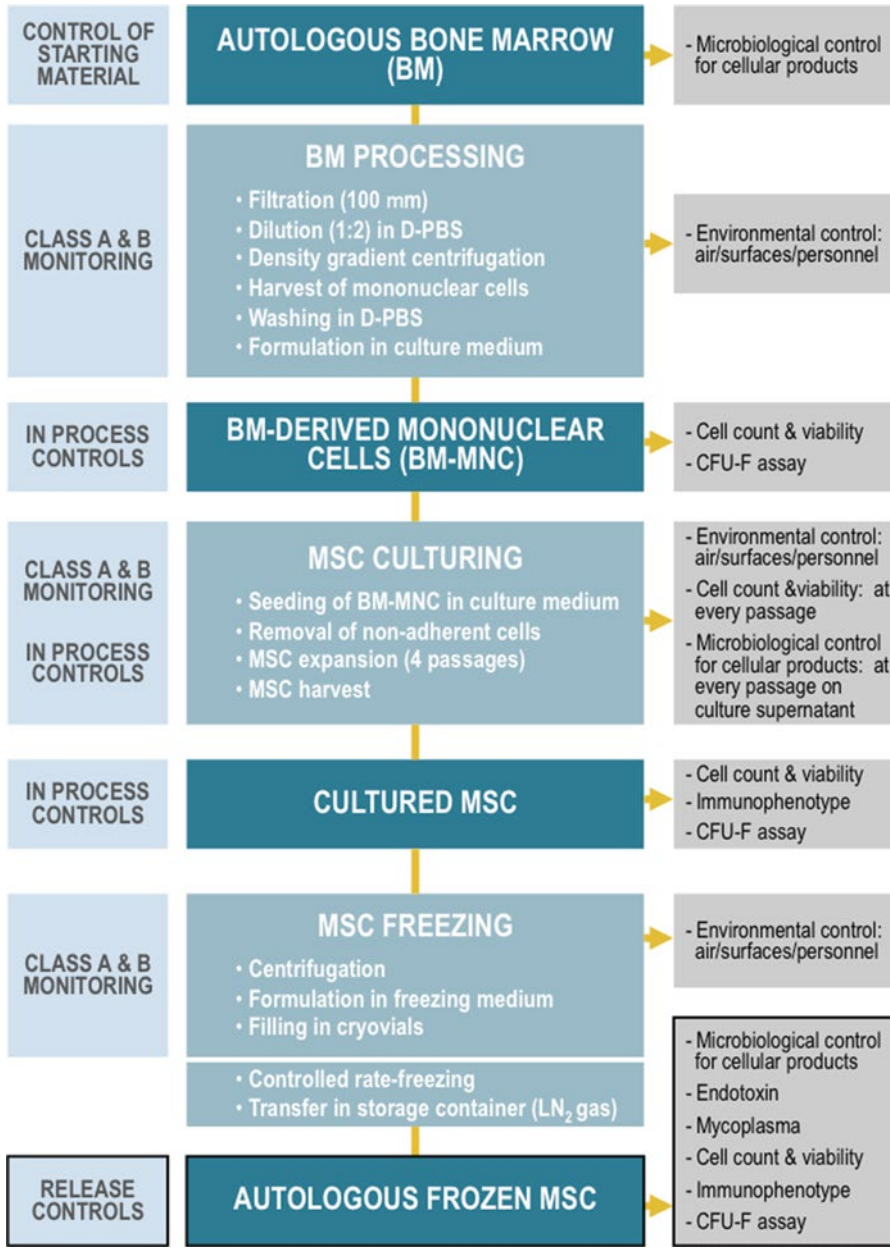

Fig. 1 Manufacturing flowchart. Process steps are summarized, as well as analytical controls performed on the starting material, in-process controls, and release controls performed on the final product consisting of autologous frozen MSC

(e.g., senescence-associated-b-galactosidase, p53/p21 or p16 expression, telomere shortening, specific DNA methylation changes [13]), confirm identity and potency (differentiation capability, i.e., for MSC the ability to differentiate toward chondrocyte, adipocyte, and osteocyte lineages [14]), and viral safety (in vitro

and in vivo test for adventitious viruses). Such tests may be outsourced to specialized companies, provided that they have a certified quality system and are regularly audited by the ATMP manufacturing license owner. A stability study, based on the release assay panel, should also be established in order to define the ATMP shelf life.

This chapter focuses on a series of analytical methods implemented and performed in our cell factory as part of the release strategy for an ATMP consisting of frozen autologous BM-derived-MSC. They are applied at different stages, as summarized in Fig. 1. For every method, test acceptance criteria have been defined on the basis of experimental data obtained during analytical development.

According to GMP guidelines [5], the QC strategy encompasses several aspects, as outlined below.

Critical **raw materials and reagents** for the manufacturing process and quality control tests are selected on the basis of parameters reported on certificates of analysis. Their quality has to be experimentally confirmed during ATMP development and validation phases. The suppliers must be qualified and their quality system checked regularly. Each lot of any critical raw material or reagent is subject to an approval procedure, based on defined written specifications. Only items released by the QC department can enter in QC and production areas. The release process is carried out on both a documentary (certificate of analysis) and experimental basis (*see* **Note 1**).

The **biological starting material** for ATMP manufacturing (in our case, the BM sample giving rise to the MSC culture) should be tested for the presence of the viruses HIV-1/2, HCV, *Treponema pallidum* (antibodies), and HBV (HBsAg), according to the relevant European Directives [15, 16]. For this purpose, a patient/donor blood sample is collected 7–30 days before the BM harvesting and tested as required. Moreover, the BM is tested for sterility according to the method described in Subheading 3.1. In-process controls (**IPC**) are performed throughout the manufacturing process, and **release controls** are applied to the final product, as outlined in Fig. 1.

Environmental monitoring for particle and microbiological contamination, a key issue during aseptic manufacturing, is carried out according to GMP Annex 1 [8]. The monitoring frequency, the number, and the location of sampling points in the clean room area are process and site specific, defined on a risk-based analysis. In any case, personnel, laminar flow box, instruments used for the manufacturing process, and the working area are always monitored, and results are taken into consideration for product release.

Equipment is qualified, calibrated, and maintained at defined intervals by appropriate procedures. Analyses are carried out in **authorized QC laboratories**, by trained **QC personnel**.

A GMP-compliant **documentation system** should be in place. Written and approved analytical methods are used, and to ensure the full traceability of the analysis, raw data (encompassing lot number of any raw materials, any data derived from instruments, any data derived from operator observation or manipulation step) are recorded by a well-identifiable and trained operator.

Analytical data are approved by the quality control head before the ATMP release by the qualified person. Any deviation or out-of-specification results are documented and investigated.

2 Materials

2.1 Microbiological Control for Cellular Products

1. BacT/ALERT FA PLUS (aerobic) (FA bottles) and BacT/ALERT FN PLUS (anaerobic) (FN bottles) (#410851 and #410852, bioMérieux, www.biomerieux.com) (*see* **Note 2**).
2. Sterile syringes and needles.
3. Agar plates: tryptic soy agar (TSA) or Columbia blood agar (CBA) and Sabouraud dextrose agar (SDA).

2.2 Endotoxin Assay

1. Endosafe® PTS™ cartridges—0.05 EU/ml sensitivity (#PTS2005F, Charles River, www.criver.com).
2. Water for injection.
3. Sterile and non-pyrogenic tubes and sterile and non-pyrogenic tips.

2.3 Mycoplasma Assay

1. Trypsin-EDTA.
2. Trypan blue.
3. Universal Mycoplasma Detection Kit (#30-1012K, ATCC, www.lgcstandards-atcc.org/) containing lysis buffer, universal master mix, universal primers, sample lysis tubes, positive control.
4. Calibrated genomic mycoplasma DNA (*M. pneumoniae* #qCRM-15531D, ATCC, or #M-1250, Bionique Testing Laboratories, www.bionique.com) as an internal control.
5. Disposable sterile pipettes.
6. Cell scraper.
7. Sterile filter tips.
8. Polymerase chain reaction (PCR) tubes or strips with caps.
9. DNA ladder 100.
10. Agarose.

11. 1.5 ml tubes, PCR clean.
12. Six-well plate, tissue culture treated.
13. Loading dye.
14. Tris-acetate-EDTA (TAE) buffer 1×.
15. SYBR Safe DNA gel stain (#S33102, Invitrogen, www.lifetechnologies.com).
16. PCR water (certified DNA-free).

2.4 Cell Count and Viability

1. Flow cytometry tubes.
2. Flow cytometry running buffer.
3. Propidium iodide (PI) solution, 100 mg/ml in Dulbecco phosphate buffered saline (D-PBS).
4. Pipette tips.

2.5 Identity Assay (Immunophenotype)

1. MSC Phenotyping Kit human (#130-095-198, Miltenyi Biotec, www.miltenyibiotec.com), including MSC Phenotyping Cocktail (containing CD73-APC, CD90-FITC; CD105-PE, CD45-PerCP, CD34-PerCP, CD14-PerCP, CD20-PerCP) and Isotype Control Cocktail (containing the corresponding isotype controls).
2. Anti-HLA-DR-PerCP (#130-095-291, Miltenyi Biotec).
3. Staining buffer: D-PBS w/o Ca^{2+} and Mg^{2+}, 0.5 % human serum albumin (HSA), 2 mM EDTA (*see* **Note 3**).
4. Flow cytometry tubes.
5. Flow cytometry running buffer (*see* **Note 4**).
6. Pipette tips.

2.6 Clonogenic Potential (CFU-F Assay)

1. StemMACS™ Medium (MSC expansion media Kit XF-Miltenyi, www.miltenyibiotec.com) (*see* **Note 5**).
2. 100 mm dishes, tissue culture treated.
3. Disposable sterile pipettes.
4. Sterile filter tips.
5. D-PBS w/o Ca^{2+} and Mg^{2+}.
6. Methanol.
7. Giemsa's azur eosin methylene blue solution.

3 Methods

3.1 Microbiological Control for Cellular Products

This assay is performed to evaluate sterility, by detecting fungal and bacterial contamination in cell-based medicinal products. It is designed to be performed on a cell suspension (on BM, as the

biological starting material test, or on frozen MSC, as a final product release test), but cell-free supernatant can also be used (as IPC) (*see* **Note 6**) provided that the assay is validated accordingly. The test is performed according to EP 2.6.27 [17]. It is preferable to the classical EP test for sterility [18], since it has better sensitivity and a broader range and may be more rapid. It is carried out using an automated microbial detection system (BacT/ALERT® 3D, BioMérieux, www.biomerieux.com) (*see* **Note 7**).

3.1.1 Procedure

The sample inoculum is performed in a clean room area (class A/background B or isolator): microbial and particle contamination should be monitored according to GMP Annex 1 [8]. The subsequent steps (cultures, subcultures, and bacteria identification) are carried out in a standard QC microbiological laboratory.

1. Remove the FA and FN bottle caps and disinfect the rubber septum.
2. With a syringe and needle, remove the test sample volume to be inoculated in one bottle (*see* **Note 8**), remove the air completely, and inoculate it in FN PLUS medium; repeat the same step for FA PLUS medium (*see* **Note 9**) and then for all the required bottles.
3. Mix the bottles well.
4. Record all data on the dedicated forms or labels (*see* **Note 10**).
5. Transfer all samples and forms outside the clean room area and then into the Bact/ALERT instrument (bioMérieux) following the supplier's instructions.
6. Check the instrument frequently and record the results.
7. At the end of the incubation period (*see* **Note 11**), print the record from the instrument (a graph should always be available showing the colorimetric signals recorded during the incubation period).
8. Evaluate results: a sample is *negative* if no growth is detected (no colorimetric signal variation), *positive* if growth is detected (variation of colorimetric signal). Liquid and solid subcultures must be performed to confirm any sample positivity.

3.1.2 Specification

The specification is:

- Negative (no growth).

3.1.3 Procedure for Subculture in the Case of Positive Results

1. Seed 1 ml of positive sample on an agar plate (*see* **Note 12**) (solid subculture) and 1 ml in a new Bact/ALERT bottle (FA or FN depending on the positive bottle) (liquid subculture).
2. Incubate the TSA or CBA plate for 3 days at 32.5°±2.5 °C for bacteria subcultures and the SDA plate for 5 days at 22.5°±2.5 °C for fungi subcultures.

3. Incubate the Bact/ALERT bottle in the instrument for the defined period (*see* **Note 11**).
4. Evaluate results: for solid subcultures, check plates for the presence of colonies (a subculture is *positive* if colonies are detected, *negative* if not); for liquid subcultures, *see* **step 8** above.

3.1.4 Final Results

If both solid and liquid subcultures are negative, the first result obtained must be considered a false-positive result, and therefore the sample can be considered negative.

If one or both subcultures are positive, the sample must be considered positive, and the microorganism's genus and species must be identified (*see* **Notes 13** and **14**).

3.2 Endotoxin Assay

This assay is performed to detect bacterial endotoxins in the final product and is based on EP 2.6.14 [19]. It is designed as a final product release test, to be performed on a frozen BM-MSC suspension. The chromogenic technique is used, relying on the development of color after cleavage of a synthetic peptide-chromogen complex by the reaction of endotoxins with limulus amoebocyte lysate (LAL). The time required for the color development (onset time) is directly related to the endotoxin concentration in the sample. The method is performed using the Endosafe®-PTS™ system (CE-certified portable spectrophotometer; Charles River, www.criver.com) [20] in combination with FDA-licensed disposable test cartridges. The assay procedure has been defined according to the Endosafe®-PTS™ system's manual.

3.2.1 Procedure

The assay is performed in a standard QC laboratory. Sample manipulation is performed in a laminar flow box.

1. Insert the PTS endotoxin cartridge into the slot of the PTS reader following the instruction manual (*see* **Notes 15** and **16**).
2. Prepare at least 100 µl of the test sample diluted with LAL reagent water (*see* **Note 17**) according to validation data.
3. Vortex the sample to prevent the endotoxin from sticking to the wall.
4. Load 25 µl of sample (*see* **Note 18**) into each of the four sample reservoirs (*see* **Note 19**).
5. Results are available in 15 min. They are displayed on the screen and can be printed.

3.2.2 Acceptance Criteria and Specification

The assay is valid (acceptance criteria) if:

- Spike recovery (*see* **Note 20**): between 50 and 200 %.
- Percent coefficient of variation (CV%) for sample and positive control: <25.

- The specification must be set according to EP 5.1.10, depending on the product dose and route of administration (*see* **Note 21**).
- The assay detection limit is expressed as the product of the sensitivity of the cartridge (e.g., λ 0.05) and the dilution factor (e.g., 100) of the validated sample (e.g., 5.00 EU/ml). The test results for samples below the detection limit are expressed as <detection limit (e.g., <5.00 EU/ml).

3.3 Mycoplasma Assay

The "Universal Mycoplasma Detection Kit" produced by ATCC (www.lgcstandards-atcc.org) is used to perform PCR for the detection of mycoplasmas in cell cultures. This kit is designed to detect mycoplasma contaminants in cell culture and contains a proprietary mix of buffers, dNTPs, and thermostable polymerase, combined with universal primers that are specific for the 16S rRNA coding region in the mycoplasma genome. It detects over 60 species of *Mycoplasma*, *Acholeplasma*, *Spiroplasma*, and *Ureaplasma* including the eight species most likely to afflict cell cultures: *M. arginini*, *M. fermentans*, *M. hominis*, *M.hyorhinis*, *M. orale*, *M. pirum*, *M. salivarium*, and *A. laidlawii*. Samples that are positive for mycoplasma are easily recognized by a distinct PCR product ranging in size from 434 to 468 bp on an agarose gel.

The protocol setup in our lab is based on the manufacturer's indications. According to EP [21], a nucleic acid amplification technology (NAT)-based method can be used as a complementary test or to replace the traditional gold standard methods (culture-based method or indicator cell culture method, EP 2.6.7) provided that some conditions are maintained (sensitivity and specificity unaffected) as discussed in Chapter 20.

The assay is used as a release test for the final product.

3.3.1 Procedure

Sample Preparation

A 20 ml sample (containing between 10^4 and 10^5 cells—*see* **Note 22**) prepared as described below is required for the assay. Sample preparation **steps 1** and **2** are carried out in a clean room and the remaining steps in a QC laboratory dedicated for cell biology testing or Pre-PCR steps (*see* **Note 23**).

1. Cells from the last split during MSC manufacturing are seeded in two wells of a six-well plate (2.5×10^3 cell/cm^2, i.e., around 2.5×10^4 cells in 5 ml medium/well) and cultured until 50–70 % confluence (according to the manufacturing method, but without any medium change in order to avoid any possible mycoplasma dilution).
2. Cell supernatant (at least 20 ml of a pool made from equal aliquots from each culture vessel) is collected at the end of the MSC manufacturing process, just before final trypsinization for cell freezing. This supernatant can be stored frozen at −80 °C and thawed at 37 °C just before use.

3. Detach cells from one well seeded in **step 1** (*see* **Note 24**), and perform a viable cell count by flow cytometry (*see* Subheading 3.4) or use the Trypan blue exclusion method (*see* **Note 25**).
4. Scrape the cells from the second well (*see* **Note 26**) and adjust the concentration to 10^4–10^5 cells/ml on the basis of the result obtained in **step 3**.
5. Dilute 1 ml of the cell suspension obtained in **step 4** in 19 ml of cell supernatant (*see* **step 2**).
6. Transfer the whole test sample (about 20 ml) to lysis tubes: 1.5–2 ml/tube.
7. Centrifuge at 18,500 × *g* for 3 min at 4 °C and carefully remove and discard the supernatant.
8. Add 50 ml of Lysis Buffer to the pellet of one tube and transfer it to all the remaining tubes in order to collect the sample in one single final tube.
9. Vortex for 10 s and incubate for 15 min at 37 °C in a water bath.
10. Heat the sample at 95 °C for 10 min.
11. Centrifuge at 16,000 × *g* at 4 °C for 5 min and transfer the supernatant (lysate) to a new 1.5 ml tube.
12. Store the lysate at –80 °C (or use it immediately for PCR).

3.3.2 PCR Mix Preparation

Mix preparation steps are carried out in a room dedicated to PCR mix preparation; positive control and samples are added in a room dedicated to nucleic acid purification (*see* **Note 23**).

1. Thaw the universal PCR mix and primers and vortex and spin down the tubes.
2. Calculate the number of PCR reactions according to the following formula (*see* **Note 27**):

Number of test samples × 2 + 1 Positive Control + 1 Internal control + 2 Negative Controls + 1

3. Prepare the PCR mix in 1.5 ml tubes using the following volumes for each PCR reaction:

Universal master mix	20 µl
Universal primers	2.5 µl
Total volume/sample	22.5 µl

4. Move the prepared mix to the room dedicated to nucleic acid purification.

3.3.3 PCR Reaction

1. Label the PCR tubes: two tubes for each test sample, A and B (e.g.,1A, 1B, 2A, 2B), negative control A and B, internal control, and positive control.

2. Thaw the positive control, the internal control, and the samples; vortex and spin down the tubes.
3. Add 22.5 µl of PCR Mix in each tube.
4. Add 2.5 µl of each sample in duplicate to the corresponding sample tubes (e.g., 2 tubes/sample: 2.5 µl of sample in tube A and 2.5 µl in tube B), mix gently with the pipette, and close the A tubes.
5. Add 2.5 µl H_2O to negative control tube A and close the tube (*see* **Note 28**).
6. Add 1 µl of a calibrated internal control (10–20 copies/µl) (*see* **Note 29**) to sample B tubes.
7. Add 1 µl of a calibrated internal control (10–20 copies/µl) (*see* **Note 29**) to the internal control tube (with 1.5 µl H_2O).
8. Add 2.5 µl of the positive control (plasmid DNA from the kit) to the positive control tube, mix gently with the pipette and close the tube.
9. Add 2.5 µl of H_2O to the negative control tube B and close the tube.
10. Store the remaining lysates at −80 °C.
11. Place the tubes in a thermal cycler and run the PCR using the following parameters:

	Temperature	Time	Cycles
Step 1	94 °C	1.5 min	1
Step 2	94 °C 70–60.5 °C[a] 72 °C	30 s 30 s 45 s	20
Step 3	94 °C 60 °C 72 °C	30 s 30 s 45 s	12
Step 4	72 °C	45 s	1
Step 5	10 °C	Hold	1

[a]Touchdown PCR steps = −0.5 °C/cycle (*see* **Note 30**)

3.3.4 Gel Electrophoresis

1. Prepare a 3 % agarose gel in 1× TAE buffer (e.g., 3 g agarose in 100 ml TAE buffer).
2. Add SYBR Safe DNA gel stain 10,000× (dilute 1:10,000: e.g., 10 µl in 100 ml 1× TAE).
3. Melt the solution in a microwave oven (SYBR Safe DNA gel stain is resistant to microwaving).
4. Insert a comb in a gel electrophoresis tray, add the melted solution, and wait until the polymerization is complete.

5. Insert the tray with the gel in the electrophoresis chamber and cover it completely with 1× TAE buffer; gently and slowly remove the comb.
6. Add 2.5 μl of 100 bp DNA ladder to 2 μl of 6× loading dye and load it in the first lane of the gel.
7. Add 10 μl of each sample to 2 μl of 6× loading dye and load the samples onto the gel, leaving an empty lane (if possible) between samples A and B.
8. Electrophorese at 80–110 V until tracking dye migrates 60–70 % the length of the gel.
9. Take a picture through a gel imaging system (*see* **Note 31** as an example) or view it with a UV illuminator. Print the picture and attach it to the lab book.
10. Evaluate results: the sample is considered *negative* if there are no visible bands in the expected range (434–468 bp) in the sample amplified without the internal control; the sample is considered *positive* if there are visible bands (434–468 bp) in the sample amplified without the internal control.

Acceptance Criteria and Specification

The assay is valid (acceptance criteria) if:

- Positive control exhibits a 464-bp band.
- Calibrated internal control exhibits its specific length band.
- There are no visible bands (434–468 bp) in the negative control lanes.

Each sample result is acceptable if:

- The sample amplified with calibrated internal mycoplasma control exhibits its specific length band (*see* **Note 32**).

The release criteria (or specification) for the mycoplasma assay is:

- Negative.

3.4 Cell Count and Viability

This assay is performed by flow cytometry [22] (*see* **Note 25**). The direct determination of cell concentration is possible with a flow cytometer equipped with a system allowing accurate uptake of sample volumes (volumetric pipetting) (*see* **Note 33**). The determination of cell concentration by other flow cytometers requires the use of fluorescence microspheres; refer to manufacturer's indications for their use. The evaluation of cell viability is based on the ability of fluorescent dyes such as PI to cross the damaged membranes of dead cells, bind to double-stranded DNA, and be detected by flow cytometry. When excited by a 488 nm laser, PI is detected both in a red fluorescence channel (PI channel) and in the yellow fluorescence channel commonly used for R-phycoerythrin (PE) detection (PE channel). The assay is applied as a release test for the final product and as IPC during cell culture.

3.4.1 Procedure

1. Thaw a final product vial (containing frozen MSC): put the vial in a bag, place in a 37 °C water bath until thawed, and then disinfect the vial surface (*see* **Note 34**).
2. Dispense 50 µl/tube of the cell suspension into two flow cytometry tubes, identified as "BLANK" and "PI."
3. Dilute the samples 1:5 by adding flow cytometry running buffer, 200 µl/tube.
4. Add 2.5 µl of PI Solution to the PI tube (final PI concentration, 1 µg/ml).
5. Acquire the samples (100 µl/tube) by flow cytometry using proper instrument settings, according to the manufacturer's indications (*see* **Note 35**).
6. Perform the analysis according to the following scheme (*see* **Note 36**). A representative analysis is shown in Fig. 2.

Plot #	Type	Parameters	Gated on	Notes
1	Dot plot	Forward scatter vs. side scatter	–	Draw a region (R1) to exclude debris; events within R1 represent cells; determine total cell concentration (count/ml in R1) (*see* Fig. 2, plot #1)
2	Dot plot	PE fluorescence vs. PI fluorescence	R1	Draw a region (R2) including the bottom and the bottom/right portion of the plot; events within R2 in the PI tube (Fig. 2, plot #2b) represent viable cells, while in the BLANK tube (Fig. 2, plot #2a), they should roughly correspond to total cells; determine viable cell concentration (count/ml in R2) and cell viability (% in R2)

7. Record results as follows:

Total cell concentration	Count/ml in R1 (value from the PI tube)
Viable cell concentration	Count/ml in R2 (value from the PI tube)
Cell viability (%)	% in R2 (value from the PI tube)
Control cell percentage (%)	% in R2 (value from the BLANK tube)

3.4.2 Acceptance Criteria and Specifications

The test is considered valid if (acceptance criteria):

- Control cell percentage (R2; blank tube) ≥95 %.

Release criteria (specification only for the final product) is:

- Cell viability: ≥70 % [23] (*See* **Note 37**).

3.5 Identity Assay (Immunophenotype)

According to the International Society for Cellular Therapy (ISCT) [14], MSC must express CD73 (ecto 5′ nucleosidase), CD90 (Thy-1), and CD105 (endoglin) and lack expression for CD45 (pan-leukocyte marker), CD34 (expressed on primitive hematopoietic progenitors and endothelial cells), CD14 or CD11b (prominently expressed on monocytes and macrophages), CD79α or

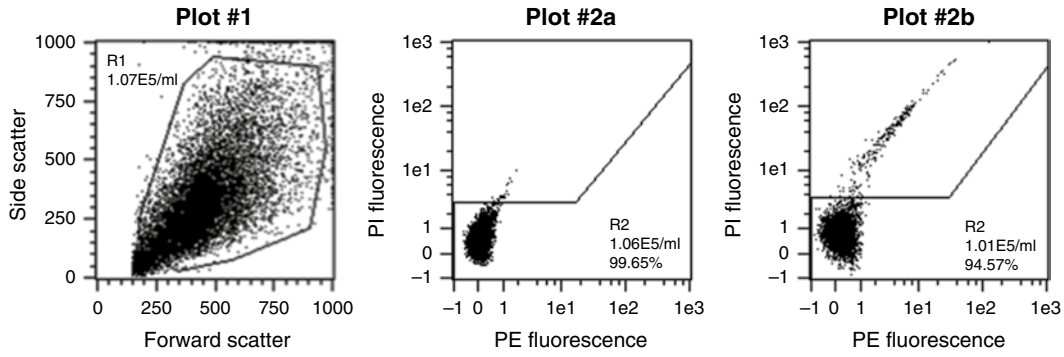

Fig. 2 Cell count and viability. An example of results is reported. Plot #1 refers to the PI sample; events in R1 represent cells; total cell concentration is shown. Plot #2a refers to the BLANK sample; control cell concentration and percentage are shown. Plot #2b refers to the PI sample; events in R2 represent viable cells; viable cell concentration and viability are shown

CD19 (markers of B cells that also express CD20), and HLA-DR surface molecules. The aim of immunophenotype characterization is to establish the identity of MSC by flow cytometry analysis [22].

The assay is applied as a release assay for the final product and as IPC during cell culture. The assay procedure has been set up in our lab according to indications provided by Miltenyi Biotec, whose monoclonal antibodies are used.

3.5.1 Procedure

1. Thaw a final product vial (containing frozen MSC): put the vial in a bag, place in a 37 °C water bath until thawed, and then disinfect the vial surface (*see* **Note 34**).
2. Determine cell concentration (*see* **Note 38**).
3. Dispense 0.25×10^6 cells/tube into two flow cytometry tubes, identified as "ISO" and "MSC," and add staining buffer up to 1 ml total volume in each tube.
4. Centrifuge the tubes at 300 × *g*, 10 min at room temperature.
5. Aspirate supernatant completely and resuspend each cell pellet in 100 µl of staining buffer.
6. Add 10 µl of MSC Phenotyping Cocktail and 10 µl of anti-HLA-DR-PerCP to the "MSC" tube; add 10 µl of Isotype Control Cocktail to the "ISO" tube.
7. Mix well (vortex 5 s) and incubate 10 min in the dark at 2–8 °C.
8. Add 2 ml of flow cytometry running buffer to each tube.
9. Centrifuge the tubes at 300 × *g*, 10 min at room temperature.
10. Completely aspirate the supernatant and resuspend each cell pellet in 200 µl flow cytometry running buffer.
11. Acquire samples on a flow cytometer using proper instrument settings and compensation, according to the manufacturer's indications.
12. Perform the analysis according to the following scheme.

Plot #	Type	Parameters	Gated on	Notes
1	Dot plot ISO	Forward scatter vs. side scatter	–	Draw a region (R1) to exclude debris
2	Histogram ISO/MSC overlay	FITC fluorescence vs. relative cell number	R1	Draw a region (R2) between the right margin of the ISO histogram and the right border of the plot, to determine % $CD90^+$ cells
3	Histogram ISO/MSC overlay	PE fluorescence vs. relative cell number	R1	Draw a region (R3) between the right margin of the ISO histogram and the right border of the plot, to determine % $CD105^+$ cells
4	Histogram ISO/MSC overlay	APC fluorescence vs. relative cell number	R1	Draw a region (R4) between the right margin of the ISO histogram and the right border of the plot, to determine % $CD73^+$ cells
5	Histogram ISO/MSC overlay	PerCP fluorescence vs. relative cell number	R1	Draw a region (R5) between the right margin of the ISO histogram and the right border of the plot, to determine % CD45/CD34/CD14/CD20/$HLA\text{-}DR^+$ cells

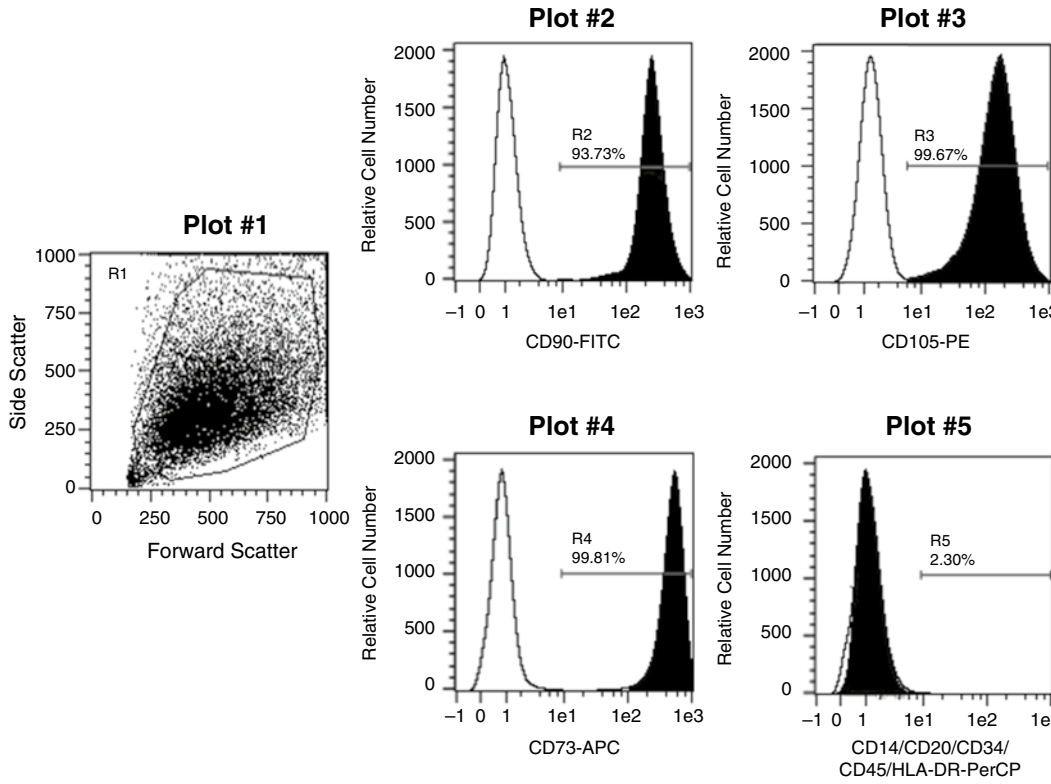

Fig. 3 Immunophenotype. An example of results is reported. Events in R1 (plot #1) represent cells. Plots #2–5 are overlaying histograms in which data from both ISO (blank peak) and MSC (colored peak) are represented. The percentages of cells positive for the following markers are shown: CD90 (plot #2, R2); CD105 (plot #3, R3); CD73 (plot #4, R4); CD14 or CD20 or CD34 or CD45 or HLA-DR (plot #5, R5)

3.5.2 Acceptance Criteria and Specifications

The test is considered valid if (acceptance criteria):

- Cells positive for all the markers in the ISO tube: ≤5 %.

Release criteria (specifications) are [14]:

- Cells positive for CD90, CD105, and CD73 in the MSC tube: ≥90 %.
- Cells positive for CD45/CD34/CD14/CD20/HLA-DR in the MSC tube: ≤10 %.

Example of results is shown in Fig. 3.

3.6 Clonogenic Potential (CFU-F Assay)

The colony-forming unit fibroblast (CFU-F) assay [24] is a functional method to assess, by limiting dilution, the frequency of mesenchymal stromal progenitor cells. It is performed on frozen MSC as a final product release test, but it can also be carried out on BM-derived mononuclear cells (BM-MNC) before cell seeding or on fresh cultured MSC (as IPC). This assay has been set up in our lab on the basis of indications published by Castro-Malaspina et al. [24].

3.6.1 Procedure

Use sterile materials and maintain sterile conditions using a laminar flow box for the cell-seeding steps and to prepare cell culture reagents. Washing and staining steps can be performed at the workbench.

3.6.2 Preparation of StemMACS MSC Supplements

1. Thaw the supplements at 37 °C.
2. Prepare aliquots in cryovials (from 0.5 to 1ml depending on the volume of medium to be prepared for each test) (*see* **Note 39**).
3. Label each tube with the following information:

StemMACS Supplements, volume (ml/vial), lot number, preparation date, expiration date (the same reported on the original bottle), storage temperature (−20 °C), and operator initials.

3.6.3 Preparation of Complete Medium

1. Thaw the StemMACS supplements aliquot(s) at 37 °C.
2. Add 0.7 ml of supplements to 50 ml of StemMACS medium and mix well.
3. Label the bottle/tube with the following information:

Complete StemMACSmedium, preparation date, expiration date (1 week after preparation), storage temperature (2–8 °C), and operator initials.

3.6.4 Cell Seeding

1. Thaw a final product vial (containing frozen MSC) and wash the cells to remove the freezing medium: put the vial in a bag, place in a 37 °C water bath until thawed, then disinfect the vial surface, transfer the vial to the laminar flow box, gently add 9 ml of culture medium, spin at $400 \times g$ for 10 min at room temperature, discard the supernatant, and resuspend the cell pellet in 1 ml of complete medium (*see* **Note 34**).
2. Determine viable cell concentration as described in Subheading 3.4 (*see* **Note 25**).
3. Dilute the cells at 1×10^3 viable cells/ml in complete medium.
4. Prepare three 100 mm dishes (A, B, and C) with 8, 9, and 9.5 ml of complete medium, respectively.
5. Add 2.0, 1.0, and 0.5 ml of the cell suspension to dishes A, B, and C, respectively; this allows the seeding of 3 dishes with 2×10^3 cells/dish (dish A), 1×10^3 cells/dish (dish B), and 0.5×10^3 cells/dish (dish C), respectively (*see* **Note 40**).
6. Place the dishes in a 37 °C humidified incubator (5 % CO_2) for 14 ± 1 days.

3.6.5 Cell Staining

1. Remove the medium from the dishes with a pipette; the colonies remain adherent to the plastic.
2. Wash the dishes twice with 8–10 ml D-PBS/dish in order to remove residual medium (*see* **Note 41**).
3. Remove D-PBS from the dishes with a pipette.

4. Fix the cells with 5 ml methanol/dish at room temperature for 5 min (*see* **Note 41**).
5. Remove methanol from the dishes with pipettes and let dishes air dry at room temperature (*see* **Note 42**).
6. Add 5 ml/dish of Giemsa solution 1:20 (*see* **Note 43**) and leave at room temperature for 20 min (*see* **Note 41**).
7. Remove the Giemsa solution from the dishes with a pipette.
8. Wash with Milli-Q water until water is clear (*see* **Note 44**) and let dry at room temperature.

3.6.6 CFU-F Colonies Enumeration

Human CFU-F colonies normally have a 1–8 mm diameter.

1. Mark, on the dish bottom, each colony observed macroscopically.
2. Count the colonies in each dish.
3. Verify the dishes microscopically (*see* **Note 45**) in order to check each marked colony for morphology and identify any possible faintly stained colony not seen at the first macroscopic examination.
4. Calculate the CFU-F frequency in each dish as CFU-F/10^3 cells seeded. Determine the average number (mean) and the coefficient of variation (CV%) (*see* **Note 46**).

3.6.7 Acceptance Criteria and Specification

The assay is valid if (acceptance criteria):

- CV% $\leq$ 25.

If CV% is >25, identify the outliers and calculate again the mean and CV% without outlier number (*see* examples in **Note 47**).

Specifications for product release are still not defined: data collected in the early phases of clinical development will be the starting point to define release criteria for more advanced clinical trial phases and for market authorization approval.

4 Notes

1. Each media lot for the microbiological assays (performed either for product testing or environmental control) is tested for sterility and growth promotion as described in EP 2.6.1 and 2.6.27.
2. These media were chosen because of the presence of an antibiotic inhibitor in their composition. The medium fertility is therefore guaranteed even for test samples potentially containing antibiotics.
3. Preparation: 8.9 ml D-PBS w/o Ca^{2+} and Mg^{2+} + 1 ml 5 % HSA + 0.1 ml 200 mM EDTA. Storage: at 2–8 °C, max 1 month.

4. Depending on the instrument, different buffers can be used; we use MACSQuant Running Buffer for the MACSQuant Analyzer.
5. Alternatively, MesenCult Proliferation Kit (StemCell Technologies, www.stemcell.com) or Alpha-MEM medium can be used.
6. Cell supernatant is used instead of a cell suspension to carry out this test as IPC: the supernatant (1–10 ml) is harvested from the culture vessel(s) at each passage, before the cell detachment procedure.
7. Alternatively, other commercially available systems may be used, such as Bactec (Becton Dickinson, www.bd.com), according to the manufacturer's recommendations and upon proper validation.
8. The minimum amount to be tested depends on the total volume of the product, and it is defined in EP 2.6.27:

Total product volume (*V*)	Inoculum volume/bottle (FA or FN medium)	Total volume to be tested (FA + FN medium)
$V \geq 10$ ml	1 % of total volume	2 % of total volume
1 ml $\leq V < 10$ ml	100 µl	200 µl
$V < 1$ ml	Not applicable	Not applicable

For a product such as frozen MSC, consisting of multiple aliquots (frozen vials), the minimum volume to be tested determines the minimum number of aliquots to be tested.

Aliquot(s) should be representative of the whole batch: they must be homogenous (the cell suspension should be well resuspended during the pre-freezing phase) and, in the case of several aliquots dedicated for microbiological assays, they have to be sampled, evenly distributed among the first, middle, and final prepared aliquots.

The maximum product volume to be inoculated in every bottle must be determined during the method's validation (*see* the accompanying Chapter 20).

9. Alternatively, the volume to be tested in both bottles may be drawn in a single syringe. In this case, completely remove the air, and first transfer the inoculum to the FN bottle (half of the volume) and then to the FA bottle (all the remaining volume and air) in order to avoid air uptake in the bottle for anaerobic culture.
10. Forms or labels (in the latter case, they can be stuck directly on the lab record book) must be sterile. Autoclaved paper or labels must be used and brought into the clean room in triple sterilized bags.

11. The incubation period at 36 ± 1 °C is usually between 7 and 14 days, and it is determined during the method's validation for each specific product.
12. Use TSA or CBA plates (or SDA plates for molds) under aerobic (for bacteria derived from FA bottles) or anaerobic (for bacteria derived from FN bottles) conditions, depending on the type of microorganism to be cultured. For the anaerobic condition, the use of anaerobic induction bags (#96118, bioMérieux) with their specific indicators is recommended. The original positive Bact/ALERT bottle will be inserted again in the Bact/ALERT system in the same location to confirm or negate the first positive result.
13. A possible identification technique is based on the use of the VITEK® 2 system (bioMérieux): the use of fresh (<24 h) and pure cultures is desirable. Briefly, a colony must be subcultured (with a sterile loop, collect only the top area of the single and well-distinguishable colony) on an appropriate plate (TSA for bacteria under aerobic or anaerobic conditions and SDA for yeast and molds), the Gram identification and morphology assessment are performed, and, according to the result, the sample is loaded on an appropriate VITEK card for the final identification.
14. A positive result always requires further investigation: data collected during environmental monitoring either performed during the manufacturing process or during sterility testing should be evaluated in order to compare the identified bacteria or fungi and to try to identify the cause of the contamination.
15. Allow the cartridge to reach room temperature in the bag before use. During cartridge manipulation, pay attention not to touch the reservoirs where the samples will be loaded: the cartridge has a rounded edge purposely designed to be touched.
16. The calibration code and the lot number required by the instrument are found in the cartridge's certificate of analysis. Several cartridges are commercially available with a sensitivity (λ) ranging between 0.005 and 0.1 EU/ml.
17. Method set up and validation (*see* Chapter 20) must be performed to define the sample dilution. Different sample's dilutions are tested with the inhibition/enhancement cartridge (PTS220 Charles River).
18. Keep the pipette tilted and do not touch the well bottom with the pipette tip. Pipette slowly in order to avoid bubble formation and squirts: they can cause nonhomogeneous samples, interfere with light transmission, and in the end produce false results.

19. Two out of four wells contain endotoxin spikes (0.5 EU/ml): they serve as positive control samples required to assess the presence of potential interference in the sample loaded.
20. The spike recovery (%) is calculated as: spike value/archived spike concentration × 100. The archived spike concentration is specific for each cartridge lot and it is defined in the certificate of analysis.
21. The specification has to be set according to Eu. Ph. 5.1.10, indicating between 0.2 and 5.0 IU per kilogram of body mass the limit for intrathecal administration or intravenous administration respectively in each single hour period. Cartridge-PTS sensitivity will be chosen accordingly; several cartridges are commercially available with a sensitivity (λ) ranging between 0.005 and 0.1 EU/ml.

    Example: assuming 40 kg as a minimum patient body mass, total endotoxin in an intravenous administered product should not exceed 200 IU; therefore, in a hypothetical infusion volume of 40 ml, the maximal endotoxin concentration in the final product should not exceed 5 IU/ml.
22. Use of more than 10^6 cells per sample may inhibit the PCR.
23. In order to avoid contamination, *do not* perform these steps in post-PCR rooms where PCR amplification products are manipulated.
24. Wash cells with 5 ml of PBS, remove PBS, add 1 ml Trysin-EDTA, incubate for 5–7 min at 37 °C, add 1 ml of complete medium (a-MEM + 2 mM Glutamine + 10 % FBS), and proceed with the cell counting.
25. As an alternative, Trypan blue cell counting [25] can be carried out, using manual systems (Bürker or Neubauer chamber) or automated systems (e.g., Cedex HiRes Analyzer, Roche, www.custombiotech.roche.com; Countess® Automated Cell Counter, Life Technologies, www.lifetechnologies.com/ch/en/home/life-science.html).
26. Trypsin or EDTA may disrupt mycoplasma: do not treat the cell sample to be tested for mycoplasma with these agents.
27. Example: 4 samples to be tested:

$4 \times 2 = 8 + 1$Positive Control + 1 Internal Control + 2 Negative Controls + **1** excess reaction = 13

    Prepare mix for 13 reactions: Master Mix (20 ml × 13 = 260 ml); Primers: (2.5 ml × 13 = 32.5 ml); Total 292.5 ml/13 tubes = 22.5 ml/tube.
28. Negative controls are in duplicate, such as the test samples: negative control A to test possible mix contamination, negative control B (Sentinel sample) to test operational contamination.

29. The calibrated internal control should be used at a concentration close to the LOD level determined during validation. Calibrated and certified genomic DNA of one mycoplasma strain suggested by EP must be used. *See* Chapter 20 where the mycoplasma test validation is described.
30. The touchdown PCR is performed to reduce nonspecific primer annealing and therefore increase specificity and sensitivity.
31. Using the Gel Doc EZ Imager/Bio-Rad, place the gel on the purple tray (UV tray) and insert the tray into the instrument. Analyze with the Image Lab Software. Protocol setup:
    - Application: SYBR safe.
    - Exposure: Automatic/faint bands.
    - Band detection sensitivity: high (better for faint bands).
32. If only the criterion 4 is not met for one or more samples, the result is considered not valid only for samples that do not meet the criterion 4 and they must be re-tested. If the problem persists, a sample dilution should be considered even though the assay sensitivity will be affected, and it has to be taken into consideration during the product release process.
33. For example, MACSQuant Analyzer (Miltenyi Biotec, www.miltenyibiotec.com) or BD FACSVerse™ (Becton Dickinson, www.bdbiosciences.com).
34. If the assay is applied as the IPC during MSC culture, skip **step 1**, using the fresh cell suspension directly for **step 2**.
35. Acquisition has to be performed just after addition of the PI; if available, use the autolabeling flow cytometer option; prolonged exposure (≥30 min) to the PI may impair the evaluation of cell viability.
36. Alternatively, with MACSQuant Analyzer, use the Express Mode, selecting Analysis/Cell count.
37. When using the assay as an in-process control during MSC culture, the number of total viable cells (TVC) is calculated at every passage according to the following formula:

$$\text{TVC} = \text{Viable cell concentration}\left(\frac{\text{Count}}{\text{ml}}\right) \times \text{Volume in which cells are suspended}\,(\text{ml})$$

Population doubling level (PDL) is determined at every passage according to the following formula:

$$\text{PDL} = \log_2\left(\frac{\text{Total viable cells at harvest}}{\text{Total viable cells at seeding}}\right) = 3.32 \times \log_{10}\left(\frac{\text{Total viable cells at harvest}}{\text{Total viable cells at seeding}}\right)$$

Cumulative population doublings (CPD) in a given period (e.g., the whole duration of a cell culture process) can be calculated by summing PDL values obtained at individual passages.

38. The cell concentration can be determined by flow cytometry (*see* Subheading 3.4) or Trypan blue exclusion (*see* **Note 25**). Total cells required: 5×10^5.
39. Store the aliquots at – 20 °C. Once thawed, the aliquots cannot be frozen again.
40. If the assay is applied to BM-MNC, higher cell-seeding densities are needed as only a fraction of the viable cell population is expected to consist of MSC; thus, prepare the suspension at 1×10^6 viable cells/ml, in order to seed three dishes with 2×10^6, 1×10^6, and 0.5×10^6 cells/dish, respectively. If the assay is applied as IPC on fresh cultured MSC, proceed as described for frozen MSC; just skip **step 1**.
41. Add any solution (PBS, methanol, or Giemsa) very slowly and on the dish's edge in order to avoid cell detachment.
42. Alternatively, 15 min under a laminar flow box is sufficient to dry the dishes completely.
43. Preparation of the Giemsa solution 1:20: mix well the Giemsa stock solution, dilute the solution 1:20 in distilled water, mix well, and let stand for 10 min. Use the 1:20 solution within the working day.
44. Washing can also be performed with distilled running water provided that the suggestion in **Note 41** is taken into account.
45. Use a grid under the dishes in order to completely score their surface (any rows and any columns). Adherent colonies containing more than 30 cells are counted at 4× magnification.
46. For the mean calculation, do not include the results obtained from dishes with more than 100 colonies; express the result as one decimal digit after the decimal point. Calculate the CV according to the following formula:

$$\mathrm{CV} = \frac{\text{standard deviation}}{\text{mean}} \times 100$$

47. Example 1:

Number of seeded cells	Number of colonies	Colonies/ 10^3 cells	Average	CV%	Acceptance criteria met
2×10^3	35	17.5	17.8	9.25	Yes
1×10^3	20	20			
0.5×10^3	8	16			

Example 2:

Number of seeded cells	Number of colonies	Colonies/ 10^3 cells	Average	CV%	Acceptance criteria met
2×10^3	41	20.5	16.2	44.6	No
1×10^3	22	22			
0.5×10^3	3	6[a]			
2×10^3	41	20.5	21.2	3.53	Yes
1×10^3	22	22			

[a]The average is calculated again without the outlier.

Acknowledgments

This work was supported by the Fondazione Cardiocentro Ticino—Lugano. The authors would like to acknowledge Maura Filippini for her excellent editing assistance.

References

1. Sharma RR, Pollock K, Hubel A et al (2014) Mesenchymal stem or stromal cells: a review of clinical applications and manufacturing practices. Transfusion 54:1418–1437
2. Ikebe C, Suzuki K (2014) Mesenchymal stem cells for regenerative therapy: optimization of cell preparation protocols. Biomed Res Int 2014:951512
3. Sensebé L, Bourin P (2009) Mesenchymal stem cells for therapeutic purposes. Transplantation 87(9 Suppl):S49–S53
4. Regulation (EC) No 1394/2007 of the European Parliament and of the Council of 13 November 2007 on advanced therapy medicinal products and amending Directive 2001/83/EC and Regulation (EC) No 726/2004
5. EudraLex – volume 4 – good manufacturing practice (GMP) guidelines – part I – basic requirements for medicinal products. http://ec.europa.eu/health/documents/eudralex/vol-4
6. Guideline on human cell-based medicinal products. EMEA/CHMP/410869/2006
7. Rayment EA, Williams DJ (2010) Concise review: mind the gap: challenges in characterizing and quantifying cell- and tissue-based therapies for clinical translation. Stem Cells 28:996–1004
8. EudraLex – volume 4 – good manufacturing practice (GMP) guidelines – annex 1 – manufacture of sterile medicinal products. http://ec.europa.eu/health/documents/eudralex/vol-4
9. Gnecchi M, Melo LG (2009) Bone marrow-derived mesenchymal stem cells: isolation, expansion, characterization, viral transduction, and production of conditioned medium. Methods Mol Biol 482:281–294
10. Wagey R, Short B (2013) Isolation, enumeration, and expansion of human mesenchymal stem cells in culture. Methods Mol Biol 946:315–334
11. Roseti L, Serra M, Bassi A (2015) Standard operating procedure for the good manufacturing practice-compliant production of human bone marrow mesenchymal stem cells. Methods Mol Biol 1283:171–186
12. Guideline on potency testing of cell based immunotherapy medicinal products for the treatment of cancer, EMEA/CHMP/410869/2006
13. Wuchter P, Bieback K, Schrezenmeier H et al (2015) Standardization of good manufacturing practice-compliant production of bone marrow-derived human mesenchymal stromal cells for immunotherapeutic applications. Cytotherapy 17:128–139
14. Dominici M, Le Blanc K, Mueller I et al (2006) Minimal criteria for defining multipotent mesenchymal stromal cells. The International Society for Cellular Therapy position statement. Cytotherapy 8:315–317

15. Commission Directive 2006/17/EC implementing Directive 2004/23/EC of the European Parliament and of the Council as regards certain technical requirements for the donation, procurement and testing of human tissues and cells
16. Directive 2004/23/EC of the European Parliament and of the Council on setting standards of quality and safety for the donation, procurement, testing, processing, preservation, storage and distribution of human tissues and cells
17. European Pharmacopoeia 8.0, Section 2.6.27 (Microbiological control for cellular products) (2014) European Directorate for the Quality of Medicines & HealthCare, Strasbourg, FR
18. European Pharmacopoeia 8.0, Section 2.6.1 (Sterility) (2014)
19. European Pharmacopoeia 8.0, Section 2.6.14 (Bacterial endotoxins) (2014) European Directorate for the Quality of Medicines & HealthCare, Strasbourg, FR
20. Endosafe – PTS Product Validation (2007) Endosafetimes – volume 13, n. 1 – Charles River Laboratories
21. European Pharmacopoeia 8.0, Section 2.6.7 (Mycoplasmas) (2014) European Directorate for the Quality of Medicines &HealthCare, Strasbourg, FR
22. European Pharmacopoeia 8.0, Section 2.7.24 (Flow Cytometry) (2010) European Directorate for the Quality of Medicines &HealthCare, Strasbourg, FR
23. US Department of Health (2008), Guidance for FDA reviewers and sponsors: content and review of chemistry, manufacturing, and control (CMC) information for human gene therapy investigational new drug applications (INDs). US Department of Health, FDA, CBER
24. Castro-Malaspina H, Ebell W, Wang S (1984) Human bone marrow fibroblast colony-forming units (CFU-F). Prog Clin Biol Res 154:209–236
25. Strober W (2001) Trypan blue exclusion test of cell viability. Curr Protoc Immunol Appendix 3B

Chapter 20

Quality Control Assays for Clinical-Grade Human Mesenchymal Stromal Cells: Validation Strategy

Marina Radrizzani, Sabrina Soncin, Sara Bolis, Viviana Lo Cicero, Gabriella Andriolo, and Lucia Turchetto

Abstract

The present chapter focuses on the validation of the following analytical methods for the control of mesenchymal stromal cells (MSC) for cell therapy clinical trials:

- Microbiological control for cellular product
- Endotoxin assay
- Mycoplasma assay
- Cell count and viability
- Immunophenotype
- Clonogenic potential (CFU-F assay)

In our lab, these methods are in use for product release, process control or control of the biological starting materials. They are described in detail in the accompanying Chapter 19.

For each method, validation goals and strategy are presented, and a detailed experimental scheme is proposed.

Key words Quality control assays, Advanced therapy medicinal products (ATMP), Good manufacturing practice (GMP), Quantitative assays, Potency assays, Specificity, Detection limit, Accuracy, Precision, Microbiological control for cellular product, Endotoxin, Mycoplasma assay, Viability, Immunophenotype, CFU-F assay

1 Introduction

Mesenchymal stromal cells (MSC) are promising therapeutic tools for immunomodulation as well as regenerative medicine applications [1] and are being employed in the context of several clinical trials [2].

According to current European regulations [3], such cell therapy products are classified as advanced therapy medicinal products (ATMP) and must be prepared according to good manufacturing

Massimiliano Gnecchi (ed.), *Mesenchymal Stem Cells: Methods and Protocols*, Methods in Molecular Biology, vol. 1416,
DOI 10.1007/978-1-4939-3584-0_20,

practice (GMP) standards. A GMP-compliant quality control (QC) strategy aiming to evaluate MSC safety, identity, purity, and potency has been designed in our lab according to current guidelines [4, 5] and described in the accompanying Chap. 19.

The present chapter focuses on methods' validation. In general, this should typically encompass the following parameters: accuracy, precision, specificity, detection limit, quantitation limit, linearity, and range [6, 7]. The ICH Q2 (R1) guideline [6] classifies the analytical methods into four categories: identification tests, quantitative tests for impurities, limit tests for the control of impurities, and quantitative assays for content/potency. The category of the analytical method determines the parameters which need to be actually evaluated (*see* **Note 1**).

Validation of analytical procedures during clinical development is seen as an evolving process [8]: for early phase studies, demonstration of the methods' suitability may be sufficient, whereas advanced phase studies require higher validation strength.

In any case, GMP analytical procedures must rely on the use of qualified equipment, calibrated and checked, at defined intervals, by appropriate methods. Furthermore, to be GMP compliant, validation activities must be carried out in QC laboratories by QC trained personnel.

For every applicable validation parameter, acceptance criteria should be defined according to European Pharmacopoeia (EP) indications and/or on the basis of experimental results obtained during assay development or setup.

A GMP-compliant documentation system is in place for validation activities: written and approved validation protocols are used; raw data (encompassing lot number of any raw materials, any data derived from instruments, any data derived from observation or manipulation step) are recorded on appropriate forms by well-defined and trained operators. Upon completion of validation activities for any given analytical procedure, a validation report is issued.

The following definitions [6] apply throughout the present chapter:

- Specificity: the ability to unequivocally assess the analyte in the presence of components which may be expected to be present.
- Detection limit: the lowest amount of analyte in a sample which can be detected but not necessarily quantitated.
- Accuracy: closeness of agreement between the value which is accepted either as a conventional true value or a reference value and the value found.

  To evaluate accuracy, the percent difference (Δ%) between any experimental value and the corresponding reference value is calculated according to the following formula:

$$\Delta\% = \left(\text{experimental value} - \text{reference value}\right) / \left(\text{reference value}\right) \times 100$$

- Precision: closeness of agreement (degree of scatter) between a series of measurements obtained from multiple sampling of the same homogeneous product under the prescribed conditions.

  Precision is expressed as the percent coefficient of variation (CV%) for a series of measurements, calculated according to the following formula:

$$\text{CV}\% = \frac{\text{standard deviation}}{\text{mean}} \times 100$$

- Repeatability (intra-assay precision): precision under the same operating conditions over a short interval of time.
- Intermediate precision: precision within laboratories during varying operating conditions (different days, different analysts, different equipment).
- Linearity: the ability (within a given range) to obtain test results which are directly proportional to the amounts of analyte in the samples.
- Range: interval between the upper and lower amounts of analyte in the sample for which a suitable level of precision, accuracy, and linearity has been demonstrated.
- Robustness: ability to remain unaffected by small but deliberate variations in the method's parameters; it provides indications on the method's reliability during normal usage.

2 Materials

A complete list of materials is reported in the accompanying Chap. 19. Specific additional materials to be used during the validation exercise are described here in Subheadings 3.1 and 3.3.

3 Methods

3.1 Microbiological Control for Cellular Products

This assay, carried out according to EP 2.6.27 [9], is designed to detect fungal and bacterial contamination in cell-based medicinal products. It is preferable to the EP test for sterility (2.6.1) [10], since it has a better sensitivity and a broader range and can be performed more rapidly. It is carried out using an automated microbial detection system (BacT/ALERT® 3D, BioMérieux, www.biomerieux.com), as described in detail in the accompanying Chap. 19, Subheading 3.1.

The assay validation approach described below has been designed according to EP 2.6.27.

The sampling volume has to be defined on the basis of the total volume of the products [11], and the maximum inoculum volume per bottle has to be experimentally determined in order to avoid any product interference with possible microorganism growth (*see* **Note 2**).

Since it is used as a detection limit assay to test impurities, this method has to be validated for the following parameters [6]:

- Specificity
- Detection limit.

Even though the test precision in terms of repeatability and intermediate precision is not required by regulators, it has been included in our validation strategy. In addition, the sterility and growth promotion test data, collected at each release of a new lot of BacT/ALERT bottles, provide information on robustness.

3.1.1 Validation Samples

- Three independent samples of bone marrow (BM) as biological starting material.
- Three independent lots of frozen MSC, at the maximum cell concentration defined for the final product.

3.1.2 Validation Materials

- The panel of microorganisms listed in EP 2.6.27 [11] (*see* **Note 3**).
- Three different lots of BacT/ALERT FA PLUS and FN PLUS bottles should be used.

3.1.3 Validation Strategy

Experiment #	Samples	Operators and assay replicates	Validation parameters
1	Three fresh BM samples (A, B, and C), to be inoculated with or without 1–10 colony-forming units (CFU) of each microorganism (*see* **Note 4**), negative control (bottles without any sample), positive controls (bottles with microorganisms only)	Two operators (I and II), two assay replicates, three lots of BacT/ALERT bottles	Specificity Detection limit Repeatability Intermediate precision
2	Three frozen MSC lots (D, E, and F), to be inoculated with or without 1–10 CFU of each microorganism (*see* **Note 4**), negative control (BacT/ALERT bottle without sample or microorganism)	Two operators (I and II), two assay replicates, three lots of BacT/ALERT bottles	Specificity Detection limit Repeatability Intermediate precision

3.1.4 Acceptance Criteria for Validation

Specificity

- Positive signal in all the bottles inoculated with microorganisms, both in the absence and presence of test samples. The microorganism identity must be confirmed at least at the genus level.
- Negative signal in the bottles inoculated only with the cell product or the negative control bottles.

Detection Limit

- <100 CFU for each microorganism. Positive signals in all the bottles inoculated with microorganisms; the number of inoculated CFU should be experimentally confirmed in order to define the corresponding detection limit (*see* **Note 4**).

Repeatability

- Positive signal in both replicates of BacT/ALERT bottles inoculated with each microorganism in all the experiments.
- Negative signal in both replicates of BacT/ALERT bottles inoculated only with the cell product or the negative control bottles in all the experiments.

Intermediate Precision

- Similar results (±2 days), in terms of time required to reach the positive signal in different test runs, for each microorganism.

3.2 Endotoxin

This assay is designed to detect bacterial endotoxin level in the final product. It is based on EP 2.6.14 [12] and relies on the Endosafe®-PTS™ system (a CE-certified portable spectrophotometer) in combination with FDA-licensed disposable test cartridges. The chromogenic technique is used, based on the development of color after cleavage of a synthetic peptide-chromogenic complex by the reaction of endotoxins with limulus amebocyte lysate (LAL). It is described in detail in the accompanying Chap. 19, Subheading 3.2.

Before assay validation, the maximum valid dilution (MVD) is calculated (*see* **Note 5**): some pre-validation test runs (with at least three product lots) are carried out in order to define the suitable sample dilution (the dilution where no interference phenomena occur) (*see* **Note 6**).

According to ICH Q2 (R1) [6], this assay, as a limit assay for the control of impurities, has to be validated for the following parameters:

- Specificity.
- Detection limit.

The cartridge sensitivity (λ) is defined by the producer and tested at release on each cartridge lot, and, as a consequence, the assay detection limit should be guaranteed when the correct MVD is used (*see* **Note 7**).

The precision and accuracy are assured by the producer within a range variability of −50/+200 % as required by the EP and United States' Pharmacopoeia (USP) and reevaluated at each cartridge lot release.

Even though the test precision in terms of repeatability and intermediate precision is not required by regulators, it has been included in our validation strategy.

3.2.1 Validation Samples

1. Three independent frozen MSC lots (A, B, and C), at the maximum cell concentration defined for the final product (*see* **Note 8**).

3.2.2 Validation Strategy

Experiment #	Samples	Operators and assay replicates	Validation parameters
1	One frozen MSC lot (A)	One operator (I), three assay replicates	Repeatability Specificity Intermediate precision
2	One frozen MSC lot (A)	One operator (I), one single assay replicate	Intermediate precision Specificity
3	Three frozen MSC lots (A, B, and C)	Two operators (I and II): each of them independently performs the assay on three lots	Specificity Intermediate precision (lot A)

Acceptance criteria for validation.

(*See* **Note 9**).

Specificity

1. Spike recovery of positive control sample between 50 and 200 % (*see* **Note 10**). This confirms that the specific sample does not cause any interference, and therefore the defined dilution factor is suitable to test the specific product.

Repeatability

1. Same result confirmed in the three assay replicates of lot A (experiment 1).
2. For results above the detection limit: individual results between −50 and +200 % of the mean value.

Intermediate Precision

1. Same result confirmed in three independent assays for lot A (experiments 1, 2, 3).
2. For results above the detection limit: individual results between 50 and 200 % of the mean value.

3.3 Mycoplasma Assay (NAT Technique)

The "Universal Mycoplasma Detection Kit" produced by ATCC (www.lgcstandards-atcc.org) is a polymerase chain reaction (PCR)-based method designed specifically to meet EP 2.6.7 [11]. It is described in detail in the accompanying Chap. 19, Subheading 3.3.

According to EP, the traditional gold standard methods (culture-based method or indicator cell culture method, EP 2.6.7) can be replaced by a nucleic acid amplification technology (NAT)-based method, like the PCR method described here, provided that the same sensitivity and specificity are guaranteed (100 CFU/ml or 10 CFU/ml depending on which standard method has to be replaced). Similar requirements are outlined in the USP and Japanese Pharmacopoeia.

Supplier's data indicate that the PCR method is able to detect over 60 species of *Mycoplasmas* in cell cultures, with detection limits ranging between 10 and 450 genomes (2.5–250 fg) depending on the species (www.lgcstandards-atcc.org); the specificity is guaranteed through the utilization of a set of primers specific to the 16S rRNA coding region in the mycoplasma genome, unable to anneal to DNA originating from other sources like bacteria (www.lgcstandards-atcc.org). Due to the PCR sensitivity, the sample volume to be tested has been increased to 20 ml of cell suspension in order to be in compliance with the above stated detection limit required by EP.

Even though, where a commercial kit is used, EP allows the utilization of the validation data provided by the supplier, the user should repeat at least part of the validation in order to prove that detection limits and sensitivity are preserved with the specific test sample. The ICH Q2 (R1) guideline [6] requires that this assay, as a limit assay to test impurities, has to be validated for the following parameters:

1. Specificity.
2. Detection limit.

Even if they are not required, the repeatability, the intermediate precision, and the robustness have also been taken into consideration as part of our validation strategy.

Moreover, to improve the reliability of our PCR-based mycoplasma assay and as part of the continuous validation, an external quality assurance program has been established and is performed on a semiannual basis (Mycoplasma Proficiency Test for Nucleic Acid Amplification Techniques, Minerva Biolabs, www.minerva-biolabs.com).

According to EP 2.6.7 [11], the detection limit can be established either as CFU or nucleic acid copies. If defined as CFU, viable or inactivated mycoplasma reference standard with a low genome copy (GC)/CFU ratio must be used. If defined as genome copy number, a calibrated and certified genomic DNA reference standard must be used (*see* **Note 11**). Due to the impossibility to operate with viable mycoplasma in our GMP facility, the validation strategy proposed relies on genomic DNA, and the detection limit is therefore expressed as GC number.

3.3.1 Validation Samples

1. Three independent frozen MSC lots.
2. 20 ml supernatant for each lot (collected from the corresponding MSC cultures just before harvest for freezing).

3.3.2 Validation Materials

1. Calibrated genomic mycoplasma DNA (ATCC mycoplasma quantitative DNA; *see* **Note 11** for alternatives).
2. Genomic bacterial DNA (ATCC; *see* **Note 11** for alternatives).
3. Three different lots of the Mycoplasma Kit should be used.

3.3.3 Validation Strategy

As the validation is based on the use of standard genomic DNA and not on viable mycoplasmas, some pre-validation tests should be performed in order to prove that the pre-PCR established steps (sample collection, centrifugations, and lysis steps) do not interfere with mycoplasma recovery.

For this reason, at least three test samples (20 ml of cell suspension harvested as described in **Note 12**) spiked with one or more inactivated mycoplasma strains at LOD (10 CFU/ml) should be tested according to the method. Alternatively, viable mycoplasma strains could be used: in this case, spiked samples should be prepared and manipulated in a proper external lab. For each sample, eight PCR reaction replicates are run. The 95 % of the spiked samples should show positive results to proceed with the validation exercise.

Validation runs should be carried out according to the following scheme:

Experiment #	Samples and replicates	Operators	Validation parameters
Minimum validation requirements (*see* **Note 13**)			
1	Test sample (cell lysate; *see* **Note 12**) from one MSC lot (A) in combination with genomic DNA of each mycoplasma and bacterial strain, positive and negative controls	One operator (I)	Detection limit (*See* **Note 14**) Specificity (*See* **Note 15**)
2	Test sample (cell lysate; *see* **Note 12**) from one MSC lot (B) in combination with genomic DNA of each mycoplasma and bacterial strain, positive and negative controls	One operator (II)	Detection limit (*See* **Note 14**) Specificity (*See* **Note 15**)
3	Test sample (cell lysate; *see* **Note 12**) from one MSC lot (C) in combination with genomic DNA of each mycoplasma and bacterial strain, positive and negative controls	One operator (I)	Detection limit (*See* **Note 14**) Specificity (*See* **Note 15**)
Additional experiments for a complete validation strategy (*see* **Note 16**)			
4	Test sample (cell lysate; *see* **Note 12**) from one MSC lot (A) in combination with eight replicates of each mycoplasma strain (ten GC/PCR reactions) (*see* **Note 17**)	One operator (I) PCR Kit 1 Thermal cycler 1	Detection limit Repeatability Intermediate precision
5	Test sample (cell lysate; *see* **Note 12**) from one MSC lot (B) in combination with eight replicates of each mycoplasma strain (ten GC/PCR reactions) (*see* **Note 17**)	One operator (II) PCR Kit 2 Thermal cycler 2	Detection limit Repeatability Intermediate precision
6	Test sample (cell lysate; *see* **Note 12**) from one MSC lot (C) in combination with eight replicates of each mycoplasma strain (ten GC/PCR reactions) (*see* **Note 17**)	One operator (I) PCR Kit 3 Thermal cycler 1	Detection limit Repeatability Intermediate precision

3.3.4 Acceptance Criteria for Validation

Specificity

1. Test samples spiked with mycoplasma exhibit 434–468 bp bands in 95 % of tested samples.
2. Each positive control exhibits a band with a similar intensity with respect to the test samples spiked with the same mycoplasma strain. This confirms that the presence of sample matrix does not interfere with the amplification reaction.
3. There are no visible bands (434–468-bp) in the negative control lanes.
4. Samples spiked with bacteria strains exhibit no visible bands (434–468-bp).

Detection Limit

1. Samples spiked with mycoplasma at LOD (ten GC/PCR reactions) exhibit 434–468 bp bands in 95 % of tested samples (*see* **Note 18**).

Repeatability

1. The results gathered from the eight replicates of each mycoplasma strain should exhibit bands with similar intensity.

Intermediate Precision

1. The validation runs performed by two operators, on different days and with three MSC lots, should confirm the specificity and detection limit with comparable results.

Robustness

1. The validation runs performed by two operators, on different days, with three lots of MSC, three lots of PCR Kit and using at least two different thermal cyclers, should confirm the specificity and detection limit with comparable results.

3.4 Cell Count and Viability

This assay is performed by flow cytometry [13], as described in detail in the accompanying Chap. 19, Subheading 3.4. The direct determination of cell concentration through flow cytometry is possible thanks to a system allowing accurate uptake of sample volumes (volumetric pipetting).

The determination of cell viability is based on the ability of fluorescent dyes such as propidium iodide (PI) to cross damaged membranes, bind to double-stranded DNA, and be detected by flow cytometry.

As a quantitative assay for content/potency, this assay should be validated for the following parameters [6]:

1. Specificity.
2. Repeatability.
3. Intermediate precision.
4. Accuracy.
5. Linearity and range.

3.4.1 Validation Samples

1. Three control bead samples, at known concentrations (Trucount Controls, Low/Medium/High, Becton Dickinson, www.bdbiosciences.com).
2. Three independent frozen MSC lots (*see* **Note 19**).
3. Control nonviable cells: stabilized human lymphocytes (CytoCOMP Cell Kit, Beckman Coulter, www.beckmancoulter.com) (*see* **Note 20**).

3.4.2 Validation Strategy

Experiment #	Samples	Operators and assay replicates	Validation parameters
1	One frozen MSC lot (A)	One operator (I), three assay replicates	Repeatability Intermediate precision
2	One frozen MSC lot (A), in combination with different proportions of nonviable cells (CytoCOMP): • MSC 100 % • MSC 75 %/nonviable c 25 % • MSC 50 %/nonviable c 50 % • MSC 25 %/nonviable c 75 % • Nonviable c 100 %	One operator (I), one single replicate	Specificity Intermediate precision Accuracy (only for cell viability) Linearity and range (only for cell viability)
3	Three frozen MSC lots (A, B, C)	Two operators (I, II) (*See* **Note 21**)	Specificity Intermediate precision
4	Three control bead samples (low/medium/high) (*See* **Note 22**)	One operator (I), one single replicate	Accuracy (only for cell counting) Linearity and range

*3.4.3 Acceptance Criteria for Validation (See **Note 9**)*

Specificity

1. Viable cells in nonviable sample (CytoCOMP: nonviable c. 100 %): ≤10 % (*see* **Note 23**).

Repeatability

1. CV% ≤20.

Intermediate Precision

1. CV% ≤20.

Accuracy

1. $-20 \leq \Delta\% \leq 20$.

Linearity and Range

1. $-20 \leq \Delta\% \leq 20$ for all the tested concentrations (*see* **Note 24**).

3.5 Identity Assay (Immunophenotype)

According to the International Society for Cellular Therapy (ISCT), MSC must express the cell surface markers CD73 (ecto 5′ nucleosidase), CD90 (Thy-1), and CD105 (endoglin) and lack expression of CD45 (pan-leukocyte marker), CD34 (expressed on

primitive hematopoietic progenitors and endothelial cells), CD14 or CD11b (prominently expressed on monocytes and macrophages), CD79α or CD19 (markers of B cells that also express CD20), and HLA-DR surface molecules [14]. The aim of the immunophenotype assay (described in detail in the accompanying Chap. 19, Subheading 3.5) is to prove the identity of MSC by flow cytometry [15]; it is used as a release assay for frozen MSC as well as an IPC during MSC culture.

As an identification assay, it has to be validated for the following parameter:

1. Specificity.

Even if the repeatability, the intermediate precision, and the accuracy are not required, they also have been taken into consideration as part of our validation strategy.

3.5.1 Validation Samples

1. Three independent frozen MSC lots (*see* **Note 25**).
2. Control non-MSC sample: stabilized human lymphocytes (CytoCOMP Cell Kit, Beckman Coulter, www.beckmancoulter.com).

3.5.2 Validation Strategy

Experiment #	Samples	Operators and assay replicates	Validation parameters
1	One frozen MSC lot (A)	One operator (I), three assay replicates	Repeatability Intermediate precision
2	One frozen MSC lot (A), in combination with different proportions of non-MSC (CytoCOMP): • MSC 100 % • MSC 75 %/non-MSC 25 % • MSC 50 %/non-MSC 75 % • MSC 25 %/non-MSC 75 % • Non-MSC 100 %	One operator (I), one single replicate	Specificity Intermediate precision Accuracy
3	Three frozen MSC lots (A, B, C)	Two operators (I, II) (*See* **Note 21**)	Specificity Intermediate precision (inter-experiments for sample A, within experiment for samples B–C)

3.5.3 Acceptance Criteria for Validation

(*See* **Note 9**).

Specificity

- Positive cells for CD90, CD105, and CD73 in MSC samples (A, B, C): ≥90 %.
- Positive cells for CD45/CD34/CD14/CD20/HLA-DR in MSC samples (A–C): ≤10 %.
- Positive cells for CD45/CD34/CD14/CD20/HLA-DR in non-MSC sample (CytoCOMP): ≥90 % (*see* **Note 26**).

Repeatability

- CV% ≤20.

Intermediate Precision

- CV% ≤20.

Accuracy

- $-20 \leq \Delta\% \leq 20$.

3.6 Clonogenic Potential (CFU-F Assay)

The colony-forming unit-fibroblast (CFU-F) assay is a functional method to assess, by limiting dilution, the frequency of mesenchymal stromal progenitor cells. It is performed on frozen MSC as a final product release test. It is described in detail in the accompanying Chap. 19, Subheading 3.6.

This assay can be considered both as an identity assay and as a quantitative assay for content/potency [6].

As an identity assay, it should be validated for the following parameter:

1. Specificity.

As a quantitative assay for content/potency, the following additional parameters should be added:

1. Repeatability.
2. Intermediate precision.
3. Accuracy.
4. Linearity and range.

Accuracy is not evaluated here, due to the lack of reference samples with known CFU-F frequency. Linearity and range will be considered only later during clinical development, on the basis of data collected during early phase clinical trials.

3.6.1 Validation Samples

- Three independent frozen MSC lots (*see* **Note 27**).

3.6.2 Validation Strategy

Experiment #	Samples	Operators and assay replicates	Validation parameters
1	One frozen MSC lot (A)	One operator (I), three assay replicates (*see* **Note 28**)	Repeatability Intermediate precision

Experiment #	Samples	Operators and assay replicates	Validation parameters
2	One frozen MSC lot (A)	One operator (I), one single assay replicate (one plate for each defined cell concentration)	Intermediate precision
3	Three frozen MSC lots (A, B,C)	Two operators (I, II) (*See* **Note 29**)	Specificity Intermediate precision (inter-experiments for sample A, within experiment for samples B–C)

3.6.3 Acceptance Criteria for Validation

(*See* **Note 9**).

Specificity

- Detectable frequency of CFU-F in all the samples.

Repeatability

- CV% ≤20.

Intermediate Precision

- CV% ≤20.

4 Notes

1. *Identification tests*: Specificity
   Quantitative tests for impurities: Accuracy, precision, specificity, limit of quantification, linearity, and range
   Limit tests for the control of impurities: Specificity and detection limit
   Quantitative assays for content/potency: Accuracy, precision, specificity, linearity, and range
2. If the sampling volume exceeds the maximum acceptable inoculum volume, it has to be split into several testing bottles.
3. *Aspergillus brasiliensis*, *Bacillus subtilis*, *Candida albicans*, *Clostridium sporogenes*, *Propionibacterium acnes*, *Pseudomonas aeruginosa*, *Staphylococcus aureus*, *Streptococcus pyogenes*, *Yersinia enterocolitica*; microorganisms previously detected in the cell products or associated with environmental contamination (bioburden) must also be used.
4. The CFU number inoculated must be verified, for each microorganism, by plating the corresponding amount in duplicate in TSA and counting the number of developed colonies. The inoculated CFU number can change according to experimental results (e.g., in case of product interference): consequently, the detection limit will be affected; a detection limit of 10–100 CFU is still considered acceptable.

5. The MVD is the maximum acceptable dilution of a sample at which the endotoxin limit can be determined. The $\text{MVD} = \frac{\text{endotoxin limit}}{\lambda}$; the endotoxin limit (EL) is determined according to EP 5.1.10 (*see* Chap. 19, **Note 21**). For example: EL = 5 endotoxin units (EU)/ml and cartridge sensitivity (λ) = 0.05 EU/ml. The MVD is $\frac{5\text{EU/ml}}{0.05\,\text{EU/ml}} = 100$. The λ is the lower concentration of endotoxin used in the standard curve.
6. Perform the test according to the accompanying Chap. 19: prepare several sample dilutions (e.g., 1:2, 1:10, 1:50, and 1:100), and load each dilution in inhibition/enhancement screening cartridges (PTS220, Charles River) containing a defined endotoxin concentration (around 0.5 EU/ml). A spike recovery between 50 and 200 % is acceptable. Spike recovery <50 % indicates negative interference, whereas spike recovery >200 % reveals positive interference. The second dilution showing no interference is chosen as the suitable dilution for the sample.
7. Each cartridge contains pre-loaded RSE (reference standard endotoxin). Alternatively, the RSE must be added to one sample, in order to show the absence of inhibiting factors under the actual test condition. The RSE should be detected within a range variability of −50/+200 % and the CV values obtained by PTS should be valid.
8. The assay is extremely sensitive to any product interference: the validation has to be carried out with the final product (with exactly the same formulation medium and at the same cell concentration). If the cell concentration specification for the final product ranges between two defined values, the assay validation has to be performed at the higher limit of the range (e.g., if the cell concentration range of the final product is $1–5 \times 10^6$ cells/ml, the endotoxin assay validation will be carried out with three samples at around 5×10^6 cells/ml).
9. The criteria indicated here have been established for the initial method's validation, on the basis of preliminary results obtained during the method's setup or development; they may be restricted in the future based on regular evaluation of the method's performance. Such criteria are acceptable for early clinical development, a phase in which demonstration of the method's suitability is required [8], while they should be restricted in view of more advanced clinical phases.

10. The spike recovery is calculated as:

$$\frac{\text{Spike value}}{\text{Archived spike concentration}} \times 100$$

The spike concentration is specific for each cartridge lot and it is defined in the certificate of analysis.

11. *ATCC*: Titered Mycoplasma Reference Strains Panel (#ATCC MP-7, low genome copy (GC)/CFU ratio); ATCC offers also genomic DNA from each mycoplasma strain with a certified genome copy number; viable bacteria or genomic DNA from all the required species are available. *Bionique Testing Laboratories*: viable (#M-1100, defined GC/CFU ratio), non-viable mycoplasma lysate (#M1200, defined GC/ml), and genomic DNA (#M-1250 defined GC/μl). *Minerva Biolabs*: 10CFU inactivated mycoplasma/vial, mycoplasma or bacteria genomic DNA extracts for all the required species. *Mycoplasma Biosafety Services*: viable with low GC/CFU ratio.
12. Thaw a vial of frozen MSC, seed cells, and collect the test sample (the cell lysate) as prescribed in Chap. 19, Subheading 3.3.
13. A validation scheme limited to experiments 1, 2, and 3 is acceptable if the PCR test has an IPC or complementary purpose only. This allows collection of suitable/preliminary data on the detection limit that has to be confirmed with experiments 4, 5, and 6 if the assay has to replace the standard cultural method.
14. For the detection limit validation, the following *Mycoplasma* species represent the selection suggested by EP: *Acholeplasma laidlawii* and *Mycoplasma fermentans*, *M. hyorhinis*, *M. orale*, *M. pneumonia* or *gallisepticum*, and *M. arginine*; the genomic DNA (1 μl) of each mycoplasma strain is added, at least in duplicate for each GC number tested (from 10^3 to 10 GC/PCR reaction), to the test samples and water (positive control) instead of the internal mycoplasma control.
15. *Clostridium*, *Lactobacillus*, and *Streptococcus* are the bacteria genera with the closest phylogenetic relation to *Mycoplasma* and therefore suitable to test and validate the assay specificity.
16. If the PCR method is designed to replace the official culture method, a comparability approach should also be taken into consideration: at least three samples, in combination with calibrated mycoplasma and bacterial strains, should be tested in parallel by PCR and culture method.
17. The EP requires for each strain, at least 24 test results (e.g., three tests with eight replicates as proposed) in order to conduct an acceptable statistical analysis and set the positive cut-off value (defined as the minimum genome copy number or CFU number that can be detected in 95 % of test runs).

18. If the detection limit is not achieved, an increase in the test sample volume should be considered and validation repeated with the new defined test conditions in order to be in compliance with EP requirements.
19. The proposed validation scheme may also be applied to fresh BM-derived mononuclear cells (BM-MNC) and fresh MSC samples obtained during MSC manufacturing, with minor modifications: for evaluation of intermediate precision, frozen BM-MNC can be used; experiment #3 can be skipped in case of limited availability of fresh samples in a single day.
20. Alternatively, nonviable MSC can be prepared in house, according to one of the following procedures: (a) thaw one vial of frozen MSC at 37 °C and then perform three freeze/thaw cycles putting the vial at −80 °C for 15 min, then at 37 °C for 15 min for each cycle, and eventually at 4 °C until use; (b) thaw one vial of frozen MSC at 37 °C and put the vial at 60 °C for 30 min and then at 4 °C until use. However, in our experience, these procedures give rise to a certain degree of cell loss and cause cell debris that may impair flow cytometry analysis.
21. Each operator independently performs staining and acquisition; both perform analysis of all the acquired samples; four results are thus generated for each sample.
22. For control beads, appropriate instrument settings should be applied during acquisition; the analysis should be performed according to the manufacturer's instructions.
23. CytoCOMP cells consist of stabilized human leukocytes and are permeable to viability dyes such as PI, appearing as dead cells.
24. The validation strategy described here allows a limited evaluation of linearity and range: for cell viability, the upper and lower limits are 75 and 25 %, respectively; for cell concentration, the upper and lower limits correspond to the nominal concentration of "high" and "low" bead samples. This approach may be justified for early clinical phases, while a more stringent validation strategy should be implemented for late phases.
25. The following validation scheme may also be applied to fresh MSC samples harvested during MSC manufacturing.
26. CytoCOMP cells consist of stabilized human leukocytes and express the pan-leukocyte marker CD45; a fraction of them may also express one or more other markers included in this analysis.
27. The following validation scheme may also be applied to fresh BM-MNC and fresh MSC samples obtained during MSC manufacturing, with minor modifications: for evaluation of intermediate precision, frozen BM-MNC can be used.

28. A complete assay = three plates with 2×10^3, three plates with 1×10^3, and three plates with $0.5 \times \times 10^3$ should be repeated three times.
29. Each operator independently performs cell seeding and staining for each sample; both perform counting of colonies in all the plates; four results are generated for each sample.

Acknowledgments

This work was supported by the Fondazione Cardiocentro Ticino—Lugano. The authors would like to acknowledge Maura Filippini for her excellent editing assistance.

References

1. Sensebé L, Bourin P (2009) Mesenchymal stem cells for therapeutic purposes. Transplantation 87:S49–S53
2. Sharma RR, Pollock K, Hubel A et al (2014) Mesenchymal stem or stromal cells: a review of clinical applications and manufacturing practices. Transfusion 54:1418–1437
3. Regulation (EC) No 1394/2007 of the European Parliament and of the Council of 13 November 2007 on advanced therapy medicinal products and amending Directive 2001/83/EC and Regulation (EC) No 726/2004
4. Guideline on human cell-based medicinal products. EMEA/CHMP/410869/2006
5. Guideline on potency testing of cell based immunotherapy medicinal products for the treatment of cancer. EMEA/CHMP/410869/2006
6. International Conference on Harmonization of technical requirements for registration of pharmaceuticals for human use (2005), ICH Harmonized Tripartite Guideline, Validation of Analytical Procedures: Text and Methodology Q2(R1)
7. U.S. Departments of Health and Human Services, Food and Drug Administration, Center for Drug Evaluation and Research (CDER), Center for Veterinary Medicine (CVM) (2001), Guidance for Industry, Bioanlytical Method Validation
8. Guideline on the requirements for quality documentation concerning biological investigational medicinal products in clinical trials. EMA/CHMP/BWP/534898/2008
9. European Pharmacopoeia 8.0, Section 2.6.27 (Microbiological control for cellular products) (2014) European Directorate for the Quality of Medicines & HealthCare, Strasbourg, FR
10. European Pharmacopoeia 8.0, Section 2.6.1 (Sterility) (2014) European Directorate for the Quality of Medicines & HealthCare, Strasbourg, FR
11. European Pharmacopoeia 8.0, Section 2.6.7 (Mycoplasma) (2014) European Directorate for the Quality of Medicines & HealthCare, Strasbourg, FR
12. European Pharmacopoeia 8.0, Section 2.6.14 (Bacterial endotoxins) (2014) European Directorate for the Quality of Medicines & HealthCare, Strasbourg, FR
13. European Pharmacopoeia 8.0, Section 2.7.29 (Nucleated cell count and viability) (2014) European Directorate for the Quality of Medicines & HealthCare, Strasbourg, FR
14. Dominici M, Le Blanc K, Mueller I et al (2006) Minimal criteria for defining multipotent mesenchymal stromal cells. The International Society for Cellular Therapy position statement. Cytotherapy 8:315–317
15. European Pharmacopoeia 8.0, Section 2.7.24 (Flow Cytometry) (2014) European Directorate for the Quality of Medicines & HealthCare, Strasbourg, FR

Chapter 21

Cryopreservation and Revival of Human Mesenchymal Stromal Cells

Mandana Haack-Sørensen, Annette Ekblond, and Jens Kastrup

Abstract

Cell-based therapy is a promising and innovative new treatment for different degenerative and autoimmune diseases, and mesenchymal stromal cells (MSCs) from the bone marrow have demonstrated great therapeutic potential due to their immunosuppressive and regenerative capacities.

The establishment of methods for large-scale expansion of clinical-grade MSCs in vitro has paved the way for their therapeutic use in clinical trials. However, the clinical application of MSCs also requires cryopreservation and banking of the cell products. To preserve autologous or allogeneic MSCs for future clinical applications, a reliable and effective cryopreservation method is required.

Developing a successful cryopreservation protocol for clinical stem cell products, cryopreservation media, cryoprotectant agents (CPAs), the freezing container, the freezing temperature, and the cooling and warming rate are all aspects which should be considered.

A major challenge is the selection of a suitable cryoprotectant which is able to penetrate the cells and yet has low toxicity.

This chapter focuses on recent technological developments relevant for the cryopreservation of MSCs using the most commonly used cryopreservation medium containing DMSO and animal serum or human-derived products for research use and the animal protein-free cryopreservation media CryoStor (BioLife Solutions) for clinical use.

Key words Mesenchymal stromal cells, Cryopreservation, Cryoprotectant, DMSO, Cooling rate, Viability, Cell recovery

1 Introduction

Cell therapy for regenerative or immunosuppressive treatment has grown substantially in the past few years, and mesenchymal stromal cells (MSCs) have been increasingly used in many preclinical as well as clinical settings [1, 2]. MSCs are multipotent stromal cells that have the capacity to differentiate into several cell lineages. They secrete many different growth factors and cytokines and have immunosuppressive properties, which make them important tools in providing an alternative medical therapy paradigm, and they may change the course of treatment for a variety of immune and degenerative disorders [3–6].

Massimiliano Gnecchi (ed.), *Mesenchymal Stem Cells: Methods and Protocols*, Methods in Molecular Biology, vol. 1416,
DOI 10.1007/978-1-4939-3584-0_21,

To develop effective cellular therapies using human autologous or allogeneic MSCs, large numbers of cells have to be manufactured according to good manufacturing practices (GMPs), cryopreserved, and stored with validated, safe, and reproducible methods and procedures that maintain desired biological functions [1, 2].

An effective and consistent cryopreservation technique is crucial, and for each particular product and application, special consideration should be paid to the cryopreservation process including the optimal selection of the cryopreservation medium, type of cell storage container, cooling rate and profile, temperature change during thawing, type of freezing device employed, and long-term storage in a liquid nitrogen tank [7].

The addition of cryoprotective agents (CPAs) to the cryopreservation medium is essential to prevent any freezing-induced cell damage. The main functions of these CPAs are stabilization of the cell membrane and minimization of osmotic effects. An ideal cryoprotection solution should be nontoxic for cells and patients and nonantigenic and provide a high survival rate after thawing and allow transplantation without washing [8]. There is a diverse choice of CPAs, ranging from low- to high-molecular-weight solutes [9]. DMSO has been extensively used as a low-molecular-weight cryoprotectant because of its high membrane permeability. It is available in clinical-grade preparations and is known to be much more successful than other CPAs. Despite the protection this cryoprotectant offers, DMSO can be potentially toxic and damage cells when used in high concentrations [10]. Nonetheless, DMSO is an indispensable component of a cryoprotectant solution, and despite toxicity considerations, the removal of DMSO from frozen-thawed cells is possible with cell washing using isotonic salts and centrifugation or just dilution. However, this action is complex and time consuming, and it introduces mechanical forces by centrifugation and osmotic stress which may damage the integrity of the cell membrane and even cause significant cell loss [11]. An alternative would be to use a lower concentration of DMSO in combination with other CPAs [9, 12–15].

Another major constituent of the cryopreservation medium is serum, which is used as a nutrient source. Fetal bovine serum (FBS) is commonly used in concentrations ranging from 5 to 90 % [16]. Nevertheless, for the storage of clinical-grade MSCs, the use of animal-free serum cryopreservation medium is desirable. As a substitute for animal serum, human serum albumin or human platelet lysate can be used, as well as commercially available, ready-to-use, defined cryopreservation products. Ginis et al. [17] have reported on the efficacy of MSC cryopreservation in a commercial, animal-free, clinically accepted, cryo-medium product: CryoStor™; however, multiple defined cryopreservation products have been marketed.

The container system used for storage of the MSCs should provide a functionally closed system to avoid contamination and

provide stability over a wide range of temperatures during the full intended shelf life [11]. Recently, a GMP-approved vial-based system, CellSeal (Regentecy), has been developed which is functionally closed, can be hermetically sealed, and remains stable throughout cryopreservation and banking procedures [18].

The cooling rate is a significant factor in the determination of viability following cryopreserved storage. Slow freezing at 1 °C/min seems to be the consensus among most laboratories for cryopreservation of MSCs. Water is the major component of all living cells and must be present for chemical reactions to occur. During cryopreservation, water changes to ice and cellular metabolism ceases. In addition, dehydration occurs, changing the concentration of salts and other metabolites, and creates an osmotic imbalance that can be detrimental to cell recovery. Intracellular ice formation (IIF) occurs during rapid cooling and can be lethal if the cell is unable to respond by exosmosis to the formation of extracellular ice and the concomitant concentration of extracellular solutes. This process results in the intracellular retention of supercooled water and an increased probability of intracellular ice nucleation [19]. For this reason, there is enormous clinical interest in avoiding IIF during cryopreservation of cells used for transplantation, and cryoprotectant solutions have been used to avoid cell and subcellular structural disruption during freezing and thawing.

Cooling devices using conventional freezing equipment, such as "Mr. Frosty" devices, are nonuniform in cooling from sample to sample and are probably unsuitable for commercial-scale cryopreservation of therapeutic cells. The use of programmed controlled-rate freezing devices is recommended to achieve uniform controlled cooling rates. Samples frozen to a predetermined temperature are eventually stored in liquid nitrogen (LN2) for extended storage.

Optimal cell recovery and membrane integrity depend on the concentration of the cells, cooling rate, exposure time and temperature of the cryoprotectant, addition and removal procedures for the cryoprotectant, and freeze/thaw protocols [7].

The objective of this chapter is to describe two useful tested and proven methods for cryopreservation of MSCs collected from the human bone marrow for preclinical and clinical applications, respectively.

2 Materials

2.1 Cell Culture and Harvest

1. Minimum essential medium alpha (αMEM, without ribonucleosides and deoxyribonucleosides).
2. Stemulate™ clinical-grade PL-SP-100 (#G35220, COOK Regentec), PL-NH-100 research grade (#G34934).
3. Penicillin/streptomycin.
4. T75 cell culture flask.

5. T600 three-layer cell culture flask.
6. T1000 five-layer cell culture flask.
7. Quantum Cell Expansion Bioreactor System (Terumo BCT, Europe, Belgium).
8. Phosphate-buffered saline (PBS) minus Ca2+ and Mg2+.
9. Glass Pasteur pipettes.
10. Serres collecting bag.
11. Membrane vacuum pump (KNF Laboport, VWR, Denmark).
12. TrypLE Select (animal origin free, Gibco, Life Technologies).
13. 10 ml centrifuge tube.
14. 50 ml centrifuge tube.
15. NucleoCounter (ChemoMetec, Denmark).
16. Bench centrifuge.
17. Inverted light microscope.

2.2 Cryopreservation of Human Mesenchymal Stem Cells for Research Applications

1. Dimethyl sulfoxide (DMSO).
2. Fetal bovine serum (FBS), Pharma Grade Gamma Irradiated AUS Origin.
3. 20 % human albumin (HA).
4. Stemulate™ research grade PL-NH-100 (#G34934, COOK Regentec).
5. Isotonic sodium chloride (9 mg/ml).
6. 1.5 ml cryovials.
7. 1 ml sterile syringe.
8. 14G needle.
9. Styrofoam ice box.
10. CoolCell freezing container (BioCision).
11. –80 °C freezer.
12. Liquid nitrogen tank, Air Liquide.

2.3 Cryopreservation of Human Mesenchymal Stem Cells for Clinical Applications

1. CryoStor CS10 (BioLife Solutions).
2. CellSeal cryovials (COOK Regentec).
3. Styrofoam ice box.
4. 5 ml sterile syringe with Luer lock.
5. 16G needle with Luer lock.
6. Heating sealer.
7. Programmable controlled-rate freezer.
8. CBS isothermal liquid nitrogen vapor storage system, V1500-AB (BioGenic Systems).

2.4 Recovery of Cryopreserved Mesenchymal Stem Cells

1. Styrofoam ice box.
2. Ziploc bags.
3. Liquid nitrogen safety gloves.
4. 70 % ethanol.
5. Heated water bath (preheated to 37 °C).
6. Ziploc bags.
7. Esprit wraps.
8. 10 ml centrifuge tubes.
9. 5 ml sterile syringe with Luer lock.
10. 16G needle with Luer lock.

2.5 Viability of Thawed Mesenchymal Stem Cells

1. NucleoCounter (ChemoMetec, Allerød, Denmark).
2. NucleoCassette (#941-0006, ChemoMetec).
3. Reagent A100 lysis buffer (#994-0003, ChemoMetec).
4. Reagent B stabilizing buffer (#994-0003, ChemoMetec).
5. Phosphate-buffered saline (PBS) minus Ca^{2+} and Mg^{2+}.
6. Trypan blue solution (0.4 %) prepared in 0.81 % sodium chloride, 0.06 % potassium phosphate.

3 Methods

The following protocols describe cryopreservation of MSCs using either clinically approved commercial GMP-manufactured CryoStor CS10 cryopreservation solution or a mixture of DMSO and FBS or human-derived products for research use (*see* **Note 1**). CryoStor CS10 is a ready-to-use solution containing 10 % DMSO and non-serum and nonanimal components.

DMSO, the most common cryoprotectant for cells (*see* **Note 2**), prevents the formation of intracellular ice during freezing and thawing. However, it is toxic for the cells at room temperature. Therefore, the cryopreservation solution should be cold before adding to the cell suspension, and it should be removed or diluted quickly after thawing. Following the guidelines below will reduce the intracellular ice formation, preserve the MSC membrane, and increase viability to maintain the MSC stemness and differentiation characteristics.

3.1 Human Mesenchymal Stem Cell Culture and Harvest for Research Applications

1. MSCs are cultured in T75 culture flasks with 15 ml complete medium and incubated at 37 °C in humidified air with 5 % CO_2. MSCs are passaged when approaching appropriate confluence (80 %) (*see* **Note 3**).
2. Remove the growth medium with a sterile Pasteur pipette connected to the membrane vacuum pump, wash with PBS, and aspirate.

3. Harvest the MSCs by incubating at 37 °C for 10 min with 3 ml TrypLE Select. To confirm that all cells are detached, check the flask under a microscope. If the cells have not begun to detach or are not fully detached, incubate for an additional 5 min at 37 °C.
4. Label a sterile 10 ml centrifuge tube with the cell line and passage number.
5. Add 7 ml complete medium to the flask to neutralize the TrypLE Select. Transfer the cell suspension to a 10 ml tube.
6. If there are more than one T75 flasks, cell suspensions can be pooled in a sterile 50 ml centrifuge tube.
7. Centrifuge at 300 × *g* for 5 min.
8. Aspirate the supernatant. Gently reconstitute the cell pellet in a known volume of complete medium.
9. The number of cells can be determined per unit volume with a NucleoCounter (*see* Subheading 3.6).

3.2 Human Mesenchymal Stem Cell Culture and Harvest for Clinical Applications

For clinical applications, a larger amount of cells is needed. The T75 flask-based cell expansion can be complicated and time consuming with an increased chance of heterogeneity in the final cell quality. Alternatively, multilayer flasks (T600 or T1000) with a larger surface area should be used. To increase the GMP compliance and safety, a fully closed and automated bioreactor system can alternatively be used; these have many advantages over traditional 2D culture systems. This can translate a research-based experimental process into a clinically relevant cell-production process (Fig. 1) (*see* **Note 4**).

1. MSCs are cultured in three-layer T600 or five-layer T1000 flasks with 120 or 200 ml complete medium and incubated at 37 °C in humidified air with 5 % CO_2. MSCs are passaged when approaching appropriate confluence (80 %) (*see* **Note 5**).
2. Culture in the automated and closed Quantum Cell Expansion Bioreactor System, by following the manufacturer's protocol (*see* **Note 6**).
3. Remove growth medium from the flasks with a sterile Pasteur pipette connected to the membrane vacuum pump, wash with PBS, and aspirate.
4. Harvest MSCs by incubating at 37 °C for 10 min with 30 ml per T600 flask and 50 ml per T1000 flask TrypLE Select. Make sure that the amount of TrypLE is equally distributed in all layers.
5. To confirm that all cells are detached, check the flasks under a microscope. If the cells have not begun to detach or are not fully detached, gently tap the side of the flask and incubate for an additional 5 min at 37 °C.

Fig. 1 Different cell expansion systems. Standard 2D culture vessel T75 flask. Millipore's Millicell HY multilayer culture flask with larger surface area. Automated, closed Quantum Cell Expansion System from Terumo BCT for manufacturing of GMP-grade MSC production for clinical application

6. Label an appropriate number of sterile 50 ml centrifuge tubes with cell line, donor ID, and passage number.
7. Add 60 ml per T600 flask or 100 ml complete medium to the T1000 flask to neutralize the TrypLE Select. Make sure that the added medium is equally distributed in all layers.
8. Transfer cell suspension to the 50 ml tubes.
9. Centrifuge at 300 × *g* for 5 min.
10. Aspirate the supernatant. Gently reconstitute the cell pellet in a known volume of complete medium.
11. The number of cells can be determined per unit volume with the NucleoCounter.

3.3 Cryopreservation of Mesenchymal Stem Cells for Research Applications

1. Make an appropriate volume of cryopreservation solution (*see* **Note 7**) and store it on ice or at 4 °C until needed. Make enough medium to allow reconstitution of the cell pellet at $0.5–5 \times 10^6$ cells/ml.
2. Label cryovials and place vials on ice until needed (*see* **Note 8**).
3. Centrifuge previously counted MSCs for 5 min at 300 × *g* to remove the culture medium.
4. Aspirate the supernatant and gently reconstitute the cell pellet in cryopreservation solution ($0.5–5 \times 10^6$ cells/ml).
5. Transfer 1 ml of cell solution to chilled cryovials and place the vials in a freezing container (Fig. 2).

Fig. 2 Freezing containers. The traditional "Mr. Frosty" isopropanol-based freezing container, where the isopropanol must be changed every few uses to ensure the controlled rate −1 °C/min. CoolCell fluid-free freezing container is easy to use and provides a highly reproducible −1 °C/min freezing rate when placed in an −80 °C temperature

6. Subject the vials to slow cooling by placing them in a −80 °C freezer. Using this protocol, samples are cooled at −1 °C/min down to −80 °C (*see* **Note 9**).
7. The following day, transfer cryovials into the liquid nitrogen tank (*see* **Note 10**).

3.4 Cryopreservation of Mesenchymal Stem Cells for Clinical Applications

To support the cryopreservation of expanded MSC for clinical applications, cells can be frozen in CellSeal cryovials, which is a closed system that can be used for long-term storage (Fig. 3).

They are designed to ensure a homogeneous, controlled-rate freeze with maximum cell viability. To support cryopreservation of MSCs in freezing cryovials, a controlled-rate freezer is used. To monitor temperature during cryopreservation, this type of freezer will utilize a temperature probe that is inserted into a control freezing cryovial and monitor the temperature of a simulated product throughout the freezing run.

1. For each donor MSC population, CellSeal vials are labeled with the date and donor name/ID.
2. All the vials are placed at 4 °C or on ice until needed.
3. After harvesting and counting MSCs (*see* Subheading 3.1), centrifuge MSCs for 5 min at $300 \times g$ and remove the supernatant.
4. Cell pellet is reconstituted in an appropriate amount of cold CryoStor CS10 corresponding to $10–20 \times 10^6$ cells/ml and gently mixed.
5. MSCs (50×10^6 or 100×10^6) are frozen in a total volume of 5 ml cryopreservation solution per CellSeal vial.

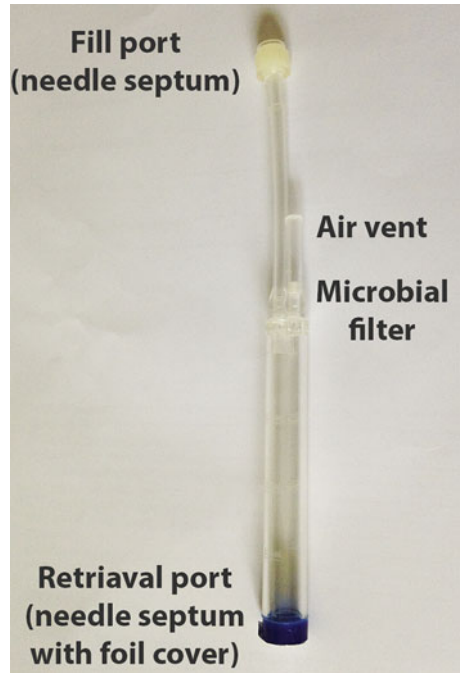

Fig. 3 Description of CellSeal vial system features

6. Draw up a 5 ml volume of cell suspension into a 5 ml syringe with a 16G needle (*see* **Note 11**). After drawing up the cells, draw up some additional air in the syringe. The air will be used to push the entire sample into the vial (Fig. 4a).
7. Thoroughly swab the top of the port with an alcohol wipe (Fig. 4b).
8. Inject 5 ml cell suspension gradually into the CellSeal vials through the first port with septum. Use the additional air in the syringe to empty the tubing (Fig. 4c).
9. This port and the second air vent are sealed using a heat sealer (designed for use with EVA tubing). Then cut the additional tubing (Fig. 4d–g).
10. The vials are placed on ice until they are transferred to the freezer.
11. Store the vials on ice for 10 min, so the samples are equilibrated in the cryopreserve solution before the freezing process is started.
12. The samples are cooled at a predetermined cooling rate to a predetermined end temperature (−80 °C). Extracellular ice nucleation occurs in the sample at around −8–9 °C (*see* **Note 12**).

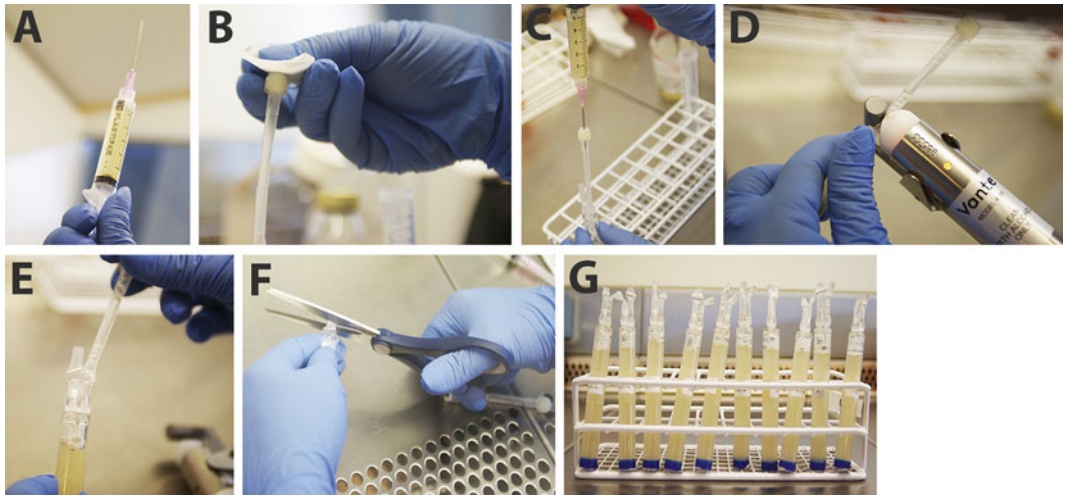

Fig. 4 CellSeal cryovial container system for packaging and storage of MSCs. (**a**) Cell suspension is drawn up in a 5 ml syringe connected to a 16G needle. (**b**) Top of the filling port is swabbed with an alcohol wipe. (**c**) The cell suspension is gradually injected into the vial. (**d**–**e**) Both the filling port and the air vent are sealed with a heat sealer. (**f**–**g**) The additional tubing is cut after sealing

Fig. 5 Cell freezing. (**a**) Programmable controlled-rate freezer. (**b**) Temperature probe is attached to control freezing vials. (**c**) All the CellSeal vials with cell suspension are placed into the freezer

13. Switch on the controlled-rate freezer (Fig. 5a). Follow the manufacturer's guidelines for machine operation (*see* **Note 13**).
14. Attach a temperature probe to the control freezing vial (Fig. 5b). Place the freezing vials into the controlled-rate freezer and follow the manufacturer's guidelines (Fig. 5c).
15. When the program is complete and the desired temperature has been achieved, the vials are removed and transferred to a liquid nitrogen tank. Use a box with dry ice for transportation from freezer device to vapor-phase nitrogen tank (*see* **Note 14**).
16. Switch off the controlled-rate freezer.

3.5 Thawing of Cryopreserved Mesenchymal Stem Cells in Cryovials

The standard procedure for thawing cells is to use a pre-warmed water bath at 37 °C.

3.5.1 Thawing of Cryopreserved MSCs in Screw Cap Cryovials

1. Take the cryovials from the liquid nitrogen container, transfer the vials to a Ziploc bag, and place the vials on ice until thawing is initiated.
2. Thaw the frozen MSCs quickly in the water bath until all ice crystals disappear. For the 1.8–2 ml cryovial, an automated thawing device can be used instead of a water bath (*see* **Note 15**).
3. Transfer the thawed cell suspension into a 10 ml centrifuge tube and dilute the cell suspension slowly (drop wise) into cold complete medium (*see* **Note 16**).
4. Centrifuge the cell suspension at 300 × *g* for 5 min (*see* **Note 17**) and reconstitute in 1 ml complete medium. Analyze cell viability manually with trypan blue or by utilizing an automated cell counter such as NucleoCounter (*see* Subheading 3.6).

3.5.2 Thawing of Cryopreserved MSCs in CellSeal

1. Take the CellSeal vial from the vapor phase nitrogen container.
2. Make sure that it is the right vial; check name and ID of the donor.
3. Transfer the vial to a Ziploc bag and place the vial on ice until thawing is initiated (Fig. 6a).

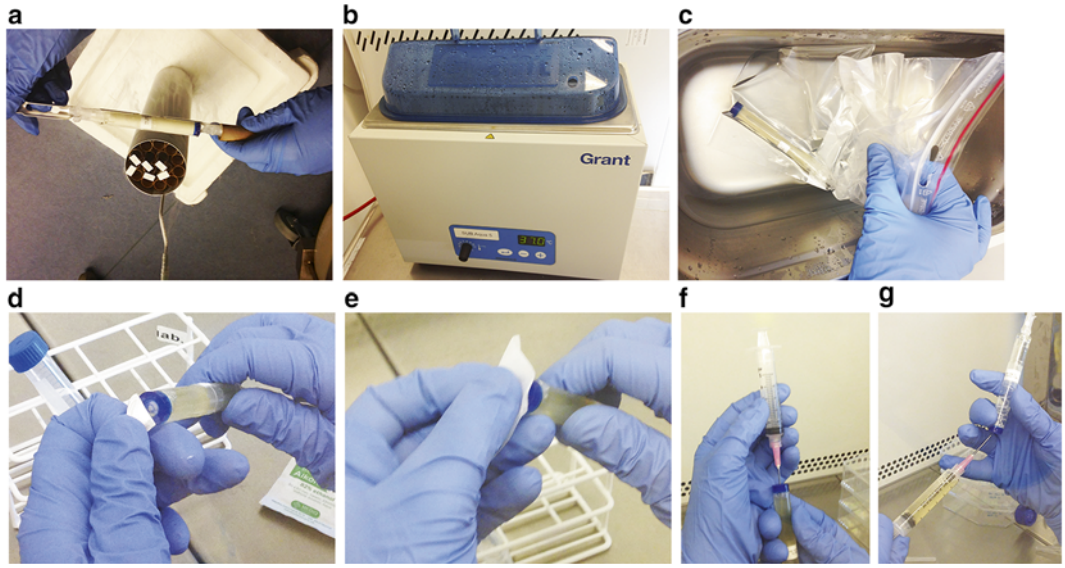

Fig. 6 Thawing of MSCs. (**a**) The frozen MSCs are removed from the nitrogen tank. (**b**) Pre-warmed water bath at 37 °C. (**c**) The vial is placed into a Ziploc bag to avoid any contamination from the environment and water. (**d**) Remove the foil cover from the bottom of the vial. (**e**) Swab with alcohol wipe. (**f**) Puncture the retrieval port with a 16G needle connected to a 5 ml syringe. (**g**) Draw the cells up

4. Thaw the frozen MSCs quickly in the pre-warmed water bath until all ice crystals disappear (Fig. 6b, c).
5. Remove the foil that covers the needle septum on the bottom of the retrieval port (Fig. 6d).
6. Thoroughly swab the port with an alcohol wipe before drawing the cells up (Fig. 6e).
7. Use a 5 ml syringe with a 16G needle to puncture the retrieval port and draw cells up (Fig. 6f, g).
8. Transfer the cells to a 10 ml centrifuge tube.
9. Cell count and viability of cells are determined with a NucleoCounter.

3.6 Viability of Thawed Mesenchymal Stem Cells

Viability of cells measured directly after thawing does not reliably estimate cryopreservation efficacy. During the post-thaw cultivation, a considerable decrease in viability will be observed. This is related to apoptotic and necrotic processes which occur within the first 24 h, and they are not evident immediately after thawing [20].

Different assessment techniques to measure cell viability include an evaluation of the structure or function of different biological elements and may give different measures of cell health and viability depending on the method. Trypan blue (TB) and other fluorescence-based viability assays are the most commonly used assays for the assessment of membrane integrity of nucleated cells (*see* **Note 18**).

3.6.1 Trypan Blue Staining

1. Mix the cell suspension with an equal volume of 0.4 % (w/v) TB solution.
2. Count live vs. dead cells using a light microscope in a Bürker cell counting chamber. Blue-stained cells are nonviable and unstained cells are viable.

3.6.2 NucleoCounter Analysis

The NucleoCounter offers an easy and reliable method to determine the total viable cell concentration in a sample. No calibration of cell size or volume is needed as the volume of the sample measured in every analysis is known. In summary, a cell sample is loaded into a NucleoCassette which contains the fluorescent dye propidium iodide (PI) immobilized inside the flow channels of the cassette. The PI is mixed with the cell sample and stains the DNA within the cell nuclei. After placement in the NucleoCounter, the stained mixture is automatically transferred to the measurement chamber where the fluorescent image is recorded. As PI stains the cell nuclei, it needs to be permeable to the dye. The dye cannot penetrate a viable cell; thus, it is necessary to lyse the cell membrane prior to staining when counting the total number of cells. As nonviable cells are permeable, they can be stained directly with the PI and counted by the NucleoCounter. Combining these two

results makes it possible to determine the cell viability of a sample. In addition, NucleoView software can be connected to the NucleoCounter; these offer a variety of advantages for the user.

1. In order to count the nonviable cells, the cell suspension must be loaded directly into the NucleoCassette without any pretreatment, and only the nonviable cells with an impaired plasma membrane are stained with PI and counted.
2. To count the total number of cells in a suspension, mix 100 µl of cell suspension with 100 µl reagent A100 lysis buffer and mix (*see* **Note 19**).
3. Mix the lysed cells (200 µl) with 100 µl reagent B stabilizing buffer (*see* **Note 19**).
4. Draw approximately 50 µl of the stabilized lysate into the NucleoCassette and place in the NucleoCounter.
5. The percent viability of MSCs can be calculated from the total number of MSCs and the number of nonviable cells.

4 Notes

1. The optimal protocol should include a low DMSO concentration and minimize the amount of time between the introduction of DMSO and initiation of the freezing protocol. The method described here uses 5 % (v/v) DMSO as the cryoprotectant for research use and 10 % (v/v) DMSO for clinical applications. The second most common constituent of the cryopreservation medium is FBS. However, it can be replaced with human albumin (HA) or human platelet lysate (hPL).
2. Cryoprotective agents (CPAs) can be classified into three different groups [9, 10] with different effects on the cell viability, which can be combined for better cryoprotection results:
   (a) Agents with low molecular weight that penetrate both the cell wall and cytoplasmic membrane include DMSO, glycerol, ethylene glycol, and propylene; these prevent intracellular ice crystal formation.
   (b) Agents that only penetrate the cell wall include glucose, sucrose, trehalose, dextrose, raffinose, hydroxyethyl starch, and albumins. Sugars are often added to dilute the medium, but they also reduce the hyperosmotic effect and prevent excessive osmotic swelling during post-thaw.
   (c) Agents that do not penetrate either the cell wall or cytoplasmic membrane include polyvinylpyrrolidone, polyvinyl alcohol, polyethylene glycol, dextran, and blood serum. These offer extracellular cryoprotection by reducing extracellular ice formation and protecting the cell membrane.

3. There is no consensus on the ideal medium for MSC culture expansion. Standard Dulbecco's Modified Eagle's medium (DMEM) or α-minimal essential medium (α-MEM) is commonly used with the addition of 10 % FBS or 5 % hPL. In our hands, MSCs proliferate better in α-MEM and 5 % hPL.
4. The culture of a high number of MSCs requires a large surface area and use of a large number of culture flasks. Therefore, decreasing the number of culture flasks is important. As shown in Fig. 1, different companies have produced large, multilayered systems that can be stacked in incubators and reduce the number of flasks needed. Decreasing the number of flasks greatly improves the microbiological safety, traceability, staff workload, and costs. However, GMP-grade MSC production in automated, closed systems such as bioreactors is preferred instead of classic flask-based cell expansion. In our laboratory, we are using both flasks and the Quantum Cell Expansion Bioreactor System for manufacturing GMP-MSCs for clinical application.
5. The standard ex vivo culture medium for MSC expansion has been 10 % FBS-supplemented medium. However, FBS shows significant batch-to-batch variability, which may negatively affect production efficiency and should be carefully tested before use [21]. Besides, its use in the clinical setting is associated with the risk of disease transmission from animals to humans. Moreover, animal serum contains xenogenic antigens which may cause immune reactions in the recipient [1, 2]. Safety requirements imply replacing FBS with more secure products such as human platelet lysate (hPL), which can be obtained from blood transfusion centers that ensure microbiological safety. Platelet lysate has been demonstrated to be an efficient alternative to FBS [22–24].
6. The Quantum Cell Expansion System is a hollow fiber-based system for automating cell culture in a functionally closed environment. Predefined, customizable settings dictate how cells are seeded onto the 2.1 m^2 surface area, fed (continuously), and eventually harvested. Additionally, the device integrates incubation and gas provision necessary to define the appropriate environment for the cells. Primary operator tasks include connecting appropriate bags (e.g., media, PBS, cells, TrypLE Select, etc.) and taking periodic samples. Both of these operations are designed to maintain the functionally closed nature of the system, i.e., via a sterile connection device and a sterile barrier filter, respectively.
7. DMSO, which prevents the formation of intracellular ice, is known to be toxic at room temperature. Therefore, it is very important that the cryopreservation solution is cold (4 °C)

before it is mixed with the cell suspension. The cryopreservation solution can be made before starting the freezing process and stored at 4 °C. These solutions can be used for cryopreservation:

(a) 95 % (v/v) FBS + 5 % (v/v) DMSO

(b) 95 % (v/v) human platelet lysate + 5 % (v/v) DMSO

(c) 10 % (v/v) 20 % human albumin + 5 % (v/v) DMSO + isotonic salt

8. Screw cap vials are the most commonly used container system for storing cell-based products but can only be used for research purposes. For clinical applications, blood bags can be hermetically sealed as a closed system and are the container of choice for most cell therapy programs. However, large volumes of cryopreservation solution with the cell product (minimum 25 ml) need to be stored in bags, and in many cases, cell products must be stored in smaller volumes that are not convenient in a bag format. Besides, bag systems can be fragile at the extreme temperatures which are imposed on samples through cryopreservation [11, 18]. Recently, a GMP-approved vial-based system (CellSeal cryovials) was developed which is functionally closed; it can be hermetically sealed and remains stable throughout cryopreservation and banking procedures [18]. In addition, the cell therapy product can be easily distributed for clinical use.
9. MSCs can be frozen in an isopropanol-jacketed freezing container "Mr. Frosty," placed in a −80 °C freezer overnight, and subsequently stored in a liquid nitrogen tank. An alternative to "Mr. Frosty" is CoolCell containers that can replace isopropanol-based freezing containers. CoolCell is a more reliable container without any fluid and provides a highly reproducible −1 °C/min freezing rate when placed in a −80 °C freezer (Fig. 2).
10. The temperature at which frozen cells are stored affects their viability after recovery. The lower the temperature, the longer the viable storage period. Cryopreservation solution containing 10 % DMSO will not fully solidify at −80 °C, and the rate of cell loss will increase with time in storage [25]. At −196 °C in liquid nitrogen, thermally driven chemical reactions are not known to occur. Therefore, it is believed that the majority of the population of stored cells will remain viable and unchanged for an indefinite period of time.
11. A bore size of 16G is used, because the bore size of the needle can have an impact on cell viability [26].
12. Extracellular ice nucleation in cells occurs at the onset of the change of state from liquid to crystalline. When this happens,

latent heat of fusion occurs and causes an increase in temperature. This heat formation can be reduced with an appropriate temperature rate (°C/min) during freezing and improve postfreeze cell viability [8].

13. Cooling is known to have the most significant influence on cell survival and recovery after thawing. A cooling rate too high or too low can result in low cell recovery due to dehydration or ice crystal formation. Several studies have shown that with an increase in the freezing rate, cell apoptosis increases drastically [17, 27]. Controlled-rate freezing before long-term storage minimizes these variables to ensure maximum viability for a wide variety of cells. Freezing of MSCs in 5 ml CryoStor in CellSeal cryovial, the profile in controlled-rate freezer starts at 6 °C; after the freezing program is started, it freezes 1 °C/min until the temperature reaches −10 °C. Thereafter, it freezes 2 °C/min until the temperature reaches −30 °C. Finally, it freezes 5 °C/min until −80 °C. The profile should be optimized with respect to the use of cryopreservation solution and volume.
14. The most robust cryo storage medium available is liquid nitrogen, where samples are stored at −196 °C and their native physiological structure and functions are preserved [28]. However, liquid nitrogen can act as a vehicle for transmission of viruses, bacteria, and fungi. Therefore, therapeutic cell products should be stored in vapor phase nitrogen tanks [18].
15. A cell that has survived freezing ultimately will not survive if it is not thawed correctly. The warming rate can equally influence survival just as the cooling rate [11, 18]. The standard method is rapid thawing in a water bath at 37 °C until all ice crystals disappear. Alternative to a water bath, an automated thawing system, ThawSTAR™ (BioCision), is available but only for 1.8–2 ml vials. It is a water- and hands-free system that monitors several parameters during the thawing process.
16. Fast addition of the dilution medium to the thawed cells will injure the cells because of changes in osmotic pressure [17].
17. Washing cells after thawing can be essential to remove the cryoprotectant (DMSO). However, washing cells by centrifugation will result in significant cell loss. Studies have observed a 30 % loss of cells post-thaw washing. Another option would be to directly seed diluted thawing cells in the culture flask containing complete medium (20–25 ml) and store the flask in the incubator until the next day, where the medium is changed. With this method, no cells are lost to centrifugation and the DMSO is diluted sufficiently to avoid toxicity.
18. Trypan blue (TB) is one of the most commonly used viability assays. TB can distinguish between viable and nonviable nucleated

cells. Cells with damaged plasma membranes absorb TB and appear blue, but TB can be toxic to human cells. Alternatively, 0.2 % nigrosin solution (Science Lab, Houston, Texas) can be used for measurement of viable MSCs. Cells with damaged plasma membranes absorb nigrosin and appear blue just like with TB [29].

19. The mixing of the cell suspension with reagent A100 lysis buffer causes permeabilization of the plasma membrane and allows the nuclei to be stained with PI. The addition of reagent B stabilizing buffer raises the pH of the mixture and allows PI to efficiently stain the nuclei.

Acknowledgments

The Aase and Ejnar Danielsens Foundation and the Research Foundation at Rigshospitalet supported the development of this protocol.

References

1. Bieback K, Kinzebach S, Karagianni M (2011) Translating research into clinical scale manufacturing of mesenchymal stromal cells. Stem Cells Int 2010:193519
2. Sensebe L, Bourin P, Tarte K (2011) Good manufacturing practices production of mesenchymal stem/stromal cells. Hum Gene Ther 22:19–26
3. Haack-Sorensen M, Friis T, Mathiasen AB et al (2013) Direct intramyocardial mesenchymal stromal cell injections in patients with severe refractory angina: one-year follow-up. Cell Transplant 22:521–528
4. Le BK, Frassoni F, Ball L et al (2008) Mesenchymal stem cells for treatment of steroid-resistant, severe, acute graft-versus-host disease: a phase II study. Lancet 371:1579–1586
5. Mathiasen AB, Jorgensen E, Qayyum AA et al (2012) Rationale and design of the first randomized, double-blind, placebo-controlled trial of intramyocardial injection of autologous bone-marrow derived mesenchymal stromal cells in chronic ischemic heart failure (MSC-HF trial). Am Heart J 164:285–291
6. Ra JC, Kang SK, Shin IS et al (2011) Stem cell treatment for patients with autoimmune disease by systemic infusion of culture-expanded autologous adipose tissue derived mesenchymal stem cells. J Transl Med 9:181
7. Thirumala S, Goebel WS, Woods EJ (2013) Manufacturing and banking of mesenchymal stem cells. Expert Opin Biol Ther 13:673–691
8. Pegg DE (2015) Principles of cryopreservation. Methods Mol Biol 1257:3–19
9. Balci D, Can A (2013) The assessment of cryopreservation conditions for human umbilical cord stroma-derived mesenchymal stem cells towards a potential use for stem cell banking. Curr Stem Cell Res Ther 8:60–72
10. Janz FL, Debes AA, Cavaglieri RC et al (2012) Evaluation of distinct freezing methods and cryoprotectants for human amniotic fluid stem cells cryopreservation. J Biomed Biotechnol 2012:649353
11. Thirumala S, Goebel WS, Woods EJ (2009) Clinical grade adult stem cell banking. Organogenesis 5:143–154
12. Li Y, Lu RH, Luo GF, Pang WJ et al (2006) Effects of different cryoprotectants on the viability and biological characteristics of porcine preadipocyte. Cryobiology 53:240–247
13. Liu Y, Xu X, Ma X et al (2010) Cryopreservation of human bone marrow-derived mesenchymal stem cells with reduced dimethylsulfoxide and well-defined freezing solutions. Biotechnol Prog 26:1635–1643
14. Rowley SD, Feng Z, Chen L et al (2003) A randomized phase III clinical trial of autologous blood stem cell transplantation comparing cryopreservation using dimethylsulfoxide vs dimethylsulfoxide with hydroxyethylstarch. Bone Marrow Transplant 31:1043–1051
15. Thirumala S, Gimble JM, Devireddy RV (2010) Evaluation of methylcellulose and

dimethyl sulfoxide as the cryoprotectants in a serum-free freezing media for cryopreservation of adipose-derived adult stem cells. Stem Cells Dev 19:513–522

16. Freimark D, Sehl C, Weber C et al (2011) Systematic parameter optimization of a Me(2) SO- and serum-free cryopreservation protocol for human mesenchymal stem cells. Cryobiology 63:67–75
17. Ginis I, Grinblat B, Shirvan MH (2012) Evaluation of bone marrow-derived mesenchymal stem cells after cryopreservation and hypothermic storage in clinically safe medium. Tissue Eng Part C Methods 18:453–463
18. Woods EJ, Thirumala S (2011) Packaging considerations for biopreservation. Transfus Med Hemother 38:149–156
19. Acker JP, Croteau IM (2004) Pre- and post-thaw assessment of intracellular ice formation. J Microsc 215(Pt 2):131–138
20. Heng BC (2009) Effect of Rho-associated kinase (ROCK) inhibitor Y-27632 on the post-thaw viability of cryopreserved human bone marrow-derived mesenchymal stem cells. Tissue Cell 41(5):376–380
21. Haack-Sorensen M, Friis T, Bindslev L et al (2008) Comparison of different culture conditions for human mesenchymal stromal cells for clinical stem cell therapy. Scand J Clin Lab Invest 68:192–203
22. Bieback K, Hecker A, Kocaomer A et al (2009) Human alternatives to fetal bovine serum for the expansion of mesenchymal stromal cells from bone marrow. Stem Cells 27:2331–2341
23. Castiglia S, Mareschi K, Labanca L et al (2014) Inactivated human platelet lysate with psoralen: a new perspective for mesenchymal stromal cell production in good manufacturing practice conditions. Cytotherapy 16: 750–763
24. Perez-Ilzarbe M, Diez-Campelo M, Aranda P et al (2009) Comparison of ex vivo expansion culture conditions of mesenchymal stem cells for human cell therapy. Transfusion 49: 1901–1910
25. Hubel A (2001) Cryopreservation of HPCs for clinical use. Transfusion 41:579–580
26. Mamidi MK, Singh G, Husin JM et al (2012) Impact of passing mesenchymal stem cells through smaller bore size needles for subsequent use in patients for clinical or cosmetic indications. J Transl Med 10:229
27. Carvalho KA, Cury CC, Oliveira L et al (2008) Evaluation of bone marrow mesenchymal stem cell standard cryopreservation procedure efficiency. Transplant Proc 40:839–841
28. Cox MA, Kastrup J, Hrubisko M (2012) Historical perspectives and the future of adverse reactions associated with haemopoietic stem cells cryopreserved with dimethyl sulfoxide. Cell Tissue Bank 13:203–215
29. Hirata AA (1968) Cytolytic antibody assay by tryptic digestion of injured cells and electronic counting. J Immunol 91:625–632

Chapter 22

Clinical-Grade Manufacturing of Therapeutic Human Mesenchymal Stem/Stromal Cells in Microcarrier-Based Culture Systems

Ana Fernandes-Platzgummer, Joana G. Carmelo, Cláudia Lobato da Silva, and Joaquim M.S. Cabral

Abstract

The therapeutic potential of mesenchymal stem/stromal cells (MSC) has triggered the need for high cell doses in a vast number of clinical applications. This demand requires the development of good manufacturing practices (GMP)-compliant ex vivo expansion protocols that should be effective to deliver a robust and reproducible supply of clinical-grade cells in a safe and cost-effective manner. Controlled stirred-tank bioreactor systems under xenogeneic (xeno)-free culture conditions offer ideal settings to develop and optimize cell manufacturing to meet the standards and needs of human MSC for cellular therapies. Herein we describe two microcarrier-based stirred culture systems using spinner flasks and controlled stirred-tank bioreactors under xeno-free conditions for the efficient ex vivo expansion of human bone marrow and adipose tissue-derived MSC.

Key words Mesenchymal stem/stromal cells, Ex vivo expansion, Spinner flask, Stirred-tank bioreactor, Microcarriers, Xenogeneic-free, Scale-up

1 Introduction

In the past few years, mesenchymal stem/stromal cells (MSC) have been extensively explored in clinical trials targeting the treatment of degenerative, genetic, and immunological diseases [1, 2]. Human MSC display several features that render these cells promising for therapeutic settings, namely, in cell-based therapies. For instance, MSC can be obtained from a wide range of sources in vivo including both adult—bone marrow (BM) and adipose tissue (AT)—and neonatal tissues, umbilical cord matrix (UCM). These cells can be isolated and expanded ex vivo and they display a high proliferative potential [3]. Additionally, MSC have the ability to differentiate toward cell types of mesodermal origin (cartilage, bone, fat, among others) [4], and, more importantly, increasingly evidence suggests that MSC migrate to sites of injury, inflammation, and tumors and

Massimiliano Gnecchi (ed.), *Mesenchymal Stem Cells: Methods and Protocols*, Methods in Molecular Biology, vol. 1416,
DOI 10.1007/978-1-4939-3584-0_22,

secrete a wide variety of bioactive factors with immunomodulatory and regenerative capacities [5–7].

Clinical trials are currently investigating systemic or local administration of both autologous and allogeneic MSC for the treatment of different conditions including acute graft-versus-host disease, acute myocardial infarction, and autoimmune disorders like Crohn's disease and type I diabetes mellitus [1, 2]. However, these experimental therapies require a vast number of MSC, typically more than one million MSC per kg of patient body weight [1]. Given the low frequency of MSC in vivo—e.g., in the BM, MSC represent 0.01 % of mononuclear cells in the newborn and decline with age to 0.001–0.0005 %—an efficient ex vivo expansion process is required in order to achieve therapeutic doses. In addition, the possibility of using allogeneic MSC in therapeutic settings makes culture-expanded MSC a desirable "off-the-shelf" cellular product that will demand cell manufacturing at a large scale according to GMP guidelines, maintaining the safety and potency of expanded cells [8–10].

Clinical doses of MSC have been generated in cumbersome multilayer planar culture systems in the presence of fetal bovine serum (FBS) or human-sourced supplements. However, these methods have serious limitations regarding cell productivity and scalability and suffer from variable culture conditions like ill-defined medium components and a heterogeneous culture environment. Moreover, cell expansion requires extensive handling and long cultivation times that are associated with safety risks (i.e., related to the potential genomic instability of cells in culture), high labor costs, and requirement for expensive infrastructure [11].

Consequently, large-scale MSC manufacturing should transit to cost-effective GMP-compliant processes that meet rigorous quality and regulatory standards and are able to robustly generate cells with well-defined characteristics and in quantities that meet clinical demands. These processes must offer optimized growth conditions for MSC, full monitoring, and control of culture conditions while featuring easy scalability.

To meet these requirements, stirred bioreactors offer significant advantages over static systems since they produce a more homogeneous culture environment and allow monitoring and control of key culture parameters (e.g., temperature, pH, dissolved oxygen). Also, stirred-tank bioreactors can be operated with different feeding modes (batch, fed-batch, or perfusion), which allow the implementation of appropriate feeding strategies that can ensure an optimal supply of the required nutrients and reduce the levels of waste metabolic products [12–14].

Therefore, significant efforts have been made in the development and optimization of microcarrier-based MSC cultures in scalable stirred bioreactors [15–22], alongside with the development and evaluation of well-defined serum- and xeno-free medium

formulations [23–26], which represent important milestones toward the clinical-scale production of MSC. In fact, we have previously demonstrated that human adipose tissue-derived stem/stromal cells (ASC) and BM MSC can be efficiently expanded in a plastic microcarrier-based culture system under xeno-free conditions, using spinner flasks [16] and controlled stirred-tank bioreactors, where different feeding regimens were evaluated [21].

Two scalable protocols for human MSC expansion under xeno-free conditions in microcarrier-based stirred culture systems at two different scales—80 mL spinner flasks and 0.8 L stirred-tank bioreactors—are described herein. These protocols have proven to be effective for MSC derived from BM and AT and can be adapted to different types of plastic microcarriers, either ready to use or with a pre-coating of adhesive substrates to facilitate initial cell adhesion.

2 Materials

2.1 Cells

1. Bone marrow aspirates are obtained from healthy donors after obtaining informed consent. Bone marrow mesenchymal stem/stromal cells (BM MSC) are isolated according to the protocol described by Dos Santos et al. [16]. Cells from different donors, at passages ranging from 3 to 6, are used.
2. Adipose tissue obtained from healthy donors after informed consent under a protocol reviewed and approved by the Pennington Biomedical Research Center (USA) Institutional Review Board. Human adipose-derived stem/stromal cells (ASC) are isolated and characterized as described previously in the literature [27]. Cells from different donors, at passages ranging from 3 to 6, are used.
3. Cell line 1301 (Instituto Nazionale per la Ricerda sul Cancro c/o CBA, Genova, Italy).

2.2 Solutions

1. Thawing medium: Iscove's Modified Dulbecco's Medium (IMDM) supplemented with 20 % fetal bovine serum (FBS) (*see* **Note 1**), 1 % of penicillin-streptomycin (10,000 units/mL penicillin + 10,000 mg/mL streptomycin), and 0.1 % of Fungizone (250 mg/mL (1000×)) (*see* **Note 1**). Store at 4 °C.
2. Expansion medium: StemPro® MSC SFM XenoFree complete medium with 1 % of GlutaMAX™-I CTS™ supplement, 1 % of penicillin-streptomycin (10,000 units/mL penicillin + 10,000 mg/mL streptomycin), and 0.1 % of Fungizone (250 mg/mL (1000×)). Store at 4 °C.
3. Phosphate-buffered saline (PBS) solution. Prepare a (1×) solution by dissolving PBS powder in 1 L of distilled water.

Filter the solution using a 0.22 mm filter and store at room temperature.

4. TrypLE™ Select CTS™ (1×) cell dissociating reagent. Store at room temperature.
5. Coating substrate: CELLstart™ CTS™. Store at 4 °C. Before using, prepare the working solution by diluting the necessary volume (1:100) in PBS.
6. Trypan blue stain 0.4 %. Store at room temperature.
7. Sigmacote®.
8. 1 % (w/v) paraformaldehyde (PFA) solution: Dissolve 1 g of PFA in 100 mL of PBS (*see* **Note 2**). Filter (0.22 μm) before use and maintain at 4 °C.
9. 1.5 μg/mL 4′,6-diamidino-2-phenylindole, dihydrochloride (DAPI) solution in PBS, store at 4 °C. Prepare from 1 mg/mL stock solution in deionized (DI) water stored at −20 °C.
10. Mouse antihuman monoclonal antibodies PE-conjugated: CD31, CD73, CD80, CD90, human leukocyte antigen (HLA-DR), CD105, and appropriate isotype controls: mouse IgG2a PE for HLA-DR and mouse IgG1 PE for the remaining (*see* **Note 3**).
11. Telomere PNA Kit/FITC for flow cytometry.
12. Transcriptor First Strand cDNA Synthesis Kit.
13. SYBR Green PCR master mix.
14. Primers: RGC32 (early osteocyte cell marker, 166 bp) (Fw) 5′-GCC ACT TCC ACT ACG AGG AG-3′, (Re) 5′-GCT GGG GTA GAG TCT GTT GG-3′; FABP4 (early adipocyte cell marker, 215 bp) (Fw) 5′-TCA TAC TGG GCC AGG AAT-3′, (Re) 5′-TCC CTT GGC TTA TGC TCT-3′, and SPP-1 (early chondrocyte cell marker, 229 bp) (Fw) 5′-CTC CAT TGA CTC GAA CGA CTC-3′, (Re) 5′-CAG GTC TGC GAA ACT TCT TAG AT-3′.

2.3 Equipment and Supplies

1. Sterile labware: pipettes, polypropylene conical tubes, Eppendorf tubes, cell strainers (100 μm), and hemocytometer.
2. Different T-flasks: Falcon tissue culture-treated flasks (T-75/T-175) and CellBIND® Surface cell culture flasks (T-75/T-175).
3. FACS tubes.
4. Nonporous microcarriers: Plastic Enhanced Attachment® and Synthemax® II microcarriers. Store at room temperature (*see* **Note 4**).
5. Lab scale.
6. Appropriate cell culture facilities.

7. Cell culture centrifuge.
8. Cell culture incubator with CO_2, temperature, and humidity control.
9. Inverted microscope equipped with ultraviolet light.
10. Temperature adjustable water bath set at 37 °C.
11. Thermomixer comfort.
12. Bellco® spinner flask with 100 mL volume, equipped with 90° normal paddles and a magnetic stir bar (*see* **Note 3**).
13. Stirring plate (30–40 rpm).
14. Schott bottle and screw cap GL45 with two ports.
15. New Brunswick BioFlo® 110 stirred-tank bioreactor (1.3 L) equipped with a three-blade pitched impeller (blades pitched 45° to vertical), dissolved oxygen (DO), pH, and temperature probes and thermal jacket.
16. Peristaltic pump volume range: 1.6–5000 mL/min.
17. Automatic analyzer YSI 7100 MBS.
18. FACSCalibur flow cytometer.
19. StepOne™.
20. UV spectrophotometry.
21. Vortex.

3 Methods

3.1 ASC and BM MSC Thawing

1. Coat Falcon tissue culture-treated flasks at least 30 min before cell thawing. Add diluted coating solution to culture plates at a final volume per surface area of 60 μL/cm^2. Incubate at 37 °C for 1 h. Before plating the cells, remove the excess of diluted coating solution.
2. Retrieve a cryogenic vial of MSC (approximately 1 mL) from the liquid nitrogen tank and quickly thaw in a 37 °C water bath.
3. Dilute the contents of the cryogenic vial in thawing medium (warmed to 37 °C) (1:4 dilution).
4. Centrifuge at $250 \times g$ for 7 min, discard the supernatant, and resuspend the pellet in expansion medium.
5. Plate thawed cells in T-75 (10 mL of expansion medium) or T-175 (20 mL of expansion medium) flasks pre-coated with coating solution, within a cell density range of $(1–3) \times 10^3$ cells/cm^2.
6. Incubate cells at 37 °C, 5 % CO_2 in a humidified atmosphere.
7. Refresh the culture medium every 3 days.

3.2 Expansion of ASC and BM MSC Under Static Conditions

1. Coat Falcon tissue culture-treated flasks at least 30 min before cell passaging according to **step 1** in Subheading 3.1.
2. Passage cells at 70–80 % cell confluence. Remove the exhausted culture medium from the flasks and add PBS (same volume as culture medium) to wash the cell layer. Remove PBS and add TrypLE™ Select CTS™ (1×) (4 and 7 mL for T-75 and T-175 flasks, respectively). Incubate at 37 °C for 7 min.
3. After complete cell detachment, transfer the cell suspension to a polypropylene tube and dilute it with twice the volume of expansion medium. Wash the flasks once with expansion medium. Centrifuge at 250 × *g* for 7 min.
4. Discard the supernatant and resuspend the pellet in culture medium. Determine cell number and viability using the trypan blue exclusion method. Mix the cell suspension with 0.4 % trypan blue stain (1:1). Viable (unstained cells) and dead cells (blue-stained cells) are identified and counted using a hemocytometer under the optical microscope.
5. Replate the cells in the appropriate T-flasks (*see* **Note 5**) within a cell density range of $1–3 \times 10^3$ cells/cm^2 until reaching the required cell number to inoculate the stirred culture (*see* **Note 6**).

3.3 Expansion of ASC and BM MSC Under Dynamic Conditions

1. Weigh 1 and 4 g of each microcarrier in a 50 mL polypropylene tube under sterile conditions for spinner flask and stirred-tank bioreactor cultures, respectively (*see* **Note 7**).
2. Wash once with PBS and expansion medium.

3.3.1 Preparation of Microcarriers

3.3.1.1 Ready-to-Use Enhanced Attachment® and Synthemax® Microcarriers

3.3.1.2 SoloHill Plastic Microcarriers

1. Weigh 1.6 and 4 g of plastic microcarriers in a 50 mL polypropylene tube for the spinner flask and stirred-tank bioreactor cultures, respectively.
2. Sterilize plastic microcarriers by autoclaving (121 °C, 20 min) in DI water.
3. Let the beads settle and wash once with PBS.
4. Prepare 10 mL of CELLstart™ CTS™ solution and add to the microcarriers (*see* **Note 8**).
5. Place the tube in the Thermomixer for 1 h at 37 °C, with a cycle of 2 min agitation followed by 10 min without agitation.
6. Wash the coated microcarriers once with PBS and expansion medium.

3.3.2 Spinner Flask Cultures

1. In order to prevent the microcarriers from sticking to the glass, the vessels (spinner flask and stirred-tank bioreactor) must be siliconized using Sigmacote (*see* **Note 9**). Add the necessary quantity of Sigmacote to the vessels in order to wet the inner glass surfaces. Remove excess Sigmacote by pipetting and allow the vessels to air dry inside the laminar flow hood. Pipet DI water to rinse the inner surfaces of the vessels and repeat this procedure three times. Autoclave the vessels with DI water (121 °C, 20 min) until further use.
2. To start the spinner flask culture, autoclave the vessel with DI water (121 °C, 20 min), remove the excess water inside the spinner, and wash it once with expansion medium.
3. Resuspend microcarriers in 25 mL of expansion medium (*see* **Note 10**) and add these to the spinner flask. Add 5 mL of expansion medium to wash the conical tube containing the microcarriers and collect any remains.
4. Add a total of 4×10^6 cells, previously expanded under static conditions in culture flasks, to the microcarriers inside the spinner flask to a final total volume of 40 mL. This yields a culture with an initial MSC concentration of around 1×10^5 cells/mL and 40 g/L of microcarriers.
5. Place the spinner flask inside the incubator with the lids slightly unscrewed to allow gas transfer, and for the first 24 h, set the agitation to 30 rpm for 18 h followed by 6 h without agitation (*see* **Note 11**). Then, set the agitation continuously at 40 rpm.
6. At day 3, add approximately 40 mL of expansion medium for a final volume of 80 mL.
7. From day 4 until day 7 replace 25 % of the medium daily.

3.3.3 Stirred-Tank Bioreactor Cultures

1. Start the spinner flask culture (*see* **Note 12**), autoclave the vessel with DI water (121 °C, 20 min), remove the excess water inside the spinner, and wash it once with expansion medium.
2. Resuspend microcarriers in 50 mL of expansion medium and add these to the spinner flask. Use an additional 20 mL of expansion medium to wash the conical tube containing the microcarriers and collect any remains.
3. Resuspend a total of 1×10^7 cells, previously expanded under static conditions in culture flasks, in 30 mL of expansion medium and gently add these to the microcarriers inside the spinner flask. This yields a culture with an initial MSC concentration of around 1×10^5 cells/mL and 40 g/L of coated plastic microcarriers.
4. Place the spinner flask inside the incubator with the lids slightly unscrewed to allow gas transfer, and for the first day, set the agitation to 30 rpm for 18 h followed by 6 h without agitation.

Then, set the agitation continuously at 40 rpm. The culture is ready to transfer to the stirred-tank bioreactor when it reaches around 2×10^5 cells/mL (2–3 days).

5. After 2 days of culture in the spinner flask, start preparing the stirred-tank bioreactor for operation: calibrate the pH probe according to the manufacturer's instructions, prepare all the connections, and sterilize the stirred-tank bioreactor by autoclaving (121 °C, 20 min).
6. Connect the DO probe and allow it to polarize overnight.
7. Before inoculating the stirred-tank bioreactor, remove the water using a peristaltic pump and add 600 mL of expansion medium. In order to maintain the process aseptic, every addition and removal of medium should be performed using a Schott bottle with a tubing connection system, and all the connections to the stirred-tank bioreactor should be performed over a flame.
8. Calibrate the DO probe by sparging the expansion medium with N_2 (0 % DO) and compressed air (100 % DO).
9. Set the culture parameters in the stirred-tank bioreactor controller at pH 7.2, temperature at 37 °C, agitation at 60 rpm, DO at 20 %, and aeration at 50 cubic centimeters per minute (ccm) (*see* **Note 13**).
10. Transfer the microcarrier-cell suspension from the spinner flask to a Schott bottle and add fresh expansion medium to reach 200 mL (the working volume in the stirred-tank bioreactor is 800 mL).
11. Seal the bottle using a screw cap with a tubing connection system and transfer the microcarrier-cell suspension to the stirred-tank bioreactor vessel using the peristaltic pump.
12. Monitor the stirred-tank bioreactor operation until the setpoints established for all culture parameters are reached.
13. In medium exchange cultures, after day 2, replace 25 % of the medium every 2 days (*see* **Note 14**). Stop the agitation and perform the medium renewal immediately after sedimentation of the microcarriers.
14. In continuous perfusion cultures, after day 2, connect Schott bottles (one containing the fresh medium and the other to collect the exhaust medium) to the stirred-tank bioreactor through the tubing connection system present in the cap. Set the pumps of the stirred-tank bioreactor at a perfusion rate of 70 μL/min.

3.4 Monitoring the Cell Culture in the Spinner Flask and Stirred-Tank Bioreactor

3.4.1 Cell Count and Viability

1. Take daily duplicate samples from the homogeneous culture suspension. For the spinner flask culture, take 0.5 mL samples (*see* **Note 15**), whereas for the stirred-tank bioreactor culture, take 2 mL samples.
2. Allow microcarriers to settle, collect the supernatant (which will be used for metabolite analysis—*see* Subheading 3.4.2), and wash with PBS.

3. Remove PBS, add 1 mL of TrypLE™ Select CTS™ (1×) to each sample, and incubate in the Thermomixer for 7–8 min at 37 °C and 750–800 rpm (*see* **Note 16**).
4. Stop the enzymatic action by adding expansion medium at a ratio of 1:3.
5. Separate the cells from the microcarriers through filtration using a cell strainer.
6. Centrifuge at 250×*g* for 7 min, discard the supernatant, and resuspend the pellet in PBS (0.5–1 mL).
7. Determine cell number and viability using the trypan blue exclusion method.

3.4.2 Metabolite Analysis

1. Collect supernatant samples every day from the spinner flask and stirred-tank bioreactor cultures and transfer to Eppendorf tubes.
2. For the spinner flask culture, allow the microcarriers to settle inside the flask and collect 1 mL of supernatant.
3. For the stirred-tank bioreactor culture, collect 1 mL of the supernatant from a 2 mL sample collected for cell counting (*see* Subheading 3.4.1). When the medium is exchanged (every 2 days), make sure to collect a supernatant sample also after medium renewal. To do this, homogenize the culture after medium addition, stop the agitation, and retrieve a 1 mL sample immediately after sedimentation of the microcarriers.
4. Centrifuge the samples for 10 min at 200×*g* and then transfer to another Eppendorf tube. Store at −20 °C until analysis.
5. Analyze the samples in an automatic analyzer YSI 7100 MBS to determine the concentration of glucose (nutrient, *see* **Note 17**), lactate, and ammonia (metabolites) throughout culture.

3.4.3 Cell Distribution in Microcarriers

1. Every 2 days, take a sample from the homogeneous culture suspension and transfer to a 24-well plate. For the spinner flask culture, take a 0.4 mL sample, whereas for the stirred-tank bioreactor culture, take a 1 mL sample.
2. Let microcarriers to settle, remove the supernatant, and wash twice with PBS.
3. Fix cells with 0.5 mL of 2 % PFA solution for 20 min at room temperature.
4. Wash twice with PBS. Add 0.5 mL of 1.5 μg/mL DAPI solution and incubate in the dark at room temperature for 5 min (*see* **Note 18**).
5. Wash three times with PBS and keep it protected from light at 4 °C until observation (maximum 7 days). Observe using a microscope under UV light.

3.5 MSC Characterization After Expansion Under Stirred Conditions

3.5.1 Immunophenotypic Analysis

1. Harvest MSC from a culture sample (*see* **Note 19**) according to the method previously described in Subheading 3.4.1.
2. Centrifuge at 250 × *g* for 7 min, discard the supernatant, and resuspend the pellet in 800 μL of PBS.
3. Split the cell suspension into eight FACS tubes (100 μL each).
4. Add the respective antibody (5 μL) to each FACS tube and incubate for 15 min at room temperature in the dark.
5. Add 2 mL of PBS to remove the excess antibody and centrifuge for 5 min at 160 × *g*.
6. Resuspend the cells, fix in 1 % PFA, and store at 4 °C until analysis is performed.
7. Analyze the cells by flow cytometry to quantitatively determine the expression of each surface marker. Collect a minimum of 1×10^4 events for each sample and use appropriate software for data acquisition and analysis.

3.5.2 Telomere Length

1. Harvest MSC from a culture sample according to the method previously described in Subheading 3.4.1 to collect a minimum of 1×10^6 cells (*see* **Note 20**).
2. To assess telomere shortening after dynamic expansion, the relative telomere size of MSC before and after dynamic cultures should be determined by telomere fluorescence in situ hybridization and flow cytometry using a telomere-specific peptide nucleic acid probe, provided by the Telomere PNA Kit/FITC for flow cytometry according to the manufacturer's instructions. In this assay, we use the 1301 cell line (Instituto Nazionale per la Ricerca sul Cancro c/o CBA, Genova, Italy) as control cells, which are tetraploid cells with very long telomeres.
3. Analyze by flow cytometry (FACSCalibur™) using logarithmic scale FL1-H for probe fluorescence and linear scale FL3-H for DNA staining. The relative telomere length (RTL) of MSC is calculated relative to the telomere length of control cells, according to the expression:

$$\mathrm{RTL} = \frac{\left(\overline{\mathrm{FL1}}_{\mathrm{sample\,w/probe}} - \overline{\mathrm{FL1}}_{\mathrm{sample\,w/o\,probe}}\right) \times \mathrm{DNA\,index\,of\,control\,cells}}{\left(\overline{\mathrm{FL1}}_{\mathrm{sample\,w/probe}} - \overline{\mathrm{FL1}}_{\mathrm{sample\,w/o\,probe}}\right) \times \mathrm{DNA\,index\,of\,sample\,cells}} \times 100$$

3.5.3 Quantitative RT-PCR Analysis of Differentiation Markers

1. Harvest MSC from a culture sample according to the method previously described in Subheading 3.4.1 to collect a minimum of 1×10^6 cells (*see* **Note 20**).
2. The primers used to assess the expression of differentiation gene code for early differentiation markers of the three main MSC differentiation lineages (RGC32, early osteocyte cell marker; FABP4, early adipocyte cell marker; SPP1, early chondrogenic

cell marker). These primers are described in Subheading 2.2, along with the metabolic housekeeping gene glyceraldehyde-3-phosphate dehydrogenase (GAPDH) used to normalize the gene expression (endogenous control).

3. Perform a two-step PCR run in a StepOne™ using a SYBR® Green PCR master mix according to the manufacturer's instructions. The two-step program consists of an initial denaturation step at 95 °C followed by 45 rounds of cycling between 10 s at 95 °C, 10 s at the respective annealing temperature, and 10 s at 72 °C.
4. The relative quantification of gene expression after dynamic culture is calculated based on the comparative CT Method (ΔΔCT Method), according to the equation:

$$\text{Relative gene expression} = 2^{-(\Delta CT_{final} - \Delta CT_{initial})}$$

where CT is the cycle threshold point defined as the number of cycles required for the fluorescent signal to cross the threshold (i.e., exceeds background level). CT levels are inversely proportional to the amount of target nucleic acid in the sample, meaning that the lower the CT level the greater the amount of target nucleic acid in the sample. ΔCT is the difference in the threshold cycles for the target gene and the endogenous control (GAPDH) in the same samples to account for differences in the amount of total cDNA added to each reaction. Relative gene expression from each microcarrier culture is quantified based on samples from the beginning (initial) and end (final) of dynamic cultures.

4 Notes

1. MSC thawing has been routinely performed in our laboratory using medium containing FBS. This is the only step of the current protocol where a xenogeneic reagent is used and is mostly due to the fact that BM MSC and ASC available in the laboratory were originally isolated using FBS (MSC qualified)-containing medium. However, the isolation of MSC under xeno-free conditions with human serum [28] or platelet lysate [29] has already been described.
2. PFA powder should be initially dissolved in a low volume of water at a high temperature (lower than 70 °C) in order to facilitate dissolution. The pH should be set at 7.3 and the final volume completed with 10× PBS.
3. The phenotypic markers analyzed are part of the criteria suggested by the International Society for Cellular Therapy to define MSC for both scientific research and preclinical studies [30].

4. Only SoloHill Plastic microcarriers need coating substrate. Enhanced Attachment® and Synthemax® II microcarriers are ready to use.
5. MSC that will be cultured afterward under stirred conditions on plastic microcarriers pre-coated with CELLstart™ CTS™ coating substrate should be replated in the pre-coated Falcon tissue culture-treated flasks. MSC that will be cultured on Synthemax® II and Enhanced Attachment® microcarriers should be replated on CellBIND® Surface cell culture flasks.
6. To initiate the stirred culture, there should be enough cells to inoculate spinner flask cultures and to perform the characterization assays prior to dynamic expansion according to the methods described in Subheading 3.5.
7. Since Enhanced Attachment® and Synthemax® II microcarriers are ready to use, the lab scale should be placed inside the laminar flow hood.
8. Other coating substrates can be used in this step, namely, a human platelet lysate supplement [31] or human fibronectin.
9. Once glassware has been siliconized, it is not necessary to repeat treatment prior to each use. In our experience, vessels should be siliconized every 20 cultures.
10. In this step, beads should be resuspended in a larger volume to minimize the amount of beads attached to the inner walls of the conical tube and pipette.
11. From our recent optimization studies, this seeding protocol prevents cell-carrier aggregation when compared with intermittent agitation [31].
12. Prior to the inoculation of the stirred-tank bioreactor, MSC are cultured in spinner flasks with a working volume of 100 mL to perform the adhesion step.
13. The addition of CO_2 is made through gentle sparging from the base of the reactor, and 1.0 M of $NaHCO_3$ is used to maintain culture pH. Aeration is achieved through gentle sparging from the base of the stirred-tank bioreactor with a mixture of N_2, air, and CO_2 gas bubbles, and the temperature is kept at 37 °C with an electric heating jacket.
14. The feeding regimen can be adjusted if nutrient depletion is verified. According to our previous study in stirred-tank bioreactors, other feeding regimens can be successfully used, namely, a fed-batch regimen with concentrated feeds [21].
15. A homogeneous sampling is essential for accurate cell number determination. Before taking 0.5 mL samples, it is important to assure an evenly mixed culture inside the spinner flask. For that purpose, a stirring plate may be used inside the laminar flow chamber to homogenize the culture inside the spinner flask before sampling.

16. In the final days of culture, larger cell-carrier aggregates are formed that require longer incubation times with TrypLE and higher agitation rates to be completely dissociated.
17. In these cultures, GlutaMAX (alanyl-l-glutamine dipeptide) is used as a glutamine substitute since it is more stable and does not spontaneously break down to form ammonia. Cells cleave the dipeptide bond to release l-glutamine as needed, and therefore, it is not possible to determine glutamine consumption during culture.
18. The well plate should be protected from light. It is also advised to turn off the laminar flow chamber light while preparing the sample.
19. The sample volume should allow the collection of enough cells to perform flow cytometry analysis. Estimate the necessary volume according to the cell concentration in culture.
20. Cells can be stored as a pellet at −80 °C until further analysis.

Acknowledgments

The authors greatly acknowledge Jeffrey M. Gimble, M.D. (Center for Stem Cell Research and Regenerative Medicine, Tulane University, New Orleans, Louisiana, USA) for kindly providing the human adipose-derived stem/stromal cells. The authors also thank the financial support from Fundação para a Ciência e a Tecnologia (FCT), Portugal, through iBB - Institute for Bioengineering and Biosciences under the project UID/BIO/04565/2013 and Programa Operacional Regional de Lisboa 2020 (Project N. 007317), projects PTDC/EQU-EQU/114231/2009 and HMSP-ICT/0001/2011 and grant SFRH/BPD/82062/2011 (awarded to AFP).

References

1. Parekkadan B, Milwid JM (2010) Mesenchymal stem cells as therapeutics. Annu Rev Biomed Eng 12:87–117
2. Trounson A, Thakar RG, Lomax G et al (2011) Clinical trials for stem cell therapies. BMC Med. doi:10.1186/1741-7015-9-52
3. da Silva Meirelles L, Chagastelles PC, Nardi NB (2006) Mesenchymal stem cells reside in virtually all post-natal organs and tissues. J Cell Sci 119:2204–2213
4. Pittenger MF, Mackay AM, Beck SC et al (1999) Multilineage potential of adult human mesenchymal stem cells. Science 284:143–147
5. Atoui R, Chiu RC (2012) Concise review: immunomodulatory properties of mesenchymal stem cells in cellular transplantation: update, controversies, and unknowns. Stem Cells Transl Med 1:200–205
6. Dittmar T, Entschladen F (2013) Migratory properties of mesenchymal stem cells. Adv Biochem Eng Biotechnol 129:117–136
7. Singer NG, Caplan AI (2011) Mesenchymal stem cells: mechanisms of inflammation. Annu Rev Pathol 6:457–478
8. Migliaccio G, Pintus C (2013) Role of the EU framework in regulation of stem cell-based products. Adv Biochem Eng Biotechnol 130:287–299
9. Bieback K, Kinzebach S, Karagianni M (2011) Translating research into clinical scale manufacturing of mesenchymal stromal cells. Stem Cells Int 2010:193519

10. Thirumala S, Goebel WS, Woods EJ (2013) Manufacturing and banking of mesenchymal stem cells. Expert Opin Biol Ther 13: 673–691
11. Bieback K, Schallmoser K, Kluter H et al (2008) Clinical protocols for the isolation and expansion of mesenchymal stromal cells. Transfus Med Hemother 35:286–294
12. Kirouac DC, Zandstra PW (2008) The systematic production of cells for cell therapies. Cell Stem Cell 3:369–381
13. Rodrigues CA, Fernandes TG, Diogo MM et al (2011) Stem cell cultivation in bioreactors. Biotechnol Adv 29:815–829
14. Dos Santos F, Andrade PZ, Silva CL et al (2013) Scaling-up ex vivo expansion of mesenchymal stem/stromal cells for cellular therapies. In: Chase LG, Vemuri MC (eds) Mesenchymal stem cell therapy. Humana Press, New York, pp 1–14
15. Eibes G, dos Santos F, Andrade PZ et al (2010) Maximizing the ex vivo expansion of human mesenchymal stem cells using a microcarrier-based stirred culture system. J Biotechnol 146:194–197
16. Dos Santos F, Andrade PZ, Abecasis MM et al (2011) Toward a clinical-grade expansion of mesenchymal stem cells from human sources: a microcarrier-based culture system under xeno-free conditions. Tissue Eng Part C Methods 17:1201–1210
17. Schop D, van Dijkhuizen-Radersma R, Borgart E et al (2010) Expansion of human mesenchymal stromal cells on microcarriers: growth and metabolism. J Tissue Eng Regen Med 4: 131–140
18. Yuan Y, Kallos MS, Hunter C et al (2014) Improved expansion of human bone marrow-derived mesenchymal stem cells in microcarrier-based suspension culture. J Tissue Eng Regen Med 8:210–225
19. Rafiq QA, Brosnan KM, Coopman K et al (2013) Culture of human mesenchymal stem cells on microcarriers in a 5 l stirred-tank bioreactor. Biotechnol Lett 35:1233–1245
20. Hewitt CJ, Lee K, Nienow AW et al (2011) Expansion of human mesenchymal stem cells on microcarriers. Biotechnol Lett 33: 2325–2335
21. Dos Santos F, Campbell A, Fernandes-Platzgummer A et al (2014) A xenogeneic-free bioreactor system for the clinical-scale expansion of human mesenchymal stem/stromal cells. Biotechnol Bioeng 111:1116–1127
22. Hupfeld J, Gorr IH, Schwald C et al (2014) Modulation of mesenchymal stromal cell characteristics by microcarrier culture in bioreactors. Biotechnol Bioeng. doi:10.1002/bit.25281
23. Miwa H, Hashimoto Y, Tensho K et al (2012) Xeno-free proliferation of human bone marrow mesenchymal stem cells. Cytotechnology 64: 301–308
24. Fekete N, Rojewski MT, Furst D et al (2012) GMP-compliant isolation and large-scale expansion of bone marrow-derived MSC. PLoS One 7:e43255
25. Kinzebach S, Bieback K (2013) Expansion of mesenchymal stem/stromal cells under xenogeneic-free culture conditions. Adv Biochem Eng Biotechnol 129:33–57
26. Lindroos B, Boucher S, Chase L et al (2009) Serum-free, xeno-free culture media maintain the proliferation rate and multipotentiality of adipose stem cells in vitro. Cytotherapy 11:958–972
27. Gimble J, Guilak F (2003) Adipose-derived adult stem cells: isolation, characterization, and differentiation potential. Cytotherapy 5: 362–369
28. Chase LG, Yang S, Zachar V et al (2012) Development and characterization of a clinically compliant xeno-free culture medium in good manufacturing practice for human multipotent mesenchymal stem cells. Stem Cells Transl Med 1:750–758
29. Bernardo ME, Avanzini MA, Perotti C et al (2007) Optimization of in vitro expansion of human multipotent mesenchymal stromal cells for cell-therapy approaches: further insights in the search for a fetal calf serum substitute. J Cell Physiol 211:121–130
30. Dominici M, Le Blanc K, Mueller I et al (2006) Minimal criteria for defining multipotent mesenchymal stromal cells. The International Society for Cellular Therapy position statement. Cytotherapy 8:315–317
31. Carmelo JG (2013) Optimizing the production of human mesenchymal stem/stromal cells in xeno-free microcarrier-based reactor systems. MSc Dissertation, Instituto Superior Técnico, Universidade de Lisboa, Lisboa

Chapter 23

GMP-Compliant Expansion of Clinical-Grade Human Mesenchymal Stromal/Stem Cells Using a Closed Hollow Fiber Bioreactor

Christina Barckhausen, Brent Rice, Stefano Baila, Luc Sensebé, Hubert Schrezenmeier, Philipp Nold, Holger Hackstein, and Markus Thomas Rojewski

Abstract

This chapter describes a method for GMP-compliant expansion of human mesenchymal stromal/stem cells (hMSC) from bone marrow aspirates, using the Quantum® Cell Expansion System from Terumo BCT. The Quantum system is a functionally closed, automated hollow fiber bioreactor system designed to reproducibly grow cells in either GMP or research laboratory environments. The chapter includes protocols for preparation of media, setup of the Quantum system, coating of the hollow fiber bioreactor, as well as loading, feeding, and harvesting of cells. We suggest a panel of quality controls for the starting material, the interim product, as well as the final product.

Key words Bioreactor, Functionally closed, Hollow fiber, Glucose consumption, Lactate generation, Mesenchymal stromal cells, Mesenchymal stem cells, MSC, Platelet lysate, GMP, Clinical application

1 Introduction

Human MSC have emerged as attractive candidates for cell therapy, tissue repair, and tissue engineering. According to a position paper of the International Society for Cell Therapy (ISCT) [1], both mesenchymal stromal cells and mesenchymal stem cells are denominated as MSC. Human MSC (hMSC) are multipotent adult progenitor cells of perivascular origin [2] present in many tissues. hMSC can be isolated from a wide range of tissues, including the bone marrow (BM), adipose tissue, and cord blood, from each of which they are readily expandable. When maintained in vitro, hMSC are defined by plastic adherence, expression of a specific set of surface markers, and the ability to differentiate into osteoblasts, adipocytes, and chondroblasts under differentiation-inducing cell culture conditions [3]. Significant ex vivo expansion

Massimiliano Gnecchi (ed.), *Mesenchymal Stem Cells: Methods and Protocols*, Methods in Molecular Biology, vol. 1416, DOI 10.1007/978-1-4939-3584-0_23,

is strictly necessary due to the low frequency of primary MSC in human tissues and the relatively large size of therapeutic cell doses. Isolation and expansion of hMSC is typically performed using classic cell culture systems, e.g., CellSTACKs (Corning) or Cell Factory Systems (Nunc). While the large surfaces offered by these systems are advantageous for the growth of adherent hMSC, difficulty in handling rapidly increases with the increase in surface area. Accordingly, various bioreactor systems have emerged in the last years, including microcarrier-based systems [4, 5], cell-stack-based systems [6], and hollow-fiber-based systems [7–10]. This chapter describes a method for GMP-compliant expansion hMSC in one of these bioreactor systems, namely, the Quantum Cell Expansion System (Terumo BCT, Lakewood, USA).

1.1 Quantum® Cell Expansion System

The Quantum system (Fig. 1a, b) is a functionally closed and automated bioreactor system, integrating incubation, fluid handling, and access to a gas supply, in addition to a touch screen interface for operation. A sterile, single-use disposable unit called the Quantum Cell Expansion Set (Fig. 2) is loaded onto the Quantum system to incorporate the hollow fiber bioreactor and fluid circuits, which will provide continuous exchange and circulation of media, as well as gas exchange. The bioreactor itself is comprised of ~11,500 hollow fibers with a total intracapillary (IC) surface area of 2.1 m^2. Typical culture manipulations (e.g., cell seeding, media exchanges, trypsinization, cell harvest, etc.) are managed by the computer-controlled system, which synchronizes pumps and valves

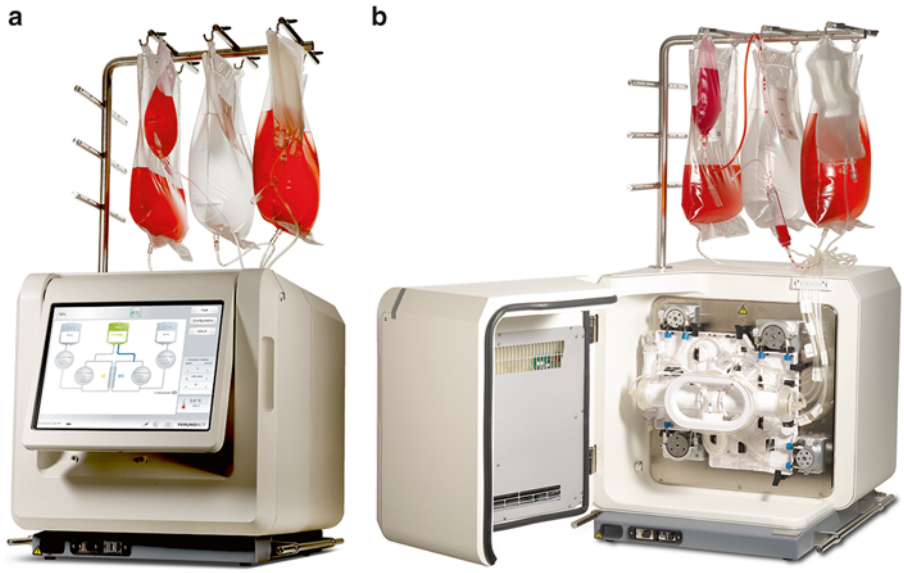

Fig. 1 Quantum® Cell Expansion System. (**a**) Closed Quantum with media bags and graphical user interface/touch screen; (**b**) Opened, with loaded cell expansion set. Both Figures: © Terumo BCT, Inc. 2014. Used with permission

Fig. 2 Cell expansion set loaded as provided by Terumo. © Terumo BCT, Inc. 2014. Used with permission

to achieve the designated task. All media and reagents are added to the system using sterile welding technology, thereby maintaining the functionally closed nature of the system. Moreover, the premixed gas supply enters the system through a sterile barrier filter, flows continually over circulating media within a hollow fiber gas transfer module, and leaves the system again via a sterile barrier filter (*see* **Note 1**). An external gas mixer may be used to supply individual gas mixtures, or gas may be supplied from a user-provided premixed gas tank which allows the user to expand cells at their optimal gas composition.

1.2 Quantum Cell Expansion System Hydraulics

The Quantum system fluid circuit is composed of two loops: the intracapillary (IC) loop and the extracapillary (EC) loop. The IC loop, which has a volume of 189 mL, is the fluid circuit including the inside of the hollow fibers. The EC loop, which has a volume of 305 mL, is the fluid circuit including the outside of the hollow fibers. A semipermeable membrane forms the hollow fibers, thus separating the IC and EC loops. Small molecules, such as glucose and dissolved gases, easily cross the membrane between the two loops. Large molecules, however, are sequestered on the side of the membrane in which they are added (or produced by the cells) (*see* **Notes 2** and **3**). For this reason, it is important to ensure that media and reagents supplying large molecules critical for the culture process (e.g., cytokines, growth factors, trypsin) are provided to the IC loop.

Five inlet lines allow for the connection of bags to the Quantum system for cell loading, media provision, and reagent addition. Though these inlet lines are named for ease of use (e.g., Cell, IC Media, Wash), the content of a bag connected to any inlet line is at the discretion of the operator. The operator can also choose to provide fluid from each of these lines to the IC loop, the EC loop, or both loops simultaneously. The fluid entering the system will necessarily displace the fluid present in the constant-volume system. This displaced fluid will exit through one of two outlets: the harvest line or the outlet line. Typically, the outlet line is used to collect process waste in a waste bag, while the harvest line is only used at the conclusion of the process to collect the harvested product.

1.3 Operation of the Quantum System

The Quantum process is analogous in many ways to a traditional cell culture process. The media (e.g., Alpha MEM plus 10 % PL), saline solution (e.g., PBS), and release agent (e.g., trypsin) can be the same (but GMP grade). Moreover, most of the process steps are logically consistent, e.g., seeding, feeding, and harvesting. However, routine operation of the Quantum system is significantly different than the repetitive flask-based or CellSTACK-based process. Instead, operation involves the following standard procedures:

1. Operating .....3the touch screen interface
2. Managing the cell expansion set
   (a) Loading the cell expansion set
   (b) Unloading the cell expansion set
3. Filling bags:
   (a) Media bags
   (b) Cell inlet bags
4. Connecting and disconnecting bags:
   (a) Use of a sterile welding device
   (b) Use of an RF (radio frequency) sealer
5. Taking samples:
   (a) From the sample port
   (b) From the sampling coil

Each of these procedures is discussed in Subheading 3 and placed in the context of the overall protocol.

The Quantum system is operated via a touch screen located on the front of the system. Via this screen, operators can configure system settings, run predefined or custom tasks, and observe the live status of the system. The live status, located on the home screen, indicates all current settings (i.e., inlet sources, outlet line, pump rates, bioreactor motion, and stop condition), temperature of the incubator, and fluid pressures. Reports including this infor-

mation, the time of all events, and the operator performing each event are also recorded for each run, enabling easier documentation and troubleshooting.

A "Task" button on the right of the touch screen provides access to a library of typical processes or tasks. Settings may be modified for all tasks, in order to meet the needs of a particular protocol. Additionally, custom tasks can be prepared to meet process needs that are not presently available in the predefined task library. Upon defining the task settings that are necessary for a particular protocol, the "Configuration" button, also on the right of the touch screen, provides the ability to save all settings.

2 Materials

Reagents and disposables should be GMP suitable, implying provision of certificates of analysis, certificates of release, certificates of origin, certification by qualified person, and/or certificates of compliance for each batch from the manufacturer, where applicable. The manufacturers should have a production license from the corresponding competent authority, an approval according to the Council Directive of the EC 93/42/EEC Annex II and/or Annex V, Article 3 concerning medical devices, and/or be certified or have an accreditation according to at least one of the following standards or directives by the corresponding competent authorities: good manufacturing practice (GMP), EN ISO 13485: 2003/AC, ISO 9001, DIN EN ISO 15189, DIN EN ISO/IEC 17025, and ISO 18001.

The materials listed in Subheadings 2.1–2.4 should be appropriate for GMP-grade isolation and expansion of hMSC as advanced therapy medicinal product (ATMP) for clinical trials.

2.1 Equipment

1. Quantum system (Quantum® Cell Expansion System), Terumo BCT, Lakewood, USA.
2. Pump or pump with pump head.
3. Sealer.
4. Sterile tubing welder.
5. Scales.
6. Lactate monitoring device.
7. Mixed gas tanks.
8. Plasma separator.

2.2 Reagents

1. DMSO.
2. Basic media as preferred by the user, e.g., Alpha MEM Eagle w/UGln1 and nucleosides or DMEM with 1 g/l glucose.
3. DPBS 0.0095 M(PO_4) w/o Ca and Mg.

4. Platelet lysate (PL).
5. TrypZean/EDTA solution.
6. Fibronectin, 5 mg/5 mL, plasma derived, GMP quality, contract manufacturing.
7. NaCl 0.9 % injectable solution.
8. 20 % HSA NaCl solution.
9. Sodium heparin.
10. Lactate test strips.

2.3 Disposables

1. Syringes (3, 10, 20 mL).
2. Sampling site coupler with needle injection site.
3. CryoMACS Freezing Bag 50 mL.
4. Transfer bag 600 mL.
5. Cell inlet bag (CIB) 0.5 L, accessory set.
6. Media bag 4 L, accessory set.
7. Sampling coil, accessory set.
8. Waste bag 4 L, accessory set.
9. In-line filter 200 μm, accessory set.
10. Cell expansion set (CES).

2.4 MSC Culture Media

Composition of complete media (*see* **Notes 4**–**7**): 90 % basic media supplemented 10 % of HPL and 1–2 IU/mL of heparin. Heparin should be added to the Alpha MEM or DMEM media first, preceding addition of the HPL.

3 Methods

3.1 Overview on the Expansion Process

The manufacture of MSC from BM is comprised of multiple expansion steps within the Quantum system. The first step includes both the isolation of hMSC from the whole bone marrow via adherence and the expansion (P0) of these primary hMSC (*see* **Note 9**). After harvest of the expanded hMSC, a portion of the pre-cultured hMSC is further expanded (P1) in a second bioreactor to generate a larger and more pure hMSC population.

Due to the functionally closed nature of the Quantum system, the system could potentially be used in lower-grade clean rooms (class C or D) than traditional cell culture processes, as per the discretion of local regulatory authorities. However, depending on the particular process design, preparation of cells, reagents, etc. may remain as open procedures, thereby requiring environments consistent with traditional cell culture procedures (e.g., a class A laminar air flow cabinet within a class B clean room environment).

Here we describe a protocol that is suitable for many autologous or small-scale allogeneic applications, from which other cell production applications can be easily derived. A few steps (*see* **Note 10**) remain as "open procedures" and are indicated accordingly.

Figures 3, 4, and 5 provide a visual summary of the overall Quantum protocol. At the top of the figure, all bags (i.e., both media bags and cell inlet bags) are illustrated, indicating their contents. The rows within the figure indicate the sequential steps of the process, highlighting the following information in the provided columns:

- The name of the task, in addition to the buttons used to locate the task. For example, "Task >> Feed and Add" indicates that the Task button should be followed by the Feed and Add button, after which the Feed Cells task can be found.
- A brief description of the task.
- The approximate duration of the task.
- An illustration of which bags are connected to each of the five inlet lines.
- A list of notes pertinent to the task.

The remainder of this section explores the details underlying the protocol.

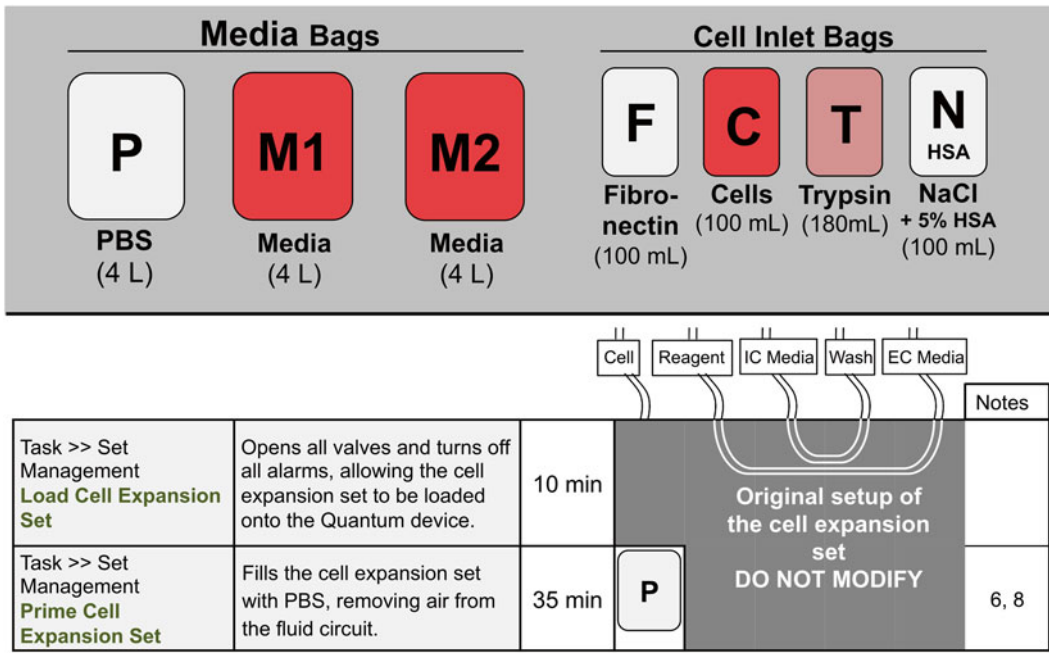

Fig. 3 Description and schematic overview of the tasks for expansion of MSC in the Quantum. © Brent Rice. Used with permission

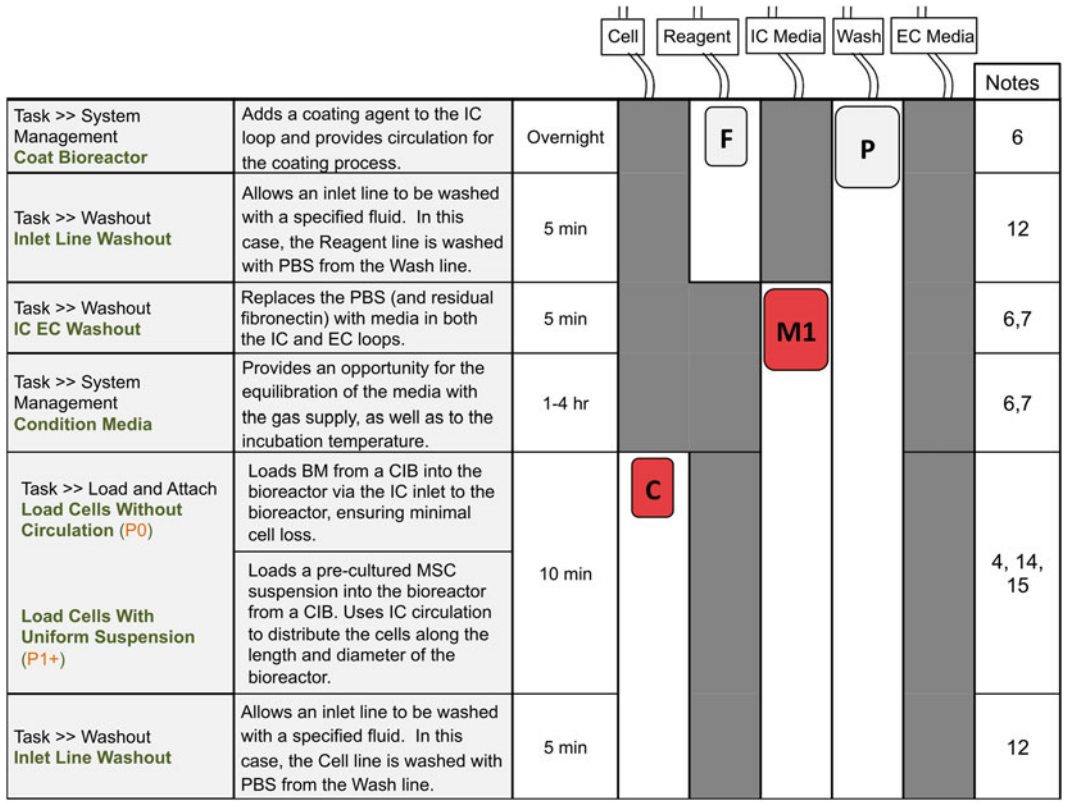

Fig. 4 Description and schematic overview of the tasks for expansion of MSC in the Quantum System. © Brent Rice. Used with permission

3.2 Tasks

Via the Quantum system touch screen (Fig. 1a, b), the user can select and modify specific tasks. A task can be considered as a programmed unit consisting of one or more consecutive steps, which are cumulatively intended to achieve a specific result (e.g., loading cells from the cell inlet bag into the bioreactor and distributing them). Each step is defined by the following settings: IC Inlet (i.e., which inlet line feeds the IC inlet pump), IC Inlet Rate, IC Circulation Rate, EC Inlet, EC Inlet Rate, EC Circulation Rate, Outlet, Rocker (i.e., stationary or in motion), and Stop Condition. Tasks are divided into seven categories: Set Management, System Management, Washout, Load and Attach, Feed and Add, Release and Harvest, and Custom.

The first six categories include tasks that are predefined as a part of the Quantum software, though the details of the tasks are flexible within the intended design of each task. The Custom category provides further flexibility when the designs of the predefined tasks do not suffice. Each of eight Custom tasks allows both maximum flexibility within each setting and the ability to add up to 99 steps.

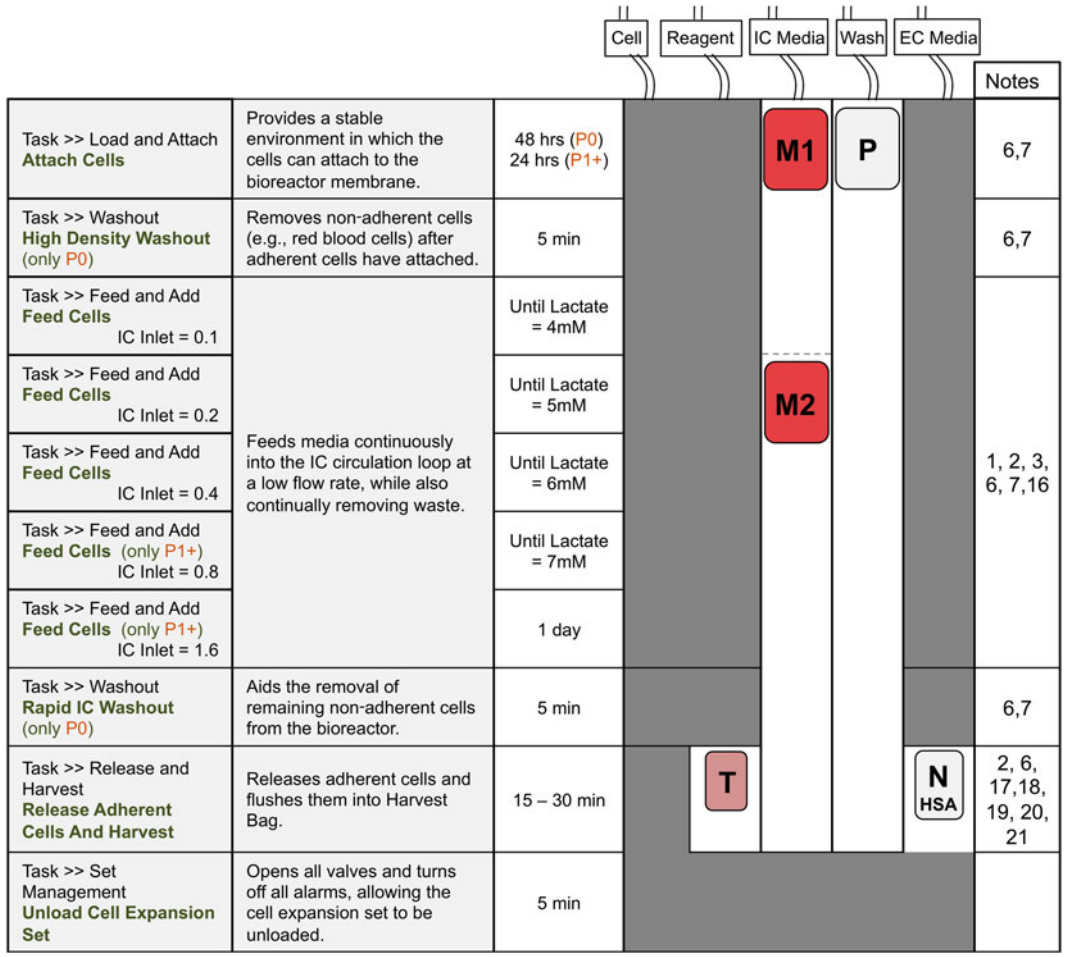

Fig. 5 Description and schematic overview on the tasks for expansion of MSC in the Quantum System. © Brent Rice. Used with permission

3.3 Loading the Cell Expansion Set (CES)

The "Load Cell Expansion Set" task opens all valves and turns off all alarms to allow the operator to load the CES onto the device, integrating it with the pumps, valves, gas supply, and fluid sensors. The primary steps are as follows:

1. Start task "Load Cell Expansion Set" which can be found in Set Management.
2. Open the incubator door.
3. Open the four pumps and the five external mounting clips.
4. Remove the CES from the packaging, and align to place the tubing organizer on the mounting plate by aligning the hole of the center of the tubing organizer with the rocker arm on the mounting plate. Rest the bioreactor on the spill tray.
5. Ensure that all five external mounting clips lock over the edges of the tubing organizer.

6. Rotate the base of the mounting clips a quarter turn counterclockwise to secure the tubing organizer in the mounting plate.
7. Ensure all tubes are pulled over the center of the corresponding pump rotors and attached behind the notch.
8. Ensure that the tubing is centered over the pump rotor on all four pumps, and close the rotor cover and lock rotor latch on each of the four pumps.
9. Load the EC inlet line into the EC fluid detector.
10. Push the rocker assembly into the rocker arm completely so the bioreactor will be in the home position.
11. Hang the waste and harvest bags on the bag pole.
12. Insert the tubing guide onto the pegs.
13. Remove the two blue and the one red caps from the CES.
14. Connect the gas inlet line to the gas quick disconnect. You should hear a click sound when you connect it. Be sure the gas inlet line is behind the bioreactor and does not hinder the rocker motion.
15. Ensure all lines are clear of the incubator door. Close the door.
16. Touch finish to complete the task.

3.4 Prime Cell Expansion Set

After loading the CES, this task is used to fill the system with PBS, removing all air. To prime the CES, the following steps need to be performed (*see* **Notes 6** and **8**):

1. Fill a media bag with PBS (*see* Subheading 3.5).
2. Turn on the external gas supply.
3. Attach the media bag containing the desired electrolyte solution to the cell line (*see* Subheading 3.7).
4. Start task "Prime Cell Expansion Set" which is located in Set Management.
5. Touch "Prime Cell Expansion Set," and on the following Setup Screen, "Prime Cell Expansion Set" touch Start.
6. Take a sample from the sample port to prime the filter (*see* Subheading 3.16).
7. After you have finished sampling, touch "Finish" and afterward "Yes."

3.5 Filling Media Bags

Media bags are used for large volume solutions up to 4 L, such as culture media or an electrolyte solution (*see* **Notes 6 and 7**) (e.g., phosphate-buffered saline or physiologic NaCl solution). Though the media bags are filled via a connected sterile barrier filter, this procedure is typically handled as an "open procedure" (*see* **Notes 10 and 11**). Complete the steps in this section to fill media bags:

1. Open the pouch that contains the media bag and take it out.

2. Remove the protective cover from the end of the tubing.
3. Connect the end of the tubing to the fluid source; for example, place the tubing into the fluid container. Use an appropriate method to exclude contamination of the fluid.
4. Load the white tube into the tubing pump.
5. Ensure that the cap on the pressure relief valve on the filter is tight.
6. Set the tubing pump to a low flow rate, such as 150 mL/min, to prime the filter. When priming the filter, hold it upright. After the filter cartridge is full and the fluid begins to flow into the bag, the flow rate may be increased up to a maximum of 500 mL/min.
7. When the last of the fluid has been pumped from the fluid source:
   (a) Set the tubing pump to a low flow rate.
   (b) Slowly pump the fluid from the white tubing into the inlet of the filter.
   (c) Stop the pump.
8. Use a tubing sealer to double seal the clear tubing. To ensure that you will have enough tubing to attach the bag to the CES using a sterile tubing welder, leave as much of the clear tubing as possible connected to the bag.
9. Separate the media bag from the filter at the double seal.
10. If the media bag will be used the same or the next day, leave it at room temperature. Store media bags in the dark.

3.6 Filling Cell Inlet Bags (CIBs)

CIBs are used for any small-volume solution less than 500 mL (e.g., BM, MSC suspension, or other reagents, such as TrypZean). Filling a CIB is an "open procedure" (*see* **Note 10**).

Complete the following steps to fill a CIB with the desired solution:

1. Open the pouch that contains the CIB and take it out.
2. Fill a syringe with as much culture media/vehicle solution as necessary to reach, together with the subsequently added liquid of interest, a final volume of 80–100 mL.

   This step does not apply for TrypZean.
3. Remove the blue cap from the luer of the CIB. Via luer, pre-fill the CIB with the culture media/vehicle solution from **step 2**.
4. Transfer the liquid of interest via luer from the syringe(s) into the CIB. Remove the syringe.
5. Via luer, push approx. 50 mL of air from a syringe into the CIB.

3.7 Loading Media Bags

Media bags are used to load cell culture media or electrolyte solution (PBS, NaCl solution) onto the Quantum bioreactor, e.g., to feed the cells or flush the system (*see* **Notes 6** and **7**).

1. Hang the media bag on the bag pole.
2. Locate the desired inlet line (typically IC inlet line or Wash line).
3. Connect the media bag tube to the inlet line via welding.

The CIB's content is usually loaded onto the Quantum bioreactor at the beginning or during a specific task (e.g., "IC EC Washout," "Condition Media").

3.8 Loading Cell Inlet Bags (CIBs)

Cell inlet bags are intended to hold any small-volume solution (i.e., <500 mL), such as cells or reagents.

1. Hang the CIB on the bag pole.
2. Locate the desired inlet line (typically cell inlet line or reagent line).
3. Connect the CIB's tube to the desired inlet line via welding.
4. The CIB's content is loaded onto the Quantum bioreactor by running an appropriate task (e.g., "Load Cells Without Circulation," "Coat Bioreactor").
5. Wash the cell line or reagent line, respectively (see Subheading 3.10).

3.9 Coating of the Bioreactor

Once the cell expansion set has been primed, the IC side of the bioreactor needs to be coated with fibronectin to promote cell adhesion (*see* **Note 6**). To coat the Quantum bioreactor, complete the following steps:

1. Aspirate the fibronectin solution into a syringe.
2. Transfer the fibronectin into a cell inlet bag (CIB; *see* Subheading 3.6). As a vehicle solution, we recommend phosphate-buffered saline (PBS) to increase the total volume to 100 mL.
3. Load the fibronectin onto the Quantum system (*see* Subheading 3.8). Connect the bag to the reagent line.
4. Coat the bioreactor by running the "Coat Bioreactor" task for 12–18 h. Remove the fibronectin bag using the RF Sealer.
5. Wash the reagent line (see Subheading 3.10).

3.10 Inlet Line Washout

This task is used to wash a line and remove possible residuals to leave a clean line for future use (*see* **Notes 10** and **12**). For example, this is helpful after a BM load or a coating procedure.

1. Choose the "Inlet Line Washout" task. In the Setup screen, choose the Inlet Source and Inlet Destination.

For an Inlet Line Washout following a **"Load Cells…"** task, use the following settings: Inlet Source: **Wash**; Inlet Destination: **Cell**.

For an Inlet Line Washout following the **"Coat Bioreactor"** task, use the following settings: Inlet Source: **Wash;** Inlet Destination: **Reagent**.

2. Lower the destination bag so that it hangs below the source bag.
3. After touching "Start" the liquid flow from the Inlet Source to the Inlet Destination. When the desired volume has reached the destination bag, touch the "Finish" button.
4. Touch "Yes" to confirm, and the home screen appears showing the system in an idle state.

3.11 IC EC Washout

After coating, the PBS and excess fibronectin should be flushed out of the bioreactor with the media (*see* **Notes 6** and 7).

1. Attach the appropriate media onto the IC media line (*see* Subheading 3.7).
2. Run the "IC EC Washout" task. Modified setting: EC Inlet = IC media.

3.12 Condition Media

In preparation for the cells, media within the system should be allowed to reach equilibrium with the attached gas mixture, as well as the temperature of the system (*see* **Notes 6** and 7).

Accordingly, run the "Condition Media" task. Modified setting: EC inlet = IC media.

3.13 Expansion of MSC from Bone Marrow (P0): Loading of BM, Removal of Non-adherent Cells, and Feeding

1. Loading BM (*see* **Notes 9, 13–15**).
   (a) Transfer 25–40 mL of unmanipulated whole BM of a healthy donor from a syringe to a CIB (*see* Subheading 3.6).
   (b) Load the BM onto the Quantum bioreactor (*see* Subheading 3.8): Start the task "Load Cells without Circulation."
2. Use the "Attach Cells" task for 48 h. Modified settings: EC inlet = IC media, rocker at 180 °C.
3. Upon completion of the 48 h attachment period, use the "High Density Washout" task to remove non-adherent cells (e.g., red blood cells). Modified settings: EC inlet = IC media.
4. Use the "Feed Cells" task to continuously feed the cells with the default inlet rate until predefined lactate concentration is observed (*see* Fig. 4). Upon reaching the next defined threshold concentration, the operator should progressively double the inlet rate as indicated in the figures.
5. When the lactate concentration reaches 6 mM at an inlet rate of 0.4, proceed to Subheading 3.18.

3.14 Expansion of MSC from Pre-cultured MSC (P1): Loading of MSC, Removal of Non-adherent Cells, and Feeding

1. Loading pre-cultured MSC (*see* **Note 9**).
   (a) Transfer the MSC suspension from a syringe to a CIB (*see* Subheading 3.6).
   (b) Load the MSC suspension onto the Quantum bioreactor (*see* Subheading 3.8): Start the task "Load Cells with Uniform Suspension."
2. Use the "Attach Cells" task for 24 h. Modified settings: EC inlet = IC media, rocker at 180 °C.
3. Use the "Feed Cells" task to continuously feed the cells with the default inlet rate until predefined lactate concentration is observed (*see* Fig. 4). Upon reaching the next defined threshold concentration, the operator should progressively double the inlet rate as indicated in the figures.
4. When the lactate concentration reaches 7 mM at an inlet rate of 0.8 mL/min, proceed to Subheading 3.18.

3.15 Taking Samples from the Sample Coil

Samples from the IC circulation loop can be taken from the sampling coil (*see* **Notes 2** and **16**).

1. If running a task, touch "Pause."
2. Open the incubator door and remove sample coil from the rocker.
3. Unravel the sample coil from the rocker and remove sample coil strain relief from sample coil line.
4. Use the sterile connection device to remove a piece of the sampling coil.
5. Open the sterile weld on the sample coil.
6. Connect sample coil relief to the sample coil, recoil it around the rocker assembly, and connect the coil strain relief to the rocker.
7. Close the incubator door.

3.16 Taking Samples from the Sample Port

The sample port gives access to the media within the EC loop which can be used for analysis of lactate and glucose levels (*see* **Note 3**).

1. Open the incubator door.
2. Use a cleansing wipe that contains an appropriate laboratory disinfectant to clean the sample port surface that will interface with the syringe. Note that this sterilization is secondary to the presence of a sterile barrier between the port and the EC loop, through which the sample is drawn.
3. Connect the syringe to the sample port.

4. Draw 3 mL of media through the filter and the sample port, and then discard the media.
5. Repeat **step 2** to clean the sample port.
6. Draw the volume of sample needed.
7. Repeat **step 2** to clean the sample port.
8. Close the incubator door.

3.17 Measuring Glucose and Lactate Concentrations

Glucose and lactate concentrations may be measured using samples taken from the either the sample port or the sampling coil (*see* Subheadings 3.15 and 3.16, **Notes 2, 3** and **16**). Concentrations can be measured by handhold devices according to the manufacturer's protocol.

3.18 Harvest of MSC

This section describes the release of MSC from the Quantum bioreactor.

1. Fill a CIB with 180 mL of TrypZean (*see* Subheading 3.6; do not dilute TrypZean). Place bag at 37 °C.
2. Fill a media bag with NaCl solution containing 5 % of HSA (*see* **Note 17**, Subheading 3.5). Weld the NaCl-HSA solution to the EC media line (*see* Subheading 3.7). Do not start a task yet.
3. For P0, run the "Rapid IC Washout" task to remove any cells remaining in suspension. Modified settings: IC inlet = wash, EC Inlet = wash. (When harvesting P1 MSC, you can directly proceed to **step 4**).
4. Weld the TrypZean to the reagent line (*see* Subheading 3.8).
5. Run the task "Release Adherent Cells and Harvest" (*see* **Note 18**). Modified settings for **step 5**: IC inlet = EC media.

3.19 Unload the Cell Expansion Set

The Unload Cell Expansion Set task opens all valves and turns off all alarms, allowing the cell expansion set to be easily removed.

1. Seal all inlet and outlet lines connected to bags.
2. Under the Task menu, choose "Set Management," followed by "Unload Cell Expansion Set." On the appearing screen, touch "Start."
3. Open the incubator door and unlock all rotor latches, open the rotor covers on the pumps, and remove the tubing from the pumps.
4. Disconnect the gas inlet line from the gas quick connect by pressing down the silver button on top of it, and turn off the external gas supply afterward.
5. Remove the bioreactor from the rocker arm.
6. Remove the tubing line guide from the pegs.

7. Rotate the base of the mounting clips a quarter turn clockwise to loosen the tubing organizer from the mounting plate.
8. Unlock the five external mounting clips and pull the tubing organizer from the mounting plate.
9. Close the rotor covers and lock the latches on all pumps.
10. Touch "Finish" and afterwards "Yes." The home screen appears showing the system status as "Idle."

3.20 Post-Processing Procedures

Subheadings 3.21–3.23 describe the procedures which are usually conducted after hMSC harvest. In summary, the quality of the cells should be confirmed, TrypZean should be washed from the suspension, and the hMSC should either be cryopreserved or prepared for immediate administration to the patient.

3.21 Taking hMSC Samples for Quality Controls

After harvest of both P0 and P1 cells, it is desirable to obtain a sample of hMSC for quality controls (*see* Tables 1 and 2). Sampling via the method described below is considered an open procedure (*see* **Note 10**).

1. Pierce a sampling site coupler with needle injection site through the membrane of the harvest bag.
2. Remove the cap from the sampling site coupler. Connect a syringe via luer and aspirate sufficient cell suspension to con-

Table 1
Proposed quality controls for passage 0 cells undergoing cryopreservation

Material tested	Type of test	Time point of sampling/test
BM aspirate (*see* **Note 13**)	Cell count and viability	Day 0
	Microbial testing	
	CFU-F assay	
Culture media (*see* **Notes 2 and 16**)	Microbial testing	Just before harvest (day 10–14)
	Mycoplasma testing	
	Endotoxin testing	
MSC	Cell count and viability	After harvest (day 10–14)
	Flow cytometry for characterization	
	CFU-F assay	
	Potency assay[a]	
MSC cryopreservant	Microbial testing	After transfer of MSC suspension to freezing bags/vials

[a]Depending on indication; *see* Table 3

Table 2
Proposed quality controls for passage 1 cells either undergoing cryopreservation or direct administration to the patient

Material tested	Type of test	Time point of sampling/test
MSC suspension (input)	Cell count and viability	Day 0
	Microbial testing	
	CFU-F assay	
Culture media (*see* **Notes 2 and 16**)	Microbial testing	Day 3–5 of expansion[a] or just before harvest
	Mycoplasma testing	
	Endotoxin testing	
MSC (harvest)	Cell count and viability	After harvest (day 15–21)
	Flow cytometry for characterization	
	CFU-F assay	
	Potency assay[b]	
Transplant[c] or cryopreservant[d]	Microbial testing	After resuspension of MSC in infusion liquid[c, e] or after transfer of MSC suspension to freezing bags/vials[d], respectively

[a]Allows for availability of results before harvest, which is particularly important when MSC are going to be administered immediately after harvest
[b]Depending on indication; suggestions for potency assays *see* Table 3
[c]In case of direct transplantation after harvest
[d]In case of intermediate cryopreservation after harvest; no mycoplasma and endotoxin testing as DMSO will interfere
[e]Results of microbial testing will only be available after administration to the patient

duct all required quality controls. Do not remove the sampling site coupler as it will be helpful again in later steps (and will leave an open bag).

3.22 Cryopreservation of P0 and P1 hMSC

The following protocol describes the cryopreservation of the complete harvested product into one freezing bag. It comprises the removal of TrypZean and resuspension of the MSC in a freezing solution consisting of NaCl with 10 % DMSO and 5 % of human serum albumin (HSA). The protocol may be easily adapted for freezing in several bags. Generally, it is recommendable not to freeze more than 1×10^7 MSC/mL. The total number of hMSC per bag depends on the number of P0-MSC to be loaded for P1 expansion (e.g., 1×10^7–2×10^7 cells) or the number of MSC to be administered to a patient in one dose after P1 (e.g., 1×10^6–5×10^6 MSC per kg body weight). It should also be noted that this protocol is one of many potential washing methods. Other options could include more automated processes that have recently become available (e.g., the Sepax from Biosafe).

1. Prepare 10 mL of a cryopreservation stock solution (CSS) by aspirating 5 mL of each solution into a syringe to produce a 50 % DMSO and 50 % NaCl solution. Place the syringe between cool packs, precooled at –20 °C.
2. Prepare a second syringe with 40 mL of a NaCl solution containing 8 % of HSA (*see* **Note 19**). Place the syringe between cool packs.
3. Weld an empty transfer bag to the harvest bag and transfer the cell suspension by gravity (*see* **Notes 20** and **21**).
4. Centrifuge the transfer bag (300 × *g*, 5 min, weak break).
5. Reconnect the transfer bag with the harvest bag by welding.
6. Immediately put the transfer bag into a plasma extractor.
7. Press the supernatant into harvest bag and disconnect the two bags by sealing. Discard the harvest bag with the supernatant.
8. Immediately resuspend the hMSC in the residual volume via manual manipulation. After resuspension, there should be no visible aggregates.
9. Tare the scale with empty transfer bag.
10. Place the transfer bag on the scale to determine the volume of the suspension by weight.
11. Remove the cap from the sampling site coupler with needle injection site (has been attached after harvest, see Subheading 3.21). Connect a syringe to the sampling site coupler and remove a sample from the hMSC suspension. Determine the cell number (counting chamber) to calculate the total amount of cells.
12. Via luer, add sufficient NaCl-8%HSA (**step 2**) solution to the cell suspension, to reach a final volume of 40 mL.
13. Recap the luer and agitate the bag carefully.
14. Remove the cap from the sampling site coupler with needle injection site. Connect a syringe via luer and aspirate the hMSC suspension.
15. Connect the syringe via luer to the freezing bag and inject the hMSC suspension.
16. Connect the syringe with the CSS (*see* **step 1**) to the freezing bag.
17. Place the freezing bag between cool packs, precooled at –20 °C.
18. Inject the CSS into the freezing bag while gently and constantly agitating the bag.
19. Connect a syringe via luer to the freezing bag. Aspirate several mL of hMSC suspension for testing (e.g., microbial testing) and retain several samples.
20. Immediately freeze bags and retain samples under controlled conditions.

3.23 Preparation of P1 hMSC for Direct Administration to the Patient

The following protocol describes the preparation of the harvested suspension for administration to the patient. It comprises the removal of TrypZean and resuspension of the hMSC in NaCl-5 % HSA. The protocol could be easily adapted for the preparation of multiple doses from a single harvested product.

1. Prepare a transfer bag with 50 mL of physiological NaCl solution containing 5 % of HSA.
   (a) Place the transfer bag on a scale. Tare the scale.
   (b) Pierce the spike of the transfer bag through the lid of a squeezable PE plastic bottle containing NaCl solution.
   (c) Squeeze the NaCl bottle to force 37.5 g of NaCl solution into the transfer bag.
   (d) Add 12.5 mL of 20 % HSA solution.
2. Conduct **steps 3–11** of Subheading 3.22.
3. Weld the transfer bag containing the NaCl-5 % HSA solution to the transfer bag with the hMSC suspension.
4. By gravity, add as much NaCl-5 % HSA solution as necessary to reach a final volume of approximately 50 mL.
5. Disconnect the two bags from each other using the sealer.
6. Pierce a sampling site coupler with needle injection site through the sample port of the transfer bag. Remove the cap from the sampling site coupler.
7. Connect a syringe to the sampling site coupler with needle injection site.
8. Aspirate several mL of hMSC suspension for, e.g., microbial testing and as retention samples for cryopreservation.
9. Use the remaining suspension in the syringe for determination of cell number (counting chamber).
10. The hMSC suspension is ready for release.

3.24 Quality Controls

Tables 1 and 2 summarize proposed quality controls that could be utilized for the isolation and expansion process. The release criteria and test methods for the ATMP must be defined in detail in both the clinical protocol and the Investigational Medicinal Product Dossier (IMPD), according to the specific requirements of the clinical trial, requests of the pertinent authorities, and the guidance of the country-specific pharmacopeia.

3.25 Release Criteria

Table 3 proposes release criteria pertaining to either the hMSC (e.g., identity) or the media in which they were cultured (e.g., sterility). Release criteria should be performed for each expansion, according to the requirements of the responsible authorities. Specifications may differ according to the therapeutic application,

Table 3
Proposed release criteria for hMSC

Feature		Test parameter	Test method	Specification P0	Specification P1
MSC immunophenotype[a]		CD105+	Flow cytometry	>60 %	>90 %
		CD73+		>50 %	>90 %
		CD90+		>70 %	>90 %
		CD45+		<20 %	<5 %
		CD34+		<10 %	<5 %
		CD14+ or CD11b+		<10 %	<5 %
		CD79α+ or CD19+		<10 %	<5 %
		HLA-DR+		<10 %	<5 %
MSC vitality		Dead cell stain	Flow cytometry	>80 %	>80 %
MSC potency assay[b]	Differentiation capacity[c]	Adipo-, chondro-, osteogenic differentiation	Staining Oil red O/ hematoxylin, methylene blue, alk. phosphatase	Detectable	Detectable
	Migration capacity[d]	Portion of migrated cells (e.g., toward HPL media, or see Garg et al.[d])	Transwell assay	Detectable; define threshold	Detectable; determine threshold
	T-cell suppressive capacity[e]	Inhibition of T-cell proliferation IDO activity/levels Treg induction IFN-γ responsivity	Flow cytometry	Detectable; define threshold	Detectable; determine threshold
	Expression/ secretion of potency markers[b]	Levels of mRNAs/ proteins relevant for indication	qPCR ELISA	Detectable; define threshold	Detectable; determine threshold
Endotoxin		Depending on test method	As per pharmacopeia	<1 EU/mL	<1 EU/mL
Mycoplasma		Depending on test method	As per pharmacopeia	Negative	Negative
Microbial tests		Growth in anaerobic and aerobic blood culture	As per pharmacopeia	Negative	Negative

[a]After dead cell exclusion; see Dominici et al. [3]
[b]Depending on indication
[c]See Dominici et al. [3]
[d]See Garg et al. [11]
[e]See Krampera et al. [12] and Menard et al. [13]

the method of delivery, and the nature of the final cell product preparation (e.g., cryopreserved vs. freshly harvested). Although genetic stability of (Quantum-derived) hMSC has been shown and the risk of tumorigenicity for hMSC is considered low [8, 10, 14], it might be advantageous to additionally analyze these parameters. Regarding the transplant itself, the endotoxin threshold is 5 EU/kg body weight per hour for intravenous administration and consider the number of transplanted leukocytes/CD45+ cells.

4 Notes

1. Daily routine should ensure that the Quantum system is still supplied with gas.
2. Samples for endotoxin, mycoplasma, and microbial testing of the culture media should be taken from the IC loop via the sampling coil. The sample port on the EC loop contains a sterile filter which limits its utility for such purposes. After having disconnected a portion of the sampling coil using the sterile connection device, culture media can be withdrawn from the coil in a sterile and safe manner by welding the filter end of a sampling coil accessory set to one end of the sample and a luer (e.g., that of an in-line filter accessory set) to the opposite end, thus allowing aspiration of the media into a syringe.
3. Samples taken from the EC loop sample port with a luer-lock syringe may be used to analyze metabolite concentrations (e.g., glucose and lactate) as an indicator of cell proliferation.
4. Any frozen solution (e.g., hMSC suspension, PL and TrypZean) should be thawed under controlled conditions, e.g., using a CE-marked plasmatherm device.
5. *Before* adding PL to the basic media, add 1–2 IU/mL heparin to the basic media and mix thoroughly, in order to avoid gelation.
6. All inlet solutions to the Quantum system should be at or above room temperature, in order to minimize bubble formation within the system.
7. If the media is light sensitive, it is important to protect the media bags from light, e.g., by wrapping them in aluminum foil.
8. Make sure that there is >2 L of electrolyte solution in the bag when priming the CES. Do not stop the "Prime Cell Expansion Set" task. If necessary, use Pause.
9. The first harvest of MSC, originating from the BM aspirate, generates *Passage 0* (P0) MSC; accordingly, expanding these cells in a second step yields *Passage 1* (P1) cells.

10. While the Quantum system is a functionally closed system and, therefore, may not require installation in a class A-C clean room, a few steps (e.g., filling CIBs and media bags) may remain open, where "open" is defined as allowing contact between the fluid and ambient air. Accordingly, these open steps should be performed in a class A clean room (e.g., class A laminar air flow in class B environment).
12. Upon arrangement, some companies can prepare their GMP-grade culture media in bags with polyurethane tubing that is compatible with the Quantum system (e.g., Biochrom, Berlin, Germany). These prefilled bags simplify handling and decrease the risk of contamination by obviating the open filling step.
13. The Inlet Line Washout task can also be used to transfer liquid from one bag to another in a sterile manner, which could be beneficial for the development of an individualized expansion protocol.
14. For BM aspiration, a variety of protocols may be used. However, care should be taken to add sufficient sodium heparin to the aspiration set.
15. It is advisable to determine cell number and viability before loading the BM onto the Quantum bioreactor, e.g., by using an automated system like Sysmex KX21-N analyzer (Sysmex Deutschland GmbH, Norderstedt, Germany).
16. It is advisable to load unmanipulated BM within 24 h after its aspiration. If intermediate storage is necessary, use a temperature range of 21 °C ± 3 °C.
17. Approximately 12.7 cm of the coil contains 1 mL of media. The total accessible length of the original sampling coil on the cell expansion set is approximately 225 cm.
18. The HSA is present to inactivate TrypZean.
19. If a noncritical alarm occurs during the "Release Adherent Cells and Harvest" task, mute it. Only press "Continue" after the task is complete, thereby avoiding repetitive alarms.
20. Final HSA concentration of the cryopreservant should be approximately 5 %.
21. The tubing connected directly to the harvest bag is made of a common polyvinyl chloride (PVC) and can, therefore, be sterile-connected to another PVC line with equal dimensions: inner diameter, 2.95 mm; outer diameter, 4.06 mm; and wall thickness, 0.56 mm.
22. The harvest bag that comes pre-attached to the cell expansion set is not suitable for centrifugation.

Acknowledgments

We appreciate the excellent technical assistance of G. Baur, T. Becker, D. Erz, S. Chester, C. Späth, C. Loechelt, and A. Wachtel. This work was supported by grants from the 7th Framework Programme of the European Commission: CASCADE (Cultivated Adult Stem Cells as Alternative for Damaged Tissue) (HEALTH-F5-2009-223236), REBORNE (Regenerating Bone Defects using New biomedical Engineering approaches) (HEALTH-2009-1.4.2-241879) to Luc Sensebé and Hubert Schrezenmeier, the von Behring-Röntgen Foundation (Cellular Interaction of Nanoparticle-Labeled MSC with Tumor Cells), and the UKGM-Kooperationsvertrag Grant (GMP-conform manufacturing of MSC) to Cornelia Brendel and Holger Hackstein.

Financial Disclosure Statement

MTR and HS work for nonprofit organizations producing platelet lysate and clinical-grade MSC. BR and SB work for Terumo BCT.

References

1. Horwitz EM, Le Blanc K, Dominici M et al (2005) Clarification of the nomenclature for MSC: The International Society for Cellular Therapy position statement. Cytotherapy 7:393–395
2. Crisan M, Yap S, Casteilla L et al (2008) A perivascular origin for mesenchymal stem cells in multiple human organs. Cell Stem Cell 3:301–313
3. Dominici M, Le Blanc K, Mueller I et al (2006) Minimal criteria for defining multipotent mesenchymal stromal cells. The International Society for Cellular Therapy position statement. Cytotherapy 8:315–317
4. dos Santos F, Andrade P, Eibes G et al (2011) Ex vivo expansion of human mesenchymal stem cells on microcarriers. In: Chase LG, Rao MS, Vemuri M (eds) Mesenchymal stem cell assays and applications. Humana Press, New York, pp 189–198
5. Schop D, Janssen FW, Borgart E et al (2008) Expansion of mesenchymal stem cells using a microcarrier-based cultivation system: growth and metabolism. J Tissue Eng Regen Med 2:126–135
6. Gottipamula S, Muttigi MS, Chaansa S et al (2014) Large-scale expansion of pre-isolated bone marrow mesenchymal stromal cells in serum-free conditions. J Tissue Eng Regen Med 2014:n/a–n/a
7. Hanley PJ, Mei Z, Durett AG et al (2014) Efficient manufacturing of therapeutic mesenchymal stromal cells with the use of the Quantum Cell Expansion System. Cytotherapy 16:1048–1058
8. Jones M, Varella-Garcia M, Skokan M et al (2013) Genetic stability of bone marrow-derived human mesenchymal stromal cells in the Quantum System. Cytotherapy 15:1323–1339
9. Nold P, Brendel C, Neubauer A et al (2013) Good manufacturing practice-compliant animal-free expansion of human bone marrow derived mesenchymal stroma cells in a closed hollow-fiber-based bioreactor. Biochem Biophys Res Commun 430:325–330
10. Rojewski MT, Fekete N, Baila S et al (2013) GMP-compliant isolation and expansion of bone marrow-derived MSCs in the closed, automated device Quantum Cell Expansion System. Cell Transplant 22:1981–2000
11. Garg A, Houlihan DD, Aldridge V et al (2014) Non-enzymatic dissociation of human mesenchymal stromal cells improves chemokine-dependent migration and maintains immunosuppressive function. Cytotherapy 16:545–559
12. Krampera M, Galipeau J, Shi Y et al (2013) Immunological characterization of multipotent mesenchymal stromal cells – The International

Society for Cellular Therapy (ISCT) working proposal. Cytotherapy 15:1054–1061
13. Menard C, Pacelli L, Bassi G et al (2013) Clinical-grade mesenchymal stromal cells produced under various good manufacturing practice processes differ in their immunomodulatory properties: standardization of immune quality controls. Stem Cells Dev 22: 1789–1801
14. Barkholt L, Flory E, Jekerle V et al (2013) Risk of tumorigenicity in mesenchymal stromal cell-based therapies – bridging scientific observations and regulatory viewpoints. Cytotherapy 15:753–759

Chapter 24

Engineering Small-Scale and Scaffold-Based Bone Organs via Endochondral Ossification Using Adult Progenitor Cells

Celeste Scotti, Beatrice Tonnarelli, Adam Papadimitropoulos, Elia Piccinini, Atanas Todorov, Matteo Centola, Andrea Barbero, and Ivan Martin

Abstract

Bone development, growth, and repair predominantly occur through the process of endochondral ossification, characterized by remodelling of cartilaginous templates. The same route efficiently supports engineering of bone marrow as a niche for hematopoietic stem cells (HSC). Here we describe a combined in vitro/in vivo system based on bone marrow-derived Mesenchymal Stem/Stromal Cells (MSC) that duplicates the hallmark cellular and molecular events of endochondral ossification during development. The model requires MSC culture with instructive molecules to generate hypertrophic cartilage tissues. The resulting constructs complete the endochondral route upon in vivo implantation, in the timeframe of up to 12 weeks. The described protocol is clearly distinct from the direct ossification approach typically used to drive MSC towards osteogenesis. Recapitulation of endochondral ossification allows modelling of stromal–HSC interactions in physiology and pathology and allows engineering processes underlying bone regeneration.

Key words Bone regeneration, Mesenchymal stem cells, Endochondral ossification, Scaffold, Hematopoietic stem cells, Osteogenesis

1 Introduction

Under normal conditions, bone tissue regenerates efficiently, through a process similar to embryonic intramembranous and endochondral ossification [1, 2]. Yet, several exogenous (e.g., prosthetic implants, high energy trauma, smoking) and endogenous factors (e.g., system diseases, aging) can disrupt local homeostasis, leading to a failure of the healing process. When this occurs, a bone grafting material is often required. We recently developed a strategy that, by recapitulating the endochondral ossification route according to a "developmental engineering"

Massimiliano Gnecchi (ed.), *Mesenchymal Stem Cells: Methods and Protocols*, Methods in Molecular Biology, vol. 1416,
DOI 10.1007/978-1-4939-3584-0_24,

paradigm [3, 4], allows the generation of mature and functional bone starting from adequately primed human adult bone marrow-derived Mesenchymal Stromal Cells (hMSC) [5–7]. The morphogenetic processes which regulate tissue formation in this model were structurally and molecularly comparable to the spatio-temporal progression of limb development [5]. Ultimately, hMSC triggered towards the endochondral route generated a fully functional "organ," consisting in the typical elements of the osseous bone compartment, including osteoid matrix, blood vessels, osteogenic and osteoclastic cells, as well as the bone marrow, including functional hematopoietic cells and long-term self-renewing Hematopoietic Stem Cells (HSC) [6]. Recent studies by other groups have confirmed and complemented our findings, overall indicating the robustness of the underlying processes [8–10]. The approach to replicate endochondral ossification by adult hMSC has the potential to determine a paradigm shift in the design of novel therapeutic options in bone regeneration, as well as for the development of models to investigate stromal niche—HSC interactions in physiology and pathology.

The method described here is clearly distinguishable from the typical protocols to engineer bone tissue, which rely on the direct differentiation of mesenchymal progenitors into osteoblastic cells [11] and thus do not capture the typical steps involved in the development and repair of most bones. Contrary to those approaches, our method implies in vitro pre-commitment of hMSC under defined culture conditions, aimed at recapitulating the first stages of endochondral ossification (i.e., cell condensation, chondrogenic differentiation, and hypertrophy) [12] (Fig. 1). Following this phase, the resulting engineered cartilage templates include all the necessary signals to autonomously activate the endochondral

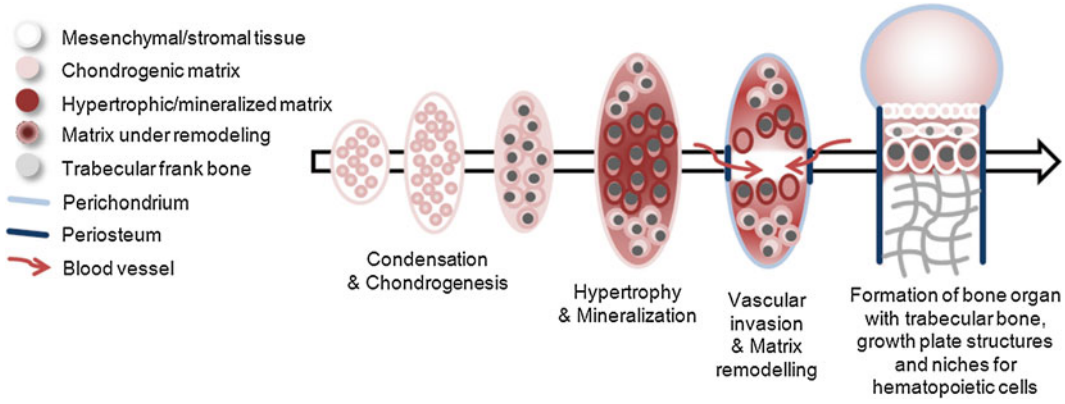

Fig. 1 Schematic representation of the endochondral ossification route during development. The process starts from condensation and subsequent chondrogenic differentiation of skeletal progenitor cells. Cell hypertrophy leads to extracellular matrix remodelling, osteoclast invasion, and vascularization. The cartilaginous template is ultimately remodelled into bone tissue containing bone marrow

route, namely vessel invasion, remodelling into bone tissue, and establishment of a functional hematopoietic microenvironment. Remarkably, such developmental processes are replicated using cells from adult organisms instead of embryonic cells, as previously reported [13].

Mineralization of the hypertrophic cartilage plays an important role in the system, as it generates a calcium-containing template, which has been shown to be essential to prime hMSC differentiation to deposit osseous matrix [8, 13]. Thus, the strategy to induce hMSC towards an endochondral as opposed to a direct ossification route circumvents the otherwise critical requirement to form bone tissue, namely the use of a ceramic-based scaffold. This feature introduces the possibility to implement the protocol in a variety of scalable configurations, without a scaffold or using a broad range of scaffold architectures and compositions, including natural or synthetic polymers.

Depending on the experimental targets and needs, here we propose two modalities of endochondral bone tissue engineering (1) small scale, scaffold-free transwell-based aggregates (6 mm-diameter, 0.5–1.5 mm-thick discs) [14]; (2) upscaled, scaffold-based tissues (up to 8 mm diameter × 3 mm thick materials) [6]. The protocol described in this chapter refers to a specific scaffold (collagen sponge, Ultrafoam™, Davel Inc.), although it is compatible with a variety of different material compositions and architectures. An increase in the tissue scale may require more time to complete the remodelling phase, yet on the other hand it offers the opportunity to better investigate spatial patterns of tissue development, to attract larger numbers of HSC and to generate larger grafts for bone repair in pre-clinical models.

A characteristic limitation of this protocol is represented by the well-known inter-individual variability of hMSC differentiation potential [15]. Importantly, until more efficient in vitro differentiation protocols are developed, the selection of a primary hMSC source with a high chondrogenic potential is a mandatory prerequisite for the successful implementation of the protocols described below.

2 Materials

2.1 Cell Culture

1. Bone marrow from human patients. Before bone marrow aspiration, protocols need to be approved by the local ethical committee and written informed consent obtained from each individual.
2. Ca2+/Mg2+-free phosphate-buffered saline.
3. Trypsin-EDTA solution.
4. Penicillin/streptomycin/glutamine mixture (PSG).
5. Dulbecco's modified Eagle's medium (DMEM).

6. Alpha modified Eagle's medium (αMEM).
7. Fetal bovine serum (FBS).
8. Hepes Buffer.
9. Sodium Pyruvate (Na Pyruvate).
10. Dithiothreitol (DTT).
11. Human Serum Albumin (HSA).
12. 0.01 % Crystal violet in PBS, pH 7.2.
13. Fibroblast growth factor-2 (FGF-2).
14. Transforming growth factor beta 3 (TGF-β3).
15. Insulin-Transferrin-Selenium-A (ITS-A).
16. L-Ascorbic acid 2-phosphate (AA).
17. Dexamethasone (Dex).
18. Beta-GlyceroPhosphate (βGP).
19. L-Thyroxine.
20. Linoleic acid.
21. Interleukin 1 beta (IL-1β).

2.1.1 Nude Mice Implantation Reagents

1. CD1 null/null nude mice (between 5 and 12 weeks old, Charles River Laboratories). All animal studies referred to in this protocol need to be approved by the local and national ethics authorities.
2. Isofluorane.
3. Disinfectant (70 % Ethanol).
4. Analgesic Buprenorphin (0.1 mg/kg/dose).
5. CO_2.

2.2 Reagent Setup

1. Media preparation for expansion, chondrogenic, and hypertrophy phases: *see* Table 1.
2. HSA preparation: prepare a stock solution of 125 mg/ml by diluting HSA 20 % in DMEM then filter-sterilize.
3. FGF-2 preparation: Prepare a stock solution of 10 μg/ml in filter-sterilized PBS containing 1 mM DTT and 1 mg/ml HSA. Prepare a working solution of 1 μg/ml in filter-sterilized DMEM containing 1.25 mg/ml HSA.
4. TGF-β3 preparation: same procedure as for FGF-2.
5. IL-1β preparation: as recommended by the manufacturer's instructions.
6. AA preparation: prepare a stock solution of 10 mM dissolving the powder in DMEM and then filter-sterilize. Handle and store protected from light.
7. Dex preparation: prepare a stock solution of 10^{-5} M (to be used for the preparation of the Chondrogenic medium) and a stock

Table 1
Media preparation for expansion, chondrogenic, and hypertrophy phases

Media Reagents	Expansion medium	Chondrogenic medium	Hypertrophic medium
DMEM		X	X
αMEM	X		
Hepes buffer	X	X	X
Na Pyruvate	X	X	X
PSG	X	X	X
FBS	X		
ITS-A		X	X
Linoleic acid		X	X
HSA		X	X
FGF-2	X		
TGF-β3		X	
AA		X	X
Dex		X	X
Thyroxine			X
βGP			X
IL-1β			X

solution of 10^{-6} M (to be used for the Hypertrophic medium) dissolving the powder in DMEM and then filter-sterilize.

8. Tyroxine preparation: prepare a stock solution of 0.05 mM dissolving the powder in 1.25 mg/ml HSA and then filter-sterilize. Handle and store protected from light.

Expansion medium: αMEM, 10 mM Hepes Buffer, 1 mM Na Pyruvate, 1 % Penicillin/streptomycin/glutamine mixture, 10 % FBS, 5 ng/ml FGF-2.

Chondrogenic medium: DMEM, 10 mM Hepes Buffer, 1 mM Na Pyruvate, 1 % Penicillin/streptomycin/glutamine mixture, 1 % ITS-A, 4.7 μg/ml Linoleic acid, 1.25 mg/ml HSA, 10 ng/ml TGF-β3, 0.1 mM AA, 10^{-7} M Dex.

Hypertophic medium: DMEM, 10 mM Hepes Buffer, 1 mM Na Pyruvate, 1 % Penicillin/streptomycin/glutamine mixture, 1 % ITS-A, 4.7 μg/ml Linoleic acid, 1.25 mg/ml HSA, 0.1 mM AA, 10^{-8} M Dex, 0.05 μM L-Thyroxine, 10 mM βGP, 50 pg/ml IL-1β.

2.3 Equipment

2.3.1 Cell Culture Equipment

1. Laminar flow biosafety cabinet (level II) equipped with UV light for decontamination.
2. Routine light microscope with phase contrast.
3. Inverted microscope.
4. Water bath with temperature control (37 °C).
5. Tissue culture flasks 150 cm^2.
6. 1.5 ml conical tubes.
7. Falcon Tubes 15 and 50 ml.
8. 6 Well and 24 well plates Clear Flat Bottom Ultra Low Attachment.
9. Transwell system (6.5 mm diameter with 0.4 μm membrane pores, 24 well plate).
10. Neubauer chamber.
11. Biopsy punch with 6 mm, 8 mm diameters.
12. Scaffolds: Avitene™ Ultrafoam™ Collagen Sponge, (3 mm thick; Davol Inc.).
13. Humified incubator at 37 °C with 20 % oxygen tension and 5 % CO_2.

2.3.2 Nude Mice Implantation Equipment

1. Animal facility and animal care staff for handling and care.
2. Small animal anesthesia vaporizer for inhalation.
3. Small animal clippers (AUTOCLIP 9 mm Wound Clips and Clip Applicator, Clay Adams).
4. Sterile surgical drapes.
5. Surgical tools for ectopic implantation (long curved blunt Metzenbaum scissors, long curved sharp Joseph scissors, fine surgical forceps, fine anatomical forceps).

3 Methods

3.1 Preparation of Human Cell Suspension

1. Isolate hMSC from BM aspirates, obtained from the iliac crests of healthy donors during routine orthopedic surgical procedures, in accordance with the local ethical committee and after informed consent.
2. Dilute and count the number of nucleated cells/ml after staining with 0.01 % crystal violet in PBS [16].
3. Expand hMSC till early passages (≤3), corresponding to ~16–18 population doublings, in tissue flasks at the seeding cell density of 3000 cells/cm^2 with αMEM supplemented with human recombinant FGF-2 (5 ng/ml) [17].
4. Obtain a single cell suspension from expanded hMSC by trypsin-EDTA digestion, following the conventional proce-

dure: remove culture medium from each flask, wash with PBS, incubate with trypsin-EDTA for 5–10 min, block with double volume of media supplemented with FBS, collect cell suspension in tubes, centrifuge at 1500 × *g* for 3 min at room temperature.

5. Count cell number with Neubauer chamber diluting the designated amount of cell suspension with trypan blue to assess cell viability.
6. Characterize hMSC, according to the positive expression of conventional markers such as CD73, CD90, CD105, clonogenic potential, and tri-lineage differentiation potential (osteogenesis, adipogenesis, and chondrogenesis), especially to assess the chondrogenic lineage which is pivotal for the endochondral protocol [16, 18, 19].

3.2 Small Scale: Transwell-Based Scaffold-Free Cell Aggregates

3.2.1 Small Scale: Transwell-Based Scaffold-Free Cell Aggregates Preparation and Culture

1. Resuspend the cells with chondrogenic medium at the cell density of 2.5×10^6 cells/ml of medium.
2. Distribute 0.2 ml of cell suspension in the top chamber of the transwell system and centrifuge the plate at 80 × *g* for 5 min at RT [5, 14]. Add 0.8 ml of chondrogenic medium in the lower chamber.
3. Place the plates in a humidified incubator at 37 °C with 20 % oxygen tension and 5 % CO_2.
4. Keep in culture in chondrogenic medium, changing it every 3–4 days for 2 weeks, to reach the onset of chondrogenesis and perform a quality control (*see* **Note 1**).
5. Culture for one additional week in chondrogenic medium to reach an early hypertrophic phenotype, then switch to hypertrophic medium; change it every 3–4 days for an additional 2 weeks (*see* **Note 2**).

3.2.2 Small-Scale Transwell-Based Scaffold-Free Cell Aggregate Nude Mice Implantation

1. Harvest aggregates after a total of 5 weeks of in vitro culture for further in vitro characterization.
2. Harvest aggregates after a total of 5 weeks of in vitro culture for in vivo ectopic implantation (*see* **Note 3**).
3. Implant cellular aggregates (max 4 per mouse) ectopically in subcutaneous pockets in the back of nude mice (one cellular aggregate per pouch): see details for ectopic implant in Subheading 3.4.
4. Retrieve after 4 weeks (to observe the matrix remodeling process) or 8 weeks (to complete bone organ formation) (Fig. 2).

3.2.3 Small Scale: Transwell-Based Scaffold-Free Cell Aggregate Characterization

1. Treat the samples, depending on the presence of calcified tissue, both for in vitro and in vivo characterization (i.e. for histological analyses, fix with PFA 4 %, if needed decalcify with 7 % EDTA-solution and embed in paraffin for further

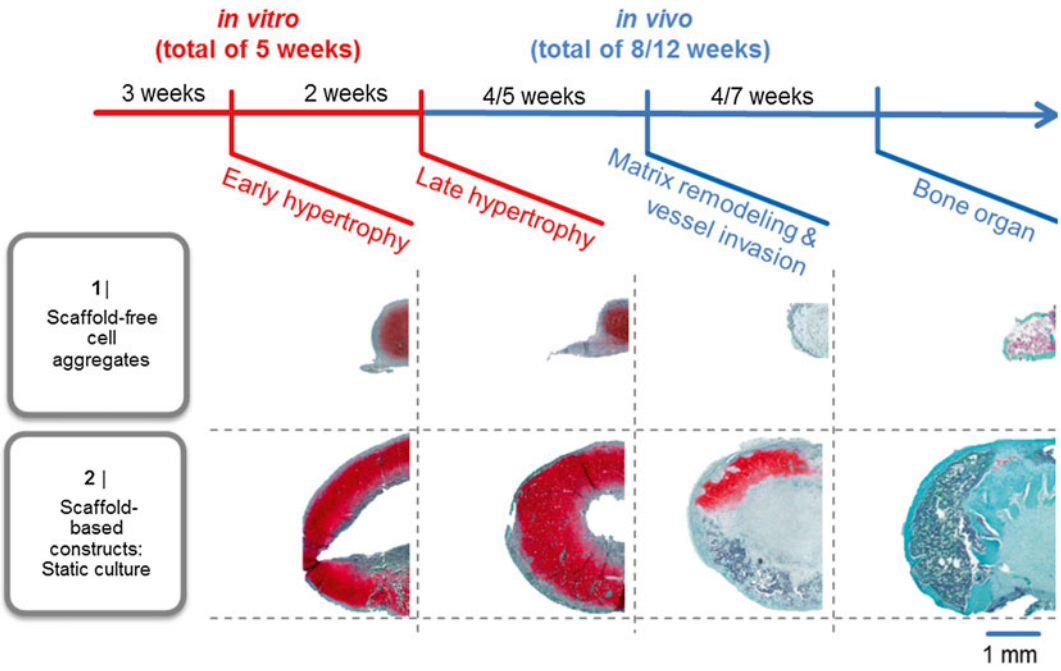

Fig. 2 Experimental design and expected outcome of the endochondral protocol for small- and large-scale constructs. The diagram indicates the typical tissue maturation stages recapitulating the endochondral ossification route at defined time points. After a total of 5 weeks of in vitro culture to reach the formation of hypertrophic cartilage, the in vivo remodelling time into a bone organ requires typically 4 + 4 weeks (total of 8 weeks) for small-scale and 5 + 7 weeks (total of 12 weeks) for large-scale constructs. The final outcome of the scaffold-free cell aggregates model is a peripheral perichondral bone tissue with an inner cavity filled with bone marrow. Scaffold-based constructs in static culture lead to a similar structure, but in a ~tenfold volume scale-up

histological and immunohistochemical stainings): Table 2 lists key markers used to characterize the typical features of the developed tissues.

3.3 Large-Scale Scaffold-Based Constructs

3.3.1 Large-Scale Scaffold-Based Construct Preparation and Culture

1. Follow instructions in Subheading 3.1 to prepare cell suspension.
2. If the scaffold does not come in the final required size (e.g., in case of sheets of Ultrafoam™), cut out discs by using the appropriate diameter biopsy punch (up to 8 mm in diameter) on a sterile Teflon surface. Press biopsy punch with slight rotation and take care not to tear the scaffold during cutting.
3. Suspend the cells with chondrogenic medium at the concentration of 114×10^6 cells/ml (e.g., 4×10^6 cells in 35 μl for 8 mm diameter scaffold).
4. Place one scaffold in each well of 6-well plates with a low adherence substrate.

Table 2
Recommended markers to characterize the typical features of the developed tissues after in vitro culture or in vivo implantation

	Matrix markers	Cellular components
Chondrogenic matrix	COLL II, GAG	Rounded cell embedded in round lacuna dispersed in dense chondorgenic matrix
Hypertrophic matrix	COLL II, GAG, COLL X, MMP13, IHH, VEGF, PTH1R	Large cells embedded in large rounded lacuna, void lacuna with apoptotic cells
Mineralized matrix	COLL II, Ca2+, BSP, OSX	"Fibroblastic-like cells" surrounded by deposits of Ca2+
Necrotic core	Picnotic cells within disorganized and loose matrix	
Matrix under remodeling	DIPEN, MMP13, MMP9, TRAP, CD31	Osteoclasts and chondroclasts, vessel ingrowth, few hypertrophic chondrocytes, and apoptotic cells
Perichondral bone	RUNX2, OSX, COLL I, BMP7	Osteocytes (host origin) embedded in dense and lamellar matrix, flattened bone-lining cells on the endosteal side
Endochondral bone	RUNX2, OSX COLL I	Osteocytes (donor origin) embedded in dense matrix remodeled by osteoclasts, cuboid osteoblasts (donor origin), bone marrow elements (adipocytes and hematopoietic cells)

Coll I Collagen type I, *Coll II* Collagen type II, *Coll X* Collagen type X, *GAG* Glycosaminoglycans, *MMP9* Metalloproteinase 9, *MMP13* Metalloproteinase 13, *Ca2+* Calcium deposits, *IHH* Indian Hedgehog, *VEGF* Vascular endothelial growth factor, *BSP* Bone sialoprotein, *PTH1R* Parathyroid hormone 1 receptor, *OSX* Osterix, *PECAM-1, CD31* Platelet endothelial cell adhesion molecule, *DIPEN* Aggrecan cryptic epitope-MMP-generated C-terminal neo-epitope, *RUNX2* Runt-related transcription factor 2, *BMP7* Bone morphogenetic protein 7, *TRAP* Tartrate-resistant acid phosphatase

5. Statically seed the cells onto the scaffold by pipetting the cell suspension as a single drop on the top of each scaffold.
6. Leave in the incubator at 37 °C with 20 % oxygen tension and 5 % CO_2 for 1 h. Do not let the scaffold dry out during the seeding phase. Make sure the construct is always wet and, if necessary, add a drop of medium around it.
7. Add 5 ml of chondrogenic medium to each well, pipetting the liquid very slowly and not directly onto the seeded scaffolds.

8. Keep in culture with the chondrogenic medium *for 3 weeks to reach an early hypertrophic phenotype, changing the medium every 3–4 days* (*see* **Note 4**).
9. After 3 weeks of chondrogenic medium, switch to hypertrophic medium; change it every 3–4 days for an additional 2 weeks (*see* **Note 5**).

3.3.2 Large-Scale Scaffold-Based Construct Nude Mice Implantation

Harvest constructs after a total of 5 weeks of in vitro culture for further in vitro characterization.

1. Harvest constructs after a total of 5 weeks of in vitro culture for in vivo ectopic implantation.
2. Implant constructs (max 4 per mouse) ectopically in subcutaneous pockets in the back of nude mice (one construct per pouch): see details for ectopic implant in Subheading 3.4.
3. Retrieve after 5 weeks (to observe the matrix remodeling process) or 12 weeks (to complete bone organ formation).

3.3.3 Large-Scale Scaffold-Based Construct Characterization

1. Treat the samples, depending on the presence of calcified tissue, both for in vitro and in vivo characterization (i.e. for histological analyses, properly fix with paraformalsehyde (PFA) 4 %, if needed decalcify with 7 % EDTA-solution and embed in paraffin for further histological and immunohistochemical stainings): Table 2 lists key markers at different experimental time-points.

3.4 Procedure for Nude Mice Implantation

1. Implant samples (4 per mouse) ectopically in the back of nude mice CD1null/null in pockets (one sample per each pouch) created between the muscle fascia and subcutaneous tissue by using surgical scissors and forceps.
2. Prolong the in vivo phase up to 8/12 weeks, according to sample size (more precisely 4/8 weeks to observe matrix remodelling process and 8/12 weeks to achieve complete bone formation).
3. During implantation, administer isofluorane anesthesia to the animal and then treat with the analgesic Buprenorphin (0.1 mg/kg/dose) every 8 h for the first 48 h.
4. Keep the animals at the animal house and follow animal care regulations.
5. Maintain groups of no more than four implanted animals in a single cage.
6. Specialized personnel should check the animals on a daily basis during the first week after surgery and twice a week thereafter.
7. At the end of the experiment, animals will be euthanized by CO_2 before harvesting the implanted tissues.

4 Notes

1. Expected outcome of disc-like cellular aggregates, 6 mm diameter/1 mm thick (in some cases discs may contract and become 1–2 mm diameter spheroids), with a stiff macroscopic consistency and smooth texture. Chondrogenic differentiation should be evident by analysis of the cells/matrix (Table 2, Fig. 2) and histological scoring (Bern score) [20]. The Bern score for the chondrogenic samples (quality control) must be ≥6 to allow further endochondral differentiation. Good chondrogenesis is a crucial prerequisite for the continuation of the experiment. A Bern score <6 should prompt interruption of the protocol and you should start again using MSC from a different primary culture.
2. Expected outcome of disc-like aggregates, 6 mm diameter/1.5 mm thick (in some cases discs may contract and become 1–2 mm diameter spheroids), with a stiff macroscopic consistency and with deposits of calcified matrix. The onset of late hypertrophy should be evident by analysis of the cells/matrix (Table 2, Fig. 2).
3. In the unlikely case that the transwell membrane comes off together with the tissue while harvesting the transwell-based aggregates from the in vitro culture, the entire construct can be implanted in order to avoid destructive manipulation. The membrane will not impair in vivo tissue formation.
4. Expected outcome of 6–7 mm diameter spheroid constructs, with a stiff macroscopic consistency and smooth texture. Chondrogenic differentiation/early hypertrophy should be evident by analysis of the cells/matrix. In such large-scale and static culture, a central necrotic core is expected to form (Table 2, Fig. 2).
5. Expected outcome of 6–7 mm diameter spheroid constructs, with a stiff macroscopic consistency and with deposits of calcified matrix and a central necrotic core. The onset of late hypertrophy should be evident by analysis of the cells/matrix (Table 2, Fig. 2).

Acknowledgments

We acknowledge support from the Swiss National Science Foundation (grant NMS1725 to IM) and from the AO Foundation (grant S-11-13P to AP).

References

1. Jakob M, Saxer F, Scotti C et al (2012) Perspective on the evolution of cell-based bone tissue engineering strategies. Eur Surg Res 49:1–7
2. Gerstenfeld LC, Cullinane DM, Barnes GL et al (2003) Fracture healing as a post-natal developmental process: molecular, spatial, and temporal aspects of its regulation. J Cell Biochem 88:873–884
3. Lenas P, Moos M, Luyten FP (2009) Developmental engineering: a new paradigm for the design and manufacturing of cell-based products. Part I: from three-dimensional cell growth to biomimetics of in vivo development. Tissue Eng Part B Rev 15:381–394
4. Lenas P, Moos M, Luyten FP (2009) Developmental engineering: a new paradigm for the design and manufacturing of cell-based products. Part II: from genes to networks: tissue engineering from the viewpoint of systems biology and network science. Tissue Eng Part B Rev 15:395–422
5. Scotti C, Tonnarelli B, Papadimitropoulos A et al (2010) Recapitulation of endochondral bone formation using human adult mesenchymal stem cells as a paradigm for developmental engineering. Proc Natl Acad Sci U S A 107:7251–7256
6. Scotti C, Piccinini E, Takizawa H et al (2013) Engineering of a functional bone organ through endochondral ossification. Proc Natl Acad Sci U S A 110:3997–4002
7. Mumme M, Scotti C, Papadimitropoulos A et al (2012) Interleukin-1β modulates endochondral ossification by human adult bone marrow stromal cells. Eur Cell Mater 24:224–236
8. Janicki P, Kasten P, Kleinschmidt K et al (2010) Chondrogenic pre-induction of human mesenchymal stem cells on beta-TCP: enhanced bone quality by endochondral heterotopic bone formation. Acta Biomater 6:3292–3301
9. Farrell E, Both SK, Odörfer KI et al (2011) In-vivo generation of bone via endochondral ossification by in-vitro chondrogenic priming of adult human and rat mesenchymal stem cells. BMC Musculoskelet Disord 12:31
10. Freeman FE, Haugh MG, McNamara LM (2013) Investigation of the optimal timing for chondrogenic priming of MSCs to enhance osteogenic differentiation in vitro as a bone tissue engineering strategy. J Tissue Eng Regen Med. doi: 10.1002/term.1793. (Epub ahead of print)
11. Meijer GJ, de Bruijn JD, Koole R et al (2007) Cell-based bone tissue engineering. PLoS Med 4:e9
12. Kronenberg HM (2003) Developmental regulation of the growth plate. Nature 423:332–336
13. Jukes JM, Both SK, Leusink A et al (2008) Endochondral bone tissue engineering using embryonic stem cells. Proc Natl Acad Sci U S A 105:6840–6845
14. Murdoch AD, Grady LM, Ablett MP et al (2007) Chondrogenic differentiation of human bone marrow stem cells in transwell cultures: generation of scaffold-free cartilage. Stem Cells 25:2786–2796
15. Mentink A, Hulsman M, Groen N et al (2013) Predicting the therapeutic efficacy of MSC in bone tissue engineering using the molecular marker CADM1. Biomaterials 34:4592–4601
16. Di Maggio N, Mehrkens A, Papadimitropoulos A et al (2012) Fibroblast growth factor-2 maintains a niche-dependent population of self-renewing highly potent non-adherent mesenchymal progenitors through FGFR2c. Stem Cells 30:1455–1464
17. Bianchi G, Banfi A, Mastrogiacomo M et al (2003) Ex vivo enrichment of mesenchymal cell progenitors by fibroblast growth factor 2. Exp Cell Res 287:98–105
18. Pittenger MF, Mackay AM, Beck SC et al (1999) Multilineage potential of adult human mesenchymal stem cells. Science 284:143–147
19. Dominici M, Le Blanc K, Mueller I et al (2006) Minimal criteria for defining multipotent mesenchymal stromal cells. The International Society for Cellular Therapy position statement. Cytotherapy 8:315–317
20. Grogan SP, Barbero A, Winkelmann V et al (2006) Visual histological grading system for the evaluation of in vitro-generated neocartilage. Tissue Eng 12:2141–2149

Chapter 25

Fabrication of Elasticity-Tunable Gelatinous Gel for Mesenchymal Stem Cell Culture

Thasaneeya Kuboki and Satoru Kidoaki

Abstract

Surface elasticity or stiffness of an underlying substrate may regulate cellular functions such as adhesion, proliferation, signaling, differentiation, and migration. Recent studies have reported on the development of biomaterials to control stem cell fate determination via the stiffness of the culture substrates. In this chapter, we provide a detailed protocol for fabricating elasticity-tunable gelatinous hydrogels for stem cell culture with photo-induced or thermo-induced crosslinking of well-developed styrenated gelatin (StG). We also include the detailed application of gelatinous gel for mesenchymal stem cell (MSC) culture and sample collection for transcriptional and proteomic analysis.

Key words Gelatinous hydrogel, Surface elasticity, MSC

1 Introduction

Several approaches have been extensively studied to control MSC self-renewal and differentiation. Recently, increasing evidence suggests that in addition to the well-studied soluble factors, mechanical stimuli such as stiffness of the culture substrate may also direct stem cell fate. Several hydrogel systems with tunable elasticity including natural and synthetic materials have increasingly been evaluated for use in stem cell biology studies [1–5]. MSC can differentiate into particular cell types when cultured on substrates with surface elasticity mimicking that of their native tissues. Natural biomaterials are the components that are typically found in the extracellular matrix (ECM) such as collagen and its derivatives, hyaluronic acid, hydroxyapatite, including those from other organisms such as alginate or chitosan. Natural materials are bioactive and biocompatible and have mechanical properties similar to the native tissues that can regulate cellular functions, but the disadvantages of using these materials include lot-to-lot variation, sterility, and difficulty in scaling up.

Massimiliano Gnecchi (ed.), *Mesenchymal Stem Cells: Methods and Protocols*, Methods in Molecular Biology, vol. 1416,
DOI 10.1007/978-1-4939-3584-0_25,

Synthetic materials greatly improve reproducibility, scalability, and safety. Popular synthetic materials including polyacrylamide, poly (ethylene glycol) diacrylates, or poly(dimethylsiloxane) have been designed and widely used for stem cell culture [6–8]. However, these materials also have several drawbacks; for example, they are not biocompatible and they require chemical cross-linking with some ECM proteins for cell culture. Though the chemical fixation of collagen onto hydrogels such as polyacrylamide gel has been widely employed, the fixed state of collagens affects the behavior and function of adhered cells [9].

The StG gel in our system was originally developed in an injectable hydrogel form for drug delivery systems [10]. The hydrogel is biocompatible, biodegradable, and suitable for cell adhesion without any chemical modification of the surface. The surface elasticity of the gelatinous gel may be precisely regulated by optimizing the concentration of photoinitiator, intensity of the light source, and the length of photoirradiation exposure.

This chapter provides a detailed methodology for the surface modification of glass substrate for gel fabrication, preparation of photocurable StG, and fabrication of elasticity-tunable gelatinous gel by photoirradiation, based on the published methods used in our laboratory [11–13]. An alternative protocol also describes the simple preparation of thermo-induced crosslinking of StG using a water-soluble azo radical initiator. The method is suitable for large-scale preparation of elasticity-tunable gels and can be applied in any laboratory that does not have photoirradiation facilities. We also provide additional details on MSC culture and characterization on hydrogels with different surface elasticity, including hydrogel sterilization methods prior to cell culture, as well as cultivation of MSCs on gelatinous gels for RNA and protein isolation.

2 Materials

2.1 Preparation of Vinylated Glass Substrates for Chemical Immobilization of StG Gel

1. Cover glass (thickness: 100–120 μm, diameter: 18 mm).
2. Vinyl methoxy silane.
3. Hydrogen peroxide, 30 % v/v aqueous solution (H_2O_2 aq).
4. Concentrated sulfuric acid (c-H_2SO_4).
5. Piranha solution: Mix 30 % H_2O_2 aq and c-H_2SO_4 at a ratio of 3:7, e.g., 30 ml 30 % H_2O_2 aq + 70 ml c-H_2SO_4.
6. Distilled water (DW).
7. Toluene.
8. Acetone.
9. Ethanol.
10. Sodium hydrogen carbonate.
11. Fine edge tweezers.

12. Metal mesh.
13. Hot air oven.
14. Shaker.

2.2 Preparation of Styrenated Gelatin (StG)

1. Gelatin (Nitta G-1070K, Nitta Gelatin NA Inc, USA).
2. Phosphate-buffered saline (PBS).
3. Water-soluble carbodiimide (WSC, 1-ethyl-3-(3-dimethylaminopropyl) carbodiimide hydrochloride).
4. *p*-Vinylbenzoic acid (VBA).
5. Sodium hydroxide (0.2 N, NaOH).
6. Hydrochloric acid (5 N, HCl).
7. Dialysis bag (MW cut-off 14,000 Da).
8. Plastic conical tube (50 ml).
9. pH meter.
10. Stirrer.
11. Oil bath.
12. UV/Vis spectrophotometer.
13. Lyophilizer.
14. Liquid nitrogen.

2.3 Preparation of Gelatin Sol Solution and Fabrication of the Gel Film

1. Lyophilized styrenated gelatin (StG).
2. Water-soluble Photo initiator, sulfonyl camphorquinone (SCQ) (C173000, Toronto Research Chemical Inc, Canada).
3. Water-soluble Azo initiator, 2,2′-Azobis[2-(2-imidazolin-2-yl) propane]dihydrochloride (VA044) (017-19362, Wako, Japan).
4. PBS.
5. Poly(*N*-isopropylacrylamide) (NIPAAm).
6. Cover glass (18 × 24 mm).
7. Cryotube (5 ml).
8. Petri dishes (35 mm and 10 cm).
9. Photo irradiation unit, metal halide lamp.
10. Laser power meter.
11. Hot plate.
12. Fine-edged tweezers.
13. Conditioning mixer (e.g., MX 201, Thinky, Japan).
14. High-speed centrifuge.
15. Water bath.
16. Vacuum aspirator.
17. Nitrogen gas and glove box.
18. Shaking incubator.

2.4 Measurement of Young's Modulus of Elasticity-Tunable Gelatin Gel by Microindentation Test with an Atomic Force Microscope

1. StG gel film fixed on cover glass.
2. Silicone adhesive material.
3. Disposable syringe (2.5 ml).
4. 200 μl Pipet tips.
5. PBS.
6. Petri dish (35 mm).
7. Fine-edged tweezers.
8. Cantilever, conical type with spring constant 0.2 N/m.
9. Atomic Force Microscope.

2.5 Characterization of MSCs on Elasticity-Tunable Gelatin Gel

2.5.1 MSC Culture

1. Primary MSC passage 3–6.
2. Tissue culture polystyrene (TCPS) dish, 10 cm.
3. Dulbecco's Modified Eagle Medium (DMEM) with low glucose.
4. Sodium hydrogen carbonate.
5. Fetal bovine serum (FBS).
6. Penicillin/streptomycin.
7. Disposable bottle top filter unit pore size 0.20 μm.
8. PBS.
9. 0.25 % Trypsin-EDTA.
10. Hemacytometer.
11. Centrifuge.
12. Class II laminar flow hood.
13. CO_2 incubator.
14. Inverted phase contrast microscope.

2.5.2 RNA Collection

1. Diethyl pyrocarbonate (DEPC).
2. RNase Away.
3. RNase-free plasticware (microcentrifuge tube, micro tips, 15 and 50 ml centrifuge tubes).
4. DEPC-treated glassware.
5. DEPC-treated PBS.
6. DEPC-treated DW.
7. TRIZOL reagent.
8. Chloroform.
9. Isopropanol.
10. 99 % Ethanol.
11. Hot air oven.
12. Centrifuge.

2.5.3 Protein Collection for Western Blotting

1. PBS.
2. 10× Protease inhibitor cocktail.
3. RIPA buffer: 20 mM Tris–HCl (pH 7.4), 2 mM EDTA, 0.15 M NaCl, Triton X-100, 1 % Na-deoxycholate, 1 % SDS 0.1 %.
4. Bio-Rad protein assay.

3 Methods

3.1 Preparation of Vinylated Glass Substrates for Chemical Immobilization of StG Gel

3.1.1 Pre-cleaning of Glass Substrate for Silane Coupling

1. Add 30 ml of H_2O_2 aq. to 300–500 ml beaker.
2. Immerse cover glasses in the H_2O_2 aq. solution and incubate for 2 h at room temperature (*see* **Note 1**).
3. Discard H_2O_2 aq. and rinse the cover glasses twice with DW.
4. Cover the beaker with plastic wrap and sonicate the cover glasses in DW for 5–10 min.
5. Discard the DW and rinse the cover glass twice with 99 % ethanol.
6. Cover the beaker with plastic wrap and sonicate the cover glasses in ethanol for 5–10 min.
7. Align the cover glasses onto the metal mesh, dry in the 50 °C oven for more than 10 min.

3.1.2 Hydroxylation of Glass Surface with Hot Piranha Treatment (in the Fume Hood)

1. Prepare the piranha solution in the 500 ml conical flask (*see* **Note 2**).
2. Carefully soak the cover glasses in piranha solution one by one with tweezers. Do not put the cover glasses into the solution all at once as this may spatter the dangerous solution on your hands (*see* **Note 3**).
3. Cover the rim of the conical flask with aluminum foil, immerse in hot oil bath at 80 °C, stir for 1 h (*see* **Note 4**).
4. Discard piranha solution in an appropriate waste container and mildly neutralize by adding an appropriate amount of sodium hydrogen carbonate.
5. Rinse the cover glasses twice with DW and transfer to a beaker.
6. Cover the beaker with plastic wrap and sonicate the cover glasses in DW for 5 min.
7. Rinse the cover glasses twice with EtOH and sonicate in EtOH for 5 min.
8. Dry the cover glasses in the 50 °C oven for more than 10 min.

3.1.3 Vinyl Silane Coupling on Glass Substrate (in the Fume Hood)

1. Add 25 ml highly dehydrated toluene into a 500 ml conical flask. Transfer the cover glasses to the solution one by one (*see* **Note 5**).
2. Discard the reagent and rinse the cover glass twice with toluene (25 ml).

3. Add 47.5 ml toluene to the flask and add 2.5 ml of vinyl methoxy silane (final concentration 5 %).
4. Cover the rim of the flask with plastic wrap and aluminum foil. Tightly secure the edge of the foil with rubber bands and adhesive tape to exclude evaporation of water into the air.
5. Incubate the cover glasses in the solution at room temperature for 3 days with gentle shaking (*see* **Note 6**).
6. Discard the solution in an appropriate waste container.
7. Rinse the cover glasses twice with toluene (25 ml) (*see* **Note 7**).
8. Add acetone/toluene 25 ml each (1:1) and sonicate for 5 min.
9. Rinse the cover glasses twice with acetone, transfer to the beaker, and sonicate for 5 min.
10. Rinse the cover glasses twice with DW, and sonicate in DW for 5–10 min (pre-heat the oven to 115 °C).
11. Rinse the cover glasses twice with EtOH, add EtOH and sonicate for 5–10 min.
12. Dry the cover glasses in the 115 °C oven for more than 10 min to completely evaporate the remaining toluene.
13. Store the functionalized vinyl glass in the desiccator.

3.2 Preparation of Styrenated Gelatin (StG)

3.2.1 StG Synthesis

1. Dissolve 10 g of gelatin in 500 ml of pre-warmed PBS in a 1 l beaker. Stir at 60 °C for 1 h.
2. Cool to room temperature and adjust the pH to 8.0.
3. Dissolve 5.25 g of VBA (10 eq. to amino groups in gelatin) in 400 ml of 0.2 N NaOH. Stir at room temperature for 1 h.
4. Adjust the pH to 8.0 with 5 N HCl (*see* **Note 8**).
5. Mix the gelatin solution with VBA solution and add the PBS to reach a final 1 l volume.
6. Confirm that the pH is 8.0.
7. Stir for 30 min at room temperature. Slowly add 6.79 g of WSC (10 eq. to amino groups in gelatin).
8. Cover the whole beaker with aluminum foil to protect the reaction from light. Continue stirring for 3 days at room temperature.
9. Confirm the pH (typically around 8.5). Filter the mixture through a 0.22 μm bottle top filter to remove large aggregates of intermolecularly reacted gelatins.
10. Pre-wet a dialysis bag in DW. Close one end of the dialysis tube with a clip and transfer the mixture to the tube (approximately 250 ml in 75 cm long).

11. Close the other end of the tube and confirm that there is no leakage. Dialyze against running tap water for 3–4 days to remove the unbound VBA and other low-molecular weight by-products.
12. After dialysis, confirm the pH (usually around 7.0) and repeat filtration using a 0.22 μm filter (*see* **Note 9**).
13. Aliquot the solution to the 50 ml conical tubes, 45 ml each.
14. Rapid freeze with liquid N_2 (*see* **Note 10**).
15. Freeze dry the sample using a lyophilizer. The lyophilized StG will appear as a white foam. Store the sample at –80 °C.

3.2.2 Measurement of the Degree of Derivatization of the StG

1. Tare the 50 ml beaker on the weighing scale.
2. Weigh 0.1 g of lyophilized StG and add 50 g of water. Stir to dissolve for more than 10 min.
3. Dilute the solution 20-fold in water (500 μl + 9.5 ml of water).
4. Measure absorbance at 268 nm and calculate the percentage of derivatization.
   From Beer-Lambert's law

$$A = \varepsilon cl$$

Where A: absorbance, ε: molar extinction coefficient, c: concentration (mol/l), l: optical path length (cm).

$$\text{Degree of derivatization}\,(\text{DD})\,(\%) = \frac{\text{concentration of styrene in StG}}{\text{concentration of Gelatin} \times \text{number of amino acid of gelatin}} \times 100$$

From the above formula, $c = A/\varepsilon$
If you dissolve X g of gelatin in Υ l of PBS

$$\text{DD}\,(\%) = \frac{A \,/\, \varepsilon 268}{\left[\dfrac{X\ \text{g}}{MStG \times \Upsilon\ \text{l}}\right] \times 35.4} \times 100$$

ε 268: molar extintion coefficient of styrene at wave length 268 nm (1.912×10^4)

If 100 % of styrene group is derivatized,

MStG = molecular weight of gelatin (100,000) + molecular weight of the bound styrene

MW of bound styrene = MW of dehydrated styrene (130.2) X amino acid of gelatin (35.4)

Therefore,

$$\text{MStG} = 100{,}000 + (130.2 \times 35.4) = 104{,}600$$

3.3 Fabrication of the Photo-Crosslinked Gelatin Gel

3.3.1 Preparation of Gelatin Sol

1. Weigh the lyophilized StG 0.9 g in a 5 ml cryotube to make a final 30 % w/v in 3 ml.
2. Prepare 10 % SCQ v/v in D.W. (*see* **Note 11**).
3. Mix 10 % SCQ and PBS in a separate tube to reach a final concentration 1.5–3 % of the gelatin concentration, add the solution to the StG in the cryotube, spin down briefly. Add the remaining solution to the tube (*see* **Note 12**).
4. Dissolve the solution by incubating in the 45 °C water bath for 1 h, vortex frequently until the gel is completely dissolved.
5. Centrifuge at 17,800 g for 1 h at 30 °C.
6. Collect the supernatant and transfer to a new tube, try not to disturb the pellet (*see* **Note 13**).
7. Degas using vacuum aspirator (0.015–0.02 MPA) for 30 min. Vortex frequently.
8. Completely defoam using the conditioning mixer for 10 min.
9. Proceed to the fabrication step or make a small aliquot of the sol solution in the 1.5 ml microcentrifuge tube. Rapid freeze the sol in liquid N_2 and store at −80 °C (*see* **Note 14**).

3.3.2 Fabrication of Photo-Crosslinked Gelatin Gel (Under Ambient Atmosphere)

1. Pre-warm the sol to 45 °C in the water bath (*see* **Note 15**).
2. Turn on the photo irradiation unit for at least 30 min before use. Measure the light intensity at 488 nm using optical power meter. The distance between the light source and the sol sample should be kept constant (*see* **Note 16**).
3. Prepare pNIPAAm-coated glass by evenly spreading 40 μl of pNIPAAm (2 % in ethanol) on 18 × 24 mm cover glass. Air-dry on a 45 °C hot plate.
4. Pre-warm the vinyl glass on the hot plate, drop 30 μl of the sol onto the vinyl glass and place on the prepared pNIPAAm-coated glass (*see* **Note 17**).
5. Place the sol sandwich on the hot plate and perform photo irradiation (Fig. 1). When preparing a new batch of the sol sample, always measure a calibration curve to check the correlation between the irradiation time and the surface elasticity. An example of the optimization experiment is shown in Fig. 2 (*see* **Note 18**).
6. After irradiation, immerse the gel sandwich in the PBS for at least 5 min (*see* **Note 19**).
7. Transfer the formed gel film fixed on vinyl glass to the new petri dish completely filled with PBS. While holding the edge of the gel with the tweezers, wash the surface by strongly paddling the gel against the buffer for at least 5 min.
8. Transfer the gel to a new petri dish, wash overnight at 28 °C with gentle rocking (*see* **Note 20**).

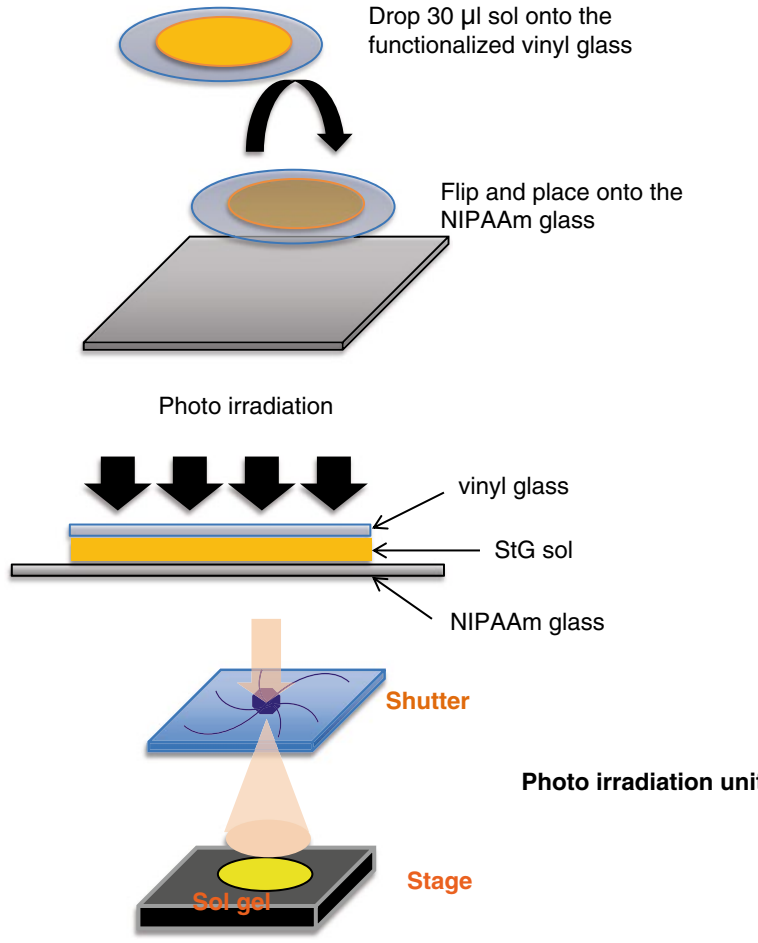

Fig. 1 Procedure for the preparation of the gel sandwich for photo irradiation and schematic display of the photo irradiation unit

3.3.3 Fabrication of Photo-Crosslinked Gelatin Gel (Under Nitrogen Atmosphere; Highly Recommended)

1. Prepare the pre-warmed and degassed sol.
2. Transfer the pNIPAAm-coated glass, vinyl glass, and other necessary materials for gel fabrication into the humidified N_2 glove box. Put the sol in the 45 °C water bath inside the chamber.
3. Pump out the air using a vacuum aspirator for 20 s (25 l/min), fill the chamber with N_2 for 1 min at 5 l/min (pressure 0.15 MPa).
4. Repeat the vacuum/N_2 for three cycles. Open the microcentrifuge tube cap to expose the sol to the N_2 for at least 30 min to exclude the dissolved oxygen under the nitrogen atmosphere.
5. Prepare the sol sandwich and take it out of the chamber. Perform the photoirradiation as described in Subheading 3.2.2. Before preparing the new sol sandwich, repeat the vacuum/N_2 cycle again.

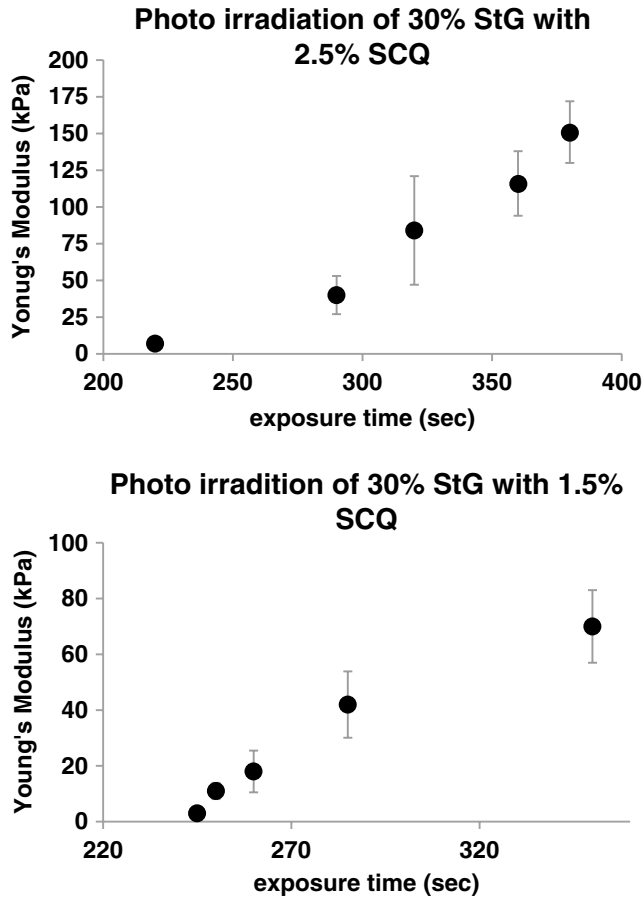

Fig. 2 Typical responses in surface elasticity of the gelatin gel regulated by the photo irradiation times under the two different concentration conditions in photo initiator SCQ

3.3.4 Fabrication of Thermally Crosslinked Gelatin Gel

1. Weigh 300 mg StG in the cryotube. Add 600 μl PBS (final concentration 33.33 % wt/v).
2. Dissolve in the 45 °C water bath for 30 min.
3. Defoam with the conditioning mixer for 5 min.
4. Pre-warm the sol in the 45 °C water bath for 5 min and centrifuge at 17,800 g for 60 min at 30 °C.
5. Transfer the supernatant to the new tube.
6. Degas the sol, then immerse in a 45 °C water bath for 60 min (0.015–0.02 Mpa). Defoam for 10 min and aliquot 300 μl to the microcentrifuge tube.
7. Dissolve 3 mg of VA044 in 97 μl PBS (30 % final concentration).

Table 1
Preparation of thermal-induced polymerization StG

	33.33 % StG sol in PBS (μl)	30 % VA044 in PBS (μl)	15 % VA044 in PBS (μl)	3 % VA044 in PBS (μl)	1.5 % VA044 in PBS (μl)
	300	33	–	–	–
	300	–	33	–	–
	300	–	–	33	–
	300	–	–	–	33
Final conc. of VA044 (per gelatin)	–	1.0 %	0.5 %	0.1 %	0.05 %

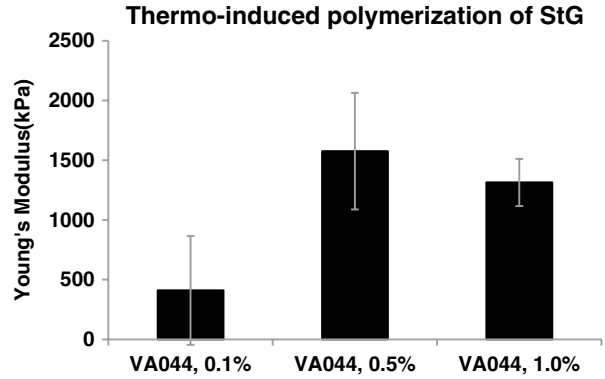

Fig. 3 Typical responses in surface elasticity of the gelatin gel regulated by the concentrations of azo initiator VA044

8. Add 33.3 μl of VA044 solution to the 300 μl StG sol (final concentration 1.0 % of StG). The concentration of VA044 can vary as shown in Table 1 (*see* **Note 21**).
9. Defoam for 10 min.
10. Make a sol sandwich by spreading 30 μl sol between the pNIPAAm-coated glass and the vinyl glass as described in Subheading 3.2.2 (*see* **Note 22**).
11. Place the sol sandwich in the humidified container and incubate overnight at 45 °C. The Young's modulus of the gels prepared with different concentrations of VA044 is shown in Fig. 3 (*see* **Note 23**).

3.4 Measurement of Young's Modulus of Elasticity-Tunable Gelatin Gel by Microindentation Test with an Atomic Force Microscope

1. Equilibrate the gel in PBS at 28 °C for several hours (*see* **Note 24**).
2. Squeeze the adhesive material into a 2.5 ml syringe connected with a 200 μl pipet tip. For AFM measurement, the sample should be well-fixed (*see* **Note 25**).
3. Apply two small spots of the adhesive material onto the bottom of the 35 mm dish (*see* **Note 26**).
4. Place the backside of vinyl glass of the gel onto the kimwipe to remove the excess PBS.
5. Attach the gel to the bottom of the dish (Fig. 4). Gently push the positions that have the adhesive material to secure the gel to the dish.
6. Perform the microindentation test in the AFM contact mode. Measure approximately ten random positions of each gel sample. Calculate the elasticity using the Hertz's model [14–16].

$$\text{Hertz's model } F_{\text{conical}}(z) = \frac{2E\tan\alpha}{\pi\left(1-\mu^2\right)}\delta^2$$

α = semivertical angle of indenter (tip), ~30°; E = Young's modulus; μ = Poisson ratio, ~0.5; δ = indentation depth.

3.5 Characterization of Mesenchymal Stem Cells on Elasticity-Tunable Gelatin Gel

3.5.1 MSC Culture on the Gelatin Gel

1. Culture the MSCs in DMEM supplement with 10 % FBS and penicillin (100 unit/ml)/streptomycin (100 μg/ml), observe the cell growth daily under a microscope until they reach about 80 % confluence (*see* **Note 27**).
2. Align one petri dish containing 70 % EtOH, two dishes of sterile PBS, and one dish with pre-warmed complete DMEM culture media.

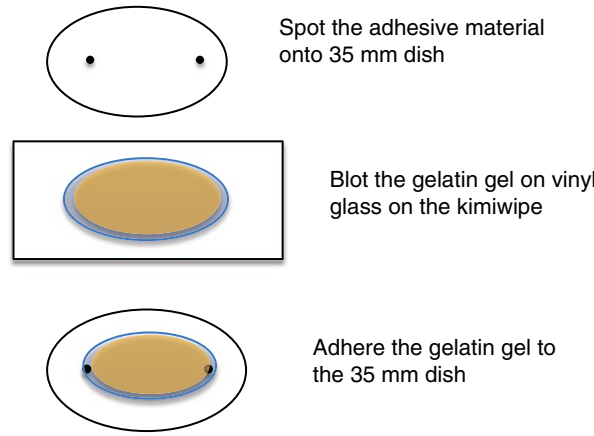

Fig. 4 Preparation of gelatin gel for AFM microindentation test

3. Sterilize the gel by dipping in 70 % EtOH. Pick up the gel using sterile tweezers, repeat dipping until the gel surface is completely saturated with EtOH (*see* **Note 28**).
4. Transfer the gel to the second dish containing PBS, shake the gel gently until the gel surface is completely saturated with PBS.
5. Transfer the gel to the third dish containing PBS and repeat washing.
6. Transfer the gel to the dish containing the culture media. Incubate the gel at 37 °C with 5 % CO_2 for at least 30 min. During incubation, prepare the cells by the trysinzation method.
7. Count the cells using a hemacytometer. The cell suspension should have a density of 1000–2500 cells per cm^2.
8. Take the gel from the incubator, discard the media, and evenly distribute the suspended cells onto the gel samples.
9. Let the cells sediment for about 1 min. Transfer the culture dish to the CO_2 incubator.
10. After 24 h, aseptically transfer the gel samples to a new dish containing fresh culture media (*see* **Note 29**).
11. Culture the cells on the gel for 4–7 days before analysis of mRNA expression. Change the culture media every 3–4 days (*see* **Note 30**).

3.5.2 RNA Collection

1. Bake the glassware (beaker, cylinder, bottle) that will be used for RNA experiments for 4–6 h at 180–200 °C. Treat the PBS and deionized DW with DEPC by adding 0.1 % v/v DEPC to the solution, shake vigorously for 1 min, and incubate at 37 °C overnight. Autoclave the solution at 120 °C for 40 min to inactivate the DEPC.
2. Inactivate any RNase contaminants on the surface of the automatic pipet or rack by spraying RNase Away on the equipment. Wipe off the solution using clean paper.
3. Discard the culture media and rinse the gels with DEPC-treated PBS.
4. Completely aspirate the PBS and directly add 1 ml TRIZOL reagent onto the gel surface (*see* **Note 31**).
5. Pipet the solution and rinse the gel area several times.
6. Collect the suspension in a 1.5 ml microcentrifuge tube, store at −80 °C or proceed to the RNA isolation step (*see* **Note 32**).

3.5.3 Protein Collection for Western Blotting

1. Prepare the cells by the trypsinization method. Collect the cell pellet and wash once with PBS.
2. Add RIPA buffer, vortex and incubate on ice for 20 min with frequent mixing.

3. Centrifuge 17,800 g at 4 °C. Transfer the supernatant to a new tube (*see* **Note 33**).
4. Determine the protein concentration by using Bio-Rad protein assay reagent according to the manufacturer's protocol (*see* **Note 34**).

4 Notes

1. Prepare a maximum of 200 pieces of the cover glasses at a time, as the surface modification will not be efficiently performed with too many samples in one container.
2. Slowly add the c-H_2SO_4 to the H_2O_2 aq., not the other way round. Heat can be generated at this step.
3. The piranha solution is a strong oxidizing agent that completely removes organic contaminants remaining from the previous cleaning step with violent bubbling.
4. Heating to 80 °C is essential for modification of the glass substrate with the hydroxyl group. Though the piranha treatment at room temperature is effective for removing organic contaminants, it has little effect on hydroxylation of the glass surface, and then fails in the following silane coupling.
5. The silane coupling reaction is easily inhibited by the contamination of water. The water contamination results in generation of polysiloxane polymers. The dehydration of toluene is essential. The flask should also be completely dry prior to use.
6. Turn on the ventilation during this process to remove toluene vapor.
7. At this step, if a high percentage of water in the atmosphere contaminated the surface modification reaction, the cover glasses will appear cloudy and stick to each other. These are the aggregates of polysiloxane polymers. This batch of cover glasses is not suitable for gel fabrication. Prepare a new batch using fully dehydrated toluene.
8. The VBA precipitates under low pH. Wait until the suspension is completely dissolved before continuing to adjust the pH. First, adjust using 5 N HCl until the pH goes down to 10. Then, adjust further using 1 N HCl to pH 8.0.
9. If the pH is still not neutral, repeat the dialysis step again.
10. Slow freezing is not recommended as the process can induce local aggregates of gelatin and reduce the reproducibility of elasticity of formed gel. Aliquots can be stored directly at −80 °C.
11. Make small aliquots and store at −80 °C.

12. The concentration of SCQ can vary, depending on the range of the desired elasticity.
13. Cut the edge of the tip for a 1 ml auto pipet and use to transfer the supernatant. Since the sol is rather viscous, slowly aspirate the solution. Do not aspirate all of the supernatant. Leave about 0.5 ml remaining solution that might contain undissolved aggregates of gelatins.
14. The frozen sol can be kept for several months. However, the sample should be freeze-dried, and it retains a lot of oxygen under low-temperatures. This storage process inevitably alters the activity of the gelation. The frozen sol sample should be used up within 1 month.
15. When sol is removed from –80 °C, repeat the degassing and defoaming step again, since a lot of oxygen may accumulate in the frozen sol.
16. Too short of a distance may cause non-homogenous elasticity distribution.
17. Use 18–20 μl of the sol to produce a thin gel layer with 30–50 μm-thickness for high-magnification fluorescence observation.
18. Make a plot between irradiation time and Young's modulus of the gel from the shortest exposure time in which gelation occurs until the longest time that the surface elasticity reaches a plateau.
19. For a very soft gel, as the gel surface is very fragile, the incubation time should be longer to allow the pNIPAAm to dissolve. Gently push the vinyl glass using fine-edged tweezers to detach the pNIPAAm-coated glass.
20. If the gel is not washed properly, the leftover NIPAAM will interfere with AFM measurement and could also be toxic to the cells.
21. The VA044 is added to the final step of sol preparation to avoid the polymerization during incubation of the sol at 45 °C. This procedure is different from the photo-crosslinking where the photo initiator (SCQ) is added to the StG at the first step.
22. The gel fabrication can be scaled up using larger sizes of vinyl glass and pNIPAAm glass.
23. The polymerization will begin after 10 min and gelation is complete after overnight incubation. The polymerization time also depends on concentration of VA044.
24. At low temperature, gelatins form a physical gel and become stiffer than the ground state of chemically crosslinked gel. Therefore, the sample and the buffers should be equilibrated at room temperature before measurement.

25. An adhesive material-filled syringe will facilitate the control of spot size of the glue.
26. The size of the adhesive glue should be large enough to fix the glass to the dish. However, too big of a spot size will make it difficult to detach the gel for the next step after AFM measurement.
27. The doubling time of the MSCs may vary significantly, depending on each donor. When cells are thawed from frozen stock, it will take generally 7–10 days for the cells to reach partial confluence. For the next passage, the doubling time will be decreased to about 4–5 days.
28. Do not immerse the gel in EtOH for too long, as this will affect the physical property of the gel.
29. After the cells have firmly attached to the gel, it is recommended to transfer the gel to a new dish to avoid the interfering effects of cytokines or secretory proteins produced by the cells that adhered to the bottom of the dish outside the gel areas.
30. Culture the MSCs on about 12 gels in a 10 cm culture dish.
31. The proliferation rate of the cells on gel is much less than the rigid TCPS. Use 1–2 ml of TRIZOL per 12 gels in 10 cm culture dish instead of 8 ml recommended by the manufacturer's instructions. For the control cells in the culture dish, use 2–3 ml of TRIZOL with a cell scrapper to dislodge the cells. If the suspension appears viscous, pass the suspension 10 times, through a 21-gauge needle connected with a syringe, to shear the genomic DNA.
32. Typically, approximately 2 μg of total RNA can be obtained from the MSCs cultured on 12 pieces of less than 10 kPa gels. For the stiffer gel substrate, the yield of total RNA increases two to three times.
33. Take care not to disturb the sticky pellet that contains the nucleic acids.
34. If the concentration of protein in the supernatant is rather high, the solution can be diluted and used directly for the protein assay. If the supernatant contains small amounts of protein, perform acetone precipitation and resuspend the pellet in PBS before protein measurement.

Acknowledgments

The authors thank Prof. Takehisa Matsuda of the Kyoto Institute of Technology (Japan) for assistance with the synthesis of styrenated gelatins. This work was supported by a Grant-in-Aid for Scientific Research (24300173, 24120007), a Management Expenses Grant

for National Universities Corporations (Nano-Macro Materials, Devices and System Research Alliance) from the Ministry of Education, Culture, Sports, Science and Technology (MEXT) of Japan.

References

1. Evans ND, Minelli C, Gentleman E et al (2009) Substrate stiffness affects early differentiation events in embryonic stem cells. Eur Cell Mater 18:1–13, discussion 13–14
2. Gilbert PM, Havenstrite KL, Magnusson KE et al (2010) Substrate elasticity regulates skeletal muscle stem cell self-renewal in culture. Science 329:1078–1081
3. Seib FP, Prewitz M, Werner C et al (2009) Matrix elasticity regulates the secretory profile of human bone marrow-derived multipotent mesenchymal stromal cells (MSCs). Biochem Biophys Res Commun 389:663–667
4. Winer JP, Oake S, Janmey PA (2009) Nonlinear elasticity of extracellular matrices enables contractile cells to communicate local position and orientation. PLoS One 4:e6382
5. Winer JP, Janmey PA, McCormick ME et al (2009) Bone marrow-derived human mesenchymal stem cells become quiescent on soft substrates but remain responsive to chemical or mechanical stimuli. Tissue Eng Part A 15:147–154
6. Engler AJ, Sen S, Sweeney HL et al (2006) Matrix elasticity directs stem cell lineage specification. Cell 126:677–689
7. Williams CG, Kim TK, Taboas A et al (2003) In vitro chondrogenesis of bone marrow-derived mesenchymal stem cells in a photopolymerizing hydrogel. Tissue Eng 9:679–688
8. Trappmann B, Gautrot JE, Connelly JT et al (2012) Extracellular-matrix tethering regulates stem-cell fate. Nat Mater 11:642–649
9. Yip AK, Iwasaki K, Ursekar C et al (2013) Cellular response to substrate rigidity is governed by either stress or strain. Biophys J 104:19–29
10. Okino H, Nakayama Y, Tanaka M et al (2002) In situ hydrogelation of photocurable gelatin and drug release. J Biomed Mater Res 59:233–245
11. Kidoaki S, Matsuda T (2008) Microelastic gradient gelatinous gels to induce cellular mechanotaxis. J Biotechnol 133:225–230
12. Kawano T, Kidoaki S (2011) Elasticity boundary conditions required for cell mechanotaxis on microelastically-patterned gels. Biomaterials 32:2725–2733
13. Kuboki T, Kantawong F, Burchmore R et al (2012) 2D-DIGE proteomic analysis of mesenchymal stem cell cultured on the elasticity-tunable hydrogels. Cell Struct Funct 37:127–139
14. Herzt H (1881) Ueber die Beruhrrung fester elastischer Korper. J Reine Angew Mathematik 92:156–171
15. Radmacher M, Fritz M, Hansma PK (1995) Imaging soft samples with the atomic force microscope: gelatin in water and propanol. Biophys J 69:264–270
16. Wu HW, Kuhn T, Moy VT (1998) Mechanical properties of L929 cells measured by atomic force microscopy: effects of anticytoskeletal drugs and membrane crosslinking. Scanning 20:389–397

Part IV

Mesenchymal Stem Cell Secretome

Chapter 26

Testing the Paracrine Properties of Human Mesenchymal Stem Cells Using Conditioned Medium

Patrizia Danieli, Giuseppe Malpasso, Maria Chiara Ciuffreda, and Massimiliano Gnecchi

Abstract

Mesenchymal stem cells (MSC) produce and secrete a great variety of cytokines and chemokines that play beneficial paracrine actions when MSC are used for tissue repair. The conditioned medium (CM) derived from MSC can be used both in vitro and in vivo to test specific paracrine effects or to screen putative paracrine/autocrine mediators by proteomics.

In this chapter, we describe a straightforward method to prepare MSC-derived CM. Furthermore, we summarize some in vitro assays useful for testing the cytoprotective, angiogenic, and regenerative activity of CM. These assays are very helpful when studying the role of MSC in cardiac repair and regeneration.

Key words Mesenchymal stem cells, Conditioned medium, Soluble factors, Paracrine effect, Hypoxia/reoxygenation, Cardioprotection, Angiogenesis, Cardiac regeneration

1 Introduction

Mesenchymal stem cells (MSC) are a cell population partly defined by their ability to differentiate into multiple cell lineages. It was originally thought that this ability for broad plasticity defined the therapeutic potential of MSC. However, an expanding body of evidence has brought growing awareness to the remarkable array of bioactive molecules produced by MSC. Nowadays, it is common opinion that the broad repertoire of secreted factors produced by MSC, generally referred to as the MSC secretome, plays a major role when these cells are administered exogenously to achieve tissue repair. This protein milieu or "secretome" comprises a diverse host of cytokines, chemokines, angiogenic factors, and growth factors. The autocrine/paracrine role of these molecules is being increasingly recognized as key to the regulation of many physiological processes including directing endogenous and progenitor cells to sites of injury as well as mediating apoptosis, scarring, and tissue revascularization. In fact, the immunomodulatory and

Massimiliano Gnecchi (ed.), *Mesenchymal Stem Cells: Methods and Protocols*, Methods in Molecular Biology, vol. 1416,
DOI 10.1007/978-1-4939-3584-0_26,

paracrine role of these molecules may predominantly account for the therapeutic effects of MSC observed in many in vitro and in vivo studies. While the study of such a vast protein array remains challenging, technological advances in the field of proteomics have greatly facilitated our ability to analyze and characterize the MSC secretome. Thus, stem cells can be considered as tunable pharmacological storehouses useful for drug manufacture and therapy. As a cell-free option for regenerative/reparative medicine, stem cell secretome has shown great potential in a variety of applications including cardiac, renal, brain, skin, tendon, and bone repair (*see* chapters of Subheading 1).

The role played by MSC in cardiac repair is of particular interest to our group. It has been demonstrated that differentiation of MSC into cardiomyocytes (CMC) occurs at a very low frequency [1], while it has been convincingly proven that MSC, through the secretion of soluble paracrine factors, protect the heart [2, 3], promote neovascularization [4], and mediate endogenous regeneration via activation of resident cardiac progenitor cells (CPC) [5]. MSC produce and secrete a broad variety of cytokines, chemokines, and growth factors that are involved in the cardiac reparative process observed after stem cell injection into damaged hearts [6]. The most convincing evidence in favor of paracrine mechanisms comes from experimental studies where the administration of conditioned medium (CM) from MSC is able to recapitulate the beneficial effects observed after stem cell therapy [7, 8].

A decade ago, we were the first to demonstrate that MSC exert cytoprotective action on ischemic CMC through secretion of soluble factors. In particular, we showed that CM from hypoxic MSC reduced apoptosis and necrosis of isolated adult rat CMC exposed to low oxygen tension [2]. The cardioprotective activity of MSC-CM was validated in a rat model of acute myocardial infarction [3]. The injection of MSC-CM into the infarct border zone of the heart essentially replicated the results observed with MSC transplantation, both in terms of infarct size and cardiac function, confirming that cytoprotection is the main mechanism of stem cell action. Afterwards, several other groups have confirmed the paracrine cytoprotective effects exerted by BM-derived stem cells on ischemic CMC [9–12].

Another important biological process positively influenced by stem cells in a paracrine fashion is neovascularization. The molecular processes leading to angiogenesis and arteriogenesis involve mediators such as nitric oxide, vascular endothelial growth factor, basic fibroblast growth factor, hepatocyte growth factor, angiopoietin, and others. It has been shown that MSC can express proangiogenic molecules [4] that may play an important role determining the increase in capillary density and collateral development observed in ischemic tissues of animals treated with stem cells.

Finally, there is evidence suggesting a further intriguing hypothesis: exogenous stem cell transplantation may activate resident CPC

and/or stimulate CMC replication via paracrine action, thus improving endogenous cardiac regeneration. The group of Hare demonstrated that MSC interact with host CPC, promoting their recruitment and/or expansion and differentiation [5].

Demonstration of the paracrine theory paves the way for cell-free molecular therapies in tissue repair. Identifying the complete scope and nature of paracrine factors involved in stem cell-mediated cardiac repair represents a demanding task, although it is extremely relevant and worth pursuing. Indeed, the administration of soluble factors instead of stem cells could be more easily translated into the clinical arena since it would bypass most of the issues associated with cell-based therapy, i.e. immune compatibility, tumorigenicity, xenozootic infections, and waiting time for the ex vivo expansion of autologous cell preparations. Such an approach would have a greater potential for the development of "off-the shelf" stem cell-derived products. Even though the road to reach optimal protein therapy presents numerous hurdles, we anticipate that the constant development and application of rational protein design technology will enable significant improvements in the efficacy and safety of existing protein therapeutics. In this case, curing myocardial infarction with a single protein or, most likely, with a cocktail of proteins may become a reality. Study of the secretome represents the most straightforward way to achieve this important goal.

The scheme in Fig. 1 illustrates the experimental flow that we will describe in detail in this chapter: from cell growth and CM production to different in vitro assays to test the properties of CM. Stem cells are typically expanded under normal conditions, even though modifications can be used in particular cases. In our laboratory, we exchange the growth medium with serum-free medium and leave the cells for 48 h under these conditions before collecting the cell secretome.

The CM can be then stored or directly tested both in vitro and in vivo. We also describe a few examples of in vitro assays normally utilized in cardiovascular research. For example, the cardioprotective effects exerted by the CM can be tested on murine CMC before and after exposure to hypoxia or to hypoxia/reoxygenation. The pro-angiogenic properties of the CM can be verified by Matrigel and migration assays using endothelial (EC) or endothelial progenitor cells (EPC). Determining how CM influences endogenous cardiac regeneration may be approached by evaluating the effects of the secretome on CPC proliferation and migration activity. CMC metabolism and contractility can also be studied with simple and reproducible in vitro assays.

The CM can also be tested in vivo using different experimental disease models. For example, the effects of CM on ischemic myocardium can be assessed in a murine model of myocardial infarction. We describe in detail a method to produce concentrated CM useful for animal experiments.

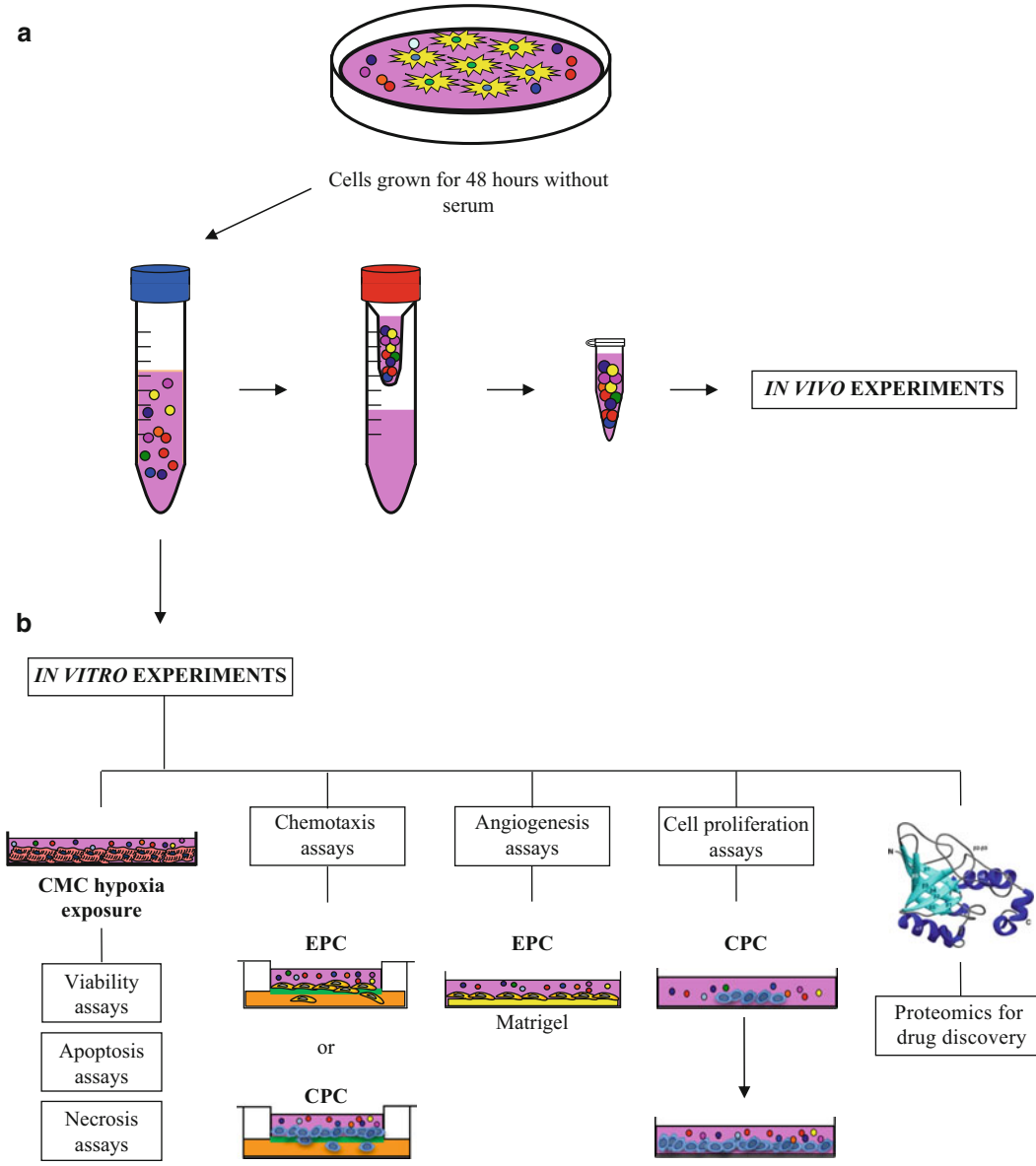

Fig. 1 Production of conditioned medium and different in vitro and in vivo assays. Stem cells are expanded under normal conditions until they are 90 % confluent. The growth medium is then exchanged with medium not containing serum and the cells are left for 48 h in a humidified 5 % CO_2 incubator. The medium is then collected and tested either in vitro or analyzed with proteomic techniques for the search of new therapeutic molecules and targets

2 Materials

2.1 General Supplies

1. Tissue culture supplies including safety hood, CO_2 incubators, a motorized pipettor, 10 ml pipettes, 15 and 50 ml centrifuge tubes, 100 mm tissue culture polystyrene dishes, manual

pipettor and tips, 1.5 ml microcentrifuge sterile tubes, and 2 ml cryovials.

2. Phosphate Buffer Saline w/o Calcium w/o Magnesium (PBS): (137 mM NaCl, 2.7 mM KCl, 10 mM Na_2HPO_4, 2 mM KH_2PO_4) pH 7.4.
3. Fetal Bovine Serum sterile-filtered, heat-inactivated (FBS).
4. Trypsin 0.25 % EDTA.
5. Penicillin and streptomycin at the final concentration of 1 U/ml and 1 μg/ml, respectively (P/S).
6. L-Glutamine at the final concentration of 2 mM.
7. Dulbecco's Modified Eagle Medium (DMEM) High Glucose.
8. Hemocytometer.
9. Inverted light microscope.
10. Refrigerated centrifuge and microcentrifuge.

2.2 Production of Conditioned Medium

1. Starvation medium: DMEM High Glucose supplemented with P/S and L-glutamine.
2. AMICON ULTRA—15 centrifugal filter device—3 K.

2.3 Cytoprotection Assays

1. H9c2(2-1) cells (ATCC® CRL-1446™).
2. Complete H9c2 medium: DMEM High Glucose supplemented with 10 % of FBS, P/S, and L-glutamine.
3. Starvation medium: as described in Subheading 2.2, **item 1**.
4. Hypoxia chamber placed inside a CO_2 incubator and properly connected with a gas controller.
5. Oxygen analyzer.
6. Ischemia medium: DMEM without glucose supplemented with P/S and L-glutamine.
7. 96 Well tissue-culture plates, transparent.
8. 96 Well tissue-culture plates, black with clear bottom (*see* **Note 1**).
9. 96 Well tissue-culture plates, white with clear bottom (*see* **Note 1**).
10. CellTiter-Blue® Cell Viability Assay.
11. Caspase-Glo® 3/7 Assay.
12. CellTox™ Green Cytotoxicity Assay.
13. Microplate 96 well reader (monochromator or filter-based) that can provide fluorescence intensity and glow luminescence detection methods.
14. 560 ± 20 nm Ex/590 ± 10 nm Em filters (for filter-based microplate readers) for CellTiter-Blue® Cell Viability Assay.
15. 485 ± 20 nm Ex/520 ± 20 nm Em (for filter-based microplate readers) for CellTox™ Green Cytotoxicity Assay.

2.4 Matrigel Assay with Human Endothelial Progenitor Cells

1. EPC.
2. Matrigel (15 mg/ml) Growth Factor-Reduced (GFR) Basement Membrane Matrix (*see* **Note 2**).
3. 48 well tissue-culture plates, transparent with flat bottom (*see* **Note 3**).
4. Endothelial Cell Growth Media, EGM™-2 BulletKit™.
5. Phase contrast microscope connected to a camera.

2.5 Migration Assay with Human Endothelial Progenitor Cells

1. EPC.
2. Transwell® permeable support 8 μm polycarbonate membrane, 6.5 mm insert, 24 well plate, tissue culture-treated, sterile.
3. 24 Well cell culture cluster, flat bottom with lid, tissue culture-treated, sterile.
4. Endothelial Cell Growth Media, EGM™-2 BulletKit™.
5. Human CXCL12/Stromal Cell-derived Factor 1 (SDF-1) active full length protein.
6. Fluorescence microscope connected with a camera.
7. Methanol, anhydrous, 99.8 %, ice-cold.
8. Hoechst 33258 (1 mg/ml stock solution).
9. PBS.

2.6 Proliferation Assay of Cardiac Progenitor Cells

1. CPC [13].
2. Complete CPC medium: Iscove's Modified Dulbecco's Medium (IMDM) supplemented with 20 % of FBS, P/S, and L-glutamine.
3. 96 Well tissue-culture plates pre-coated with fibronectin (*see* **Note 4**).
4. CellTiter 96® AQueous One Solution Cell Proliferation Assay.
5. Microplate 96 well reader (monochromator or filter-based) that can record absorbance values at 490 nm.

2.7 Cardiac Progenitor Cell Migration Assay

1. CPC.
2. Complete CPC medium: IMDM supplemented with 20 % of FBS, P/S, and L-glutamine.
3. Transwell® permeable support 8 μm polycarbonate membrane, 6.5 mm insert, 24 well plate, tissue culture-treated, sterile.
4. 24 well cell culture cluster flat bottom with lid, tissue culture-treated, sterile.
5. IMDM.
6. Phase contrast microscope connected to a camera.

7. Methanol, anhydrous, 99.8 %, ice-cold.
8. Hoechst 33258 (1 mg/ml stock solution).
9. PBS.

3 Methods

3.1 Conditioned Medium

1. Use 90 % confluent cells from passage 4–5.
2. Aspirate the growth medium and wash three times with PBS.
3. Add 5 ml of starvation medium. Incubate the cells in the CO_2 incubator for 48 h. This will be the CM.
4. At the same time, incubate 5 ml of starvation medium in a dish without cells. This will serve as the control medium (CTRL-M).
5. Transfer CM and CTRL-M with 10 ml pipettes from dishes to centrifuge tubes.
6. Centrifuge CM and CTRL-M at 4000 × *g* for 5 min at 20 °C to remove debris.
7. Transfer CM and CTRL-M to clean tubes, paying attention not to aspirate the cell debris at the bottom of the tube.
8. Check a small aliquot of CM at the microscope for the presence of debris.
9. MSC are trypsinized and counted to assess the CM concentration (*see* **Notes 5** and **6**).
10. The CM can be tested immediately in different assays or transferred to cryovials and frozen at –80 °C until future use (*see* **Note 7**).

3.2 Concentrated Conditioned Medium

1. Repeat **steps 1–9** reported in Subheading 3.1.
2. Transfer the CM into AMICON ULTRA centrifugal filter devices.
3. Centrifuge at 4,000 × *g* for 30 min at 4 °C (*see* **Note 8**).
4. Immediately recover the concentrate using a 200 μl pipette.
5. Proceed by desalting the concentrate (*see* **Note 9**).
6. The concentrated CM (ultrafiltrate) can be placed in 1.5 ml microcentrifuge tubes on ice and used immediately or stored in 2 ml cryovials at –80 °C until use.

3.3 Cytoprotection Assay

1. Seed 5,000 H9c2 cells/well in 96 well tissue-culture plates in complete H9c2 medium. Seed at least five replicates/treatment per assay.
2. At the same time, seed at least five replicates of H9c2 basal controls (5,000 H9c2 cell/well) for each experiment/assay. Basal controls should be fed with complete H9c2 medium and

cultured in the CO_2 incubator in a normoxic environment throughout the whole experiment.

3. Culture for 24 h in a CO_2 incubator.
4. Remove culture medium and wash the cells twice with PBS.
5. Starve the cells with 100 μl/well starvation medium.
6. After 24 h, remove starvation medium and wash the cells twice with PBS.
7. Put 100 μl/well ischemia medium.
8. Incubate the plates for 6 h in the hypoxia chamber (placed inside the CO_2 incubator) filled with N_2 gas. Monitor the oxygen concentration with an oxygen analyser: O_2 concentration should be kept <0.5 %.
9. Remove ischemia medium and:
   (a) Put 100 μl/well of CM or CTRL-M for CellTiter-Blue® Cell Viability and Caspase-Glo® 3/7 assay.
   (b) Put 50 μl of CM or CTRL-M and 50 μl CellTox™ Green Cytotoxicity assay reagent in each well for CellTox™ Green Cytotoxicity assay.
10. Incubate H9c2 cells in a normoxic environment in a CO_2 incubator for 18 h.
11. Perform CellTiter-Blue® Cell Viability, Caspase-Glo® 3/7 and CellTox™ Green Cytotoxicity assays according to the manufacturer's instructions (*see* **Notes 10–12**).
12. Record fluorescence or luminescence values with the microplate reader and proceed to proper data calculations and statistical analysis.

3.4 Angiogenesis Assays

3.4.1 Matrigel Assay

1. Place the vial of Matrigel on ice and thaw at 4 °C overnight. Keep Matrigel on ice before usage and use pre-cooled pipettes and 48-well culture plate (*see* **Note 13**).
2. Keep the culture plate on ice during the coating process.
3. Add 60 μl/well of Matrigel to a 48-well plate. Coat the required wells for the experiment.
4. Place the plate in a 37 °C incubator for 30 min.
5. While the Matrigel-coated plate incubates, trypsinize the EPC culture and count the cells.
6. Seed 30,000 EPC/well. For seeding, re-suspend the cells directly in the treatment media: complete EGM™-2 medium (CTRL+), CTRL-M, or CM. Perform at least three replicates/experimental condition.
7. Incubate the plate(s) in a humidified 5 % CO_2 incubator at 37 °C.
8. Examine the plates after 6 and 24 h.

9. Capture images of the wells with a camera connected to a phase contrast microscope and score the number of branch points and/or capillary length per field. Evaluate at least five wells/experimental condition.

3.4.2 Endothelial Progenitor Cell Migration Assay

1. Trypsinize the EPC and count the cells.
2. Seed 20,000 EPC on each polycarbonate membrane (8 μm pores) of a 24-well transwell plate in EGM™-2 medium alone (CTRL+) or supplemented with 10 ng/ml SDF-1α, CTRL-M or CM. Perform at least three replicates/experimental condition.
3. Incubate the plate(s) in a humidified 5 % CO_2 incubator at 37 °C.
4. Examine the plate(s) after 10 h.
5. Fix the cells in ice-cold methanol for 10 min at 4 °C.
6. Wash the plates(s) with PBS for 5 min. Repeat the PBS wash.
7. Stain EPC nuclei with Hoechst 33258 (200 μg/ml in PBS) for 5 min at RT.
8. Wash the plates(s) with PBS for 5 min. Repeat the PBS wash.
9. Capture images of the wells with a camera connected to a phase contrast microscope and score the number of EPC that have migrated to the lower side of the membrane at least in five random microscopic fields.

3.5 Regeneration Assays

3.5.1 Cardiac Progenitor Cell Proliferation Assay

1. Trypsinize the culture of CPC and count the cells.
2. Seed 3,000 CPC/well in 96 well tissue-culture plates in complete CPC medium. Seed at least five replicates (5 wells per 96 well tissue-culture plate) for each experimental condition/time point.
3. Culture the cells for 24 h in a humidified 5 % CO_2 incubator.
4. Replace complete culture medium with 100 μl/well complete CPC medium (CTRL+), CTRL-M (negative CTRL), or CM with the addition of 5 % FBS (*see* **Note 14**).
5. Place the wells inside a humidified 5 % CO_2 incubator at 37 °C.
6. Assess the number of metabolically active cells with CellTiter96® Aqueous One Solution Cell assay after 2 h (baseline), 24, 48 and 72 h following the manufacturer's instructions (*see* **Note 15**).
7. Data calculation: normalize the absorbance value recorded at 24, 48, and 72 h vs. absorbance recorded at baseline for each experimental condition (*see* **Note 16**).

3.5.2 Cardiac Progenitor Cell Migration Assay

1. Trypsinize the CPC and count the cells.
2. Repeat **steps 2–9** reported in Subheading 3.4.2 using CPC.

4 Notes

1. 96-Well white and black plates differ in their reflective properties. We recommend white plates for luminescent assays since they maximize the light output signal and black plates for fluorescent assays, because they absorb light and reduce background and crosstalk. Furthermore, we suggest using clear bottom plates to examine the cells by microscopy during the course of the experiment.
2. Use a defined Growth Factor Reduced (GFR) Matrigel to avoid any possible confounding effects of interfering growth factors contained in the matrix on the CM actions.
3. For the Matrigel assay, we recommend using plates with a flat bottom to ensure a smooth Matrigel surface for the growth of cells.
4. As an alternative, standard 96 well tissue-culture plates can be coated with 1 μg/cm^2 fibronectin from human plasma according to the manufacturer's instructions.
5. To compare media conditioned by two different cell types (e.g. MSC and fibroblasts), we suggest normalizing their concentration by the number of cells. To do so, count the cells after collecting the CM and adjust their volumes according to the cell number.
6. We suggest administering CM to H9c2, EPC, and CPC starting with a 1:1 ratio (i.e. give MSC CM (produced from 5,000 cells) to 5,000 H9c2/EPC/CPC). Adjust this ratio according to your specific cell type and/or experimental condition. In addition, dose-response assays can be performed with increasing CM concentrations (e.g. 1×, 10×, 20×…).
7. The use of fresh CM is preferred. Otherwise, CM can be frozen at −80 °C, thawed ONLY ONCE at 37 °C, and used immediately. Multiple freeze/thaw cycles should be avoided since they will result in growth factor/cytokine degradation and consequently loss of CM efficacy.
8. This centrifugation will collect a 200 μl retentate volume starting from a 15 ml sample; adjust the centrifugation time accordingly.
9. Desalting is accomplished by reconstituting the concentrate to the original sample volume with any desired solvent (we suggest PBS) and concentrate again.
10. The CellTiter-Blue® Cell Viability Assay provides a fluorometric method for estimating the number of viable cells present in multiwell plates. It uses the indicator dye resazurin to measure

the metabolic capacity of cells, an indicator of cell viability. Viable cells retain the ability to reduce resazurin into resorufin, which is pink and highly fluorescent (579 nm Ex/584 nm Em). Nonviable cells rapidly lose metabolic capacity, and thus do not reduce the indicator dye.

11. The Caspase-Glo® 3/7 Assay includes a single reagent that performs cell lysis, followed by caspase cleavage of the substrate (tetrapeptide sequence DEVD) and generation of a "glow-type" luminescent signal, produced by luciferase. Luminescence is proportional to the amount of caspase activity present.
12. The CellTox™ Green Cytotoxicity Assay is based on the use of an asymmetric cyanine dye that is excluded from viable cells, but preferentially stains the dead cells' DNA. When the dye binds DNA its fluorescent properties are substantially enhanced, whereas viable cells produce no appreciable increase in fluorescence. Therefore, the fluorescent signal produced is proportional to cytotoxicity.
13. Matrigel solidifies rapidly at 22–35 °C. Always thaw Matrigel on ice, since it may gel at slightly elevated temperatures in a refrigerator. Follow the manufacturer's instructions for general handling procedures.
14. A minimum percentage of FBS (we suggest 5 %) should be added to each CM or control media to ensure detectable CPC proliferation over time.
15. The CellTiter 96® AQueous One Solution Cell Proliferation Assay consists of a MTS tetrazolium compound that is bioreduced by NADPH or NADH produced by dehydrogenase enzymes of metabolically active cells into a colored soluble formazan product. The quantity of the formazan product, as measured by the absorbance at 490 nm, is directly proportional to the number of living cells in culture.
16. Alternatively, it is possible to draw the growth curves, calculate the linear regression equations with the slopes and the R2 values.

Acknowledgments

This work was supported by the Ministero Italiano della Sanità [Grant number GR-2008-1142871 and GR-2010-2320533]; the Fondazione Cariplo [Grant number 2007-5984], and the Ministero Italiano degli Affari Esteri [Grant number ZA11GR2].

References

1. Noiseux N, Gnecchi M, Lopez-Ilasaca M et al (2006) Mesenchymal stem cells overexpressing akt dramatically repair infarcted myocardium and improve cardiac function despite infrequent cellular fusion or differentiation. Mol Ther 14:840–850
2. Gnecchi M, He H, Liang OD et al (2005) Paracrine action accounts for marked protection of ischemic heart by akt-modified mesenchymal stem cells. Nat Med 11: 367–368
3. Gnecchi M, He H, Noiseux N et al (2006) Evidence supporting paracrine hypothesis for akt-modified mesenchymal stem cell-mediated cardiac protection and functional improvement. FASEB J 20:661–669
4. Kinnaird T, Stabile E, Burnett MS et al (2004) Marrow-derived stromal cells express genes encoding a broad spectrum of arteriogenic cytokines and promote in vitro and in vivo arteriogenesis through paracrine mechanisms. Circ Res 94:678–685
5. Hatzistergos KE, Quevedo H, Oskouei BN et al (2010) Bone marrow mesenchymal stem cells stimulate cardiac stem cell proliferation and differentiation. Circ Res 107:913–922
6. Caplan AI, Dennis JE (2006) Mesenchymal stem cells as trophic mediators. J Cell Biochem 98:1076–1084
7. Gnecchi M, Zhang Z, Ni A et al (2008) Paracrine mechanisms in adult stem cell signaling and therapy. Circ Res 103:1204–1219
8. Mirotsou M, Jayawardena TM, Schmeckpeper J et al (2011) Paracrine mechanisms of stem cell reparative and regenerative actions in the heart. J Mol Cell Cardiol 50:280–289
9. Kubal C, Sheth K, Nadal-Ginard B et al (2006) Bone marrow cells have a potent anti-ischemic effect against myocardial cell death in humans. J Thorac Cardiovasc Surg 132:1112–1118
10. Takahashi M, Li TS, Suzuki R et al (2006) Cytokines produced by bone marrow cells can contribute to functional improvement of the infarcted heart by protecting cardiomyocytes from ischemic injury. Am J Physiol Heart Circ Physiol 291:H886–H893
11. Uemura R, Xu M, Ahmad N et al (2006) Bone marrow stem cells prevent left ventricular remodeling of ischemic heart through paracrine signaling. Circ Res 98:1414–1421
12. Xu M, Uemura R, Dai Y et al (2007) In vitro and in vivo effects of bone marrow stem cells on cardiac structure and function. J Mol Cell Cardiol 42:441–448
13. Messina E, De Angelis L, Frati G et al (2004) Isolation and expansion of adult cardiac stem cells from human and murine heart. Circ Res 95:911–921

Chapter 27

Tips on How to Collect and Administer the Mesenchymal Stem Cell Secretome for Central Nervous System Applications

F.G. Teixeira, S.C. Serra, and A.J. Salgado

Abstract

Human mesenchymal stem cells (hMSCs) have been proposed as possible therapeutic agents for central nervous system (CNS) disorders. Recently, it has been suggested that their effects are mostly mediated through their secretome, which contains a number of neuroregulatory molecules capable of increasing cell proliferation, differentiation, and survival in different physiological conditions. Here, we present an overview of the hMSC secretome as a possible candidate in the creation of new cell-free therapies, demonstrating the process of its collection and route of administration, focusing our attention on their effects in CNS regenerative medicine.

Key words Mesenchymal stem cells, Conditioned media, Secretome, Central nervous system, In vivo

1 Introduction

1.1 Mesenchymal Stem Cells

The use of mesenchymal stem cells (MSCs) as a new strategy for cell-based therapies has shown promising results in a variety of health-related problems, including neurodegenerative disorders [1–3]. This great potential has been associated with their widespread availability in the human body, along with the fact that, when isolated, they display great proliferative potential with minimal senescence after multiple passages [4, 5]. The definition introduced by the International Society for Cell Therapy (ISCT) includes some minimal criteria for the identification of MSCs populations, such as adherence to plastic under standard culture conditions; positive expression for specific markers CD73, CD90, CD105 and negative expression for hematopoietic markers CD34, CD45, HLA-DR, CD14 or CD11B, CD79α or CD19; and in vitro differentiation into at least osteoblasts, adipocytes, and chondroblasts [6]. Following the early studies of Friedenstein and colleagues, several reports have confirmed that MSCs are present not

Massimiliano Gnecchi (ed.), *Mesenchymal Stem Cells: Methods and Protocols*, Methods in Molecular Biology, vol. 1416,
DOI 10.1007/978-1-4939-3584-0_27,

only within the bone marrow but also in other tissues: adipose tissue [7, 8], dental pulp [9, 10], placenta [11, 12], umbilical cord blood [13] and Wharton Jelly [14, 15], and brain [16]. Although all these populations meet the defined criteria for MSCs, they do present subtle differences, specifically in their membrane antigen markers. Indeed, studies have shown that such diversity can result from different cell culture isolation and expansion protocols or, alternatively, be related to the tissue source from where they were isolated [17, 18]. Besides the membrane antigens proposed by the ISCT (CD73, CD90, and CD105) for the characterization of MSCs, CD29, CD44, CD51, CD71, CD106, and Stro-1 have also been associated with MSCs' definition [17, 19, 20]. In addition to these findings, further studies have demonstrated that all the MSC populations mentioned may be subpassaged and differentiated in vitro into different cell lineages such as osteoblasts, chondrocytes, adipocytes, and myoblasts [20, 21]. Curiously, several reports have shown that MSCs may also differentiate into neuronal and epithelial populations [20, 22–25]. While differentiation into epithelial cells is widely accepted, the differentiation of MSCs into functional neuronal lineages is still a matter of intense debate [20, 26].

In addition to the necessity to clarify the phenotypic identity of MSCs and the best culture parameters for their handling, other studies have proposed that it is also important to characterize the MSCs secretome, which has been described as the main effector of their therapeutic actions [27–31].

1.2 Mesenchymal Stem Cell Secretome

It has been proposed that the regenerative effects mediated by MSCs are mainly associated with their capacity to secrete a wide panel of bioactive molecules into the extracellular milieu, that is, their secretome [27, 31, 32]. The secretome is defined as the proteins that are released by a cell, tissue, or organism, which are crucial to the regulation of different cell processes [33]. Today it is believed and accepted that in response to injury, apart from cell–cell interactions, the MSC secretome is the main agent of their immunomodulation and regenerative capacity at the lesion site [34–37]. On the other hand, it has been suggested that the MSC transcriptome/secretome can be modulated under different environmental conditions. As such, it is important to analyze to what extent these changes are relevant according to the normal or pathological conditions in which they are being applied [26, 38].

Several studies have shown that MSCs from bone marrow, umbilical cord, adipose tissue, dental pulp, or from other sources are able to secrete trophic factors such as BDNF, β-NGF, IGF-1, HGF, VEGF, TGF-β, GDNF, FGF-2, SCF, G-CSF, and SDF-1 both in vitro and in vivo [32, 34, 39–42]. In some cases most of these factors are considered the main effectors in the modulation of a variety of mechanisms such as immune system suppression, inhibition of apoptosis, increased angiogenesis, and stimulation of

adjacent tissue cells [40]. For instance, in bone regeneration, the MSCs secretome has revealed promising results [43]. Actually, it has been demonstrated that after transplantation of MSCs into femurs of animal models of *osteogenesis imperfecta*, these cells are able to secrete some growth factors (i.e., BMP-2, PEDF and SDF-1) that facilitate the differentiation/recruitment of osteogenic progenitors contributing to bone repair and regeneration of host tissue [43]. In another setting, the trophic action of MSCs in acute lung injury also provided benefits in the regeneration process [44]. The secretion of Ang-1, KGF, HGF, PGE_2, and IL-10 by MSCs into lung tissue had an effect on the regulation of endothelial and epithelial permeability, decreased inflammation, and inhibited bacterial growth, leading to an increase in lung tissue repair [44, 45]. Also in myocardial infarction, MSC-derived factors presented promising results [30, 46]. In fact, both studies with transplanted cells and conditioned media have shown that MSCs are able to secrete many factors such as epiregulin, endothelin, FGF-16, IL-1α, sFRP-1, sFRP-4, TIMP-2, and VEGF. These factors are attributed with the stimulation of angiogenesis, suppression of cardiomyocyte apoptosis, increased efficiency of cardiomyocyte metabolism, and modulation of the interstitial matrix composition through improved survival of myocytes by affecting the activity of ion channels [30, 41, 46, 47].

Concerning the action of MSCs in the central nervous system (CNS), studies have shown that MSCs are able to secrete a wide panel of trophic factors leading to increased neuronal survival and neurogenesis both in vitro and in vivo [48–51]. Even in neurodegenerative disorders such as Parkinson's Disease, spinal cord injury, or stroke, it has been demonstrated that MSCs are able to survive in brain tissue and secrete trophic factors such as BDNF, FGF-2, GDNF, and IGF-1. This fact could explain not only the increase in neuronal survival but also the improved animal behavior upon cell transplantation [52–59]. In addition to these promising results in the CNS, bone, lung, and heart, positive trophic action by MSCs has also been observed in other diseases such as kidney injury, inflammation, diabetes, and cancer [60–62].

Besides the soluble proteic fraction, which includes most of the known growth factors and cytokines, the MSC secretome also contains a vesicular fraction. The latter is composed of microvesicles (MVs) and exosomes and seems to play an important role in the cell and tissue modulatory actions mediated by MSCs [63–68].

A thorough characterization of the MSC secretome is necessary not only to identify the full range of released factors but also to clarify if in fact the molecules released are able to modulate not only the immune response but also different cell processes such as cell proliferation, differentiation, and survival in different physiological settings [69–71]. At the same time, new protocols must be developed to examine the MSC secretome in vivo, as well as

strategies to modulate it [30]. By doing this, it will be possible to understand if in fact the MSC secretome may be used as a new therapeutic strategy in the field of regenerative medicine.

In this chapter, methods for the collection of the MSC secretome and its in vivo applications are presented.

2 Materials

2.1 Mesenchymal Stem Cell Secretome Collection for Proteomic Analysis

1. PBS 1× without Ca^{2+}/Mg^{2+}.
2. Trypsin.
3. Cell culture medium.
4. 10 and 25 ml pipettes.
5. Pipettor.
6. Hemocytometer.
7. T75 cell culture flasks.
8. 50 ml Falcon tubes.

2.2 Mesenchymal Stem Cell Secretome Transplantation in the Dentate Gyrus (DG) of the Hippocampus

1. *Wistar rats.*
2. Anesthetics (ketamine hydrochloride and medetomidine).
3. Anti-sedation (100 μl of anti-sedan solution—Orion Pharma, Finland).
4. Stereotaxic and injector apparatus (Stoelting).
5. Hamilton syringe (0.5 μl).
6. Scalpels, scissors, drill, suturing thread, needles, syringes (1 ml), and disinfectant.
7. Eye protection solution.
8. hMSC secretome.

3 Methods

3.1 Mesenchymal Stem Cell Secretome Collection for Proteomic Analysis

1. All procedures must be conducted under sterile conditions.
2. Expand cells to the desired passage. Upon trypsinization and counting of selected cells, seed them again at a density of 12,000 cells/cm^2 and culture in appropriate growth medium.
3. After 72 h remove growth medium and wash the cells (*see* **Note 1**) five times with 7 ml (*see* **Note 2**) of PBS 1× without Ca^{2+}/Mg^{2+} (at room temperature).
4. Wash (*see* **Note 1**) two additional times with 7 ml (*see* **Note 2**) of cell culture medium (pre-warmed to 37 °C) with *only* 1 % antibiotic.
5. Add 16 ml (*see* **Note 2**) of cell culture medium (pre-warmed to 37 °C) with *only* 1 % antibiotic.

6. After the intended conditioning time collect the total volume of medium into a falcon tube.
7. Snap freeze in liquid nitrogen and store at −80 °C.

3.2 Mesenchymal Stem Cell Secretome Transplantation in the Dentate Gyrus (DG) of the Hippocampus

1. All procedures must be conducted in accordance with the guidelines for the care and handling of laboratory animals: Directive 2010/63/EU of the European Parliament.
2. Prepare and sterilize all materials required for the stereotaxic surgery: scalpels, scissors, drill, suturing thread, needles, syringes (1 ml), stereotaxic and injector apparatus, Hamilton syringe (0.5 μl), anesthesia, disinfectant, and eye protection solution.
3. Determine the coordinates for the brain region of interest according to the Paxinos and Watson atlas [72]. For example, rat coordinates for the hippocampal dentate gyrus (DG) are: Anterior/Posterior (AP) = 3.5 mm, Dorsal/Ventral = 3.5–3.1 mm, Lateral (L) = 2.0 mm.
4. Anesthetize the animals with a mixed solution of ketamine (150 mg/kg) and medetomidine (0.3 mg/kg), injecting 300 μl intraperitoneally.
5. When the animal is sleeping, put one drop of eye protection solution in both eyes (repeat this procedure as needed during the surgery).
6. Accommodate the animal properly in the stereotaxic apparatus and disinfect the head, always protecting its eyes.
7. With a scalpel make a fine incision on the head just enough to expose the Bregma (the incision should be as small as possible).
8. Define the Bregma, mark it with a pen, and set the coordinates: $X = 0$; $Y = 0$; $Z = 0$ using the Hamilton syringe.
9. Starting from the Bregma, find the region of interest with the Hamilton syringe corresponding to the previously established coordinates. Mark the exact position with a pen on the skull.
10. Using a drill, make a small hole at the appropriate skull coordinates.
11. Confirm with the Hamilton syringe that the hole was made at the correct coordinates.
12. Fill the Hamilton syringe with MSC secretome (0.5 μl) and inject slowly (injection rate should be 0.250 μl/min) in the desired area (*see* **Note 3**).
13. Remove the Hamilton syringe slowly and remove the animal from the stereotaxic apparatus (*see* **Note 4**).
14. Suture the animal and inject 100 μl of anti-sedan. Put it back in the cage on top of paper to avoid direct contact with the animal bedding. Check that the animal wakes up properly and behaves normally during the day.

4 Notes

1. When collecting the MSC secretome, special care should be taken during the washing steps. These have to be done thoroughly, but carefully. Thorough washing aims to eliminate all traces of previous media that the cells were in contact with, particularly those supplemented with fetal bovine serum. The proteins of the latter commonly adsorb to TCP. Even in trace amounts, some components may have some effect on the cells and thus interfere with the expected effect of the secretome itself. At this stage, it is important that the cells are disturbed as little as possible. Avoid pipeting the solutions directly on top of the cells. Also, be aware that even a slightly cooler temperature might be enough to make cells detach from the flask.
2. All volumes indicated are adjusted to T75 flasks.
3. Regarding the in vivo procedure for the application of the MSC secretome, one of the biggest challenges (which is still under debate) is the search for the best delivery method (i.e., intracranial, intravenous, intramuscular). Moreover, dosing has not been established. For example, to reach the desired effect is one injection or multiple injections of the secretome necessary?
4. Intracranial injection is the most common strategy described in the literature for the transplantation of MSCs and it has also been used in the application of the MSC secretome. However, this procedure is invasive, especially when the procedure needs to be repeated, for instance, in a multiple injection process. In order to overcome this technical limitation, we first need to establish the best strategy for injecting the MSC secretome in vivo. If the intracranial strategy results as the best method, procedures must be adopted to minimize the level of surgical invasion (i.e., exposition of the animal skull). In addition, if multiple injections are necessary, instead of performing consecutive surgeries, cannulas could be inserted as a more permanent delivery system.

References

1. Gogel S, Gubernator M, Minger SL (2011) Progress and prospects: stem cells and neurological diseases. Gene Ther 18:1–6
2. Wang S, Qu X, Zhao RC (2011) Mesenchymal stem cells hold promise for regenerative medicine. Front Med 5:372–378
3. Hirai H (2002) Stem cells and regenerative medicine. Hum Cell 15:190–198
4. Uccelli A, Benvenuto F, Laroni A et al (2011) Neuroprotective features of mesenchymal stem cells. Best Pract Res Clin Haematol 24: 59–64
5. Uccelli A, Laroni A, Freedman MS (2011) Mesenchymal stem cells for the treatment of multiple sclerosis and other neurological diseases. Lancet Neurol 10:649–656
6. Dominici M, Le Blanc K, Mueller I et al (2006) Minimal criteria for defining multipotent mesenchymal stromal cells. The International Society for Cellular Therapy position statement. Cytotherapy 8:315–317
7. Zuk PA, Zhu M, Ashjian P et al (2002) Human adipose tissue is a source of multipotent stem cells. Mol Biol Cell 13:4279–4295

8. Zuk PA, Zhu M, Mizuno H et al (2001) Multilineage cells from human adipose tissue: implications for cell-based therapies. Tissue Eng 7:211–228
9. Gronthos S, Mankani M, Brahim J et al (2000) Postnatal human dental pulp stem cells (DPSCs) in vitro and in vivo. Proc Natl Acad Sci U S A 97:13625–13630
10. Shi S, Gronthos S (2003) Perivascular niche of postnatal mesenchymal stem cells in human bone marrow and dental pulp. J Bone Miner Res 18:696–704
11. Fukuchi Y, Nakajima H, Sugiyama D et al (2004) Human placenta-derived cells have mesenchymal stem/progenitor cell potential. Stem Cells 22:649–658
12. Abumaree MH, Al Jumah MA, Kalionis B et al (2013) Phenotypic and functional characterization of mesenchymal stem cells from chorionic villi of human term placenta. Stem Cell Rev 9:16–31
13. Erices A, Conget P, Minguell JJ (2000) Mesenchymal progenitor cells in human umbilical cord blood. Br J Haematol 109: 235–242
14. Wang HS, Hung SC, Peng ST et al (2004) Mesenchymal stem cells in the Wharton's jelly of the human umbilical cord. Stem Cells 22:1330–1337
15. Weiss ML, Troyer DL (2006) Stem cells in the umbilical cord. Stem Cell Rev 2:155–162
16. Paul G, Özen I, Christophersen NS et al (2012) The adult human brain harbors multipotent perivascular mesenchymal stem cells. PLoS One 7:e35577
17. Chamberlain G, Fox J, Ashton B et al (2007) Concise review: mesenchymal stem cells: their phenotype, differentiation capacity, immunological features, and potential for homing. Stem Cells 25:2739–2749
18. Meirelles Lda S, Fontes AM, Covas DT et al (2009) Mechanisms involved in the therapeutic properties of mesenchymal stem cells. Cytokine Growth Factor Rev 20:419–427
19. Phinney DG (2007) Biochemical heterogeneity of mesenchymal stem cell populations: clues to their therapeutic efficacy. Cell Cycle 6:2884–2889
20. Phinney DG, Prockop DJ (2007) Concise review: mesenchymal stem/multipotent stromal cells: the state of transdifferentiation and modes of tissue repair – current views. Stem Cells 25:2896–2902
21. Kolf CM, Cho E, Tuan RS (2007) Mesenchymal stromal cells. Biology of adult mesenchymal stem cells: regulation of niche, self-renewal and differentiation. Arthritis Res Ther 9:204
22. Mitchell KE, Weiss ML, Mitchell BM et al (2003) Matrix cells from Wharton's jelly form neurons and glia. Stem Cells 21:50–60
23. Alaminos M, Pérez-Köhler B, Garzón I et al (2010) Transdifferentiation potentiality of human Wharton's jelly stem cells towards vascular endothelial cells. J Cell Physiol 223: 640–647
24. Liqing Y, Jia G, Jiqing C et al (2011) Directed differentiation of motor neuron cell-like cells from human adipose-derived stem cells in vitro. Neuroreport 22:370–373
25. Baer PC, Geiger H (2012) Adipose-derived mesenchymal stromal/stem cells: tissue localization, characterization, and heterogeneity. Stem Cells Int 2012:812693
26. Maltman DJ, Hardy SA, Przyborski SA (2011) Role of mesenchymal stem cells in neurogenesis and nervous system repair. Neurochem Int 59:347–356
27. Teixeira FG, Carvalho MM, Sousa N et al (2013) Mesenchymal stem cells secretome: a new paradigm for central nervous system regeneration? Cell Mol Life Sci 70: 3871–3882
28. Drago D, Cossetti C, Iraci N et al (2013) The stem cell secretome and its role in brain repair. Biochimie 95:2271–2285
29. Estrada R, Li N, Sarojini H et al (2009) Secretome from mesenchymal stem cells induces angiogenesis via Cyr61. J Cell Physiol 219(3):563–571
30. Ranganath SH, Levy O, Inamdar MS et al (2012) Harnessing the mesenchymal stem cell secretome for the treatment of cardiovascular disease. Cell Stem Cell 10:244–258
31. Salgado AJ, Gimble JM (2013) Secretome of mesenchymal stem/stromal cells in regenerative medicine. Biochimie 95:2195
32. Meyerrose T, Olson S, Pontow S et al (2010) Mesenchymal stem cells for the sustained in vivo delivery of bioactive factors. Adv Drug Deliv Rev 62:1167–1174
33. Skalnikova H, Motlik J, Gadher SJ et al (2011) Mapping of the secretome of primary isolates of mammalian cells, stem cells and derived cell lines. Proteomics 11:691–708
34. Chen L, Tredget EE, Wu PY et al (2008) Paracrine factors of mesenchymal stem cells recruit macrophages and endothelial lineage cells and enhance wound healing. PLoS One 3, e1886
35. Block GJ, Ohkouchi S, Fung F et al (2009) Multipotent stromal cells are activated to reduce apoptosis in part by upregulation and secretion of stanniocalcin-1. Stem Cells 27: 670–681

36. Shi Y, Hu G, Su J et al (2010) Mesenchymal stem cells: a new strategy for immunosuppression and tissue repair. Cell Res 20:510–518
37. Kode JA, Mukherjee S, Joglekar MV et al (2009) Mesenchymal stem cells: immunobiology and role in immunomodulation and tissue regeneration. Cytotherapy 11:377–391
38. Puissant B, Barreau C, Bourin P et al (2005) Immunomodulatory effect of human adipose tissue-derived adult stem cells: comparison with bone marrow mesenchymal stem cells. Br J Haematol 129:118–129
39. Bonfield TL, Nolan Koloze MT, Lennon DP et al (2010) Defining human mesenchymal stem cell efficacy in vivo. J Inflamm (Lond) 7:51
40. Caplan AI, Dennis JE (2006) Mesenchymal stem cells as trophic mediators. J Cell Biochem 98:1076–1084
41. Rehman J, Traktuev D, Li J et al (2004) Secretion of angiogenic and antiapoptotic factors by human adipose stromal cells. Circulation 109:1292–1298
42. Nakano N, Nakai Y, Seo TB et al (2010) Characterization of conditioned medium of cultured bone marrow stromal cells. Neurosci Lett 483:57–61
43. Li F, Whyte N, Niyibizi C (2012) Differentiating multipotent mesenchymal stromal cells generate factors that exert paracrine activities on exogenous MSCs: Implications for paracrine activities in bone regeneration. Biochem Biophys Res Commun 426:475–479
44. Lee JW, Fang X, Krasnodembskaya A et al (2011) Concise review: mesenchymal stem cells for acute lung injury: role of paracrine soluble factors. Stem Cells 29:913–919
45. Xu J, Qu J, Cao L et al (2008) Mesenchymal stem cell-based angiopoietin-1 gene therapy for acute lung injury induced by lipopolysaccharide in mice. J Pathol 214:472–481
46. Nguyen BK, Maltais S, Perrault LP et al (2010) Improved function and myocardial repair of infarcted heart by intracoronary injection of mesenchymal stem cell-derived growth factors. J Cardiovasc Transl Res 3:547–558
47. Shabbir A, Zisa D, Suzuki G et al (2009) Heart failure therapy mediated by the trophic activities of bone marrow mesenchymal stem cells: a noninvasive therapeutic regimen. Am J Physiol Heart Circ Physiol 296:H1888–H1897
48. Ribeiro CA, Fraga JS, Grãos M et al (2012) The secretome of stem cells isolated from the adipose tissue and Wharton jelly acts differently on central nervous system derived cell populations. Stem Cell Res Ther 3:18
49. Ribeiro CA, Salgado AJ, Fraga JS et al (2011) The secretome of bone marrow mesenchymal stem cells-conditioned media varies with time and drives a distinct effect on mature neurons and glial cells (primary cultures). J Tissue Eng Regen Med 5:668–672
50. Salgado AJ, Fraga JS, Mesquita AR et al (2010) Role of human umbilical cord mesenchymal progenitors conditioned media in neuronal/glial cell densities, viability, and proliferation. Stem Cells Dev 19:1067–1074
51. Crigler L, Robey RC, Asawachaicharn A et al (2006) Human mesenchymal stem cell subpopulations express a variety of neuro-regulatory molecules and promote neuronal cell survival and neuritogenesis. Exp Neurol 198: 54–64
52. Jin GZ, Cho SJ, Lee YS et al (2010) Intrastriatal grafts of mesenchymal stem cells in adult intact rats can elevate tyrosine hydroxylase expression and dopamine levels. Cell Biol Int 34: 135–140
53. McCoy MK, Martinez TN, Ruhn KA et al (2008) Autologous transplants of adipose-derived adult stromal (ADAS) cells afford dopaminergic neuroprotection in a model of Parkinson's disease. Exp Neurol 210:14–29
54. Fu YS, Cheng YC, Lin MY et al (2006) Conversion of human umbilical cord mesenchymal stem cells in Wharton's jelly to dopaminergic neurons in vitro: potential therapeutic application for Parkinsonism. Stem Cells 24:115–124
55. Gu W, Zhang F, Xue Q et al (2010) Transplantation of bone marrow mesenchymal stem cells reduces lesion volume and induces axonal regrowth of injured spinal cord. Neuropathology 30:205–217
56. Lopatina T, Kalinina N, Karagyaur M et al (2011) Adipose-derived stem cells stimulate regeneration of peripheral nerves: BDNF secreted by these cells promotes nerve healing and axon growth de novo. PLoS One 6:e17899
57. Yang CC, Shih YH, Ko MH et al (2008) Transplantation of human umbilical mesenchymal stem cells from Wharton's jelly after complete transection of the rat spinal cord. PLoS One 3:e3336
58. Wakabayashi K, Nagai A, Sheikh AM et al (2010) Transplantation of human mesenchymal stem cells promotes functional improvement and increased expression of neurotrophic factors in a rat focal cerebral ischemia model. J Neurosci Res 88:1017–1025
59. Koh SH, Kim KS, Choi MR et al (2008) Implantation of human umbilical cord-derived mesenchymal stem cells as a neuroprotective therapy for ischemic stroke in rats. Brain Res 1229:233–248
60. Sasportas LS, Kasmieh R, Wakimoto H et al (2009) Assessment of therapeutic efficacy and

fate of engineered human mesenchymal stem cells for cancer therapy. Proc Natl Acad Sci U S A 106:4822–4827

61. Semedo P, Palasio CG, Oliveira CD et al (2009) Early modulation of inflammation by mesenchymal stem cell after acute kidney injury. Int Immunopharmacol 9:677–682
62. Abdi R, Fiorina P, Adra CN et al (2008) Immunomodulation by mesenchymal stem cells: a potential therapeutic strategy for type 1 diabetes. Diabetes 57:1759–1767
63. Baglio SR, Pegtel DM, Baldini N (2012) Mesenchymal stem cell secreted vesicles provide novel opportunities in (stem) cell-free therapy. Front Physiol 3:359
64. Huang YC, Parolini O, Deng L (2013) The potential role of microvesicles in mesenchymal stem cell-based therapy. Stem Cells Dev 22:841–844
65. Lai RC, Arslan F, Lee MM et al (2010) Exosome secreted by MSC reduces myocardial ischemia/reperfusion injury. Stem Cell Res 4:214–222
66. Lai RC, Chen TS, Lim SK (2011) Mesenchymal stem cell exosome: a novel stem cell-based therapy for cardiovascular disease. Regen Med 6:481–492
67. Lai RC, Yeo RW, Tan KH et al (2013) Mesenchymal stem cell exosome ameliorates reperfusion injury through proteomic complementation. Regen Med 8:197–209
68. Zhou Y, Xu H, Xu W et al (2013) Exosomes released by human umbilical cord mesenchymal stem cells protect against cisplatin-induced renal oxidative stress and apoptosis in vivo and in vitro. Stem Cell Res Ther 4:34
69. Rivera FJ, Siebzehnrubl FA, Kandasamy M et al (2009) Mesenchymal stem cells promote oligodendroglial differentiation in hippocampal slice cultures. Cell Physiol Biochem 24:317–324
70. Sadan O, Shemesh N, Cohen Y et al (2009) Adult neurotrophic factor-secreting stem cells: a potential novel therapy for neurodegenerative diseases. Isr Med Assoc J 11:201–204
71. English K, French A, Wood KJ (2010) Mesenchymal stromal cells: facilitators of successful transplantation? Cell Stem Cell 7: 431–442
72. Paxinos G, Watson C (2004) Rat brain in stereotaxic coordinates, 5th edn. Academic, San Diego

Chapter 28

Soluble Factors from Human Fetal Bone Marrow-Derived Mesenchymal Stem Cells: Preparation of Conditioned Medium and Its Effect on Tumor Cells

Jerry K.Y. Chan and Paula Lam

Abstract

Mesenchymal stem cells (MSCs) possess some unique features (inherent tumor tropism, anti-inflammatory and immunosuppressive properties) that are not commonly found in conventional anti-cancer agents. These cells are known to secrete a vast array of proteins including growth factors, cytokines, chemokines, extracellular matrix metalloproteinases, and their corresponding inhibitors which exhibit profound effects on the microenvironment. However, the lack of a uniform method for culturing MSCs and their paracrine factors has hindered our understanding of MSC biology. In this chapter, we describe methods for the isolation, in vivo expansion, and phenotypic characterization of MSCs. In addition, methods for the collection and concentration of conditioned medium from these MSCs are described. Using tumor cells that constitutively express fluorescence reporter proteins, the effect of conditioned medium on tumor cell viability can be easily tested in vitro.

Key words Human fetal MSCs, Conditioned medium, Tumor cell viability

1 Introduction

Human mesenchymal stem cells or mesenchymal stromal cells (MSCs) are a rare population of fibroblast-like, nonhematopoietic stromal cells (approximately 0.0001–0.001 % of nucleated cells) first identified in the bone marrow [1] and later identified in many tissues such as brain, adipose tissue, lung, heart, umbilical cord, and fetal tissues [2]. MSCs are identified according to the criteria set forth by the International Society for Cell Therapy (ISCT; 2006) that describe MSCs as plastic adherent cells, negative for the hematopoietic markers CD45 and CD34, monocyte, and macrophage markers CD14 and HLA-DR. MSCs are positive for the expression markers including CD73 (known as ecto 5′nucleotidase and originally recognized by the monoclonal antibody (MAb) SH3/4), CD105 (known as endoglin and originally recognized by the MAb SH2), and CD90 (Thy-1) and differentiate

Massimiliano Gnecchi (ed.), *Mesenchymal Stem Cells: Methods and Protocols*, Methods in Molecular Biology, vol. 1416,
DOI 10.1007/978-1-4939-3584-0_28,

into adipocytes, chondrocytes, and osteoblasts under standard in vitro differentiating conditions [3]. There is currently no evidence that a combination of the above-mentioned markers with other surface makers could enhance the isolation of a pure population of MSCs, thus posing difficulties in the large-scale isolation and clinical application of these MSCs. Fetal MSCs have emerged as a possible alternative source of MSCs, as these cells have enhanced plasticity, proliferation rate, and expansion potential compared with adult MSCs [4]. This allows for the expansion of large amounts of cells without age-related senescence.

Fetal MSCs can be isolated from prenatal and extra-embryonic tissues consisting of bone marrow, liver, amniotic fluid, and umbilical cord blood; these MSCs have active telomerase and express pluripotency markers although comparatively lower than embryonic stem cells. In addition, fetal MSCs lack intracellular HLA class II and have lower class I expression compared to adult MSCs, indicating that these cells may be immunologically inert and alluding to their potential in allogeneic transplantation paradigms [5]. MSCs are now in various stages of clinical trials for the treatment of severe osteogenesis imperfecta, osteoarthritis, graft-versus-host disease, Crohn's disease, multiple sclerosis, and liver cirrhosis [6–8].

The drawback of using MSCs for cancer therapy is that its role in tumorigenesis is not well understood. Some authors have reported that MSCs could promote tumor progression, while others report that MSCs exhibit an anti-tumor effect [9]. An evolving scientific concept is that the various paracrine and trophic factors secreted by MSCs exhibit profound direct/indirect effects on local cellular dynamics. Factors secreted by MSCs at high levels include angiogenic factors, pro- and anti-inflammatory cytokines, chemokines, growth factors and their regulators, extracellular matrix metalloproteinases and their corresponding inhibitors [10]. In fact, a number of studies have shown that the therapeutic effect of CM is, in part, mediated by membrane-bound and intracellular proteins; however this topic is beyond the scope of this chapter [11, 12]. When considering studies of the paracrine factors secreted by MSCs, it is worth noting that many studies are based on the secretome in vitro. It is likely that findings will differ in vivo as many other cell types such as macrophages, T cells, fibroblasts, and endothelial cells are also capable of secreting similar factors. Intravenously administered MSCs have been shown to home and inhibit tumor growth in a model of Kaposi's sarcoma [13]. The corresponding inhibition of Akt activation by MSCs was demonstrated in vitro in some but not all tumor cells, suggesting the possible involvement of immunomodulatory properties of MSCs in the tumor microenvironment. Others have shown that MSCs may exert an anti-proliferative effect through the secretion of DKK-1 (dickkopf-1), which subsequently suppresses the canonical WNT signaling pathway, including attenuated β-catenin accumulation [14–16]. We have shown that the co-administration of MSCs with

glioma cells resulted in significant reduction in tumor volume and vascular density, which was not observed when MSCs were injected with immortalized normal human astrocytes [17]. The anti-tumor effect of MSCs is mediated through an impaired recruitment of endothelial progenitor cells and reduced production of angiogenic factors which affects the PDGF/PDGFR signaling axis, a key player in glioma angiogenesis. Very recently, Yang and colleagues have shown that conditioned media from MSCs could cause the differentiation of glioma cells towards a normal glial cell phenotype, thus inhibiting glioma cell proliferation [18]. In contrast, MSCs have also been reported to promote tumor growth through upregulation of proangiogenic factors including VEGF [19–21] and bone morphogenetic protein 2 [22]. Thus, it is of great importance to culture MSCs in a safe and effective manner, including the standardization of conditioned media or microvesicles derived from MSCs for further investigation and clinical development.

2 Materials

2.1 Isolation of Human Fetal MSC (hfMSC)

1. 21G needle.
2. 15 ml falcon.
3. 70 μm cell strainer.
4. Trypan blue.
5. Ficoll-Paque.

2.2 Culture and Expansion of hfMSC

1. Dulbecco's Modified Eagle Medium (DMEM).
2. Phosphate buffered saline solution (PBS).
3. Trypsin.
4. Penicillin-streptomycin (P/S).
5. Fetal bovine serum (FBS) heat inactivated.
6. Dimethyl sulfoxide (DMSO).
7. D10 medium: DMEM, 10 % FBS, 1 % P/S.
8. Freezing medium: 60 % DMEM, 30 % FBS, 10 % DMSO.

2.3 Characterization of hfMSC

1. Monoclonal antibodies CD14, CD34, CD45, CD31, Collagen I and II.
2. Monoclonal antibodies CD73, CD105, CD90.
3. B-glycerophosphate.
4. Ascorbic acid.
5. Dexamethasone.
6. Insulin.
7. Indomethacin.
8. Transforming growth factor-β3.

9. Sodium pyruvate.
10. Proline.
11. ITS-Plus.
12. Safranin O.
13. Toluidine blue staining.
14. *Osteogenic differentiation medium*: D10 medium, 10 mM β-glycerophosphate, 0.2 mM ascorbic acid, 10^{-8} M dexamethasone.
15. Adipogenic medium: D10 medium, 5 μg/ml insulin, 10^{-6} dexamethasone, 60 μM indomethacin.
16. Chondrogenic medium: DMEM, 10 ng/ml transforming growth factor-β3, 100 nM dexamethasone, 50 μg ml ascorbic acid, 100 μg/ml sodium pyruvate, 40 μg/ml proline, ITS-plus 1×.

2.4 Production and Concentration of Conditioned Medium from hfMSC

1. Filtration device Vivaspin 20.
2. Bradford protein assay.
3. Cell Counting Kit-8 (CCK-8) solution (Dojindo Molecular Technologies, Japan).

3 Isolation of Fetal Mesenchymal Stem Cells

1. The long bones (femur and humerus) are stripped of any attached musculature, the epiphyseal ends are cut, and the marrow compartment flushed with a 21G needle with sterile DMEM into 15 ml centrifuge tubes (*see* **Note 1**).
2. The collected marrow is vortexed and passed through a 70 μm cell strainer and spun down at 400 × *g* for 5 min. The BM aspirate can be subjected to Ficoll gradient density centrifugation depending on the extent of red blood cell contamination.
3. The supernatant is then discarded and the resulting pellet resuspended in 1–2 ml of DMEM and viable mononuclear cells (MNC) are enumerated using Trypan blue.
4. A total of 10^6 MNC per ml are plated in 10 ml of D10 medium on a 10 cm plate or equivalent, and incubated in a humidified incubator at 37 °C in 5 % CO_2 (*see* **Note 2**).
5. A change of D10 medium is performed on Day 3 to remove remaining red cells and at this point, emerging colonies of spindle-shaped cells should be noticeable.
6. CFU assessment of the plates can be made on Day 7 and a decision can be made to replate them when colonies are over 1 cm in diameter. Otherwise, the medium should be replaced every 3–4 days until replating becomes necessary at 50–70 % confluence.

3.1 Expansion of hfMSC

1. hfMSC should be replated when confluency reaches 70 % (*see* **Note 3**).
2. For replating, the growth medium is aspirated from the plate and washed twice with 1× PBS.

   1× Trypsin is added to cover the cells and the plates are returned to the incubator for 5 min at 37 °C.
3. The trypsinization reaction is quenched by the addition of 10 ml of D10 medium and the cells are transferred into a 15 ml or 50 ml centrifuge tube, and spun down at 400 × *g* for 5 min. The resulting pellet is resuspended in 1–5 ml of media and enumerated.
4. Replating of hfMSC is performed by seeding 2500 cells per cm^2 surface area. Media needs to be changed every 3–4 days (*see* **Note 3**).
5. For cryopreservation, after recovering the cell pellet, resuspend the cells at 10^6 per ml of freezing medium in cryovials before placement in a slow freezing container (Mr. Frosty, with isopropanol) for slow controlled freezing in a −20 °C freezer overnight. The cryovial is transferred to liquid nitrogen the following day.
6. For thawing, 1–2 ml cryovials are recovered from the liquid nitrogen storage and immersed into a 37 °C water bath until thawing is complete. With a pipette, the cells are added slowly to warm growth medium (1 ml of cryopreserved cells to 10 ml of warm D10 medium). This will then be spun down at 5000 × *g* for 5 min, the pellet is recovered, and cells are seeded at 2500 cells per cm^2 in plates or flasks.

3.2 Characterization of hfMSC

1. hfMSC grow as spindle-shaped plastic adherent cells; they express the markers: CD44, CD73, CD90, and CD105 and are negative for CD31 and CD45; thus they are nonendothelial and nonhemopoeitic. hfMSC are able to form clonal colonies when plated at low density in CFU-F assays, and differentiate into the standard mesenchymal lineages of bone, fat, and cartilage under permissive conditions as previously described.
2. CFU Capacity—hfMSC are plated at 100 cells in 10 ml of D10 medium in a 10 cm plate and the medium is replaced every 3–4 days. The plates are recovered for crystal violet staining after 10–14 days and the number of colonies containing more than 100 cells (>2 mm diameter) enumerated. Healthy low passage hfMSC have a CFU capacity of 40–70 % (40–70 colonies formed from 100 seeded cells).
3. Osteogenic Differentiation—hfMSC are seeded at 20,000 cells/cm^2 in osteogenic differentiation medium and the medium is changed every 3–4 days. Extracellular crystals can be seen from Day 3 of culture and staining for evidence of osteogenic differentiation can be undertaken after 7–10 days

of differentiation. Von Kossa staining with silver nitrate is performed by decanting the medium, washing two times with distilled water, and 2 % silver nitrate in distilled water is added to the culture plate; the plate is then exposed to bright sunlight or a 100 W incandescent bulb for 60 min. Mineralization is evidenced by black precipitates of silver phosphate at the end of this reaction as previously described [23].

4. Adipogenic Differentiation—hfMSC are seeded at 20,000 cells/cm^2 onto fibronectin-coated plates in adipogenic medium; the medium is changed every 3–4 days. Evidence of adipogenic differentiation can be seen after 2–4 weeks of adipogenic culture, with lipid laden adipocytes visualized under phase contrast microscopy. These lipid inclusion bodies will stain red with fresh Oil Red O as previously described [24].
5. Chondrogenic Differentiation—hfMSC are grown as a micromass pellet culture in a polypropylene tube in serum-free chondrogenic differentiation media over 3–4 weeks in this assay. 100,000 hfMSC are centrifuged at 400 × *g* for 5 min in a polypropylene tube to generate a pellet. The pellet is then covered with 1 ml of serum-free chondrogenic medium; the medium is changed twice a week for 4 weeks. At the end of differentiation, the pellet is formalin fixed and paraffin embedded, and sectioned for staining of anionic proteoglycans with Safranin O and toluidine blue stain [24]; the presence of Collagen I and II is determined through immunocytochemistry [25].

3.3 Production of Conditioned Medium from hfMSC

1. hfMSC from early passage numbers are cultured as described in Subheading 3.2. The same culture medium is used as a control (*see* **Note 4**).
2. After 48 h of incubation, transfer the medium to a 15 ml centrifuge tube.
3. The conditioned medium will then be centrifuged at 2500 × *g* for 10 min at 4 °C to ensure removal of cellular debris.
4. Transfer the conditioned medium to a new 15 ml centrifuge tube, paying attention not to aspirate the cellular debris at the bottom of the tube.
5. The conditioned medium can then be concentrated or immediately snap frozen and stored at −80 °C until further use.

3.3.1 Concentrated Conditioned Medium from hfMSC

1. Repeat **steps 1–5** as in Subheading 3.4.
2. Transfer the conditioned medium and the control medium to a filtration device Vivaspin 20 (*see* **Note 5**).
3. Centrifuge at 3000 × *g* for 30 min at 4 °C (*see* **Note 6**).
4. Recover the concentrate using a 200 µl pipette (*see* **Note 7**).
5. Aliquot the concentrated conditioned medium, snap-freeze in liquid nitrogen, and store at −80 °C until use.

3.4 Assay Conditioned Medium Effect on Tumor Cell Viability

1. Seed tumor cells in a 48-well dish (*see* **Note 8**).
2. Remove a small aliquot of the conditioned medium, approximately 15 μl for the standard Bradford protein assay measurement (*see* **Note 9**).
3. Rinse cells once with serum-free DMEM, add 2850 μg of total protein obtained from the conditioned medium per well. The volume of each well is kept at a maximum of 300 μl per well with serum-free DMEM.
4. Incubate tumor cells treated with conditioned medium for 48 h.
5. After 48 h, add 30 μl of cell counting solution -8 (CCK-8) to each well (*see* **Note 10**).
6. Incubate the plate for 1–4 h in the incubator.
7. Measure the absorbance at 450 nm using a microplate reader.

4 Notes

1. Fetal tissue collection was approved by the Domain Specific Review Board of National University Hospital, Singapore, in compliance with international guidelines regarding the use of fetal tissue for research.
2. For efficient cellular proliferation and CFU capability, batch-selected FBS is used.
3. Keep cells at a relatively undifferentiated state, as overconfluency can activate osteogenic programing of the cells.
4. The propagation of hfMSC and collection of conditioned medium can also be performed using serum-free culture medium. Culture medium with serum is used when animal studies are needed.
5. Vivaspin 20 handles up to 20 ml and is designed to fit into rotors that can accommodate Falcon 50 ml conical bottom tubes. Ensure that the tubes are balanced prior to centrifugation.
6. Adjust the centrifugation time accordingly to obtain a final 30-fold concentration.
7. Manually pipet the concentrated solute up and down twice to achieve a homogenous mixture.
8. Depending on the cell size, for Huh7.DsRed2 we seed 1.5×10^4 cells/48 wells.
9. Typical dilution for a 30-fold concentrated CM is 1:1000.
10. Be careful not to introduce bubbles into the wells, since they interfere with the O.D. reading.

Acknowledgements

Paula Lam is funded by the Singapore Ministry of Health's National Medical Research Council (NMRC/1201/2009) and the Singapore Stem Cell Consortium (SSCC/08/013). Jerry Chan received salary support from the National Medical Research Council, Singapore (NMRC/CSA/043/2012).

References

1. Friedenstein AJ, Chailakhjan RK, Lalykina KS (1970) The development of fibroblast colonies in monolayer cultures of guinea-pig bone marrow and spleen cells. Cell Tissue Kinet 3:393–403
2. van den Berk LC, Jansen BJ, Siebers-Vermeulen KG et al (2011) The tissue origin and culture history of mesenchymal stem cells affect their performance in osteoblastic differentiation. Tissue Eng Regen Med 8:96–105
3. Dominici M, Le Blanc K, Mueller I et al (2006) Minimal criteria for defining multipotent mesenchymal stromal cells. Cytotherapy 8:315–317
4. Guillot PV, Gotherstrom C, Chan J et al (2007) Human first-trimester fetal MSC express pluripotency markers and grow faster and have longer telomeres than adult MSc. Stem Cells 25:646–654
5. Gotherstrom C, West A, Liden J et al (2005) Difference in gene expression between human fetal liver and adult bone marrow mesenchymal stem cells. Haematologica 90:1017–1026
6. Zhang ZY, Teoh SH, Hui JH et al (2012) The potential of human fetal mesenchymal stem cells for off-the-shelf bone tissue engineering application. Biomaterials 33:2656–2672
7. Kim N, Cho SG (2013) Clinical applications of mesenchymal stem cells. Korean J Intern Med 28:387–402
8. Gotherstrom C, Westgren M, Shaw SW et al (2014) Pre and postnatal transplantation of fetal mesenchymal stem cells in osteogenesis imperfecta: a two-center experience. Stem Cells Transl Med 3:255–264
9. Klopp AH, Gupta A, Spaeth E et al (2011) Concise review: dissecting a discrepancy in the literature: do mesenchymal stem cells support or suppress tumor growth? Stem Cells 29: 11–19
10. Galderisi U, Giordano A (2014) The gap between the physiological and therapeutic roles of mesenchymal stem cells. Med Res Rev 34:1100–1126
11. Sze SK, de Kleijn DP, Lai RC et al (2007) Elucidating the secretion proteome of human embryonic stem cell-derived mesenchymal stem cells. Mol Cell Proteomics 6:1680–1689
12. Katsuda T, Kosaka N, Takeshita F, Ochiya T (2013) The therapeutic potential of mesenchymal stem cell-derived extracellular vesicles. Proteomics 13:1637–1653
13. Khakoo AY, Pati S, Anderson SA et al (2006) Human mesenchymal stem cells exert potent antitumorigenic effects in a model of Kaposi's sarcoma. J Exp Med 203:1235–1247
14. Qiao L, Xu ZL, Zhao TJ et al (2008) Dkk-1 secreted by mesenchymal stem cells inhibits growth of breast cancer cells via depression of Wnt signalling. Cancer Lett 269:67–77
15. Zhu Y, Sun Z, Han Q et al (2009) Human mesenchymal stem cells inhibit cancer cell proliferation by secreting DKK-1. Leukemia 23:925–933
16. Hou L, Wang X, Zhou Y et al (2014) Inhibitory effect and mechanism of mesenchymal stem cells on liver cancer cells. Tumour Biol 35:1239–1250
17. Ho IA, Toh HC, Ng WH et al (2013) Human bone marrow-derived mesenchymal stem cells suppress human glioma growth through inhibition of angiogenesis. Stem Cells 31:146–155
18. Yang C, Lei D, Ouyang W et al (2014) Conditioned media from human adipose tissue-derived mesenchymal stem cells and umbilical cord-derived mesenchymal stem cells efficiently induced the apoptosis and differentiation in human glioma cell lines in vitro. Biomed Res Int 2014:109389
19. Zhang T, Lee YW, Rui YF et al (2013) Bone marrow-derived mesenchymal stem cells promote growth and angiogenesis of breast and prostate tumors. Stem Cell Res Ther 4:70
20. Zhu W, Huang L, Li Y et al (2011) Mesenchymal stem cell-secreted soluble signaling molecules potentiate tumor growth. Cell Cycle 10:3198–3207

21. Suzuki K, Sun R, Origuchi M et al (2011) Mesenchymal stromal cells promote tumor growth through the enhancement of neovascularization. Mol Med 17:579–587
22. Raida M, Heymann AC, Günther C (2006) Role of bone morphogenetic protein 2 in the crosstalk between endothelial progenitor cells and mesenchymal stem cells. Int J Mol Med 18:735–739
23. Zhang ZY, Teoh SH, Chong MS et al (2009) Superior osteogenic capacity for bone tissue engineering of fetal compared to perinatal and adult mesenchymal stem cells. Stem Cells 27:126–137
24. Lee ES, Chan J, Shuter B et al (2009) Microgel iron oxide nanoparticles for tracking human fetal mesenchymal stem cells through magnetic resonance imaging. Stem Cells 27:1921–1931
25. Li CH, Chik TK, Ngan AH et al (2011) Correlation between compositional and mechanical properties of human mesenchymal stem cell-collagen microspheres during chondrogenic differentiation. Tissue Eng Part A 17:777–788

Chapter 29

Isolation and Characterization of Exosome from Human Embryonic Stem Cell-Derived C-Myc-Immortalized Mesenchymal Stem Cells

Ruenn Chai Lai, Ronne Wee Yeh Yeo, Jayanthi Padmanabhan, Andre Choo, Dominique P.V. de Kleijn, and Sai Kiang Lim

Abstract

Mesenchymal stem cells (MSC) are currently the cell type of choice in many cell therapy trials. The number of therapeutic applications for MSCs registered as product IND submissions with the FDA and initiation of registered clinical trials has increased substantially in recent years, in particular between 2006 and 2012. However, defined mechanisms of action underpinning the therapeutic efficacy of MSCs are lacking, but they are increasingly attributed to MSC trophic secretion rather than their differentiation potential. A promising secreted therapeutic candidate is an extracellular vesicle (EV) known as the exosome. The use of exosomes instead of cells as a therapeutic agent provides several advantages. A critical advantage is the prospect of a conventional pharmaceutical manufacturing process that is highly scalable and amenable to the stringent manufacturing process. For example, MSCs used as producers of therapeutics, and not as therapeutics per se, could be immortalized to generate infinitely expansible clonal lines to enhance the reproducible production of therapeutic exosomes. In this chapter, we will describe the immortalization of MSCs, and the production, isolation, and characterization of exosomes from immortalized MSC.

Key words Mesenchymal stem cells, Immortalization, Exosome

1 Introduction

Mesenchymal stem cells (MSCs) are currently the most used cell type in the field of cell therapy. Between 2006 and 2012, there was a threefold increase in MSC-based product FDA IND submissions [1]. There were also 246 MSC-based clinical trials registered in this same period. These cells are being tested for a wide range of clinical indications with the most common ones being cardiovascular and neurological diseases. Despite the intensive clinical testing of MSCs, the mechanism of action responsible for their therapeutic efficacy remains nebulous. The initial rationale was based on the differentiation potential of MSCs and has become increasingly redundant, particularly in light of new insights from clinical and

Massimiliano Gnecchi (ed.), *Mesenchymal Stem Cells: Methods and Protocols*, Methods in Molecular Biology, vol. 1416,
DOI 10.1007/978-1-4939-3584-0_29,

animal studies [2]. Recent demonstrations that MSCs elicit their therapeutic effects through secreted factors have radically revolutionized the field [3–12].

Paracrine secretion by MSCs was first described almost two decades ago when Haynesworth et al. [13] reported that MSCs synthesize and secrete a broad spectrum of growth factors, chemokines and cytokines, that exert significant effects on cells in their vicinity. This was followed by numerous reports that these secreted factors enhance arteriogenesis [14], protect against ischemic renal and limb tissue injury [15], promote neovascularization [16], and increase angiogenesis [17, 18]. Gnecchi et al. demonstrated that intramyocardial injection of culture medium conditioned by MSCs overexpressing the Akt gene reduced infarct size in a rodent model of AMI to the same extent as the Akt-MSC cells themselves [3]. Our group subsequently demonstrated that human embryonic stem cell-derived MSCs (hESC-MSC) secrete more than 200 unique gene products [19] into the culture medium and this conditioned culture medium reduces reperfusion injury in a pig model of myocardial ischemia/reperfusion [6]. Fractionation studies of the conditioned medium led to the identification of exosomes as the active therapeutic agent in the MSC secretome [7]. Since then MSC exosomes have been implicated in the therapeutic efficacy of MSCs against graft-versus-host disease [20, 21], cerebral ischemia [22], liver fibrosis [23], hypoxic pulmonary hypertension [24], acute kidney injury [25], and acute liver injury [26].

The exosome is an extracellular vesicle with a diameter of 50–100 nm, which can be differentiated from other extracellular vesicles through several biophysical and biochemical parameters, e.g., flotation density of 1.1–1.19 g/mL, the presence of tetraspanin proteins, Alix, and TSG101 as summarized by Thery et al. [27]. Exosomes were first reported to be secreted by sheep reticulocytes in 1983 as a means to discard unwanted protein [28]. Exosomes are now known to be secreted by many cell types and to exert a wide spectrum of functional activities that have been implicated in both therapeutic and pathological processes [2]. The discovery that the cardioprotective activity of MSCs was mediated by exosomes introduced a new perspective to current MSC stem cell-based therapies, and engenders novel approaches in the development of cell-free tissue repair.

Exosome-based therapy offers tremendous advantages over cell-based therapy. It is nonviable; therefore it is safer, easier to store, transport, and administer (*see review* [2]). However, MSCs have limited expansion capability. In the long term, large-scale production of MSC exosomes could be sustained only by constant replenishment with new sources of MSCs either from new donors or, in the case of hES-MSC, repeated derivation from hESC. Such replenishment is not only costly as each new source will have to be

tested and validated, but also the batch quality and reproducibility of the exosome production could also be compromised.

We had previously proposed MYC immortalization of hESC-MSC to generate infinitely expansible clonal cell lines for exosome production as a means to overcome the obstacle of limited cell supply [29]. This approach virtually ensures that MSC exosomes will be generated from the same MSC source and therefore, minimize batch-to-batch variation. Here we provide detailed protocols on how to immortalize MSCs, produce, purify, and characterize their exosomes, thus enabling researchers to produce sufficient MSC exosomes to evaluate their therapeutic efficacy.

2 Materials

2.1 Generation of Lentivirus Particles Carrying MYC

1. DMEM High Glucose.
2. OPTI-MEM I.
3. Sodium pyruvate.
4. MEM Non-essential amino acids (MEM NEAA).
5. Penicillin-Streptomycin-Glutamine (PSG).
6. Fetal bovine serum, ESC qualified (FBS).
7. Phosphate buffered saline, pH 7.4 (PBS).
8. Trypsin, 0.05 % EDTA.
9. Lipofectamine.
10. 0.1 % Gelatin in water.
11. HEK293T cells.
12. Plasmids: pMDLg/pRRE, pCMV-VSV-G, pRSV-Rev, pLVX-MYC-puro.
13. Amicon Ultra Centrifugal Filters Ultracel 100 K.
14. Corning T175 flasks.
15. 0.45 μm Minisart Syringe Filter.
16. 50 mL Precise Syringe.

2.2 MYC Immortalization of Human Embryonic Stem Cell-Derived Mesenchymal Stem Cells

1. DMEM High Glucose.
2. Sodium pyruvate.
3. MEM Non-essential amino acids (MEM NEAA).
4. Penicillin-Streptomycin-Glutamine (PSG).
5. Fetal bovine serum, ESC qualified (FBS).
6. Phosphate buffered saline, pH 7.4 (PBS).
7. Trypsin, 0.05 % EDTA.
8. Hexadimethrine bromide (Polybrene).

9. Puromycin dihydrochloride.
10. 0.1 % Gelatin in water.
11. Dimethyl sulfoxide (DMSO).
12. HuES9.E1 cells.
13. *MYC* lentivirus particles.
14. Corning T25, T75, 175 flasks.
15. 6, 12, 48 Well Cell Culture Cluster.
16. Pyrex cloning cylinder.

2.3 Mesenchymal Stem Cell Expansion

1. hES-MSC Medium: DMEM supplemented with 10 % FBS, 1× PSG, 1 mM sodium pyruvate, 1× MEM NEAA.
2. Dulbecco's Phosphate Buffered Saline without Calcium and Magnesium Chloride (PBS-).
3. Serum-Free Medium: DMEM without phenol red supplemented with 1× insulin, transferrin, and selenium (ITS-X), 5 ng/mL FGF2, 5 ng/mL PDGFAB, and 1× β-mercaptoethanol, 1× NEAA, 1× l Glutamine, 1 mM Sodium pyruvate.
4. Virus collection medium: DMEM supplemented with 1 % FBS, 1× PSG, 1 mM sodium pyruvate, 1× MEM NEAA.
5. Trypsin, 0.05 % EDTA.
6. 0.1 % Gelatin in Water.
7. Cell Stack.

2.4 HPLC Isolation of Mesenchymal Stem Cell Exosome

1. 1× Phosphate buffered saline (PBS) for tangential flow filtration (TFF): 137 mM sodium chloride, 2.7 mM potassium chloride, 1.8 mM potassium phosphate monobasic, 10 mM disodium hydrogen phosphate, pH 7.4.
2. Size exclusion chromatography (SEC) buffer preparation:
   (a) Measure 5.52 g sodium dihydrogen phosphate (Mr = 137.99) and 11.94 g sodium chloride (Mr = 58.44) separately into a weighing boat.
   (b) Transfer and dissolve all salts into a 2000 mL volumetric flask containing ~1900 mL ultrapure water. Mix well.
   (c) Adjust the pH to 7.2 using ~7 mL of 4 M NaOH and top up to the final volume of 2000 mL using ultrapure water.
   (d) Remove particulate matter by vacuum filtration through a 0.1 μm 47 mm PESU membrane filter (Sartorius) into a clean, labeled 2000 mL glass bottle.
   (e) Degas the buffer in a sonicator for 5 min.
3. Sartoflow Slice 200 Benchtop crossflow filtration system.
4. ÄKTA explorer 100 system with UNICORN software.
5. Shimadzu HPLC system with Class VP and ASTRA V (for Light Scattering Detector) software.

6. Multi-Angle Light Scattering (MALS) Detector.
7. Quasi Elastic Light Scattering (QELS) Detector.
8. Refractive Index (RI) Detector.
9. ≥99.5 % Sodium chloride.
10. >99 % Sodium dihydrogen phosphate.
11. ≥98 % Sodium hydroxide.
12. ≥99% Disodium hydrogen phosphate.
13. Ultrapure water (18.2 MΩ).
14. ≥99.5% Potassium chloride.
15. ≥99.5 % Potassium phosphate monobasic.
16. Custom Size Exclusion Chromatography Column (TSKgel G3000SW; 13 μm, 600 mm × 7.5 mm, Tosoh).
17. HPLC Size Exclusion Chromatography Column (TSKgel G3000SWxl; 5 μm, 300 mm × 7.8 mm, Tosoh).
18. PESU membrane filter; 0.1 μm.
19. Minisart® NML Syringe Filters; 0.2 μm.
20. Vivaspin 20; 30,000 kDa MWCO PES.
21. Hydrosart® ultrafiltration membrane; 100 kDa MWCO, 0.1 m^2.

2.5 Exosome Protein Quantification

1. 96 Well flat bottom transparent microplate.
2. Bio-rad Protein Assay Kit.

2.6 Sucrose Density Gradient Assay

1. 1 M Tris–HCl, pH 7.4.
2. Sucrose.
3. 4 mL ultracentrifuge tube.
4. SW60Ti rotor.

2.7 NanoSight

1. NanoSight LM10.
2. NanoSight syringe pump.
3. NTA 2.3 analytical software.
4. 0.22 μm syringe filter.

3 Methods

3.1 Generation of Lentivirus Particles Carrying MYC

3.1.1 Lentivirus Production

1. Coat the entire surface of a T175 flask with 5 mL of gelatin for 20 min at room temperature (RT) and aspirate to dryness.
2. *Day 1*: Seed 1.2×10^7 HEK293T cells in the coated T175 flask with 35 mL hES-MSC medium. Incubate at 37 °C, 5 % CO_2 overnight.
3. *Day 2*: Prepare two tubes of OPTI-MEM I, 8 mL per tube

Label tube 1 as "Plasmids" and add the following and vortex mix.

(a) pMDLg/pRRE 27 μg.

(b) pCMV-VSV-G 9 μg.

(c) pRSV-Rev 9 μg.

(d) pLVX-MYC-puro 27 μg.

Label tube 2 as "Lipofectamine" and add 108 μL lipofectamine, invert gently, and incubate the mixture at RT for 5 min.

4. Add tube 1 to tube 2, invert gently. Incubate at RT for 20 min.
5. Flask seeded with HEK293T cells should be 80–90 % confluent. Remove spent medium and wash cells twice with PBS.
6. Add the contents of the combined tubes 1 and 2 gently onto the cells, pour evenly across entire flask surface. Incubate the flask at 37 °C, 5 % CO_2 for 6 h.
7. Remove transfection medium, replace with 24 mL virus collection medium. Run medium down the walls of the dish slowly to prevent cells from dislodging.
8. *Days 4 and 5* (*see* **Note 1**): 48 h after transfection, collect the first harvest of 24 mL virus-rich medium. Replace with fresh 24 mL virus collection medium.
9. Centrifuge virus-rich medium at 300×*g* for 10 min at 4 °C, filter supernatant through a 0.45 μm syringe filter. Store at 4 °C.
10. 72 h after transfection, collect the second harvest of 24 mL virus-rich medium.
11. Centrifuge virus-rich medium at 300×*g* for 10 min at 4 °C, filter supernatant through a 0.45 μm syringe filter. Combine both harvests to obtain 48 mL of virus-rich medium.
12. Prewet 100 kDa Amicon Ultra Centrifugal Filters by adding 10 mL PBS and centrifuge at 4000×*g* for 1 min.
13. Remove filtrate, load filter with 10 mL virus-rich medium, centrifuge at 4000×*g* for 15 min. Repeat this process until the 48 mL of medium is reduced to 600 μL.
14. Split virus concentrate into 60 μL aliquots. Use immediately for infection or store at −80 °C.
15. Determine virus concentration using the Lenti-X™ qRT-PCR Titration Kit according to the manufacturer's instructions. Viral titer should be at least 10^{11} copies per mL.

3.1.2 MYC Immortalization of hES-MSC

1. *Day 1* Target cell infection:

(a) Coat the surface of a 6-well plate with gelatin for 20 min at RT, aspirate and allow to dry.

(b) Seed HuES9.E1 cells at 2.5×10^5 cells per well in hES-MSC medium, incubate at 37 °C, 5 % CO_2.

2. *Day 2:*

(a) 24 h after seeding HuES9.E1 cells, wells should be 70–80 % confluent.

(b) If using a frozen virus aliquot, remove a vial of virus from −80 °C and thaw on ice. Calculate the volume of virus concentrate required to infect HuES9.E1 cells at an MOI of 5. Add this to 1.5 mL of hES-MSC medium.

(c) To this, add 1.5 μL of polybrene (4 mg/mL in water) and mix by pipetting (*see* **Note 2**).

(d) Remove spent medium from HuES9.E1 cells, add virus-containing medium drop by drop distributing the medium evenly over the cell culture.

(e) Use one well of cells as an uninfected control. Replace the medium with 1.5 mL of fresh medium containing 1.5 μL of polybrene.

(f) Incubate at 37 °C, 5 % CO_2 overnight.

3. *Day 3*: Transfer cells from each of the wells into T75 flasks. Incubate in fresh hES-MSC medium at 37 °C, 5 % CO_2 for 24 h.

4. Antibiotic selection and population expansion.

5. Prepare selection medium by diluting 10 mg/mL puromycin in hES-MSC medium to obtain 1 μg/mL concentration.

6. Replace spent medium with selection medium for both infected and uninfected cells.

7. Change selection medium once every 2 days until complete cell death is observed with the uninfected cells.

8. Puromycin-resistant MYC-transfected HuES9.E1 cells (E1MYC) should be observable after 3–4 days of selection. Replace selection medium with fresh medium.

9. Expand the population from a T75 flask to a T175 flask. Freeze cells in freezing medium (10 % DMSO, 20 % FBS, and 70 % hES-MSC) at −80 °C overnight. Transfer cells to −150 °C thereafter.

3.1.3 Clonal Selection

1. Seed 10^4 cells in a gelatin-coated T175 flask.

2. Once visible, round, colonies have formed, isolate colonies by trypsinization in cloning cylinders. Transfer each colony to a single well in a 48-well plate.

3. Expand colonies from a 12-well to 48-well plate, to T25 and finally to T175 flasks. Label cells as P1 and freeze cells as per (Subheading 3.1.2, **step 9** above).

3.2 Passaging hES-MSCs

1. Upon reaching 80 % confluence, passage E1MYCs at 1:3 or 1:4 split ratio (*see* **Note 3**).
2. Aspirate spent medium from T175 flask and rinse cells with 10 mL PBS (−).
3. Aspirate PBS (−), add 3.0 mL Trypsin per T175 flask, and rotate flask gently to ensure liquid covers the entire cell surface.
4. Return flask to the incubator, for 3–5 min.
5. Remove flask and gently tap sides to dislodge cells.
6. Add 6–7 mL of hES-MSC media to neutralize Trypsin, and gently wash the sides of the flask.
7. Transfer cell suspension into 15 mL tube. Wash flask again with 3–5 mL media.
8. Pool cell suspension, and centrifuge at 800 × *g* for 5 min.
9. Aspirate supernatant, resuspend pellet in 4 mL hES-MSC media and then transfer to a new T175 flask with 30 mL fresh hES-MSC media.
10. Replace spent medium with fresh medium every 2 days.
11. It is always recommended to maintain E1MYC between 25 and 80 % confluence or ~15–50,000 cells per cm^2.

3.3 Expansion of E1MYC Using a Cell Stack

1. Start this procedure with ten T175 flasks of 90–100 % confluent E1MYC.
2. Gelatinize the cell stack (500 mL gelatin/stack) for 30 min.
3. Warm hES-MSC medium and Trypsin in a water bath for at least 20 min.
4. Aspirate spent medium from flask and wash once with 10 mL PBS (−).
5. Aspirate PBS (−), add 3.0 mL Trypsin per T175 flask, and rotate flask gently to ensure liquid covers the entire cell surface.
6. Return flasks to the incubator for 3–5 min.
7. Remove flasks and gently tap sides to dislodge cells.
8. Add 6–7 mL of media to neutralize Trypsin and gently wash the sides of the flask.
9. Transfer cell suspension into a 15 mL tube. Wash flask again with 3–5 mL of medium.
10. Pool cell suspension and centrifuge at 800 × *g* for 5 min.
11. Aspirate the supernatant and resuspend the pellet in 4 mL hES-MSC medium.
12. Pool pellets (from 10× T175 cm^2 flasks) into 50 mL hES-MSC medium and then transfer to 1 L growth medium.

13. Pour out gelatin from cell stack.
14. Add 1 L medium with cells into the cell stack. Distribute evenly.
15. Transfer the cell stack to 37 °C incubator and check for adherence 24 h later.

3.4 Conditioning of E1MYC

1. Start this procedure when E1MYC are 80 % confluent in a cell stack.
2. Pour out spent medium and wash once with 500 mL PBS (+) per cell stack.
3. Add 1 L serum-free medium (*see* Subheading 2.3, **item 3**) per stack.
4. 24 h later, pour out medium and wash once with 500 mL PBS (+).
5. Add 1 L serum-free medium per cell stack.
6. Return the cell stack to incubator for 72 h.
7. Carefully pour out conditioned medium into a sterile bottle.
8. Pass through a 0.22 μm filter before further processing.

3.5 HPLC Purification of Mesenchymal Stem Cell Exosomes

3.5.1 Tangential Flow Filtration

1. Clamp the ultrafiltration membrane to the holding device at a torque of 20 Nm as per the manufacturer's recommendations.
2. Connect the above assembly to a peristaltic pump, pressure sensors at the feed, attach retentate and filtrate streams to the corresponding tubing.
3. Flush the cassette with warm 1 M sodium hydroxide for 30 min at a crossflow rate of 8 L/(min m^2) with both the retentate and filtrate valves fully open to sanitize it.
4. Measure the clean water flux of the sanitized cassette as a reference for the performance of a clean cassette. At a transmembrane pressure (TMP) of 0.8 bar, the filtrate flux is 4 L/(min m^2).
5. Flush the cassette with 1× PBS to equilibrate the pH of the cassette. Equilibration is complete when the filtrate measures pH 7.4.
6. Perform ultrafiltration of the exosome-containing conditioned medium at TMP = 0.8–1.0 bar, with a filtrate flux of 2–1.5 L/(min m^2). Reduce sample volume from 5000 mL to around 100 mL including dead volume.
7. If desired, change the retentate to 1× PBS with 5–10× volume.
8. Pour out the retentate in the reservoir and drain it from the tubing and cassette into a clean bottle.

9. Flush the cassette with 1× PBS to remove the majority of the proteins in the tubing and cassette.
10. Next, flush the cassette with warm (50 °C) 1 M sodium hydroxide for 1 h, according to the manufacturer's recommendations. Fully open both retentate and filtrate valves.
11. Measure the clean water flux again at TMP = 0.8 bar. The cassette is considered clean if the measured clean water flux is between 70 and 110 % of that measured in **step 4**. The cassette may still be dirty and require further cleaning if the clean water flux is less than that before use, or its integrity may be compromised if the clean water flux exceeds that before use.
12. Disassemble the filter assembly and store the cassette in 0.1 M sodium hydroxide. Wash the holding device with water. Wash the tubing and reservoir with soapy water.

3.5.2 Size Exclusion Chromatography and Concentration

1. Connect the custom Size Exclusion Column to the AKTA Explorer.
2. Prime the AKTA Explorer using SEC buffer and then equilibrate the column for 30 min at a flow rate of 4 mL/min.
3. Connect one outlet to a GE Fraction Collector Frac-950 for collecting the purified sample at 4 °C.
4. Using a 3 mL syringe, inject 1.5 mL of sample into the sample loop.
5. The program used for size exclusion chromatography can be found in Appendix. Table 1 summarizes the ATKA run conditions.
6. The first peak, P1, at the detection wavelength of UV 280 nm will correspond to the purified exosome (*see* Fig. 1).
7. Using the fraction collector, collect P1 in 0.5 mL fractions.
8. Pool these fractions into one tube. Mix well.
9. Use a Vivaspin 20 to concentrate the pool by 20×.

Table 1
AKTA run conditions

Column	TSKgel G3000SW (13 μm), 600 mm × 7.5 mm
Column temperature	25 °C
Fraction collector temperature	4 °C
Flow rate	1 mL/min
Injection volume	1.5 mL
Fraction volume	0.5 mL
Run time	50 min

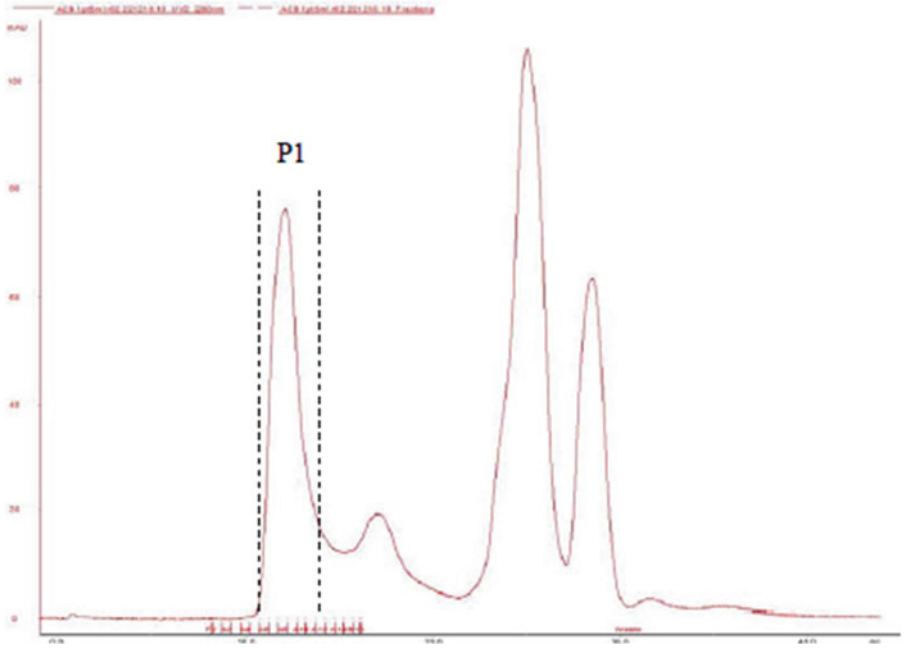

Fig. 1 Typical AKTA chromatogram of exosome purification

3.5.3 Analysis of Purified Exosomes

1. Connect the HPLC Size Exclusion Column to the Shimadzu HPLC.
2. Prime the HPLC using SEC buffer and then equilibrate the column for 30 min at a flow rate of 0.5 mL/min.
3. Inject 20 μL of 20× concentrated and purified exosomes into the column.
4. Follow Table 2 for HPLC run conditions: The elution time for exosomes is ~12 min at the detection wavelength of UV 220 nm (*see* Fig. 2).
5. Upon completion of the run, ASTRA V software is used to determine the hydrodynamic radius, Rh, of the purified exosomes. The Rh of exosomes normally ranges between 50 and 60 nm.

3.6 Exosome Protein Quantification

3.6.1 BSA Standard Preparation

1. Prepare 32 μg/mL BSA standard by adding 8 μL 2 mg/mL BSA to 492 μL distilled water in a 1.5 mL microcentrifuge tube.
2. Serially dilute 220 μL of 32 μg/mL BSA with 220 μL distilled water to generate 16, 8, 4, and 2 μg/mL BSA standards in 1.5 mL microcentrifuge tubes.
3. Aliquot 220 μL distilled water in a 1.5 mL microcentrifuge tube as the blank control.

Table 2
HPLC run conditions

Column	TSKgel G3000SWxl 300 mm × 7.8 mm
Column temperature	25 °C
Flow rate	0.5 mL/min
Injection volume	20 μL
Run time	40 min
No. of replicate injections	2
No. of blank runs as negative control between samples	1

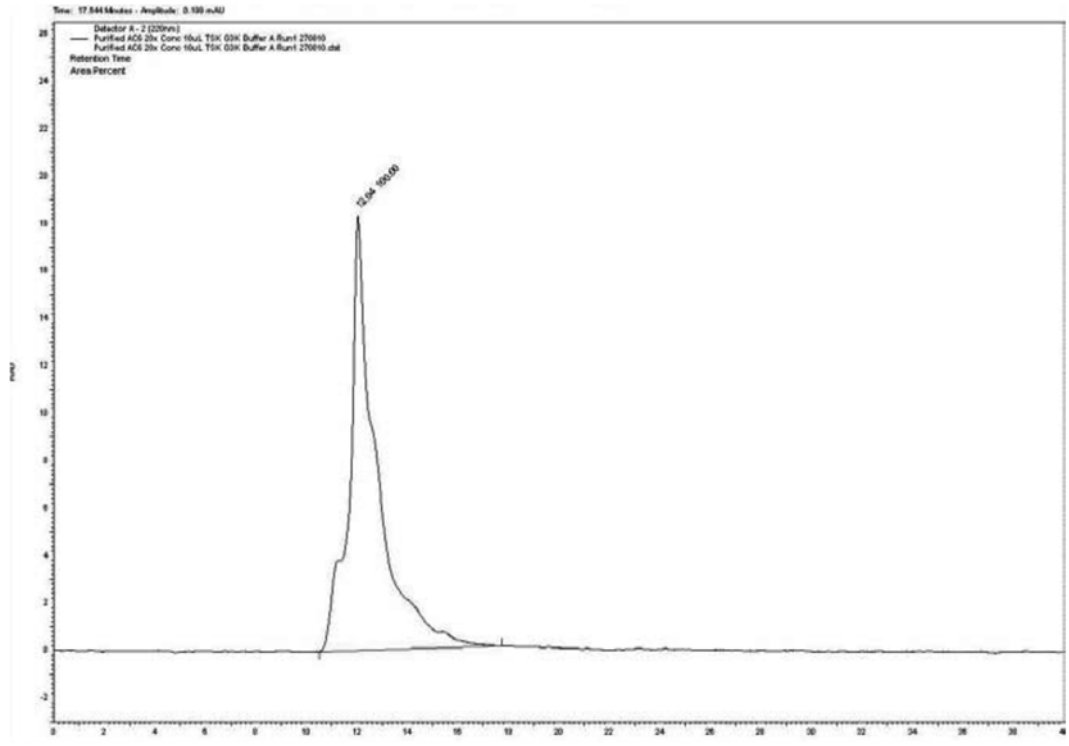

Fig. 2 Typical HPLC chromatogram of purified exosomes

4. Transfer 200 μL of standards and blank control to a 96 well flat bottom transparent microplate.

3.6.2 Sample Preparation

1. Dilute exosome sample 10× by adding 20 μL exosome to 180 μL distilled water.

2. Add 10, 20, 30 μL of the diluted exosome sample to 96 well flat bottom transparent microplate. Add distilled water to a final volume of 200 μL for each well. Prepare each well of the diluted exosome sample in triplicate.

3.6.3 Absorbance Measurement

1. Add 50 μL 1× dye reagent to each well. Mix well.
2. Measure absorbance of each well at 595 nm using a microplate reader.

3.6.4 Protein Concentration Calculation

1. Subtract the absorbance value of the blank from that of each standard and sample. The net absorbance of each standard is plotted against its known protein concentration to generate a standard curve. Set the X- and Y-axis intercept to 0 and plot the best-fit linear graph. The linear regression coefficient, r^2, must be >0.95. Otherwise, the assay should be repeated.
2. Calculate the sample protein concentration (x) by the following equation:

$$x = \frac{v \times d}{m}$$

where v is the net absorbance value, d is the dilution factor (if 10 μL of diluted exosomes was used, the dilution factor is $200/1 = 200$), and m is the slope of the standard curve.

3.7 Sucrose Density Gradient Assay

1. Prepare 50 mL of 20 mM Tris–HCl, pH 7.4 by diluting 1 mL of 1 M Tris–HCl, pH 7.4–50 mL with distilled water.
2. Weigh 2 g of sucrose and put in a 15 mL tube labeled as Tube A and 6 g of sucrose into a 15 mL tube labeled as Tube B.
3. Dissolve the sucrose in Tube A and Tube B with 7 mL of 20 mM Tris–HCl, pH 7.4 before slowly topping to 10 mL with the same buffer (*see* **Note 4**).
4. Filter the sucrose solutions using a 0.22 μm syringe filter.
5. Aliquot sucrose solution from Tube A and Tube B into each of 14 labeled 1.5 mL microcentrifuge tubes as shown in Table 3.
6. Vortex each of the 14 labeled 1.5 mL microcentrifuge tubes to mix the two sucrose solutions.
7. Prepare the sucrose gradient in a 4 mL ultracentrifuge tube by first loading 0.45 mL sucrose solution from tube 1 before layering 0.25 mL sequentially from tubes 2–14. Repeat to prepare a second sucrose density gradient (*see* **Note 5**).
8. Load 0.5 mL exosome sample on top of the gradient. Sample can be diluted with 20 mM Tris–HCl, pH 7.4 if the volume is less than 0.5 mL.
9. Carefully load the ultracentrifuge tube in a SW60 Ti rotor.

Table 3
Preparation of sucrose solution

Label	Tube A (mL)	Tube B (mL)
1	1	0.00
2	0.93	0.07
3	0.86	0.14
4	0.79	0.21
5	0.72	0.28
6	0.65	0.35
7	0.57	0.43
8	0.5	0.5
9	0.43	0.57
10	0.36	0.64
11	0.29	0.71
12	0.22	0.78
13	0.15	0.85
14	0.07	0.93

10. Spin overnight (≥16.5 h) 200,000 × *g* at 4 °C using slow acceleration. Deceleration should be slow or preferably without the brake.
11. After ultracentrifugation, carefully take out the ultracentrifuge tube from the rotor.
12. Carefully pipette 320 μL from the top of the ultracentrifuge tube into preweighed 1.5 mL Eppendorf tubes to collect 13 fractions (*see* **Note 6**).
13. Weigh each tube. After subtracting the weight of the tube, the density of each fraction is calculated using the following equation:

$$\text{density} = \frac{\text{mass}}{\text{volume}}$$

14. Take an identical aliquot volume from each of the 13 tubes containing the sucrose gradient. Detect the presence of exosomes markers (e.g., CD9) in each fraction by western blot hybridization. The density ranges of the sucrose where

exosome markers are detected represent the density range of the exosomes.

15. Figure 3 gives an overview of the whole assay.

3.8 Nanosight

1. Calibrate the NanoSight LM10 using 100 nm polystyrene beads as per the manufacturer's instruction before measuring the size distribution of the exosome sample.
2. Dilute the purified exosome to a particle number concentration of between 10^8 and 10^9 particles per mL (*see* **Note 7**).
3. Open the NTA 2.3 Analytical Software, navigate to the capture screen, select basic mode, and set the camera level to 10.
4. Aspirate the diluted exosome with a 1 mL syringe and slowly inject the sample into the viewing unit device (*see* **Note 8**).
5. Hold the syringe in place by loading it into the syringe holder of the NanoSight Syringe Pump.
6. Set the infusion rate to 1000, click "load," after 10 s change the infusion rate to 20.
7. Using the script control function, set 3× 60 s recording time and click "run."

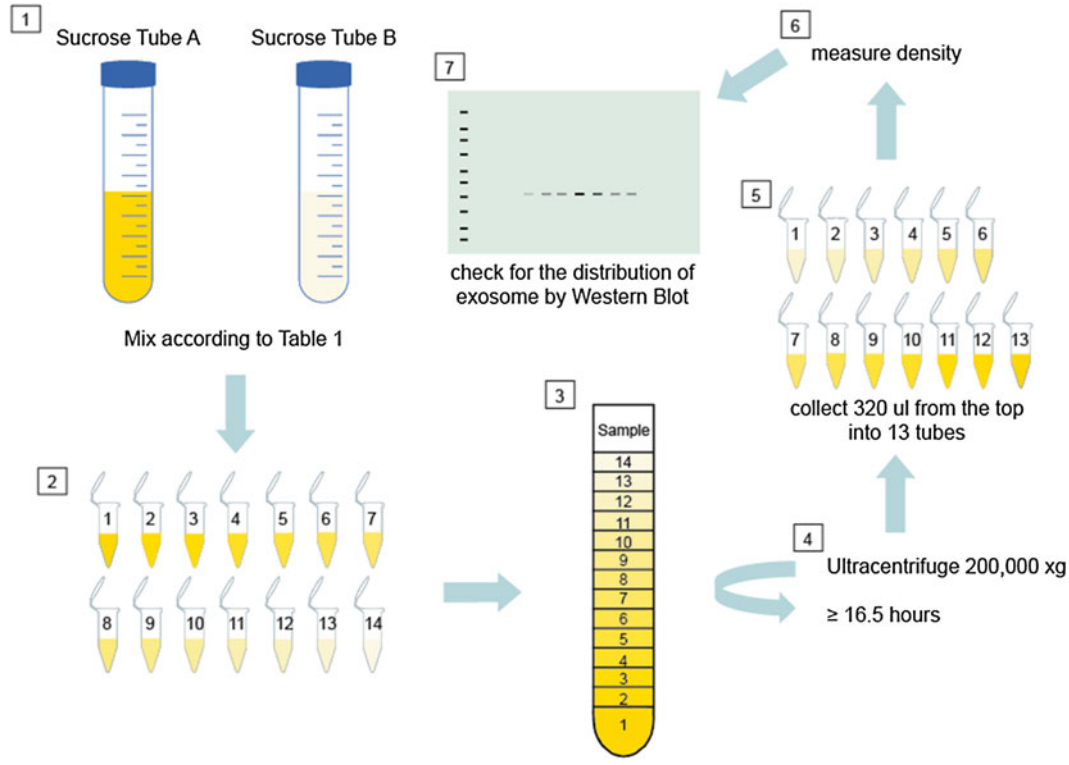

Fig. 3 Flow chart of the sucrose density gradient assay

8. Make sure that 20–100 particles can be seen in the field of view; if not, dilute or concentrate the sample accordingly.
9. After the recording, analyze the recording according to the user's manual to estimate the size distribution.

4 Notes

1. When handling live virus, wear proper personal protective equipment and soak all used disposable culture ware, tubes, serological pipettes in bleach solution for at least one hour before disposing as per regular biological waste.
2. This virus-containing medium is enough for 1 well (in a 6 well plate) only. Prepare more according to the user's needs.
3. It is recommended to always maintain hESC-derived MSCs between 25 and 80 % confluency or ~15–50,000 cells per cm^2. Upon reaching 80 % confluence, it is recommended to passage hES-MSCs at a 1:3 or 1:4 split ratio.
4. It takes about 10 min to fully dissolve the sucrose.
5. Cut 5 mm off the pipette tip before using it. After loading each layer of sucrose gradient, the interface between the layers should be visible.
6. Cut 5 mm off the pipette tip before using it. Aspirate the sample slowly and steadily.
7. 1000–10,000× dilution with PBS will be sufficient to achieve the concentration.
8. Care should be taken to avoid the introduction of bubbles at this stage.

Acknowledgments

This work was supported by funding from A*STAR. We thank members of our laboratories for their contribution to this work.

5 Appendix: Purification Method

Main method:

¤ (Main)
0.00 Base CV (26.5)#Column_volume [31] Any
0.00 Flow 1 {mL/min}
0.00 Watch_Pressure Greater_Than 2.9 [32] PAUSE
0.00 BufferValveA1 A12
0.00 ColumnPosition Position3

0.00 Alarm_Pressure Enabled 2.9 [32] 0.00 [32]
0.00 Wavelength 220 {nm} 280 {nm} 260 {nm}
¤ 0.00 Block Equilibration
(Equilibration)
0.00 Base SameAsMain
0.5 AutoZeroUV
0.50 End_Block
¤ 0.00 Block Sample_injection
(Sample_injection)
0.00 Base Volume
0.00 InjectionValve Inject
1.5 InjectionValve (Load)#Load_volume
1.50 End_Block
¤ 0.00 Block Fractionation
(Fractionation)
0.00 Base SameAsMain
0.25 OutletValve F2
0.25 Fractionation 12 mm 0.5 [31] FirstTube Volume
0.55 FractionationStop
0.55 OutletValve WasteF1
1.10 End_Block
¤ 0.00 Block Reequilibration
(Reequilibration)
0.00 Base SameAsMain
0.5 End_Block
0.00 End_method

References

1. Mendicino M, Bailey AM, Wonnacott K et al (2014) MSC-based product characterization for clinical trials: an FDA perspective. Cell Stem Cell 14:141–145
2. Lai RC, Chen TS, Lim SK (2011) Mesenchymal stem cell exosome: a novel stem cell-based therapy for cardiovascular disease. Regen Med 6:481–492
3. Gnecchi M, He H, Noiseux N et al (2006) Evidence supporting paracrine hypothesis for Akt-modified mesenchymal stem cell-mediated cardiac protection and functional improvement. FASEB J 20:661–669
4. Gnecchi M, He H, Noiseux N et al (2005) Paracrine action accounts for marked protection of ischemic heart by Akt-modified mesenchymal stem cells. Nat Med 11:367–368
5. Mirotsou M, Zhang Z, Deb A et al (2007) Secreted frizzled related protein 2 (Sfrp2) is the key Akt-mesenchymal stem cell-released paracrine factor mediating myocardial survival and repair. Proc Natl Acad Sci U S A 104:1643–1648
6. Timmers L, Lim SK, Arslan F et al (2007) Reduction of myocardial infarct size by human mesenchymal stem cell conditioned medium. Stem Cell Res 1:129–137
7. Lai RC, Arslan F, Lee MM et al (2010) Exosome secreted by MSC reduces myocardial ischemia/reperfusion injury. Stem Cell Res 4:214–222
8. Lai RC, Arslan F, Tan SS et al (2010) Derivation and characterization of human fetal MSCs: an alternative cell source for large-scale production of cardioprotective microparticles. J Mol Cell Cardiol 48:1215–1224
9. Bi B, Schmitt R, Israilova M et al (2007) Stromal cells protect against acute tubular injury via an endocrine effect. J Am Soc Nephrol 18:2486–2496
10. Parekkadan B, van Poll D, Suganuma K et al (2007) Mesenchymal stem cell-derived

molecules reverse fulminant hepatic failure. PLoS One 2, e941

11. Timmers L, Lim SK, Hoefer IE et al (2011) Human mesenchymal stem cell-conditioned medium improves cardiac function following myocardial infarction. Stem Cell Res 6: 206–214
12. Schafer R, Northoff H (2008) Cardioprotection and cardiac regeneration by mesenchymal stem cells. Panminerva Med 50:31–39
13. Haynesworth SE, Baber MA, Caplan AI (1996) Cytokine expression by human marrow-derived mesenchymal progenitor cells in vitro: effects of dexamethasone and IL-1 alpha. J Cell Physiol 166:585–592
14. Kinnaird T, Stabile E, Burnett MS et al (2004) Bone-marrow-derived cells for enhancing collateral development: mechanisms, animal data, and initial clinical experiences. Circ Res 95:354–363
15. Patschan D, Plotkin M, Goligorsky MS (2006) Therapeutic use of stem and endothelial progenitor cells in acute renal injury: ca ira. Curr Opin Pharmacol 6:176–183
16. Miyahara Y, Nagaya N, Kataoka M et al (2006) Monolayered mesenchymal stem cells repair scarred myocardium after myocardial infarction. Nat Med 12:459–465
17. Min JY, Sullivan MF, Yang Y et al (2002) Significant improvement of heart function by cotransplantation of human mesenchymal stem cells and fetal cardiomyocytes in postinfarcted pigs. Ann Thorac Surg 74:1568–1575
18. Kinnaird T, Stabile E, Burnett MS et al (2004) Marrow-derived stromal cells express genes encoding a broad spectrum of arteriogenic cytokines and promote in vitro and in vivo arteriogenesis through paracrine mechanisms. Circ Res 94:678–685
19. Sze SK, de Kleijn DP, Lai RC et al (2007) Elucidating the secretion proteome of human embryonic stem cell-derived mesenchymal stem cells. Mol Cell Proteomics 6:1680–1689
20. Kordelas L, Rebmann V, Ludwig AK et al (2014) MSC-derived exosomes: a novel tool to treat therapy-refractory graft-versus-host disease. Leukemia 28:970–973
21. Ludwig AK, Kordelas L, Rebmann V et al (2012) Exosomes – from bench to bedside. Klin Padiatr 224:A6
22. Xin H, Li Y, Buller B et al (2012) Exosome-mediated transfer of miR-133b from multipotent mesenchymal stromal cells to neural cells contributes to neurite outgrowth. Stem Cells 30:1556–1564
23. Li T, Yan Y, Wang B et al (2013) Exosomes derived from human umbilical cord mesenchymal stem cells alleviate liver fibrosis. Stem Cells Dev 22:845–854
24. Lee C, Mitsialis SA, Aslam M et al (2012) Exosomes mediate the cytoprotective action of mesenchymal stromal cells on hypoxia-induced pulmonary hypertension. Circulation 126: 2601–2611
25. Reis LA, Borges FT, Simões MJ et al (2012) Bone marrow-derived mesenchymal stem cells repaired but did not prevent gentamicin-induced acute kidney injury through paracrine effects in rats. PLoS One 7:e44092
26. Tan CY, Lai RC, Wong W et al (2014) Mesenchymal stem cell-derived exosomes promote hepatic regeneration in drug-induced liver injury models. Stem Cell Res Ther 5:76, Epub ahead of print
27. Thery C, Ostrowski M, Segura E (2009) Membrane vesicles as conveyors of immune responses. Nat Rev Immunol 9:581–593
28. Pan BT, Johnstone RM (1983) Fate of the transferrin receptor during maturation of sheep reticulocytes in vitro: selective externalization of the receptor. Cell 33:967–978
29. Chen TS, Arslan F, Yin Y et al (2011) Enabling a robust scalable manufacturing process for therapeutic exosomes through oncogenic immortalization of human ESC-derived MSCs. J Transl Med 9:47

Chapter 30

Transcriptomic Analysis of Adult Renal Derived Mesenchymal Stem-Like Cells

Jose Gomez, Jeffrey Schmeckpeper, and Maria Mirotsou

Abstract

Mesenchymal stem cells (MSC) from bone marrow or adult tissues are widely studied to evaluate their potential for tissue repair. Differences in tissue of origin, donor variation, or in vitro handling exist and it is still unclear how they affect cell function and regenerative potential. Large-scale gene expression analysis of these cells not only allows researchers to compare and contrast the differences between each MSC subset but also allows for the development of better analytical tools for their characterization and utilization. Here, we describe a protocol for transcriptomics analysis of MSC-like cells derived from adult kidneys.

Key words Renal MSC-like cells, RNA analysis, In vitro characterization

1 Introduction

Mesenchymal stem cells (MSC) were first described over 40 years ago as a population of bone marrow cells that develop colony forming units after plastic adherence [1]. While much excitement has been directed at the use of bone marrow derived MSC for therapeutic use, their clinical utility has been hampered by inconsistent protocols for their isolation, in vitro handling, and characterization. Moreover, the mode of action underlying their reparative effects is still under investigation and clear markers of their therapeutic potency are poorly defined. Recently, MSC-like cells have been isolated from a multitude of adult tissues, including lung [2], skeletal muscle [3], heart [4], and kidney [5, 6]. These tissue-resident MSC, like their bone marrow counterparts, not only show great potential for ex vivo expansion and multilineage differentiation but also may have a more specific differentiation capacity and secretome profile attributed to the tissue from which they arise. The ability to identify and isolate these tissue-resident MSCs based on specific marker expression will not only allow researchers to compare and contrast the subtle differentiation potential each subset has to offer and better understand how these cells contribute to

Massimiliano Gnecchi (ed.), *Mesenchymal Stem Cells: Methods and Protocols*, Methods in Molecular Biology, vol. 1416,
DOI 10.1007/978-1-4939-3584-0_30,

tissue homeostasis and repair, but also provide the analytical tools for their utilization in cell therapy approaches.

Here, we report protocols on the isolation and characterization of mesenchymal stromal like cells from adult mouse kidneys and gene profiling assays to characterize this population. Kidney MSC participate in the response to blood pressure changes in vivo and in vitro. They represent a population of primary cells that may be used to investigate the mechanisms of renin expression and release. [6].

Various methods from microarray profiling to RNA sequencing and single-cell gene expression studies can be used for this purpose. Still, heterogeneity and reproducibility create challenges in evaluating these cells and the protocols for their growth and characterization are crucial for any follow-up studies.

2 Materials

2.1 Mouse Kidney Harvest

1. Wild-type male C57BL/6 mice, 8 weeks old (The Jackson Laboratory, Bar Harbor, ME, USA) or C57BL/6 Ren1c YFP mice, 8 weeks old (kindly provided by Dr. Ariel Gomez Virginia University Medical Center).
2. Appropriate sterilized surgical instruments. The instruments needed include: a pair of surgical scissors, two forceps, one 10 ml syringe, one hypodermic 27G needle, drapes, paper wipes, cotton swaps, and sterile gloves.
3. 1 ml syringe and Ketamine hydrochloride injection U.S.P. 100 mg/ml stored at 4–8 °C protected from light. Xylazine hydrochloride injection U.S.P. 20 mg/ml stored at 4–8 °C protected from light.
4. Water bath (37 °C) with temperature control and shaker.
5. Cell culture facility consisting of tissue culture hood, tissue culture room with positive pressure, and incubator with temperature and carbon dioxide (CO_2) control.
6. Cell culture materials including a motorized pipettor, 5, 10, and 25 ml pipettes, 10 cm plastic tissue culture dishes, and 50 ml conical tubes.
7. Sterile alcohol Prep Pads and 70 % ethyl alcohol.
8. Hanks' Balanced Salt Solution (HBBS).
9. Collagenase type I 10 % w/v in HBSS. Aliquoted and stored at –20 °C.
10. 1000 and 200 μL pipettors with respective pipet tips.

2.2 Isolation, Expansion, and Cryopreservation

1. Tissue culture supplies including a motorized pipettor, 10 and 25 ml pipettes, 15 and 50 ml centrifuge tubes, and 35, 60, and 100 mm plastic tissue culture dishes.
2. Hanks' Balanced Salt Solution (HBBS).

3. Phosphate-buffered saline (PBS).
4. Fetal bovine serum (FBS), heat inactivated.
5. Penicillin–streptomycin (P/S).
6. Dulbecco's Modified Eagle Medium (DMEM). Complete DMEM consisting of DMEM 10 % FBS and 1× P/S.
7. Trypsin 0.05 % in EDTA.
8. CD44-APC Antibody.
9. 7-Amino-Actinomycin D 7AAD.
10. Refrigerated centrifuge.
11. Embryomax cell culture freezing media with DMSO (Cat# S-002-D, Millipore, Billerica, MA, USA).
12. Fluorescence Activated Cell Sorting (FACS) Staining buffer: 0.05 % w/v Bovine Serum Albumin (BSA) in PBS.
13. FACS buffer: 2 mM EDTA, 2 % FBS, 1× P/S in PBS.
14. MesenPRO RS™ MSC growth media (Cat# 12746-012, Gibco).
15. Cryotubes.
16. Cell freezing storage container.

Media (*see* **Note 1**)

Adipogenic culture medium: DMEM supplemented with heat inactivated 10 % v/v Fetal bovine serum (FBS), 1 μM dexamethasone, 10 μM insulin, 200 μM indomethacin, and 0.5 mM 3-Isobutyl-1-methylxanthine (IBMX).

Osteogenic culture medium: DMEM containing 10 % FBS, 0.1 μM dexamethasone, and 50 μg/ml ascorbic acid-2-phosphate.

Muscle cell culture medium: DMEM containing 10 % FBS, 2.5 ng/ml TGF-β1, and 10 ng/ml PDGF.

Mouse renal cell differentiation medium: DMEM supplemented with heat inactivated 10 % v/v Fetal bovine serum (FBS) and 1× Penicillin–streptomycin (P/S).

2.3 Characterization: Immunophenotyping

Various cell surface markers can be used for cell characterization: CD44, CD105, CD11b, CD73, CD14, CD117 (c-Kit), CD166, CD31, CD54, CD45, and CD40. Negative controls for antibody type can be performed by using isotype control immunoglobulin G with their respective fluorescence label. FACS analysis can be performed on a FACS Vantage SE or a FACSCalibur flow cytometer. List of antibodies:

1. CD44-APC Antibody.
2. CD105 Alexa Fluor 488 Antibody.
3. CD11b-APC Antibody.
4. CD14-FITC Antibody.

5. CD45-FITC Antibody.
6. CD73-PE Antibody.
7. CD166-PE Antibody.
8. CD31-APC Antibody.
9. C-Kit-PE Antibody.
10. CD54-PE Antibody.
11. CD40-PE Antibody.

3 Methods

3.1 Mouse Kidney Collection

1. Warm 50 ml DMEM 10 % FBS and 1× P/S per mouse in 37 °C water bath and place a 60 mm dish with sterile ice-cold HBSS on ice for each mouse kidney isolation

   Anesthetize the animal with ketamine/xylazine. Use the following dose: ketamine 100 mg/kg and xylazine 10 mg/kg by intraperitoneal injection (IP). Mix 0.5 ml (50 mg) ketamine + 0.25 ml (5 mg) xylazine + 4.25 ml sterile water or saline. Mouse dose is 0.1 ml/10 g body weight (*see* **Note 2**).
2. After anesthetic injection wait for enough time to allow complete sedation before proceeding to isolate the kidneys.
3. Wear sterile gloves and, using the alcohol pads, clean the skin with unidirectional movements from the abdomen to the chest (*see* **Note 3**).
4. Scrub the mouse abdomen using the povidone–iodine pads USP swab sticks.
5. Fill a 10 mL syringe with sterile PBS for kidney perfusion.
6. Using surgical scissors open the abdomen and move the intestines onto a PBS wet gauze and open the chest cavity to expose the heart.
7. Once the heart is accessible, make an incision in the aorta at the top of the heart and insert the syringe needle, prefilled with PBS, into the left ventricle.
8. Slowly inject the PBS to flush the blood (containing circulating stem cells). As the PBS enters into the circulation, the organs will change color from reddish to pallid yellow; this means the perfusion is working.
9. Wearing fresh sterile gloves, cut both kidneys and keep them in ice-cold HBSS on a 60 mm tissue culture dish (3 mL of HBSS per isolation). From two kidneys the amount of CD44+ MSCs may range from 250,000 to 500,000 cells (*see* **Note 4**).
10. Repeat isolation steps if more than one animal is used.
11. Once all the kidneys are on ice-cold HBSS, proceed to mince the organs and isolate the CD44+ MSC.

3.2 Mouse Kidney CD44+ Mesenchymal Stem Cell FACSorting (*See* Note 5)

1. Using clean sterile scissors mince into pieces the kidneys in the 60 mm tissue culture dish. Make sure to cut the kidneys into small pieces of about 1–3 mm each to ensure good collagenase digestion. Keep minced tissue on ice until the next collagenase digestion step.
2. Transfer the minced kidneys to a 50 mL conical tube and wash the tissue culture dish with ice-cold HBSS and set the tube on ice. Bring the volume to 20 mL if needed.
3. Add 200 μL of collagenase (10 % w/v) to each tube, to digest the tissue.
4. Transfer to the 37 °C water bath and incubate for 20–30 min with rocking, and every 5 min mix with a plastic transfer pipet.
5. Stop the collagenase digestion by adding 20 mL of DMEM complete media and move the final mixture to an ice bath.
6. Centrifuge the digested kidneys at 300 × *g* for 5 min at 4 °C. Discard the supernatant and add 5 mL of red cells lysis buffer per isolation. Lyse remaining red blood cells on ice for 5 min.
7. Centrifuge at 300 × *g* for 5 min at 4 °C. Discard the supernatant and wash with ice-cold PBS and proceed to the next step.
8. Centrifuge the digested kidneys at 300 × *g* for 5 min at 4 °C. Discard the supernatant and resuspend the pellet in 1000 μL of staining buffer (resuspended cells). Divide samples as follows: for every set of samples run at the same time, 100 μL of resuspended cells plus 0.5–1.0 μg CD44–APC conjugated antibody sample without 7AAD (nuclear staining to discriminate dead cells), 100 μL of resuspended cells plus the corresponding isotype—APC conjugated antibody (0.5–1.0 μg per tube) plus and minus 7AAD, and 800 μL 0.5–1.0 plus μg CD44–APC conjugated antibody sample with 7AAD. These samples serve as controls. The other samples will be labeled with CD44-APC conjugated antibody using 0.5–1.0 μg per 1000 μL of resuspended cells (*see* **Notes 6** and **7**).
9. Incubate the samples with the antibodies for 1 h at 4 °C with rocking.
10. While the cells are labeled with the antibody prepare the tubes for collection of the FACSorted cells. Into the tubes pour 1 mL of complete DMEM media with 5× P/S to avoid contamination during the sorting procedure.
11. Centrifuge cells at 300 × *g* for 5 min at 4 °C. Discard the supernatant and resuspend the pellet in 1000 μL PBS.
12. Centrifuge cells at 300 × *g* for 5 min at 4 °C. Discard the supernatant and resuspend the pellet in 1000 μL FACS buffer.
13. Add the 7AAD (5 μL 7AAD/1000 μL cells suspension) to respective samples.

14. Pour the samples into polypropylene FACS tubes.
15. FACSort the cells. The CD44+ MSCs are isolated by two cycles of FACS sorting via specific gates, and the purity of CD44+ cells is confirmed before use. Dead cells are excluded with 7AAD, doublets are excluded on the basis of three hierarchical gates (forward/side scatter area, forward scatter height/width, and side scatter height/width). Proceed to Mouse kidney CD44+ MSC culture, expansion, and stocks.

3.3 Mouse Kidney CD44+ Mesenchymal Stem Cell Culture, Expansion, and Stocks

1. Collect the cells and centrifuge them at 300 × *g* for 5 min at 4 °C. Discard the supernatant and resuspend the pellet in 2 mL of MSC growth media MesenPRO RS™. Culture the cells in a 35 mm tissue culture dish in an incubator at 37 °C 5 % CO_2.
2. Culture in MSC growth medium. During culture, renal CD44+ cells will float, and within 24–72 h a fraction of cells will adhere to the culture dish; the remaining nonattached fraction consists of hematopoietic cells, floating cell aggregates, and dead round cells.
3. Exchange the medium every 3 days to discard dead and floating cells. Within 7 days, the CD44+ MSCs culture consists of an adherent population of small round cells, whereas spindle-like and elongated shapes start to appear and increase with time (about 14 days). Isolated cells are grown for two to three passages until sufficient cells are obtained for study. At the same time, CD44– cells are also isolated and cultured for comparison.
4. Culture the cells in the 35 mm dish until 90 % confluence and split the cells.
5. Wash cells with warm (37 °C) PBS and detach cells with 0.05 % Trypsin EDTA solution incubating for 5 min at 37 °C. Once cells are detached, inactivate the trypsin by adding 2 mL of complete DMEM media.
6. Centrifuge the cells at 300 × *g* for 5 min. Discard the supernatant and seed the cells from each 35 mm dish into two 60 mm tissue culture dishes.
7. Repeat the growth cycle until 90 % confluent and split the cells into 100 mm tissue culture dishes. Seed 250,000 cells per dish.

   Grow the cells to 90 % confluence and at this point they can be used in different experiments, characterization, and liquid nitrogen stocks (*see* **Note 8**).
8. Count the cells and at this point divide the cells into three different groups:
   (a) Cells for MSC characterization. The multilineage characterization of mouse renal MSC is discussed in detail in the next section.

(b) Cells for expansion.

(c) Cells for frozen liquid nitrogen stocks.

9. Freeze 10^6 cells in Embryomax cell culture freezing media with DMSO. Pour the cells into a cryotube and place the tube in the cell freezing storage container. Once the cells are in the container start the freezing process at −80 °C overnight and then store the cells in liquid nitrogen.

Continue the cell expansion for use in differentiation experiments as well as for characterization (*see* **Notes 9–11**).

3.4 Determination of Mesenchymal Stem Cell Multipotency

1. Grow cells in growth medium and expand for three passages. At passage three grow cells to 95 % confluence (*see* **Note 12**).
2. Trypsinize and replate onto tissue culture plates or slide chambers at a density of $5 \times 10^4/\text{mm}^2$ for adipogenic and osteogenic differentiation, and $5 \times 10^3/\text{mm}^2$ for differentiation into smooth muscle cells.
3. The cells are incubated in a small amount of growth medium for 1 day to promote adherence to the plates.
4. After cells have adhered, cells are placed in the induction medium.
   (a) For enhancement of adipogenic differentiation, use adipogenic culture medium.
   (b) Osteogenic differentiation is induced in osteogenic medium
   (c) The differentiation into smooth muscle cells is induced with muscle cell medium for 6 days. The medium is changed every 2 days.
5. After treatment differentiation is determined as follows:
   (a) Adipogenic differentiation is assessed by Oil Red O staining 2 weeks after initial adipogenic induction as described.
   (b) Alkaline phosphatase staining is used to detect osteogenic differentiation after 3 weeks of induction of differentiation according to the manufacturer's recommendations.
   (c) To detect the differentiation of smooth muscle cells, immunohistochemistry can be performed after 6 days of induction to detect smooth muscle cell markers such as α-SMA.

3.5 Mouse Kidney CD44+ Mesenchymal Stem Cell Differentiation to Renin Expressing Cells with cAMP

Mouse renal MSC are promoted with mouse renal cell differentiation medium (*see* **Note 13** and Table 1).

1. cAMP concentration will be induced in the cells with a combination of small molecules: 3-Isobutyl-1-methylxanthine (IBMX) and Forskolin. DMSO is used as solvent control (*see* **Note 14**).

Table 1
Experimental conditions for mouse renal CD44+ MSC isolated from C57BL/6 Ren1c YFP transgenic mice

MSC CD44+ derived from	Sample	Final concentration
C57BL6 Ren1c YFP mouse	No treatment	N/A
C57BL6 Ren1c YFP mouse	DMSO solvent	N/A
C57BL6 wild type	No treatment	N/A
C57BL6 wild type	Forskolin IBMX	10 μM 0.1 mM

2. Seed CD44+ MSCs into 6 well plates and start treatment once the cells are 95–100 % confluent. Seed 11,565 cells/cm^2 (150,000 cells/well). It is important to use MSC that have been passaged no more than 5 times (Cell survival is measured by Trypan blue).
3. C57Bl6 wild-type mouse kidney MSC CD44+ are seeded under the same conditions to be treated as the MSC CD44+ derived from the Ren1c YFP mouse. The wild-type derived cells will serve as a control for autofluorescence during FACSorting or fluorescence microscopy.
4. Determine cell confluence and when they reach 95–100 % confluence, start treatments based on the experimental design. It is important to add the same volume of each compound to keep the solvent volume constant, which is used in the solvent control sample. Respective dilutions of each compound may be needed. Make sure to document the starting date of treatment.
5. Before treatment, acquire images with the fluorescence microscope as controls for each sample in the experimental setting.
6. Prepare in separate tubes the mix of complete DMEM media plus IBMX and Forskolin, DMSO, and media (untreated sample).
7. Differentiate the cells and replenish the compounds every day by adding compounds to the medium in about 10 % of the medium in the well plus the drugs needed—taking into account the 10 % extra medium (for a total of 1200 μL per well, mix the drugs with 120 μL of medium; add drugs up to a 1320 μL total volume), and at day 3 exchange medium with fresh complete medium containing compounds.
8. Continue the treatment for 7 days analyzing the expression of YFP as a surrogate for renin expression. If wild-type cells are used in the experiment, at day 7, the expression of renin can be analyzed by immunocytochemistry (*see* **Note 15**).

9. At day 7, FACSort Renin-YFP positive and YFP negative cells for following experiments or acquire images to document YFP expression (*see* **Note 16**).

3.6 Mouse Kidney Mesenchymal Stem Cell Flow Cytometry Characterization

1. For MSC cell surface markers analysis, 100,000 freshly isolated or cultured cells are incubated with the antibodies in 100 μL of staining buffer for 60 min at 4 °C.
2. Primary antibodies (PE, FITC, or APC conjugated) are used at a dilution of 1:50 or 1:100 following the dilution recommended by the manufacturer.
3. Dead cells are excluded with 7AAD, doublets are excluded on the basis of three hierarchical gates (forward/side scatter area, forward scatter height/width, and side scatter height/width). For each reaction, 75,000 events are counted.
4. Antibodies used are: anti-mouse CD44, CD105, CD11b, CD73, CD14, CD117 (c-Kit), CD166, CD31, CD54, CD45, and CD40.
5. FACS analysis is performed on a FACS Vantage SE or a FACSCalibur flow cytometer.
6. Expression of the different markers is analyzed using the flow cytometry software FloJo.

3.6.1 RNA Isolation (RNeasy Plus Micro)

1. For cells grown in a monolayer do not use more than 5×10^5 cells. Take samples from the −80 °C freezer and thaw them on ice. Spin down cells plus RNA at $5000 \times g$ for 10 min at room temperature (RT).
2. Discard RNA, and disrupt the cells by adding 350 μL buffer RLT plus, loosen the cell pellet by vortexing the tube for 1 min to lyse cells (if less than 1×10^5 cells use 75 μL RTL buffer).
3. Transfer the homogenized lysate to a gDNA eliminator spin column placed in a 2 mL collection tube. Centrifuge for 30 s at $\geq 8000 \times g$ ($\geq$10,000 rpm).
4. Discard the column and save the flow-through.
5. Add 1 volume (350 μL) of fresh 70 % ethanol (EtOH) to the flow-through from **step 4**, and mix well by pipetting up and down. Do not centrifuge and go immediately to **step 6**.
6. Transfer the sample including any precipitate that may have formed to an RNeasy MinElute spin column placed in a 2 mL collection tube. Close the lid gently and spin for 15 s at $\geq 8000 \times g$. Discard flow-through.
7. Add 700 μL of buffer RW1 to the RNeasy minElute column. Close the lid gently and spin for 15 s at $\geq 8000 \times g$. Discard flow-through.

8. Add 500 μL of buffer RPE to the RNeasy minElute column. Close the lid gently and spin for 15 s at ≥8000 × *g* to wash the spin column membrane. Discard flow-through.
9. Add 500 μL of fresh 80 % EtOH to the RNeasy minElute column. Close the lid gently and spin for 2 min at ≥8000 × *g* to wash the spin column membrane. Discard the collection tube with the flow-through.
10. Place the RNeasy MinElute spin column in a new 2 mL collection tube. Open the lid of the column and centrifuge at full speed (14,000 rmp) for 5 min. Discard the collection tube with the flow-through.
11. Place the RNeasy MinElute spin column in a new 1.5 mL tube prelabeled with sample ID. Add 20 μL RNase-free water directly to the center of the spin column membrane, close the lid gently, and centrifuge for 1 min at full speed (14,000 rmp) to elute the isolated RNA.

3.6.2 RNA Isolation (PicoPure RNA Isolation) (See Notes 17 *and* 18*)*

RNA Extraction from Cell Pellets

1. For cells grown in a monolayer do not use more than 5×10^5 cells. Take samples from the −80 °C freezer and thaw them on ice. Spin down cells plus RNA later at 5000 × *g* for 10 min at RT.
2. Discard the RNA and resuspend the pellet in 1 mL of PBS (prepared in RNase-free water and 0.2 μm filtered). Do not vortex.
3. Pellet cells by spinning down at 3000 × *g* for 5 min at RT, discard the supernatant.
4. Extract the RNA with 100 μL of Extraction Buffer (XB). Resuspend the cell pellet gently by pipetting. Do not vortex. Incubate at 42 °C for 30 min, spin samples at 3000 × *g* for 2 min at RT, pipette the supernatant containing the extracted RNA into a new microcentrifuge tube (provided), avoid picking-up the pellet.

RNA Isolation

1. Preconditioning of the RNA purification column.
   (a) Pipette 250 μL Conditioning Buffer (CB) onto the purification column filter membrane.
   (b) Incubate the RNA purification column with conditioning buffer for 5 min at RT.
   (c) Centrifuge the purification column in the provided collection tube at 16,000 × *g* for 1 min.
2. Pipette 100 μL of 70 % EtOH into the cell extract from **step 8** (RNA extraction part). Mix well by pipetting up and down. Do not centrifuge.
3. Pipette the cell extract and EtOH mixture into the preconditioned purification column. The cell extract and EtOH will have a combined volume of approximately 200 μL.

4. To bind RNA, centrifuge for 2 min at 100 × *g*, immediately followed by a centrifugation at 16,000 × *g* for 30 s to remove flow-through.
5. Pipette 100 μL wash buffer 1 (W1) into the purification column and centrifuge for 1 min at 8000 × *g*.
   (a) DNase treatment: RNase-free DNase set
   - Pipette 10 μL DNase I stock solution into 30 μL buffer RDD (provided with kit). Mix by gently inverting.
   - Pipette 40 μL DNase incubation mix directly onto the purification column membrane. Incubate at RT for 15 min.
   - Pipette 40 μL PicoPure RNa kit wash buffer 1 (W1) onto the purification column membrane. Centrifuge at 8000 × *g* for 15 s.
6. Pipette 100 μL wash buffer 2 (W2) onto the purification column and centrifuge for 1 min at 8000 × *g*.
7. Pipette another 100 μL wash buffer 2 (W2) into the purification column and centrifuge for 2 min at 16,000 × *g*, check the purification column for any residual wash buffer. If wash buffer remains, recentrifuge at 16,000 × *g* for 1 min.
8. Transfer the purification column to a new 0.5 mL microcentrifuge tube provided in the kit.
9. Pipette elution buffer (EB) directly onto the membrane of the purification column (gently touch the tip of the pipette tip to the surface of the membrane while dispensing the elution buffer to ensure maximum absorption of EB onto the membrane). 11 μL for less than 1000 cells, 25 μL for 3000–5000 cells, and 50 μL for 15,000–20,000 cells and values in between if different cell number. Incubate the column for 1 min at RT.
10. Centrifuge the column for 1 min at 1000 × *g* to distribute EB onto the column, and spin for 1 min at 16,000 × *g* to elute RNA. Measure [RNA]. Store RNA at −80 °C.

Gene Expression Profiling

RNA is used to produce cDNA for further analysis using the high capacity cDNA reverse transcription kit following the manufacture's recommended protocol. cDNA can then be used for gene profiling with the Affymetrix Mouse 430 2.0 array.

Alternatively, samples can be prepared for whole-transcriptome analysis with total RNA sequencing (total RNA-Seq) to allow for a broader range of detection including both coding and noncoding RNA species. For small noncoding RNAs (such as miRNAs) the Illumina TruSeq small RNA library preparation protocol can be used. Various analysis packages such as DeSeq can be applied for data analysis. Further annotation data analyses can be performed using various packages such as Ingenuity, David, or Toppgene.

4 Notes

1. Test the FBS before use in the growth, expansion, and differentiation of MSCs. One serum may be optimal for growth, while another may be optimal for differentiation.
2. All animal procedures should be conducted in accordance with animal care policies and must be approved by the institutional animal care committee.
3. Unless stated otherwise, all procedures should be conducted with the utmost adherence to aseptic technique.
4. Keep the volume of HBSS to about 3 mL; this improves the handling of kidneys during mincing.
5. Use very stringent settings during the Fluorescence Activated Cell Sorting to ensure that the sorted cells are a homogeneous population. If the sorted cells are to be stored, always store at −80 °C.
6. Prepare and label the samples for the 7AAD control; however, the nuclear dye will be added at the end of the procedure before Fluorescence Activated Cell Sorting (FACS).
7. If cells from a transgenic mouse line with a specific cell reporter are used, it is important to include a wild-type control to account for transgene variability. This wild-type control can be used for nuclear staining and isotype antibody controls.
8. At this point it is important to characterize the MSC for multilineage capacity, expression of different MSC markers, and clonogenicity.
9. The MSC can be used up to passage 6 for differentiation experiments as they conserve their progenitor characteristics.
10. Some of the MSC markers will decrease or disappear with culture and passage of cells.
11. The initial population of MSC will have a spindle-like morphology and will grow slowly during the first passage. Passage cells only until 95 % confluent to ensure better survival afterwards.
12. During differentiation use fresh compounds as well as fresh media. Do not use medium for more than 1 month.
13. FBS from Hyclone is used for differentiation. Before the FBS is used to differentiate mouse renal MSC into renin expressing cells, different batches of FBS are tested to ensure that there is no interference of the serum with the differentiation.
14. IBMX and Forskolin are dissolved in DMSO and kept at −20 °C at a concentration of 1000×, the concentration used in treatment.

15. Expression of YFP peaks at day 7; however in the initial stages follow YFP expression closely as the treatment is performed and recommended to assess the differentiation process.
16. At this point the renin expressing cells can be characterized as juxtaglomerular like cells as reported in [6].
17. When isolating RNA from sorted cells keep the working bench clean, use dedicated filter tips, and a dedicated set of pipettors for this procedure.
18. Always perform RNA and cDNA PCR reactions on the same day to avoid RNA degradation.
19. Cells FACSorted for microarray should be pelleted by centrifugation, followed by suspension in RNA later for later use.

References

1. Friedenstein AJ, Gorskaja JF, Kulagina NN (1976) Fibroblast precursors in normal and irradiated mouse hematopoietic organs. Exp Hematol 4:267–274
2. Martin J, Helm K, Ruegg P et al (2008) Adult lung side population cells have mesenchymal stem cell potential. Cytotherapy 10: 140–151
3. Boppart MD, De Lisio M, Zou K et al (2013) Defining a role for non-satellite stem cells in the regulation of muscle repair following exercise. Front Physiol 4:310
4. Chong JJ, Chandrakanthan V, Xaymardan M et al (2011) Adult cardiac-resident MSC-like stem cells with a proepicardial origin. Cell Stem Cell 9:527–540
5. Bruno S, Bussolati B, Grange C et al (2009) Isolation and characterization of resident mesenchymal stem cells in human glomeruli. Stem Cells Dev 18:867–880
6. Wang H, Gomez JA, Klein S et al (2013) Adult renal mesenchymal stem cell-like cells contribute to juxtaglomerular cell recruitment. J Am Soc Nephrol 24:1263–1273

Chapter 31

Proteomic Analysis of Mesenchymal Stem Cells

Vitor Marcel Faça, Maristela Delgado Orellana, Lewis Joel Greene, and Dimas Tadeu Covas

Abstract

Mesenchymal stem or stromal cells (MSCs) are of great interest in biomedical sciences and disease treatment because of their multipotency and wide range of applications for tissue repair and suppression of the immune system. Proteomic analysis of these unique cells has contributed to the identification of important pathways utilized by MSCs to differentiate into distinct tissues as well as important proteins responsible for their special function in vivo and in vitro. However, comparison of proteomic studies in MSCs still suffers from the heterogeneity of MSC preparations. In addition, as proteomics technology advances, several studies can be revisited in order to increase the depth of analysis and, therefore, elucidate more refined mechanisms involved in MSC functionalities. Here, we present detailed protocols to obtain MSCs, as well as protocols to perform in-depth profiling and quantification of alterations in MSC proteomes.

Key words Mesenchymal stem cells, Bone marrow, Umbilical cord vein blood, Proteomics, Protein fractionation, Mass spectrometry

1 Introduction

Mesenchymal stem or stromal cells (MSCs) were claimed to differentiate into specialized mesenchymal tissues including bone, cartilage, muscle, marrow stroma, tendon, ligament, fat, and other connective tissues, when first discovered [1]. More recently, site-specific roles of these progenitor cells have been evidenced, indicating more restricted roles and differentiation capabilities of MSCs, depending on their tissue of origin [2]. MSCs are mainly present in bone marrow in adults, but can also be found around blood vessels, in fat, skin, muscle, and a variety of locations during tissue development [1–5].

Regenerative medicine and tissue engineering have focused attention on MSCs based on their capacity to grow, expand, and differentiate ex vivo. A large number of clinical trials have already shown the efficacy of MSCs in cell therapy. Furthermore, there

Massimiliano Gnecchi (ed.), *Mesenchymal Stem Cells: Methods and Protocols*, Methods in Molecular Biology, vol. 1416,
DOI 10.1007/978-1-4939-3584-0_31,

is strong evidence supporting the notion that crucial cellular functions such as proliferation, differentiation, communication, and migration are strictly regulated by the MSC secretome. Investigation of the stem cell secretome is continuously increasing, given the potential of large-scale cell by-product production in regenerative medicine [6–8].

The variety of sources as well as clinical applications makes MSCs extremely interesting subjects of proteomic studies to elucidate pathways involved in differentiation [9, 10], comparisons of different sources [11], and characterization of secretomes [12]. However, there is some debate about the criteria to define an MSC cell population and a homogeneous MSC cell preparation. Minimal requirements have already been established to define MSCs: the cells should adhere to plastic; test positive for cell surface markers CD73, CD90, and CD105 and negative for CD11b or CD14, CD19 or CD79a, CD34, CD45 and HLA-DR, with the capacity to differentiate into osteoblasts, adipocytes, and chondroblasts in vitro [13].

Profiling MSC proteomes and secretomes is a challenging task, since they are very dynamic and susceptible to extracellular conditions, allowing posttranslational modification and degradation. On the other hand, proteomics technology has evolved significantly in the last decade, especially in terms of instrumentation, which allows faster, more sensitive and more accurate mass measurements [14, 15]. This evolution drives comprehensive studies that are just recently capable of elucidating over thousands of proteins in complex mixtures such as the MSC secretome [16]. To our knowledge, protein fractionation plus state-of-the-art mass spectrometry has achieved the best results in terms of secretome coverage [17, 18]. In addition, bioinformatics workflows have also helped to uncover secreted proteins using better-annotated databases, appropriate data filtering, and improved prediction of signal sequences [19, 20]. Here, we present a strategy for profiling and relative quantitation of MSC proteomes obtained from different sources.

2 Materials

Prepare fresh solutions using MilliQ water on the day of use and maintain at room temperature, unless indicated otherwise.

2.1 Cell Isolation and Culture Components

1. Cell culture medium: alpha-minimal essential medium supplemented with 10 % fetal bovine serum (FBS), 2 mM L-glutamine, and 100 U penicillin/100 µg streptomycin (*see* **Note 1**).
2. Tissue culture flasks for adherent cell culture (25 and 75 cm^2).
3. Collagenase solution: collagenase type 1A at 5 mg/mL, prepared in Dulbecco's modified essential medium.

4. Trypsin/EDTA (0.05 % trypsin/EDTA/PBS).
5. Adipocyte differentiation medium: α-MEM supplemented with 15 % FBS, 2 mM L-glutamine, 100 U/mL penicillin, 100 μg/mL streptomycin, and 2 g/L sodium bicarbonate, with 10 μM dexamethasone, 10 μg/mL insulin, and 100 mM indomethacin.
6. Osteocyte differentiation medium: use the same base α-MEM medium with 15 % FBS, 2 mM L-glutamine, 100 U/mL penicillin, 100 μg/mL streptomycin and supplement with 0.1 μM dexamethasone, 100 μM ascorbic acid, and 10 mM β glycerophosphate.

2.2 Components for Sample Preparation and Proteomic Analysis

1. Complete protease inhibitor cocktail tablets (Roche Diagnostics, Germany).
2. Bradford quantification kit.
3. Denaturation buffer: Urea 8 M, Tris–HCl 0.15 M, pH 8.5. Weigh 1.5 g of urea and 454 mg of trizma-base, dilute with 15 ml of water. Mix until solids are completely dissolved and adjust pH with HCl (diluted 1:1 in water). Transfer to a 25 ml volumetric flask and adjust the volume.
4. Trypsin solution: Sequencing grade modified trypsin (20 μg/ml). Resuspend one vial containing 20 μg of sequence grade modified trypsin in 1 mL of 0.1 M ammonium bicarbonate solution (dissolve 395 mg of ammonium bicarbonate in 50 ml of water and filter through a 0.22 μm syringe filter).
5. Reducing and acrylamide isotopic labeling solutions: Dissolve 10 mg of dithiothreitol in 1 mL of 0.15 M Tris–HCl, pH 8.5 solution. For light acrylamide alkylating solution, dissolve 7.1 mg of light acrylamide ($^{12}C_3$) in 0.2 mL 0.15 M Tris–HCl, pH 8.5. For heavy acrylamide alkylating solution, dissolve 7.4 mg of heavy acrylamide ($^{13}C_3$), in 0.2 mL 0.15 M Tris–HCl, pH 8.5 (*see* **Note 2**).
6. Solid phase purification tips: solid-phase-extraction reversed-phase C_{18} microcolumns. Equilibration solution is 95 % water/5 % acetonitrile/0.1 % formic acid. Elution solution is 30 % water/70 % acetonitrile/0.1 % formic acid.
7. LTQ-ORBITRAP mass spectrometer series coupled to a nanoflow chromatography system.
8. Chromatographic column: 25 cm long column (Picofrit 75 mm ID, New Objectives, packed in-house with Magic C_{18} resin).
9. Solvents for reversed-phase chromatography: Aqueous solvent (A)—5 % acetonitrile/95 % water/0.1 % formic acid; Organic solvent (B)—95 % acetonitrile/5 % water/0.1 % formic acid.

10. Commercial precast SDS-PAGE gels (12 %) and compatible buffers (*see* **Note 3**).
11. Light microscope equipped with an AxioCam camera.

3 Methods

3.1 Isolation and Culture of Mesenchymal Stem Cells from Umbilical Cord Veins (See Note 4*)*

1. Isolate MSCs from human umbilical cord veins (UCV-hMSCs) by washing twice internally and externally with 20 mL of phosphate-buffered saline. After clamping the distal end of the cord, fill the vein with 3–5 mL of collagenase type 1A solution, clamp the proximal extremity and incubate for 30 min at 37 °C, immerse in a flask containing 100 mL of PBS (*see* **Note 5**).
2. Harvest the detached cells by adding the collagenase solution and performing additional washing of the vein with 20 mL of α-MEM supplemented with 5 % FBS, 2 mM L-glutamine, and 100 U penicillin/100 μg streptomycin.
3. Collect cells from endothelial and subendothelial umbilical cord layers by centrifugation at 400 × *g*, at 5 °C for 10 min.
4. Resuspend the cell pellet in α-MEM medium and culture. Transfer the cell resuspension directly to a 75 cm^2 culture flask and allow MSCs to adhere for 96 h in an incubator at 37 °C and 5 % CO_2 (*see* **Note 6**).
5. Remove the medium from the flask and expand cells in tissue culture flasks with α-MEM medium supplemented with 15 % FBS, 2 mM L-glutamine, and 100 U penicillin/100 μg streptomycin until 80–90 % confluency.
6. After expansion, trypsinize cells with 5 mL of 0.05 % trypsin–EDTA/PBS solution, resuspend cells in 20 mL of α-MEM medium, and centrifuge cell suspension at 400 × *g* (*see* **Note 7**).
7. Wash the cell suspension twice with PBS, resuspend cells in 25 mL α-MEM medium, and expand cells in tissue culture flasks for 3–4 passages (*see* **Note 8**).

3.2 Isolation and Culture of Mesenchymal Stem Cells from Bone Marrow (See Note 4*)*

1. Isolate MSCs from human bone marrow (BM) iliac crest aspirates (BM-hMSCs) by gradient separation in Ficoll-Hypaque 1077. Collect the mononuclear cell layer, wash twice with PBS, and centrifuge at 400 × *g* for 10 min at 5 °C (*see* **Note 9**).
2. Resuspend the cell pellet in α-MEM medium, transfer directly to a 25 cm^2 culture flask, and allow MSCs to adhere for 96 h in an incubator at 37 °C and 5 % CO_2.
3. Obtain the adherent cells by culturing initially in 25 cm^2 culture tissue flasks in α-MEM medium and then expand cells in 75 cm^2 tissue culture flasks for 3–5 passages (*see* **Note 8**).

3.3 Immunophenotypical and Functional Characterization

1. Wash approximately 1×10^5 UCV-hMSCs or BM-hMSCs cells with PBS, and label with each of the following monoclonal antibodies for immunophenotyping by flow cytometry: CD13, CD14, CD29, CD34, CD90, CD49e, CD51/61, CD73, CD90, CD105, conjugated with phycoerythrin (PE), CD31, CD45, HLA-DR and the corresponding controls y1/y2 conjugated with fluorescein (FITC) (*see* **Note 10**).
2. Analyze cells in duplicate on a FACSCalibur flow cytometer and then evaluate the results with CELLQuest™ software (*see* **Note 11**).
3. For functional characterization, induce MSC adipogenic or osteogenic differentiation (*see* **Note 12**).
4. After 15 days, differentiated cells are fixed and adipocytes are stained by Sudan II and Scarlet stains (for fat accumulation) and osteocytes are stained with the von Kossa method (for calcium deposition) [3]. Cells are analyzed by light microscopy equipped with an AxioCam camera.

3.4 Proteomic Analysis

1. Perform the MSC culture expansion according to appropriate cell culture conditions until approximately 5×10^6 cells are obtained (*see* **Note 13**).
2. If secretome analysis is of interest, remove supplemented cell medium from flasks and replace with 6 ml of fresh α-MEM medium, without FBS and other additives. Keep cells in culture for an additional 24–48 h to collect cellular secretion.
3. Pool the cellular conditioned media containing secreted proteins, immediately add complete protease inhibitor cocktail (1 tablet/10 ml of pooled media), and remove cells and debris first by centrifugation at $5000 \times g$ and then by filtration through a 0.22 mm filter.
4. Concentrate conditioned media to approximately 1 ml using centrifuge concentrators, with molecular weight cutoff of 3 kDa. Store solution at 4 °C until fractionation (*see* **Note 14**).
5. Add 500 μL denaturation buffer, containing complete protease inhibitor cocktail (1 tablet/5 ml of solution), to the remaining cells attached to the flask. Collect cells using a cell scraper and combine extracts from different plates if required. Additional cellular protein extraction is obtained by sonication of solution using an ultrasound probe with 3 alternating cycles of 30 s of sonication and ice bath. Centrifuge solution at $20{,}000 \times g$ to remove cellular debris. Store at 4 °C until processing.
6. Quantify concentrated conditioned media and cellular extract using the Bradford Assay kit according to the manufacturer's instructions (*see* **Note 15**).

7. Aliquot 50 μg of both conditioned media and total cell extract and perform protein reduction by adding 5 μL of reduction solution and maintaining the reaction at 37 °C for 1 h. Right after that, perform protein alkylation by adding 10 μL of alkylating solution and maintain the reaction at room temperature for one additional hour.
8. Fractionate the complex protein mixtures of conditioned media and total cell extract using SDS-PAGE in a 12 % precast gel, according to the manufacturer's instructions (*see* **Note 16**).
9. Split each gel lane into the desired number of fractions (*see* **Note 17**).
10. Perform in-gel trypsin digestion of the gel fragments. First, wash the gel fragments 3 times with 200 μL of 0.1 M ammonium bicarbonate and 50 % acetonitrile solution. Agitate vigorously in between washes and discard the washing solution. Add 200 μL of acetonitrile. To dehydrate gel pieces, discard the solution and further dry gel fragments in a speedvac. Add 20 μL of trypsin solution and let gel fragments hydrate for 15 min. Then cover the band with approximately 100 μL of 0.1 M ammonium bicarbonate solution. Carry out the digestion for 18 h or overnight at 37 °C. Collect the solution and save. Extract peptides from gel pieces with three further washes with 200 μL of 0.1 M ammonium bicarbonate and 50 % acetonitrile solution. Pool the extraction solutions collected from each band. Dry extracted solutions in a speedvac (*see* **Note 18**).
11. Centrifuge extracted peptide solutions at 12,000 × *g* for 15 min and transfer to mass spectrometry compatible injection tubes (*see* **Note 19**).
12. Carry out the high-throughput LC-MS/MS data collection for each individual fraction obtained from conditioned media and total cell extract. Analyze samples over a 90 min linear gradient from 5 to 35 % of organic solvent at 350 nl/min (*see* **Note 20**).
13. Process LC-MS/MS files through data bank search, protein inference, and quantitative analysis (*see* **Note 21**). Figure 1 illustrates a proteomic study comparing BM-hMSCs and UCV-hMSCs that demonstrates MSCs isolated from both sources share high similarity in metabolic and functional processes relevant to their therapeutic potential [11].
14. When applicable, match the lists of proteins identified in the conditioned media (secretome) and proteins identified in the total cell extract and select secreted proteins based on the higher value of enrichment obtained from the ratio of spectral counts observed in conditioned media profile/total cell extract profile (*see* **Note 22**).

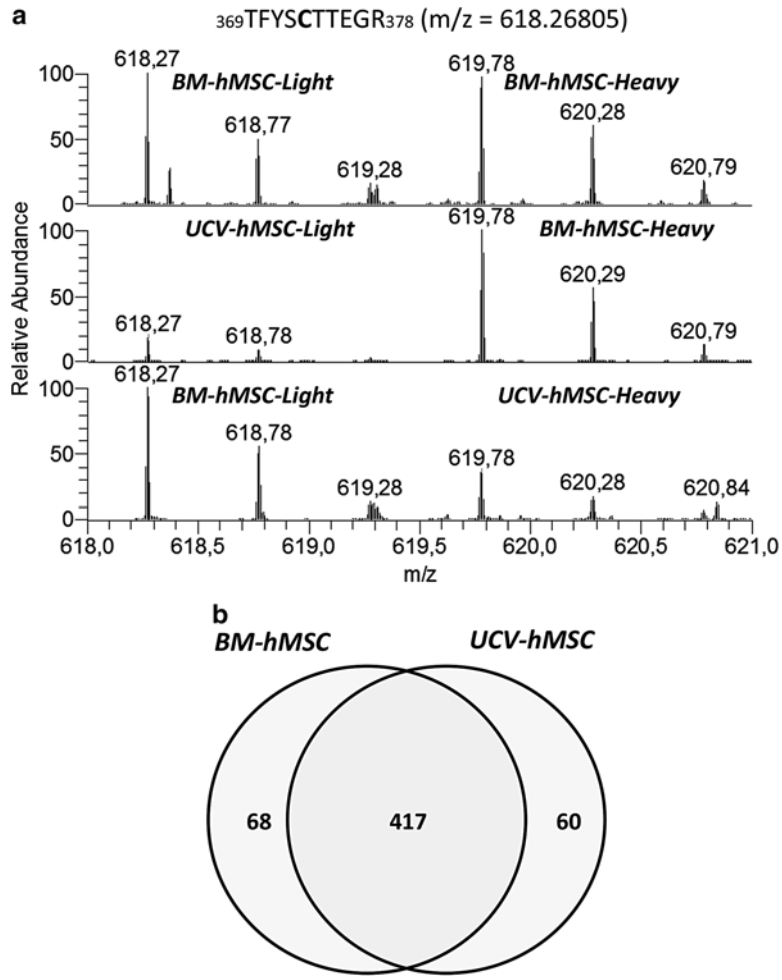

Fig. 1 Proteomic comparison of BM-hMSC and UCV-hMSC. Cells obtained from BM and UCV were compared using the proteomic approach described here. Total cell extracts were labeled with heavy or light acrylamide isotopes. *Panel* (**a**) illustrates the relative quantification of a peptide from fibronectin 1 (FN1), which was detected at higher levels (~3-fold) in BM-hMSCs. Label swapping shows the reliability of the alkylation with acrylamide isotopes. In the study, more than 1500 proteins were confidently identified and 545 presented cysteine containing peptides, which allowed accurate relative quantification. Results in *panel* (**b**) showed that BM-hMSCs and UCV-hMSCs share a high degree of similarity, since only 128 proteins were detected with protein abundance differences greater than 1.5-fold [11]

4 Notes

1. MSC cell culture in α-MEM can be used for most cell types obtained directly from patients. MSC-derived cell lines should use appropriate media formulations. See ATCC (www.atcc.org) for detailed specifications.

2. Always prepare fresh dithiothreitol and acrylamide solutions to guarantee efficient reduction and alkylation of cysteine residues. Do not store these solutions and avoid long reaction times, since nonspecific amine labeling can also occur. Please *see* Faça et al. [21] for more detailed information.
3. Commercial precast SDS-PAGE gels have much better quality controls to allow reproducible separations and less environmental protein contamination, such as with keratins.
4. Approval by the local ethics committee and informed written consent was obtained from all donors in our studies.
5. Use a sterile 250 ml beaker to immerse umbilical cord in 100 ml of PBS and incubate it in a water bath at 37 °C covered with parafilm.
6. Cells are typically resuspended at 2.5×10^5 cells/ml of medium. A total of 20 ml of cell suspension is transferred to a 75 cm^2 cell culture flask. One umbilical cord usually contains 5×10^6 total cells. At passage one, 8–10 days after the isolation of MSC, around 5.0×10^6 MSCs are recovered.
7. Before MSC treatment with 0.05 % trypsin-EDTA, remove total medium from the culture flasks, wash twice with PBS, then add 5.0 ml of 0.05 % trypsin-EDTA to each culture flask. Incubate culture flasks at 37 °C for 2–5 min. Detach the cells from culture flasks with gentle shaking. Wash the cell suspension twice with PBS by centrifugation at $400 \times g$, 5 °C for 10 min.
8. After 3–4 passages, MSCs still retain most of their original characteristics. Avoid further expansion, since cell culture, FBS components, and manipulation can stimulate in vitro differentiation. Cells can be stored at −80 °C until proteomic analysis.
9. Mononuclear cells from BM are typically resuspended at 3.0×10^6 cells/ml of medium. 5 mL of cell suspension is transferred to a 25 cm^2 cell culture flask, while 20ml of the suspension can be directly transferred to a 75 cm^2 cell culture flask. Usually, 3 mL of bone marrow from one donor contains 1.0×10^7 cells.
10. MSCs are expected to be positive for: CD29, CD44, CD49e, CD73, CD90, and HLA class I, while negative for: CD34, CD33, CD45, CD14, CD31, KDR, CD51/61, and HLA-DR class II cell surface markers.
11. Cell sorting based on the CD73 marker can be carried out to increase homogeneity of cell populations used in experiments and proteomic analysis. CD73 is important because it is constitutively and continuously expressed during in vitro MSC culture.

12. For differentiation studies, approximately 5×10^4 cells are cultured in 24 well plates. Differentiation is initiated 24 h after the initial cell plating and at approximately 50 % confluence when regular medium is replaced with the differentiation induction medium.
13. Upon cellular confluence, approximately $2–5 \times 10^6$ cells per 75 cm^2 flask are expected. Multiple patient samples can be pooled if necessary to obtain enough material for proteomic studies.
14. Concentrated conditioned medium must be fractionated quickly in order to avoid precipitation. It is recommended to perform reduction, alkylation with acrylamide isotopes, and SDS-PAGE fractionation on the same day as conditioned medium collection.
15. The procedure described for total protein extraction provides 1.8–2.5 mg of protein per 1×10^7 cells, according to the Bradford method. For conditioned medium, protein concentrations range from 5 to 20 μg/mL after 24 h protein secretion in a confluent 75 cm^2 culture flask.
16. To each lane, 50 μg of protein extract is loaded. When nonlabeling quantification methods are applied for MSC comparison, 3 replicate lanes are loaded. For comparisons in which acrylamide labeling is used, two lanes are loaded, representing both combinations of isotopic labeling.
17. Split the gel lane into fragments of equal sizes, in order to obtain approximately the same amount of protein. Gel fragments containing intense bands can be further split and analyzed individually. This strategy is used to maximize the number of identifications in the following LC-MS/MS step. The number of pools is dependent on the time available for LC-MS/MS data collection. Routinely 6–8 gel fragments provide deep proteome coverage, representing over a 1000 identified proteins.
18. The in-gel digestion procedure described estimates a total of 5–10 μg protein in each gel fragment. By adding 400 ng of trypsin to each pool we guarantee a minimal enzyme to substrate ratio of 1:25.
19. Desalting is required when the LC-MS/MS system does not operate with trapping columns. De-salting can be performed according to commercial C_{18} zip-tips or home-made stage tips, described elsewhere.
20. Using the described conditions and instrumentation, it is expected that each run contains at least 200 good protein identifications. When all fractions from the conditioned media and total cell extracts are taken together, this procedure is expected to generate a list of confident identifications containing more than 2000 protein hits.

21. Acquired data can be automatically processed by the open-source Labkey Server (www.labkey.org) platform, which employs the TransProteomic Pipeline, developed at the Institute of Systems Biology [22]. Search data against the most recent version of the human proteome database (Uniprot) or other appropriate human protein database of your choice. A fixed modification of 71.03712 and a variable modification of 3.01006 mass units are added to cysteine residues for database searches in order to account for incorporation of the light and heavy acrylamide isotopes into alkylated proteins. To estimate the significance of peptide and protein matches, we apply the tools PeptideProphet [23] and ProteinProphet [24]. Identifications with a PeptideProphet probability greater than 0.75 are selected and submitted to ProteinProphet to account for the protein inference problem. Overall, false discovery rates for this procedure are less than 2 %. Protein quantification can also be performed automatically with the Q3 tool available in the distribution of labkey server [21].
22. The spectral counting method can be used to estimate protein secretion enrichment as previously described [18]. Briefly, the total number of spectral counts for each protein group output by ProteinProphet for secreted profile over the spectral counts output for the total cell extract profile is used for a semiquantitative enrichment analysis. The total number of counts in the entire experiment is used as a normalization parameter for each profile.

Acknowledgements

This work was supported by the São Paulo State Research Foundation, Brazil, grant 2011/09740-1; CNPq (Conselho Nacional de Desenvolvimento Científico e Tecnológico), Brazil, Investigator Fellowship grant 301570/2011-6, Center for Integrative Systems Biology, University of São Paulo, grant 12.1.17598.1.3, and Center for Cell-Based Therapy (CTC-CEPID), grant 2013/08135-2.

References

1. Caplan AI (1991) Mesenchymal stem cells. J Orthop Res 9:641–650
2. Bianco P (2014) Stem cells and bone: a historical perspective. Bone 70:2–9
3. Pittenger MF, Mackay AM, Beck SC et al (1999) Multilineage potential of adult human mesenchymal stem cells. Science 284: 143–147
4. Jiang Y, Jahagirdar BN, Reinhardt RL et al (2002) Pluripotency of mesenchymal stem cells derived from adult marrow. Nature 418:41–49
5. da Silva Meirelles L, Chagastelles PC, Nardi NB (2006) Mesenchymal stem cells reside in virtually all post-natal organs and tissues. J Cell Sci 119:2204–2213

6. Lavoie JR, Rosu-Myles M (2013) Uncovering the secretes of mesenchymal stem cells. Biochimie 95:2212–2221
7. Makridakis M, Roubelakis MG, Vlahou A (2013) Stem cells: insights into the secretome. Biochim Biophys Acta 1834:2380–2384
8. Faça VM (2012) Human mesenchymal stromal cell proteomics: contribution for identification of new markers and targets for medicine intervention. Expert Rev Proteomics 9: 217–230
9. Granéli C, Thorfve A, Ruetschi U et al (2014) Novel markers of osteogenic and adipogenic differentiation of human bone marrow stromal cells identified using a quantitative proteomics approach. Stem Cell Res 12:153–165
10. Ishihara T, Kakiya K, Takahashi K et al (2014) Discovery of novel differentiation markers in the early stage of chondrogenesis by glycoform-focused reverse proteomics and genomics. Biochim Biophys Acta 1840:645–655
11. Miranda HC, Herai RH, Thomé CH et al (2012) A quantitative proteomic and transcriptomic comparison of human mesenchymal stem cells from bone marrow and umbilical cord vein. Proteomics 12:2607–2617
12. Rocha B, Calamia V, Casas V et al (2014) Secretome analysis of human mesenchymal stem cells undergoing chondrogenic differentiation. J Proteome Res 13:1045–1054
13. Choi YH, Kurtz A, Stamm C (2011) Mesenchymal stem cells for cardiac cell therapy. Hum Gene Ther 22:3–17
14. Cox J, Mann M (2011) Quantitative, high-resolution proteomics for data-driven systems biology. Annu Rev Biochem 80:273–299
15. Bensimon A, Heck AJ, Aebersold R (2012) Mass spectrometry-based proteomics and network biology. Annu Rev Biochem 81: 379–405
16. Kim JM, Kim J, Kim YH et al (2013) Comparative secretome analysis of human bone marrow-derived mesenchymal stem cells during osteogenesis. J Cell Physiol 228:216–224
17. Faca V, Pitteri SJ, Newcomb L et al (2007) Contribution of protein fractionation to depth of analysis of the serum and plasma proteomes. J Proteome Res 6:3558–3565
18. Faça VM, Ventura AP, Fitzgibbon MP et al (2008) Proteomic analysis of ovarian cancer cells reveals dynamic processes of protein secretion and shedding of extra-cellular domains. PLoS One 3:e2425
19. Emanuelsson O, Brunak S, von Heijne G et al (2007) Locating proteins in the cell using TargetP, SignalP and related tools. Nat Protoc 2:953–971
20. Petersen TN, Brunak S, von Heijne G et al (2011) SignalP 4.0: discriminating signal peptides from transmembrane regions. Nat Methods 8:785–786
21. Faca V, Coram M, Phanstiel D et al (2006) Quantitative analysis of acrylamide labeled serum proteins by LC-MS/MS. J Proteome Res 5:2009–2018
22. Rauch A, Bellew M, Eng J et al (2006) Computational Proteomics Analysis System (CPAS): an extensible, open-source analytic system for evaluating and publishing proteomic data and high throughput biological experiments. J Proteome Res 5:112–121
23. Keller A, Nesvizhskii AI, Kolker E et al (2002) Empirical statistical model to estimate the accuracy of peptide identifications made by MS/MS and database search. Anal Chem 74:5383–5392
24. Nesvizhskii AI, Keller A, Kolker E et al (2003) A statistical model for identifying proteins by tandem mass spectrometry. Anal Chem 75: 4646–4658

Chapter 32

Unraveling Mesenchymal Stem Cells' Dynamic Secretome Through Nontargeted Proteomics Profiling

Sandra I. Anjo, Ana S. Lourenço, Matilde N. Melo, Cátia Santa, and Bruno Manadas

Abstract

The modulatory and regenerative potential shown by the use of MSC secretomes has emphasized the importance of their proteomics profiling. Proteomic analysis, initially focused on the targeted analysis of some candidate proteins or the identification of the secreted proteins, has been changing to an untargeted profiling also based on the quantitative evaluation of the secreted proteins.

The study of the secretome can be accomplished through several different proteomics-based approaches; however this analysis must overcome one key challenge of secretome analysis: the low amount of secreted proteins and usually their high dilution.

In this chapter, a general workflow for the untargeted proteomic profile of MSC's secretome is presented, in combination with a comprehensive description of the major techniques/procedures that can be used. Special focus is given to the main procedures to obtain the secreted proteins, from secretome concentration by ultrafiltration to protein precipitation. Lastly, different proteomics-based approaches are presented, emphasizing alternative digestion techniques and available mass spectrometry-based quantitative methods.

Key words MSC secretome, Quantitative proteomics, Mass spectrometry

1 Introduction

The secretome – proteins released by cells, tissues, or organisms – has been shown to be important for the regulation of different cell processes [1]. In particular, the regenerative potential of mesenchymal stem cells (MSCs) and their secretome has been studied for potential applications in the central nervous system (CNS), which has a low regenerative potential [2].

The study of the secretome can be accomplished through several different proteomics-based technologies including gel and liquid approaches, as well as targeted and nontargeted quantification (Fig. 1). However this must overcome one key challenge of secretome analysis, which is the low amount of secreted proteins,

Massimiliano Gnecchi (ed.), *Mesenchymal Stem Cells: Methods and Protocols*, Methods in Molecular Biology, vol. 1416,
DOI 10.1007/978-1-4939-3584-0_32,

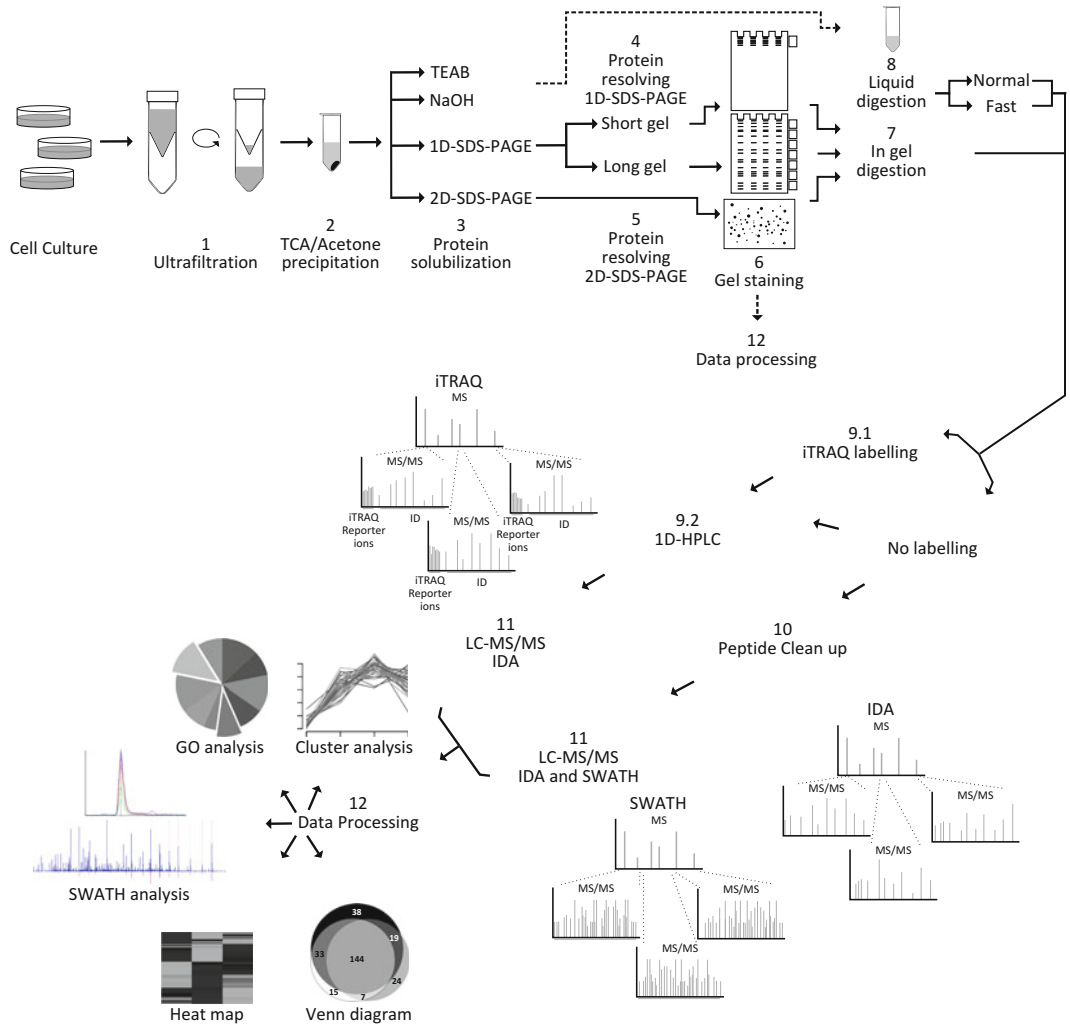

Fig. 1 General workflow for untargeted analysis of secretome

and in the case of cell culture, their high dilution in the culture medium [1]. Thus, a reduction in sample volume to concentrate the contained proteins is mandatory before analysis [1]. This can be achieved by using ultrafiltration, or even ultrafiltration followed by trichloroacetic acid (TCA) and acetone precipitation [1, 3, 4].

After protein precipitation, the choice of the buffer used must take into consideration the downstream applications. If liquid (or in solution) digestion is chosen, then a buffer without (or with low amounts of) detergents and salts should be considered. If the protein pellet is difficult to solubilize or if some sample separation is desired, then a more stringent buffer could be used followed by 1D- or 2D-Isoelectric Focusing-Sodium Dodecyl Sulfate Polyacrylamide Gel Electrophoresis (1D-SDS-PAGE or 2D-IEF-SDS-PAGE) and in gel digestion.

Due to the high complexity of diverse biological samples, various separation and fractionation techniques have been developed for proteins, or resulting proteolytic digests, in order to make mass spectrometry (MS)-based proteomics profiling more efficient and sensitive.

Fractionation at the protein level (by SDS-PAGE) has proven effective to improve the comprehensiveness of proteomics profiling, mainly by providing a simple and cost-effective procedure for sample prefractionation that results in a significant proteome complexity and dynamic range improvement [5–7]. Moreover, 1D-SDS-PAGE also comprises other appealing characteristics such as (1) its ability to efficiently remove low molecular weight contaminants, such as detergents and buffer components, that can interfere with protein digestion; (2) when combined with MS-compatible protein staining it provides visual quality control of the samples by estimating the relative protein amount and assesses sample complexity, which are beneficial to separate complex protein mixtures into several fractions; (3) it is preceded by a highly efficient denaturation method and is very robustly applied to a large variety of sample types; and (4) it can be applied to challenging samples, such as protein pellets which require the use of more stringent buffers for solubilization, such as 1D-SDS-PAGE buffer or the addition of high amounts of detergent [6–9]. Another advantage of using polyacrylamide gels for downstream protein identification is that SDS-PAGE gels are good containers for handling, concentrating, and storing proteins down to the femtomolar range [9].

If greater protein resolution is required, two-dimensional gel electrophoresis (2D-IEF-SDS-PAGE) represents a powerful method to separate a complex mixture of proteins [10]. This method is based on two separation processes: isoelectric focusing (IEF), which separates proteins according to their isoelectric point; and SDS-PAGE, which separates proteins according to their molecular weight [11]. With this technique, it is possible to resolve more than 5000 distinct protein spots when a combination of narrow pH range gels is used; while around 1000–3000 protein spots may be visualized when broad pH range gels are used (IPG 3-10 or IPG 4-7) [12]. Two-dimensional electrophoresis provides a way to discover differences in the protein expression of different experimental conditions, and allows the detection of protein isoforms and post-translational modifications [10].

To visualize the separated proteins (after both 1D- or 2D-IEF-SDS-PAGE) several protein staining methods are available and their selection is based on their sensitivity (detection limit), the linear dynamic range (for quantitative accuracy), the reproducibility, and compatibility with protein identification by MS [13]. Some examples include anionic dyes (e.g., Coomassie Blue), negative staining with metal cations (e.g., zinc imidazole), silver staining, and fluorescence staining. The most accurate results in terms of

sensitivity are obtained with silver nitrate and fluorescence staining; however, fluorescence staining – like Flamingo™ fluorescence gel stain (Bio-Rad) – is more suitable for quantification, since it exhibits a larger linear range.

Before MS analysis, samples must be subjected to a digestion protocol, which is a critical step in proteomics studies and several studies have tried to improve this process [8, 14]. The protocol comprises protein denaturation, reduction, alkylation, and tryptic digestion. Each one of these steps is critical to achieve good digestion: denaturation and reduction aim to unfold the proteins by breaking intramolecular forces and disulfide bonds; alkylation is crucial to block the cysteines responsible for the disulfide bonds; and lastly, and probably the most important step, digestion with an enzyme (usually trypsin) is used to enzymatically cleave the proteins into peptides, conventionally for 16 h at 37 °C [15] in liquid samples and overnight at room temperature for in gel digestion. In total, the preparation of a sample from protein to peptide mixture can take more than 18 h and it is a laborious procedure with much sample handling [8], although many efforts have been made to accelerate this process [16–19].

After a complex mixture of peptides is obtained, other substances may be present in a biological sample, like salts or detergents, which may influence the liquid chromatography coupled to mass spectrometry (LC-MS) analysis [20]. In order to avoid a decrease in the ionization efficiency, sensitivity and smaller detection dynamic range, a peptide purification or "cleanup" procedure should be performed [20]. For this purpose several commercial devices are available specifically for this application; the most widely used ones are based on a solid phase extraction technique. These can be adapted in 10 μL or 100 μL micropipette tips, making the sample cleanup procedure fast and easy. These tips are provided with several sorbents which should be chosen according to the application desired; and in the case of peptide mixtures the most widely used sorbent is C18.

Liquid chromatography coupled to tandem mass spectrometry (LC-MS/MS) is considered the method of choice for discovery/nontargeted proteomics studies where the major aim is the deep characterization of proteome changes across several samples. As most of those biological changes result in slight perturbations only detectable at the quantitative level, LC-MS/MS methods for identification and quantification of proteins are commonly applied [21]. For identification, the MS instrument is operated in information-dependent acquisition (IDA)/data-dependent acquisition (DDA) mode, where the fragment ions spectra are acquired for selected precursor ions detectable in a survey scan and used for peptide identification by sequence database searching. Shotgun proteomics is the method of choice for discovering the maximum number of proteins from one or a few samples; however this method has limited

quantification capabilities in large sample sets because of stochastic and irreproducible precursor ion selection [14].

Recently, major advances have been achieved in quantitative methods for proteomic workflows, mainly divided into two groups: label and label-free methods. The most common labeling methods include metabolic labeling such as SILAC; and labeling with heavy compounds, for example with ^{18}O labeling, or chemical labeling with isobaric compounds such as iTRAQ. The latter reagents are able to globally code the amino-terminal and lysine residues of all peptides in one sample making it possible to generate information on the relative and absolute peptide abundance for hundreds of proteins [22]. It also has the great advantage of allowing the simultaneous labeling of several biological or analytical replicates that are compared in one single LC-MS analysis, reducing the technical variability observed when several LC runs are necessary [6]. Each of the multiplexed samples is labeled with isotopic probes that when subjected to fragmentation will result in reporter ions with different m/z, which will make it possible to compare the relative abundances of a given peptide in up to eight samples in the same MS/MS spectra. This leads to an increase in sample complexity [6] and a 2D-LC-MS approach, with two peptide fractionation steps, should be used instead of the standard LC-MS approach. In order to perform this 2D-LC-MS analysis, several fractionation techniques can be chosen as the first dimension, such as strong cation exchange with salt or pH gradient and reversed phase at high pH [23, 24].

Label-free quantitative techniques have also become more robust over the last few years, mainly through the improvement of MS instrumentation and data processing algorithms. Such label-free methods measure protein abundance based on the analysis of integrated chromatographic peak areas of peptides or the number of MS/MS spectra (spectral counting) in a LC-MS/MS run. Among label-free technologies, the SWATH-MS method is a particularly promising quantitative method for routine high-throughput screening, due to its ability to combine the information acquired from shotgun proteomics to identify proteins and data-independent acquisition to accurately quantify a larger number of peptides [14]. SWATH-MS is a data-independent (DIA) label-free method where data are acquired by repeatedly cycling through sequential isolation windows over the whole chromatographic elution range. This generates a complete recording of the fragment ions spectra of all peptides detectable in a biological sample for which the precursor ion signals are within a user defined m/z vs. retention time (t_R) window [14, 25]. Therefore SWATH-MS allows relative and absolute quantification of thousands of peptides and proteins in a single LC-MS/MS run [22].

Once proteins have been detected and quantified, statistical analysis needs to be performed in order to find significant

differences between the groups of samples under study. Due to the complex patterns provided by proteomics screenings, the use of efficient and robust methods is fundamental [26]. Two approaches are mainly used to compare the relative protein levels in proteomics: univariate and multivariate analysis [27]. The univariate methods (e.g., Student's *t*-test, Mann-Whitney test, and ANOVA) consider the different proteins as independent measurements [27]. Multivariate analyses (as Principal Component Analysis, Linear Discriminant Analysis, and Clustering Analysis) consist of statistical techniques that exhibit the inter-relationship between a large number of variables, and are able to correlate multiple proteins with a specific experimental group [27]. To perform this type of analysis several software packages are available such as SPSS (Statistical Package for the Social Sciences) and Matlab.

Further meaningful biological information can be obtained by gene ontology analysis (for instance using GoMiner™, UniProt, PANTHER, or GOrilla for enrichment analysis) or other tools targeted for pathway elucidation (such as Ingenuity Pathway Analysis, DAVID, or Reactome).

2 Materials

2.1 Secretome Concentration

1. Centrifuge tubes.
2. Refrigerated centrifuge.
3. Centrifugal concentrators.

2.2 TCA/Acetone Precipitation

1. Laboratory deep freezer (–80 °C).
2. Sonicator with cuphorn (e.g., 750 W sonicator).
3. Refrigerated centrifuge.
4. Vortex.
5. Centrifuge tubes.
6. Micropipettes and micropipette tips.
7. Trichloroacetic acid (TCA).
8. Acetone (prechilled to –20 °C).

2.3 Protein Solubilization

2.3.1 Protein Solubilization for 1D-SDS-PAGE

1. Laemmli buffer: (6× concentrated) 350 mM/0.28 % Tris–HCl/SDS pH 6.8, 30 % (v/v) Glycerol, 10 % (w/v) SDS, 0.93 % (w/v) dithiothreitol (DTT), bromophenol blue; or commercially available Laemmli buffer (e.g., 2× Laemmli buffer, Bio-Rad, composition: 65.8 mM Tris–HCl, pH 6.8, 2.1 % SDS, 26.3 % (w/v) glycerol, 0.01 % bromophenol blue).
2. Micropipettes and micropipette tips.
3. Vortex.
4. Spin.

5. Sonicator with cuphorn (e.g., 750 W sonicator).
6. Thermomixer.

2.3.2 Protein Solubilization for 2D-IEF-SDS- PAGE

1. 2D-Sample buffer: 6 M Urea, 1.5 M Thiourea, 3 % (w/v) CHAPS, 1.2 % (v/v) Destreak, 1.5 % (v/v) IPG buffer, bromophenol blue.
2. 2-D Quant Kit (GE Healthcare).
3. Vortex.
4. Spin.
5. Sonicator with cuphorn (e.g., 750 W sonicator).

2.3.3 Protein Solubilization for Liquid Digestion

1. 0.5 M TriEthyl Ammonium Bicarbonate buffer (TEAB).
2. 20 mM Sodium hydroxide (NaOH).
3. Water (LC Grade) – (H_2O).
4. Sonicator with cuphorn (e.g., 750 W sonicator).
5. Sonicator with 3 mm tip.

2.4 Protein Resolving by 1D-SDS-PAGE

1. Vertical protein gel electrophoresis system.
2. Power supply.
3. Commercially available precast polyacrylamide gels.
4. Commercially available 10× concentrated Tris/Glycine/SDS Buffer: 250 mM Tris, 1.92 M Glycine, 1 % (w/v) SDS, pH 8.3.
5. Molecular weight marker (commercially available).
6. Micropipettes and micropipette tips.
7. Vortex.
8. Spin.

2.5 Protein Resolving by 2D-IEF-SDS-PAGE

1. IPG strips pH 4–7.
2. Protean IEF cell.
3. Focusing tray 24 cm.
4. Equilibrium buffer: 50 mM Tris-HCl pH 8.8, 30 % (v/v) glycerol, 2 % (w/v) SDS.
5. 1 % (w/v) dithiothreitol (DTT).
6. 2.5 % (w/v) iodoacetamide (IAA).
7. Rehydration/equilibration trays 24 cm.
8. Protean Plus Hinged spacer plates and combs.
9. 10 % Polyacrylamide gel.
10. 0.5 % (w/v) low melting agarose.
11. Protean plus Dodeca cell.
12. Power supply.

2.6 Gel Staining

2.6.1 Flamingo Staining

1. 40 % (v/v) ethanol.
2. 10 % (v/v) acetic acid.
3. Flamingo™ fluorescence gel stain.
4. Box (to put the gel in).
5. Double deionized water (ddH_2O).
6. Laser-based fluorescence scanner capable of exciting and detecting near 510 and 540 nm, respectively, or a system based on the UV transilluminator and CCD camera.

2.6.2 Colloidal Coomassie Staining

1. Scale.
2. Magnetic stirrer plate.
3. Orbital shaker.
4. Beakers.
5. Box (to put the gel in).
6. Graduated cylinder.
7. Micropipettes and micropipette tips.
8. Magnetic stirrer.
9. Methanol.
10. Ammonium sulfate.
11. 85 % (v/v) Orthophosphoric acid.
12. Coomassie Brilliant Blue G-250.
13. ddH_2O.
14. Fixation solution: 10 % (v/v) orthophosphoric acid (85 %), 10 % (w/v) ammonium sulfate, and 20 % (v/v) methanol.

2.7 In Gel Digestion and Peptide Extraction

1. 20 % (w/v) SDS.
2. 0.01 μg/μL Trypsin.
3. Ammonium bicarbonate.
4. Acetonitrile (ACN).
5. Formic acid (FA).
6. Scale.
7. Concentrator (vacuum centrifuge).
8. Thermomixer.
9. Vortex.
10. Laminar flow hood.
11. Destaining solution for Colloidal Coomassie Staining: 50 mM ammonium bicarbonate and 30 % (v/v) Acetonitrile.
12. Spin.
13. Low binding microcentrifuge tubes.
14. Centrifuge tubes.

15. Micropipettes and micropipette tips.
16. Scalpel blade.
17. Plastic sheet.
18. ddH_2O and LC grade water.
19. Disposable grid cutter, 2 mm × 7 mm lanes, 25 rows.
20. Spot picking station.

2.8 Liquid Digestion

1. Sonicator with cuphorn (e.g., 750 W sonicator).
2. Vortex.
3. Thermomixer.
4. Concentrator (vacuum centrifuge).
5. Low binding microcentrifuge tubes.
6. Microcentrifuge tubes carrier.
7. Micropipettes and micropipette tips.
8. 0.5 M TEAB.
9. Water (LC Grade) – (H_2O).
10. 50 mM Tris-(2-CarboxyEthyl)Phosphine – (TCEP).
11. 200 mM Methyl MethaneThioSulfonate (in isopropanol) – (MMTS).
12. 0.5 μg/μL Trypsin.
13. Formic Acid.
14. Methanol.

2.9 iTRAQ

2.9.1 iTRAQ Sample Preparation

1. Microcentrifuge tubes.
2. Sonicator with cuphorn (e.g., 750 W sonicator).
3. Concentrator (vacuum centrifuge).
4. Micropipettes and micropipette tips.
5. iTRAQ kit (8-plex or 4-plex).
6. Spin.
7. 1 M TEAB.
8. Water (LC Grade).
9. Isopropanol (LC Grade) – (H_2O).
10. Acetonitrile (LC Grade).

2.9.2 iTRAQ 1D-LC or 2D-LC-MS/MS Analysis

1. Microcentrifuge tubes.
2. Sonicator with cuphorn (e.g., 750 W sonicator).
3. Concentrator (vacuum centrifuge).
4. Spin.
5. Micropipettes and micropipette tips.

6. C18 columns: 2 Aeris XB-C18 Phenomenex® (2.1 mm ID × 15 cm length, 3.6 μm particles).
7. Mobile phases for HPLC:
   (a) Mobile Phase A: 72 mM TEAB in water.
   (b) Mobile Phase B: 72 mM TEAB in ACN.

2.10 Peptide Cleanup by C18 Solid Phase Extraction

1. Bench-top Centrifuge.
2. Sonicator with cuphorn (e.g., 750 W sonicator).
3. Concentrator (vacuum centrifuge).
4. Micropipettes and micropipette tips.
5. SPE Tips with C18 matrix (e.g., OMIX tip C18 100 μL).
6. Microcentrifuge tubes (500 μL).
7. Low binding microcentrifuge tubes (500 μL or 1500 μL).
8. CombiTip (with precut end).
9. 50 % Acetonitrile.
10. 2 % Acetonitrile in 1 % Formic Acid.
11. 70 % Acetonitrile in 0.1 % Formic Acid.

2.11 LC-MS/MS Data Acquisition in IDA and DIA

1. Sonicator with cuphorn (e.g., 750 W sonicator).
2. Centrifuge.
3. Vials.
4. Micropipettes and micropipette tips.
5. Mass spectrometer: Triple TOF™ 5600 System operated by Analyst® TF 1.7.
6. Electrospray ionization source.
7. HPLC: nanoLC Ultra 2D.
8. iRT Kit (Biognosys).
9. ChromXP™ C18AR reversed phase column (300 μm ID × 15 cm length, 3 μm particles, 120 Å pore size) for protein identification and iTRAQ analysis.
10. Halo Fused-Core™ C18 reversed phase column (300 μm ID × 15 cm length, 2.7 μm particles, 90 Å pore size) for protein identification and SWATH analysis.
11. Mobile phase for sample preparation: 2 % ACN in 0.1 % FA.
12. Mobile phases for HPLC:
    (a) Mobile Phase A: 0.1 % FA in water.
    (b) Mobile Phase B: 0.1 % FA in ACN.

2.12 Data Processing

1. Computer.
2. ProteinPilot™ software or another software for protein database search and/or iTRAQ relative quantification.
3. PeakView™ v1.1 with Protein Quantification 1.0 MicroApp or another software for label-free quantification.
4. PeakView™ v2.0.01 with SWATH™ processing plug-in.

3 Methods

3.1 Secretome Concentration

1. Collect 20–30 mL of cellular secretome (also called conditioned medium) into a centrifuge tube (*see* **Note 1**).
2. Centrifuge at 290 × *g*, for 5 min at 4 °C, to remove intact cells.
3. Transfer the supernatant to a new tube.
4. Concentrate the secretome using a low molecular weight cut-off concentrator in order to retain proteins.
5. Once the desired concentration is achieved, recover sample from the bottom of the concentrator pocket with a micropipette and transfer to a new tube [2].

3.2 TCA/Acetone Precipitation

1. Add 100 % TCA to the sample in order to obtain a final 20 % concentration.
2. Incubate in the –80 °C freezer, adapting the time to the sample (30 min to overnight).
3. Thaw the mixture slowly on ice.
4. Centrifuge at 15,000–20,000 × *g* for 20 min at 4 °C.
5. Discard the supernatant and add 100 μL of acetone (–20 °C) to the pellet.
6. Sonicate using the cuphorn with 1 s on, 1 s off pulses at 20 % intensity for 5 min.
7. Centrifuge at 15,000–20,000 × *g* for 20 min at 4 °C.
8. Discard the acetone and add the appropriate buffer, such as Laemmli buffer when 1D-SDS-PAGE is the next step; the 2D-Sample buffer for 2D-IEF-SDS-PAGE; or TEAB when liquid digestion follows and dissolve the pellet [2].

The TCA/acetone precipitation can produce pellets that are difficult to dissolve. To avoid this problem, the acetone precipitation procedure [28] can be used or the protein pellet can be solubilized in a more stringent buffer [29].

3.3 Protein Solubilization

3.3.1 1D-SDS-PAGE Protein Solubilization

1. Prepare 1× or 2× Laemmli buffer solution from the 6× concentrated solution or prepare the desired volume of the commercial buffer by adding the proper amount of DTT (according to the manufacturer's indications) (*see* **Note 2**).

2. Add 20–30 μL of sample buffer (1× or 2× concentrated) to the protein pellets, vortex and spin.
3. Sonicate using the cuphorn with 1 s on, 1 s off pulses at 20 % intensity for 5 min (*see* **Note 3**).
4. Denature samples at 95 °C for 5 min (*see* **Note 4**).
5. Allow samples to reach room temperature and add acrylamide to a final concentration of 1 % (v/v).
6. The total protein concentration must be assessed with compatible assays for all buffer components.
7. Apply the entire sample, or an equal amount of protein per sample, in a polyacrylamide gel for 1D-SDS-PAGE and in gel digestion.

3.3.2 2D-IEF-SDS-PAGE Protein Solubilization

1. Solubilize proteins in the 2D-Sample buffer. Urea/thiourea is required to convert proteins into single conformations, contributing to hydrophobic protein solubilization and it also avoids protein-protein interactions. CHAPS is a zwitterionic detergent that increases the solubility of hydrophobic protein; the destreak reagent is a cocktail of reducing agents, containing DTT, β-mercaptoethanol, and TCEP; the IPG buffer, which is designed for generating pH gradients, improves the solubility of proteins by substituting ionic buffers.
2. Keep samples on ice and sonicate to improve protein recovery [29] (*see* **Note 5**).
3. Centrifuge samples at 20,000×*g* for 15 min to remove the insoluble material.
4. Assess the total protein concentration with specific assays compatible with the sample buffer reagents, such as the 2-D Quant Kit.

3.3.3 Solubilization for Liquid Digestion

1. Add the desired volume of 0.5 M TEAB (*see* **Note 6**).
2. Sonicate samples for 2 min with 20 % amplitude and 1 s on, 1 s off cycles. Repeat until a good solubilization is achieved (*see* **Note 7**).
3. The total protein concentration must be assessed with compatible assays for the different buffer components.

The choice of buffer in which the proteins must be solubilized prior to the digestion is very important. TEAB is MS-friendly and also compatible with iTRAQ labeling. Alternatively, NaOH may also be used to efficiently solubilize more difficult precipitated protein samples [30]; however it is a salt buffer with an extreme pH, which makes it necessary to adjust the pH prior to protein digestion and a desalting step prior to LC-MS analysis.

When dealing with more difficult samples, such as membrane proteins, the use of a small percentage of organic solvents, such as 10 % (v/v) methanol, may be beneficial in this solubilization step.

3.4 Protein Resolution by 1D-SDS-PAGE

1. Prepare samples (*see* Subheading 3.1) (*see* **Note 8**).
2. Prepare the precast gel(s) as recommended by the manufacturer. Gradient gels should be used to promote a better separation of proteins from complex mixtures. The use of precast gels and commercially available solutions will reduce sample contamination with keratin, and increase the reproducibility of the experiments.
3. Prepare the desired volume of 1× Tris/Glycine/SDS buffer from the 10× concentrated solution.
4. Place the gel cassette(s) onto the gel supports.
5. Transfer the holder to the electrophoresis system tank and fill the chamber and the tank with 1× running buffer (Tris/Glycine/SDS solution).
6. Wash the wells with running buffer.
7. Load the samples and the molecular weight markers. Leave one empty lane between samples in order to avoid cross contamination and fill the empty lane with an equal volume of 1× Laemmli buffer (*see* **Note 9**).
8. Run at 150–200 V (constant voltage) until the tracking dye reaches the bottom of the gel. The electrophoretic run should be stopped as soon as the tracking dye reaches the bottom of the gel in order to retain low molecular weight proteins that could be lost in the SDS-PAGE separation. For a similar reason, the stacking gel should also be maintained and analyzed in order to assess the high molecular weight proteins (*see* **Note 10**).
9. Open the gel cassette, remove the gel, and place it into a container with ddH_2O.
10. Stain the gel with the appropriate staining in order to visualize protein separation.

3.5 Protein Resolution by 2D-IEF-SDS-PAGE

1. Rehydrate 300 μg of protein for 12 h at 50 V using pH 4–7 strips of 24 cm.
2. Isoelectric focus the proteins as follows: 500 V (500 V h step and hold (SH)), 1000 V (1000 V h SH), 10,000 V (15,000 V h with linear increase), and final focusing at 10,000 V during 14 h, using a Protean IEF cell with a current limit of 50 μA per strip.
3. Incubate the IPG strip in the reducing equilibration buffer in the presence of 1 % (w/v) DTT for 15 min.
4. Incubate the IPG strip for an additional 15 min step in the alkylation equilibration buffer in the presence of 2.5 % (w/v) iodoacetamide.
5. Place the IPG strips on top of a 10 % acrylamide gel, and overlay with 0.5 % (w/v) low melting agarose.
6. Run the gel at 3 W/gel for 30 min, followed by 200 V for 6 h, at 20 °C.

3.6 Gel Staining

3.6.1 Flamingo Staining

1. Fix the gel overnight in 40 % (v/v) ethanol and 10 % (v/v) acetic acid.
2. Stain the gel for 8 h in 1× Flamingo staining solution.
3. Equilibrate the gel overnight in distilled water under agitation with an orbital shaker.
4. Acquire the gel image using a laser-based fluorescence scanner or a system based on the UV transilluminator and CCD camera.
5. Store in ddH_2O [for long period storage add NaN_3 at a final concentration of 0.1 % (w/v)].

3.6.2 Colloidal Coomassie Staining

1. Prepare the fixation solution.
2. Wash the gel with ddH_2O in an appropriate support (box) for 1 min.
3. Remove the water and add the fixation solution.
4. Incubate with agitation using an orbital shaker at low speed.
5. Add 100 mg of coomassie to the solution using a strainer, in order to prevent the formation of clusters.
6. Incubate with agitation for 1–2 h to visualize the protein staining.
7. Discard the solution in an appropriate disposal recipient and put the gel in a new box with ddH_2O.
8. Incubate with agitation using an orbital shaker at low speed.
9. Change the ddH_2O until the gel background is clear.
10. Store in ddH_2O [for long period storage add NaN_3 at a final concentration of 0.1 % (w/v)] [31].

Visual analysis of the patterns obtained after the staining frequently provides the first indications of possible differences between the conditions in the study as well as possible interesting bands. The staining is also very useful to verify if the amount of protein loaded was similar, and to define which bands should be analyzed and/or how gel bands will be combined for posterior analysis by mass spectrometry.

3.7 In Gel Digestion and Peptide Extraction

1. Wash gloves and an acetate sheet with SDS.
2. Perform gel band cutting as follows (*see* **Note 11**):
   - Place the acetate sheet in the laminar flow hood.
   - Transfer the gel to the acetate sheet.
   - Cut the gel lane with a scalpel blade or for equal sized bands use a disposable gridcutter.
   - Put 1 mL of ddH_2O in a clean microcentrifuge tube.

- Divide each band into small pieces and transfer them to the microcentrifuge tube.

3. For 2D gel spots, proceed with a similar protocol using a pre-cut micropipette tip larger than the spot size, or use an automated spot picking station.
4. Perform gel band/spot destaining as follows:
   - Prepare the destaining solution for Colloidal Coomassie Staining.
   - Remove the water from the microcentrifuge tube and add 1 mL of destaining solution.
   - Agitate for 15 min at 25 °C and ≈850 rpm.
   - Remove the destaining solution and verify if all the stain has been removed, otherwise repeat the process.
   - Add 1 mL of water (to wash) and shake for 10 min at 25 °C and ≈850 rpm.
5. Dry the gel pieces using a Concentrator ("speedvac"/vacuum centrifuge) for 1 h (*see* **Note 12**).
6. Perform the tryptic digestion as follows:
   - Prepare a 10 mM ammonium bicarbonate solution.
   - Prepare trypsin solution (0.01 μg/μL) by dissolving the powder in the ammonium bicarbonate solution.
   - Prepare several aliquots of the trypsin solution to prevent frequent freeze/thaw cycles.
   - Add trypsin until all the band pieces are covered with the solution (≈30 μL/gel band or spot).
   - Incubate for about 10 min at 4 °C, until the gel pieces are rehydrated and if necessary add more ammonium bicarbonate solution until all band pieces are covered with the solution.
   - Incubate overnight at room temperature in the dark (see Note 13).
7. Perform peptide extraction as follows:
   - Prepare the extraction solutions (in LC grade water):
     - Solution A: 30 % Acetonitrile, 1 % Formic Acid.
     - Solution B: 50 % Acetonitrile, 1 % Formic Acid.
     - Solution C: 98 % Acetonitrile, 1 % Formic Acid.
8. Remove excess solution from gel pieces (containing trypsin and some peptides) and transfer to a low binding microcentrifuge tube.
9. Add 40 μL of Solution A to the gel pieces and agitate for 15 min at 25 °C and 1050 rpm.

10. Transfer the solution with peptides to the same low binding microcentrifuge tube referred above.
11. Add 40 μL of Solution B to the gel pieces and agitate for 15 min at 25 °C and 1050 rpm.
12. Transfer the solution with peptides to the same low binding microcentrifuge tube referred above.
13. Add 40 μL of Solution C to the gel pieces and agitate for 15 min at 25 °C and 1050 rpm.
14. Transfer the solution with peptides to the same low binding microcentrifuge tube referred above.
15. Evaporate the peptides' extraction solutions, almost completely, using a vacuum concentrator.
16. Proceed to C18 cleanup protocol or iTRAQ labeling [28, 32] (*see* **Note 14**).

3.8 Liquid Digestion

3.8.1 Standard Procedure

1. Pipette the amount of necessary protein (from 10 to 100 μg) from each sample to a low binding microcentrifuge tube.
2. Add 0.5 M TEAB to reach a 45 μL of volume.
3. Vortex and spin.
4. Add 4 μL of 50 mM TCEP.
5. Vortex and spin.
6. Sonicate with the cuphorn for 1 min with low amplitude, 1 s on, 1 s off cycles.
7. Add 2 μL of 200 mM MMTS and incubate for 10 min at room temperature.
8. Add 0.5 M TEAB to reach a final volume for the tryptic reaction of 100 μL (include the volume of trypsin to be added afterwards).
9. Vortex and spin.
10. Add trypsin in a defined ratio [from 1:20 (w/w) to 1:50 (w/w)].
11. Mix in a Thermomixer at 600 rpm for 1 min.
12. Incubate for 16 h at 37 °C, if possible in a wet chamber.
13. After 16 h, add 2 μL of 100 % formic acid to stop the digestion (*see* **Note 15**).
14. Vortex and spin.
15. Evaporate the sample in a vacuum concentrator.
16. Proceed to C18 cleanup protocol or iTRAQ labeling.

3.8.2 Fast Procedure

1. Perform the first seven steps of the standard procedure.
2. Add 10 μL of methanol.

3. Add 0.5 M TEAB to reach a final volume for the tryptic reaction of 100 μL (include the volume of trypsin to be added afterwards).
4. Vortex and spin.
5. Add trypsin in a defined ratio [from 1:20 (w/w) to 1:50 (w/w)].
6. Sonicate with the cuphorn for 15 min with low amplitude, 1 s on, 1 s off cycles.
7. Add 2 μL of 100 % formic acid to stop the digestion (*see* **Note 15**).
8. Vortex and Spin.
9. Evaporate the sample in the vacuum concentrator.
10. Proceed to C18 cleanup protocol or iTRAQ labeling.

3.9 iTRAQ

3.9.1 iTRAQ Sample Preparation

1. Prepare a solution with 70 % (v/v) isopropanol and 30 % (v/v) 1 M TEAB.
2. Add 75 μL of the solution prepared in **step 1** to the evaporated peptides (after liquid digestion of 20–100 μg of protein) (*see* **Note 16**).
3. Sonicate at 20 % amplitude for 10 min with 1 s on, 1 s off cycles.
4. Spin all samples.
5. Thaw iTRAQ reagent vials and bring to room temperature.
6. Spin iTRAQ vials.
7. Add the first sample to the first vial (write down which sample belongs to each iTRAQ channel).
8. Vortex and spin.
9. Add 10 μL of 70 % (v/v) isopropanol in TEAB to the sample tube.
10. Rinse and spin.
11. Transfer to the iTRAQ vial (*see* **Note 17**).
12. Repeat last 5 steps for the remaining samples and iTRAQ vials.
13. Incubate for 2 h at room temperature.
14. Add 100 μL of water to each vial.
15. Vortex and spin.
16. Incubate for 30 min at room temperature.
17. Combine all samples in one low binding microcentrifuge tube (mix sample).
18. Add 100 μL of 50 % ACN to the first vial.
19. Rinse and spin.
20. Transfer the solution to the second vial.

21. Rinse and spin.
22. Repeat the last four steps until all vials have been "cleaned."
23. Combine the "wash" with the mix.
24. Prepare the mix for LC-MS/MS, 2D-LC-MS/MS analysis or keep at –80 °C until further analysis.

3.9.2 iTRAQ 1D-LC Peptide Fractionation

1. Prepare the necessary mobile phases: (a) 72 mM TEAB; (b) 72 mM TEAB in ACN.
2. After peptide labeling, evaporate the iTRAQ mix.
3. Resuspend in 280 μL (or desired volume) of the first dimension mobile phase, 2 % ACN in 72 mM TEAB (pH 8.5).
4. Sonicate for 2 min with 20 % amplitude with 1 s on, 1 s off cycles.
5. Centrifuge for 5 min at 14,100 × *g*.
6. Transfer the supernatant to a new microcentrifuge tube and discard the pellet (if any).
7. Inject the sample into the HPLC system with 2 online C18 reversed phase columns with the proper LC method (e.g., a 60 min linear gradient from 2 % ACN to 45 % ACN in 72 mM TEAB followed by a wash and an equilibration step).
8. Collect fractions as defined for your samples (e.g., the first fraction corresponds to the first 10–12 min; then collect one fraction per minute; and the last fraction would correspond to the last 10 min).
9. Combine fractions, either consecutive fractions or preferably interpolated fractions.
10. Evaporate all fractions.
11. Proceed to LC-MS/MS analysis.

3.10 Peptide Cleanup by C18 Solid Phase Extraction

1. Prepare all necessary solutions (*see* Subheading 2.10).
2. To the evaporated peptide mixture, add 100 μL of 2 % ACN in 1 % FA or adjust the sample to 2 % ACN in 1 % FA (*see* **Note 18**).
3. Sonicate in the cuphorn for 2 min with low amplitude and 1 s on, 1 s off cycles.
4. Wet the C18 tip by adding 100 μL of 50 % ACN from above.
5. Push the sample through the tip with the help of the precut CombiTip. Discard the flow through.
6. Repeat once more.
7. Equilibrate the tip by adding, from above, 100 μL of 2 % ACN in 1 % FA.
8. Push the sample through the tip with the help of the precut CombiTip. Discard the flow through.

9. Repeat two more times.
10. Apply the sample to the tip from above.
11. Push the sample through the tip with the help of the precut CombiTip. Transfer to the same sample microcentrifuge tube.
12. Repeat four more times.
13. Wash the tip by adding, from above, 100 μL of 2 % ACN in 1 % FA.
14. Push the sample through the tip with the help of the precut CombiTip. Transfer the flow through to a clean 500 μL microcentrifuge tube (*see* **Note 19**).
15. Elute peptides by adding, from above, 100 μL of 70 % ACN in 0.1 % FA (*see* **Note 20**).
16. Push the sample through the tip with the help of the precut CombiTip. Transfer the flow through to a new low binding microcentrifuge tube.
17. Repeat three more times.
18. Evaporate all samples.

3.11 LC-MS/MS Data Acquisition in IDA and DIA Modes

1. Spike cleaned/desalted samples with iRT peptides. iRT peptides can be used as internal standards to account for sample losses and/or t_R alignment (*see* **Note 21**).
2. Resuspend samples in mobile phase (2 % ACN in 0.1 % FA) to the desired volume. The volume should be adjusted according to sample amount and application. For example resuspend samples or each fraction in 30 μL of mobile phase.
3. Vortex and spin.
4. Sonicate using the cuphorn with 1 s on, 1 s off cycles at 20 % intensity for 5 min.
5. Centrifuge samples for 5 min at 14,000 × *g* to remove insoluble material.
6. Transfer the collected sample to the proper vial for LC-MS/MS.

3.11.1 LC Method

1. Inject the desired amount of sample. Usually 5–10 μL (from 30 μL of sample), depending on the sample concentration and/or application.
2. Resolve the peptide mixture on a C18 reversed phase column at 5 μL/min. The column should be chosen according to the application (*see* Subheading 2.11).
3. Elute peptides into the mass spectrometer with an acetonitrile gradient from 2 to 35–40 % ACN in 0.1 % FA. The length of the gradient should be adjusted according to sample complexity and application: for samples with a reduced complexity or those divided into a large number of fractions (GeLC-MS/

MS analysis) use a 25 min gradient; for samples with higher complexity or fewer number of fractions, such as liquid digestion, SWATH, and iTRAQ samples, use a 45 min gradient (*see* **Note 22**).

3.11.2 Information-Dependent Acquisition (IDA) Method for Identification/ Label-Free Quantification and for iTRAQ

For information-dependent acquisition (IDA), set the mass spectrometer with the proper parameters according to the application:

1. Scan full spectra from 350 to 1250 m/z for 250 ms.
2. Scan up to 20 or 30 MS/MS spectra from 100 to 1500 m/z for 75 to 100 ms accumulation time each. For iTRAQ always scan 30 MS/MS with 100 ms accumulation time.
3. For fragmentation, isolate the candidate ions that have a charge state between +2 and +5 and counts above a minimum threshold of 70 counts per second.
4. Exclude the candidate ion for 15–20 s after 1 MS/MS spectra is collected for normal IDA experiments or 2 MS/MS spectra in the case of iTRAQ.
5. Use rolling collision with a collision energy spread of 5 eV. For iTRAQ select the "iTRAQ rolling collision energy" option (*see* **Note 23**).

3.11.3 Data-Independent Acquisition: SWATH (Sequential Windowed Data-Independent Acquisition of the Total High-Resolution Mass Spectra) Acquisition Method

1. Analyze samples in two phases:
   - One third of the sample should be used for information-dependent acquisition (IDA) to build the library of precursors and fragments for data analysis (*see* **Note 24**).
   - Two thirds of the sample should be used in SWATH acquisition mode.
2. For SWATH-MS-based experiments, the mass spectrometer is operated in a looped product ion mode. The instrument is specifically tuned to allow quadrupole resolution of a specific mass selection. By using an isolation width plus 1 Da and by containing 1 m/z of overlap, a complete transmission is achieved [33]. A typical SWATH acquisition method should comprise the following parameters:
   - Scan full spectra from 350 to 1250 m/z for 50 ms accumulation time.
   - 30 Overlapping windows of 25 Da width across the range of 350–1100 m/z.
   - Scan MS/MS spectra from 100 to 1500 m/z for 100 ms accumulation time each.
   - Rolling collision energy spread of 15 eV with a collision energy for each window determined for a charge +2 ion centered upon the window (*see* **Notes 23** and **25**).

3.12 Data Processing

3.12.1 2D Image Analysis

Once the images are acquired, a computer-assisted analysis of 2D gels is performed using dedicated software such as PDQuest™, to identify differential protein expression across multiple experimental conditions.

The steps for gel analysis using PDQuest™ can be summarized as follows:

1. Image filtering: removes noise features on the image while leaving larger features (such as spots) unaffected. To reduce this high-frequency background noise, the signal is extracted by applying a Gaussian smoothing filter.
2. Automated spot detection: the faintest spot is selected first (this will set the sensitivity and minimum peak value parameters), followed by selection of the largest spot on the image.
3. Image alignment: gels are aligned via polynomial image warping. First the landmarks on each image are identified and the reference gel is then chosen. The alignment algorithm attempts to superimpose these landmarks by stretching and shrinking the images.
4. Spot matching: groups of gels can be edited and matched to one another in a match set. A match set consists of gel spot files and gel images, where protein spots are matched to each other.
5. Normalization: when comparing gels in a match set, there is often some variation in spot size and intensity between gels that is not due to differential protein expression. This variation can be caused by a number of factors including pipetting errors during sample preparation and loading, variations in sample density, inconsistencies in staining, etc. To accurately compare spot volume between gels, the data should be normalized to compensate for these nonexpression variations in spot intensity. One example is the local regression model algorithm, the most sophisticated normalization method available in PDQuest™, which is less susceptible to outliers than a simple linear regression and also corrects for differences in labeling efficiency resulting from differences in the total amount of protein loaded. This normalization method calculates a curve in the scatter plot, which minimizes the distance to all points in the plot.

3.12.2 Protein Identification Using ProteinPilot™ Software

1. Perform peptide identification by searching the IDA files with ProteinPilot™ software using the following search parameters:
   - Protein database: UniProtKB/Swiss-Prot database (fasta file) (nonredundant database).
   - Species: Search against all species or restrict the search to a specific species (*see* **Note 26**).
   - Alkylating agent: MMTS, Acrylamide, IAA, or other.
   - Enzyme: usually trypsin.

- Special factors (optional): such as Gel-based ID and Urea denaturation (*see* **Note 27**).

2. Perform a False Discovery Rate (FDR) analysis by using the target-decoy approach provided with ProteinPilot™ software. This analysis will assess the quality of the identifications. Positive identifications should be considered when both proteins and peptides identified reach a 5 % local FDR confidence [34, 35].

3.12.3 Protein Quantification

Relative Peptide Query (rPQ)

1. Perform peptide identification as described in "Protein Identification Using ProteinPilot™ Software" (*see* Subheading 3.12.2)
2. Calculate the rPQ for each protein identified by performing the ratio between the unique peptides identified in the two samples [36].

Area Under the Curve (AUC) of Precursor Ions

1. Use the files obtained in IDA mode to create a specific library of precursor masses. To obtain the library, perform peptide identification as described in "Protein Identification Using ProteinPilot™ Software" (*see* Subheading 3.12.2). The library can be created by:
   - Combining all files from the IDA experiments (all fractions from all samples analyzed).
   - Use the IDA from the pool of all samples.
2. Process data using the Protein Quantification plug-in for PeakView™:
   - Upload the library file, i.e., the *.group file obtained in ProteinPilot™ database search.
   - Indicate the number of proteins to analyze. This number should correspond to the proteins detected with 5 % local FDR.
   - Import the IDA files.
   - Exclude peptides with biological modifications and/or peptides shared between different protein entries/isoforms.
   - Define the peptide confidence. This number should correspond to the confidence at 5 % local FDR from ProteinPilot™ searches.
   - Define the Peak Area Options:
     - XIC Display Window: this value should be adjusted to accommodate the entire chromatographic peaks, usually around 5 min.
     - XIC width (AMU): dependent on instrument mass error, usually around 0.07 Da.

3. Extract areas. Areas will be calculated at two different levels: peptide and protein level. The protein areas correspond to the sum of all the peptides areas.
4. Filter the data according to the experimental setup, usually only considered non-null peptides in at least two biological replicates.
5. Estimate the levels of the proteins in the study. Protein levels correspond to the sum of all peptides areas that were retained after filtering (an adaptation of [37]).
6. If necessary, normalize the data using the most appropriate method. Different methods for normalization can be used, such as:
   - Normalization for the more stable internal standard (if available) or for a specific protein.
   - To the total intensity of each sample.
7. After analyzing the results, export them into generic text files; this will make it possible to perform other analyses (such as functional analysis, clustering, among others).

SWATH Data

1. Use the files obtained in IDA mode and the resulting ID file to create a specific library of precursor masses and fragments. To obtain the library, perform peptide identification as described in "Protein Identification Using ProteinPilot™ Software" (*see* Subheading 3.12.2). The library can be created by:
   - Combining all files from the IDA experiments (all fractions from all samples analyzed).
   - Use the IDA from the pool of all samples.
2. Process SWATH data using the SWATH™ processing plug-in for PeakView™:
   - Upload the library file, i.e., the *group file obtained in ProteinPilot™ database search.
   - Indicate the number of proteins to analyze. This number should correspond to the proteins detected with 5 % local FDR.
   - Exclude peptides with biological modifications and/or peptides shared between different protein entries/isoforms.
   - Import the SWATH files.
   - If necessary perform t_R alignment. To that, select the iRT peptides (if the samples were spiked with them) or several peptides along the chromatographic run from a protein present in all samples using the "RT+ Cal" icon. This will add a new protein (Retention time calibration protein) to the protein list. Select this protein to apply the t_R calibration to the remaining data set.

- Define the Processing Setting:
  - Peptide filter: use up to 15 peptides identified below the 5 % local FDR from ProteinPilot™ searches with up to five transitions per peptide.
  - XIC options:
    (i) XIC Extraction Window (min): Should be adjusted to accommodate entire chromatographic peaks. Usually around 3–5 min.
    (ii) XIC width (ppm or Da): Dependent on instrument mass error, usually around 0.02 Da or 10–100 ppm.
  - Peptides are confirmed by finding and scoring peak groups, which are a set of fragment ions for the peptide. Target fragment ions are automatically selected and peak groups scored following the criteria previously described [38]. Peak group confidence threshold is determined based on an FDR analysis using the target-decoy approach and 1 % extraction FDR threshold should be used for all the analyses.

3. Extract areas and peptides for FDR analysis. Note that areas will be calculated at three different levels: transition, peptide, and protein level. Peptide areas correspond to the sum of all the transitions areas and protein areas correspond to the sum of all the peptides areas.
4. Filter the data according to the experimental setup, usually only consider (1) non-null transitions/fragment ions and (2) peptides that meet the 1 % FDR in at least two biological replicates.
5. Estimate the levels of the proteins in the study. Protein levels correspond to the sum of all the transitions from all the peptides that were retained after filtering (an adaptation of [37]).
6. If necessary normalize the data using the most appropriate method. Different methods for normalization can be used, such as:
   - Normalization for the more stable internal standard (if available) or for a specific protein.
   - To the total signal of each sample.
7. After analyzing, export them into generic text files; this will make it possible to perform other analyses (such as functional analysis, clustering, among others).

3.12.4 iTRAQ Labeled Peptide Relative Quantification

1. Perform peptide identification and quantification by searching the IDA files with ProteinPilot™ software using the appropriate search parameters as in "Protein Identification Using ProteinPilot™ Software" (*see* Subheading 3.12.2); select "quantitate," "bias correction," and "background correction";

fill the iTRAQ isotope correction factors (standard definition already written but can be corrected for batch variances).

2. Perform an FDR analysis as described in "Protein Identification Using ProteinPilot™ Software" (*see* Subheading 3.12.2). Peptides used for quantification are automatically chosen (it is possible to alter these parameters although it is not recommended).
3. If not previously selected, perform Bias correction to correct for differences in total protein loading and background correction, use the last only when you are conducting a differential expression study. There is always the possibility of recalculating the search with and without these corrections.
4. Choose the channel to be used as the denominator for protein relative quantification (if dealing with several batches this channel should be the one with the same sample that is repeated throughout all batches). (*see* **Note 28**).
5. After analyzing the results with the software, export them into generic text files; this will make it possible to perform other analyses (such as functional analysis, clustering, among others).

4 Notes

1. This volume must be optimized for each cell culture type.
2. Sample buffer composition can be adjusted to increase the desired solubility of the proteins. In general, an increase in detergent and/or reducing agents can help to promote more efficient solubilization.
3. Repeat the sonication step if necessary to dissolve the pellets.
4. Protein denaturation promotes more efficient protein solubilization.
5. The sonication step is performed with increasing amplitude, starting from zero to 40 kHz, in five cycles of 10 s. Each cycle consists of 5 s of sonication followed by an interval of 5 s (to keep the samples at low temperature).
6. TEAB is a volatile buffer with the proper pH for trypsin enzymatic activity.
7. If the protein pellet is too hard to solubilize, then we suggest using NaOH and/or to sonicate for 30 s with the 3 mm tip at low amplitude and 1 s on, 1 s off cycles. If necessary, use the tip to disrupt the pellet to accelerate the solubilization.
8. Always denature and alkylate samples before SDS-PAGE.
9. Sample volumes should be similar, if necessary adjust the volume with Laemmli buffer (1×) and fill empty wells with the same volume of Laemmli buffer (1×).

10. As an alternative to the complete electrophoretic separation, a short run (as presented in [39, 40]) could be performed to allow the samples to enter into the gel. This will allow the use of more stringent buffers to solubilize the protein pellets and remove some sample contaminants that interfere with the digestion, while reducing the sample processing and improving reproducibility.
11. All precautions should be taken to avoid direct contact of the band with any potential dirty surface. Always wash the gloves after touching any potential dirty surface.
12. Dried gel pieces should be white.
13. When the digestion protocol is being performed in MW plates, place them in a box with water soaked paper in order to create a humid atmosphere and prevent spots from drying.
14. All reagents should be compatible with the iTRAQ protocol if this approach is used.
15. TEAB reacts with acid so some "bubbling" will be observed.
16. The organic solvent content of the buffer must be kept high (above 65 %); otherwise the labeling reaction will be quenched.
17. These five steps should be performed as quickly as possible once the labeling reaction starts.
18. The micropipette tips adapted for SPE applications have a known amount of sorbent, so do not exceed the correct amount of sample to be applied; otherwise some loss of peptides of interest can occur due to matrix saturation.
19. Store the wash until the LC-MS/MS analysis is finished, and discard it afterwards.
20. With this ACN percentage the solution will drop by gravity, so put the tip inside the respective microcentrifuge tube before adding the elution solution to the tip.
21. Concentration of iRT peptides in the sample can be 10× lower than that recommended by the manufacturer.
22. A typical LC method should comprise the following phases: (a) equilibration of the column (this phase is linked to the injection step); (b) gradient of organic solvent (could be linear or stepwise); (c) column wash with high organic content, and (d) re-equilibration of the column with high hydrophilic content of the mobile phase.
23. Some parameters of the acquisition method, such as the number of candidate ions and the accumulation time, should be adapted according to the sample and the chromatographic peak width, in order to be able to acquire the maximum information within a cycle time compatible with the chromatographic separation. A minimum of eight points should be acquired across the chromatographic peak to obtain a good

peak profile for quantitative purposes. In order to determine the compatible cycle time, the peak width should be divided by 8 (or by the desired number of points per peak). With the indicated chromatographic conditions, the cycle time is usually around 3 s.

24. Two approaches can be used to build the library: (a) individual analysis of all samples in the experimental setup or (b) single analysis of a pool of all the samples in the study. In both cases, the sample(s) can be analyzed unfractionated (if the complexity is not too great) or fractionated (in the case of a more complex sample).
25. Recent improvements in the SWATH acquisition algorithm allow the definition of windows with variable width across the chromatographic run. These improvements allow the design of more customized methods specific for the sample under analysis.
26. If the samples were spiked with iRT peptides (non-natural peptides), their sequence should be added to the database.
27. Alkylating agent and enzyme should be selected according to the digestion performed.
28. More than one batch of iTRAQ 8-plex can be used if the experimental design requires more than eight samples. In order to compare results from several batches, the same sample (usually a mix of all the samples to be analyzed, to theoretically guarantee that all the identified peptides are present in this sample) should be labeled with one channel in each batch and during the analysis this should be the channel used for normalization. If the samples to be analyzed are not too complex, one dimension LC followed by MS analysis (refer to LC-MS procedure) can be performed after the labeling and mixture cleanup (refer to C18 cleanup procedure).

Acknowledgments

This work was supported by Fundação para a Ciência e Tecnologia (FCT) (PTDC/SAU-NEU/103728/2008, PTDC/NEU-NMC/0205/2012, PEst-C/SAU/LA0001/2013–2014, and UID/NEU/04539/2013) and co-financed by "COMPETE Programa Operacional Factores de Competitividade," QREN; the European Union (FEDER – Fundo Europeu de Desenvolvimento Regional) and by The National Mass Spectrometry Network (RNEM) (REDE/1506/REM/2005). Sandra I. Anjo, Ana S. Lourenço, and Cátia Santa are supported by FCT PhD fellowships (SFRH/BD/81495/2011, SFRH/BD/78585/2011, and SFRH/BD/88419/2012).

References

1. Skalnikova H, Motlik J, Gadher SJ et al (2011) Mapping of the secretome of primary isolates of mammalian cells, stem cells and derived cell lines. Proteomics 11:691–708
2. Fraga JS, Silva NA, Lourenço AS et al (2013) Unveiling the effects of the secretome of mesenchymal progenitors from the umbilical cord in different neuronal cell populations. Biochimie 95:2297–2303
3. Jiang L, He L, Fountoulakis M (2004) Comparison of protein precipitation methods for sample preparation prior to proteomic analysis. J Chromatogr A1023:317–320
4. Isaacson T, Damasceno CM, Saravanan RS et al (2006) Sample extraction techniques for enhanced proteomic analysis of plant tissues. Nat Protoc 1:769–774
5. Jafari M, Primo V, Smejkal GB et al (2012) Comparison of in-gel protein separation techniques commonly used for fractionation in mass spectrometry-based proteomic profiling. Electrophoresis 33:2516–2526
6. Vowinckel J, Capuano F, Campbell K et al (2014) The beauty of being (label)-free: sample preparation methods for SWATH-MS and next-generation targeted proteomics. F1000Res 2, doi: 10.12688/f1000research.2-272.v2
7. Granvogl B, Ploscher M, Eichacker LA (2007) Sample preparation by in-gel digestion for mass spectrometry-based proteomics. Anal Bioanal Chem 389:991–1002
8. Switzar L, Giera M, Niessen WM (2013) Protein digestion: an overview of the available techniques and recent developments. J Proteome Res 12:1067–1077
9. Lundby A, Olsen JV (2011) GeLCMS for in-depth protein characterization and advanced analysis of proteomes. Methods Mol Biol 753:143–155
10. Carrette O, Burkhard PR, Sanchez JC et al (2006) State-of-the-art two-dimensional gel electrophoresis: a key tool of proteomics research. Nat Protoc 1:812–823
11. Magdeldin S et al (2014) Basics and recent advances of two dimensional-polyacrylamide gel electrophoresis. Clin Proteomics 11:16
12. Rogowska-Wrzesinska A, Le Bihan MC, Thaysen-Andersen M et al (2013) 2D gels still have a niche in proteomics. J Proteomics 88:4–13
13. Gorg A, Weiss W, Dunn MJ (2004) Current two-dimensional electrophoresis technology for proteomics. Proteomics 4:3665–3685
14. Gillet LC, Navarro P, Tate S et al (2012) Targeted data extraction of the MS/MS spectra generated by data-independent acquisition: a new concept for consistent and accurate proteome analysis. Mol Cell Proteomics 11(O111):016717
15. Capelo JL, Carreira R, Diniz M et al (2009) Overview on modern approaches to speed up protein identification workflows relying on enzymatic cleavage and mass spectrometry-based techniques. Anal ChimActa 650:151–159
16. Lopez-Ferrer D, Capelo JL, Vazquez J (2005) Ultrafast trypsin digestion of proteins by high intensity focused ultrasound. J Proteome Res 4:1569–1574
17. Russell WK, Park ZY, Russell DH (2001) Proteolysis in mixed organic-aqueous solvent systems: applications for peptide mass mapping using mass spectrometry. Anal Chem 73:2682–2685
18. Zhang N, Chen R, Young N et al (2007) Comparison of SDS- and methanol-assisted protein solubilization and digestion methods for Escherichia coli membrane proteome analysis by 2-D LC-MS/MS. Proteomics 7:484–493
19. Blonder J, Chan KC, Issaq HJ et al (2006) Identification of membrane proteins from mammalian cell/tissue using methanol-facilitated solubilization and tryptic digestion coupled with 2D-LC-MS/MS. Nat Protoc 1:2784–2790
20. Jehmlich N, Golatowski C, Murr A et al (2014) Comparative evaluation of peptide desalting methods for salivary proteome analysis. Clin Chim Acta 434:16–20
21. Ong SE, Mann M (2005) Mass spectrometry-based proteomics turns quantitative. Nat Chem Biol 1:252–262
22. Craft GE, Chen A, Nairn AC (2013) Recent advances in quantitative neuroproteomics. Methods 61:186–218
23. Manadas B, English JA, Wynne KJ et al (2009) Comparative analysis of OFFGel, strong cation exchange with pH gradient, and RP at high pH for first-dimensional separation of peptides from a membrane-enriched protein fraction. Proteomics 9:5194–5198
24. Manadas B, Mendes VM, English J et al (2010) Peptide fractionation in proteomics approaches. Expert Rev Proteomics 7:655–663
25. Liu Y, Hüttenhain R, Surinova S et al (2013) Quantitative measurements of N-linked glycoproteins in human plasma by SWATH-MS. Proteomics 13:1247–1256
26. Marengo E, Robotti E, Bobba M (2008) 2D-PAGE maps analysis. Methods Mol Biol 428:291–325

27. Carpentier SC, Panis B, Swennen R et al (2008) Finding the significant markers: statistical analysis of proteomic data. Methods Mol Biol 428:327–347
28. Vitorino R, Guedes S, Manadas B et al (2012) Toward a standardized saliva proteome analysis methodology. J Proteomics 75:5140–5165
29. Manadas BJ, Vougas K, Fountoulakis M et al (2006) Sample sonication after trichloroacetic acid precipitation increases protein recovery from cultured hippocampal neurons, and improves resolution and reproducibility in two-dimensional gel electrophoresis. Electrophoresis 27:1825–1831
30. Nandakumar MP, Shen J, Raman B et al (2003) Solubilization of trichloroacetic acid (TCA) precipitated microbial proteins via NaOH for two-dimensional electrophoresis. J Proteome Res 2:89–93
31. Candiano G, Bruschi M, Musante L et al (2004) Blue silver: a very sensitive colloidal Coomassie G-250 staining for proteome analysis. Electrophoresis 25:1327–1333
32. Correia S, Vinhas R, Manadas B et al (2012) Comparative proteomic analysis of auxin-induced embryogenic and nonembryogenic tissues of the solanaceous tree Cyphomandra betacea (Tamarillo). J Proteome Res 11:1666–1675
33. Gillet LC, Navarro P, Tate S et al (2012) Targeted data extraction of the MS/MS spectra generated by data-independent acquisition: a new concept for consistent and accurate proteome analysis. Mol Cell Proteomics 11:O111.016717
34. Tang WH, Shilov IV, Seymour SL (2008) Nonlinear fitting method for determining local false discovery rates from decoy database searches. J Proteome Res 7:3661–3667
35. Sennels L, Bukowski-Wills JC, Rappsilber J (2009) Improved results in proteomics by use of local and peptide-class specific false discovery rates. BMC Bioinformatics 10:179
36. Santos SD, Manadas B, Duarte CB et al (2010) Proteomic analysis of an interactome for long-form AMPA receptor subunits. J Proteome Res 9:1670–1682
37. Collins BC, Gillet LC, Rosenberger G et al (2013) Quantifying protein interaction dynamics by SWATH mass spectrometry: application to the 14-3-3 system. Nat Methods 10:1246–1253
38. Lambert JP, Ivosev G, Couzens AL et al (2013) Mapping differential interactomes by affinity purification coupled with data-independent mass spectrometry acquisition. Nat Methods 10:1239–1245
39. Paulo JA, Kadiyala V, Brizard S et al (2013) Short gel, long gradient liquid chromatography tandem mass spectrometry to investigate the urine proteome of chronic pancreatitis. Open Proteomics J 6:1–13
40. Anjo SI, Santa C, Manadas B (2014) Short GeLC-SWATH: a fast and reliable quantitative approach for proteomic screenings. Proteomics. doi:10.1002/pmic.201400221

Chapter 33

Identification of Factors Produced and Secreted by Mesenchymal Stromal Cells with the SILAC Method

Beatriz Rocha, Valentina Calamia, Francisco J. Blanco, and Cristina Ruiz-Romero

Abstract

Mesenchymal stromal cells (MSCs) secrete a large variety of proteins and factors, which shape the secretome. These proteins participate in multiple cellular functions, including the promotion of regenerative processes in the damaged tissue. Secretomes derived from either undifferentiated MSCs or these cells undergoing osteogenic, chondrogenic, or adipogenic differentiation have been characterized using different liquid chromatography tandem mass spectrometry (LC-MS/MS)-based quantitative proteomic approaches. In this chapter, we describe the use of the Stable Isotope Labeling by Amino Acids in Cell culture (SILAC) strategy for the identification and relative quantification of the mesenchymal stromal cell secretome, specifically during chondrogenesis.

Key words SILAC, Secretome, Conditioned medium, Mesenchymal stromal cells, Proteomics, Mass spectrometry, Chondrogenesis

1 Introduction

Protein secretion is a common, complex, and well-controlled process. Normally, cells react to different stimuli and signals that they receive from their environment, and consequently activate or inactivate the secretion of a number of bioactive molecules, including proteins. Protein secretion balance is essential for normal cell function. Thus, misbalance or alterations in the protein secretion profile (or secretome) can be indicative of a pathological condition [1]. Furthermore, the secretome also reflects the functional status of a cell in a given environment; hence secretomics is a very attractive approach for discovering novel diagnostic or prognostic biomarkers, and also putative therapeutic targets.

Secretomics is a recent proteomic approach that seeks to describe the secretome. The term *secretome* was introduced for the first time by Tjalsma et al. in a study of those proteins secreted by *Bacillus subtilis* [2]. It essentially describes the global set of

Massimiliano Gnecchi (ed.), *Mesenchymal Stem Cells: Methods and Protocols*, Methods in Molecular Biology, vol. 1416,
DOI 10.1007/978-1-4939-3584-0_33,

proteins secreted by a cell, tissue, or organism at any given time or under certain conditions through various secretory mechanisms. In addition, it is considered to be encoded by approximately 10 % of the human genome [3, 4]. The secretome constitutes an important class of proteins, including components of the extracellular matrix (ECM) and regulatory molecules. These play essential roles in several physiological and pathophysiological processes, such as cell signaling, differentiation, cell adhesion, angiogenesis, or apoptosis [5]. Mesenchymal stromal cells (MSCs) and other types of stromal cells have recently become targets of secretome profiling studies aiming to discover proteins regulating cell survival, proliferation, differentiation, or the inflammatory response. In fact, a variety of several different molecules, including growth factors and proteins binding to them, pro-inflammatory and anti-inflammatory cytokines, chemokines, ECM structural proteins and remodeling enzymes, have been identified in the secretomes of MSCs [6].

The secretome is a rather complex sample, mainly because of the difficulties in its collection and preparation for protein analysis. However, a fairly high number of proteomic studies have focused on its characterization in the past few years [7–9]. This illustrates the growing interest in the MSC secretome, which is largely due to the potential applications of these cells in regenerative medicine. Attempts to explore the MSC secretome have been promoted by relevant improvements in proteomic platforms and mass spectrometry (MS) instrumentation, together with advances in the protocols for MSC isolation, expansion, and differentiation. Different proteomic approaches, mainly MS-based quantitative strategies, are being employed for the large-scale analysis of the proteins secreted by MSCs. Quantitative proteomics analyses can be performed either by label-free approaches or via isotopic labeling (SILAC, ICAT, iTRAQ). In the latter workflow, stable isotopes can be incorporated into cellular proteomes by in vivo metabolic labeling (SILAC) or by in vitro labeling using chemical reagents (iTRAQ/ICAT).

We will focus on the application of SILAC (Stable Isotope Labeling by Amino acids in Cell culture) to identify proteins secreted by MSCs. This strategy is based on the incorporation of stable isotopically labeled amino acids into the newly synthesized proteins during cell culture [10]. SILAC has a higher quantitative accuracy than other labeling methods, considering that the conditions to be compared can be mixed at the cellular or protein level prior to any further sample preparation, thus minimizing handling errors. Furthermore, one of the major benefits of the SILAC approach in secretome studies is that contaminating proteins from the fetal bovine serum (FBS), normally employed in cell culture

media, can be easily discriminated from the MSC-derived proteins by their absence of stable isotope incorporation [11]. Due to these advantages, SILAC labeling has been recently employed for the study of protein secretion during osteogenesis [12] and chondrogenesis [13], and also to study the effects of basic fibroblast growth factor (bFGF) on MSC secretion [14]. Table 1 summarizes the proteomic studies performed to date on MSC secretomes using the SILAC approach.

In this chapter, we describe a double-SILAC strategy combined with liquid chromatography tandem mass spectrometry analysis (LC-MS/MS) for the identification and relative quantification of secreted proteins by MSCs (Fig. 1). Procedures for cell culture and labeling, sample preparation, digestion of proteins, separation and analysis of the corresponding peptides by nanoLC-MS/MS in a LTQ-Orbitrap, and finally data analysis using MaxQuant software are illustrated. The protocol provided below could potentially be applied to the study of any given cell secretome.

Table 1
Studies on mesenchymal stem cell (MSCs) secretomes using the SILAC approach

Origin	MSC source	Cell treatment	Cond. time[a]	Sample type	Proteomic technique	Ref.
Mouse	BM-MSCs	bFGF	32 h	Serum-free CM	SILAC + 1D SDS PAGE + LC-MS/MS	[14]
Human	hMSC-TERT cells (BM-MSCs)	Osteogenic differentiation	18 h	Serum-free CM	SILAC + 1D SDS PAGE + LC-MS/MS	[12]
Human	BM-MSCs	Chondrogenic differentiation	24 h	Serum-free CM	SILAC + 1D SDS PAGE + LC-MS/MS	[13]
Human	Adipose tissue	None	48–114 h (72 h for SILAC)	Serum-free CM	SILAC + 1D SDS PAGE + LC-MS/MS/SELDI	[11]
Mouse	3T3-L1 preadipocytes	Adipogenic differentiation	18 h at the end of 0, 1, 3, 5, and 7 days	Serum-free CM	SILAC + LC-MS/MS	[17]

CM conditioned medium, *BM-MSCs* bone marrow-derived mesenchymal stem cells, *bFGF* basic fibroblast growth factor, *LC-MS/MS* liquid chromatography–tandem mass spectrometry, *SDS PAGE* sodium dodecyl sulfate polyacrylamide gel electrophoresis, *SELDI* surface-enhanced laser desorption/ionization, *SILAC* stable isotopic labeling by amino acids in cell culture

[a]Conditioning (incubation) time

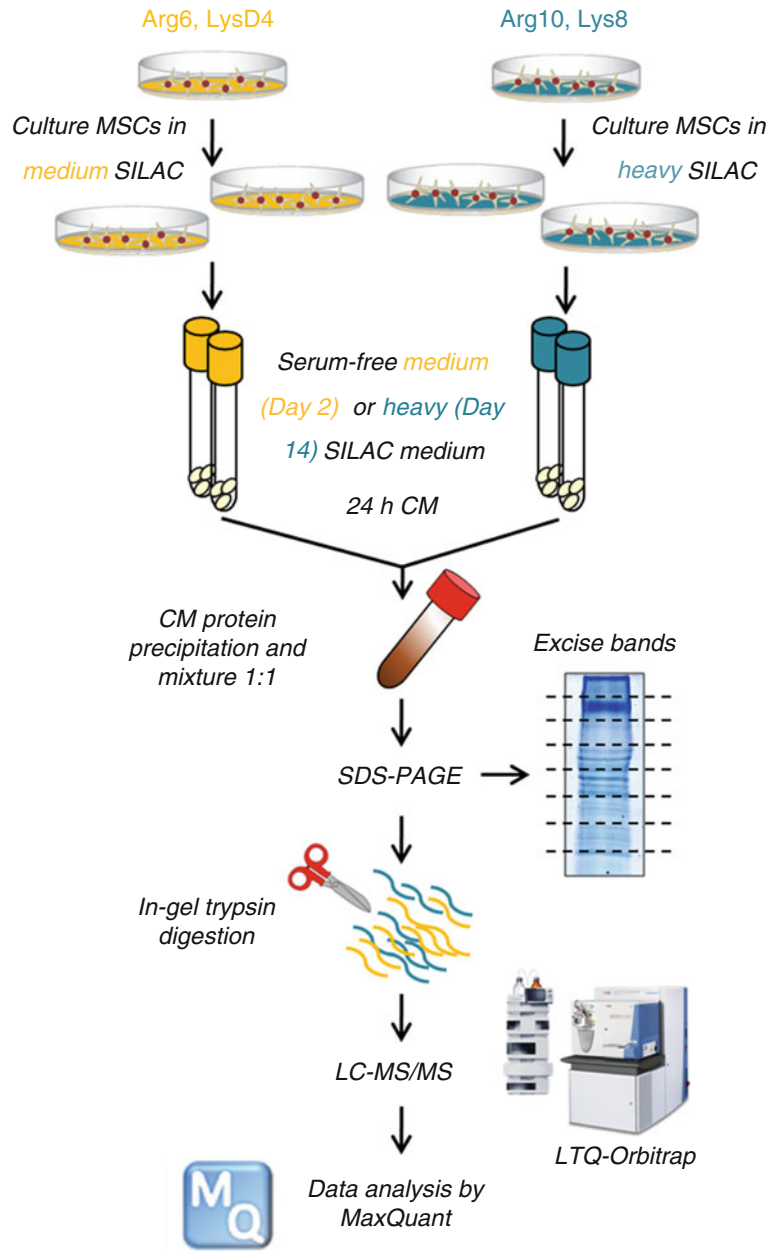

Fig. 1 Experimental workflow of a double-SILAC strategy applied to study the secretome of mesenchymal stromal cells (MSCs) during chondrogenic differentiation [13]. Two populations of MSCs were cultured with isotope variants of lysine and arginine (Arg6, Lys4 for the "medium" labeling and Arg10, Lys8 for the "heavy" labeling) over 6 weeks. The labeled populations were then subjected to differentiation in 3D cultures (micromasses) supplemented with chondrogenic inducers for 2 or 14 days. Proteins in the conditioned media (CM) from the two time points of differentiation were precipitated, combined at a 1:1 ratio, and resolved into eight fractions by SDS-PAGE. Gel bands were excised, subjected to in-gel digestion, and analyzed by LC-MS/MS. Data analysis was performed using the MaxQuant software

2 Materials

Prepare all solutions using Mass spectrometry (MS)-grade water and analytical grade reagents. Prepare and store all reagents at room temperature (unless indicated otherwise).

2.1 Cell Culture and SILAC Labeling

1. Human mesenchymal stromal cells (MSCs) isolated from trabecular bone marrow samples [15].
2. SILAC medium: Dulbecco's modified Eagle's medium (DMEM), 4.5 g/L glucose, without lysine and arginine.
3. Supplements: Dialyzed fetal bovine serum (dFBS), l-glutamine (200 mM), penicillin-streptomycin (P/S, 5000 U/ml-5000 μg/ml).
4. Heavy stable isotopes of amino acids: l-lysine-HCl-4,4,5,5-D_4 (Lys4), l-lysine-HCl-$^{13}C_6{}^{15}N_2$ (Lys8), l-arginine HCl-$^{13}C_6$ (Arg6), and l-arginine-HCl-$^{13}C_6{}^{15}N_4$ (Arg10) (all from Silantes GmbH, Mering, Germany). Dissolve 0.1 g of each amino acid in 1 mL of distilled water (100 mg/mL). Store at 4 °C.
5. Trypsin-EDTA solution (10×).
6. Tissue culture supplies, including cell culture flasks (25, 75, and 162 cm^2) and 15 mL conical polypropylene tubes.

2.2 Collection of Conditioned Media and Preparation of Protein Extracts

1. Protease inhibitors: protease inhibitor cocktail and 100 mM phenylmethylsulfonyl fluoride (PMSF) solution in isopropanol: dissolve 174.2 mg PMSF in 10 mL of isopropanol. Store both at −20 °C.
2. Prepare 0.2 % sodium deoxycholate (DOC) solution in water: dissolve 20 mg in 10 mL of distilled water.
3. Absolute trichloroacetic acid (TFA 99 % LC-MS).
4. Acetone (stored at −20 °C).
5. Urea lysis buffer: 6 M urea, 2 M thiourea, 4 % CHAPS, 30 mM Tris base. Dissolve 0.36 g of urea for electrophoresis (≥99 %), 0.15 g of thiourea (≥99 %), 40 mg of 3-[(3-cholamidopropyl) dimethylammonio]-1-propanesulfonate (CHAPS), and 3.63 mg of Tris base (≥99 %) in 1 mL of water (*see* **Note 1**). Make 100 μL aliquots and store them at −20 °C.
6. Bradford assay reagent and albumin standard, for protein quantification. Make 2 mg/mL aliquots and store them at 4 °C.
7. Syringe filters (0.22 μm pore size, PVDF).
8. Protein LoBind microcentrifuge tubes.
9. Refrigerated microcentrifuge.

2.3 Separation and Visualization of Proteins by SDS-PAGE and Gel Staining

1. Running buffer (10×): 250 mM Tris base, 1.92 M glycine, 1 % sodium dodecyl sulfate (SDS) in water. Dissolve 30.3 g of Tris base (≥99 %), 144 g of glycine, and 10 g of SDS in 1 L of distilled water.
2. Sample buffer (5×): 10 % SDS, 200 mM Tris–HCl pH 6.8, 50 % glycerol, 0.1 % bromophenol blue, 10 % β-mercaptoethanol. Mix all reagents except β-mercaptoethanol: 1 g SDS, 4 mL 200 mM Tris–HCl pH 6.8, 5 mL glycerol, and 100 μL bromophenol blue. Make 900 μL aliquots and store them at RT. Add 100 μL of β-mercaptoethanol to each aliquot before use.
3. Reagents for electrophoresis: 30 % acrylamide/bis-acrylamide solution, 2 M Tris base (≥99 %) pH 8.8, 1 M Tris base (≥99 %) pH 6.8, 10 % SDS solution, 20 % ammonium persulfate (PSA) solution, *N*,*N*,*N*′,*N*′-tetramethylethylenediamine (TEMED).
4. Coomassie Blue G-250.
5. Fixing solution: mix 24 mL distilled water, 25 mL ethanol, and 1 mL phosphoric acid.
6. Staining solution: mix 32 mL distilled water, 16.5 mL methanol, 1.5 mL phosphoric acid, 8.5 g ammonium sulfate, and 33 mg Coomassie blue G-250 (*see* **Note 2**).
7. Mini PROTEAN® 3 System (Bio-Rad, catalog number 1653311) or similar equipment for protein electrophoresis.
8. Plastic container for gel staining.

2.4 In-Gel Protein Digestion

1. 25 mM ammonium bicarbonate (AmBi, ≥99 %) in water: dissolve 19 mg in 10 mL of HPLC water (*see* **Note 3**).
2. 10 mM Dithiothreitol stock (DTT, ≥99 %) in 25 mM AmBi: dissolve 1.54 mg DTT in 1 mL of 25 mM AmBi.
3. 50 mM Iodoacetamide solution (IAA, ≥99 %): dissolve 9.25 mg IAA in 1 mL of 25 mM AmBi (*see* **Note 3**).
4. 0.1 % TFA solution: Add 1 μL of trifluoroacetic acid (TFA 99% LC-MS) to 999 μL of water.
5. 0.1 % TFA, 50 % ACN solution: Add 500 μL of ACN (ACN LC-MS CHROMASOLV, Sigma) and 1 μL of TFA to 499 μL of water.
6. Spectrometry grade trypsin stock (1 μg/μL in 0.01% TFA). Use trypsin solution at 6.66 ng/μL in 25 mM AmBi at 4 °C (*see* **Note 4**).
7. Sonication bath.
8. Thermoblock.
9. Vacuum microcentrifuge.

2.5 NanoLC-MS/MS and Data Analysis

1. Buffer A: 5 % Methanol (MeOH)/1 % Formic acid (FA) in LC-MS grade water. Add about 94 mL of water to a 100 mL graduated cylinder and bring the volume to 99 mL with MeOH. Transfer to a bottle and add 1 mL of FA.
2. Buffer A_1: 0.1 % FA in LC-MS grade water. Add about 100 mL of ACN to a 100 mL graduated cylinder. Transfer to a bottle and add 100 μL of FA.
3. Buffer B_1: 0.1 % FA in ACN. Add about 100 mL of ACN to a 100 mL graduated cylinder. Transfer to a bottle and add 100 μL of FA.
4. LC microvials.
5. C_{18} precolumn (5 × 0.3 mm, 5 μm, 300 Å; Agilent Technologies, Barcelona, Spain).
6. C_{18} column (75 μm id, 10 cm; Vydac MS Columns, Grace Davison Discovery Sciences).
7. Agilent 1200 nanoflow system (Agilent Technologies).
8. LTQ-Orbitrap XL mass spectrometer (ThermoFisher) equipped with a nanoelectrospray ion source (Proxeon Biosystems, Odense, Denmark).
9. Xcalibur 2.0.7. Orbitrap software.
10. MaxQuant software for data analysis.

3 Methods

3.1 Cell Culture and SILAC Labeling

1. Prepare SILAC medium by adding different isotope variants of Lys and Arg to DMEM 4.5 g/L glucose without Lys and Arg at a final concentration of 73 and 28 mg/L, respectively (*see* **Note 5**). Supplement the media with 10 % dFBS, 4 mM l-glutamine, and 1 % P/S.
2. Seed the MSCs (5×10^4) in two 25 cm^2 culture flasks (for the medium and heavy conditions).
3. After reaching 80 % confluence, wash the cells twice using PBS, and recover the cells from the culture flasks using a trypsin-EDTA solution (2×).
4. Subculture the MSCs using 75 cm^2 and then 162 cm^2 culture flasks (usually passages 5–6), until achieving complete incorporation of the labeled amino acids (*see* **Note 6**).
5. Induce MSC differentiation. For chondrogenic induction, place 2.5×10^5 cells in 15 mL conical polypropylene tubes and centrifuge at 400 × *g* for 10 min. Incubate the cell pellets in 500 μL of chondrogenic medium [15]. Change chondrogenic medium every 2 days.

3.2 Collection of Conditioned Media

1. At the selected differentiation time points, wash the cells carefully at least five times in serum-free media to remove the FBS-contaminating proteins.
2. Add SILAC medium without FBS.
3. After 24 h of incubation, aspirate the medium and place it into a 1.5 mL microcentrifuge tube.
4. Collect the conditioned medium (CM) by centrifugation at 400×*g* for 5 min (*see* **Note 7**).
5. Pass CM through a 0.2 μm filter (*see* **Note 8**).
6. Add 0.1 % of 100 mM PMSF solution and 0.1 % protease inhibitor cocktail to the CM sample.
7. The CM can be used immediately or stored at −80 °C.

3.3 Preparation of Secretome Extracts and SDS-PAGE

1. Add 1/10 (v/v) of 0.2 % DOC solution to the CM sample. Vortex thoroughly. Incubate on ice for 10 min.
2. Add 1/10 (v/v) of 100 % TCA. Vortex thoroughly. Let the sample precipitate for a minimum of 1 h at 4 °C, but preferably overnight.
3. Centrifuge samples at 14,000×*g* in a precooled centrifuge for 10 min, and remove the supernatant.
4. Wash the pellet with ice-cold acetone, vortex, and keep at −20 °C for at least 10 min. Repeat **step 3**.
5. Air-dry the protein pellet (with the tube open) less than 15 min to prevent complete desiccation. This will make resolubilization much more difficult.
6. Solubilize the pellet (approx. 1:10 w/v) in urea lysis buffer. Vortex thoroughly. Sonicate 3×20 s and burst on ice, with a 1 min chilling interval.
7. Centrifuge samples at 14,000×*g* in a precooled centrifuge for 10 min, transfer the supernatant to a new microcentrifuge tube and discard the pellet.
8. Proceed to protein quantification. Determine total protein concentration of each CM using the Bradford (or equivalent) protein assay. Make the standard curve using known concentrations of BSA.
9. Mix collected CMs in a 1:1 ratio according to measured protein concentrations. Add 5× loading buffer to the samples, and water to a final volume of 30 μL.
10. Perform a standard SDS-PAGE fractionation in an 8 % SDS-PAGE gel (maximum thickness 1 mm). Load the samples in the center lanes of the gel, leaving a blank well between them to avoid contamination. Mark a line 1–2 cm below the stacking gel (*see* **Note 9**).

11. Run the gel at 80 V, constantly, for approximately 45 min or until the dye front reaches the marked line.
12. Prepare 50 mL of fixing solution in a clean plastic bottle. Stop the electrophoresis and transfer the gel to a plastic container with fixing solution. Incubate in an orbital shaker for 30 min.
13. Prepare 50 mL of staining solution in a clean plastic bottle. Remove the fixing solution and replace it with staining solution. Incubation time depends on the sensitivity required, but it is recommended to discard the staining solution after observing colored bands (30 min–1 h).
14. Destain the gel in distilled water, exchanging the water multiple times.
15. Cut the entire gel lanes into slices with a clean scalpel and transfer gel pieces into 0.5 mL microcentrifuge tubes containing 100 μL of water. Each slice can be cut in half in order to obtain a technical duplicate of the sample. To improve protein recovery, minimize the size of excised bands (cut each band into small cubes). Note that smaller pieces could clog pipette tips (*see* **Note 10**).

3.4 In-Gel Protein Digestion

Volumes can be scaled up or down based on the size of the gel pieces.

1. Destain gel pieces: add 50 μL of 25 mM AmBi/ACN (1:1, v/v) and incubate at RT with occasional vortexing for 30 min (*see* **Note 11**).
2. Wash four times with 100 μL of water, 5 min each.
3. Add 50 μL of ACN and incubate at RT with occasional vortexing, until pieces become white and shrink. Discard ACN and evaporate the bands to dryness.
4. Add 10 mM DTT solution to completely cover gel pieces. Incubate for 1 h at 37 °C.
5. Add 50 μL of ACN and incubate for 10 min at RT, then remove all liquid.
6. Add 50 mM IAA solution and incubate the resultant mixture for 45 min at RT in darkness.
7. After alkylation wash gel pieces with 25 mM AmBi and dehydrate using ACN. Repeat twice. Air-dry 5 min on ice.
8. Add 12.5 ng/mL trypsin in 25 mM AmBi. Let them saturate with the enzyme (2–3 h on ice) and then cover the gel pieces with 25 mM AmBi. Perform trypsin digestion overnight at 37 °C.
9. Transfer the supernatant to a new 0.5 μL microcentrifuge tube and then add 30 μL of 50 % ACN/0.1 % TFA solution to extract the peptides. Vortex 30 min and sonicate 5 min. Repeat this **step 3** times, combining the peptides extracts (*see* **Note 12**).

10. Dry the extracts in a vacuum centrifuge for approximately 3 h (*see* **Note 13**).

3.5 NanoHPLC-MS/MS

1. Ensure that the reservoirs for the mobile phase in the nanoflow HPLC are not empty. In case they need to be filled, add the mobile phase gradually with a pipette to avoid air bubbles.
2. Prime the binary pump with a syringe before operating the HPLC. Disconnect the mobile phase tube from the pump and connect the syringe adapter to the tube. Slowly pull the syringe to draw up at least 40 mL of the mobile phase in order to flush out gas bubbles and completely fill the tubings to the pump inlet. Disconnect the syringe adapter from the solvent tube and connect it to the binary pump (*see* **Note 14**).
3. Place the micro-switch valve to inject position. Perform the equilibration of the column at a flow of 400 nL/min changing the mobile phase from 3 to 100 % of buffer B_1. Then, gradually decrease the percentage of buffer B_1 until reaching initial conditions.
4. Dissolve the dried peptide samples in 40 μL of buffer A and transfer to an LC microvial.
5. Place the micro-switch valve to load position to inject the samples in the C_{18} precolumn. Inject 20 μL of the samples at a flow rate of 20 μL/min over 10 min to remove salts and other impurities.
6. Place the micro-switch valve to inject position. Load the desalted peptide mixture to a C_{18} column at a constant flow rate of 400 nL/min to perform the peptide separation.
7. Separate the peptides over 120 min using a multi-segment linear gradient of buffer B_1 (*see* **Note 15**). Finally, equilibrate the nanoHPLC system with 97 % buffer A_1 for 15 min.
8. Perform the MS analysis in the LTQ-Orbitrap. Specify tune settings in the Xcalibur 2.0.7 software as follows: spray voltage of 1.8 kV and temperature of the heated capillary at 200 °C.
9. Operate Orbitrap analyzer as follows: set full scan mode, resolution of 100.000 and range mass/charge (m/z) of 400–1800. Each full MS scan is followed by ten dependent MS/MS scans, in which the ten most abundant peptide ions are dynamically selected, with a dynamic exclusion window of 45 s.
10. Perform MS/MS analysis in CID mode, with a normalized collision energy of 35 %, isolation width of 3.0, activation Q of 0.250, and activation time of 30 ms. Set the minimum signal threshold to 100.
11. Repeat **steps 3–10** to analyze the technical replicate of the samples, if required.

3.6 Data Analysis

1. Process the acquired raw data using MaxQuant (version 1.2.2.5).
2. Configure the Andromeda search engine: (a) In the General tab, press the plus sign button to add a new database; (b) Load the protein sequence fasta file; (c) Specify the "Select rule" by choosing a predefined rule from the available list (>.*\|(.*)\| for Uniprot); (d) Press the update button to select the desired rule from the rules panel.
3. In the Raw files tab of MaxQuant, press the load files button to upload raw files.
4. Create an experimental design file template in a folder named "combined." The folder should be in the same location as raw files. Add fraction and experiment information.
5. In the Modifications & Labels tab, select methionine oxidation and protein N-terminal acetylation as "Variable modifications."
6. Set the "Multiplicity" according to the number of labels in your experiment. Select 3 for double and triple SILAC labeling.
7. Select 3 as the maximum number of labeled amino acids per peptide.
8. Select Trypsin/P as digestion enzyme.
9. Set the "Type" according to the mass spectrometer: select "Standard" for LTQ-Orbitrap.
10. Select the labeled amino acids used in our experiment. Select Lys 4 and Arg 6 from "Medium labels" panel and Lys 8 and Arg 10 from "Heavy labels" panel.
11. Select 2 as maximum number of missed cleavage sites per peptide.
12. Keep the default values of the options main and first search ppm, maximum charge per peptide, maximum number of modifications, and individual peptide mass tolerance.
13. In the MS/MS & sequences tab, press "Add file" button in order to load a protein sequence fasta file preconfigured previously in Andromeda.
14. Introduce Carbamidomethyl (C) as "Fixed modifications."
15. Check the "Include contaminants" box to add known contaminants to the search database file. Check the "I=L" box to use isoleucine and leucine as indistinguishable during the MaxQuant analysis.
16. In the "Identification & Quantification" tab, set the peptide and protein FDR values to 1%.

17. Set 6 value to the minimum peptide length. Shorter peptides are not taken into account for identification or quantification.
18. Load the experimental design template which was modified in **step 4**.
19. Select the minimum number of peptide ratios for protein quantification.
20. Specify which peptides should be used for protein ratio calculation. Check "Use unique and razor peptides" option.
21. In the Site quantification panel, select "Normalized ratios" option to use the normalized peptide ratios.
22. Check the "Re-quantify" option to calculate the ratio for isotopic patterns not assembled as SILAC pairs. The missing isotope pattern will be reconstructed based on the shape of the found isotope pattern, the expected shift among the *m/z* retention time plane, and the intensities integrated over these regions (*see* **Note 16**).
23. Select the "Match between runs" option to transfer MS/MS identifications across different LC-MS/MS runs (replicates). Specify the size of the time window in which the program can align the two retention times of the medium and heavy peptide. The default value is 2 min.
24. Select the number of threads (1–4) that will be used for MaxQuant processing.
25. Press the "Start" button and go to the "Performance" tab to evaluate the state of the processing.
26. MaxQuant results are stored in .txt files in the combined folder created in **step 7** (*see* **Note 17**).

4 Notes

1. Urea solutions must not be heated above 30 °C, as this may produce protein carbamylation. Thiourea is insoluble in water; therefore first dissolve the urea, then the thiourea, and finally the rest of the reagents.
2. Filter the Coomassie Blue solution before use. The dye can be reused. However, for protein identification by MS it is preferable to prepare a fresh solution.
3. Make AmBi and IAA solutions shortly before use; discard unused volume.
4. Trypsin stock (1 μg/μL) can be kept frozen in aliquots at −20 °C.
5. Titration of a suitable Arg concentration in SILAC medium is required. Several studies using SILAC have described the

metabolic conversion of Arg to proline (Pro) in certain cell lines [16]. This conversion process can reduce the intensity of the labeled peptides (heavy) affecting protein ratios. One strategy to minimize this problem is to reduce the Arg concentration in the SILAC medium.

6. Cells should be expanded for at least five cell doublings in order to obtain 100 % labeling efficiency. To determine the incorporation rate of labeled amino acids, as well as the conversion of Arg to Pro, cell lysates should be independently analyzed by LC-MS/MS.
7. CM volume depends on the cellular culture system. We perform the chondrogenic differentiation of MSCs in a micromass (3D) culture system [13]. In this case, more than one cell pellet can be combined in the same polypropylene tube in order to reduce the SILAC medium. We usually recover 1 mL of CM (around 6–10 μg of protein) from each experimental condition.
8. CMs are filtered using 0.2 μm filters to remove cell debris and remaining particles present in the medium. In addition, this step reduces the CM contamination with intracellular proteins.
9. CM can be fractionated by SDS-PAGE to reduce sample complexity. We usually separate proteins from the secretome in a few fractions (4–6 bands). It is important to use gels of 1 mm thick (or less) to avoid problems with protein digestion and to facilitate gel destaining.
10. Take special care to avoid contamination of samples with keratins. For the excision of gel bands, it is recommended to rinse the glass plates with ethanol before use, and to change gloves frequently.
11. Band destaining is necessary for successful LC-MS/MS analysis. The duration of the washing steps depends on the staining intensity. Wash the gel pieces at least three times. If the gel pieces are still blue, continue with the protocol, since it will not interfere with protein digestion.
12. Extracted peptides from each gel piece are pooled in the same microcentrifuge tube. Do not discard extracted gel pieces until MS analysis has been performed. If the digestion fails, the protocol can be repeated using the same gel pieces.
13. Dried peptide extracts can be safely stored at −20 °C for a few months until LC-MS/MS analysis.
14. Make sure that buffer A reservoir is full before priming the binary pump.
15. The specific gradient we use is given in Table 2.

Table 2
Multi-segment linear gradient

Time (min)	A_1 (%)	B_1 (%)
0	97	3
10	97	3
100	60	40
105	60	40
106	10	90
120	0	100
121	97	3

16. This option is highly recommended to quantify proteins with high ratios, where one of the SILAC partners is below noise level.
17. Among the MaxQuant .txt output files, the "proteinGroups" table contains the list of the identified and quantified proteins. In this table, the quantitative information of each protein is given by the normalized ratio *H/M* (*H*: heavy; *M*: medium labels). The ratio *H/M* column can directly be used to calculate significance B (a *p*-value dependent on the protein intensities) using Perseus software.

References

1. Hathout Y (2007) Approaches to the study of the cell secretome. Expert Rev Proteomics 4:239–248
2. Tjalsma H, Bolhuis A, Jongbloed JD et al (2000) Signal peptide-dependent protein transport in Bacillus subtilis: a genome-based survey of the secretome. Microbiol Mol Biol Rev 64:515–547
3. Makridakis M, Vlahou A (2010) Secretome proteomics for discovery of cancer biomarkers. J Proteomics 73:2291–2305
4. Pavlou MP, Diamandis EP (2010) The cancer cell secretome: a good source for discovering biomarkers? J Proteomics 73:1896–1906
5. Mustafa SA, Hoheisel JD, Alhamdani MS (2011) Secretome profiling with antibody microarrays. Mol Biosyst 7:1795–1801
6. Skalnikova H, Motlik J, Gadher SJ et al (2011) Mapping of the secretome of primary isolates of mammalian cells, stem cells and derived cell lines. Proteomics 11:691–708
7. Choi YA, Lim J, Kim KM, Acharya B, Cho JY, Bae YC, Shin HI, Kim SY, Park EK (2010) Secretome analysis of human BMSCs and identification of SMOC1 as an important ECM protein in osteoblast differentiation. J Proteome Res 9:2946–2956
8. Kim S, Min WK, Chun S et al (2010) Protein expression profiles during osteogenic differentiation of mesenchymal stem cells derived from human umbilical cord blood. Tohoku J Exp Med 221:141–150
9. Lee MJ, Kim J, Kim MY, Bae YS, Ryu SH, Lee TG, Kim JH (2010) Proteomic analysis of tumor necrosis factor-alpha-induced secretome of human adipose tissue-derived mesenchymal stem cells. J Proteome Res 9:1754–1762
10. Ong SE, Blagoev B, Kratchmarova I et al (2002) Stable isotope labeling by amino acids in cell culture, SILAC, as a simple and accurate approach to expression proteomics. Mol Cell Proteomics 1:376–386

11. Alvarez-Llamas G, Szalowska E, de Vries MP et al (2007) Characterization of the human visceral adipose tissue secretome. Mol Cell Proteomics 6:589–600
12. Kristensen LP, Chen L, Nielsen MO et al (2012) Temporal profiling and pulsed SILAC labeling identify novel secreted proteins during ex vivo osteoblast differentiation of human stromal stem cells. Mol Cell Proteomics 11:989–1007
13. Rocha B, Calamia V, Casas V et al (2014) Secretome analysis of human mesenchymal stem cells undergoing chondrogenic differentiation. J Proteome Res 13:1045–1054
14. Tasso R, Gaetani M, Molino E et al (2012) The role of bFGF on the ability of MSC to activate endogenous regenerative mechanisms in an ectopic bone formation model. Biomaterials 33:2086–2096
15. Rocha B, Calamia V, Mateos J et al (2012) Metabolic labeling of human bone marrow mesenchymal stem cells for the quantitative analysis of their chondrogenic differentiation. J Proteome Res 11:5350–5361
16. Van Hoof D, Pinkse MW, Oostwaard DW et al (2007) An experimental correction for arginine-to-proline conversion artifacts in SILAC-based quantitative proteomics. Nat Methods 4:677–678
17. Molina H, Yang Y, Ruch T et al (2009) Temporal profiling of the adipocyte proteome during differentiation using a five-plex SILAC based strategy. J Proteome Res 8:48–58

INDEX

Massimiliano Gnecchi (ed.), *Mesenchymal Stem Cells: Methods and Protocols*, Methods in Molecular Biology, vol. 1416, DOI 10.1007/978-1-4939-3584-0, © Springer Science+Business Media New York 2016

D

E

F

G

H

I

K

L

M

N

O

P

R

S

T

U

V

W

X